

Dissertation zur Erlangung des Doktorgrades der
Fakultät für Chemie und Pharmazie der
Ludwig-Maximilians-Universität München

**Effect of Collapse
on Pharmaceutical Protein Lyophilizates**

Kathrin Brigitte Schersch

aus Kiel

München 2009

Erklärung

Diese Dissertation wurde im Sinne von § 13 Abs. 3 bzw. 4 der Promotionsordnung vom 29. Januar 1998 von Herrn Prof. Dr. G. Winter betreut.

Ehrenwörtliche Versicherung

Diese Dissertation wurde selbständig, ohne unerlaubte Hilfe erarbeitet.

München, den 18.09.2009

A handwritten signature in black ink, appearing to read 'Kathrin Schersch', written in a cursive style. Below the signature is a horizontal dotted line.

Kathrin Schersch

Dissertation eingereicht am: 22.09.2009

1. Gutachter: Prof. Dr. G. Winter

2. Gutachter: Prof. Dr. W. Frieß

Mündliche Prüfung am: 23.10.2009

ACKNOWLEDGMENTS

The present thesis was prepared at the Department of Pharmacy, Pharmaceutical Technology and Biopharmaceutics at the Ludwig-Maximilians-University (LMU) in Munich, Germany under the supervision of Prof. Dr. Gerhard Winter.

First of all, I would like to express my deepest gratitude to my supervisor Prof. Dr. Gerhard Winter for giving me the possibility to join his team and to work in this fascinating field of research, for his professional and dedicated guidance of my work and for all his scientific and also personal advice over the last years. Also I would like to thank him for providing outstanding working conditions and for the opportunity to present my work at numerous international conferences and meetings. I am deeply thankful for making possible my research stay in the lab of Prof. Pikal.

I would like to thank Prof. Dr. Wolfgang Frieß for his continuous enthusiasm and interest in my work, the scientific input and advice over the last years and for kindly being co-referee of this thesis.

I would like to thank Prof. Winter and Prof. Frieß for creating an outstanding working climate that made the preparation of this thesis a precious and exciting time.

Boehringer-Ingelheim Pharma GmbH & Co.KG is gratefully acknowledged for scientific, financial and material support. My very special thanks go to the whole group of A BP Process Sciences in Biberach for their very warm welcome and for their great support during this project. Especially, I would like to thank Ortrud Betz, for her never-fading understanding and all the support and practical help over the last years. My very special thanks are also expressed to Dr. Silke Mühlau, Dr. Patrick Garidel and Dr. Stefan Bassarab for all their scientific and personal contributions to the success of this exciting project and their constant interest in this work. Thanks are extended to all other groups at Boehringer-Ingelheim that contributed to this project during the last years.

I am deeply grateful to Prof. Dr. Michael Pikal for giving me the great opportunity to work for three months in his lab at the University of Connecticut. I would also like to thank him for his enthusiasm and his extremely valuable scientific input into my work. I would like to express my profound appreciation to the entire research group at UConn for their very warm welcome, all the help and support and also for simply having a great time. My special thanks go to Johanna Rivera. I very much enjoyed our trips in New England. JoAnne Ronzello from

the Institute of Materials Science, University of Connecticut is gratefully acknowledged for support with the DRS measurements.

The Dr. August und Dr. Anni Lesmüller-Foundation is thanked for their generous financial support.

Many thanks are expressed to all the colleagues from the research groups of Prof. Winter and Prof. Frieß who shared the time with me in Munich, to Ahmed, Alice, Andrea, Angelika, Gerd, Jan, Julia, Kathrin, Klaus, Martin, Michael, Sandra and Virginie and the entire crew. Thank you for the many inspiring discussions, for all the help and support and for the numerous activities also off the job. Especially, I would like to thank Stefan and Rainer for the great time we had - and for the music.

Wolfgang Wünschheim is acknowledged for his help with the powder diffractometer and Tina Reuther for performing the BET measurements.

Alice Pahnke is acknowledged for the good job she has done during her bachelor thesis.

Thanks are extended to Prof. Dr. A. Vollmar, Prof. Dr. F. Bracher, Prof. Dr. F. Paintner and PD Dr. S. Zahler for kindly serving as a member of my thesis advisory committee.

I am very thankful to Patrick Garidel, Sandra Schulze, Julia Myschik and Tim Serno for proof-reading this thesis.

To my parents, my sisters Stephanie and Caroline and my grand-parents: Thank you for all your encouragement and support, thank you for always being there for me.

Finally, I would like to thank Tim, for all your help and support. And for your love.

For my parents

TABLE OF CONTENTS

CHAPTER 1: GENERAL INTRODUCTION

1	INTRODUCTION	1
2	FREEZE-DRYING OF PROTEINS	3
2.1	THE FREEZE-DRYING PROCESS IN BRIEF	3
2.2	FREEZE-DRYING OF PROTEIN PHARMACEUTICALS	6
3	THE COLLAPSE PHENOMENON	9
3.1	DEFINITION.....	9
3.2	MECHANISM	10
3.3	THE COLLAPSE TEMPERATURE	12
3.4	DETERMINANTS OF COLLAPSE.....	14
3.4.1	Viscosity.....	14
3.4.2	Time scale	15
3.4.3	Pore radius	17
3.5	THE OCCURRENCE OF COLLAPSE	17
3.5.1	Collapse during freeze-drying.....	17
3.5.2	Collapse during storage.....	18
3.6	EFFECTS OF COLLAPSE: CURRENT OPINION	18
3.7	PRO & CONTRA OF DRYING CLOSE TO THE COLLAPSE TEMPERATURE: WHY IT IS WORTH INVESTIGATING THE COLLAPSE PHENOMENON IN DETAIL	21
4	STABILITY OF PROTEIN PHARMACEUTICALS IN THE SOLID STATE	24
4.1	FACTORS AFFECTING STABILITY OF PROTEINS IN THE SOLID STATE	24
4.1.1	Water replacement hypothesis	24
4.1.2	Vitrification hypothesis	25
4.1.3	Temperature	25
4.1.4	Moisture	26
4.1.5	Hydrogen ion activity	26
4.2	IMPLICATIONS OF COLLAPSE FOR THE CONCEPTS OF SOLID STATE PRESERVATION.....	26
4.2.1	Effect of collapse on thermodynamic stabilization concepts.....	26
4.2.2	effect of collapse on kinetic stabilization concepts	26
4.3	CHARACTERISTICS OF GLASSY SYSTEMS	27
4.3.1	Temperature dependence of molecular mobility.....	28
4.4	STABILITY OF GLASSY SYSTEMS	31
4.5	CORRELATION OF MOLECULAR MOBILITY AND PROTEIN STABILITY	33

4.5.1	Global mobility	34
4.5.2	Local mobility	34
5	REFERENCES	36

CHAPTER 2: OBJECTIVES OF THE THESIS

OBJECTIVES OF THE THESIS	47
---------------------------------------	-----------

CHAPTER 3: MATERIALS AND METHODS

1	MATERIALS	51
1.1	IGG ₀₁	51
1.2	L-LACTIC DEHYDROGENASE (LDH)	52
1.3	PA ₀₁	52
1.4	FREEZE-DRYING EXCIPIENTS	53
1.5	FURTHER CHEMICALS AND REAGENTS	54
2	METHODS	55
2.1	FREEZE-DRYING	55
2.1.1	Process monitoring	55
2.1.2	Preparation of solutions for freeze-drying	55
2.1.3	The collapse-cycle	56
2.1.4	Conservative freeze-drying cycles	57
2.2	SAMPLE PROCESSING AFTER FREEZE-DRYING	61
2.2.1	Annealing in the solid dried state	61
2.2.2	Stability studies	61
2.2.3	Liquid storage stability	62
2.3	CHARACTERIZATION OF PROTEIN STABILITY	62
2.3.1	High pressure size-exclusion chromatography (HP-SEC)	62
2.3.2	One-chain/two-chain material PA ₀₁	63
2.3.3	Asymmetric flow field flow fractionation (AF4)	63
2.3.4	Dynamic light scattering (DLS)	66
2.3.5	Light obscuration	66
2.3.6	Turbidity	67
2.3.7	Sodium dodecyl sulphate polyacrylamide gel electrophoresis (SDS-PAGE) ..	67
2.3.8	Transmission Fourier Transform infrared (FTIR) spectroscopy	68
2.3.9	Intrinsic protein fluorescence spectroscopy	68
2.3.10	High resolution UV 2 nd derivative absorbance spectroscopy (2DUV)	69
2.3.11	Color of reconstituted solution	69
2.3.12	Activity assays	70

2.4	CHARACTERIZATION OF LYOPHILIZATE CHARACTERISTICS	71
2.4.1	Differential scanning calorimetry (DSC).....	71
2.4.2	Freeze-dry microscopy (FDM)	72
2.4.3	X-ray powder diffraction (XRD).....	72
2.4.4	Karl Fischer residual moisture determination	72
2.4.5	Near infrared spectroscopy (NIRS).....	73
2.4.6	Scanning electron microscopy (SEM).....	75
2.4.7	Digital microscopy.....	75
2.4.8	Macroscopic classification of the extent of collapse	75
2.4.9	Specific surface area (SSA) measurement.....	76
2.4.10	Mercury (HG) porosimetry	76
2.4.11	Helium pycnometry	76
2.4.12	Glucose quantification (Trinder assay)	77
3	REFERENCES	78
 CHAPTER 4: CONTROLLED GENERATION OF COLLAPSED LYOPHILIZATES		
1	INTRODUCTION	81
2	COLLAPSIBILITY	82
2.1	DETERMINATION OF CRITICAL MATERIAL PROPERTIES	82
2.2	TENTATIVE EXPERIMENTS	85
2.2.1	Effect of process parameters and formulation variables in formulations comprising a crystalline bulking agent.....	85
2.2.2	Effect of formulation variables in formulations lacking a crystalline bulking agent.....	87
2.3	THE COLLAPSE-CYCLE	89
2.3.1	Collapse-drying protocol	89
2.3.2	Appearance of collapsed cakes	89
3	CHARACTERIZATION OF THE COLLAPSE CYCLE AND THE DRYING BEHAVIOR OF COLLAPSED LYOPHILIZATES	91
3.1	FACTORS AFFECTING THE DRYING BEHAVIOR OF COLLAPSED LYOPHILIZATES	91
3.1.1	Formulation variables	91
3.1.2	Matrix structure: Partially crystalline and amorphous cakes	93
3.2	DRYING KINETICS	94
3.2.1	Effect of N ₂ -injections.....	94
3.2.2	Mass-spectrometric monitoring of drying in the collapsed state	95
3.2.3	Monitoring the drying process by gravimetric determination.....	98
3.2.4	Monitoring the drying process by visual inspection	99

3.3	CONCLUSION: OPTIMIZATION OF THE COLLAPSE-CYCLE	100
4	SUMMARY AND CONCLUSION	100
5	REFERENCES	102

CHAPTER 5: METHODS FOR THE QUANTIFICATION OF THE EXTENT OF COLLAPSE IN FREEZE-DRIED CAKES

1	INTRODUCTION	105
2	MACROSCOPIC AND MICROSCOPIC EVALUATION OF THE CAKE APPEARANCE	106
2.1	PARTIALLY CRYSTALLINE LYOPHILIZATES: FROM NON-COLLAPSED TO COMPLETELY COLLAPSED CAKES.....	106
2.2	AMORPHOUS LYOPHILIZATES	109
3	SPECIFIC SURFACE AREA (SSA) DETERMINATION	110
3.1	PARTIALLY CRYSTALLINE LYOPHILIZATES	110
3.2	AMORPHOUS LYOPHILIZATES	111
4	MERCURY POROSIMETRY.....	112
4.1	PARTIALLY CRYSTALLINE LYOPHILIZATES	112
5	HELIUM PYCNOMETRY	113
5.1	EFFECT OF COLLAPSE ON THE INTACT CAKE: PARTIALLY CRYSTALLINE LYOPHILIZATES	114
5.1.1	Porosity	114
5.1.2	Density	116
5.2	EFFECT OF COLLAPSE ON THE PARTICLE DENSITY: AMORPHOUS LYOPHILIZATES	117
6	SUMMARY AND CONCLUSION	118
7	REFERENCES	119

CHAPTER 6: EFFECT OF RESIDUAL MOISTURE ON IGG₀₁-STABILITY IN THE LYOPHILIZED STATE

1	INTRODUCTION	121
2	PHYSICOCHEMICAL MATERIAL-PROPERTIES	122
2.1	CAKE APPEARANCE	122
2.2	RESIDUAL MOISTURE	122
2.3	GLASS TRANSITION & CRYSTALLIZATION	126
3	PHYSICAL PROTEIN STABILITY OF IGG ₀₁ IN RECONSTITUTED LYOPHILIZATES	128
4	CONFORMATIONAL STABILITY OF IGG ₀₁ IN RECONSTITUTED LYOPHILIZATES	132
5	EXCURSUS: DISTRIBUTION OF RESIDUAL MOISTURE IN COLLAPSED AND ELEGANT CAKES	133

6	SUMMARY AND CONCLUSION	135
7	REFERENCES	137
 CHAPTER 7: EFFECT OF COLLAPSE ON PROTEIN STABILITY I: STABILITY AFTER FREEZE-DRYING		
1	INTRODUCTION	139
2	IgG₀₁	140
2.1	AMORPHOUS SYSTEMS.....	140
2.1.1	Physicochemical characteristics of lyophilizates.....	141
2.1.2	Physical protein stability of IgG ₀₁ in reconstituted lyophilizates.....	143
2.1.3	Binding activity of IgG ₀₁ in reconstituted lyophilizates.....	148
2.1.4	Conformational stability of IgG ₀₁ in reconstituted lyophilizates.....	149
2.1.5	Conformational stability of IgG ₀₁ in freeze-dried cakes.....	154
2.2	PARTIALLY CRYSTALLINE: FROM ELEGANT TO COMPLETELY COLLAPSED.....	155
2.2.1	Physicochemical characteristics of lyophilizates.....	158
2.2.2	Physical protein stability of IgG ₀₁ in reconstituted lyophilizates.....	162
2.2.3	Binding activity of IgG ₀₁ in reconstituted lyophilizates.....	167
2.2.4	Conformational stability of IgG ₀₁ in reconstituted lyophilizates.....	168
2.2.5	Conformational stability of IgG ₀₁ in freeze-dried cakes.....	170
2.2.6	Is there a delayed effect? short term stress stability of reconstituted IgG ₀₁ lyophilizates.....	171
3	L-LACTIC DEHYDROGENASE (LDH)	173
3.1	PHYSICOCHEMICAL PROPERTIES OF COLLAPSED AND NON-COLLAPSED LYOPHILIZATES.....	173
3.2	ENZYME ACTIVITY OF LDH IN RECONSTITUTED LYOPHILIZATES.....	176
3.3	PHYSICAL PROTEIN STABILITY OF LDH IN RECONSTITUTED LYOPHILIZATES.....	178
3.4	CONFORMATIONAL STABILITY OF LDH IN RECONSTITUTED LYOPHILIZATES.....	181
3.5	EXCURSUS I: COMPARISON OF DIFFERENT DISACCHARIDES.....	185
3.6	EXCURSUS II: IS THERE A MINIMUM MOLECULAR WEIGHT REQUIRED? EFFECT OF MOLECULAR WEIGHT OF PEG ON THE PRESERVATION OF LDH STABILITY IN COLLAPSED AND NON-COLLAPSED LYOPHILIZATES.....	188
3.6.1	Residual moisture.....	189
3.6.2	Physical protein stability.....	190
3.6.3	Conformational stability.....	191
3.6.4	Enzyme activity.....	192
3.7	SUMMARY AND CONCLUSION.....	193
4	TISSUE-TYPE PLASMINOGEN ACTIVATOR (PA₀₁)	194

4.1	PHYSICO-CHEMICAL PROPERTIES OF COLLAPSED AND NON-COLLAPSED LYOPHILIZATES	194
4.2	CATALYTIC ACTIVITY OF PA ₀₁ IN RECONSTITUTED LYOPHILIZATES.....	195
4.3	PHYSICAL STABILITY OF PA ₀₁ IN RECONSTITUTED LYOPHILIZATES	196
4.4	CONFORMATIONAL STABILITY OF PA ₀₁ IN RECONSTITUTED LYOPHILIZATES.....	199
5	FINAL SUMMARY AND CONCLUSION.....	201
6	REFERENCES	203

CHAPTER 8: EFFECT OF COLLAPSE ON PROTEIN STABILITY II: STABILITY OF LYOPHILIZATES DURING STORAGE AT ELEVATED TEMPERATURES

1	INTRODUCTION.....	213
2	IGG ₀₁	215
2.1	AMORPHOUS SYSTEMS I - TREHALOSE-BASED LYOPHILIZATES: THE EFFECT OF COLLAPSE DURING LYOPHILIZATION	215
2.1.1	Physicochemical characteristics of lyophilizates.....	215
2.1.2	Physical protein stability of IgG ₀₁ in reconstituted lyophilizates	217
2.1.3	Binding activity of IgG ₀₁ in reconstituted lyophilizates.....	221
2.1.4	Conformational stability of IgG ₀₁ in reconstituted lyophilizates	222
2.1.5	Summary and conclusion	223
2.2	AMORPHOUS SYSTEMS II – SUCROSE-BASED LYOPHILIZATES: THE EFFECT OF COLLAPSE DURING STORAGE.....	224
2.2.1	Physicochemical characteristics of lyophilizates.....	224
2.2.2	Physical protein stability of IgG ₀₁ in reconstituted lyophilizates	238
2.2.3	Binding activity of IgG ₀₁ in reconstituted lyophilizates.....	247
2.2.4	Conformational stability of IgG ₀₁ in reconstituted lyophilizates	248
2.2.5	Excursus: In-depth investigation of crystallization and non-enzymatic browning in initially collapsed and initially non-collapsed sucrose-based lyophilizates	250
2.2.6	Summary and conclusion	255
2.3	PARTIALLY CRYSTALLINE SYSTEMS: THE EFFECT OF PARTIAL COLLAPSE.....	257
2.3.1	Physicochemical characteristics of lyophilizates.....	258
2.3.2	Physical protein stability of IgG ₀₁ in reconstituted lyophilizates	259
2.3.3	Binding activity of IgG ₀₁ in reconstituted lyophilizates.....	262
2.3.4	Conformational stability of IgG ₀₁ in reconstituted lyophilizates	263
2.3.5	Summary and conclusion	265
3	L-LACTIC DEHYDROGENASE (LDH)	266

3.1	PHYSICO-CHEMICAL PROPERTIES OF COLLAPSED AND NON-COLLAPSED LYOPHILIZATES	267
3.2	ENZYME ACTIVITY OF LDH IN RECONSTITUTED LYOPHILIZATES.....	272
3.2.1	Collapsed versus non-collapsed lyophilizates	272
3.2.2	Collapsed versus partially collapsed lyophilizates	273
3.3	PHYSICAL PROTEIN STABILITY OF LDH IN RECONSTITUTED LYOPHILIZATES	274
3.3.1	Collapsed versus non-collapsed lyophilizates: Trehalose-based formulations	275
3.3.2	Collapsed versus partially collapsed lyophilizates: Sucrose-based formulations	278
3.4	CONFORMATIONAL STABILITY OF LDH IN RECONSTITUTED LYOPHILIZATES	281
3.4.1	Collapsed versus non-collapsed lyophilizates: Trehalose-based lyophilizates	281
3.4.2	Collapsed versus partially collapsed lyophilizates: Sucrose-based lyophilizates	285
3.5	SUMMARY AND CONCLUSION.....	288
4	TISSUE-TYPE PLASMINOGEN ACTIVATOR (PA₀₁)	290
4.1	PHYSICO-CHEMICAL PROPERTIES OF COLLAPSED AND NON-COLLAPSED LYOPHILIZATES	290
4.2	CATALYTIC ACTIVITY OF PA ₀₁ IN RECONSTITUTED LYOPHILIZATES.....	292
4.3	PHYSICAL PROTEIN STABILITY OF PA ₀₁ IN RECONSTITUTED LYOPHILIZATES ..	293
4.4	CONFORMATIONAL STABILITY OF PA ₀₁ IN RECONSTITUTED LYOPHILIZATES.....	299
4.5	SUMMARY AND CONCLUSION.....	301
5	FINAL SUMMARY AND CONCLUSION.....	303
6	REFERENCES	306

CHAPTER 9: GLASSY DYNAMICS OF COLLAPSED AND NON-COLLAPSED LYOPHILIZATES

1	INTRODUCTION.....	315
2	SPECIAL MATERIALS AND METHODS.....	318
2.1	FREEZE-DRYING	318
2.1.1	Solutions for freeze-drying	318
2.1.2	Collapsed lyophilizates	318
2.1.3	Non-collapsed lyophilizates	318
2.2	ANNEALING AFTER FREEZE-DRYING.....	319
2.3	ISOTHERMAL MICROCALORIMETRY (THERMAL ACTIVITY MONITOR (TAM)).....	319
2.4	DIELECTRIC RELAXATION SPECTROSCOPY (DRS)	321

2.5	DIFFERENTIAL SCANNING CALORIMETRY (DSC)	325
2.5.1	Determination of T_g and $\Delta c_p (T_g)$	325
2.5.2	Determination of fragility	326
2.6	POWDER DENSITY MEASUREMENTS.....	326
2.7	KARL FISCHER RESIDUAL MOISTURE DETERMINATION	326
2.8	SOLID STATE FOURIER TRANSFORM INFRARED (SS-FTIR) SPECTROSCOPY	327
2.9	SPECIFIC SURFACE AREA (SSA) MEASUREMENT	327
2.10	HIGH PRESSURE SIZE-EXCLUSION CHROMATOGRAPHY (HP-SEC)	327
2.11	POLARIZED LIGHT MICROSCOPY	328
3	GLOBAL DYNAMICS OF COLLAPSED AND NOT COLLAPSED LYOPHILIZATES	329
3.1	GLOBAL DYNAMICS FROM CALORIMETRIC DATA.....	329
3.1.1	Sucrose-based freeze-dried systems	329
3.1.2	Trehalose based freeze-dried systems.....	332
3.2	GLOBAL DYNAMICS FROM SPECTROSCOPIC DATA.....	333
3.2.1	Experimental Set-Up: Benefit of the insertion of a Teflon-Sheet	333
3.2.2	The α -relaxation process	336
4	LOCAL DYNAMICS OF COLLAPSED AND NOT COLLAPSED LYOPHILIZATES	342
5	FRAGILITY OF COLLAPSED AND NOT COLLAPSED LYOPHILIZATES	354
5.1	FRAGILITY FROM CALORIMETRIC METHODS	355
5.2	FRAGILITY FROM SPECTROSCOPIC METHODS.....	355
6	IS IT JUST ANNEALING OR IS THERE A “COLLAPSE EFFECT”?	357
6.1	EFFECT OF ANNEALING ON GLASSY DYNAMICS OF NON-COLLAPSED CAKES	357
6.2	CORRELATION OF GLASSY DYNAMICS TO STORAGE STABILITY	358
7	SUMMARY	364
8	REFERENCES	366

CHAPTER 10: FINAL SUMMARY AND CONCLUSION

FINAL SUMMARY AND CONCLUSION	371
---	------------

LIST OF ABBREVIATIONS

2DUV	Second derivative UV-absorption spectroscopy
AF4	Asymmetrical flow field-flow fractionation
BSA	Bovine serum albumine
DLS	Dynamic light scattering
DRS	Dielectric relaxation spectroscopy
DSC	Differential scanning calorimetry
DTT	Dithiothreitol
FDA	U.S. Food and Drug Administration
FDM	Freeze-dry microscopy
FNU	Formazine Nephelometric Units
FTIR	Fourier transformed infrared spectroscopy
Hmw	high molecular weight
Ig	Immunoglobulin
IgG	Immunoglobulin class G
LDH	L-lactic dehydrogenase
M	Mannitol
mAb	Monoclonal antibody
NIRS	Near infrared spectroscopy
NNLS	Non-negative least squares
PAGE	Poly(acrylamide) gel electrophoreses
PBS	Phosphate-buffered saline
PDI	Polydispersity index
PEG	Poly(ethylene glycol)
Ph.Eur.	European Pharmacopoeia
rpm	rounds per minute
S	Sucrose
SD	Standard deviation
SDS	Sodium Dodecyl Sulphate
SE	Standard error
SE-HPLC	Size exclusion high performance liquid chromatography
SEM	Scanning electron microscopy
SPR	Surface plasmon resonance spectroscopy
SSA	Specific surface area
ss-FTIR	solid state Fourier transformed infrared spectroscopy
τ	relaxation time constant

T_0	Temperature of zero mobility
TAM	Thermal Activity Monitor
T_c	Collapse temperature
T_f	Fictive temperature
T_g	Glass transition temperature
T_g'	Glass transition temperature of the maximally freeze-concentrated solution
T_m	Melting temperature
T_{cryst}	Crystallization temperature
USP	United States Pharmacopoeia
XRD	X-Ray powder diffraction

CHAPTER 1

GENERAL INTRODUCTION

1 INTRODUCTION

Starting in the early 1970s, the improved understanding of the biomolecular roots of human diseases (due to advances made in the fields of molecular biology and genetic engineering) paired with the development of new biotechnological techniques opened the door to tremendous possibilities of using proteins as pharmaceuticals to alleviate illnesses^{1,2}. With the first production of rDNA (Paul Berg in 1972)³ and the first recombinant plasmid transformation of E.coli (Herbert Boyer's team in 1973)⁴ the era of recombinant protein pharmaceuticals began.

Since the FDA-approval of the first human recombinant protein in 1982, (Humulin, Genentech) protein pharmaceuticals have become increasingly important in state of the art pharmacotherapy. Today more than 130 different proteins or peptides are approved for clinical use by the FDA and many more are under development². The treatment of manifold diseases, such as diabetes mellitus, hemophilia or other enzyme deficiency diseases, various cancer afflictions, immune mediated diseases such as Multiple sclerosis or Hepatitis B/C as well as emergency medication such as clotlysis after acute myocardial infarctions has been tremendously improved by protein pharmaceuticals.

However, the same properties that contribute to the proteins' high potential as pharmaceuticals, their complexity and compositional variety, also cause their high susceptibility to various stresses. Therefore, finding a formulation that stabilizes the protein during purification, production, storage and final application is one of the major challenges during biopharmaceutical development.

Because liquid formulations are more cost-conscious to handle during manufacturing, the desired drug product would be a stable liquid. What is more, liquids are more convenient for the patient⁵. Although efforts have been made to develop stable liquid formulations for biopharmaceuticals the method of choice for the stabilization of many protein pharmaceuticals is still lyophilization (e.g. Activase[®] (Alteplase), ReFacto[®] (Factor VIII), Enbrel[®] (Etanercept), Avonex[®] (Interferon beta-1a)⁶).

The freeze-dried state bears some advantages over the liquid state. As the protein ingredient is immobilized in the solid state the rate constant of most chemical and physical degradation reactions is decreased dramatically in the glassy state⁷⁻⁹. As the product thus becomes more stable, this might permit suitable long term storage at 5 °C or ambient temperatures (25 °C), leading to simplified product handling during storage and shipping, where exact temperature

control is not always feasible and considerably increases costs of goods. Another merit is that the risk of damage during abidance at sub-zero temperatures is eliminated. Furthermore the risk of interfacial-stress, e.g. during agitation is eliminated as the product is solid^{5,7}.

One major constraint of lyophilization is the time-consuming and costly production cycles. It is good pharmaceutical freeze-drying practice to keep the product at a low product temperature during the lyophilization process¹⁰. A rise in product temperature above the glass transition temperature of the maximally freeze concentrated protein-exciipient solution (T_g') or even above the collapse temperature (T_c) is regarded as detrimental for product quality although data fully confirming this assumption is rare and not clear. The major purpose of this approach is to avoid the onset of structural cake collapse during the primary or secondary drying stage¹¹⁻¹⁴. The onset of gross collapse in a protein pharmaceutical product causes the loss of the whole batch as reprocessing of collapsed material is not an option at the moment.

With the entry of biogenerics into the pharmaceutical market the development of stable and safe but cost-conscious products becomes even more important. "Conservative" freeze-drying cycles usually take several days up to a week to finish. Special attention has to be paid to optimization of lyophilization because any increase in product temperature dramatically decreases primary drying time¹⁵. Recently, there have been several patent applications, claiming the application of high primary drying temperatures to shorten drying times¹⁶⁻¹⁸.

However, in order not to jeopardize product stability, exact monitoring of the freeze-drying process using state of the art process analytical technology (PAT) is important. Even more crucial is the thorough revision of the conventional approach of freeze-drying at low product temperatures. A detailed investigation of the implications of high product temperatures and collapse on protein stability during freeze-drying and the stability of such products during subsequent storage has to be performed in order to allow for a scientifically sound evaluation of the effect of collapse on protein stability and to provide a broad basis for the responsible handling and reprocessing of collapsed batches.

2 FREEZE-DRYING OF PROTEINS

2.1 THE FREEZE-DRYING PROCESS IN BRIEF

Lyophilization is a unit operation commonly employed as a drying technology in the food and pharmaceutical industry¹⁹. Freeze-drying was first mentioned by Ray in 1976²⁰. Jennings gave the first definition to the term lyophilization emphasizing the intention to stabilize (heat-) sensitive materials by reducing the amount of solvent (most commonly water²¹) to a level that no longer allows biological growth or chemical reactions²². Lyophilization in its simplest form is defined as a process where the solution that shall be dried is first frozen and concomitantly the solvent is removed by first sublimation (primary drying) and second by desorption (secondary drying)^{22,23}.

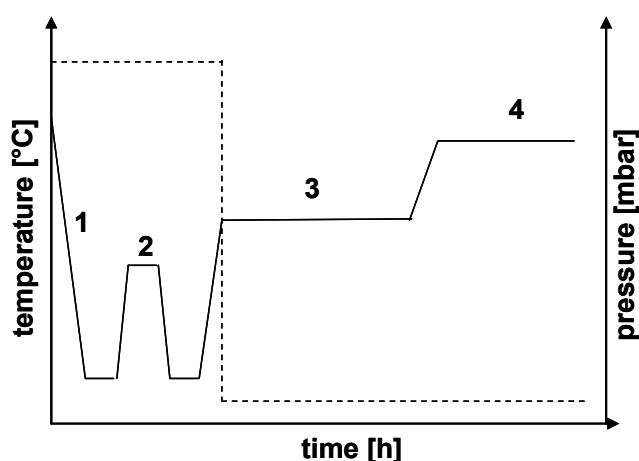


Figure 1.1: Scheme of a typical freeze-drying cycle.

Temperature (solid black line) and pressure (dashed black line) course during the different process stages: 1 = freezing, 2 = annealing (optional), 3 = primary drying, 4 = secondary drying.

The freeze-drying process can be divided into three major process stages, i.e. freezing, primary drying and secondary drying. An optional annealing step can be included between the freezing and the drying steps. Figure 1.1 depicts a scheme of a typical freeze-drying protocol.

In the following paragraph each step's key parameters are briefly described, focusing on characteristics important with regards to the collapse phenomenon.

FREEZING

During the freezing step, the temperature of the freeze-drying system is lowered below its solid-liquid phase transition temperature. Thereby the solvent is separated from the solute²³. Figure 1.2 depicts the typical behavior of an amorphous system upon cooling:

Upon lowering the temperature either crystallization of both solvent and solute, forming an eutectic mixture below the eutectic temperature (T_{eut} in Figure 1.2), or crystallization of the solvent alone, resulting in phase separation and the formation of a crystalline ice-phase and an amorphous solute-phase, occur. In the case of phase separation, an increase in

concentration in the remaining solution (so-called freeze-concentration) is observed. Freeze-concentration continues until the viscosity exceeds a critical value, that defines the glass transition of the maximally freeze-concentrated solution (T_g' in Figure 1.2). Below the glass transition, the amorphous phase is solid and is referred to as a glass in the interstitials of the ice crystals²¹.

The freezing step during lyophilization is considered at least as important for product quality as the drying steps due to its potential effect on protein stability²⁴. The key parameter hereby is the cooling rate or rather the ice nucleation rate²⁵. In general, a faster freezing rate results in smaller ice crystals^{26,27}. Fast freezing causes a greater degree of super cooling, i.e. the retention of the liquid state below the equilibrium freezing point of the solution. Super cooling limits the ability to control the freezing rate by manipulation of shelf temperature, because the greater the degree of super cooling, the faster is the effective freezing rate once ice crystals nucleate²⁸⁻³⁰. Slow freezing in return results in larger ice crystals because ice crystal growth continues after ice crystal nucleation. However, a slow freezing rate also was observed to result in considerable super-cooling³¹ and thus a fast effective freezing rate. Slow freezing also has the potential to increase the system's tendency for phase separation and prolongs the time where the protein exists in a highly concentrated fluid state³². In general, the ability to control the freezing rate is limited and an intermediate freezing rate is recommended³².

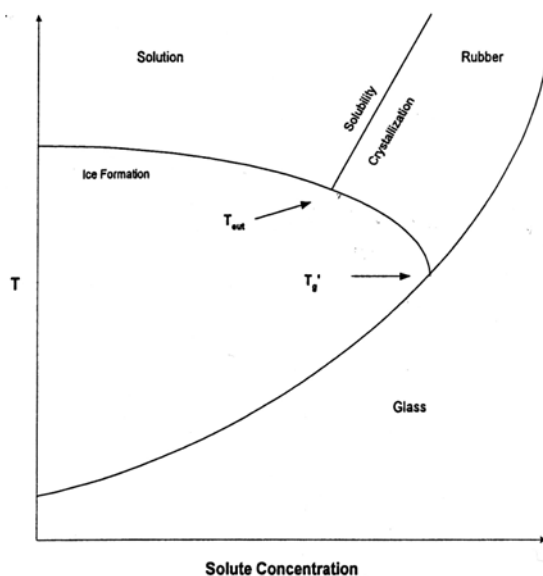


Figure 1.2: Theoretical phase diagram showing ice formation, solute crystallization, the eutectic melting point and the glass transition during freezing of an amorphous system. ^{25,28}

Small crystals generate small pores, as pores originate from sublimed ice crystals. During drying, water vapor has to diffuse through these pores out of the cake. Small pores oppose a higher resistance to water vapor flow than larger pores (a phenomenon referred to as dried layer resistance), thus decreasing the sublimation rate and turning primary drying less efficient. In contrast, larger pores greatly reduce the dry layer resistance to water vapor and

render primary drying more efficient. Annealing is sometimes applied to increase the size of ice crystals formed during the freezing step by Ostwald ripening and thus increase the efficiency of primary drying.

However, small pores also add up to a larger specific surface area as compared to large pores, resulting in a more efficient secondary drying³³.

PRIMARY-DRYING

During primary-drying the frozen solvent is removed from the product by sublimation. This is initiated by lowering the chamber pressure to a level lower than the vapor pressure of ice at the product temperature. The energy required for the phase transition is provided by adjusting the shelf temperature. Because the energy input is consumed by sublimation the resulting product temperature is much lower than the shelf temperature. Differences of up to 30 Kelvin (K) are not unusual. The product temperature approaching the shelf temperature due to the end of sublimation is a common way to detect the end of primary drying.

There are three mechanisms accounting for the heat transfer from the shelf to the vial: conduction, convection and radiation.

In order to prevent collapse the product temperature has to be maintained below the collapse temperature. When the collapse temperature is unknown, the glass transition or the eutectic melting temperature in amorphous or crystalline systems, respectively, is used as maximum allowable product temperature³³. On the other hand, as each 1°K increase in product temperature decreases primary drying time by about 13%¹⁵, the drying temperature should be maintained as high as possible.

The process is characterized by the sublimation rate v that can be expressed as:

$$v = \frac{A_p (P_p - P_0)}{R_p} \quad (1.1)$$

A_p is the cross sectional area of the vial, P_p is the product's vapor pressure at the sublimation front, P_0 is the partial vapor pressure in the vial and R_p is the dried layer resistance to water vapor flow^{33,34}.

The resistance of the already dried product, accounting for 90% of the total resistance to vapor flow, increases with progressing drying and can cause an increase of product temperature possibly leading to cake collapse³⁵. However, the occurrence of small-scale collapse may decrease R_p and increase the sublimation rate³⁶.

SECONDARY DRYING

At the end of primary drying, only non-frozen water is present in the freeze-dried cake. This water cannot be removed by sublimation but has to be removed by desorption. Thus more energy is applied during secondary drying. To further promote the drying process some

authors advise to further decrease the chamber pressure in order to increase the concentration gradient of water vapor from the product to its surroundings.

Especially at the beginning of secondary drying it is important to bear in mind that the glass transition temperature is a function of residual moisture. As the residual moisture content at the end of primary drying can be as high as 30%, a too rapid increase in shelf temperature may cause the product temperature to rise above the collapse temperature resulting in cake collapse³⁷.

The residual moisture decreases rapidly during the first hours of secondary drying, approaching an equilibrium level dependent only on the shelf temperature and the specific surface area of the cake. It is independent of the chamber pressure or the height of the dried product layer³⁸.

2.2 FREEZE-DRYING OF PROTEIN PHARMACEUTICALS

Proteins are complex and labile molecules, sensitive towards various degradation pathways. As for economic viability a shelf life of 18-24 months is desirable³⁹, lyophilization is often the method of choice to develop stable market formulations for biopharmaceuticals. 46% of the FDA-approved biopharmaceuticals in 2003 were lyophilizates⁴⁰.

Although freeze-drying is used to stabilize labile products, the process itself generates both freezing and drying stresses and might often be harmful for the protein pharmaceutical⁴¹. Thus the careful development of a formulation that thoroughly stabilizes the active ingredient is as important as the lyophilization cycle development itself⁴⁰.

The formulation shall provide stability during manufacturing, freeze-drying, shipping, storage reconstitution and finally during administration of the final product in the patient. Degradation pathways of proteins are diverse and complex. Smallest amounts of degradation products can have severe consequences, for example as intermediates for further degradation, as e.g. oxidized species or heterogeneous nucleation sites as metals shed from vial filling pumps. Alternatively aggregated species may cause immune responses. Hence the formulation has to provide the highest possible level of stabilization⁴².

In principle, a formulation for freeze-drying is composed of protein stabilizers (so-called cryo- and lyo-protectants), specific stabilizers as antioxidants or surfactants, bulking agents, tonicifiers and buffer agents^{25,40}. Generally the total amount of solids in the formulation makes up between 2 and 10 % of the solution before freeze-drying, combining a sufficient mass to ensure a stable cake but allowing for good processability as well^{5,43}.

The choice of excipients is particularly governed by the level of stabilization required by the specific protein drug. If the concentration of active ingredient is low, a bulking agent like mannitol or glycine has to be used to ensure an elegant and mechanically stable cake with satisfying drying behavior. Furthermore, salts either serving as pH buffers or giving the required tonicity, should be added⁹. The addition of specific stabilizers such as surfactants,

antioxidants or preservatives can be necessary as well. To achieve a sufficiently short reconstitution time and adequate solubility, a solubilizer like arginine can be added.

The compatibility of the protein drug with excipients and container materials has to be kept in mind as well. Furthermore, the regulatory status of excipients, the route of administration or a desired modified release has to be taken into account.

The different components of freeze-drying formulations will be discussed in more detail below. Before, a short description of the stress situation arising during lyophilization is given.

During freezing, the decreasing temperature can cause cold denaturation, as the solubility of hydrophobic groups in water increases with decreasing temperature concurrently decreasing intramolecular hydrophobic interactions determining the protein's tertiary and quaternary structure^{9,44-46}. Oligomeric proteins often show cold denaturation. One factor accounting for this phenomenon is, that association is amongst others determined by hydrophobic interactions^{27,46}.

Other instabilities arise due to the formation of ice crystals: Most obviously the formation of ice crystals creates new interfaces that are able to cause surface-induced denaturation⁴⁷.

Furthermore, due to the continuous freeze- concentration of the remaining amorphous phase the solution can change to a degree that might damage the protein. For example the manifold increase in ionic strength or destabilizing species such as oxygen might be deteriorating²⁷. The relative concentration of formulation compounds can be changed as well, due to selective crystallization, causing e.g. pH changes or phase separation.

During drying the protein is subjected to dehydration stresses. As the level of residual moisture achieved after lyophilization is usually lower than the water content in the protein's hydration shell (0.3 - 0.35 g * g⁻¹ protein^{25,48}), this may disrupt the native state and cause changes in the protein's structure.

Various excipients are used to stabilize protein pharmaceuticals during freeze-drying and during subsequent storage. They can be classified into cryo- and lyo-protectants according to their ability to protect the protein during freezing and drying, respectively.

Although there are some proteins that do not need much stabilization and that can be dried without the addition of excipients, most biopharmaceuticals do need either cryo- or lyo-preservation or both⁴⁹.

CRYO-PROTECTANTS

The most widely accepted mechanism by which cryo-protection is mediated is preferential exclusion, meaning that the interaction between protein and excipient is thermodynamically unfavorable, leading to an accumulation of water molecules at the protein's surface (preferential hydration) as well as to a more compact structure of the molecule, burying the hydrophobic backbone^{7,50-53}.

Other mechanisms providing stabilization during freezing are modification of size of ice crystals, reduction of surface tension and restriction of diffusion of reacting molecules due to an increase in viscosity.

Commonly used cryo-protectants are polymers like polyvinylpyrrolidone (PVP), polyethylene glycol, e.g. PEG 3350, amino acids such as glycine or human serum albumin (HSA).

LYO-PROTECTANTS

Lyo-protection is mediated by two mechanisms: First, the lyo-protectant acts as a water substitute, forming hydrogen bonds with the protein's hydrophilic groups upon the removal of water^{54,55}. This theory was first formulated by Crowe et al. and Allison et al. and is referred to as water replacement theory⁵⁶⁻⁵⁹. Because the interaction between carbohydrates and proteins necessarily requires both to be in the same (amorphous) phase, crystallization often has a destabilizing effect on solid protein formulations.

Excipients stabilizing by this mechanism are polyols and sugars, especially disaccharides, because with increasing molecular weight the steric hindrance renders effective hydrogen bonding more and more ineffective^{5,7}. Sucrose and trehalose are most commonly used. Some amino acids, such as proline, arginine or sodium glutamate are used as well^{55,60}.

A second mechanism that stabilizes proteins in the dried state is vitrification: the active ingredients and all possible reacting species are immobilized in the glassy state where molecular mobility is strongly decreased. Common excipients stabilizing by this mechanism are high molecular weight carbohydrates like maltodextrins or polymers like polyvinylpyrrolidone (PVP).

The use of a disaccharide and a high molecular weight excipient together combines effective hydrogen bonding with a sufficiently high glass transition temperature (T_g) leading to maximum stabilization.

In contrast to this theory, Cicerone et al. reported that the addition of a plasticizer, e.g. glycerol to the amorphous phase leads to increased stability. The authors ascribe this observation to the filling of holes left by the glass former by the smaller plasticizer, thereby decreasing the fast glassy dynamics and increasing stability^{61,62}.

3 THE COLLAPSE PHENOMENON

3.1 DEFINITION

Collapse is the macroscopic or microscopic change in structure of a dehydrated material as a response to environmental stresses⁶³.

One of the first descriptions of collapse was given by Shackell, who freeze-dried various food products early in the era of freeze-drying^{19,64}. Among these he tried to freeze-dry beef, but observed a significant degree of shrinkage upon drying. When he mixed the beef with sand before drying, this shrinkage could be reduced. Although Shackell gave no explanation for this phenomenon himself, Jennings elucidates this observation with the retardation of the drying process and the maintaining of a completely frozen state during the drying process^{23,23}.

Collapse is most evidently characterized by loss of cake structure⁶⁵ either during drying or during subsequent storage. Collapse usually results in a cake whose volume is less than the volume of the initial frozen matrix²³. Furthermore a reduction of the mean pore size and porosity as well as an increase in bulk density can be observed^{65,66}.

Macroscopic characteristics of collapse can range from simple retractions from the vial wall to slow sporadic bubbling over foaming to beading. Cavitations and fenestrations can be formed to the point of gross collapse⁶⁷. But definition of collapse and especially a scientific based measure of quantification has not been proposed yet. Although Rambhatla et al. defined cake shrinkage not as classic collapse; shrinkage nevertheless is caused by the same mechanism. Cake shrinkage is a common feature for freeze-dried excipients with a low T_c and is affected by the temperature difference to T_g as well⁶⁸.

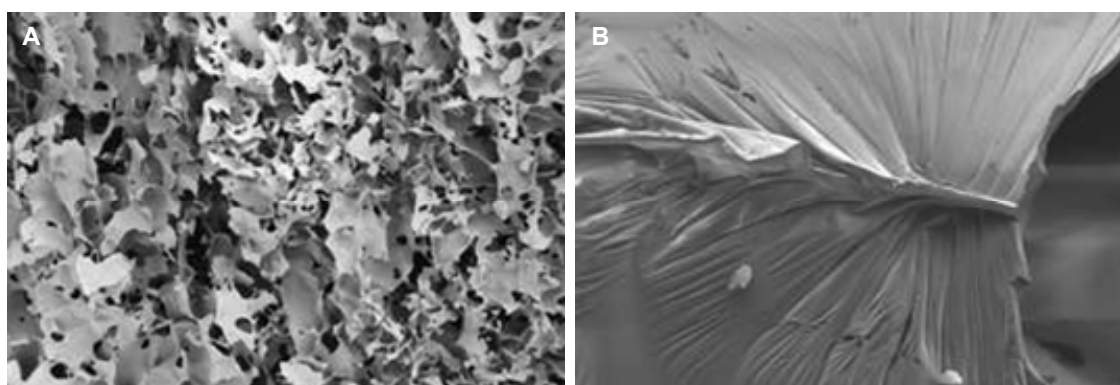


Figure 1.3: Scanning electron microscopic pictures of non-collapsed (A) and collapsed (B) trehalose lyophilizates.

SEM-magnification: 100 x.

First observed upon drying of food materials, chemically very different systems, such as penicillin, orange juice or plasma protein fractions that were incompletely purified from ethanol, have been described to easily collapse during freeze-drying⁶⁷. Usually the occurrence of collapse is regarded as detrimental for the product quality as it will be

described in detail in section 3.6 of this chapter. However, the observation of collapse phenomena is not limited to freeze-drying but is described for various other drying technologies as well: The sticking of spray-dried powder to the dryer wall at too high operating temperatures or too high humidities⁶⁹ is also considered to be a collapse phenomenon.

Occasionally the collapse phenomenon is used in a controlled way. For example for the production of instant powders collapse is applied by raising the moisture content of powders to a degree, where the surface gets sticky, so that the particles form clusters. Then these powders are dried to the desired moisture content⁷⁰.

3.2 MECHANISM

Generally speaking, collapse is a dynamic process caused by viscous flow over a finite distance.

More specifically, collapse during lyophilization is caused by viscous flow of the freeze-concentrated amorphous phase over the distance of a pore diameter at the time-scale of freeze-drying.

As described above, there is a phase separation taking place upon freezing, leading to a crystalline solvent phase and a concentrated amorphous phase containing the solutes and a certain amount of unfrozen water, called the CAS (concentrated amorphous solute)⁷¹. With decreasing temperature the viscosity of the amorphous phase increases, first because of the direct effect of temperature on viscosity, second because of the increasing degree of freeze-concentration due to crystallization of ice. At the T_g' , a critical viscosity of 10^{12} Pas is exceeded and the system passes through a glass transition, turning from a rubbery into a glassy state in which mobility is greatly decreased and therefore it is regarded as a solid state.

At the glass transition the viscosity changes by several orders of magnitude within a narrow temperature range. The relationship between viscosity and temperature around T_g is described by the Williams-Landel-Ferry equation⁷²:

$$\log_{10}\left(\frac{\eta}{\eta_g}\right) = \frac{-C_1 \cdot (T - T_g)}{C_2 + (T - T_g)} \quad (1.2)$$

In equation (1.2) η is the viscosity, η_g the viscosity at the glass transition temperature, T the temperature and T_g the glass transition temperature. C_1 and C_2 are experimental constants that equal to $C_1 = 17$ and $C_2 = 51$ for many polymeric glass formers⁷².

Above the glass transition temperature the molecular mobility increases dramatically. This is due to the decrease of viscosity⁷³ with increasing temperature. At temperatures above the melting temperature of ice, the dilution of the freeze-concentrated solution with melted ice has a contribution as well^{70,74}.

Mackenzie further examined the thermal behavior of certain concentrated solutions (total solid content approx. 30-60 % w/w), vitrified by rapid cooling, upon slow rewarming, observing several thermal events preceding the completion of the melting process. First the system undergoes a devitrification, which is the spontaneous freezing of the glass, causing a phase separation into ice and the more concentrated amorphous phase. Upon further heating, the system undergoes antemelting and incipient melting. These are thermal transitions that are observable using differential thermal analysis. Mackenzie identified these transitions at slightly lower temperatures than the collapse temperature itself, as the origins of collapse⁶⁷.

Due to the increased molecular mobility the whole cake structure becomes more flexible. This renders the highly porous plug mechanically instable. Due to the force of gravity, the cake is no longer able to support its own complex structure.

The second, more important physical power causing the cake's collapse is surface tension^{67,75}. The cake's highly porous, sponge-like structure is formed by sublimation of the ice crystal lattice, leaving wholes and channels where the ice crystals have been. This is possible only because ice like most solids exhibits a very low surface tension. With the transition from the solid into the rubbery, i.e. liquid state, the ambition to minimize the system's surface area is evoked.

Kistler et al. analyzed the collapse behavior of cellular structures during freeze-drying as a preparation for scanning electron microscopy. They found the Brownian movement as major reason for the three-dimensional structures to collapse⁷⁶.

Rambhatla et al. described collapse in a model based upon the works of Pikal, describing collapse as viscous flow over a finite distance x during the measurement time⁶⁸, where x is the distance the flow has to cover to cause collapse, e.g. the pore diameter, γ is the surface tension, t the time, η the viscosity and T the temperature :

$$\delta x = 2\gamma \int_0^t \frac{\delta t}{\eta(T, t)} \quad (1.3)$$

Equation 1.3 explicitly shows the determinants of collapse:

- viscosity (influenced by the temperature)
- timescale of the incident
- distance the flow has to cover to cause collapse, e.g. pore radius

A special form of collapse is the small scale of microscopic collapse⁶⁹. Mackenzie also refers to this form of collapse as modified or limited collapse⁶⁷. Small scale collapse describes a form of collapse where the macroscopic form of the cake is preserved and thus collapse can only be detected microscopically. This manifestation of collapse is observed in cakes being formulated with a combination of crystalline and amorphous excipients. The crystalline part of the matrix provides a supporting scaffold for the amorphous phase to collapse on^{68,77}. Micro-

collapse was also reported to enhance the drying properties of the product by decreasing the dried layer resistance^{36,67,78}.

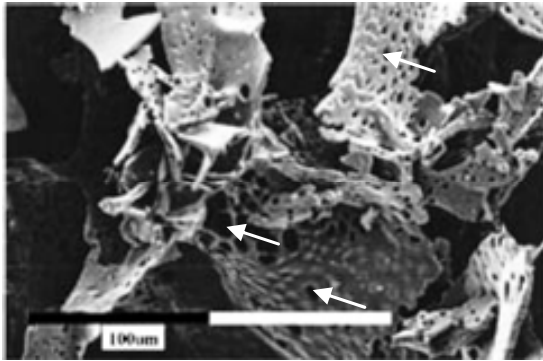


Figure 1.4: Small-scale collapse: Scanning microscopic image of a sucrose-based lyophilizate that underwent small-scale collapse as indicated by the small holes (2-20 μm) in the structure of the lyophilized disaccharide.³⁶

Completely crystalline systems sometimes may collapse as well. Here collapse coincides with the melting of the whole system, thus occurs at the system's eutectic melting temperature⁷⁸.

3.3 THE COLLAPSE TEMPERATURE

The temperature at which collapse occurs is called the collapse temperature T_c ⁷⁹ and usually it is about 1-3 K higher than T_g' , although there are some publications describing aberrations as much as 30 K⁶⁷. Systems containing cells do not show any correlation between T_c and T_g' . The difference between these systems' T_c and T_g' is more than 10 K⁸⁰. Formulations comprising high protein concentrations show a discrepancy in T_g' and T_c with increasing protein concentration as well¹⁶. Furthermore, the loss of structure can be further classified into onset and complete loss of structure, leading to two characteristic temperatures $T_{c\text{ onset}}$ and $T_{c\text{ complete}}$ ¹⁶. Because the glass transition temperature is determined in a closed container (DSC-crucible) after freezing, where no drying occurs during the determination, whereas collapse is a dynamic process taking place during freeze-drying, a difference in the two temperatures comes as no surprise⁸⁰. A more detailed comparison of analytical methods addressing the determination of T_c and T_g' and the relevance of both methods for the freeze-drying process, is given in Chapter 5 of this thesis.

The collapse temperature represents the maximum allowable operating temperature during primary drying. Thus it is one of the key parameters during lyophilization cycle development and there has always been a special interest in its reliable determination. A lot of methods for the determination of T_c have been investigated, ranging from thermal methods like differential thermal analysis, to optical methods, as freeze-drying microscopy and mechanical methods, as thermal mechanical analysis⁸¹. Despite all the effort made, so far no 100% reliable method has been established and there are some pitfalls to be aware of. Most frequently

however, freeze-dry-microscopy (FDM) is applied to assess the maximum allowable operating temperature⁸².

Since collapse is a dynamic process, the experimental measurement time has an effect on the determined collapse temperature: T_c decreases with increasing measurement time⁸³. Furthermore, since collapse is defined as flow over a certain distance, the geometrical dimensions of the specimen are of importance as well. Small pores collapse more easily than larger pores. A common way to determine the collapse temperature is freeze-drying microscopy. Here, a small amount (approximately 10 μ l) of sample is placed between two cover slides located in a pressure- and temperature- controlled microscope stage, where freeze-drying can be performed under visual observation. The sample is then ramped up slowly in temperature until collapse occurs. Although the method itself is robust and reproducible, the determined T_c s sometimes do not correlate well with the T_c s observed for the same formulation in an actual vial. This deviation is presumably caused by the very different three dimensional structures.

Mackenzie states that the collapse temperature is neither dependent on the thermal history of the sample after the completion of the freezing process, nor on the freezing rate or the initial solute concentration⁶⁷, although a small effect of the freezing rate was reported by Tsourouflis et al.⁶³.

Because the definition of collapse is the loss of structure, a property not easily assessed by a physical measure, most methods determining the collapse temperature are based upon optical judgment of the sample, imposing the risk of operator-dependent deviations. Therefore, often not the collapse temperature but the glass transition temperature as determined by differential scanning calorimetry or dielectric relaxation spectroscopy is used.

The collapse temperature is affected by the molecular weight of the solutes, as well as the structure and composition of the solute⁶⁷. It increases with increasing molecular weight⁷¹.

The collapse temperature of a mixture of several solutes is influenced by the collapse temperatures of the single components and their weight ratio as demonstrated by the following equation^{80,80,84}:

$$T_{cm} = \frac{\sum T_{ci} \cdot C_i}{\sum C_i} \quad (1.4)$$

Where T_{cm} is the collapse temperature of the mixture, T_{ci} refer to the collapse temperatures of each single component and C_i is the weight ratio of the single components.

This equation correlates to the Gordon-Taylor-equation (1.5)⁸⁵ describing the relationship between the glass transition temperatures of mixed amorphous systems, their phase composition and the glass transition temperatures of the pure substances.

$$T_{g_{mix}} = \frac{[(m_1 \cdot T_{g1}) + (k \cdot m_2 \cdot T_{g2})]}{(m_1 + k \cdot m_2)} \quad (1.5)$$

Where m_1, m_2 are the weight fractions, T_{g1}, T_{g2} are the glass transition temperatures of the pure components, k is the ratio of the free volumes of the two components, calculated from the density and the change in thermal expansivity at T_g ⁸⁶.

Table 1.1: Glass transition temperatures of the maximally freeze-concentrated solution (T_g') and collapse temperatures (T_c) of selected freeze-drying excipients.

Excipient	T_g'	T_c	Reference
L-Arginine		-34	Ito ⁸⁷
Dextran 2000		-9	MacKenzie ⁶⁷
Fructose	-42 ^{a)}	-48 ^{b)}	^{a)} Wisniewski ²⁷ , ^{b)} MacKenzie ⁶⁷
Glucose	-43 ^{a)}	-40 ^{b)}	^{a)} Franks 1990, ^{b)} MacKenzie ⁶⁷
Lactose		-31	MacKenzie ⁶⁷
Mannitol	-27 ^{a)}	-2 (T_{eut}) ^{b)}	^{a)} Lueckel et al. ⁸⁸ , ^{b)} Johnson et al. ⁸⁹
PEG 6000		-13	Willemer ⁹⁰
PVP (40 kDa)		-24	Adams and Ramsay ⁴¹
Sorbitol	-41 ^{a)}	-54 ^{b)}	^{a)} Kerr ⁹¹ , ^{b)} Adams and Ramsay ⁴¹
Sucrose	-32 ^{a)}	-32/ -25 ^{b)}	^{a)} Kasraian et al. ⁹² , ^{b)} Ito ⁹³
Trehalose	-30 ^{a)}	-29 ^{b)}	^{a)} Levine and Slade ⁹⁴ , ^{b)} Adams and Ramsay ⁴¹

Besides the collapse temperature, some authors like Fonseca define a micro-collapse temperature. That is the temperature, where local loss of structure can be observed for the first time^{36,80}. This temperature corresponds to the collapse temperature as described by Mackenzie⁶⁷

A list of experimental collapse temperatures is given by^{25,67,71,93}, the T_g' and T_c values of selected representative freeze-drying excipients are summarized in Table 1.1.

3.4 DETERMINANTS OF COLLAPSE

As derived from equation (1.3) the primary determinants of the collapse phenomenon are viscosity, time and the pore radius. As these variables are affected by other parameters again, in the following section a brief overview of the parameters influencing the incidence of collapse shall be given.

3.4.1 VISCOSITY

As collapse is caused by viscous flow, viscosity undershooting a certain minimum viscosity is the key parameter in the causation of collapse.

Figure 1.5 shows the relationship between viscosity and collapse temperature for various sugar solutions: With increasing equilibrium viscosity the solutions tend to collapse at higher temperatures⁷¹.

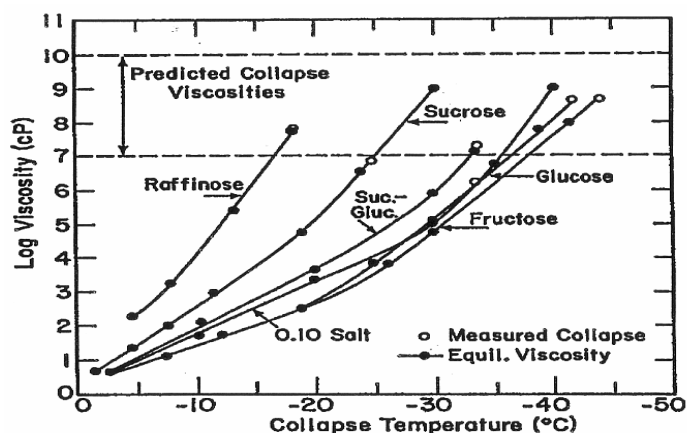


Figure 1.5: Equilibrium viscosity curves for various sugar solutions.⁷¹

TEMPERATURE

Viscosity itself is strongly affected by temperature, as the molecules' higher inner energies at higher temperatures raise the probability of overcoming the intermolecular van-der-Waals forces^{71,95}.

WATER CONTENT

Water acts as a plasticizer of amorphous solids^{94,96}, depressing the system's glass transition temperature about 5-20 K for every 1 % of residual water¹⁰. As the glass transition is inherently linked to a viscosity value of 10^{12} Pa s, decreasing the glass transition temperature also decreases the viscosity of a system at a given temperature.

One has to keep in mind that this is only applicable for systems having an even moisture distribution, which during freeze-drying is true only during secondary drying. During primary drying frozen water, that was separated from the amorphous phase during freezing, is sublimed. However, unfrozen water that remained in the amorphous phase and acts as a plasticizer of the amorphous phase is not sublimed during primary drying but is desorbed during secondary drying. Thus, although there is a considerable decrease of the average moisture content during primary drying, there is almost no increase in glass transition temperature during primary drying.

ADDITION OF HIGH OR LOW MOLECULAR WEIGHT EXCIPIENTS

Excipients with high molecular weights, such as dextran, PVP or gelatin increase the viscosity of the amorphous phase by increasing the structural viscosity of the system. This in turns increases the formulation's T_g . Excipients with low molecular weight, like sodium chloride and glycerol, decrease the formulation's T_g by acting as a plasticizer of the amorphous phase^{35,63,67}.

3.4.2 TIME SCALE

Another important factor when dealing with the collapse phenomenon is the experimental observation time or the drying time at a certain temperature.

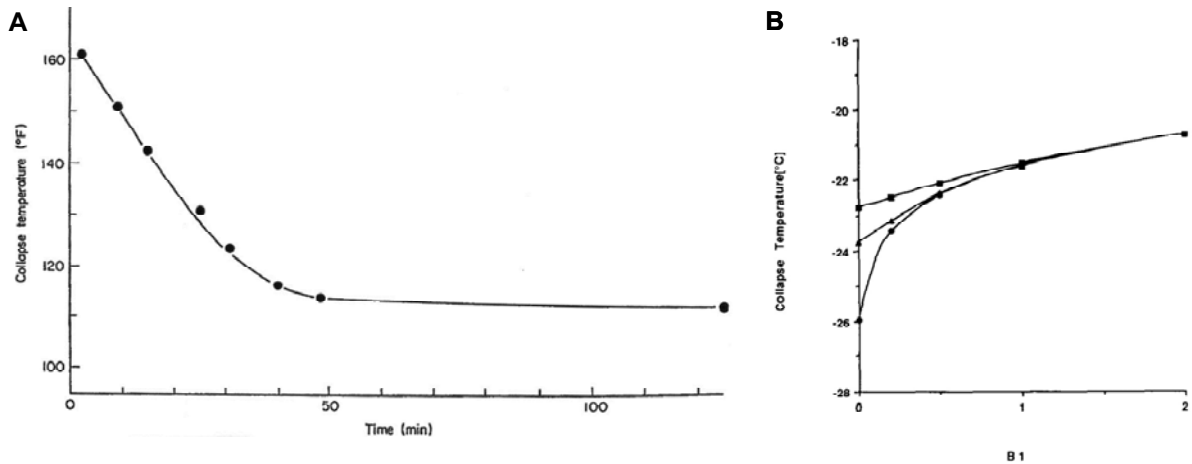


Figure 1.6: Time required to cause complete collapse in a dried sucrose system held at different temperature levels⁶³ (A); dependence of the determined collapse temperature on the drying rate parameter B1 as a function of measurement time (0.2 h: squares; 0.5 h: triangles, 5 h: circles)⁸³ (B).

Tsourouflis et al. tested the relationship between collapse temperature and measurement time by heating ampoules containing freeze-dried cakes from 2 mL orange-juice in a water bath. They found that the determined collapse temperature approaches a minimum value after 45 minutes of holding for given moisture content. Figure 1.6 A shows this alteration of collapse temperature with observation time for dry sucrose⁶³. Figure 1.6 B shows the dependency of determined collapse temperature on the sublimation rate (denoted as drying rate parameter B1) and observation time. The experimental observation time is especially important at low drying rates.

The different determinants of collapse were summarized in equation (1.6) stated by Bellows and King where t is the sublimation time, η the viscosity, R the pore radius and γ the surface tension⁷¹:

$$t = \frac{\eta R}{2\gamma} \quad (1.6)$$

Using general values (for frozen liquid foods) they calculated the critical viscosity for collapse to take place. They assumed the usual pore radius to be 20 μm , the surface tension 70 dyn/cm and the time needed for sublimation of water in common freeze dryers 1-10³ seconds. So the critical viscosity would be 10⁷ – 10¹⁰ cPoise.

Thus, shortening the time needed for sublimation would lower the critical viscosity and thereby raising the possible maximum operating temperature.

Another implication of this relationship is that collapse temperatures determined e.g. using a freeze-drying microscope are strongly dependent on the time of the experiment^{65,83,97} with the risk of artificially high collapse temperatures when this time is too short.

3.4.3 PORE RADIUS

Because collapse can be described as viscous flow over the distance of a pore radius, the bigger the radius, the longer the time or the higher the temperature needed for this flow to take place.

Tsourouflis et al. also found that a system with a smaller internal surface area is presumably less sensitive to collapse, because the surface tension as the driving force for collapse is less grave in systems with smaller surface areas⁶³.

A further important aspect when regarding the pore radius is the effect of freezing-rate. As mentioned above, a fast freezing rate leads to small pores and thus to high cake resistance and less efficient primary drying. Additionally the distance over which the viscous flow has to occur to cause collapse is small. Thus, fast frozen systems should be more sensitive to collapse.

Tsourouflis et al. found, the effect of freezing rate appears to have a significant but relatively small effect. Furthermore, they did not find a homogenous pattern of behavior. The authors concluded that the thickness of the matrix between the pores has different effects related to different bonding arrays of different excipients⁷⁰.

3.5 THE OCCURRENCE OF COLLAPSE

Collapse of lyophilizates can occur either during the freeze-drying process itself or during subsequent storage.

3.5.1 COLLAPSE DURING FREEZE-DRYING

During the lyophilization process, collapse can occur in either one of the two drying steps of the process, during primary or during secondary drying.

As described in detail above, the onset of collapse is governed by the viscosity of the freeze-dried system, the timescale of the drying process and the pore diameter in the freeze-dried cake.

During the freeze-drying process the time period during that collapse is likely to occur is dictated by the time it takes for the lamellae between the ice crystals to dry. This is usually $1-10^3$ seconds in commercial freeze-dryers⁷¹. As this parameter depends mostly on the freeze-dryer model and the process parameters shelf temperature and chamber pressure, the variable time remains more or less constant during the lyophilization process. The onset of collapse is hence influenced by the viscosity of the amorphous phase of the drying cake and by the pore diameter. The latter has a less pronounced effect than the former.

The viscosity of the amorphous phase is affected by the product temperature, determined by chamber pressure and shelf temperature itself. Whenever the product temperature rises above a critical temperature, the collapse temperature T_c , collapse occurs.

During primary drying, where frozen water is sublimed and the water content of the amorphous phase does not change, the maximum allowable operating temperature is the predetermined collapse temperature. During secondary drying, where the residual moisture content of the amorphous phase is decreased and thus the glass transition temperature, as a function of the residual water content, is increased, drying can be performed at increasingly high temperatures. Collapse during secondary drying was termed “retrograde collapse” by Mackenzie, because of its observation behind the sublimation front in freeze-drying microscopy⁶⁷.

Because drying at higher temperatures is also often mandatory to achieve short drying protocols and sufficiently low residual moistures, Franks suggest to raise the shelf temperature step-wise⁹⁸, where other researchers recommend to raise the temperature during a slow ramp. As the cake at the end of primary drying often has up to 30 % residual moisture, even 50% water are reported for some amorphous formulations, a slow ramp has to be applied in order not to provoke collapse³⁷.

As the pore radius has an effect on the readiness of a system to collapse, the freezing rate affects the occurrence of collapse as well, with fast freezing leading to small ice crystals and small resulting pores that might more readily collapse⁶³.

3.5.2 COLLAPSE DURING STORAGE

Collapse during storage most evidently occurs whenever a product is stored above its glass transition temperature, when the temperature is either too high, e.g. when a cooling system during transportation is defect, or when the glass transition temperature of the system is lowered to temperatures below the storage temperature^{99,100}, e.g. by moisture transfer from incorrectly dried stoppers²³ or from the outside through moisture permeable closure systems. Another reason for increased residual moisture levels can be the anhydrous crystallization of an excipient from the amorphous state, leaving the remaining amorphous phase with a higher percentage of water. Some developers therefore use excipients that crystallize as a hydrate¹⁰¹.

Regarding collapse during storage, called stickiness by food researchers^{74,102}, the timescale becomes dominant. As timescales are long, collapse can occur even at temperatures well below the system’s collapse temperature.

3.6 EFFECTS OF COLLAPSE: CURRENT OPINION

Usually the occurrence of collapse is regarded as detrimental for product quality. In the production of biopharmaceuticals the onset of collapse in a freeze-dried batch leads to rejection of that batch⁸⁰.

One important issue is that collapse causes the loss of “pharmaceutical elegance”^{15,94,103}. But there are more severe concerns regarding the product’s drying behavior, its ability to sufficiently stabilize the active ingredient and reconstitution after storage^{29,104,105}.

Collapse is caused by viscous flow of the glassy matrix, increasing the density of the cake structure and eventually resulting in blockage of pores. This leads to increased product resistance to water vapor flow, decreased sublimation rates and thus retarded primary drying¹⁰⁶. Due to the complete closure of pores some authors say that drying is completely reduced to evaporative mechanisms, rendering the drying highly ineffective⁶³.

In contrast, “small-scale” collapse of formulations containing a crystalline bulking agent leads to a decreased water vapor resistance and an increased drying rate and is reported to be intentionally employed for optimization of freeze-drying protocols^{32,36}.

The loss of porosity also results in reduced specific surface area, slowed desorption and thereby slowed secondary drying²⁸. Increased density hinders diffusion of water molecules in the dried matrix, yielding the same effect. Adams et al. found good correlation between the extent of collapse and the residual moisture content during freeze-drying at a certain point of time³⁵. Mackenzie claims that drying of collapsed material is almost impossible⁶⁷. In addition, the moisture-distribution within the collapsed cake is very likely to be uneven, with the structure itself being irregular¹⁰⁷.

Poor rehydration behavior might be caused by the reduced surface area as well^{63,67,71}. A correlation between the reconstitution time and the extent of collapse was given by Adams et al.³⁵.

A loss in microstructure due to cake collapse is reflected by the loss of the ability to entrap volatiles and aroma substances^{63,71}. In contrast, To and Flink state, that the observed decreased ability to keep volatiles is due to recrystallization of the system’s amorphous components¹⁰⁸. Indeed, an increased tendency of amorphous substances to crystallize in collapsed matrices has been observed by other authors as Darcy et al. and Izutsu and co-workers^{105,109}.

Concerning the stability of protein pharmaceuticals in dried matrices, stabilization does not necessarily require a porous cake-structure. Vacuum- and spray-drying, lacking the formation of a cake upon drying, have been successfully employed for protein-stabilization^{60,110-113}. Recently, the concept of foam drying was applied to stabilize proteins in the dried state¹¹⁴. Also, investigations by Abdul-Fattah et al. and by Hsu and coworkers indicate that a formulation with a smaller surface area might in certain cases be more stable^{114,115}. Regarding the specific effect of collapse on the stability of incorporated proteins, collapse is usually believed to be detrimental for product quality. Although there are only a few publications pointing out a clear negative effect on stability^{77,80,116}, a collapsed product is not released to the market. Nevertheless, studies suggest that collapse itself does not

necessarily result in loss of protein stability^{31,107,117}. A review of the currently available scientific literature on the effect of collapse on protein lyophilizates shall be given in the following section.

Adams et al. investigated the stability of *Erwinia* L-Asparaginase upon freeze-drying with different sugars and various amounts of sodium chloride. Although the authors found a correlation between the onset of collapse and instability when using glucose and mannitol as excipients, they did not see a reduced stability upon the occurrence of collapse when using lactose and sodium chloride as excipients^{35,41}.

Although Izutsu et al. showed a correlation between the onset of collapse, the crystallization of inositol and the decrease in recovery of β -galactosidase, the stability-affecting factor is the crystallization of the lyo-protectants, because collapse had no effect when crystallization was prevented by addition of polymers.¹⁰⁵

In a study investigating the effect of process variables on the stability of IL-6, the authors found a decreased stability of collapsed sucrose-glycine cakes upon storage at temperatures above the glass transition temperature, but no differences in the aggregation level immediately after freeze-drying. Furthermore, not-collapsed cakes incubated at comparable residual moisture levels after lyophilization showed a decreased physical stability upon storage as well¹¹⁶.

The studies described above did not explicitly investigate the effect of collapse on protein stability but observations were collected during process and formulation development studies. Investigations intentionally dealing with the effect of collapse on protein stability are rare:

Jiang and Nail scrutinized the effect of process conditions on protein activity by freeze-drying various proteins from buffer alone forgoing the use of any stabilizers. The recovery of activity decreased continuously during primary drying without a sharp drop with the onset of collapse. However, a more pronounced decrease in recovery of activity was observed for higher product temperatures and the rate of activity loss increased with proceeding drying. Whether this was caused by the decreasing level of moistures alone, or if this is somehow a delayed effect of collapse has to be further investigated. It is highly likely that variables such as freezing rate, protein concentration, the availability of adequate stabilizers and a certain minimum residual moisture level have more pronounced effects than the onset of collapse³¹.

In another study Wang and co-workers caused collapse by omitting the annealing step in a partially crystalline formulation consisting of sucrose and glycine and compared these collapsed samples with elegant samples dried with annealing and at primary drying shelf temperatures either below or above the glass transition temperature of the formulation. They found no difference in the long term stability of all formulations but even an increased stability of some collapsed samples at high storage temperatures (40 °C for up to 18 months)¹¹⁷.

The same observation was made by Chatterjee et al. when they freeze-dried formulations containing raffinose and trehalose with varying amounts of crystallizing glycine, causing collapse depending on the weight ratio of the crystalline to the amorphous component at primary drying temperatures below and above the collapse temperature. The authors saw no difference in recovery of enzyme activity no matter whether the material had collapsed or not¹⁰⁷.

However, some researchers observed a clear stability-abating effect of collapse.

Fonseca et al.⁸⁰ found a decreased activity of *Lactobacillus* suspensions when freeze-dried above the system's collapse temperature. Passot and coworkers⁷⁷ found a decreased long-term stability of proteins primary-dried at temperatures above T_g' , although there was no effect detectable on stability immediately after lyophilization. However, the decreased long-term stability was not correlated with the occurrence of collapse but with the primary drying temperature. Cakes that did not collapse (either because of the use of a crystalline bulking agent or because T_c was not sufficiently exceeded) exhibited a decreased stability as well⁷⁷.

Taking together conclusions from published investigations, structural collapse leads to a variety of changes in cake properties of both esthetical and stability-related concerns. Doubtless, the loss of pharmaceutically elegant cake structure diminishes the product's appeal. But the decrease in porosity, causing inferior drying behavior and thus increased residual moisture levels can cause more severe stability issues. However, by adding crystalline components or by application of high drying temperatures, the residual moisture levels of collapsed cakes can be reduced to amounts comparable to conventionally dried lyophilizates^{89,107}.

A variety of proteins has been investigated but there have been no publications so far on the effect of collapse on monoclonal antibody lyophilizates. Since this is the most important protein pharmaceutical class today, the study of implication of collapse on antibodies is of utmost interest.

As there is no inevitable detrimental effect of collapse on protein stability documented, drying at elevated temperatures in order to shorten drying time may well be an option.

3.7 PRO & CONTRA OF DRYING CLOSE TO THE COLLAPSE TEMPERATURE: WHY IT IS WORTH INVESTIGATING THE COLLAPSE PHENOMENON IN DETAIL

Good freeze-drying practice implies maintaining shelf temperature and chamber pressure at a level that avoids product temperature to rise above the system's collapse temperature during primary drying¹¹⁸. This may result in drying protocols that could take days or even a week to finish¹⁵.

For economic reasons it is highly desirable to shorten drying times as much as possible. Furthermore, as the freeze-drying process itself might be harmful for the protein drug, stability is a second motivation for drying cycle optimization.

As each 1 K increase in product temperature during primary drying decreases the primary drying time by about 13 %¹⁵, drying should be performed at temperatures as high as possible. Tang and Pikal suggest a safety margin of 2-5 K of the product temperature to the collapse temperature, depending on the primary drying time³². However, in systems with a very low collapse temperature, primary drying at very low shelf temperatures would be rendered highly inefficient. Here, Tang et al. suggest to perform drying at product temperatures above T_g using a crystalline bulking agent to avoid the onset of macroscopic collapse. The authors did not observe a strong increase in protein denaturation rate, most probably due to the sufficiently high viscosity of a freeze-concentrated carbohydrate system at low temperatures to avoid protein unfolding in the time frame of freeze-drying. The half-life of protein unfolding can be correlated to viscosity by the following mathematical expression:

$$t_{1/2} = A * \eta^\alpha \quad (1.7)$$

Where $t_{1/2}$ is the protein unfolding half-life, A is a constant of proportionality, η is the system's viscosity and α is the coupling constant¹¹⁹.

With the first approvals of biosimilars and biogenerics who even more rely on cost-efficiency the need for highly optimized freeze-drying cycles is growing. Recently, there have been several patent applications claiming the application of high primary drying temperatures to shorten drying times¹⁶⁻¹⁸.

Common understanding of the freeze-drying process is that the product temperature is controlled by both chamber pressure and shelf temperature. A recent investigation analyzed the effect of process variables on primary drying time and maximum product temperature during primary drying. A significant effect was only found for the shelf temperature. Therefore the only way to optimize freeze-drying cycles is to increase drying temperatures especially during primary drying as it is the most time consuming step¹⁶. This further points out the importance of a sound investigation of the effects of collapse, because drying close to the collapse temperature without good understanding of the possible implications on product stability would put product stability on risk.

Many authors state that macroscopic collapse has to be prevented under all circumstances. The most common means in doing so during freeze-drying at high primary drying temperatures is using a crystalline bulking agent^{89,120,121}. Bearing in mind the findings of Passot et al., this approach has to be carefully evaluated. Passot et al. found a decreased long-term stability of protein lyophilizates after exposure to temperatures above T_g' during the drying process⁷⁷. Lückel assigns this to the extended time in a high molecular mobility environment, having observed similar instabilities after annealing¹¹⁶. Using a crystalline bulking agent, collapse, as the macroscopic manifestation of a too high molecular mobility, would be masked²³.

Dealing with highly concentrated protein formulation drying above T_g' with retention of cake structure might be possible without the use of crystalline bulking agent. Due to the dense packaging and the high viscosity of the freeze-concentrated phase the freedom of movement is low causing the described divergence of glass transition and collapse temperature¹⁶.

Another concept to process optimization is the use of annealing, i.e. to increase product temperature above the glass transition temperature in the frozen state. During annealing viscosity is decreased to a degree at which reorganization of the solids can take place. Due to the presence of ice, only a localized collapse occurs, causing the ice crystals to grow and the amorphous phase to consolidate¹²². Doing so sublimation rate heterogeneities are reduced and primary drying rates can be 3.5 fold increased¹²².

An even more drastic approach to shorten drying times would be the application of "collapse-drying" There is no publication describing the use of this procedure so far. Collapse-drying is considered to be similar to foam-drying. Foam-drying is a drying procedure similar to vacuum drying. In contrast to freeze-drying the solution is not frozen initially but pressure is lowered immediately. Contrary to vacuum drying, the pressure is lowered to a degree that induces the foaming of the solution. This situation usually is avoided during vacuum drying. Foam-drying comprises of primary and secondary drying similar to freeze-drying, but the underlying drying mechanism is evaporative drying during both stages.

Foam-drying has been successfully used to dry protein pharmaceuticals by Abdul-Fattah et al. ^{114,123} and there are several patent applications describing the stabilization of bioactive material by foam drying¹²⁴⁻¹²⁶.

4 STABILITY OF PROTEIN PHARMACEUTICALS IN THE SOLID STATE

Drying proteins from aqueous solutions to stabilize them in the solid state is common practice in the pharmaceutical industry. Although formulations may contain a variety of different components (as described in detail above) the premise for stabilization is the formation of a glassy matrix where the protein is molecularly dispersed. The most commonly used stabilizers are low molecular weight sugars or a mixture of a low molecular weight sugar and a polymeric excipient.

The properties of these dried products depend on the characteristics of the amorphous state perhaps as much as upon the behavior of the protein itself¹¹⁹.

This chapter provides an overview about the factors influencing the solid state stability of proteins and the underlying stabilizing mechanisms. Because the most important protein stabilizing systems are glasses, the characteristics of glassy systems in the context of protein stabilization will be discussed. Emphasis will be put onto the phenomenon of molecular mobility and its relationship to protein stability both below and above the system's glass transition temperature.

4.1 FACTORS AFFECTING STABILITY OF PROTEINS IN THE SOLID STATE

Protein stability in the solid state is influenced by a variety of factors. These can be distinguished into either intrinsic or extrinsic factors. Intrinsic factors involve the structure of the protein itself, such as the primary sequence. Formulation, processing and storage conditions are considered as extrinsic factors¹²⁷.

This chapter deals with the extrinsic factors only.

Provided formulation and process development have been successful, a stable dried product is obtained at the end of the freeze-drying cycle. Stability in the solid state is governed by similar factors as stability during the drying process.

There are two proposed mechanisms by which excipients are believed to stabilize the protein in the amorphous state.

4.1.1 WATER REPLACEMENT HYPOTHESIS

The water replacement hypothesis states that stabilization results from the preservation of native structure in the dried state due to hydrogen bonding between the stabilizer and the protein. The native conformation is thermodynamically more stable and therefore more resistant towards degradation during storage. Stabilization as a result of the native structure preservation offers a thermodynamic explanation for the stabilization mechanism^{54,58,128}.

4.1.2 VITRIFICATION HYPOTHESIS

A second approach is the vitrification hypothesis that is called the glass dynamics mechanism by some authors¹²⁹. The theory proposes that stabilization is provided by immobilization of the molecules in the solid state thereby oppressing global motions, also known as α -relaxations. α -relaxations occur mainly due to translational and rotational motions. They therefore strongly influence the diffusion of reactive molecular species. As every degradation reaction is dependent on molecular motion of some kind, degradation processes thus are kinetically inhibited^{130,131}. Thermodynamic instability is irrelevant because the system is prevented from moving towards equilibrium. Thus this theory offers a kinetic explanation for the stabilization mechanism in contrast to the thermodynamic explanation listed above.

There are various investigations analyzing the validity of each of these hypotheses. Some found a better predictability for storage stability when assuming structural preservation^{129,132}, whereas others found a better correlation with molecular mobility¹³³⁻¹³⁵. Yoshioka et al. found contributions of both, thermodynamic and kinetic factors. They stated an equation quantitatively describing this relationship^{135,136}.

$$k = k_{act} \left(\frac{\alpha T \left(\frac{1}{\tau} \right)^\zeta}{k_{act} + \alpha T \left(\frac{1}{\tau} \right)^\zeta} \right) \quad (1.8)$$

Where k is the rate constant of the degradation reaction, k_{act} is the rate constant without restriction of diffusion, α is a constant describing the coupling between k and τ , T is the temperature and ζ is a parameter that represents coupling between D and τ .

Some authors state that local dynamics rather than the global mobility as assessed by τ are predictive for stability.

A detailed discussion about the effect of molecular mobility on protein stabilization in the solid state is given in section 4.5 of this chapter.

There are further factors affecting the solid state stability of proteins.

4.1.3 TEMPERATURE

The effect of temperature in general is often described by the Arrhenius law.

$$k = A \exp\left(\frac{-E_A}{R * T}\right) \quad (1.9)$$

Where k is the rate constant, A is a constant, E_A is the activation energy, R is the gas constant and T is the temperature.

Whenever there are secondary effects such as phase transitions, protein denaturation or limitation of diffusion, deviations from Arrhenius behavior are observed¹³⁷.

The most prominent deviation is the irreversible thermal denaturation caused by the increase in entropy. This favors the formation of reversibly unfolded intermediates that aggregate due to intermolecular interactions.

4.1.4 MOISTURE

Water acts as a plasticizer of the amorphous state, decreasing T_g and thereby increasing molecular mobility. Furthermore, water can participate directly in degradation reactions either as a reactant (i.e. hydrolysis) or as a catalyst. Moreover, water can serve as solvent or reaction medium¹³⁷.

4.1.5 HYDROGEN ION ACTIVITY

As there is no definition for pH in the solid state, the 'pH' or effective pH is defined as the pH of the solution prior to lyophilization or upon reconstitution. However, there are several experimental setups under investigation directly assessing the pH in the solid state.

There are publications correlating the pH to physical and chemical degradation reactions, as aggregation or deamidation¹³⁸⁻¹⁴¹.

4.2 IMPLICATIONS OF COLLAPSE FOR THE CONCEPTS OF SOLID STATE PRESERVATION

4.2.1 EFFECT OF COLLAPSE ON THERMODYNAMIC STABILIZATION CONCEPTS

Most studies investigating the effect of collapse dealt with the direct effect of collapse on product quality. This approach is governed by the widespread concern that collapse causes the immediate damage of the embodied protein drug, i.e. a thermodynamic destabilization. Depending on the extent of disturbance this was supposed to either cause an instantaneous or a delayed instability reaction.

4.2.2 EFFECT OF COLLAPSE ON KINETIC STABILIZATION CONCEPTS

Since the characteristics of the glassy state are strongly influenced by the way of its formation and the thermal history of the glass, collapse representing a change in thermal history with respect to the conventionally dried product might have an effect on the nature of the glass.

Exposure to elevated temperatures, so called annealing, causes relaxation of the glass towards its equilibrium state. The occurrence of collapse, which indicates a rise of product temperature above T_c , thus implicates that a collapsed product was exposed to elevated temperatures. This might cause alterations in relaxation time constants and thereby a change in diffusivity of reacting species. What is more the temperature dependence of the relaxation time constants, i.e. the system's fragility, might be changed.

As collapse might have an effect on residual moisture as explained above, this might have an effect on stabilization as well. Increased levels of moisture in the lyophilizate can cause instabilities in one of the ways described above. Furthermore, the activity of water molecules in collapsed cakes might be different from that in an intact cake.

In the following sections the formation and characteristics of glassy systems shall be presented in some detail because these concepts might be new in the context of collapsed protein lyophilizates.

4.3 CHARACTERISTICS OF GLASSY SYSTEMS

A glass is an amorphous solid state that lacks the long-range order of crystalline solids. It is formed during cooling of a liquid through the glass transition. A glass is regarded as thermodynamically unstable with respect to the crystalline solid state due to its increased configurational entropy.

Figure 1.7 shows a schematic plot of enthalpy vs. temperature illustrating the behavior of a glass-forming system upon cooling:

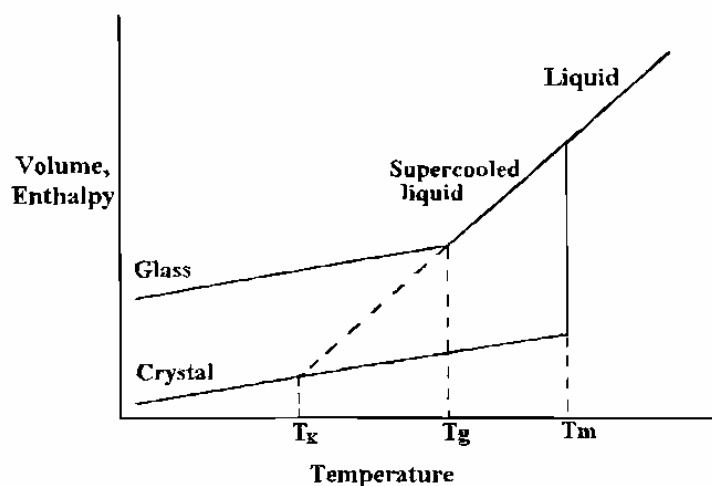


Figure 1.7: Schematic depiction of the variation of enthalpy (or volume) with temperature.¹⁴²

Cooling from ambient temperatures, the liquid experiences undercooling to a degree dependent on the purity of the sample. The undercooled sample behaves like a liquid with increasing viscosity with decreasing temperature. It can either crystallize or solidify as an amorphous solid. A glass is formed during the passage of the glass transition temperature (T_g in Figure 1.7). The slope of the entropy curve changes at the glass transition temperature, classifying it as a second order transition. A crystalline state is formed by spontaneous crystallization at the melting temperature (T_m in Figure 1.7).

Because the crystalline state is more stable usually the formation of a glass is thermodynamically unfavored. Only when the viscosity around the melting point is high enough to hinder crystallization a glass will be formed rather than a crystal. High viscosity

can be caused e.g. by a low melting point due to crystal lattices with little stability or by addition of high molecular weight excipients.

In the liquid state, the system is in equilibrium with its surroundings, but upon solidifying, the system falls out of this equilibrium state into the metastable glassy state. Thereby the absolute enthalpy level of the glass is not fixed but dependent on the way of preparation of the glass. For example the cooling rate influences the velocity with which the system passes through the glass transition. Upon solidifying the structure of the liquid is frozen in and preserved in the glass. A glass prepared with a high cooling rate exhibits more defects in the glassy structure and thereby has a higher level of enthalpy.

With annealing or aging transitions to lower enthalpy levels occur as will be described in more detail below¹⁴³.

The theoretical extension of the liquid curve (dashed line in Figure 1.7) gives the enthalpy state of the ideal or equilibrium glass. This describes the glass being in equilibrium with its surroundings and is the preferred state where the real glass relaxes towards.

The temperature named T_K in Figure 1.7 is the Kauzmann temperature. At this temperature the entropy of the supercooled liquid state falls below the entropy of the crystalline state. Because this is a theoretical situation never encountered in reality but prevented by crystallization by any means, this is called also the Kauzmann's paradox. The Kauzmann temperature is regarded as the lower limit of the experimental glass transition by some authors. It is sometimes associated with the zero mobility temperature T_0 , the temperature below that all mobility ceases and placed approx. 50 K below T_g ¹⁴³.

The glassy state is described by the following parameters:

- Viscosity (η)
- Molecular mobility (τ)
- Fragility

The viscosity at the glass transition temperature is $10^{12} - 10^{14}$ Pa*s. α -relaxation times at the glass transition are around 100 s. Hence, the glassy state is characterized by a viscosity higher than 10^{12} Pa*s and α -relaxation times slower than 100 s. Viscosity and molecular motions are obviously coupled. However, sometimes there are deviations from that coupling. Because molecular motions are more indicative for degradation reactions than viscosity values, analytical methods aiming at the mobility rather than the viscosity are usually more significant. Analytical methods approaching molecular mobility will be the topic of discussion in a separate chapter of this thesis (Chapter 9).

4.3.1 TEMPERATURE DEPENDENCE OF MOLECULAR MOBILITY

A. TEMPERATURE DEPENDENCE ABOVE T_g

The temperature dependence of the molecular mobility near and above T_g is termed fragility. Glasses exhibiting a steep change of their physical properties with temperature are termed

fragile. Glasses showing roughly Arrhenius-like temperature dependence in their molecular mobility are designated strong. Proteins are an example for strong glass formers.

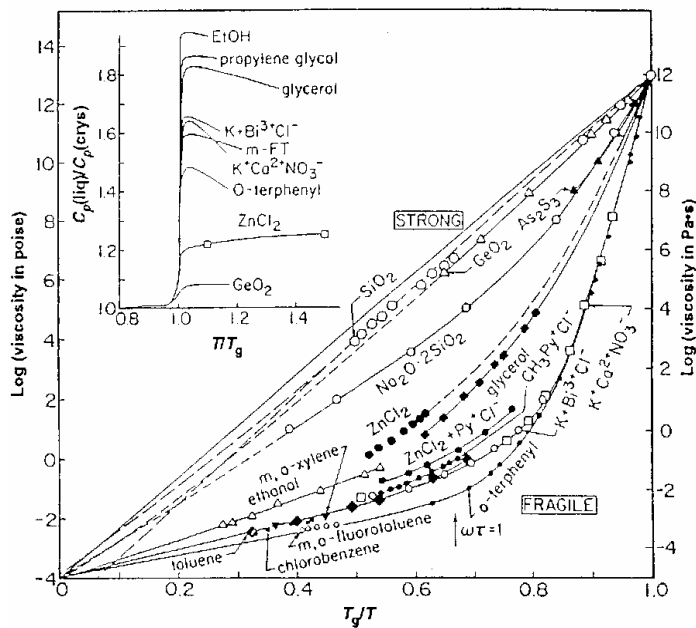


Figure 1.8: Molecular mobility (or viscosity) as a function of normalized temperature above T_g .^{142,144,145}

The fragility of glass formers is commonly depicted in a Kauzmann-type plot (Figure 1.8). Strong glasses show an approximately linear change of apparent activation energy with the inverse of temperature whereas fragile glasses show a more bent curve progression. There are several variations of Kauzmann-type plots depicting either of the physical characteristic properties describing the glassy state with changing temperature, i.e. viscosity or molecular mobility. Figure 1.8 shows the change in viscosity with changing inverse temperature normalized for the glass transition temperature, i.e. T_g/T .

Another way to classify a glass as fragile or strong is to study the change in heat capacity at T_g : Strong glasses show a small change in heat capacity whereas fragile ones show a large change.

The temperature dependence of molecular motions directly determines many important properties including the location of the glass transition temperature and the ease of glass formation. The temperature dependence of molecular mobility is commonly described by the empirical Vogel-Tamman-Fulcher (VTF) equation¹⁴⁴⁻¹⁴⁶:

$$\tau = \tau_0 \exp\left(\frac{DT_0}{T - T_0}\right) \quad (1.10)$$

Where τ is the mean molecular relaxation time, T is the temperature and τ_0 , D and T_0 are constants as described in the following section:

Some authors equate T_0 with the Kauzmann temperature (T_K) described above. τ_0 can be related to the relaxation time constant of the unrestricted material^{144,145} ($\sim 10^{-14}$ s¹⁴³). D ,

(called Angell's parameter by some authors^{147,148}) directly refers to the fragility of a material. Presuming a constant relaxation time of roughly 100 s at the glass transition temperature for all glasses and further insisting that τ is the same for all glasses at the extreme high-temperature limit (i.e. 16 orders of magnitude change between T_g and the high-temperature limit¹¹⁹), a relationship between D and T_0 can be stated¹⁴⁹:

$$\frac{T_g}{T_0} = 1 + \frac{D}{36.85} \quad (1.11)$$

Large values for D (>100) are indicative for strong glasses, small values (<10) are indicative for fragile glass-forming tendencies¹⁴².

Other methods to estimate the fragility of a glassy system is to calculate the offset between T_g and T_0 with $(T_g - T_0) > 50$ typical for strong glasses¹⁴². A "rule of thumb" to assess the fragility without relaxation time data on hand is the ratio of the melting temperature and the glass transition temperature with $T_m/T_g > 1.5$ indicating a strong glass^{144,145}.

The temperature dependence of the viscosity is described by the William-Landel-Ferry (WLF) equation listed above. The WLF equation is a special form of the VTF equation where C_1 and C_2 are equivalent to $DT_0/(T_g - T_0)$ and $(T_g - T_0)$, respectively.

B. TEMPERATURE DEPENDENCE BELOW T_g

Because the equations derived above assume that the configurations are in equilibrium, they are not valid below the glass transition as the configurations in a glass are not in thermal equilibrium.

The extent of a glass's deviation from equilibrium is strongly dependent on the way it was formed. Thus the temperature dependence of the molecular motions below the glass transition temperature is influenced by the glass's formation conditions. The temperature dependence is usually less pronounced than above the T_g , thus some authors even propose an Arrhenius-like relationship.

However, most frequently, the temperature dependence of the relaxation time below the glass transition is described by the Adam-Gibbs-Vogel (AGV) equation:

$$\tau = \tau_0 \exp\left(\frac{DT_0}{T - (T/T_f)T_0}\right) \quad (1.12)$$

Where τ is the mean molecular relaxation time, T is the temperature, τ_0 , D and T_0 are constants and refer to the relaxation time constant of the unrestricted material, the Angell's parameter and the Kauzmann temperature, respectively, as described above. T_f is the fictive temperature, i.e. the temperature where the ideal glass has the same configurational entropy as the real glass at the temperature T . The introduction of T_f , accounts for the conditions of glass formation.

The molecular relaxation processes that are an important characteristic of the glassy state are discussed in detail in the following section.

4.4 STABILITY OF GLASSY SYSTEMS

As already described in detail above, the glassy state is a metastable state as compared to the crystalline state as well as compared to the equilibrium glass. The extent of metastability, i.e. the offset between the entropy of the real glass and the equilibrium glass, is affected by the conditions of glass formation.

During storage, the metastable system relaxes towards the equilibrium state by rearranging the molecular short range order to minimize the free volume and the enthalpy of the system. The molecular basis for these rearrangements is molecular motions. Commonly seen as solid matter, there is still mobility in the glassy state although the motions are slow and the apparent activation enthalpies for any motion to appear are high.

Relaxations commonly are described by exponential decay functions. Because a glass is composed of various sub-states with different relaxation types and times and because the molecular motions in the glassy state are highly cooperative the mean molecular relaxation time of the whole system follows a nonexponential function. This distribution of relaxation times is best described by the empirical Kohlrausch-William-Watts (KWW) stretched exponential function:

$$\phi(t) = \exp\left(-\left(\frac{t}{\tau}\right)^\beta\right) \quad (1.13)$$

Where $\phi(t)$ is the extent of relaxation at time t , τ is the mean molecular relaxation time and β is a constant. β describes the distribution of relaxation times with a value close to unity for a single relaxation time and a small value indicating a wide distribution of relaxing substates. It is often referred to as “stretching parameter”¹⁵⁰.

In search for a better explanation of experimental data several variations and advancements of the KWW equation, e.g. the Cole-Davidson and Cole-Cole equation, have been stated. They will be discussed in detail in the results and discussion part presented in Chapter 9 of this thesis.

Molecular mobility is imparted by different relaxation processes. Figure 1.9 schematically shows the different relaxation processes as observed by dielectric relaxation spectroscopy (DRS).

Global dynamics or α -relaxations are processes that are highly cooperative (i.e. requiring the simultaneous motion of relatively large regions in the glass) and therefore highly coupled to viscosity^{119,145,151}. The glass transition is ascribed to α -relaxations, below the glass transition the motions become cooperative to the degree that they are unlikely to occur at all. The structural relaxation time as described by the KWW equation usually means the time

constant for α -motions^{119,152}. α -relaxations exhibit a non-Arrhenius temperature dependence¹⁵¹. Fragility usually refers to the temperature dependence of α -relaxations.

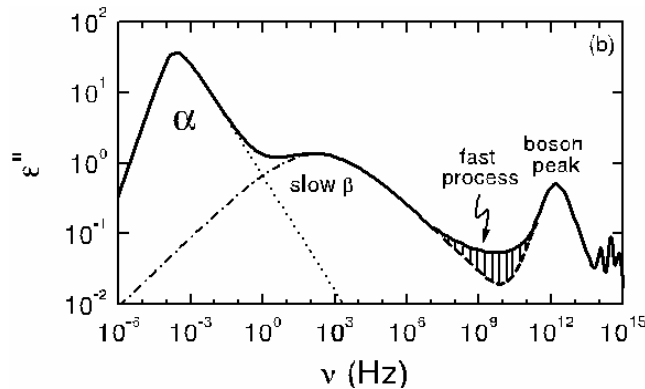


Figure 1.9: Schematic view of the frequency dependent dielectric loss in glass-forming materials as observed with DRS spectroscopy showing peaks characteristic for α - and β -relaxations.¹⁵⁶

Local dynamics or β -relaxations precede the α -process and occur at lower temperatures. They are usually weaker than the α -relaxation and can be further diminished by annealing¹⁵¹ although some pharmaceuticals as sorbitol are found to exhibit surprisingly strong β -relaxations^{153,154}. It is representative for fast dynamics, i.e. faster and more localized motions that involve specific parts of the molecule rather than whole glass regions. Fast dynamics occur over a broad range of timescales anywhere between vibrational and rotational motions. β -relaxations show an Arrhenius temperature dependence¹⁵¹. Some authors regard β -relaxations as more relevant to protein stability than α -relaxations^{61,62,155}. Some authors describe γ - and δ -processes as well. These processes represent fast dynamics, too, but they are usually weaker than β -relaxations¹⁵⁷.

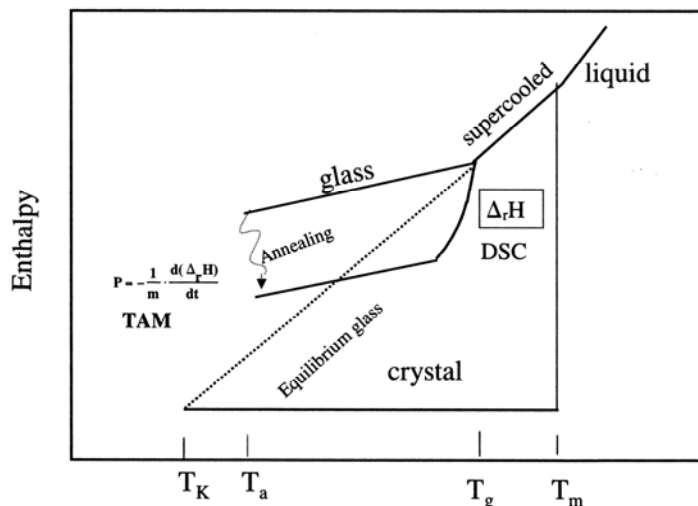


Figure 1.10: Enthalpy relaxation of amorphous solids: enthalpy diagram depicting the aging of a glassy material.¹⁶²

The process of relaxation towards the equilibrium state is called aging or annealing. This either happens unintentionally during storage or deliberately during holding at elevated temperatures in order to increase stability. Annealing causes relaxation of the glass towards

the equilibrium glass, as schematically depicted in Figure 1.10. It enforces a change in molecular glass dynamics and leads to the retardation of structural relaxation times. Therefore some authors describe an impact of annealing on protein stability¹⁵⁸⁻¹⁶¹. The relationship between glassy dynamics and protein stability will be discussed in the following section.

4.5 CORRELATION OF MOLECULAR MOBILITY AND PROTEIN STABILITY

Regarding protein stability in the solid state, dynamics are important because every reaction, such as aggregation, oxidation or non-enzymatic browning requires some degree of mobility¹¹⁹.

In pharmaceutical protein lyophilizates there are two types of dynamics relevant to stability: the dynamics of the amorphous matrix and the internal protein dynamics. Only when the protein is molecularly dispersed in the matrix, there is a coupling of the two types of dynamics. Coupling however is of utmost importance, because this is the premise for retardation of protein degradation by the use of excipients.

Concerning degradation reactions it is differentiated between those that occur within one protein molecule and those that are bimolecular and thus dependent on diffusion.

The latter type of reaction is obviously more affected by molecular mobility. Reactions with minor contributions from molecular mobility cannot be inhibited by reducing molecular mobility¹³⁶.

As mobility and the system's viscosity are interrelated, the Stokes-Einstein equation (1.14) gives a rough approximation of the reactivity.

$$D = \frac{kT}{6\pi\eta a} \quad (1.14)$$

Where D is the translational diffusion coefficient, k is the Boltzman's constant, T is temperature, η is the viscosity and a is the hydrodynamic radius of the diffusing species.

The diffusion coefficient of the reacting species and the reaction rate constant of the degradation reaction are proportionally related, thus equation (1.14) can predict the reaction rate.

As the Stokes-Einstein equation is not entirely appropriate for highly viscous systems and because not all types of mobility are coupled to viscosity, perfect coupling is not always observed¹⁶³.

It was found that a correlation of reaction rates and viscosity and global mobility works best for reactions demanding motion on a larger scale¹¹⁹.

However, the contribution of molecular mobility to the rates of chemical degradation or physical reactions is difficult to evaluate quantitatively, because thermodynamic factors

always affect these rates as well¹³⁵. As described above, the reactivity of amorphous solids is affected by both molecular mobility and energy of activation for a certain reaction.

If reactivity is found to be affected mainly by molecular mobility as described by the glass transition, then this factor can be used to predict stability. However, if there is no correlation then stability cannot be predicted by molecular mobility.

Degradation rates in amorphous materials often show a non-Arrhenius behavior around T_g . It is important to bear in mind the fact that predictions of storage stability from accelerated stability testing at higher temperatures cannot be concluded without explicit knowledge of the temperature dependence of molecular mobility.

4.5.1 GLOBAL MOBILITY

Investigations analyzing the impact of molecular mobility on chemical and physical stability, mostly considered global mobility. They used either the difference of storage temperature and glass transition temperature ($T-T_g$) or directly assessed the structural relaxation time. Good correlation was found for physical degradation reactions such as the dimer formation of monoclonal antibody-vinca conjugates¹⁶⁴, the aggregation of bovine γ -globulin¹⁶⁵, human growth hormone or IgG1¹⁶⁶. Chemical degradation rates showed contributions of molecular mobility as well. Correlation is reported for the chemical decomposition of mab-vinca conjugates¹⁶⁴ or the deamidation of Asn-hexapeptide¹⁶⁷.

A correlation of mobility and stability is also suggested from findings in which an increased formulation- T_g led to an increased stability. A decreased aggregation rate was observed for lyophilized recombinant interleukin-2¹⁶⁸, actin¹⁶⁹ as well as for bovine γ -globulin¹⁷⁰ after increase of the formulation's T_g .

However, sometimes no correlation between structural relaxation time and reaction rates is found^{171,172}.

Recently there have been suggestions that local mobility as expressed by β -dynamics is more predictive for stability than global mobility^{129,155}.

4.5.2 LOCAL MOBILITY

The molecular motion required for a reaction to proceed varies depending on the reaction mechanism. Correlation between reactivity and local mobility has been shown for several amorphous pharmaceuticals although there are fewer reports than for the correlation of global mobility and stability.

Local mobility can be assessed through solid state NMR measurements, dielectric relaxation spectroscopy (DRS) or incoherent elastic neutron scattering using the high flux backscattering spectrometer (HFBS).

The deamidation and dimerization of lyophilized insulin has been found to correlate with relaxation times determined using NMR¹⁷³. The group of M. Cicerone studied the effect of

addition of small molecular weight plasticizers like glycerol on stability. They found an even increased stability with decreased structural relaxation time but decreased local mobility as determined with neutron scattering techniques^{61,62,155}.

However, whereas many studies have demonstrated a possible relationship between molecular mobility and chemical and physical stability, there are a lot of reports where no apparent correlation could be established^{171,172}. In some of these studies other factors could be identified as responsible for this lack of correlation. The role of excipients as reactant and the complex effects of water or the heterogeneity of the amorphous phase can explain a deviation of reactivity from molecular mobility¹³⁶.

Summing up, there are several publications reporting a correlation between the molecular mobility on the one hand and chemical and physical stability on the other hand. However, stability of amorphous pharmaceuticals is determined by the relative effects of both molecular mobility and the activation energy barrier E_A for degradation reactions. An increase in E_A reduces the significance of mobility.

The significance of mobility is also influenced by the degradation mechanism. Global mobility is especially important in bimolecular reactions; whereas local mobility is more vital in degradations that include smaller-scale motions.

It is important to remember that mobility changes greatly around the glass transition. Thus the temperature dependence of reaction rates that are influenced by molecular mobility may change as well.

Another important conclusion of these considerations is the fact that only formulations exhibiting instabilities that are affected by mobility can be stabilized by the addition of antiplasticizers.

5 REFERENCES

1. Pavlou, A.K. and Reichert, J.M. Recombinant protein therapeutics-success rates, market trends and values to 2010. *Nature Biotechnology*, **22** (12): 1513-1519 (2004)
2. Leader, B., Baca, Q.J., and Golan, D.E. Protein therapeutics: a summary and pharmacological classification. *Nature Reviews Drug Discovery*, **7** (1): 21-39 (2008)
3. Singer, M. and Berg, P. Recombinant DNA: NIH Guidelines. *Science*, **193** (4249): 186-188 (1976)
4. Cohen, S.N., Chang, A.C.Y., Boyer, H.W., and Helling, R.B. Construction of biologically functional bacterial plasmids in vitro. *Proceedings National Academy of Sciences USA*, **70** (11): 3240-3244 (1973)
5. Carpenter, J.F., Pikal, M.J., Chang, B.S., and Randolph, T.W. Rational design of stable lyophilized protein formulations: some practical advice. *Pharmaceutical Research*, **14** (8): 969-975 (1997)
6. Schwegman, J.J., Hardwick, L.M., and Akers, M.J. Practical formulation and process development of freeze-dried products. *Pharmaceutical Development and Technology*, **10** (2): 151-173 (2005)
7. Arakawa, T., Prestrelski, S.J., Kenney, W.C., and Carpenter, J.F. Factors affecting short-term and long-term stabilities of proteins. *Advanced Drug Delivery Reviews*, **46** (1-3): 307-326 (2001)
8. Manning, M.C., Patel, K., and Borchardt, R.T. Stability of protein pharmaceuticals. *Pharmaceutical Research*, **6** (11): 903-918 (1989)
9. Franks, F. Freeze-drying of bioproducts: putting principles into practice. *European Journal of Pharmaceutics and Biopharmaceutics*, **45** (3): 221-229 (1998)
10. Lechuga-Ballesteros, D., Miller, D.P., and Duddu, S.P. Thermal analysis of lyophilized pharmaceutical peptide and protein formulations. *Biotechnology: Pharmaceutical Aspects*, **2** (Lyophilization of Biopharmaceuticals): 271-335 (2004)
11. Wang, W. Lyophilization and development of solid protein pharmaceuticals. *Int.J.Pharm.*, **203** (1-2): 1-60 (2000)
12. Franks, F. Freeze-drying of bioproducts: putting principles into practice. *Eur.J.Pharm.Biopharm*, **45** (3): 221-229 (1998)
13. Pikal, M.J. Freeze-drying of proteins: process, formulation, and stability. *ACS Symp.Ser.*, **567** (Formulation and Delivery of Proteins and Peptides): 120-133 (1994)
14. MacKenzie, A.P. Collapse during freeze drying - qualitative and quantitative aspects. *Freeze Drying Adv.Food Technol., [Int.Course]*, 277-307 (1975)
15. Pikal, M.J. Freeze-drying of proteins. Part I: process design. *BioPharm (Duluth, MN, United States)*, **3** (8): 18-20, 22 (1990)
16. Colandene, J.D., Maldonado, L.M., Creagh, A.T., Vrettos, J.S., Goad, K.G., and Spitznagel, T.M. Lyophilization cycle development for a high-concentration monoclonal antibody formulation lacking a crystalline bulking agent. *Journal of Pharmaceutical Sciences*, **96** (6): 1598-1608 (2007)
17. Lewis, L.M. Lyophilized formulations of modified antibodies, TNFalpha specific humanized antibody CDP870, and methods of making the same. **2003-US24413** (2004019860): 34(20040311)
18. Passot, S., Fonseca, F., and Marin, M. Composition for the freeze-drying of proteins. **2005-791** (2881139): 36(20060728)
19. Trappler, E.D. Lyophilization equipment. *Biotechnology: Pharmaceutical Aspects*, **2** (Lyophilization of Biopharmaceuticals): 3-41 (2004)
20. Rey, L.R. Glimpses into the fundamental aspects of freeze-drying. *Developments in Biological Standardization*, **36** 19-27 (1976)
21. Oetjen, G.W. and Haseley, P. Freeze-Drying. **2** *Wiley-VCH* (2004)

22. Jennings, T.A. and Duan, H. Calorimetric monitoring of lyophilization. *PDA journal of pharmaceutical science and technology / PDA*, **49** (6): 272-282 (1995)
23. Jennings, T.A. Lyophilization: Introduction and Basic Principles. *Informa Healthcare* (1999)
24. Willemer, H. Measurements of temperatures, ice evaporation rates and residual moisture contents in freeze-drying. *Developments in Biological Standardization*, **74** (Biol. Prod. Freeze-Drying Formulation): 123-136 (1992)
25. Wang, W. Lyophilization and development of solid protein pharmaceuticals. *International Journal of Pharmaceutics*, **203** (1-2): 1-60 (2000)
26. Eckhardt, B.M., Oeswein, J.Q., and Bewley, T.A. Effect of freezing on aggregation of human growth hormone. *Pharmaceutical Research*, **8** (11): 1360-1364 (1991)
27. Wisniewski, R. Large-scale cryopreservation of cells, cell components, and biological solutions. *BioPharm (Eugene, Oreg.)*, **11** (9): 42-49,61 (1998)
28. Nail, S.L., Jiang, S., Chongprasert, S., and Knopp, S.A. Fundamentals of freeze-drying. *Pharmaceutical Biotechnology*, **14** (Development and Manufacture of Protein Pharmaceuticals): 281-360 (2002)
29. Pikal, M.J. Freeze-drying of proteins: process, formulation, and stability. *ACS Symposium Series*, **567** 120-133 *ACS Symposium Series* (1994)
30. House, J.A. and Mariner, J.C. Stabilization of rinderpest vaccine by modification of the lyophilization process. *Developments in Biological Standardization*, **87** 235-244 (1996)
31. Jiang, S. and Nail, S.L. Effect of process conditions on recovery of protein activity after freezing and freeze-drying. *European Journal of Pharmaceutics and Biopharmaceutics*, **45** (3): 249-257 (1998)
32. Tang, X. and Pikal, M.J. Design of Freeze-Drying Processes for Pharmaceuticals: Practical Advice. *Pharmaceutical Research*, **21** (2): 191-200 (2004)
33. Bindschaedler, C. Lyophilization process validation. *Drugs and the Pharmaceutical Sciences*, **96** (Freeze-Drying/Lyophilization of Pharmaceutical and Biological Products): 373-408 (1999)
34. Nail, S.L. and Johnson, W. Methodology for in-process determination of residual water in freeze-dried products. *Developments in Biological Standardization*, **74** (Biol. Prod. Freeze-Drying Formulation): 137-151 (1992)
35. Adams, G.D.J. and Irons, L.I. Some implications of structural collapse during freeze-drying using *Erwinia carotovora* L-asparaginase as a model. *Journal of Chemical Technology and Biotechnology*, **58** (1): 71-76 (1993)
36. Overcashier, D.E., Patapoff, T.W., and Hsu, C.C. Lyophilization of Protein Formulations in Vials: Investigation of the Relationship between Resistance to Vapor Flow during Primary Drying and Small-Scale Product Collapse. *Journal of Pharmaceutical Sciences*, **88** (7): 688-695 (1999)
37. Franks, F. Freeze-Drying of Pharmaceuticals and Biopharmaceuticals. *Royal Society of Chemistry* (2008)
38. Pikal, M.J., Shah, S., Roy, M.L., and Putman, R. The secondary drying stage of freeze drying: drying kinetics as a function of temperature and chamber pressure. *International Journal of Pharmaceutics*, **60** (3): 203-217 (1990)
39. Chang, B.S. and Hershenson, S. Practical approaches to protein formulation development. *Pharmaceutical Biotechnology*, **13** (Rational Design of Stable Protein Formulations): 1-25 (2002)
40. Costantino, H.R. Excipients for use in lyophilized pharmaceutical peptide, protein, and other bioproducts. *Biotechnology: Pharmaceutical Aspects*, **2** (Lyophilization of Biopharmaceuticals): 139-228 (2004)
41. Adams, G.D.J. and Ramsay, J.R. Optimizing the Lyophilization Cycle and the Consequences of Collapse on the Pharmaceutical Acceptability of *Erwinia* L-Asparaginase. *Journal of Pharmaceutical Sciences*, **85** (12): 1301-1305 (1996)

42. Randolph, T.W. and Carpenter, J.F. Engineering challenges of protein formulations. *AIChE Journal*, **53** (8): 1902-1907 (2007)
43. Hatley, R.H.M. Glass fragility and the stability of pharmaceutical preparations-excipient selection. *Pharmaceutical Development and Technology*, **2** (3): 257-264 (1997)
44. Dill, K.A., Alonso, D.O.V., and Hutchinson, K. Thermal stabilities of globular proteins. *Biochemistry*, **28** (13): 5439-5449 (1989)
45. Graziano, G., Catanzano, F., Riccio, A., and Barone, G. A reassessment of the molecular origin of cold denaturation. *Journal of Biochemistry*, **122** (2): 395-401 (1997)
46. Jaenicke, R. Protein structure and function at low temperatures. *Philos.Trans.R.Soc.London, B*, **326** (1237): 535-553 (1990)
47. Chang, B.S., Kendrick, B.S., and Carpenter, J.F. Surface-induced denaturation of proteins during freezing and its inhibition by surfactants. *Journal of Pharmaceutical Sciences*, **85** (12): 1325-1330 (1996)
48. Kuhlman, B., Yang, H.Y., Boice, J.A., Fairman, R., and Raleigh, D.P. An exceptionally stable helix from the ribosomal protein L9: implications for protein folding and stability. *Journal of Molecular Biology*, **270** (5): 640-647 (1997)
49. Overcashier, D.E., Brooks, D.A., Costantino, H.R., and Hsu, C.C. Preparation of Excipient-Free Recombinant Human Tissue-Type Plasminogen Activator by Lyophilization from Ammonium Bicarbonate Solution: An Investigation of the Two-Stage Sublimation Phenomenon. [Erratum to document cited in CA126:242793]. *Journal of Pharmaceutical Sciences*, **86** (7): 880(1997)
50. Arakawa, T., Kita, Y., and Carpenter, J.F. Protein-solvent interactions in pharmaceutical formulations. *Pharmaceutical Research*, **8** (3): 285-291 (1991)
51. Lin, T.Y. and Timasheff, S.N. On the role of surface tension in the stabilization of globular proteins. *Protein Science*, **5** (2): 372-381 (1996)
52. Timasheff, S.N. The control of protein stability and association by weak interactions with water: How do solvents affect these processes? *Annu.Rev.Biophys.Biomol.Struct.*, **22** 67-97 (1993)
53. Timasheff, S.N. Control of protein stability and reactions by weakly interacting cosolvents: the simplicity of the complicated. *Adv.Protein Chem.*, **51** (Linkage Thermodynamics of Macromolecular Interactions): 355-432 (1998)
54. Carpenter, J.F. and Crowe, J.H. An infrared spectroscopic study of the interactions of carbohydrates with dried proteins. *Biochemistry*, **28** (9): 3916-3922 (1989)
55. Carpenter, J.F., Crowe, J.H., and Arakawa, T. Comparison of solute-induced protein stabilization in aqueous solution and in the frozen and dried states. *Journal of Dairy Science*, **73** (12): 3627-3636 (1990)
56. Allison, S.D., Dong, A., and Carpenter, J.F. Counteracting effects of thiocyanate and sucrose on chymotrypsinogen secondary structure and aggregation during freezing, drying, and rehydration. *Biophysical Journal*, **71** (4): 2022-2032 (1996)
57. Allison, S.D., Randolph, T.W., Manning, M.C., Middleton, K., Davis, A., and Carpenter, J.F. Effects of drying methods and additives on structure and function of actin: mechanisms of dehydration-induced damage and its inhibition. *Archives of Biochemistry and Biophysics*, **358** (1): 171-181 (1998)
58. Crowe, J.H., Crowe, L.M., and Carpenter, J.F. Preserving dry biomaterials: the water replacement hypothesis. Part 1. *BioPharm (Eugene, Oreg.)*, **6** (3): 28-9, 32 (1993)
59. Crowe, J.H., Crowe, L.M., and Carpenter, J.F. Preserving dry biomaterials: The water replacement hypothesis. Part 2. *BioPharm (Eugene, Oreg.)*, **6** (4): 40-43 (1993)
60. Mattern, M., Winter, G., Kohnert, U., and Lee, G. Formulation of proteins in vacuum-dried glasses. II. Process and storage stability in sugar-free amino acid systems. *Pharmaceutical Development and Technology*, **4** (2): 199-208 (1999)

61. Cicerone, M.T., Tellington, A., Trost, L., and Sokolov, A. Substantially improved stability of biological agents in dried form: the role of glassy dynamics in preservation of biopharmaceuticals. *Bioprocess International*, **1** (1): 36-38, 40, 42, 44, 46 (2003)
62. Cicerone, M.T. and Soles, C.L. Fast dynamics and stabilization of proteins: Binary glasses of trehalose and glycerol. *Biophysical Journal*, **86** (6): 3836-3845 (2004)
63. Tsourouflis, S., Flink, J.M., and Karel, M. Loss of structure in freeze-dried carbohydrates solutions: effect of temperature, moisture content and composition. *Journal of the Science of Food and Agriculture*, **27** (6): 509-519 (1976)
64. Shackell, L.F. An improved method of desiccation, with some applications to biological problems. *AJP - Legacy*, **24** (3): 325-340 (1909)
65. Levi, G. and Karel, M. Volumetric shrinkage (collapse) in freeze-dried carbohydrates above their glass transition temperature. *Food Research International*, **28** (2): 145-151 (1995)
66. Krokida, M.K., Karathanos, V.D., and Maroulis, Z.B. Effect of freeze-drying conditions on shrinkage and porosity of dehydrated agricultural products. *Journal of Food Engineering*, **35** 369-380 Elsevier Science Limited (1998)
67. MacKenzie, A.P. Collapse during freeze drying - qualitative and quantitative aspects. *Freeze Drying Adv.Food Technol., [Int.Course]*, 277-307 (1975)
68. Rambhatla, S., Obert, J.P., Luthra, S., Bhugra, C., and Pikal, M.J. Cake shrinkage during freeze drying: a combined experimental and theoretical study. *Pharmaceutical Development and Technology*, **10** (1): 33-40 (2005)
69. Mizrahi, S., Zimmermann, G., Berk, Z., and Cogan, U. The use of isolated soybean proteins in bread. *Cereal Chemistry*, **44** (2): 193-203 (1967)
70. Tsourouflis, S., Flink, J.M., and Karel, M. Loss of structure in freeze-dried carbohydrates solutions: effect of temperature, moisture content and composition. *Journal of the Science of Food and Agriculture*, **27** (6): 509-519 (1976)
71. Bellows, R.J. and King, C.J. Freeze-drying of aqueous solutions: Maximum allowable operating temperature. *Cryobiology*, **9** (6): 559-561 (1972)
72. Williams, M.L., Landel, R.F., and Ferry, J.D. The temperature dependence of relaxation mechanisms in amorphous polymers and other glass-forming liquids. *Journal of the American Chemical Society*, **77** 3701-3707 (1955)
73. Ferry, J.D. Viscoelastic Properties of Polymers. 3rd Ed. 641 *John Wiley & Sons* (1980)
74. Karel, M., Anglea, S., Buera, P., Karmas, R., Levi, G., and Roos, Y. Stability-related transitions of amorphous foods. *Thermochimica Acta*, **246** (2): 249-269 (1994)
75. Richard James Bellows Freeze drying of liquid foods: dependence of collapse temperature on composition and concentration. (*Ph.D.in Chemical Engineering*)--University of California, Berkeley, (1972)
76. Kistler, J. and Kellenberger, E. Collapse phenomena in freeze-drying. *Journal of ultrastructure research*, **59** (1): 70-75 (1977)
77. Passot, S., Fonseca, F., Barbouche, N., Marin, M., arcon-Lorca, M., Rolland, D., and Rapaud, M. Effect of Product Temperature During Primary Drying on the Long-Term Stability of Lyophilized Proteins. *Pharmaceutical Development and Technology*, **12** (6): 543-553 (2007)
78. Ito, K. Freeze drying of pharmaceuticals. Eutectic temperature and collapse temperature of solute matrix upon freeze drying of three-component systems. *Chemical & Pharmaceutical Bulletin*, **19** (6): 1095-1102 (1971)
79. MacKenzie, A.P. Basic principles of freeze-drying for pharmaceuticals. *Bulletin of the Parenteral Drug Association*, **20** (4): 101-130 (1966)

80. Fonseca, F., Passot, S., Cunin, O., and Marin, M. Collapse Temperature of Freeze-Dried *Lactobacillus bulgaricus* Suspensions and Protective Media. *Biotechnology Progress*, **20** (1): 229-238 (2004)
81. To, E.C. and Flink, J.M. 'Collapse', a structural transition in freeze dried carbohydrates. I. Evaluation of analytical methods. *Journal of Food Technology*, **13** (6): 551-565 (1978)
82. Meister, E. and Gieseler, H. Freeze-dry microscopy of protein/sugar mixtures: Drying behavior, interpretation of collapse temperatures and a comparison to corresponding glass transition Data. *Journal of Pharmaceutical Sciences*, **98** (9): 3072-3087 (2009)
83. Pikal, M.J. and Shah, S. The collapse temperature in freeze drying: dependence on measurement methodology and rate of water removal from the glassy phase. *International Journal of Pharmaceutics*, **62** (2-3): 165-186 (1990)
84. Fonseca, F., Obert, J.P., Beal, C., and Marin, M. State diagrams and sorption isotherms of bacterial suspensions and fermented medium. *Thermochimica Acta*, **366** (2): 167-182 (2001)
85. Gordon, M. and Taylor, J.S. Ideal copolymers and the second-order transitions of synthetic rubbers. I. Noncrystalline copolymers. *J.Appl.Chem.(London)*, **2** 493-500 (1952)
86. Duddu, S.P. and Dal Monte, P.R. Effect of glass transition temperature on the stability of lyophilized formulations containing a chimeric therapeutic monoclonal antibody. *Pharmaceutical research*, **14** (5): 591-595 (1997)
87. Ito, K. Freeze drying of pharmaceuticals. Macroscopic appearance of frozen and dried samples in connection with the growth of the eutectic crystals. *Chemical & Pharmaceutical Bulletin*, **18** (8): 1519-1525 (1970)
88. Lueckel, B., Bodmer, D., Helk, B., and Leuenberger, H. Formulations of sugars with amino acids or mannitol-influence of concentration ratio on the properties of the freeze-concentrate and the lyophilizate. *Pharm.Dev.Technol.*, **3** (3): 325-336 (1998)
89. Johnson, R.E., Kirchhoff, C.F., and Gaud, H.T. Mannitol-sucrose mixtures-versatile formulations for protein lyophilization. *Journal of Pharmaceutical Sciences*, **91** (4): 914-922 (2002)
90. Willemer, H. Experimental freeze-drying: procedures and equipment. *Drugs Pharm.Sci.*, **96** (Freeze-Drying/Lyophilization of Pharmaceutical and Biological Products): 79-121 (1999)
91. Kerr, W.L., Lim, M.H., Reid, D.S., and Chen, H. Chemical reaction kinetics in relation to glass transition temperatures in frozen food polymer solutions. *Journal of the Science of Food and Agriculture*, **61** (1): 51-56 (1993)
92. Kasraian, K., Spitznagel, T.M., Juneau, J.A., and Yim, K. Characterization of the sucrose/glycine/water system by differential scanning calorimetry and freeze-drying microscopy. *Pharmaceutical Development and Technology*, **3** (2): 233-239 (1998)
93. Ito, K. Freeze drying of pharmaceuticals. Change in the macroscopic appearance during freezing and the critical temperature necessary for freeze drying. *Chemical & Pharmaceutical Bulletin*, **18** (8): 1509-1518 (1970)
94. Levine, H. and Slade, L. Thermomechanical properties of small-carbohydrate-water glasses and 'rubbers': kinetically metastable systems at sub-zero temperatures. *Journal of the Chemical Society, Faraday Transactions 1: Physical Chemistry in Condensed Phases*, **84** (8): 2619-2633 (1988)
95. Atkins, P.W. Physical Chemistry, 6th Edition. 1014 *Oxford University Press* (1998)
96. Roos, Y. and Karel, M. Plasticizing effect of water on thermal behavior and crystallization of amorphous food models. *Journal of Food Science*, **56** (1): 38-43 (1991)
97. Flink, J. and Karel, M. Retention of organic volatiles in freeze-dried solutions of carbohydrates. *Journal of Agricultural and Food Chemistry*, **18** (2): 295-297 (1970)
98. Shalaev, E.Y. and Franks, F. Structural glass transitions and thermophysical processes in amorphous carbohydrates and their super-saturated solutions. *Journal of the Chemical Society, Faraday Transactions*, **91** (10): 1511-1517 (1995)

99. Fitzpatrick, S. and Saeklatvala, R. Understanding the physical stability of freeze dried dosage forms from the glass transition temperature of the amorphous components. *Journal of Pharmaceutical Sciences*, **92** (12): 2495-2501 (2003)
100. Seager, H. Drug-delivery products and the Zydys fast-dissolving dosage form. *Journal of pharmacy and pharmacology*, **50** (4): 375-382 (1998)
101. Aldous, B.J., Auffret, A.D., and Franks, F. The crystallization of hydrates from amorphous carbohydrates. *Cryo-Letters*, **16** (3): 181-186 (1995)
102. Lazar, M.E., Chapin, E.O., and Smith, G.S. Freeze-drying of apples; new developments in the work method. *Food Technology (Chicago)*, **15** (Jan.): 32-36 (1961)
103. Nail, S.L., Jiang, S., Chongprasert, S., and Knopp, S.A. Fundamentals of freeze-drying. *Pharmaceutical Biotechnology*, **14** (Development and Manufacture of Protein Pharmaceuticals): 281-360 (2002)
104. Craig, D.Q., Royall, P.G., Kett, V.L., and Hopton, M.L. The relevance of the amorphous state to pharmaceutical dosage forms: glassy drugs and freeze dried systems. *International Journal of Pharmaceutics*, **179** (2): 179-207 (1999)
105. Izutsu, K., Yoshioka, S., and Kojima, S. Physical stability and protein stability of freeze-dried cakes during storage at elevated temperatures. *Pharmaceutical Research*, **11** (7): 995-999 (1994)
106. Wang, D.Q., Hey, J.M., and Nail, S.L. Effect of collapse on the stability of freeze-dried recombinant factor VIII and α -amylase. *J.Pharm.Sci.*, **93** (5): 1253-1263 (2004)
107. Chatterjee, K., Shalaev, E.Y., and Suryanarayanan, R. Partially crystalline systems in lyophilization: II. Withstanding collapse at high primary drying temperatures and impact on protein activity recovery. *Journal of Pharmaceutical Sciences*, **94** (4): 809-820 (2005)
108. To, E.C. and Flink, J.M. 'Collapse', a structural transition in freeze dried carbohydrates. III. Prerequisite of recrystallization. *Journal of Food Technology*, **13** (6): 583-594 (1978)
109. Darcy, P. and Buckton, G. The influence of heating/drying on the crystallization of amorphous lactose after structural collapse. *International Journal of Pharmaceutics*, **158** (2): 157-164 (1997)
110. Adler, M. and Lee, G. Stability and Surface Activity of Lactate Dehydrogenase in Spray-Dried Trehalose. *Journal of Pharmaceutical Sciences*, **88** (2): 199-208 (1999)
111. Mattern, M., Winter, G., Rudolph, R., and Lee, G. Formulation of proteins in vacuum-dried glasses. Part 1. Improved vacuum-drying of sugars using crystallizing amino acids. *European Journal of Pharmaceutics and Biopharmaceutics*, **44** (2): 177-185 (1997)
112. Maury, M., Murphy, K., Kumar, S., Mauerer, A., and Lee, G. Spray-drying of proteins: effects of sorbitol and trehalose on aggregation and FT-IR amide I spectrum of an immunoglobulin G. *European Journal of Pharmaceutics and Biopharmaceutics*, **59** (2): 251-261 (2005)
113. Schuele, S., Schulz-Fademrecht, T., Garidel, P., Bechtold-Peters, K., and Friess, W. Stabilization of IgG1 in spray-dried powders for inhalation. *European Journal of Pharmaceutics and Biopharmaceutics*, **69** (3): 793-807 (2008)
114. Abdul-Fattah, A.M., Truong-Le, V., Yee, L., Nguyen, L., Kalonia, D.S., Cicerone, M.T., and Pikal, M.J. Drying-induced variations in physico-chemical properties of amorphous pharmaceuticals and their impact on stability (I): stability of a monoclonal antibody. *Journal of Pharmaceutical Sciences*, **96** (8): 1983-2008 (2007)
115. Hsu, C.C., Nguyen, H.M., Yeung, D.A., Brooks, D.A., Koe, G.S., Bewley, T.A., and Pearlman, R. Surface denaturation at solid-void interface—a possible pathway by which opalescent particulates form during the storage of lyophilized tissue-type plasminogen activator at high temperatures. *Pharmaceutical Research*, **12** (1): 69-77 (1995)
116. Lueckel, B., Helk, B., Bodmer, D., and Leuenberger, H. Effects of formulation and process variables on the aggregation of freeze-dried interleukin-6 (IL-6) after lyophilization and on storage. *Pharmaceutical Development and Technology*, **3** (3): 337-346 (1998)

117. Wang, D.Q., Hey, J.M., and Nail, S.L. Effect of collapse on the stability of freeze-dried recombinant factor VIII and α -amylase. *Journal of Pharmaceutical Sciences*, **93** (5): 1253-1263 (2004)
118. Pikal, M.J. Freeze-drying of proteins part II: formulation selection. *BioPharm (Duluth, MN, United States)*, **3** (9): 26-30 (1990)
119. Pikal, M.J. Mechanisms of Protein Satbilization during Freeze-Drying and Storage: The Relative Importance of Thermodynamic Stabilization and Glassy State Relaxation Dynamics.(3): 63-108 *Freeze-Drying/ Lyophilization of Pharmaceutical and Biological Products (Drugs and the Pharmaceutical Sciences Volume 137)* (2004)
120. Hora, M.S., Rana, R.K., and Smith, F.W. Lyophilized formulations recombinant tumor necrosis factor. *Pharmaceutical Research*, **9** (1): 33-36 (1992)
121. Pikal, M.J., Dellerman, K.M., Roy, M.I., and Riggan, R.M. The effects of formulation variables on the stability of freeze-dried human growth hormone. *Pharmaceutical Research*, **8** (4): 427-436 (1991)
122. Searles, J.A., Carpenter, J.F., and Randolph, T.W. Annealing to optimize the primary drying rate, reduce freezing-induced drying rate heterogeneity, and determine Tg' in pharmaceutical lyophilization. *Journal of Pharmaceutical Sciences*, **90** (7): 872-887 (2001)
123. Abdul-Fattah, A.M., Truong-Le, V., Yee, L., Pan, E., Ao, Y., Kalonia, D.S., and Pikal, M.J. Drying-Induced Variations in Physico-Chemical Properties of Amorphous Pharmaceuticals and Their Impact on Stability II: Stability of a Vaccine. *Pharmaceutical Research*, **24** (4): 715-727 (2007)
124. Truong-Le, V., Yee, L., Lechuga-Ballesteros, D., and Ohtake, S. Formulations for preservation of rota virus.**2008-US11169** (2009042202): 30pp(20090402)
125. Vehring, R. Preservation of bioactive materials by freeze dried foam and method for prepg. stable dry foam composition.**2008-US5840** (2008143782): 70pp(20081127)
126. Vu, T.L. Preservation of bioactive materials by freeze dried foam.**2003-US10989** (2003087327): 72(20031023)
127. Lai, M.C. and Topp, E.M. Solid-state chemical stability of proteins and peptides. *Journal of Pharmaceutical Sciences*, **88** (5): 489-500 (1999)
128. Prestrelski, S.J., Arakawa, T., and Carpenter, J.F. Structure of proteins in lyophilized formulations using Fourier transform infrared spectroscopy. *ACS Symposium Series*, **567** (Formulation and Delivery of Proteins and Peptides): 148-169 (1994)
129. Chang, L., Shepherd, D., Sun, J., Tang, X., and Pikal, M.J. Effect of sorbitol and residual moisture on the stability of lyophilized antibodies: Implications for the mechanism of protein stabilization in the solid state. *Journal of Pharmaceutical Sciences*, **94** (7): 1445-1455 (2005)
130. Franks, F., Hatley, R.H.M., and Mathias, S.F. Materials science and the production of shelf-stable biologicals. *BioPharm (Eugene, Oreg.)*, **4** (9): 38, 40-2, 55 (1991)
131. Slade, L. and Levine, H. Beyond water activity: recent advances based on an alternative approach to the assessment of food quality and safety. *Critical Reviews in Food Science and Nutrition*, **30** (2-3): 115-360 (1991)
132. Chang, L., Shepherd, D., Sun, J., Ouellette, D., Grant, K.L., Tang, X., and Pikal, M.J. Mechanism of protein stabilization by sugars during freeze-drying and storage: Native structure preservation, specific interaction, and/or immobilization in a glassy matrix? *Journal of Pharmaceutical Sciences*, **94** (7): 1427-1444 (2005)
133. Shamblin, S.L., Hancock, B.C., and Pikal, M.J. Coupling Between Chemical Reactivity and Structural Relaxation in Pharmaceutical Glasses. *Pharmaceutical Research*, **23** (10): 2254-2268 (2006)
134. Yoshioka, S., Tajima, S., Aso, Y., and Kojima, S. Inactivation and Aggregation of beta -Galactosidase in Lyophilized Formulation Described by Kohlrausch-Williams-Watts Stretched Exponential Function. *Pharmaceutical Research*, **20** (10): 1655-1660 (2003)

135. Yoshioka, S. and Aso, Y. A Quantitative Assessment of the Significance of Molecular Mobility as a Determinant for the Stability of Lyophilized Insulin Formulations. *Pharmaceutical Research*, **22** (8): 1358-1364 (2005)
136. Yoshioka, S. and Aso, Y. Correlations between molecular mobility and chemical stability during storage of amorphous pharmaceuticals. *Journal of Pharmaceutical Sciences*, **96** (5): 960-981 (2007)
137. Stotz, C.E., Winslow, S.L., Houchin, M.L., D'Souza, A.J.M., Ji, J., and Topp, E.M. Degradation pathways for lyophilized peptides and proteins. *Biotechnology: Pharmaceutical Aspects*, **2** (Lyophilization of Biopharmaceuticals): 443-479 (2004)
138. Costantino, H.R., Langer, R., and Klibanov, A.M. Moisture-induced aggregation of lyophilized insulin. *Pharmaceutical Research*, **11** (1): 21-29 (1994)
139. Liu, W.R., Langer, R., and Klibanov, A.M. Moisture-induced aggregation of lyophilized proteins in the solid state. *Biotechnology and Bioengineering*, **37** (2): 177-184 (1991)
140. Oliyai, C., Patel, J.P., Carr, L., and Borchardt, R.T. Solid state chemical instability of an asparaginyl residue in a model hexapeptide. *Journal of Pharmaceutical Science and Technology*, **48** (3): 167-173 (1994)
141. Oliyai, C. and Borchardt, R.T. Chemical pathways of peptide degradation. VI. Effect of the primary sequence on the pathways of degradation of aspartyl residues in model hexapeptides. *Pharmaceutical Research*, **11** (5): 751-758 (1994)
142. Hancock, B.C. and Zografi, G. Characteristics and Significance of the Amorphous State in Pharmaceutical Systems. *Journal of Pharmaceutical Sciences*, **86** (1): 1-12 (1997)
143. Hancock, B.C., Shamblin, S.L., and Zografi, G. Molecular mobility of amorphous pharmaceutical solids below their glass transition temperatures. *Pharm.Res.*, **12** (6): 799-806 (1995)
144. Angell, C.A. The old problems of glass and the glass transition, and the many new twists. *Proceedings National Academy of Sciences USA*, **92** (15): 6675-6682 (1995)
145. Angell, C.A. Formation of glasses from liquids and biopolymers. *Science (Washington, D.C.)*, **267** (5206): 1924-1935 (1995)
146. Ediger, M.D., Angell, C.A., and Nagel, S.R. Supercooled Liquids and Glasses. *Journal of Physical Chemistry*, **100** (31): 13200-13212 (1996)
147. Angell, C.A. The glass transition. *Current Opinion in Solid State and Materials Science*, **1** (4): 578-585 (1996)
148. Angell, C.A. Why $C_1 = 16-17$ in the WLF equation is physical - and the fragility of polymers. *Polymer*, **38** (26): 6261-6266 (1997)
149. Angell, C.A. Structural instability and relaxation in liquid and glassy phases near the fragile liquid limit. *Journal of Non-Crystalline Solids*, **102** (1-3): 205-221 (1988)
150. Shamblin, S.L., Hancock, B.C., Dupuis, Y., and Pikal, M.J. Interpretation of relaxation time constants for amorphous pharmaceutical systems. *Journal of Pharmaceutical Sciences*, **89** (3): 417-427 (2000)
151. Yu, L. Amorphous pharmaceutical solids: preparation, characterization and stabilization. *Advanced Drug Delivery Reviews*, **48** (1): 27-42 (2001)
152. Hancock, B.C., Shamblin, S.L., and Zografi, G. Molecular mobility of amorphous pharmaceutical solids below their glass transition temperatures. *Pharmaceutical Research*, **12** (6): 799-806 (1995)
153. Olsen, N.B. Scaling of beta -relaxation in the equilibrium liquid state of sorbitol. *Journal of Non-Crystalline Solids*, **235-237** 399-405 (1998)
154. Wagner, H. and Richert, R. Spatial uniformity of the beta -relaxation in D-sorbitol. *Journal of Non-Crystalline Solids*, **242** (1): 19-24 (1998)

155. Cicerone, M.T., Soles, C.L., Chowdhuri, Z., Pikal, M.J., and Chang, L. Fast dynamics as a diagnostic for excipients in preservation of dried proteins. *American Pharmaceutical Reviews*, **8** (6): 22, 24-22, 27 (2005)
156. Lunkenheimer, P. and Loidl, A. Dielectric spectroscopy of glass-forming materials: alpha -relaxation and excess wing. *Chemical Physics*, **284** (1-2): 205-219 (2002)
157. Liu, Y., Bhandari, B., and Zhou, W. Glass Transition and Enthalpy Relaxation of Amorphous Food Saccharides: A Review. *Journal of Agricultural and Food Chemistry*, **54** (16): 5701-5717 (2006)
158. Abdul-Fattah, A.M., Kalonia, D.S., and Pikal, M.J. The challenge of drying method selection for protein pharmaceuticals: product quality implications. *Journal of Pharmaceutical Sciences*, **96** (8): 1886-1916 (2007)
159. Luthra, S.A., Hodge, I.M., and Pikal, M.J. Investigation of the impact of annealing on global molecular mobility in glasses: optimization for stabilization of amorphous pharmaceuticals. *Journal of Pharmaceutical Sciences*, **97** (9): 3865-3882 (2008)
160. Luthra, S.A., Hodge, I.M., and Pikal, M.J. Effects of annealing on enthalpy relaxation in lyophilized disaccharide formulations: mathematical modeling of DSC curves. *Journal of Pharmaceutical Sciences*, **97** (8): 3084-3099 (2008)
161. Wang, B., Tchessalov, S., Warne, N.W., Cicerone, M.T., and Pikal, M.J. Impact of Sucrose level on Storage Stability of Proteins in Freeze-dried Solids: II. Correlation of Aggregation Rate with protein Structure and Molecular Mobility. *Journal of Pharmaceutical Sciences*, **9999 published online** (9999): n/a-n/a (2008)
162. Pikal, M.J. Chemistry in Solid Amorphous Matrices: Implications for Biostabilization. 257-272 *The Royal Society of Chemistry* (2008)
163. Angell, C.A. Dynamic processes in ionic glasses. *Chemical Reviews*, **90** (3): 523-542 (1990)
164. Roy, M.L., Pikal, M.J., Rickard, E.C., and Maloney, A.M. The effects of formulation and moisture on the stability of a freeze-dried monoclonal antibody-vinca conjugate: a test of the WLF glass transition theory. *Developments in Biological Standardization*, **74** (Biol. Prod. Freeze-Drying Formulation): 323-340 (1992)
165. Yoshioka, S., Aso, Y., Nakai, Y., and Kojima, S. Effect of High Molecular Mobility of Poly(vinyl alcohol) on Protein Stability of Lyophilized gamma -Globulin Formulations. *Journal of Pharmaceutical Sciences*, **87** (2): 147-151 (1998)
166. Levine, H. and Editor. Amorphous Food and Pharmaceutical Systems. (Proceedings of the Symposium held at Churchill College, Cambridge 15-17 May 2001.) [In: Spec. Publ. - R. Soc. Chem., 2002; 281].351(2002)
167. Sun, W.Q., Davidson, P., and Chan, H.S.O. Protein stability in the amorphous carbohydrate matrix: relevance to anhydrobiosis. *Biochimica et Biophysica Acta, General Subjects*, **1425** (1): 245-254 (1998)
168. Prestrelski, S.J., Pikal, K.A., and Arakawa, T. Optimization of lyophilization conditions for recombinant human interleukin-2 by dried-state conformational analysis using Fourier-transform infrared spectroscopy. *Pharmaceutical Research*, **12** (9): 1250-1259 (1995)
169. Allison, S.D., Manning, M.C., Randolph, T.W., Middleton, K., Davis, A., and Carpenter, J.F. Optimization of storage stability of lyophilized actin using combinations of disaccharides and dextran. *Journal of Pharmaceutical Sciences*, **89** (2): 199-214 (2000)
170. Yoshioka, S., Aso, Y., and Kojima, S. Dependence of the molecular mobility and protein stability of freeze-dried gamma -globulin formulations on the molecular weight of dextran. *Pharmaceutical Research*, **14** (6): 736-741 (1997)
171. Chang, B.S., Beauvais, R.M., Dong, A., and Carpenter, J.F. Physical factors affecting the storage stability of freeze-dried interleukin-1 receptor antagonist: glass transition and protein conformation. *Archives of Biochemistry and Biophysics*, **331** (2): 249-258 (1996)
172. Davidson, P. and Sun, W.Q. Effect of sucrose/raffinose mass ratios on the stability of co-lyophilized protein during storage above the Tg. *Pharmaceutical Research*, **18** (4): 474-479 (2001)

173. Yoshioka, S., Miyazaki, T., and Aso, Y. beta -Relaxation of Insulin Molecule in Lyophilized Formulations Containing Trehalose or Dextran as a Determinant of Chemical Reactivity. *Pharmaceutical Research*, **23** (5): 961-966 (2006)

CHAPTER 2

OBJECTIVES OF THE THESIS

Freeze-drying is commonly applied to stabilize sensitive materials such as proteins. It is thereby considered good freeze-drying practice to maintain the product at a low temperature during processing to avoid cake collapse. Collapsed vials are usually sorted out and the occurrence of gross collapse leads to categorical rejection of the whole batch, since collapsed lyophilizates are regarded as inferior products with irregularly distributed residual moisture and compromised protein stability, although there is no comprehensive systematic investigation on this topic performed so far. Also, collapsed lyophilizates are regarded as “pharmaceutically unacceptable” due to their optical appearance. Recently, study results pointing towards collapse not having a detrimental effect on protein stability were reported¹⁻⁴. Also, as it was lately reported for other drying-techniques, such as vacuum- or foam-drying, adequate protein stabilization does not necessarily require a porous cake structure^{5,6}.

It was thus the major aim of this work to analyze and understand the effect of lyophilized cake collapse on the quality characteristics and storage stability of incorporated proteins in order to provide a scientific basis for the rational handling of collapsed lyophilizates. It was intended to assess collapse in a way that supports a sound and fact-based decision on the release of collapsed batches for reprocessing. A second objective was the evaluation of the feasibility of performing freeze-drying at higher temperatures, both with and without the onset of collapse in order to shorten production cycles and render them more cost-efficient. Deliberately collapsed lyophilizates were to be compared to non-collapsed lyophilizates in order to get insight into the effects of collapse and in order to learn about the applicability of a new drying technique, herein referred to as collapse-drying.

After freeze-drying, lyophilizates are usually stored refrigerated, also in order to avoid cake collapse during storage, greatly complicating storage and distribution of lyophilized products. It was therefore a further goal of this thesis to investigate the effect of lyophilizate collapse during storage at elevated temperatures on protein stability.

Recently, the importance of thermal history (for instance defined by the applied drying technology) on the solid state characteristics, especially on the molecular mobility of dried materials was described. It was consequently a further major aim of this thesis to disclose the effect of collapse and the effect of the applied drying-protocol on the glassy dynamics of collapsed lyophilizates and to correlate the results to the stability of incorporated proteins.

More precisely, the main objectives of the thesis were:

1. Understanding the mechanism and the determinants of lyophilizate collapse as well as the drying kinetics of collapsed cakes in order to generate collapsed lyophilizates in a controlled and reproducible way (Chapter 4).
2. Characterization of collapsed lyophilizates with focus on quality characteristics that are supposed to change with the onset of collapse in order to develop a scientific and up-scalable analytical technique to quantify the degree of collapse (Chapter 5).
3. Characterization of the distribution of residual moisture in collapsed cakes and investigation of the effect of residual moisture on mAb-stability to allow for a clear discrimination of effects of collapse from effects of moisture (Chapter 6).
4. Characterization of the effect of lyophilizate collapse on protein stability with a focus on biological, physical and conformational protein stability as well as on physicochemical stability of the lyophilized formulation both immediately after freeze-drying (Chapter 7) and during storage at elevated temperatures (Chapter 8).
5. Comparison of lyophilizates that were intentionally collapsed during freeze-drying and lyophilizates that collapsed during storage at elevated temperatures with a focus on the physicochemical excipient stability and the stability of incorporated proteins (Chapter 8).
6. Characterization of the global and local glassy dynamics of collapsed versus non-collapsed lyophilizates and correlation to the stability of incorporated protein pharmaceuticals (Chapter 9).

REFERENCES

1. Chatterjee, K., Shalaev, E.Y., and Suryanarayanan, R. Partially crystalline systems in lyophilization: II. Withstanding collapse at high primary drying temperatures and impact on protein activity recovery. *Journal of Pharmaceutical Sciences*, **94** (4): 809-820 (2005)
2. Izutsu, K., Yoshioka, S., and Kojima, S. Physical stability and protein stability of freeze-dried cakes during storage at elevated temperatures. *Pharmaceutical Research*, **11** (7): 995-999 (1994)
3. Jiang, S. and Nail, S.L. Effect of process conditions on recovery of protein activity after freezing and freeze-drying. *European Journal of Pharmaceutics and Biopharmaceutics*, **45** (3): 249-257 (1998)
4. Wang, D.Q., Hey, J.M., and Nail, S.L. Effect of collapse on the stability of freeze-dried recombinant factor VIII and α -amylase. *Journal of Pharmaceutical Sciences*, **93** (5): 1253-1263 (2004)
5. Abdul-Fattah, A.M., Truong-Le, V., Yee, L., Nguyen, L., Kalonia, D.S., Cicerone, M.T., and Pikal, M.J. Drying-induced variations in physico-chemical properties of amorphous pharmaceuticals and their impact on stability (I): stability of a monoclonal antibody. *Journal of Pharmaceutical Sciences*, **96** (8): 1983-2008 (2007)
6. Mattern, M., Winter, G., Kohnert, U., and Lee, G. Formulation of proteins in vacuum-dried glasses. II. Process and storage stability in sugar-free amino acid systems. *Pharmaceutical Development and Technology*, **4** (2): 199-208 (1999)

CHAPTER 3

MATERIALS AND METHODS

1 MATERIALS

1.1 IgG₀₁

A humanized monoclonal antibody of the IgG₁ class was provided by Boehringer Ingelheim Pharma GmbH.

Monoclonal antibodies are Y-shaped glycoproteins of the immune system. There are 5 types of immunoglobulins in the human immune system differentiated by their different glycosylation of the heavy chain: IgG, IgM, IgA, IgD, IgE. The immunoglobulin types can be further classified into subclasses. IgG is the largest and most important group of immunoglobulins.

Antibodies are composed of two longer (heavy) chains and two shorter (light) chains connected by disulfide bonds. They have a molecular weight of about 150 kDa¹. By the point of cleavage of papain, two F_{ab}-parts and one F_c-part of the antibody can be distinguished. The F_{ab}-fragment (fragment antigen binding) consists of a light chain and part of one heavy chain and is responsible for the antigen-binding properties of antibodies. The F_{ab}-fragment can be further divided into a constant part and a variable part, the F_v-part². The F_c - fragment (fragment crystallizable) consists of the remaining parts of the two heavy chains and mediates most of the effector functions of the antibody³.

All currently approved antibody products are of the IgG class^{4,5}. The secondary structure of IgGs as determined by FTIR spectroscopy is predominantly β -sheet structure (60 %) with the remainder in unordered motifs such as turns⁶. The IgG₀₁ molecule contains 14 tryptophan residues.

The IgG₀₁ bulk solution used in this thesis contained 4.99 mg/mL protein, based on UV-metric concentration determination, formulated in 10 mM phosphate buffered saline at a pH of 6.2. Diafiltration was used to change the buffer system to a 10 mM sodium succinate buffer adjusted to a pH of 5.5 using an Ultrac[®] Lab PES 30 membrane (Schleicher & Schuell/ General Electric Biosciences Whatman Schleicher Schuell, Kent, UK) and the GUC system (Pall, Dreieich, Germany) equipped with a cassette holder from Pall (Pall, Dreieich, Germany). Subsequently, the protein content was adjusted to approximately 20 mg/mL by appending an ultrafiltration step using the same equipment. The protein solution was filtered using a 0.22 μ m Durapore PVDF Sterivex filter unit with a filling bell (Millipore, Schwalbach, Germany) and the protein content was determined photometrically at 280 nm according to

the European Pharmacopoeia (2.2.25) using a Lambda 950 spectrophotometer (Perkin Elmer, Waltham, MA, USA) .

For freeze-drying formulations the protein concentration was adjusted to 4.0 mg/mL and various excipients, such as sucrose, trehalose, mannitol (as cryo- and lyo-protectants) and polysorbate 20 as surfactant were added. A detailed description of the investigated formulations is given in Chapters 6 to 8 in the sections dealing with the IgG₀₁.

1.2 L-LACTIC DEHYDROGENASE (LDH)

L-Lactic Dehydrogenase (LDH) was used as a second model protein because of its well documented sensitivity towards stress situations arising both during freezing⁷⁻⁹ and during drying^{10,11}. The application of LDH as a sensitive model protein in freeze-drying¹²⁻¹⁴ as well as spray- and vacuum-drying experiments was described by several researchers¹⁵⁻¹⁸.

LDH is a tetrameric protein that is ubiquitously present in the cytoplasm of both animals and plants. It catalyzes the reduction of pyruvate to lactate while oxidizing the reduced form of β -nicotinamide adenine dinucleotide (β -NADH) to its oxidized counterpart β -NAD. Thereby it allows the regeneration of NAD as vital substance for the glycolysis in the absence of oxygen. LDH is composed of two different types of subunits, the M and the H type. The organ-specific expression of these isozymes permits the use of LDH as a diagnostic marker to localize pathological conditions.

LDH is composed of 36.8 % helical structures, 11.3 % β -sheet structures and 14.3 % turn structures as determined from X-ray diffraction¹⁹. There are six tryptophan molecules present in each subunit^{20,21}.

L-Lactic Dehydrogenase (LDH) Type II from rabbit muscle was purchased from Sigma-Aldrich (Steinheim, Germany) as aqueous ammonium sulfate suspension and dialyzed overnight against 10 mM potassium phosphate buffer adjusted to a pH of 7.5 using Slide-A-Lyzer® dialysis cassettes (cutoff of 10 kDa, volume of 12-30 mL) from Pierce (Perbio Science Deutschland GmbH, Bonn, Germany).

Dialysis was performed immediately before freeze-drying to ensure optimum stability. After dialysis the protein solution was filtered using a 0.22 μ m Durapore PVDF Sterivex filter unit (Millipore, Schwalbach, Germany).

As excipients for freeze-drying formulations sucrose and trehalose as lyo-protectants and PEG 1500, 3350, 8000 as cryo-protectants were added. A detailed description of the formulations investigated is given in Chapter 8 and Chapter 9 in the section dealing with LDH.

1.3 PA₀₁

Tissue-type plasminogen activator (PA₀₁) was investigated as a third model protein in this thesis. PA₀₁ was provided by Boehringer Ingelheim Pharma GmbH. The protein was

formulated at a concentration of 2.5 mg/mL together with arginine as solubilizer and Tween[®] 80 as surfactant. After thawing, the bulk was filtered using a 0.22 µm Durapore PVDF Sterivex filter unit with a filling bell (Millipore, Schwalbach, Germany). The protein concentration was determined using UV-spectroscopy at 280 nm.

The bulk was freeze-dried without further modification as described in section 2.1.

1.4 FREEZE-DRYING EXCIPIENTS

Table 3.1: Excipients used for freeze-drying experiments.

Excipient	Description	Supplier
L-Arginine	>98%, Ph.Eur.	Kyowa Hakko Europe GmbH (Duesseldorf, Germany)
H ₃ PO ₄	Ph.Eur. 85%	Merck KGaA (Darmstadt, Germany)
KH ₂ PO ₄	p.A.	Merck KGaA (Darmstadt, Germany)
KOH	Ph.Eur. 5.0	Caesar & Lorentz GmbH (Hilden, Germany)
Mannitol	Ph.Eur.	Cerestar (Cargill Europe BVBA, Mechelen, Belgium)
NaOH	50%	Merck KGaA (Darmstadt, Germany)
Na-Succinat * 6 H ₂ O	p.A.	Dr.Paul Lohmann (Emmerthal, Germany)
Poly(ethylene glycol) 1500		Clariant (Sulzbach, Germany)
Poly(ethylene glycol) 3350	ultra	Sigma Aldrich Chemie GmbH Steinheim, Germany)
Poly(ethylene glycol) 8000		Clariant (Sulzbach, Germany)
Sucrose	p.A.	Suedzucker AG (Mannheim, Germany)
α,α-Trehalose dihydrate	high purity, low endotoxin	Ferro Pfanstiehl Lab., Inc. (Waukegan, IL, USA)
Tween 20	Ph.Eur.	Uniquema (Emmerich, Germany)
Tween 80	Ph.Eur.	Croda (Nettetal Kaldenkirchen, Germany)

1.5 FURTHER CHEMICALS AND REAGENTS

Table 3.2: Significant fine chemicals.

Reagent	Description	Supplier
Apura [®] Water Standard Oven 1%	1% water	Merck KGaA (Darmstadt, Germany)
BSA	min. 96%	Sigma Aldrich Chemie GmbH Steinheim, Germany)
CoCl ₂ * 6 H ₂ O	99.99%, ACS	Acros Organics BVBA (Geel, Belgium)
FeCl ₃ * 6 H ₂ O	99% p.A.	VWR International GmbH (Darmstadt, Germany)
H ₃ PO ₄ 85%	Ph.Eur., 85%	Merck KGaA (Darmstadt, Germany)
Hydranal [®] Methanol dry	Riedel-de Haën, ≤0.01% water	Sigma Aldrich Chemie GmbH Steinheim, Germany)
Hydranal [®] Formamide dry	Riedel-de Haën, ≤0.02% water	Sigma Aldrich Chemie GmbH Steinheim, Germany)
Hydranal [®] Water Standard 1.00	Riedel-de Haën, 0.1% water	Sigma Aldrich Chemie GmbH Steinheim, Germany)
Hydranal [®] Coulomat AG	Riedel-de Haën	Sigma Aldrich Chemie GmbH Steinheim, Germany)
KCl	p.A.	Merck KGaA (Darmstadt, Germany)
KH ₂ PO ₄	p.A.	Merck KGaA (Darmstadt, Germany)
NaCl	p.A.	Merck KGaA (Darmstadt, Germany)
β – NADH	98%	Sigma Aldrich Chemie GmbH Steinheim, Germany)
NaH ₂ PO ₄ * 2 H ₂ O	p.A.	Merck KGaA (Darmstadt, Germany)
NaN ₃	p.A.	VWR International GmbH (Darmstadt, Germany)
NaOH	50%	Merck KGaA (Darmstadt, Germany)
Na-Pyruvat	99%	Sigma Aldrich Chemie GmbH Steinheim, Germany)
Sodium dodecyl sulphate (SDS)	>99%, ACS	Sigma Aldrich Chemie GmbH Steinheim, Germany)

2 METHODS

2.1 FREEZE-DRYING

Freeze-drying was performed using either a Christ Epsilon 2-12D freeze-dryer or a Christ Epsilon 2-6D pilot scale freeze-dryer (Christ, Osterode am Harz, Germany). Samples investigated for the analysis of glassy dynamics were prepared in a FTS Systems Durastop freeze-dryer (Stone Ridge, New York, USA).

1 mL (IgG₀₁ and LDH formulations) and 0.91 mL (PA₀₁ formulation) aliquots of the solutions for freeze-drying, respectively, were filled into 2 R blow back vials glass type I from Schott (Schott, Mainz, Germany) and partially stoppered with cross-linkable high molecular weight polydimethylsiloxane-coated rubber-lyophilization stoppers (B2-44, West, Eschweiler, Germany). For storage stability studies vials were washed with water for injection and heat sterilized. Stoppers were autoclaved and dried at 90 - 110 °C using vacuum for at least 7 hours.

In order to produce collapsed and elegant lyophilizates, 2 different freeze-drying protocols, an aggressive and a gentle cycle, respectively, were applied. After lyophilization the chamber was vented with dry nitrogen to a pressure of 800 mbar and the vials were stoppered by lowering the shelves. The vials were crimped with flip off seals.

2.1.1 PROCESS MONITORING

Throughout the drying process, the product temperature was monitored using thermocouples placed in selected vials of each formulation positioned both in the middle of a full shelf and at the edge of the shelf to detect the extent of edge effects. At the end of primary drying the product temperature approached the temperature of the shelves or even rose above this temperature. The end of primary drying was further detected by the approach of the pressure curves determined by Pirani and MKS sensors. The drying process of selected runs was additionally monitored using a mass spectrometer (PT50-MS, Oerlikon Leybold Vacuum, Cologne, Germany) that was connected to the freeze-drying chamber by a heated hose connection. Signals from water vapor, nitrogen and oxygen were detected additionally to the determination of the total pressure. The end of primary drying is characterized by a sharp drop in the water vapor signal versus time curve.

2.1.2 PREPARATION OF SOLUTIONS FOR FREEZE-DRYING

Formulations for freeze-drying were prepared by mixing the protein bulk solution with excipient stock solutions and buffer. The solutions were then filtered through 0.22 µm PVDF filters and immediately filled into vials as described above. An aliquot of each formulation was kept for analysis to determine the exact characteristics of the starting material.

2.1.3 THE COLLAPSE-CYCLE

Figure 3.1 depicts the drying protocol used to produce collapsed lyophilizates in a controlled way. It was developed following literature investigating the collapse behavior of formulations containing mannitol²². Samples were loaded onto the shelves at ambient temperature and were frozen to -50 °C at a cooling rate of 0.8 K/min. Primary as well as secondary drying was conducted at shelf temperatures of 45 °C and a chamber pressure of 2 mbar. The pressure was controlled using a Pirani sensor except for the drying of PA₀₁ lyophilizates where a MKS sensor was employed. Vials were placed directly on the shelf, no freeze-drying trays were used and the vials were surrounded by a stainless steel frame.

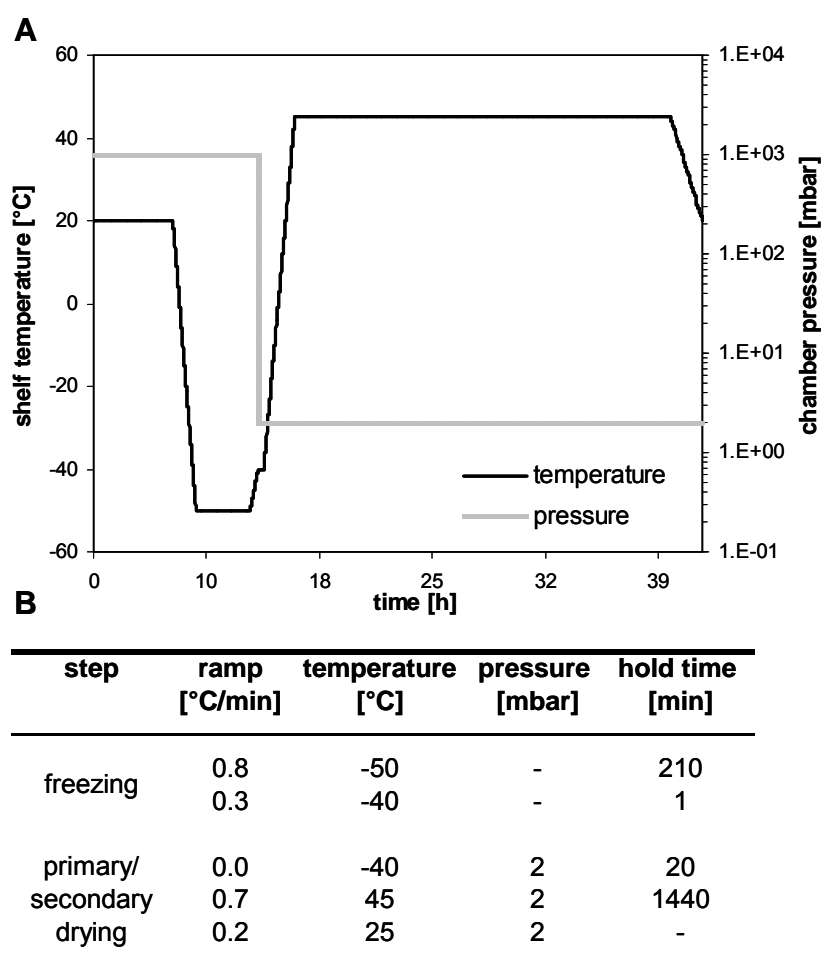


Figure 3.1: The “collapse-cycle”: Representative freeze-drying protocol used for the production of collapsed sucrose based IgG₀₁ lyophilizates. Time-dependent pressure-temperature profiles (A), table listing the parameters of the drying cycle (B).

All formulations were collapse-dried using the same protocol but with varying drying durations at 45 °C in order to achieve similar residual moisture levels. Figure 3.1 shows the drying protocol used to freeze-dry sucrose-based IgG₀₁ formulations, which is representative for all collapse-drying-cycles.

Table 3.3: Duration of drying at 45°C and additional variations of drying procedures used for the different investigated formulations in order to achieve the desired residual moisture level.

protocol	protein	formulation	drying time @ 45 °C	further secondary drying step
I	IgG01	sucrose	24 h	-
II		trehalose	24 h	20h/45°C/0.001 mbar
III	LDH	trehalose	44 h	} dry nitrogen injections
IV		sucrose + PEG	24 h	
V		trehalose + PEG	24 h	
VI	PA01	arginine	14 h	48h/50°C/0.0041 mbar dry nitrogen injections

Table 3.3 lists the different durations of drying at 45 °C and further variations in the secondary drying step used to dry the varying formulations under investigation, in order to achieve comparable residual moisture levels.

2.1.4 CONSERVATIVE FREEZE-DRYING CYCLES

FREEZE-DRYING OF IgG₀₁

SUCROSE-BASED AND MANNITOL-BASED FORMULATIONS

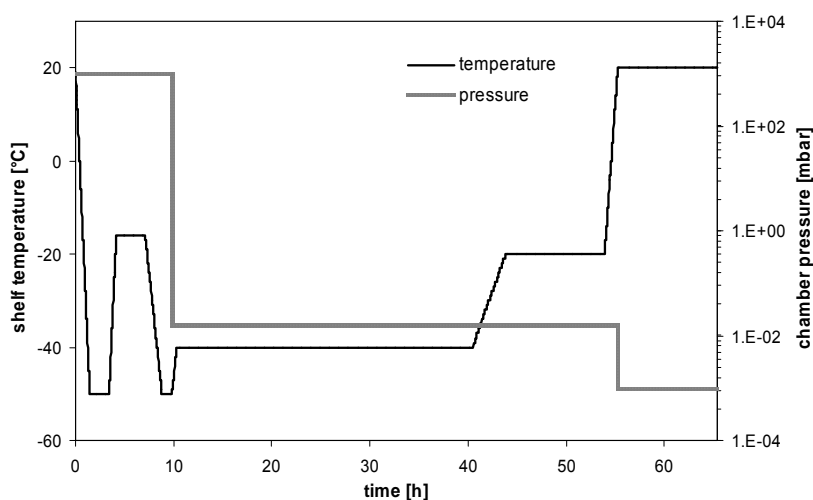


Figure 3.2: Freeze-drying protocol applied for the production of elegant sucrose based IgG₀₁ lyophilizates.

Figure 3.2 depicts the freeze-drying cycle used to produce pharmaceutically elegant lyophilizates. Samples were frozen at the same cooling rate (i.e. 0.8 K/min) that was applied during the “collapse-cycle”. To ensure complete mannitol crystallization, an annealing step at -16 °C was included. Primary Drying was performed at -40 °C and -20 °C, secondary drying was performed at 20°C. The pressure was maintained at 0.016 mbar throughout the primary drying process and lowered to 0.0001 mbar during secondary drying. The chamber pressure was controlled using a MKS sensor. Drying was performed on lyophilization trays with a thickness of 1.3 mm. The vials were surrounded by a stainless steel frame.

Conservatively-dried mannitol-sucrose based lyophilizates composed of different ratios of mannitol to sucrose were freeze-dried at 0 °C and 0.15 mbar during primary drying. During secondary drying, shelf temperatures were increased to 30 °C and the pressure was maintained constant. In order to increase the number of collapsed formulations with a conservative freeze-drying protocol (as discussed in Chapter 4), an additional freeze-drying run at 15 °C shelf temperature instead of 0 °C was performed. All other parameters were kept constant.

TREHALOSE-BASED FORMULATIONS

For freeze-drying of trehalose-based formulations the drying protocol was adapted to the different drying behavior of trehalose-based lyophilizates as compared to sucrose-based formulations. An additional secondary drying step at 35 °C and 0.001 mbar was appended after the 20 °C-step to sufficiently decrease the residual moisture level and drying at this temperature was performed for 10 hours.

In order to avoid mixing up effects of production variables and effects of collapse, critical process parameters were maintained constant. Therefore, the freezing step remained unchanged, i.e. the freezing rate and the annealing step, although an annealing step was not mandatory given the absence of mannitol.

PREPARATION OF DIFFERENT RESIDUAL MOISTURE LEVELS

Trehalose-based formulations with various residual moisture levels were produced using the single-shelf-seal function of the Christ Epsilon 2-12D freeze-dryer. Primary-drying was performed at -40 °C and 0.016 mbar according to the conservative drying-protocol used for preceding experiments. Secondary drying was done at -20, -17, -7 and 15 °C, respectively. Each temperature step was held for at least 20 hours to ensure a homogeneous residual moisture distribution of the vials throughout the shelf.

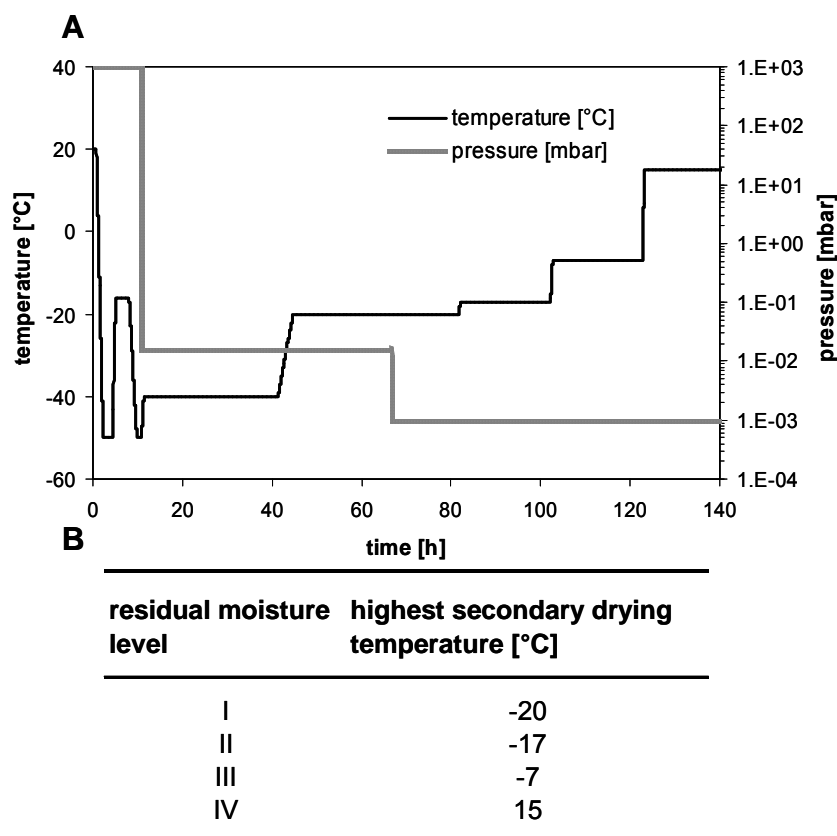


Figure 3.3: Freeze-drying cycle used to prepare lyophilizates with various levels of residual moistures. Time-dependent pressure-temperature profile (A), table listing the different secondary drying temperatures used for the preparation of different residual moisture levels (B).

Vials were freeze-dried on lyophilization trays with a thickness of 1.3 mm and were surrounded by a lyophilization frame. The 2 outermost rows of vials were dummy vials filled with placebo used to keep edge effects on the sample vials small.

Vials were stoppered under full vacuum, as the vials were closed after different secondary drying times during the freeze-drying cycle in order to produce lyophilizates with different residual moisture levels. Leak tests were performed prior to this experiment to ensure the tightness of the stoppers during storage under full vacuum.

FREEZE-DRYING OF LDH

Pharmaceutically elegant lyophilizates containing LDH as a model protein were produced using the protocol depicted in Figure 3.4. Samples were frozen to $-50\text{ }^{\circ}\text{C}$ with a cooling rate of 0.8 K/min and held for 3 hours. Primary drying was performed at a shelf temperature of $-40\text{ }^{\circ}\text{C}$ and $-20\text{ }^{\circ}\text{C}$ and a pressure of 0.04 mbar . Secondary drying was done at $10\text{ }^{\circ}\text{C}$ and 0.04 mbar . An additional secondary drying step at $15\text{ }^{\circ}\text{C}$ and 0.04 mbar was attached to adjust the residual moisture level of the formulations based on pure trehalose.

Vials were stoppered under full vacuum, because vials were closed after different drying times in order to adapt residual moisture levels of amorphous and partially crystalline formulations using the single-shelf-seal function of the Christ Epsilon 2-12D freeze-dryer.

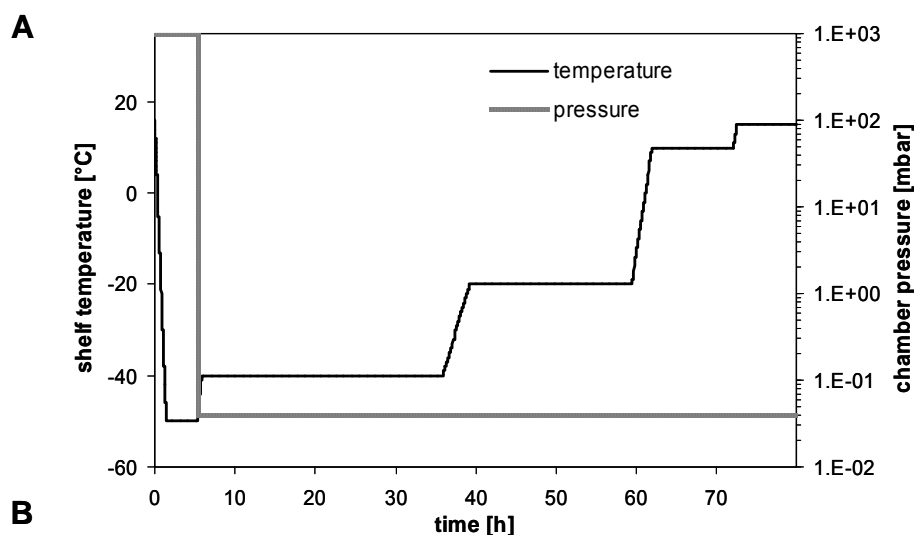


Figure 3.4: Freeze-drying cycle applied to prepare elegant LDH lyophilizates. Time-dependent pressure-temperature profiles (A), Table listing the process parameters (B).

Freeze-drying was done on lyophilization trays as described before. The first two rows of each shelf consisted of placebo lyophilizates serving as dummy vials reducing edge effects.

FREEZE-DRYING OF PA₀₁

Figure 3.5 depicts the freeze-drying protocol used for the generation of elegant PA₀₁ lyophilizates.

Vials were put on shelves precooled to 5 °C and frozen to -50 °C using two freezing rates. Primary drying was performed at a shelf temperature of -20 °C and secondary drying was performed at a shelf temperature of 5 °C. Chamber pressure was controlled by a MKS sensor at 0.09 mbar. Vials were freeze-dried directly on the shelves enclosed by a lyophilization frame.

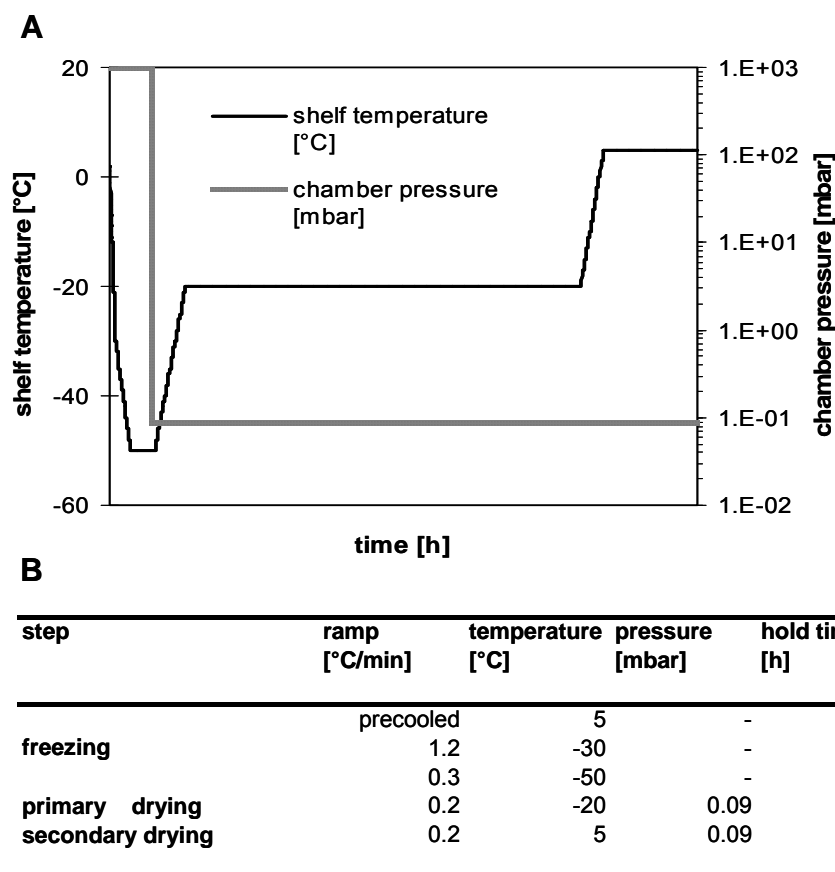


Figure 3.5: Freeze-drying cycle used to prepare elegant PA₀₁ lyophilizates. Time-dependent pressure-temperature profiles (A), table listing the process parameters (B).

2.2 SAMPLE PROCESSING AFTER FREEZE-DRYING

2.2.1 ANNEALING IN THE SOLID DRIED STATE

In order to investigate the impact of annealing effects that may be exerted by freeze-drying at high temperatures during the drying cycle, sucrose-based non-collapsed IgG₀₁ lyophilizates were subjected to a post-drying thermal treatment mimicking the collapse drying-protocol. Vials were placed in a Delta 9023 oven (Delta Design, temperature control ± 0.2 °C) and kept for 24 hours at 45 °C, i.e. the same period of time, the collapsed cakes were dried during primary and secondary drying of the collapse cycle. A beaker with silica gel was put into the oven to reduce the relative humidity.

2.2.2 STABILITY STUDIES

In order to compare the performance of collapsed and not collapsed lyophilizates during long term storage, samples were stored at elevated temperatures levels for up to 6 months. Samples were stored in the described 2R class I glass vials sealed with the specified B2-coated rubber-lyophilization stoppers. PA₀₁-containing lyophilizates were additionally sealed in aluminum bags.

IgG₀₁ lyophilizates were stored at 40 °C and 50 °C, reference samples were stored in the refrigerator (2-8 °C). Samples were analyzed immediately after freeze-drying and after 2, 4, 6, 9, 12 and 15 weeks of storage.

LDH lyophilizates were stored at 25 °C and 40 °C, reference samples were stored at 2-8 °C. Samples were analyzed after freeze-drying and after 2, 4, 6, 9, 15 and 25 weeks.

PA₀₁ lyophilizates were stored at 50 °C and reference samples were stored at 2-8 °C. Samples were analyzed after freeze-drying and after 4, 9 and 15 weeks of storage.

2.2.3 LIQUID STORAGE STABILITY

Reconstituted lyophilizates composed of IgG₀₁ and varying amounts of mannitol and sucrose were stored at 37 °C and were slightly shaken (40 rpm) for up to 8 days. Samples were stored in Eppendorf reaction tubes.

2.3 CHARACTERIZATION OF PROTEIN STABILITY

2.3.1 HIGH PRESSURE SIZE-EXCLUSION CHROMATOGRAPHY (HP-SEC)

Protein aggregation was determined by HP-SEC. Analytics were performed on a Spectra-Physics System equipped with a TSKgel G3000SWxl column (Tosoh Biosep, Stuttgart, Germany). The injection volume was 50 µl.

Samples were centrifuged or filtrated prior to injection in order to remove insoluble aggregates. Sample recovery was determined using an external standard calibration curve to check for insoluble aggregates. Standard calibration curves were run at least at the beginning and at the end of each sequence run composed of 5 known concentrations of the analyzed protein. Two lyophilizates were analyzed for each time point and each temperature and each sample was injected twice.

The proteins were detected spectrophotometrically ($\lambda = 280$ nm, UV1000, Thermo Electron Corporation, Dreieich, Germany).

The chromatograms were integrated manually using the ChromQuest software (Thermo Electron Corporation, Dreieich, Germany). Aggregation in % was determined by comparing the area under the curve (AUC) of dimers, trimers and higher molecular weight aggregates with the total AUC. Recovery of monomer and amount of fragments were considered as well.

IgG₀₁

The running buffer for HP-SEC analysis of IgG₀₁ was composed of 50 mM NaH₂PO₄ and 600 mM NaCl (adjusted to pH 7.0 with sodium hydroxide). The analytics were performed at a flow rate of 1 mL/min.

Samples were diluted to a concentration of 1.0 mg/mL with running buffer. Standard calibration curves were collected in a concentration range of 0.5 – 1.5 mg/mL.

LDH

The running buffer for LDH analysis was composed of 10 mM NaH₂PO₄ and 150 mM NaCl (adjusted to a pH of 6.9 with potassium hydroxide) and the flow rate was 0.8 mL/min. The samples were diluted to a concentration of 0.25 mg/mL with running buffer and standard curves were recorded in a concentration range of 0.125 – 1.0 mg/mL.

PA₀₁

Aggregation status of PA₀₁ was monitored using a running buffer composed of 230 mM NaH₂PO₄ and 1 % (m/m) SDS (adjusted to a pH of 6.8 with sodium hydroxide). Samples were injected without further dilution. Standard calibration curves were collected in a concentration range from 0.25 – 1.5 mg/mL.

2.3.2 ONE-CHAIN/TWO-CHAIN MATERIAL PA₀₁

For PA₀₁, the amino acid bond between amino acid 275 and 276 is susceptible to cleavage. By the intactness of that bond 1-chain material and 2-chain material can be distinguished. After cleavage, the two fragments are connected only by disulfide-bonds. After reduction with dithiothreitol (DTT), the two fragments can be separated using HP-SEC.

The Spectra-Physics System equipped with a TSKgel G3000SWxl column (Tosoh Biosep, Stuttgart, Germany) was used for analysis. The running buffer was composed of 230 mM NaH₂PO₄ and 1 % (m/m) SDS (adjusted to a pH of 6.8 with sodium hydroxide). Analytics were performed at a flow rate of 0.5 mL/min and the protein was detected spectrophotometrically at 210 nm.

Prior to injection the samples were diluted with 0.02 M DTT and heated to 85 °C for 8 minutes. Two lyophilizates were analyzed for each time point and each temperature and each sample was injected twice.

Integration was performed using the ChromQuest software (Thermo Electron Corporation, Dreieich, Germany). One-chain material, two-chain material as well as remaining peaks (the peaks eluting before the one-chain material) were considered and the relative area in percent was calculated.

2.3.3 ASYMMETRIC FLOW FIELD FLOW FRACTIONATION (AF4)

Protein aggregation was further monitored using asymmetrical flow field-flow fractionation (AF4). AF4 is a one-phase chromatography technique separating sample fractions in a channel by applying a parabolic laminar Newtonian flow profile (the carrier flow) and a cross flow perpendicular to the carrier flow. In this study AF4 is used as a complementary analytical method to HP-SEC to characterize insoluble aggregates.

Figure 3.6 illustrates the principle of AF4:

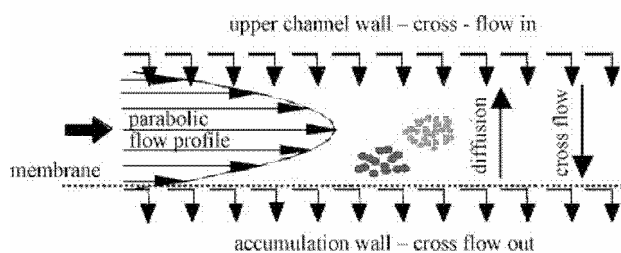


Figure 3.6: Separation principle of AF4.²³

Molecules eluting in the parabolic flow are forced downwards into slower-flowing regions of the flow profile by the cross flow. Due to the established concentration gradient a diffusion movement in the reverse direction is induced and an equilibrium position in the flow profile is reached depending on the size of the sample. Small molecules that have higher diffusion coefficients and are less strongly affected by the cross flow therefore elute more rapidly than large molecules that have their equilibrium position in more parietal regions of the flow profile^{24,25}.

Analysis was performed using a Wyatt Eclipse2 system (Wyatt Technology Europe GmbH, Dernbach, Germany) connected to an Agilent 1100 HPLC system (isocratic pump, autosampler, degasser, UV- and RI-detector, Agilent Technologies, Böblingen, Germany). Sample fractions were detected using a Wyatt DAWN EOS MALS detector, an Agilent UV-detector ($\lambda = 280$ nm) and an Agilent RI-detector.

IgG₀₁

For the separation of IgG₀₁ a 25 cm long channel equipped with a 350 μm -spacer of medium width and a regenerated cellulose membrane with a 10 kDa cutoff was used. The running buffer was the same as the one used for the HP-SEC experiments.

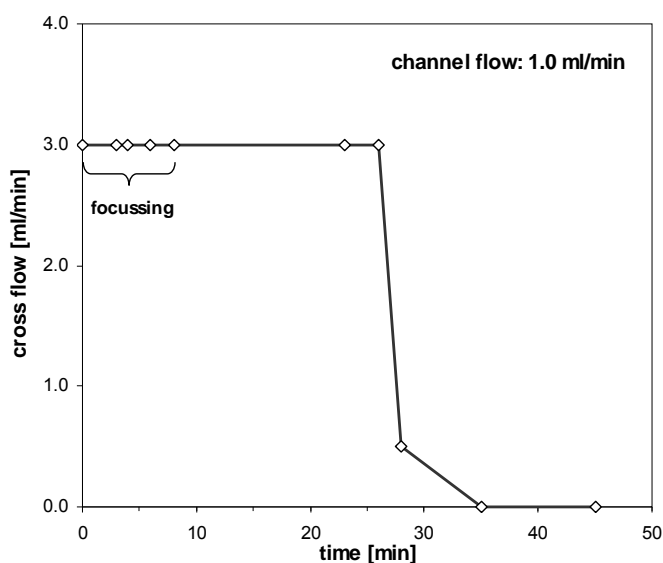


Figure 3.7: AF4 cross flow profile applied for the separation of IgG₀₁ sample fractions.

Samples preparation was identical to the HP-SEC samples as well except for the centrifugation/filtration step. For every time point and temperature 2 vials were analyzed. Selected samples were injected both before and after filtration to assess the extent of insoluble aggregates.

Figure 3.7 depicts the cross flow profile applied for the separation of IgG₀₁ fractions: The channel flow was set to 1 mL/min and the injection flow was set to 0.2 mL/min. 10 µg IgG₀₁ were injected. The total focusing time was 4 minutes at a focus flow of 3 mL/min. For the separation an initial cross-flow of 3 mL/min was applied for 15 minutes and it was then lowered to 0.5 mL/min within 3 minutes and subsequently to 0.0 mL/min within 2 more minutes. Detection was continued for ten more minutes.

LDH

For the separation of LDH a 25 cm long channel equipped with a 350 µm-spacer of medium width and a regenerated cellulose membrane with a 5 kDa cutoff was used. The running buffer was the same as the one used for HP-SEC experiments. Samples preparation was identical to the HP-SEC samples except for the centrifugation/filtration step, which was not performed during AF4 sample preparation. For every time point and temperature 2 vials were analyzed.

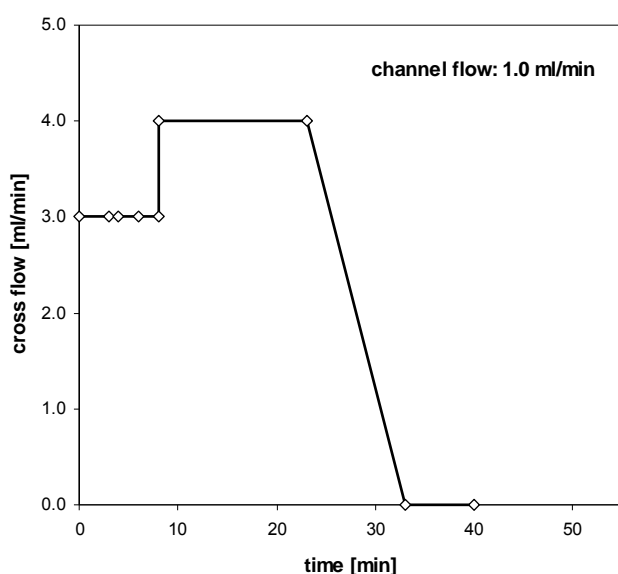


Figure 3.8: AF4 cross flow profile applied for the separation of LDH sample fractions.

Figure 3.8 depicts the method used for LDH fractionation: The channel flow was set to 1.0 mL/min and the focus flow to 0.2 mL/min. 10 µg LDH were injected and focused for 4 minutes with a focus flow of 3 mL/min. Then a cross flow of 4 mL/min was applied for 15 minutes and then lowered to 0.0 mL/min within 10 minutes. Detection was continued for ten more minutes.

2.3.4 DYNAMIC LIGHT SCATTERING (DLS)

Dynamic Light Scattering (DLS) was used to measure the size and size distribution of protein molecules and particles in the sub micron region (1 nm – 1 µm). Measurements were performed on a Malvern Zetasizer Nano ZS (Malvern, Herrenberg, Germany). The Zetasizer Nano is operating with a 4 mW He-Ne-Laser at 633 nm and non-invasive backscattering technique (NIBS) at a constant temperature of 25°C. Standard values for the viscosity and refractive indices of aqueous protein solutions were used ($\eta=0.8872$, $RI_{(\text{dispersant})}=1.33$, $RI_{(\text{protein})}=1.45$). The measurements were performed in the manual mode with 20 sub runs of 20 seconds each. The laser beam was directed in the centre of the cuvette. Each sample was analyzed twice. The size distribution of the hydrodynamic radius by intensity and by volume were calculated from the correlation function using the multiple narrow modes of the Dispersion Technology Software (DTS) from Malvern (version 5.00) based on a non-negative least square (NNLS) algorithm. The polydispersity index (PDI) and the mean size (Z-average diameter) were calculated from the correlation function by performing the cumulants analysis.

2.3.5 LIGHT OBSCURATION

The concentration and distribution of particles in the range of 1 - 200 µm was analyzed by light obscuration using a SVSS-C40 apparatus (PAMAS GmbH, Rutesheim, Germany). The system was flushed with particle free water until there were less than 100 particles > 1 µm/mL. The system was calibrated annually. To check the performance of the system, size standards were measured at regular intervals. At the beginning and at the end of each measurement sequence test measurements with particle free water were performed.

The average value of each measurement was calculated and the amount of mean counted particles $\geq 1 \mu\text{m}$ / $\geq 4.1 \mu\text{m}$ / $\geq 10 \mu\text{m}$ / $\geq 25 \mu\text{m}$ was correlated to a sample volume of 1 mL. After each measurement the system was flushed with 5 mL of particle free water to exclude cross contamination. After this cleaning procedure less than 100 particles larger or equal then 1 µm/mL were detected.

IGG₀₁: SUCROSE-STABILITY/ TREHALOSE-STABILITY/MANNITOL-FORMULATIONS

About 2 mL of liquid formulation or 2 pooled vials of reconstituted lyophilizate were analyzed. The system was flushed with 0.4 mL of sample liquid and subsequently 3 aliquots of 0.4 mL of each sample were analyzed.

IGG₀₁: RESIDUAL MOISTURE STABILITY

3 vials were pooled into two cuvettes and mixed carefully by inversion. The system was flushed with 0.4 mL of sample and then 3 measurements analyzing 0.3 mL each were performed.

LDH

3 vials were pooled into two cuvettes and mixed carefully by inversion. The system was flushed with 0.4 mL of sample and then 3 measurements analyzing 0.3 mL each were performed.

PA₀₁

3 vials were pooled into a 10 mL cryo tube and mixed carefully by inversion. The system was flushed with 3 mL of sample volume and then 5 measurements of 0.5 mL aliquots were analyzed.

2.3.6 TURBIDITY

The turbidity of the samples in formazine nephelometric units (FNU) was measured by 90° light scattering at $\lambda = 860$ nm with a NEPHLA turbidimeter (Dr. Lange, Düsseldorf, Germany) as described in the European Pharmacopoeia (method 2.2.1)²⁶.

About 2 mL of the pre-lyophilization solutions or 2 pooled vials of reconstituted lyophilizate, respectively were analyzed.

2.3.7 SODIUM DODECYL SULPHATE POLYACRYLAMIDE GEL ELECTROPHORESIS (SDS-PAGE)

Non-reducing denaturing SDS-PAGE was used as an additional method to monitor the aggregation and fragmentation of the protein formulations. Analysis was performed using an XCell II Mini cell system (Novex, San Diego, CA, USA). Reconstituted lyophilizates were diluted to a final concentration of 0.05 mg/ml in a pH 6.8 Tris-buffer containing 2 % SDS and 2 % glycerine. The samples were denatured at 95 °C for 20 minutes and then 20 μ l of the solutions were loaded to the gel wells.

Gels were stained with the SilverXPress® Silver Staining Kit (Invitrogen, Karlsruhe, Germany). To check the performance of the system a standard was analyzed on each gel. To determine the molecular weight of the detected bands a molecular weight standard was analyzed on each gel as well (Mark 12 Unstained Standard, Invitrogen, Karlsruhe, Germany).

IgG₀₁

Electrophoresis of IgG₀₁ samples was performed using NuPAGE® Pre-Cast 7 % Tris-Acetate gels 1mm, 10 wells and NuPAGE® Tris-Acetate running buffer. Separation was accomplished with a constant voltage of 150 V and running time was approximately 45 min.

LDH

Electrophoresis of LDH samples was performed using NuPAGE® Pre-Cast 10 % Bis-Tris gels 1mm, 10 wells and NuPAGE® MES running buffer. Separation was done at a constant voltage of 200 mV and running time was approximately 35 min.

PA₀₁

Electrophoresis of PA₀₁ samples was performed using the same system as for the separation of LDH samples. Additionally, reduced SDS-PAGE was performed by adding dithiothreitol (DTT) to the sample buffer and incubating the samples at 95 °C as described above.

2.3.8 TRANSMISSION FOURIER TRANSFORM INFRARED (FTIR) SPECTROSCOPY

FTIR spectroscopy was used to monitor the conformational stability of the proteins both prior to lyophilization and after reconstitution. Analysis was done using a Tensor 27 FTIR spectrometer (Bruker Optics, Ettlingen, Germany) equipped with a calcium fluoride flow through cell (Aquaspec 1110 M, Bruker Optics, Ettlingen, Germany) with a path length of 6.5 µm and a nitrogen-cooled photovoltaic MCT (mercury-cadmium-telluride) detector. The temperature was kept constant at 20 °C. For each spectrum 240-scan interferograms from 4000 to 850 cm⁻¹ were collected at a single-beam mode with a resolution of 4 cm⁻¹. The collected interferograms were Fourier transformed and the spectrum of the corresponding placebo solution was subtracted using the scaled subtraction function of the Opus software (version 5.5 and version 6.5, Bruker Optics, Ettlingen, Germany). Using the Opus software, the amide I region of the spectra (1720 – 1580 cm⁻¹) was further vector normalized (i.e. area normalized) and the second derivative was calculated (with 17 smoothing points according to the Savitzky-Golay algorithm).

Each sample was injected at least twice and the mean spectrum was calculated and visually compared to standard spectra and spectra of the liquid formulation before lyophilization. Additionally, the so-called β-ratio was calculated for selected formulations of the IgG₀₁ as described by Abdul-Fattah et al.²⁷.

2.3.9 INTRINSIC PROTEIN FLUORESCENCE SPECTROSCOPY

Intrinsic protein fluorescence was determined to monitor the proteins' tertiary structure using a Varian Cary Eclipse fluorescence spectrometer (Varian, Inc., Darmstadt, Germany) at a constant temperature of 20 °C. Samples were equilibrated for at least 15 minutes in order to ensure adequate tempering. Protein solutions were diluted to a final concentration of 0.05 mg/mL with formulation buffer in order to prevent internal quenching effects. Sample solutions and buffers were filtered through a 0.2 µm filter prior to analysis to prevent the interference of particles. Solutions were measured either in 3.0 mL cuvettes or in black 96-well plates with a fill volume of 300 µl. Analysis in cuvettes was done in duplicates and analysis in 96-well plates was done in triplicates.

Spectra were recorded and further processed using the Scan application of the Cary Eclipse Software (version 1.0, Varian, Inc., Darmstadt, Germany).

The excitation wavelength was set to 280 nm with an excitation slit of 10 nm. The emission was recorded from 260 to 450 nm and from 300 to 450 nm for different studies, respectively

at an emission slit of 10 nm. After recording all samples were further processed by calculating the mean spectrum and smoothing the spectra with 17 smoothing points according to the Savitzky-Golay algorithm.

IGG₀₁

For experiments in cuvettes the scanning rate was set to 600 nm/min with an averaging time of 0.1 s and a data interval of 1 nm. The PMT voltage of the detector was set to 500 V. For measurements performed in 96-well plates, the scan rate was 30 nm/min using an averaging time of 1 s and a data interval of 0.5 nm. For these experiments the PMT voltage of the detector was set to 600 V.

LDH

LDH samples were analyzed in cuvettes at a scan rate of 120 nm/min with an averaging time of 0.5 s and a data interval of 1 nm.

2.3.10 HIGH RESOLUTION UV 2ND DERIVATIVE ABSORBANCE SPECTROSCOPY (2DUV)

High resolution UV 2nd derivative absorbance spectroscopy (2DUV) was used to analyze the tertiary structure of PA₀₁. Measurements were performed using an Agilent 8453 UV-visible Spectrophotometer (Agilent Technologies, Waldbronn, Germany). Samples were diluted to a final concentration of 0.1 mg/mL with placebo solution and spectra were recorded from 190 to 1100 nm using a data interval of 1 nm and an integration time of 0.5 s at a constant temperature of 20 °C.

Spectral analysis was conducted using Chemstation™ software (Agilent) according to the procedure described by Kueltzo et al.^{28,29}. Second derivative spectra were calculated using a nine-point data filter and a fifth degree Savitzky-Golay polynomial. Afterwards, spectra were fitted to a cubic function with 99 interpolated points per raw data point. This procedure allows a resolution of 0.01 nm²⁸. Peak positions were determined from these curves using Origin 7.0 software (OriginLab, Northampton, MA, USA).

2.3.11 COLOR OF RECONSTITUTED SOLUTION

The color of the PA₀₁ solutions after reconstitution of the lyophilizate was determined according to the method 2.2.2 described in the European Pharmacopoeia by comparing the sample solutions with standard solutions³⁰. A stock solution was prepared by mixing acidic solutions (0.9 % HCl) of FeCl₃ (45 mg/mL) and CoCl₂ (59.6 mg/mL) at a ratio of 4:1. The reference solutions were prepared by further diluting the stock solution with hydrochloric acid 1 % according to Table 3.4. The color of the sample solutions was determined by direct visual comparison in front of a white background (minimum volume of 2 mL in a disposable cuvette).

Table 3.4: Composition of the yellow reference solutions according to method 2.2.2 Ph.Eur. ³⁰

reference solution	diluted stock solution [ml]	HCl 1% [ml]	degree of yellow
G5	1.25	8.75	yellowish (\leq G5)
G6	0.5	9.5	slightly yellowish ($<$ G6)
G7	0.25	9.75	colorless ($<$ G7)

2.3.12 ACTIVITY ASSAYS

IgG₀₁

The biologic activity of the IgG₀₁ was assessed by determination of the specific binding of the IgG₀₁ to its target using surface plasmon resonance. The target receptor was coupled to the carboxylated dextran matrix of a Biacore CM5 sensor chip (Biacore AB, Uppsala, Sweden) via amine coupling prior to the measurement. The specific binding of the IgG₀₁ to the coupled target structure was monitored using a Biacore Q system (Biacore, Freiburg, Germany). by the change in angle intensity of reflected plasmon waves due to changes of the refractive index of the chip surface caused by the binding reaction.

The IgG₀₁ was diluted to at least 5 different concentrations ranging from 1 μ g/mL to 7.8 ng/mL with 10mM HBS (Hepes Buffered Saline), pH 7,4 and was flushed over the surface of the chip with a defined flow rate of 10 μ l/min for 3.5 minutes. The amount of binding antibody was quantified.

LDH

The enzymatic activity of LDH was determined by monitoring the decrease of absorption at 340 nm using the enzyme assay provided by Sigma-Aldrich (Sigma-Aldrich, Steinheim, Germany). A mixture of sodium pyruvate (69 mM) and β -NADH (0.13 mM) was equilibrated at 37 °C for at least 30 minutes in a waterbath (Memmert, Schwabach, Germany). Samples were diluted to a final LDH concentration of 0.5 μ g/mL (according to \sim 0.25-0.75 units/mL) with a 1 % BSA solution, in order to prevent protein loss due to adsorption on reaction vessels. LDH was added to the sodium pyruvate and β -NADH mixture and the absorption was recorded over a period of 4 minutes using an Agilent 8453 UV-visible Spectrophotometer (Agilent Technologies, Waldbronn, Germany). A linear slope was calculated by regression and the activity was calculated using equation (3.1).

$$a[\text{units} / \text{ml}_{\text{enzyme}}] = \frac{(\Delta A_{340\text{nm}} / \text{min}_{\text{sample}} - \Delta A_{340\text{nm}} / \text{min}_{\text{blank}}) * 3 * f}{(6.22) * (0.1)} \quad (3.1)$$

3 (mL) is the total volume of the assay, f is the dilution factor, 6.22 is the millimolar extinction coefficient of β -NADH at 340 nm and 0.1 (mL) is the volume of the enzyme solution added to the assay.

The activity in units per mg protein was calculated according to equation (3.2):

$$a \left[\text{units} / \text{mg}_{\text{protein}} \right] = \frac{a \left[\text{units} / \text{ml}_{\text{enzyme}} \right]}{\text{mg}_{\text{protein}} / \text{ml}_{\text{enzyme}}} \quad (3.2)$$

To correct for day to day fluctuations the activity in units/ mg enzyme was divided by the activity of a standard solution. The standard solution was prepared by diluting the LDH suspension as purchased from Sigma-Aldrich with the BSA-1%-solution to a final concentration of ~ 0.6 µg/mL (according to ~ 0.25-0.75 units/mL).

The activity of reconstituted lyophilizates was further related to the activity prior to lyophilization and the recovery of activity in % was calculated.

CLOT LYSIS (PA₀₁)

The activity of PA₀₁ was determined with the clot lysis assay as described by Carlson et al.³¹. Fibrinogen, plasminogen, thrombin and PA₀₁ were mixed in a micro centrifuge, in-situ generating a fibrin clot and activating plasminogen by PA₀₁ at the same time. The lysis of the clot is monitored photometrically measuring the optical density at 340 nm. The time taken for the lysis is then considered to calculate the activity.

2.4 CHARACTERIZATION OF LYOPHILIZATE CHARACTERISTICS

2.4.1 DIFFERENTIAL SCANNING CALORIMETRY (DSC)

Differential Scanning Calorimetry (DSC) was used to assess the physicochemical characteristics of the lyophilized cakes. The glass transition temperature of the maximally freeze-concentrated solution and the lyophilizates was determined using a Netzsch Differential Scanning Calorimeter 204 Phoenix (Netzsch, Selb, Germany). The melting temperature of the formulated sugar components and the degree of crystallinity of excipients was considered as well. The instrument was calibrated annually using indium heated from 0 – 150 °C with a heating rate of 10 K/min.

For the determination of T_g' approximately 20 µl were weighed into aluminum crucibles. The samples were cooled to -90 °C and subsequently heated up to 10 °C at a heating rate of 10 K/min. The mid point of the glass transition (point of inflection) was determined.

For determination of T_g the lyophilizates were ground in an agate mortar in a glove box flushed with dry nitrogen. 5 -10 mg of the powder were weighed into an aluminum crucible and cold-sealed in the dry atmosphere. The reference pan was empty and was sealed in the same way. Samples were cooled down to -20 °C and subsequently heated up to 90 °C to 100 °C (depending on the excipient) at a rate of 10 °C/min. After cooling down again, a second heating scan was performed up to 200 °C -230 °C, depending on the formulation.

The thermal events were analyzed in the heating scans. Glass transitions (point of inflection), melting endotherms, crystallization exotherms and relaxation events were considered.

2.4.2 FREEZE-DRY MICROSCOPY (FDM)

Freeze-dry microscopy was performed using an Olympus BX50 microscope (Olympus Deutschland GmbH, Hamburg, Germany) equipped with a Linkham THM600S freeze-drying stage (Linkham Scientific Instruments, Surrey, UK) with a liquid nitrogen cooling system (Linkham LNP 93/2), a programmable temperature controller (Linkham TMS 93) and a vacuum pump (Edwards 1.5 Two Stage; Edwards Hochvakuum GmbH, Marburg, Germany). Pictures were taken with a DG-03 digital camera and analyzed with the analysis 3.0 software. Pressure was monitored with a Pirani sensor and temperature was determined via a thermocouple in the silver block oven used to temperate the sample. This thermocouple was calibrated prior to the measurements using liquids with well-defined melting points (water, n-dodecane, n-decane, n-octane).

5 μl of liquid sample were placed in a quartz crucible and covered with a glass cover slide (diameter 14.3 mm). The set-up was placed on the silver block oven. Between the silver block and the crucible about 5 μl of silicone oil were added to optimize thermal contact.

The collapse temperature was determined using the following procedure: Samples were cooled to $-50\text{ }^{\circ}\text{C}$ with 10 and 20 K/min and held 10 minutes to ensure complete thermal equilibration. Vacuum was applied and sublimation was observed. Then samples were heated to a temperature about 2-5 K lower than the expected collapse temperature with a heating rate of 5 K/min and held for approximately 3 minutes, allowing sublimation to occur. Temperature was increased stepwise in one degree increments with three minutes hold times in between to observe sublimation. Upon the observation of collapse, the sample was cooled down again and the procedure was repeated to confirm observations.

2.4.3 X-RAY POWDER DIFFRACTION (XRD)

The morphology of the lyophilized cakes was analyzed using X-ray powder diffraction (XRD). Analysis was carried out on a Seifert X-ray diffractometer XRD 3000 TT (Seifert, Ahrensburg, Germany) equipped with a copper anode (40 kV, 30 mA, $\lambda = 154.17\text{ pm}$). Experiments were conducted from $5\text{-}40\text{ }^{\circ}2\text{-}\theta$ at a resolution of $0.02\text{ }^{\circ}2\text{-}\theta$ and a duration of 2 s per step.

The crystallinity of lyophilizates containing sucrose and mannitol in varying ratios was analyzed using a STOE STADI P X-ray diffractometer equipped with a position sensitive detector and a $\text{CuK}\alpha$ anode (40 kV, 40 mA, $\lambda = 154.17\text{ pm}$) (STOE & Cie, Darmstadt, Germany) using the same experimental set-up.

2.4.4 KARL FISCHER RESIDUAL MOISTURE DETERMINATION

KARL FISCHER HEADSPACE-SETUP

The residual moisture of the samples was determined with a coulometric Karl Fischer titration using the Aqua 40.00 titrator (Analytik Jena AG, Halle, Germany) equipped with a headspace oven. For the measurement the whole lyophilized cake in a 2R vial was heated to $80\text{ }^{\circ}\text{C}$ in an

oven connected to the reaction vessel via a tubing system flushed with dry nitrogen. The evaporated water was transferred with the dry nitrogen flow into the titration solution and the amount of water was determined. The measurement was performed for at least 5 minutes until no more water evaporation is detectable as indicated by a drop of the drift below the start value ($7 \mu\text{g}/\text{min} + 2 \mu\text{g}/\text{min}$).

At the start and at the end of each measurement sequence a solid water standard (Apura[®] water standard oven 1.0, Merck, Darmstadt, Germany) was analyzed. A blank value was determined from at least 3 empty vials analyzed with the same routine.

To determine the optimum temperature to evaporate all water from the cake, selected samples were heated up stepwise in the range from 80 °C to 140 °C and the amount of detected water was considered.

To evaluate the effect of cake structure on the accuracy of the residual moisture determination, samples were analyzed without sample preparation (i.e. analyzing the intact cake), after grinding to a powder in a dry nitrogen atmosphere (10-30 mg) and after dissolving in 0.5 mL dry formamide (Hydranal[®] - Formamide dry, Fluka, Sigma-Aldrich, Steinheim, Germany), respectively. All sample handling was done in a dry nitrogen atmosphere. For this specific experiment an oven temperature of 100 °C was used.

KARL FISCHER DIRECT METHANOL EXTRACTION-SETUP

Residual moisture content was determined using a Karl Fisher coulometric titrator (652-KF Coulometer and a 737 KF Coulometer, Metrohm, Filderstadt, Germany). 3 mL of dry methanol (Hydranal[®] -Methanol dry, Fluka, Sigma-Aldrich, Steinheim, Germany) were added to the sealed lyophilizate by injection. Samples were dispersed in the dry methanol and water was extracted for 20 minutes prior to injecting a 1 mL aliquot of the methanol into the reaction vessel. The measurement was performed until the drift dropped below the start value.

At least 6 blank measurements were performed at the beginning of each measurement series. At the start and at the end a water standard was analyzed to check the system performance (Hydranal[®] water standard 1.00, Riedel-de-Haën, Sigma-Aldrich, Steinheim, Germany). Each sample was measured at least in triplicate.

2.4.5 NEAR INFRARED SPECTROSCOPY (NIRS)

NIRS was used to determine the residual moisture content in lyophilizates during the study of the effect of residual moisture on the IgG₀₁ stability. NIRS bears several advantages over Karl Fischer moisture determination, the most important is its non-destructive character. Because of this, the same samples that were analyzed with NIRS for moisture can be assessed with another stability-indicating analytical method allowing direct correlation of

residual moisture level and stability. Furthermore, NIRS is fast, no sample preparation is required and no hazardous chemicals are used.

NIRS has long been used for the identification and residual moisture determination of dry bulk goods³² and for the process control of granulation processes³³. The use of NIRS for the residual moisture determination of lyophilized products has been investigated by several researchers. They have shown a good correlation between the residual moisture values determined by NIRS measuring through the vial bottom and the residual moisture values determined by Karl Fischer titration³⁴⁻³⁸.

There are three absorption bands caused by water that can be utilized in the determination of residual moisture by NIRS: The combination band of OH stretching and HOH bending at 1900-1950 nm, the first overtone of the OH stretch at 1400-1450 nm and the second overtone of the OH stretch at 960-980 nm^{35,39,40}.

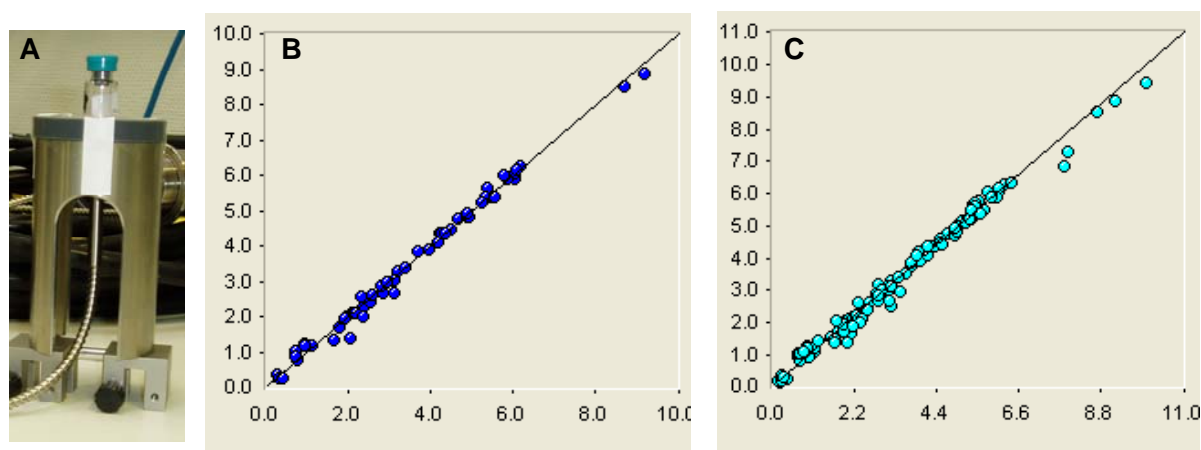


Figure 3.9: Experimental set-up for NIRS measurements (A), calibration: plot of the calculated residual moisture (RM) contents (x-axis) versus RM contents as determined by Karl Fischer (y-axis) used to set-up the equation (B), validation: plot of calculated RM contents (x-axis) versus RM contents determined by Karl Fischer (y-axis) used to validate the proposed equation (C).

Analytics were performed with a Foss NIR 6500 Online spectrometer (Foss, Rellingen, Germany) in reflection mode. Highly diffuse reflecting PTFE (Spectralon[®]) was used as external reference; the external reference was recorded every day. Samples were analyzed in the sample holder depicted in Figure 3.9 A: Spectra were recorded through the base of the vial using a NIR reflection probe that was connected by optical fibers to the spectrometer. The probe was adjusted to the centre of the vial. Spectra recording and all further data processing were done using the Vision software (Version 3.1.0.0, Foss, Rellingen, Germany).

Spectra were recorded from 850-2100 nm and each spectrum was the average of 32 scans. The intensity around the water band at 1950 nm (1700 – 2088 nm) was used for calibration. The spectra were treated by multiple scatter correction (MSC) to remove absorbance offsets. Then a standard normal variate was applied to correct for differences in porosity of the samples.

For calibration standard sample sets of more than 100 vials with residual moisture levels ranging from 0.2 % to 9 % were analyzed. The standard samples were then analyzed by Karl Fischer analysis using the Metrohm 652-KF Coulometer (Metrohm, Filderstadt, Germany) as described above. Subsequently the Karl Fischer results were assigned to their corresponding NIR spectra through the chemometric part of the Vision software. A partial least square regression with 3 factors was accomplished (representative calibration plot shown in Figure 3.9 B). A cross validation was carried out to evaluate the model performance as follows (representative validation plot shown in Figure 3.9 C): One standard was removed from the calibration set at a time and the model was then recalibrated and the residual moisture in the excluded standard was predicted. This process was repeated until all standards had been excluded once. The accuracy and precision of the calibration model were expressed by the r^2 of cross validation and the root mean square error of cross validation (RMSECV), respectively. Values of $r^2 = 0.9924$ and RMSECV = 0.1865 were achieved. In addition to cross validation an external validation was carried out. The root mean square error of prediction (RMSEP) was used to judge the future predictability of the calibration. A value of RMSEP = 0.223 was achieved.

2.4.6 SCANNING ELECTRON MICROSCOPY (SEM)

SEM pictures were recorded to examine the morphology of the freeze-dried cakes. Analytics were carried out using a scanning electron microscope SUPRA 55 VP (Zeiss SMT, Oberkochen, Germany) or a Joel JSM-6500F (Joel, Ebersberg, Germany).

Samples were fixed with a double-sided adhesive carbon tape (Bal-tec GmbH, Witten, Germany) and sputtered with carbon under vacuum (MED 020, Bal-tec GmbH, Witten, Germany).

2.4.7 DIGITAL MICROSCOPY

Lyophilizate morphology was further evaluated using digital microscopy. Analysis was performed using the Keyence VHX-600 (Keyence GmbH, Neu-Isenburg, Germany). Lyophilizates were extracted from the vials preserving the intact cake structure and the surface of the cake (top, wall and bottom section) as well as the cake's cross section were examined.

2.4.8 MACROSCOPIC CLASSIFICATION OF THE EXTENT OF COLLAPSE

The extent of collapse was classified by macroscopic and microscopic examination using a stereo-microscope. First, the lyophilizate in the vial was inspected, and then the cake was carefully removed from the vial by breaking the bottleneck.

The top, wall and bottom of the cake were examined for deformations and shiny patches. Then a cross section was made using a scalpel cutting the edge and breaking the lyophilizate in half. This procedure ensured the preservation of the porous structure. In the

cross section porosity and the existence of cavities were considered. Furthermore, the mechanical stability of the cakes was assessed.

The appearance of the cake is classified on a scale from 1 to 10. 1 means that the cake is either mechanically unstable (the cake loses its structure when the vial is turned upside down or when the cake is sliced into half) or mostly collapsed (the cake show a high degree of cavities in the cross section). 10 means that the cake is mechanically stable and shows a homogeneous porous structure in the cross section.

2.4.9 SPECIFIC SURFACE AREA (SSA) MEASUREMENT

BET (Brunauer Emmett Teller) specific surface area (SSA) analysis was performed using an Autosorb-1 analyzer (Quantachrome, Odelzhausen, Germany) purged with Krypton 4.8. Samples were degassed under vacuum at 25 °C over night prior to the measurement. The Brunauer Emmett and Teller (BET) equation was used to fit data of krypton adsorption at 77 K over a relative pressure range of 0.05 – 0.3 employing 10 measurement points. Samples mass was at least 200 mg and each formulation was analyzed at least in duplicate.

2.4.10 MERCURY (HG) POROSIMETRY

Pore size distribution of collapsed and non-collapsed lyophilizates was analyzed using mercury porosimetry. Measurements were performed on a Poremaster (Quantachrome, Odelzhausen, Germany). The contact angle used was 140 °. Mercury intrusion and extrusion experiments were performed on intact cakes over a wide range of pressures starting from 0.2 psi to 60000 psi.

2.4.11 HELIUM PYCNOMETRY

Density of collapsed and non-collapsed lyophilizates was determined with helium pycnometry using an Accupyc 1330 Gas Pycnometer (Micromeritics, Mönchengladbach, Germany).

Lyophilizates were analyzed either as intact cake or ground to a powder using an agate mortar in a dry nitrogen atmosphere.

Intact cakes were extracted from the vial by breaking the bottleneck, immediately weighed and transferred into the measurement cell. Analysis was performed using the 10 cm³ cell of the pycnometer. The geometric volume of none-collapsed cakes was determined as well using a digital caliper ruler (Digimatic CD-15CD, Mitutoyo, Oberndorf, Germany) to measure sample height and diameter and the porosity was calculated.

Sucrose and trehalose based lyophilizates were also analyzed after homogenization with a spatula, grinding in an agate mortar and transfer into the 1 cm³ aluminum sample cell. Afterwards the surface was flattened and the sample was slightly compressed with a steel stab and the mass was determined. Sample preparation and sample handling was performed in a dry nitrogen atmosphere, with the humidity controlled at below 2 %. Then the cell was mounted into the analysis chamber. The sample was first purged with helium for about 30

minutes with the purge fill pressure adjusted to 134 kPa (19.5 psig). Then the sample was analyzed 20 times with the helium equilibration rate set to 34 Pa/min (0.005 psig/min). The pycnometer was tested for accuracy and precision using crystalline sucrose.

2.4.12 GLUCOSE QUANTIFICATION (TRINDER ASSAY)

To analyze the extent of sucrose decomposition into glucose during storage, reconstituted lyophilizates were analyzed photometrically according to the Trinder method using a glucose determination kit (Reference No GAGO20, Sigma-Aldrich, Steinheim, Germany).

The kit contains the enzymes glucose oxidase and peroxidase, the colorless dianisidine and sulfuric acid. Glucose peroxidase oxidizes glucose to D-gluconic acid and hydrogen peroxide (as a by product). Hydrogen peroxide then reacts with (reduced) dianisidine in the presence of the enzyme peroxidase and the brown (oxidized) o-dianisidine is formed. Oxidized o-dianisidine reacts with sulfuric acid to form a more stable pink product that can be quantified by its absorption at 540 nm. Its concentration is proportional to the original glucose concentration.

Glucose standard solutions at 5 different concentrations ranging from 20 – 80 µg glucose/mL were analyzed to give a calibration curve. Reconstituted lyophilizates were diluted 10 fold and 100 fold, respectively, depending on the expected glucose concentration to get glucose concentrations between 20 and 80 µg/mL. The reaction was started by addition of the assay reagent to the samples, tubes were then incubated at 37 °C for 30 minutes and the reaction was stopped by the addition of sulfuric acid. Photometric analysis was performed at 540 nm using an Agilent 8453 UV-visible Spectrophotometer (Agilent Technologies, Waldbronn, Germany). Water mixed with assay reagent identically processed was used as blank. Glucose concentration was calculated from the calibration curve.

3 REFERENCES

1. van Dijk, M.A. and Vidarsson, G. Monoclonal antibody-based pharmaceuticals. *Pharm.Biotechnol.*(2nd Ed.), 283-299 (2002)
2. Piggee, C. Therapeutic antibodies coming through the pipeline. *Analytical Chemistry*, **80** (7): 2305-2310 (2008)
3. Vollmar, A. and Dingermann, T. Immunologie: Grundlagen und Wirkstoffe. *Wissenschaftliche Verlagsgesellschaft mbH Stuttgart* (2005)
4. Roskos, L.K., Davis, C.G., and Schwab, G.M. The clinical pharmacology of therapeutic monoclonal antibodies. *Drug Development Research*, **61** (3): 108-120 (2004)
5. Wang, W., Singh, S., Zeng, D.L., King, K., and Nema, S. Antibody structure, instability, and formulation. *Journal of Pharmaceutical Sciences*, **96** (1): 1-26 (2007)
6. Costantino, H.R., Andya, J.D., Shire, S.J., and Hsu, C.C. Fourier-transform infrared spectroscopic analysis of the secondary structure of recombinant humanized immunoglobulin G. *Pharmaceutical Sciences*, **3** (3): 121-128 (1997)
7. Bhatnagar, B.S., Pikal, M.J., and Bogner, R.H. Study of the individual contributions of ice formation and freeze-concentration on isothermal stability of lactate dehydrogenase during freezing. *Journal of Pharmaceutical Sciences*, **97** (2): 787-803 (2008)
8. Mi, Y., Wood, G., and Thoma, L. Cryoprotection mechanisms of polyethylene glycols on lactate dehydrogenase during freeze-thawing. *AAPS Journal*, **6** (3): e22(2004)
9. Nema, S. and Avis, K.E. Freeze-thaw studies of a model protein, lactate dehydrogenase, in the presence of cryoprotectants. *J.Parenter.Sci.Technol.*, **47** (2): 76-83 (1993)
10. Moreira, T., Pendas, J., Gutierrez, A., Pomes, R., Duque, J., and Franks, F. Effect of sucrose and raffinose on physical state and on lactate dehydrogenase activity of freeze-dried formulations. *Cryo-Letters*, **19** (2): 115-122 (1998)
11. Kawai, K. and Suzuki, T. Stabilizing Effect of Four Types of Disaccharide on the Enzymatic Activity of Freeze-dried Lactate Dehydrogenase: Step by Step Evaluation from Freezing to Storage. *Pharmaceutical Research*, **24** (10): 1883-1890 (2007)
12. Carpenter, J.F., Prestrelski, S.J., and Arakawa, T. Separation of freezing- and drying-induced denaturation of lyophilized proteins using stress-specific stabilization. I. Enzyme activity and calorimetric studies. *Archives of Biochemistry and Biophysics*, **303** (2): 456-464 (1993)
13. Mi, Y. and Wood, G. The application and mechanisms of polyethylene glycol 8000 on stabilizing lactate dehydrogenase during lyophilization. *PDA journal of pharmaceutical science and technology / PDA*, **58** (4): 192-202 (2004)
14. Prestrelski, S.J., Arakawa, T., and Carpenter, J.F. Separation of freezing- and drying-induced denaturation of lyophilized proteins using stress-specific stabilization. II. Structural studies using infrared spectroscopy. *Archives of Biochemistry and Biophysics*, **303** (2): 465-473 (1993)
15. Adler, M. and Lee, G. Stability and Surface Activity of Lactate Dehydrogenase in Spray-Dried Trehalose. *Journal of Pharmaceutical Sciences*, **88** (2): 199-208 (1999)
16. Mattern, M., Winter, G., Kohnert, U., and Lee, G. Formulation of proteins in vacuum-dried glasses. II. Process and storage stability in sugar-free amino acid systems. *Pharmaceutical Development and Technology*, **4** (2): 199-208 (1999)
17. Miller, D.P., Anderson, R.E., and De Pablo, J.J. Stabilization of lactate dehydrogenase following freeze-thawing and vacuum-drying in the presence of trehalose and borate. *Pharmaceutical Research*, **15** (8): 1215-1221 (1998)

18. Engstrom, J.D., Simpson, D.T., Cloonan, C., Lai, E.S., Williams, R.O., Kitto, G.B., and Johnston, K.P. Stable high surface area lactate dehydrogenase particles produced by spray freezing into liquid nitrogen. *European Journal of Pharmaceutics and Biopharmaceutics*, **65** (2): 163-174 (2007)
19. Baumruk, V., Pancoska, P., and Keiderling, T.A. Predictions of secondary structure using statistical analyses of electronic and vibrational circular dichroism and Fourier transform infrared spectra of proteins in H₂O. *Journal of Molecular Biology*, **259** (4): 774-791 (1996)
20. Pan, Y.C., Sharief, F.S., Okabe, M., Huang, S., and Li, S.S.L. Amino acid sequence studies on lactate dehydrogenase C4 isozymes from mouse and rat testes. *Journal of Biological Chemistry*, **258** (11): 7005-7016 (1983)
21. Torikata, T., Forster, L.S., O'Neal, C.C., Jr., and Rupley, J.A. Lifetimes and NADH quenching of tryptophan fluorescence in pig heart lactate dehydrogenase. *Biochemistry*, **18** (2): 385-390 (1979)
22. Johnson, R.E., Kirchhoff, C.F., and Gaud, H.T. Mannitol-sucrose mixtures-versatile formulations for protein lyophilization. *Journal of Pharmaceutical Sciences*, **91** (4): 914-922 (2002)
23. Fraunhofer, W. and Winter, G. The use of asymmetrical flow field-flow fractionation in pharmaceutics and biopharmaceutics. *European Journal of Pharmaceutics and Biopharmaceutics*, **58** (2): 369-383 (2004)
24. Fraunhofer, W. and Winter, G. The use of asymmetrical flow field-flow fractionation in pharmaceutics and biopharmaceutics. *Eur.J.Pharm.Biopharm.*, **58** (2): 369-383 (2004)
25. Wyatt Technology Corp. How Asymmetric Field Flow Fractionation (AF4) Theory Works. <http://www.wyatt.com/theory/fieldflowfractionation/>, (2007)
26. Ph.Eur. 2.2.1 Clarity and degree of opalescence of liquids, 6th edition. *European Directorate for the Quality of Medicine (EDQM)*, (2008)
27. Abdul-Fattah, A.M., Truong-Le, V., Yee, L., Nguyen, L., Kalonia, D.S., Cicerone, M.T., and Pikal, M.J. Drying-induced variations in physico-chemical properties of amorphous pharmaceuticals and their impact on stability (I): stability of a monoclonal antibody. *Journal of Pharmaceutical Sciences*, **96** (8): 1983-2008 (2007)
28. Kuelzto, L.A., Ersoy, B., Ralston, J.P., and Middaugh, C.R. Derivative absorbance spectroscopy and protein phase diagrams as tools for comprehensive protein characterization: A bGCSF case study. *Journal of Pharmaceutical Sciences*, **92** (9): 1805-1820 (2003)
29. Kuelzto, L.A., Wang, W., Randolph, T.W., and Carpenter, J.F. Effects of solution conditions, processing parameters, and container materials on aggregation of a monoclonal antibody during freeze-thawing. *Journal of Pharmaceutical Sciences*, **97** (5): 1801-1812 (2008)
30. Ph.Eur. 2.2.2 Degree of coloration of liquids.(European Directorate for the Quality of Medicine (EDQM)): (2008)
31. Carlson, R.H., Garnick, R.L., Jones, A.J.S., and Meunier, A.M. The determination of recombinant human tissue-type plasminogen activator activity by turbidimetry using a microcentrifugal analyzer. *Analytical Biochemistry*, **168** (2): 428-435 (1988)
32. Burns, D.A., Ciurczak, E.W., and Editors. Handbook of Near-Infrared Analysis, Second Edition, Revised and Expanded. [In: Pract. Spectrosc., 2001; 27].814(2001)
33. Frake, P., Greenhalgh, D., Grierson, S.M., Hempenstall, J.M., and Rudd, D.R. Process control and end-point determination of a fluid bed granulation by application of near infrared spectroscopy. *International Journal of Pharmaceutics*, **151** (1): 75-80 (1997)
34. Derksen M.W.J., van de Oetelaar Piet J.M., and Maris Frans A. The Use of near-infrared Spectroscopy in the efficient prediction of a specification for the residual moisture content of a freeze-dried product. *Journal of Pharmaceutical and Biomedical Analysis*, **1998** (17): 473-480 (1997)
35. Lin, T.P. and Hsu, C.C. Determination of residual moisture in lyophilized protein pharmaceuticals using a rapid and non-invasive method: near infrared spectroscopy. *PDA journal of pharmaceutical science and technology / PDA*, **56** (4): 196-205 (2002)

36. Jones, J.A., Last, I.R., MacDonald, B.F., and Prebble, K.A. Development and transferability of near-infrared methods for determination of moisture in a freeze-dried injection product. *Journal of Pharmaceutical and Biomedical Analysis*, **11** (11-12): 1227-1231 (1993)
37. Kamat, M.S., Lodder, R.A., and DeLuca, P.P. Near-infrared spectroscopic determination of residual moisture in lyophilized sucrose through intact glass vials. *Pharm.Res.*, **6** (11): 961-965 (1989)
38. Last, I.R. and Prebble, K.A. Suitability of near-infrared methods for the determination of moisture in a freeze-dried injection product containing different amounts of the active ingredient. *Journal of Pharmaceutical and Biomedical Analysis*, **11** (11-12): 1071-1076 (1993)
39. Presser, I. Innovative Online-Messverfahren zur Optimierung von Gefriertrocknungsprozessen. *Dissertation Ludwig-Maximilians-Universität München* (2003)
40. Radtke, G., Knop, K., and Lippold, B.C. Near infrared (NIR) spectroscopy. Fundamentals and application from a pharmaceutical point of view. *Pharmazeutische Industrie*, **61** (9): 848-857 (1999)

CHAPTER 4

CONTROLLED GENERATION OF COLLAPSED LYOPHILIZATES

1 INTRODUCTION

Collapse usually occurs unintentionally either during a freeze-drying run or during subsequent storage at elevated temperatures. In order to systematically investigate the collapse phenomenon and its effect on protein stability, the ability to generate collapsed cakes in a controlled and reproducible manner is an essential prerequisite. Furthermore, as the solid state stability of proteins is known to be affected by a variety of factors, such as the formulation, pH and the residual moisture level^{1,2}, the consistency of all these factors in collapsed and non-collapsed samples is highly desirable in order to allow for a clear discrimination between the effect of collapse on protein stability and the impact of other variables.

Generally, lyophilizate collapse can be provoked by increasing the product temperature above the formulation's collapse temperature (T_c). This can be achieved by either lowering the system's collapse temperature below the product temperature observed during an existing process or by varying the process parameters, in order to raise the product temperature above the collapse temperature.

This leads to two basic approaches to the provocation of collapse:

- variation of the formulation
- variation of the freeze-drying process

By the addition of low molecular weight excipients, such as sodium chloride, the T_g' and thus the T_c of the formulation can be significantly decreased³. Also, leaving out crystalline bulking agents considerably increases the susceptibility towards collapse^{4,5}. However, one major drawback of this approach is that the composition of the collapsed lyophilizates differs from that of the non-collapsed lyophilizates.

In contrast, process variations, i.e. the increase of primary and secondary drying shelf temperature or chamber pressure, bears the potential to produce collapsed and non-collapsed lyophilizates of the same formulation. However, thermal history of these samples differs, as they are produced with different drying protocols⁶.

In most published investigations dealing with the effect of collapse on protein stability, collapse was not intentionally provoked, but occurred accidentally due to inappropriate excipient/freezing-dry-protocol combinations⁷⁻⁹. In the few studies in which collapse was triggered on purpose, process variations rather than formulation variations were applied:

Wang et al. caused collapse by omitting the annealing step during freeze-drying of a partially crystalline formulation¹⁰. This caused a decrease in T_g' of the amorphous phase due to incomplete excipient crystallization during the freezing step. Jiang et al. provoked collapse by freeze-drying low- T_g' formulations at high drying temperatures¹¹.

This chapter summarizes the development of a standardized approach to generate collapsed lyophilizates in a controlled and reproducible manner. In order to understand the limits of the freeze-drying process, both formulation and process parameters were varied and the impact on the occurrence and extent of collapse was analyzed.

After thorough consideration of the effects of process and formulation variables, collapsed lyophilizates were chosen to be generated by an aggressive drying protocol, referred to as the “collapse-cycle”, because this approach allowed for the comparison of collapsed and non-collapsed cakes of identical composition. However, because the importance of thermal history on solid state stability was recently reported^{12,13}, in a second approach collapsed cakes were produced by stepwise variation of the ratio of crystalline mannitol to amorphous sucrose and the application of an aggressive freeze-drying protocol⁵.

During pharmaceutical routine production of lyophilized products, collapse most often occurs during ramping from primary to secondary drying when sublimation is not yet complete. While causing collapse during this process step would have been an even more realistic model, the controlled and reproducible provocation of collapse in this stage would not have been feasible. Thus collapse was caused during the primary drying stage of the process as described above in order to generate collapsed lyophilizates in a controlled and reproducible way.

The extensive characterization of the collapse-cycle and the resulting optimization regarding the residual moisture content of the resulting cakes are also described in this chapter.

2 COLLAPSIBILITY

In order to get further insight into the determinants of collapse, process as well as formulation parameters were varied and their impact on the occurrence and the extent of collapse was analyzed. The overall goal was to define parameters that could provoke collapse in a reproducible way in a wide range of formulations.

2.1 DETERMINATION OF CRITICAL MATERIAL PROPERTIES

When dealing with collapse phenomena, the determination of the maximum allowable operation temperature, i.e. the temperature above which collapse occurs, is important. Here, there are three different approaches that have been recently reviewed and compared¹⁴. Freeze-dry literature most frequently reports the glass transition temperature of the maximally freeze-concentrated solution (T_g') determined by differential scanning calorimetry (DSC)^{9,15} as the maximum allowable operation temperature. In addition, collapse

temperature (T_c) values determined by freeze-dry microscopy (FDM) are sometimes given^{16,17}. FDM simulates the actual freeze-drying process at a microscopic scale and thus resulting T_c -values are more relevant than T_g' values determined by DSC, as T_g' values reflect only the amorphous phase of a formulation. Although T_c was usually found to be 2-5 °C higher than T_g' ^{18,19}, the difference was reported to increase with increasing protein concentration^{16,20}. Recently, the performance of primary drying above T_g' without the occurrence of collapse has been applied by several researches in order to shorten drying times^{16,17}, stressing the importance of FDM for the realistic determination of the maximum allowable operating temperature. Freeze-drying behavior of partially crystalline formulations, which is affected by the formation of a crystalline scaffold preventing the macroscopic collapse of the amorphous component²¹ and allowing for freeze-drying at high primary drying temperatures²² is also poorly predicted by the T_g' from a DSC measurement. Although the different geometries between the FDM set-up and a vial during an actual freeze-drying run also affect the collapse temperature, the resulting T_c from an FDM experiment is still more representative for actual collapse than T_g' .

Besides the two experimental approaches, the Gordon-Taylor equation as a theoretical approach allows the calculation of a mixture's T_g' from the T_g' 's of the pure components²³.

COLLAPSE TEMPERATURE T_c

Figure 4.1 and Figure 4.2 exemplarily show the freeze-drying behavior of two mannitol-sucrose-based formulations in the FDM at different temperatures (A-D). The frozen part of the sample can be seen at the bottom part of the picture (pink and purple), the already dried part can be recognized at the top part (green). The pink holes in the already dried part of the sample show a loss of structure indicative for collapse.

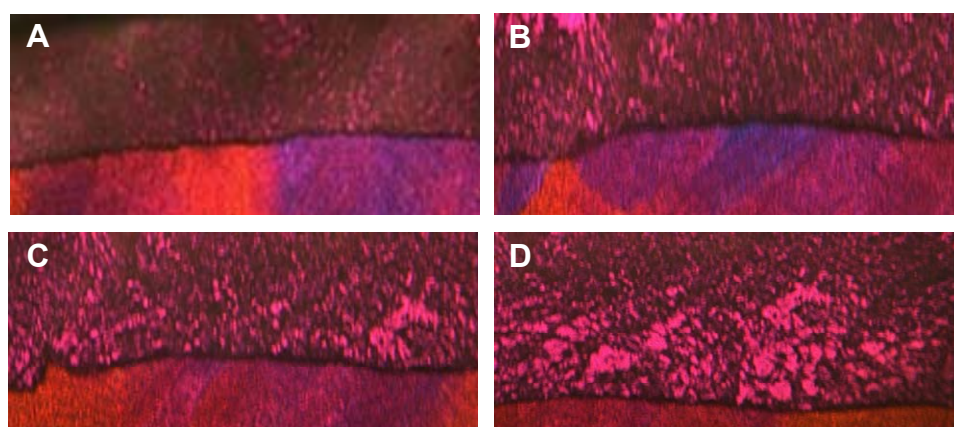


Figure 4.1: Freeze-dry-microscopic pictures of the freeze-drying process of a 10 µl aliquot of a 1:4 (m:m) mannitol-sucrose solution at -40.0 °C (A), -38.0 °C (B), -37.0 °C (C) and -36.0 °C (D).

Figure 4.1 shows a formulation composed of 40 mg/mL sucrose and 10 mg/mL mannitol. Due to the large overage of sucrose, freeze-drying behavior is mostly determined by sucrose. At -40 °C (Figure 4.1 A) first signs of loss of structure can be seen. At -36 °C

(Figure 4.1 D), the product forms no coherent product layer adjacent to the sublimation front, indicating full collapse. Thus the formulation's collapse temperature T_c is $-36\text{ }^\circ\text{C}$.

Figure 4.2 shows the freeze-drying behavior of a formulation composed of 40 mg/mL mannitol and 10 mg/mL sucrose. Due to the overage of mannitol, the freeze-drying behavior of this formulation is mainly influenced by mannitol. The first visual indication of collapse is observed at $-34.5\text{ }^\circ\text{C}$ as small pockets (Figure 4.2 B). At $-32.9\text{ }^\circ\text{C}$ the samples is completely collapsed with no coherent structure adjacent to the freeze-drying front observed, a criterion that was recently proposed by Meister et al. for the definition of complete collapse in FDM¹⁴.

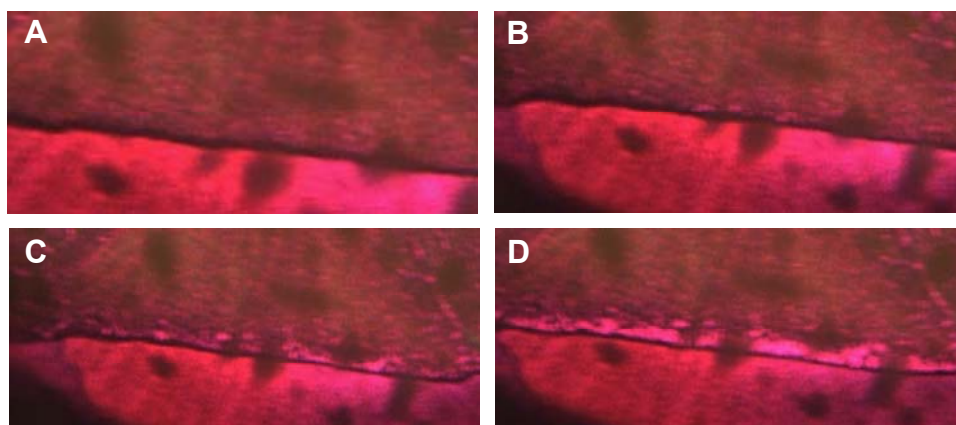


Figure 4.2: Freeze-dry-microscopic pictures of the freeze-drying process of a 10 μl aliquot of a 4:1 (m:m) mannitol-sucrose solution at $-35.1\text{ }^\circ\text{C}$ (A), $-34.5\text{ }^\circ\text{C}$ (B), $-33.3\text{ }^\circ\text{C}$ (C) and $-32.9\text{ }^\circ\text{C}$ (D).

COMPARISON OF T_c AND T_g'

Comparing the determined T_c values with T_g' values measured by DSC that are summarized in Table 4.1, a difference between the two values is observed. The sucrose-rich formulation, has a T_c of $-36\text{ }^\circ\text{C}$ and a T_g' of $-39\text{ }^\circ\text{C}$, thus a difference of $3\text{ }^\circ\text{C}$ is observed, corresponding well to the commonly reported offset of $2 - 5\text{ }^\circ\text{C}$ ¹⁹.

Table 4.1: Glass transition temperatures of the maximally freeze-concentrated solution, T_g' of formulations comprising different ratios of mannitol to sucrose.

ratio mannitol: sucrose (m:m)	T_g' [$^\circ\text{C}$]
4:1	-43.4
3.5:1.5	-42.7
3:2	-42.5
1:1	-40.5
2:3	-39.2
1.5:3.5	-40.2
1:4	-39.0

In contrast, the mannitol-rich formulation shows a large difference between T_c and T_g' of $10.5\text{ }^\circ\text{C}$. This difference is most probably caused by the special freeze-drying behavior of formulations containing a crystalline bulking agent, such as mannitol, as explained above.

However, as investigations performed during this thesis mostly dealt with amorphous formulations where a reasonable correlation with an acceptable offset of 3 °C between T_g' and T_c was shown, DSC was accomplished as the standard analytical technique for the determination of the maximum allowable operating temperature, i.e. T_g' . Additionally, FDM was performed on selected formulations. Table 4.2 summarizes T_g' 's of selected formulations investigated during this thesis.

Table 4.2: Glass transition temperatures of the maximal freeze-concentrated solution, T_g' of selected formulations investigated in this thesis (average +/- SD, n = 2).

formulation	$T_g' \pm SD$ [°C]
sucrose 5%	-40.1 ± 0.6
trehalose 5%	-36.0 ± 0.8
trehalose 3.2% + PEG 3350 1.8%	-39.5 ± 1.1
sucrose 3.2% + PEG 3350 1.8%	-39.5 ± 1.8
arginine 8.7%	-25.6 ± 0.1

2.2 TENTATIVE EXPERIMENTS

2.2.1 EFFECT OF PROCESS PARAMETERS AND FORMULATION VARIABLES IN FORMULATIONS COMPRISING A CRYSTALLINE BULKING AGENT

As discussed above, there are two different approaches to produce collapsed lyophilizates, i.e. the variation of the process and the variation of the formulation.

Table 4.3: Freeze-drying protocols applied for the production of collapsed lyophilizates and formulations that collapsed during the cycle.

protocol	primary drying		secondary drying		collapsed formulations ²	
	shelf temperature [°C]	chamber pressure [mbar]	shelf temperature [°C]	chamber pressure [mbar]	partially	completely
1 ¹	45	2	45	2	2-4	5-7
2	0	0.15	30	0.15	5,6	7
3	15	0.28	30	0.15	5,6	7

¹ developed according to Johnson et al⁵; referred to as "collapse-cycle"

² formulations referenced as indicated in Table 4.4 (column ID)

In order to investigate the effect of process and formulation variables on the occurrence of collapse three different freeze-drying protocols (Table 4.3) were used to freeze-dry formulations composed of the stabilizers mannitol and sucrose in different mass-ratios as summarized in Table 4.4.

Table 4.4: Partially crystalline mannitol-sucrose formulations investigated regarding their collapse-behavior.

ID	ratio mannitol:sucrose	further excipients
1	4:1	
2	3.5:1.5	
3	3:2	
4	1:1	0.04% PS20 10 mM
5	2:3	sodium succinate, pH 5.5
6	1.5:3.5	
7	1:4	

PS20 = polysorbate 20, ID = sample designation

Protocol 1 applies very high shelf temperatures immediately after the freezing step and primary and secondary drying are performed at the same, high temperature. Protocol 2 and 3 resemble conventional freeze-drying protocols, but shelf temperatures during primary drying are higher.

EFFECT OF PROCESS PARAMETERS

Table 4.3 lists the formulations that partially or completely collapsed during freeze-drying at the indicated conditions. Only a minor part of the formulations completely collapsed during the protocols that resemble conventional freeze-drying cycles and applied a primary and a secondary drying step. Interestingly, there was no difference in the number of collapsed formulations, no matter whether primary drying was performed at 0 °C or 15 °C. In contrast, protocol 1, resulted in partially or complete collapse of the majority of the formulations.

EFFECT OF FORMULATION-VARIABLES

The ratio of crystalline to amorphous formulation component had a strong impact on the formulation's collapse-behavior. High amounts of crystalline bulking agent prevented the system from macroscopic collapse even at very high drying temperatures (as e.g. experienced in protocol 1). With decreasing amount of crystalline component, the system's susceptibility towards collapse increased.



Figure 4.3: Lyophilizates composed of different ratios of mannitol to sucrose (as listed in Table 4.4) aggressively freeze-dried from 10 mM Tris-HCl buffer at pH 7.5 according to protocol 1 (Table 4.3).

Figure 4.3 depicts lyophilizates composed of different ratios of mannitol to sucrose freeze-dried with the aggressive protocol 1. Note that the formulation buffer is Tris-HCl and thus is

different from the sodium-succinate buffer used in the process variation experiment described in the section above, resulting in slightly differing collapse-behavior.

2.2.2 EFFECT OF FORMULATION VARIABLES IN FORMULATIONS LACKING A CRYSTALLINE BULKING AGENT

EFFECT OF BUFFER-TYPE

Figure 4.4 illustrates the effect of buffer type on the collapse behavior of different formulations. While there was no difference when applying a conservative freeze-drying protocol (Figure 4.4 B), sodium-succinate based lyophilizates collapsed more readily than Tris-HCl based cakes when subjected to aggressive freeze-drying (Figure 4.4 A). Note that if no bar is displayed in Figure 4.4, no collapse occurred.

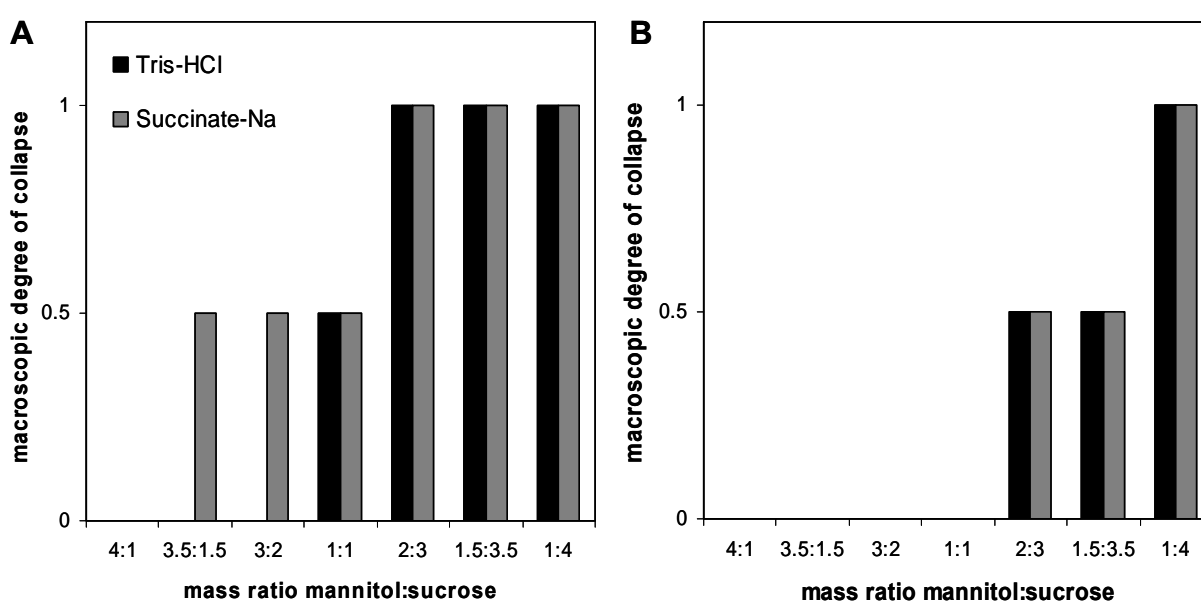


Figure 4.4: Effect of buffer type on collapse behavior of lyophilizates: macroscopic degree of collapse after visual evaluation of formulations comprising of different ratios of mannitol to sucrose freeze-dried using an aggressive (protocol 1, Table 4.3) (A) and a conservative (protocol 2, Table 4.3) (B) protocol, respectively.

EFFECT OF TOTAL SOLID CONCENTRATION

Figure 4.5 illustrates the effect of the total solid concentration on the collapse behavior. At low solid content, the cake collapsed into a coherent layer. With increasing solid content, the system started to foam with the onset of collapse.



Figure 4.5: Effect of total solid concentration on the collapse propensity of arginine-based lyophilizates. 1: 17.4 mg/mL arginine; 2: 34.8 mg/mL arginine; 3: 52.3 mg/mL arginine; 4: 69.7 mg/mL arginine; 5: 87.1 mg/mL arginine.

FURTHER VARIABLES

Comparing placebo and active lyophilizates, placebo consistently collapsed more readily than protein-containing formulations. This can be related to the higher T_g' of protein-containing formulations, as pure protein has a high T_g' ($-11\text{ }^{\circ}\text{C}^{20}$) and thus increases the T_g' of a mixture according to the Gordon-Taylor equation²³.

Furthermore, fill volume and cake height have an impact as well. Comparing 10 R vials with a 5 mL fill and 2 R vials with a 1 mL fill, larger volumes collapsed more readily.

CONCLUSION FROM COLLAPSIBILITY EXPERIMENTS

Table 4.5 summarizes the effect of the investigated parameters on the susceptibility of a given formulation towards collapse during a freeze-drying run. After consideration of the effects of process and formulation variation, two approaches to investigate the effect of collapse on protein stability were chosen.

The first approach comprised producing collapsed lyophilizates by variation of process parameters. Here, collapsed cakes were generated by applying the protocol 1 described above (Table 4.3), which is now referred to as the “collapse-cycle”. This aggressive process was chosen in order to reliably exceed collapse temperature regardless of the actual T_g' of the freeze-dried formulations. Corresponding non-collapsed lyophilizates were produced by conventional freeze-drying cycles. This approach bears the advantage that collapsed and non-collapsed lyophilizates have the identical composition. However, achieving comparable residual moisture levels might not always be perfectly feasible, as will be discussed in detail in Chapter 6 of this thesis. Furthermore, the drying protocol itself has an impact on the glassy dynamics of the lyophilizate. This matter will be approached in Chapter 9 of the thesis.

Table 4.5: Summary of effect of different parameters on the susceptibility towards collapse during a freeze-drying run.

Parameter	Effect on collapsibility
crystalline bulking agent ↓	collapse ↑
buffer type (succinate-Na ↑)	collapse ↑
solid concentration ↑	collapse ↓
protein concentration (placebo vs. verum) ↓	collapse ↑
fill volume ↑	collapse ↑

In a second approach, collapsed and non-collapsed lyophilizates were produced within one freeze-drying run, by stepwise variation of the ratio of a crystalline and an amorphous excipient, as described in Table 4.4. By comparing lyophilizates that were collapsed to different degrees and that were produced with different drying protocols outlined in Table 4.3, the impact of drying procedure and the impact of collapse are investigated. In this approach, sodium succinate based formulations were investigated, because they exhibited a stronger susceptibility towards collapse than Tris-HCl based formulations.

2.3 THE COLLAPSE-CYCLE

2.3.1 COLLAPSE-DRYING PROTOCOL

Figure 4.6 depicts the pressure-temperature profile of a typical aggressive freeze-drying protocol that was applied throughout the thesis to generate collapsed lyophilizates. After the freezing step, the shelf temperature is rapidly increased to 45 °C and primary as well as secondary drying are conducted at the same temperature. Chamber pressure is controlled at 2 mbar throughout the cycle. Thus the protocol combines the application of high temperature and high pressure to increase the product temperature above the collapse temperature. Due to the high energy input primary drying is short. The end of primary drying, as indicated by the rise of product temperature to the shelf temperature and the convergence of capacitance and Pirani pressure gauge reading (comparative pressure measurement), is reached after five hours. Product temperature during sublimation is around -10 °C and the maximum product temperature during primary drying is around 15 °C as determined according to Colandene et al. as the point of inflection of the thermocouple traces approaching the shelf temperature¹⁶.

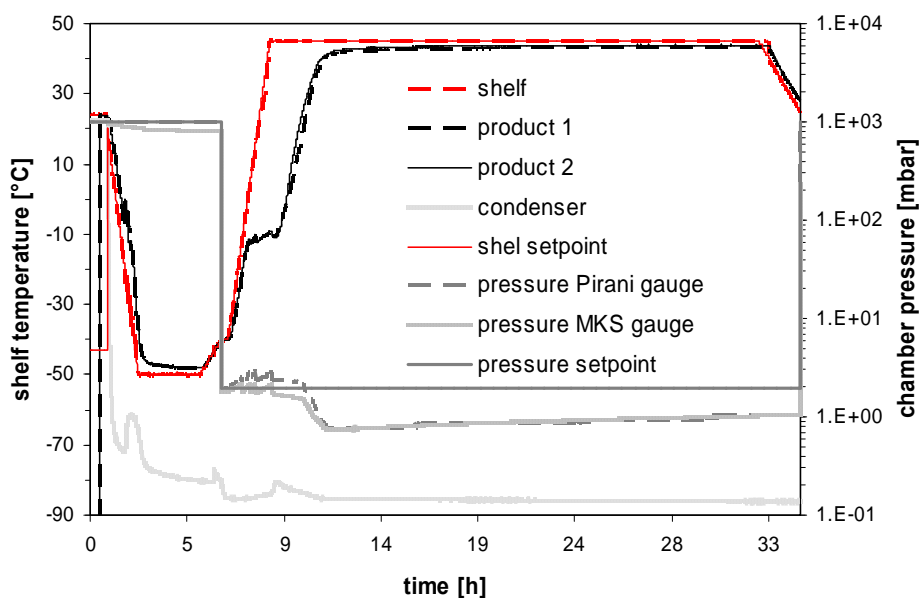


Figure 4.6: Pressure-temperature profile of a typical aggressive freeze-drying cycle as adapted from Johnson et al.⁵

The drying behavior of collapsed cakes is discussed in more detail in section 3 of this chapter.

2.3.2 APPEARANCE OF COLLAPSED CAKES

Figure 4.7 and Figure 4.8 illustrate the microscopic appearance of non-collapsed and collapsed cakes in the scanning electron and the digital microscope, respectively. Clearly, the strongly decreased porosity of collapsed cakes stands out. Non-collapsed lyophilizates

show a porous, sponge-like structure (Figure 4.7 A & D). In contrast collapsed lyophilizates (Figure 4.7 B, C, E & F) have fewer pores with strongly increased pore diameters.

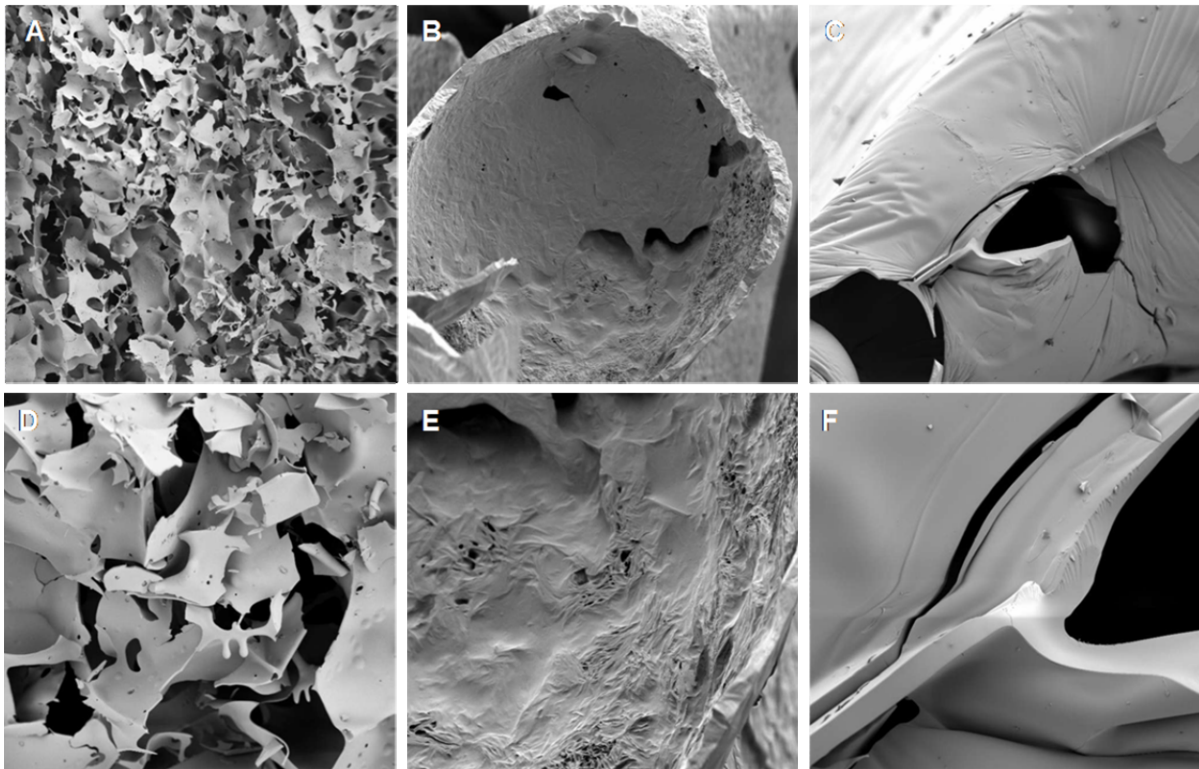


Figure 4.7: Scanning electron microscopic pictures of non-collapsed trehalose-PEG-lyophilizates (100x: A; 500x: D), collapsed trehalose-PEG-lyophilizates (150x: B; 400x: E) and collapsed trehalose-lyophilizates (100x: C; 500x: F).

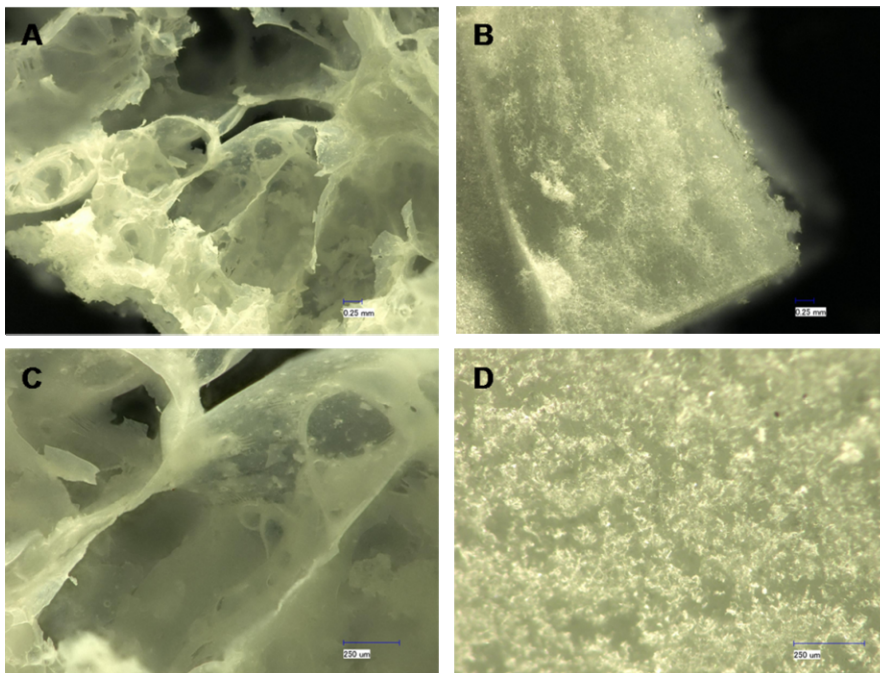


Figure 4.8: Digital microscopic pictures of collapsed (50x: A; 150x: C) and non-collapsed (50x: B; 200x: D) sucrose-based lyophilizates.

The digital-microscopic pictures additionally highlight the different matrix characters: Whereas non-collapsed lyophilizates (Figure 4.8 B & D) appear matt-white, collapsed cakes (Figure 4.8 A & C) look shiny and glassy.

Interestingly, partially crystalline collapsed systems show a less dense and less compact structure (Figure 4.7 B & E) than purely amorphous cakes (Figure 4.7 C & F). A similar observation was also reported for partially crystalline vacuum dried glasses²⁴ and was related to the formation of a crystalline scaffold coated with the amorphous component. This dramatically reduced the diffusion path length for desorbed water and strongly enhanced vacuum drying, an observation that was confirmed during collapse-drying experiments (see section 3.1 for details).

3 CHARACTERIZATION OF THE COLLAPSE CYCLE AND THE DRYING BEHAVIOR OF COLLAPSED LYOPHILIZATES

After the definition of the parameters of the collapse protocol (see Table 4.3 protocol 1), the process was further optimized, especially with respect to the final residual moisture content of the freeze-dried cakes. In order to avoid mixing up the possible effect of collapse and the effect of residual moisture on protein stability, it is crucial to closely monitor and match the moisture content of collapsed and non-collapsed cakes.

One major concern regarding collapsed lyophilizates frequently expressed in literature is that collapsed lyophilizates cannot be sufficiently dried^{10,25}, because drying may be rendered highly ineffective due to obliteration of pores. Thus a strong increase of water vapor resistance could result. However, it is reported that low residual moisture levels can be achieved by processes such as vacuum-drying and foam-drying, that also lack the porous structure of a freeze-dried cake^{13,24}

3.1 FACTORS AFFECTING THE DRYING BEHAVIOR OF COLLAPSED LYOPHILIZATES

3.1.1 FORMULATION VARIABLES

Experience from vacuum-drying and warm-air drying of micro-drops show that decreasing the diffusion path length dramatically increases drying efficiency^{24,26}. The onset of foaming also results in a reduction of the effective diffusion path length.

ADDITION OF POLYSORBATE/ BUFFER TYPE/ PH

Because polysorbates (PS) are commonly known to reduce the surface tension and can introduce the formation of foam, an effect on the foaming during collapse-drying might well be expected. Indeed, this was found to be true during vacuum-drying²⁴. During collapse-drying, no difference in macroscopic foam formation was observed with and without the addition of either PS 20 or PS 80. However, a significant effect of PS-addition on the residual moisture content of collapse-dried lyophilizates was detected. Figure 4.9 A displays the

residual moisture content of collapse-dried trehalose-lyophilizates that additionally contained PS 20 or PS 80 as compared to a purely trehalose-based cake. A 1.5 and 1.3 fold reduction of the residual moisture content was achieved after 23 hours of drying at 45 °C (collapse-drying) as compared to the formulation without the addition of PS (black bars in Figure 4.9 A). In contrast, conventional freeze-drying efficiency was not significantly affected by the addition of PS and even showed higher residual moisture contents in formulations containing PS (grey bars in Figure 4.9 A). Note that conventional freeze-drying cycles applied here were designed to match the higher residual moisture contents of collapse-dried lyophilizates and therefore used uncommonly low drying temperatures (i.e. -10 °C for secondary drying). The low drying conditions applied here could result in inhomogeneities in drying and larger standard deviations possibly skewing the effect of PS addition in the conventionally freeze-dried samples.

A 1.3 fold reduction of residual moisture content upon the addition of PS 20 was also observed for 10 mM sodium succinate buffer pH 5.5 (data not shown).

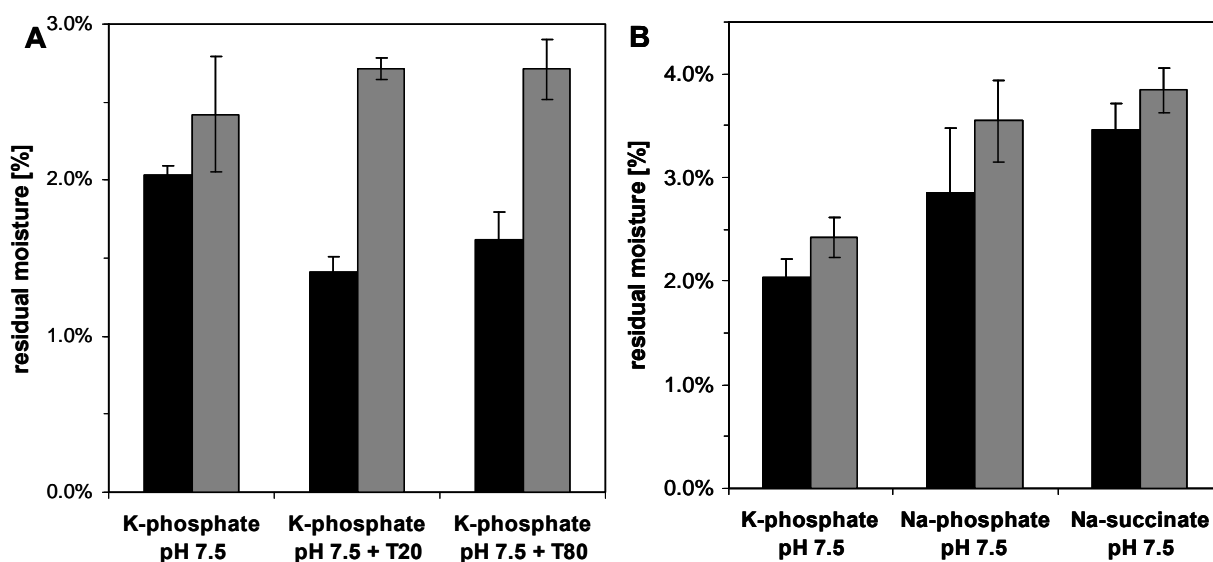


Figure 4.9: Effect of the addition of polysorbate 20 (T20) and polysorbate 80 (T80) on the residual moisture content of collapse-dried lyophilizates (A); effect of buffer type on the residual moisture content of collapse-dried lyophilizates (B)

Black bars represent residual moisture levels after collapse-drying for 23 hours at 45 °C and grey bars represent residual moisture levels after conventional freeze-drying at -40 °C/ -20 °C and -10 °C. Lyophilizates contained 50 mg/mL trehalose and 10 mM of the designated buffer at the specified pH.

Figure 4.9 B depicts the effect of buffer type on the residual moisture content of the freeze-dried cake. 10 mM solutions of potassium phosphate, sodium phosphate and sodium succinate were investigated. In order to rule out the effect of pH, which was investigated in a separate experiment, all buffers were adjusted to pH 7.5.

A significant impact of buffer type on the final moisture level is observed. Interestingly, this effect is found in both, collapse- and conventionally freeze-dried lyophilizates.

In order to assess the effect of pH value on the drying behavior of lyophilizates, 10 mM sodium succinate and potassium phosphate buffers were additionally freeze-dried at a pH of

5.5. A 1.2 and 1.4 fold reduced residual moisture content was found for the pH 5.5 sodium succinate lyophilizates aggressively and conventionally freeze-dried, respectively. In contrast, a 1.6 fold increased residual moisture content was found for the collapse-dried pH 5.5 potassium phosphate buffer. No effect of pH was observed for the conventionally freeze-dried potassium phosphate samples. Thus in summary, no consistent effect of pH on the drying behavior of collapse- and conventionally freeze-dried lyophilizates can be concluded.

3.1.2 MATRIX STRUCTURE: PARTIALLY CRYSTALLINE AND AMORPHOUS CAKES

As already demonstrated in Figure 4.7, partially crystalline and purely amorphous collapsed lyophilizates show different matrix structures. This led to tremendous differences in the drying behavior as well. Figure 4.10 displays the residual moisture contents of amorphous and partially crystalline collapse-dried cakes. Partially crystalline cakes showed significantly lower residual moisture contents after the same drying time. The benefit of the addition of crystallizing amino acids on the drying efficiency during vacuum drying was already mentioned earlier²⁴. Mattern et al. described that a crystalline scaffold coated by the amorphous formulation component²⁴ was formed, rendering drying more efficient.

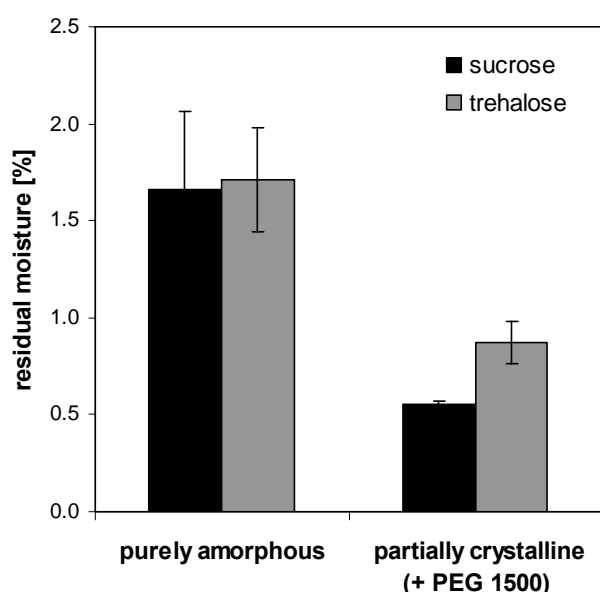


Figure 4.10: Difference in drying behavior of purely amorphous and partially crystalline collapsed lyophilizates: Residual moisture contents of collapsed cakes after drying with the collapse-cycle (protocol 1, Table 4.3); average +/- SD, n = 2.

Most probably, the more efficient drying of partially crystalline collapsed lyophilizates was related to the same fact. As it is widely acknowledged that collapse leads to constriction of pores, thereby significantly slowing down sublimation rates^{25,27} and eventually reducing drying to evaporative mechanisms¹⁰, shortening the diffusion path length becomes especially important.

In order to adequately reduce the residual moisture content of purely amorphous formulations, special optimization of the process had to be accomplished, as described in the next section.

3.2 DRYING KINETICS

3.2.1 EFFECT OF N₂-INJECTIONS

Chamber pressure during freeze-drying can be additionally controlled using a regulated flow of dry nitrogen in order to allow for the correction of pressures below the set-point. Too low pressures usually occur when sublimation rates are high and sublimation ends abruptly. Due to sublimation, pressure increases constantly during primary drying. At the end of primary drying, no more water vapor is generated and thus the pressure is easily decreased to levels below the set-point. In a process set-up without the possibility to adjust the vacuum by nitrogen injections, pressure remains too low during the remaining process time. This is illustrated in Figure 4.11 A. In contrast, the use of nitrogen allows for a controlled pressure adaptation to the set-point (Figure 4.11 B).

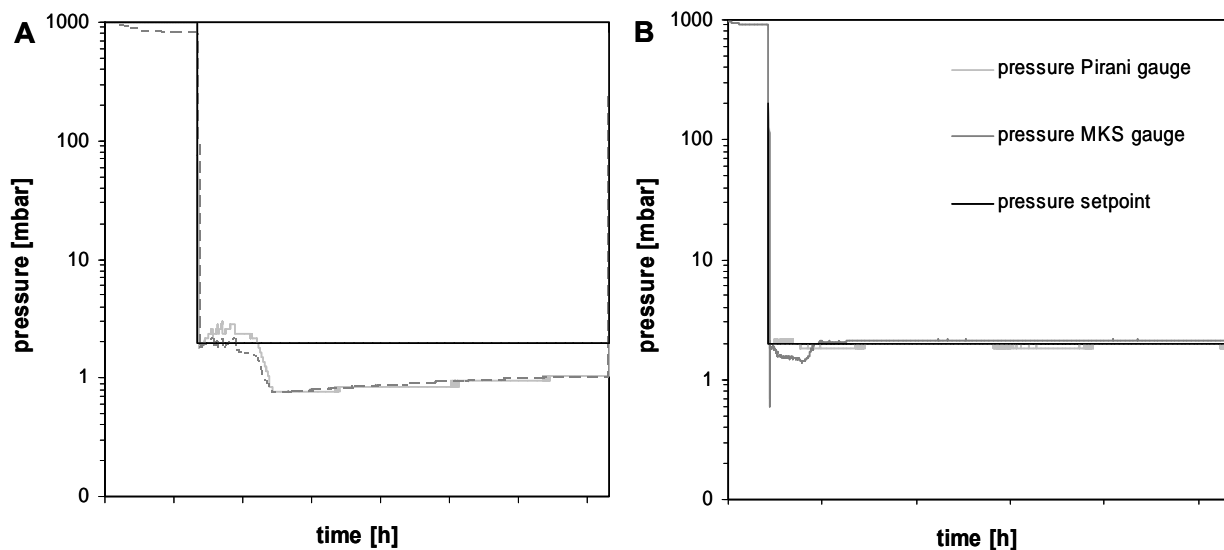


Figure 4.11: Pressure course during collapse-drying without (A) and with (B) pressure control by nitrogen injections.

In addition to improved control of the chamber pressure, the introduction of a constant flow of dry nitrogen enhances the water vapor transport from the samples to the condenser and exerts an additional drying effect. Figure 4.12 illustrates the impact of the introduction of dry nitrogen to the collapse-drying process on the drying kinetics of different formulations. No matter which sample composition is chosen, samples dried with additional nitrogen injections (open symbols) showed lower residual moisture levels than samples dried without the additional nitrogen injections (closed symbols).

This effect was especially pronounced in amorphous samples that had a denser structure and that were thus difficult to dry. Lyophilizates composed of sucrose & PEG 3350 showed

slightly increased residual moisture levels after freeze-drying with nitrogen injections for 33 hours as compared to drying without nitrogen injections. However, this fact most probably reflected slight batch to batch variations in drying. As the residual moisture content of this formulation was generally low, the impact of nitrogen injections on the drying performance was less pronounced. At the end of the investigation, i.e. after 53 hours of drying, residual moisture content is low, confirming the overall benefit of nitrogen injections.

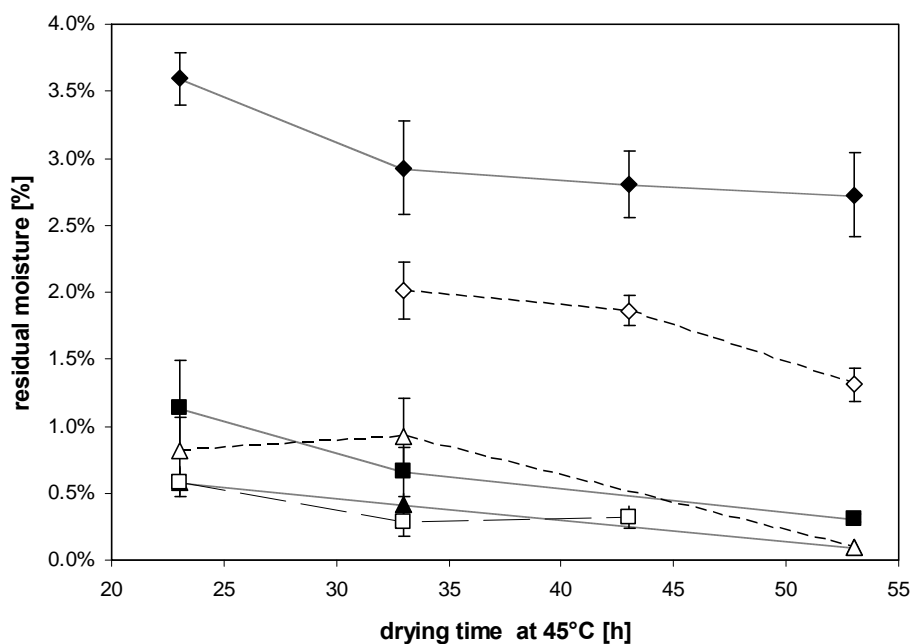


Figure 4.12: Effect of introduction of dry nitrogen during collapse-drying: residual moisture content versus drying time at 45 °C of collapsed lyophilizates formulated with trehalose & PEG 3350 (squares), trehalose (diamonds) and sucrose & PEG 3350 (triangles) with (open symbols) and without (closed symbols) pressure control by nitrogen injections; n = 2 or n = 3.

3.2.2 MASS-SPECTROMETRIC MONITORING OF DRYING IN THE COLLAPSED STATE

The use of mass spectrometry to monitor the freeze-drying process was first described by Jennings in 1980²⁸. In 1993 Connelly applied mass spectrometry to detect the end point of primary drying²⁹ and Presser further refined the method and proposed an online detection method for the end of secondary drying³⁰.

Figure 4.13 depicts a typical collapse-drying run that also includes the relative mass spectrometric signal of water vapor in the freeze-drying chamber, in order to monitor the course of sublimation and desorption.

At the beginning of the primary drying stage, sublimation rates rapidly increase with increasing shelf temperature with a maximum of 86 % water vapor in the drying chamber. Due to the rapid drying, the sublimation stage is short. The end of primary drying is indicated by a steep decrease of the water vapor fraction in the chamber after only five hours. The mass spectrometric signal is in perfect accordance with other methods commonly used to detect the end point of primary drying, i.e. the thermocouples reaching the shelf temperature,

the convergence of the signal of capacitance and Pirani pressure gauge (comparative pressure measurement) and the decrease of the ice condenser temperature to its minimum¹⁶.

The steep decrease of the water vapor signal indicates a homogeneous sublimation of vials distributed over the shelf, because all vials reach the end of sublimation within a narrow time frame.

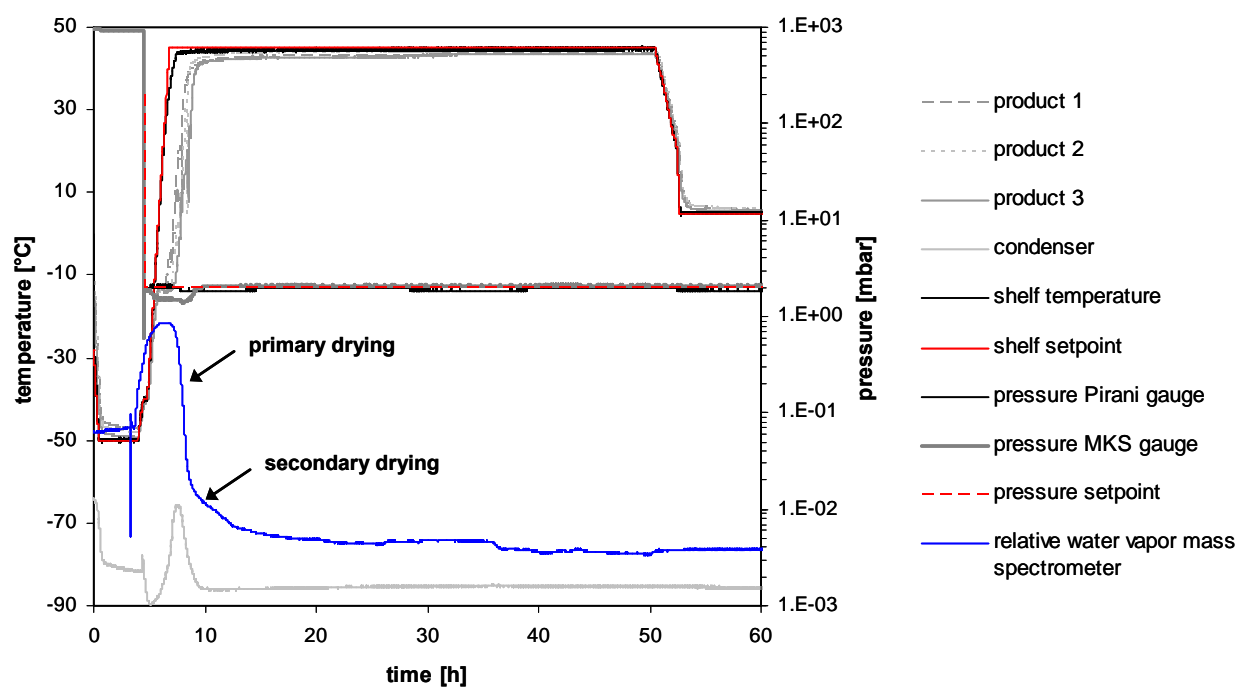


Figure 4.13: Pressure-temperature profile of a collapse-drying run including the relative mass spectrometric signal of water vapor in order to monitor the drying process.

Lyophilizates were composed of 50 mg/mL trehalose, 32 mg/mL trehalose + 18 mg/mL PEG 3350 or 50 mg/mL sucrose in 10 mM potassium phosphate buffer pH 7.5, respectively.

Primary drying is followed by a slow secondary drying step, as indicated by the shoulder observed in the mass spectrometric signal that levels into a plateau after about three hours. The absence of a second peak, as usually observed during secondary drying³⁰, indicates that the extent of secondary drying is small, most probably due to the strongly reduced surface area of the collapsed cakes. However, some drying still proceeds and after 22 hours the signal levels into its final plateau.

Figure 4.14 displays the pressure-temperature profiles of a conventional (Figure 4.14 A) and a collapse freeze-dry cycle (Figure 4.14 B) of arginine-based lyophilizates that were designed to yield in comparable residual moisture contents in order to allow for a direct comparison of the drying kinetics of collapsed and non-collapsed lyophilizates. Primary drying in a conventional freeze-drying cycle is not as rapid as in the collapse-cycle, as can be deduced from the observation of a plateau-phase rather than a peak in the water vapor MS signal during primary drying. The less steep decrease of the water vapor curve at the end of primary drying indicates that sublimation is less homogeneous in a conventional cycle. This

observation contravenes the wide-spread belief that collapse per se results in inhomogeneous drying. At least at high shelf temperatures, as applied during the collapse-cycle, drying is not affected by the onset of collapse.

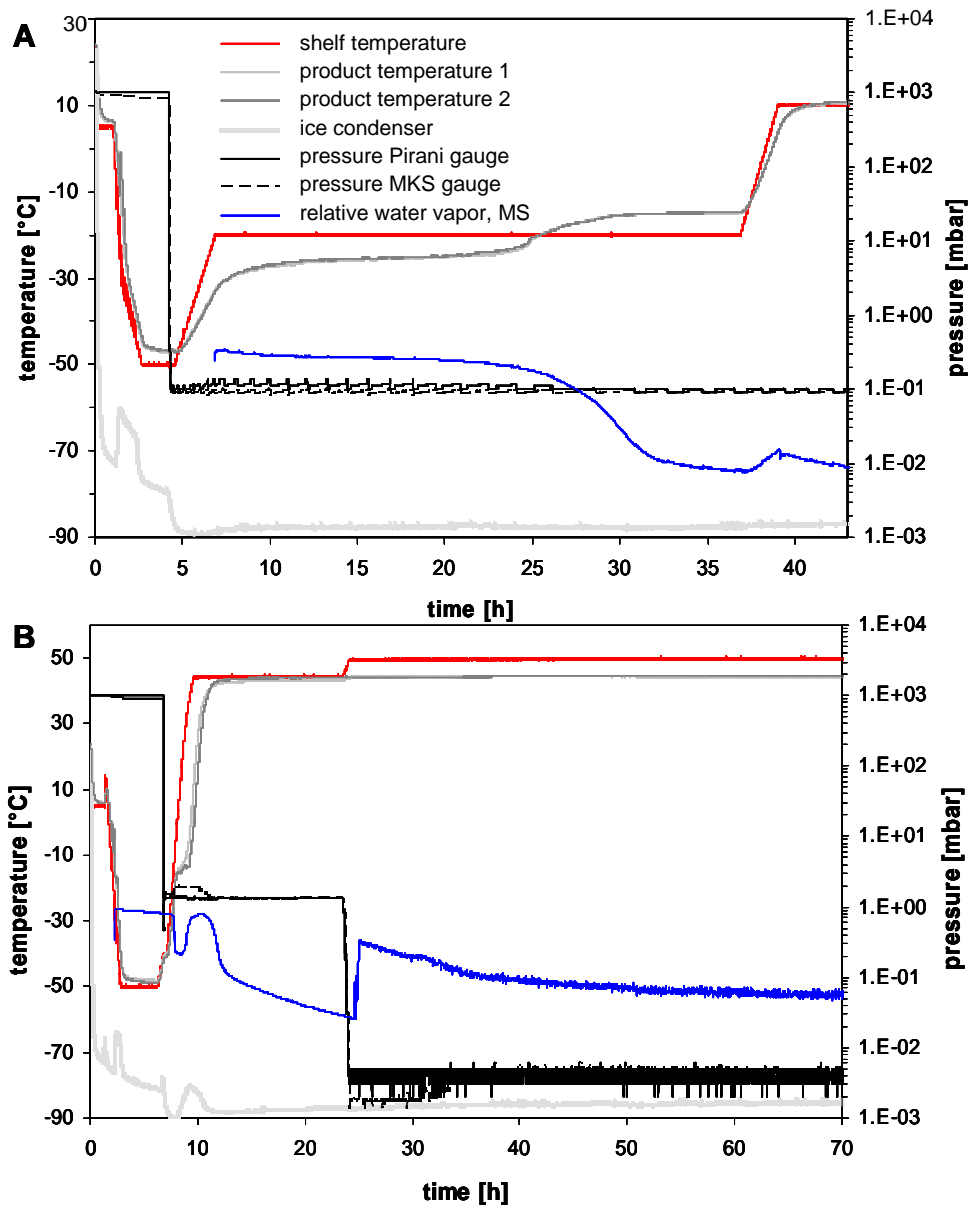


Figure 4.1: Pressure-temperature profiles including water vapor partial pressure courses of a conventional freeze-drying cycle (A) and a collapse-cycle (B) of arginine-based lyophilizates.

Lyophilizates were composed of 2.5 mg/mL PA₀₁, 87.1 mg/mL L-arginine, 0.0255 % PS 80 adapted to a pH of 7.3 with phosphoric acid.

The increase of the shelf temperature to the secondary drying stage in the conventional freeze-drying cycle results in a second, smaller peak caused by the evaporation of adsorbed water. In contrast to the cycle shown in **Fehler! Verweisquelle konnte nicht gefunden werden.**, the increase of shelf temperature and concomitant decrease of chamber pressure in the collapse cycle depicted in Figure 4.1 B results in a noticeable desorption peak in the MS signal. However, a plateau rather than a peak is observed, indicating that desorption is much slower than in non-collapsed

lyophilizates. This further confirms the widespread opinion that collapse leads to an inferior secondary drying.

3.2.3 MONITORING THE DRYING PROCESS BY GRAVIMETRIC DETERMINATION

In order to further investigate the effect of the onset of cake collapse on the sublimation rate, vials were closed after defined periods of time during primary drying and extracted from the freeze-dryer with a sample-thief. The amount of sublimed water was determined gravimetrically.

Figure 4.15 shows the amount of sublimed water during primary drying in both the collapse-cycle and a conventional freeze-drying cycle with a constant shelf temperature of $-20\text{ }^{\circ}\text{C}$. In the conventional protocol, water is constantly sublimed, but at a low rate, as indicated by the linear curve with a low slope.

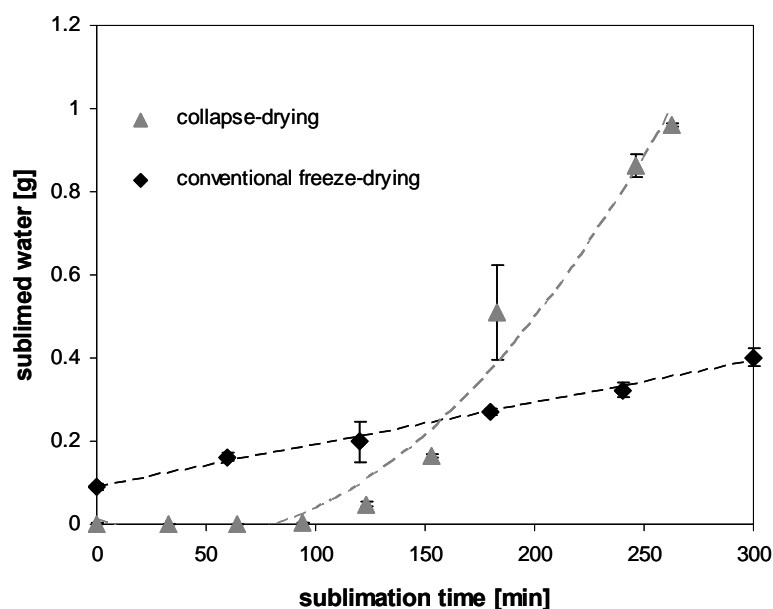


Figure 4.15: Amount of sublimed water during the primary drying stage of a conventional freeze-drying run (at $-20\text{ }^{\circ}\text{C}$) and the collapse-cycle (ramping from $-40\text{ }^{\circ}\text{C}$ to $45\text{ }^{\circ}\text{C}$ within 120 minutes followed by holding at $45\text{ }^{\circ}\text{C}$).

Sublimed water values were determined by the difference in weight prior to freeze-drying and after a defined period of freeze-drying; vials were extracted during the freeze-drying run using a sample-thief. Symbols are calculated average values of 2 vials. Vials contained 5 % sucrose in 10 mM sodium succinate buffer pH 5.5.

In contrast, sublimation in the collapse-cycle is low at the beginning of the ramp, but rapidly increases towards the end of the ramp. This is in good agreement with the amount of water vapor in the freeze-drying chamber as detected by mass spectrometry (Figure 4.11). Interestingly, the visual observation of the drying process, discussed in the following section, led to a different observation: The elevation of the lyophilized cake from the vial bottom was related to a strong stream of water vapor caused by rapid sublimation. The existence of strong sublimation is also indicated by the low product temperatures showing self-cooling. A possible explanation might be the fact that the initially sublimed water is trapped in the vial below the elevated remaining cake. When the cake eventually falls to the bottom of the vial,

water vapor is released out of the vial and is then detected by mass spectrometry and loss in weight.

3.2.4 MONITORING THE DRYING PROCESS BY VISUAL INSPECTION

Figure 4.16 shows the appearance of sucrose-based lyophilizates during the primary drying phase of the collapse-cycle, i.e. during the 120 minutes ramp from $-40\text{ }^{\circ}\text{C}$ to $45\text{ }^{\circ}\text{C}$ and during the subsequent hold period at $45\text{ }^{\circ}\text{C}$.



Figure 4.16: Sucrose lyophilizates during the primary drying phase of the collapse-cycle.

- 1: 20 minutes primary drying (PD); product temperature (PT) $-32\text{ }^{\circ}\text{C}$, shelf temperature (ST) $-25\text{ }^{\circ}\text{C}$
- 2: 35 min PD, $-18\text{ }^{\circ}\text{C}$ to $-21\text{ }^{\circ}\text{C}$ PT; $-14\text{ }^{\circ}\text{C}$ ST
- 3: 65 min PD, $-10\text{ }^{\circ}\text{C}$ PT, $9\text{ }^{\circ}\text{C}$ ST
- 4: 80 min PD, $-8\text{ }^{\circ}\text{C}$ to $-7\text{ }^{\circ}\text{C}$ PT, $18\text{ }^{\circ}\text{C}$ ST
- 5: 110 min PD, $-8\text{ }^{\circ}\text{C}$ to $-7\text{ }^{\circ}\text{C}$ PT, $40\text{ }^{\circ}\text{C}$ ST
- 6: 125 min PD, $+3\text{ }^{\circ}\text{C}$ to $+7\text{ }^{\circ}\text{C}$ PT, $45\text{ }^{\circ}\text{C}$ ST
- 7: 140 min PD, $+9\text{ }^{\circ}\text{C}$ to $11\text{ }^{\circ}\text{C}$ PT, $45\text{ }^{\circ}\text{C}$ ST
- 8: 155 min PD, $+12\text{ }^{\circ}\text{C}$ to $15\text{ }^{\circ}\text{C}$ PT, $45\text{ }^{\circ}\text{C}$ ST
- 9: 316 min PD, $41\text{ }^{\circ}\text{C}$ PT, $45\text{ }^{\circ}\text{C}$ ST

First signs of collapse can be observed already after 35 minutes of primary drying at the bottom of the cakes at a product temperature of $-21\text{ }^{\circ}\text{C}$ to $-18\text{ }^{\circ}\text{C}$. In the course of primary drying, during ramping to $45\text{ }^{\circ}\text{C}$, the bottom part of the cakes becomes more and more collapsed. The remaining cake structure is elevated, most probably by the water vapor stream caused by the rapid sublimation. At the end of the drying process, the cake residues fall back to the bottom of the vial.

The direct observation of the cakes allowed the determination of the exact time point of collapse. With first indications of collapse already observed at the very beginning of primary drying, this further shows that collapse does not result in a decrease of sublimation in this special cycle.

3.3 CONCLUSION: OPTIMIZATION OF THE COLLAPSE-CYCLE

After thorough characterization of the drying behavior of collapsed lyophilizates, the collapse cycle was optimized with respect to the drying time at 45 °C and the pressure applied during secondary drying. For arginine-based formulations, shelf temperature during secondary drying was increased to 50 °C.

The overall aim was to produce collapsed lyophilizates with residual moisture contents matching those of non-collapsed cakes. Details on the optimized protocols are given in the materials and methods section of this thesis (Chapter 3).

4 SUMMARY AND CONCLUSION

Different approaches towards the controlled generation of collapsed lyophilizates were tested and investigated towards their suitability for the analysis of the effect of collapse on protein stability. As solid state protein stability is known to be affected by a variety of factors, such as formulation variables or residual moisture, the final approach was designed to keep most of these variables as constant as possible. Thus collapsed lyophilizates were chosen to be produced by variation of process parameters rather than by variation of formulation variables. However, because the effect of drying technology on solid state stability was recently highlighted^{6,13}, lyophilizates with different formulations that collapsed to different extents produced in one freeze-drying run were also investigated in a second approach.

The chosen aggressive freeze-drying cycle is referred to as collapse-cycle, representing a special form of freeze-drying protocol, as applied shelf temperatures and chamber pressures were controlled at much higher values than usually observed during conventional freeze-drying protocols, in order to reproducibly cause collapse. The drying behavior of collapsed lyophilizates was characterized and the drying protocol was further optimized regarding the residual moisture content by adapting the time of drying at 45 °C, as described in detail in Chapter 3. Sublimation was shown not to be relevantly reduced by the onset of collapse during application of this special drying-protocol. In contrast, sublimation rates in the collapse cycle were much higher than sublimation rates observed in conventional freeze-drying protocols due to the high shelf temperatures.

However, secondary drying was observed to be strongly affected by the onset of collapse. The addition of crystalline excipients strongly improved drying behavior, as also described for vacuum-dried glasses by Mattern et al.²⁴. Also, the introduction of dry nitrogen during freeze-drying strongly improved secondary drying.

In summary, a freeze-drying cycle for the controlled and reproducible generation of collapsed lyophilizates was developed. The protocol was optimized to yield collapsed lyophilizates with low residual moistures, comparable to non-collapsed lyophilizates of identical composition. This provided the basis for the sound investigation of the effect of collapse on protein stability. Moreover, the optimization of the collapse-cycle rebutted current opinion that collapse renders drying highly inefficient and inhomogeneous and that collapsed lyophilizates cannot be dried to adequate residual moisture levels.

5 REFERENCES

1. Lai, M.C. and Topp, E.M. Solid-state chemical stability of proteins and peptides. *Journal of Pharmaceutical Sciences*, **88** (5): 489-500 (1999)
2. Stotz, C.E., Winslow, S.L., Houchin, M.L., D'Souza, A.J.M., Ji, J., and Topp, E.M. Degradation pathways for lyophilized peptides and proteins. *Biotechnology: Pharmaceutical Aspects*, **2** (Lyophilization of Biopharmaceuticals): 443-479 (2004)
3. Kilmartin, P.A., Reid, D.S., and Samson, I. The measurement of the glass transition temperature of sucrose and maltose solutions with added NaCl. *Journal of the Science of Food and Agriculture*, **80** (15): 2196-2202 (2000)
4. Chatterjee, K., Shalaev, E.Y., and Suryanarayanan, R. Partially crystalline systems in lyophilization: II. Withstanding collapse at high primary drying temperatures and impact on protein activity recovery. *Journal of Pharmaceutical Sciences*, **94** (4): 809-820 (2005)
5. Johnson, R.E., Kirchhoff, C.F., and Gaud, H.T. Mannitol-sucrose mixtures-versatile formulations for protein lyophilization. *Journal of Pharmaceutical Sciences*, **91** (4): 914-922 (2002)
6. Abdul-Fattah, A.M., Kalonia, D.S., and Pikal, M.J. The challenge of drying method selection for protein pharmaceuticals: product quality implications. *Journal of Pharmaceutical Sciences*, **96** (8): 1886-1916 (2007)
7. Adams, G.D.J. and Irons, L.I. Some implications of structural collapse during freeze-drying using *Erwinia caratovora* L-asparaginase as a model. *Journal of Chemical Technology and Biotechnology*, **58** (1): 71-76 (1993)
8. Adams, G.D.J. and Ramsay, J.R. Optimizing the Lyophilization Cycle and the Consequences of Collapse on the Pharmaceutical Acceptability of *Erwinia* L-Asparaginase. *Journal of Pharmaceutical Sciences*, **85** (12): 1301-1305 (1996)
9. Lueckel, B., Helk, B., Bodmer, D., and Leuenberger, H. Effects of formulation and process variables on the aggregation of freeze-dried interleukin-6 (IL-6) after lyophilization and on storage. *Pharmaceutical Development and Technology*, **3** (3): 337-346 (1998)
10. Wang, D.Q., Hey, J.M., and Nail, S.L. Effect of collapse on the stability of freeze-dried recombinant factor VIII and α -amylase. *Journal of Pharmaceutical Sciences*, **93** (5): 1253-1263 (2004)
11. Jiang, S. and Nail, S.L. Effect of process conditions on recovery of protein activity after freezing and freeze-drying. *European Journal of Pharmaceutics and Biopharmaceutics*, **45** (3): 249-257 (1998)
12. Abdul-Fattah, A.M., Truong-Le, V., Yee, L., Pan, E., Ao, Y., Kalonia, D.S., and Pikal, M.J. Drying-Induced Variations in Physico-Chemical Properties of Amorphous Pharmaceuticals and Their Impact on Stability II: Stability of a Vaccine. *Pharmaceutical Research*, **24** (4): 715-727 (2007)
13. Abdul-Fattah, A.M., Truong-Le, V., Yee, L., Nguyen, L., Kalonia, D.S., Cicerone, M.T., and Pikal, M.J. Drying-induced variations in physico-chemical properties of amorphous pharmaceuticals and their impact on stability (I): stability of a monoclonal antibody. *Journal of Pharmaceutical Sciences*, **96** (8): 1983-2008 (2007)
14. Meister, E. and Gieseler, H. Freeze-dry microscopy of protein/sugar mixtures: Drying behavior, interpretation of collapse temperatures and a comparison to corresponding glass transition Data. *Journal of Pharmaceutical Sciences*, **98** (9): 3072-3087 (2009)
15. Wang, W. Lyophilization and development of solid protein pharmaceuticals. *International Journal of Pharmaceutics*, **203** (1-2): 1-60 (2000)
16. Colandene, J.D., Maldonado, L.M., Creagh, A.T., Vrettos, J.S., Goad, K.G., and Spitznagel, T.M. Lyophilization cycle development for a high-concentration monoclonal antibody formulation lacking a crystalline bulking agent. *Journal of Pharmaceutical Sciences*, **96** (6): 1598-1608 (2007)
17. Passot, S., Fonseca, F., arcon-Lorca, M., Rolland, D., and Marin, M. Physical characterisation of formulations for the development of two stable freeze-dried proteins during both dried and liquid storage. *European Journal of Pharmaceutics and Biopharmaceutics*, **60** (3): 335-348 (2005)

18. Fonseca, F., Passot, S., Cunin, O., and Marin, M. Collapse Temperature of Freeze-Dried *Lactobacillus bulgaricus* Suspensions and Protective Media. *Biotechnology Progress*, **20** (1): 229-238 (2004)
19. Pikal, M.J. and Shah, S. The collapse temperature in freeze drying: dependence on measurement methodology and rate of water removal from the glassy phase. *International Journal of Pharmaceutics*, **62** (2-3): 165-186 (1990)
20. Meister, E. and Gieseler, H. Freeze-dry microscopy of protein/sugar mixtures: Drying behavior, interpretation of collapse temperatures and a comparison to corresponding glass transition Data. *Journal of Pharmaceutical Sciences*, **9999** (9999): n/a-n/a (2008)
21. Overcashier, D.E., Patapoff, T.W., and Hsu, C.C. Lyophilization of Protein Formulations in Vials: Investigation of the Relationship between Resistance to Vapor Flow during Primary Drying and Small-Scale Product Collapse. *Journal of Pharmaceutical Sciences*, **88** (7): 688-695 (1999)
22. Tang, X. and Pikal, M.J. Design of Freeze-Drying Processes for Pharmaceuticals: Practical Advice. *Pharmaceutical Research*, **21** (2): 191-200 (2004)
23. Gordon, M. and Taylor, J.S. Ideal copolymers and the second-order transitions of synthetic rubbers. I. Noncrystalline copolymers. *Journal of Applied Chemistry (London)*, **2** 493-500 (1952)
24. Mattern, M., Winter, G., Rudolph, R., and Lee, G. Formulation of proteins in vacuum-dried glasses. Part 1. Improved vacuum-drying of sugars using crystallizing amino acids. *European Journal of Pharmaceutics and Biopharmaceutics*, **44** (2): 177-185 (1997)
25. Tsourouflis, S., Flink, J.M., and Karel, M. Loss of structure in freeze-dried carbohydrates solutions: effect of temperature, moisture content and composition. *Journal of the Science of Food and Agriculture*, **27** (6): 509-519 (1976)
26. Stabenau, A. Drying process and stabilization of proteins by means of warm air drying and application of micro drops. *Dissertation Ludwig-Maximilians-Universität München* (2003)
27. MacKenzie, A.P. Collapse during freeze drying - qualitative and quantitative aspects. *Freeze Drying Adv. Food Technol., [Int. Course]*, 277-307 (1975)
28. Jennings, T.A. Residual gas analysis and vacuum freeze drying. *J. Parenter. Drug Assoc.*, **34** (1): 62-69 (1980)
29. Connelly, J.P. and Welch, J., V Monitor lyophilization with mass spectrometer gas analysis. *J. Parenter. Sci. Technol.*, **47** (2): 70-75 (1993)
30. Presser, I. Innovative Online-Messverfahren zur Optimierung von Gefriertrocknungsprozessen. *Dissertation Ludwig-Maximilians-Universität München* (2003)

CHAPTER 5

METHODS FOR THE QUANTIFICATION OF THE EXTENT OF COLLAPSE IN FREEZE-DRIED CAKES

1 INTRODUCTION

As discussed in detail in the general introduction (Chapter 1) of this thesis, the occurrence of collapse is one of the most common aberrations experienced during a freeze-drying run. Since collapsed lyophilizates are frequently associated with having increased and irregularly distributed residual moisture contents¹, prolonged reconstitution times² and compromised protein stability³⁻⁵, a collapsed product is usually not released to the market.

So far, lyophilizates are evaluated by judgement of their macroscopic and microscopic appearance and then divided into not collapsed, partially collapsed and completely collapsed cakes⁶. However, as collapse is known to exist in a variety of manifestations, ranging from slight shrinkage commonly observed during freeze-drying of low T_g '-carbohydrates⁷, over partial and total collapse to melt-back phenomena, this simple classification lacks scientific differentiation and needs improvement. Besides the occurrence in freeze-drying, collapse is also observed during spray-drying, during the production of agglomerates and during storage of amorphous solids at elevated temperatures. Thus an accurate and distinctive method to evaluate the degree of collapse is of utmost importance.

To assess the structure of freeze-dried cakes, a variety of approaches was described. For example, the homogeneity of the dried cake structure was examined by fluorescence microscopy of cakes that were previously embedded in rhodamine-containing wax⁸. There are few publications trying to describe the collapse phenomenon in a rational way. As the onset of collapse is accompanied by a decrease in specific volume and an increase in bulk density, these properties can be exploited as an analytic measure to quantify the degree of collapse: The degree of volume reduction during storage of dehydrated whey and dairy products was measured by determining the geometric dimensions of compressed samples by Burin et al. and Prado et al.^{9,10}. Buera and co-workers assessed the volume of dried solids by liquid pycnometry¹¹. A similar approach was described by Katekawa¹². Levi and co-workers as well as Aguilera used the glass beads displacement method first introduced by Hwang and Hayakawa¹³ to describe shrinkage during food production^{14,15}. In this method, the amount of glass beads that is displaced by the lyophilizate is measured gravimetrically and the cake volume is calculated using the density of these beads.

Krokida et al. described the application of a pycnometric method to evaluate the true density of the dried solids and an exponential correlation was found to the drying temperature¹⁶.

Another material property that is affected by the occurrence of collapse is the porosity¹⁷ and its application in the quantitative description of collapse during drying of food systems was reported by Krokida et al. and Rassis and co-workers^{16,18}.

However, a method to quantify the degree of collapse in pharmaceutically relevant lyophilizates on a scientific and up-scalable basis has rarely been described yet. Rambhatla et al. described the use of specific surface area measurements and mercury intrusion porosimetry measurements to assess the degree of shrinkage during freeze-drying of sucrose-based lyophilizates⁷.

While this is an excellent approach, the authors did not fully exploit the method in order to establish an analytic measure to evaluate the degree of collapse of a given product. In order to set up a scientific basis to decide whether a lyophilized cake has collapsed, and if so, to what extent, a method to quantify the degree of collapse is of utmost importance. After thorough data collection, product properties such as the mean specific surface area for a certain product and the maximum allowable deviation from this average value could be defined and used as a quality control method.

In order to evaluate different material properties to be utilized as a quantitative analytic measure for the degree of collapse, lyophilizates with different macroscopic degrees of collapse were produced by stepwisely reducing the amount of a crystalline bulking agent, mannitol, and concurrently increasing the amount of the amorphous excipient sucrose. Purely sucrose- and trehalose-based lyophilizates were analyzed as a second sample set.

2 MACROSCOPIC AND MICROSCOPIC EVALUATION OF THE CAKE APPEARANCE

2.1 PARTIALLY CRYSTALLINE LYOPHILIZATES: FROM NON-COLLAPSED TO COMPLETELY COLLAPSED CAKES



Figure 5.1: Lyophilizates consisting of different ratios of mannitol to sucrose freeze-dried with the collapse-cycle resulting in different degrees of collapse.

1 - mannitol-sucrose (M:S) 4:1; 2 - M:S 3.5:1.5; 3 - M:S 3:2; 4 - M:S 1:1; 5 - M:S 2:3; 6 - M:S 1.5:3.5; 7 - M:S 1:4.

Further formulation components: polysorbate 20 (0.04 %), sodium succinate (10 mM, pH 5.5)

In the production of pharmaceutical lyophilizates, the degree of collapse is usually assessed by visual macroscopic and microscopic inspection. Thus the visual evaluation of the cake appearance was performed as a starting point in order to compare results gained by other techniques to this standard procedure.

Table 5.1: Criteria for the macroscopic and microscopic evaluation of the degree of collapse by visual inspection.

appearance	top	side	bottom	cross section	cake-stability
not collapsed	matt white, porous	matt white, porous, only slightly shrunken or detached of the vial wall	matt white, porous, only slightly shrunken or detached of the vial wall	homogeneous	stable
partially collapsed <i>(possibly recognisable at cross section only)</i>	matt white – increasingly glossy-vitreous, increasingly cavernous – sponge-like, no coherent structure	increasingly shrunken, increasingly glossy-vitreous, increasingly vertical cavernous-/sponge-like structures, cavernous	increasingly shrunken, increasingly glossy-vitreous, increasingly vertical cavernous-/sponge-like structures, cavernous	inhomogeneous, not coherent, cavernous	increasingly instable
completely collapsed	rudimental or not existing, glossy-vitreous, no coherent structure	rudimental or not existing, glossy-vitreous, no coherent structure, sometimes looking like foam	rudimental or not existing, glossy-vitreous, molten down, sometimes looking like foam	no cross section possible	instable resp. stable because cake has collapsed and molten down

Figure 5.1 depicts the mannitol-sucrose-based lyophilizates under investigation. The degree of mannitol was reduced stepwisely and the amount of sucrose was concurrently increased. Then the formulations were freeze-dried using an aggressive freeze-drying protocol (as described in section 2.1.3, Chapter 3).

The degree of collapse was assigned following a thorough macroscopic and microscopic visual evaluation according to the criteria listed in Table 5.1. Figure 5.2 shows representative views of non-collapsed, partially collapsed and completely collapsed cakes, regarding the top, the cross-section and the bottom of the lyophilizates using a stereo-microscope and a seven-fold magnification.

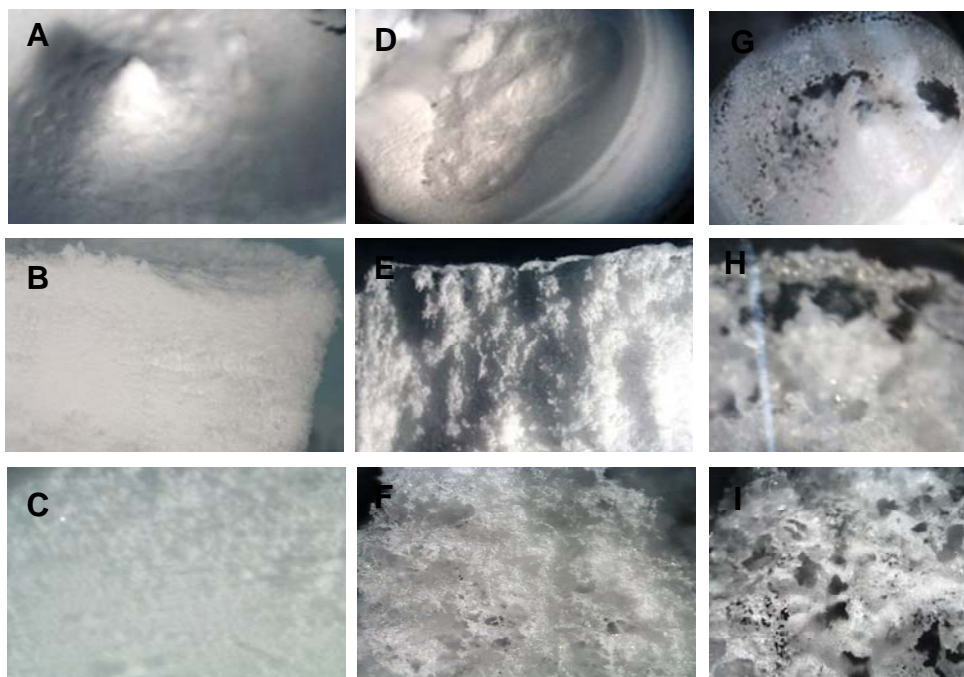


Figure 5.2: Microscopic appearance of non-collapsed (A – C), partially collapsed (D – F) and completely collapsed (G – I) using a stereo-microscope and a 7-fold magnification.

Top of the lyophilizates (A, D, G), cross section (B, E, H) and bottom of the lyophilizates (C, F, I).

Most obviously, the cake becomes less mechanically stable and more cavernous with increasing degrees of collapse. The top changes from a homogenous surface area to an increasingly translucent and pitted layer. Most sensitive towards the onset of collapse is the cross-section, in which holes and caverns are well detectable long before the outside of the cake shows any signs of collapse. With increasing degrees of collapse, the geometric cake dimensions vanish and a holey and incoherent material is formed. In addition, the matrix appearance changes from matt white to vitreous and translucent. The bottom of the cake loses integrity as well and becomes holier.

By visual evaluation, the lyophilizates depicted in Figure 5.1 were classified into three categories based on the degree of collapse. They are non-collapsed, partially collapsed and completely collapsed cakes, presented by a 0 to 1 scale in Figure 5.3.

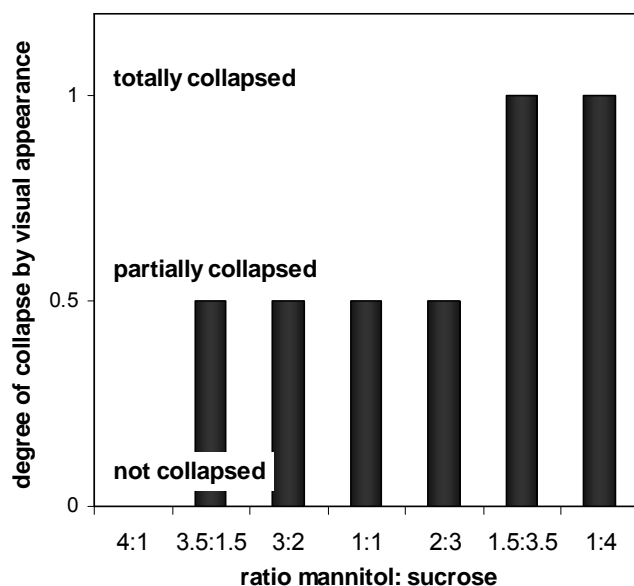


Figure 5.3: Degree of collapse of mannitol-sucrose-based lyophilizates after collapse-drying as determined by macroscopic and microscopic visual inspection.

0: not collapsed, 0.5: partially collapsed, 1: totally collapsed

Due to the aggressiveness of the applied drying cycle, only the formulation comprising the highest amount of crystalline component did not collapse. The two formulations with the lowest amount of crystalline bulking agent experienced complete collapse. This is in good agreement with literature describing a minimum weight ratio of crystalline bulking agent to amorphous stabilizer in order to prevent macroscopic collapse^{19,20}.

2.2 AMORPHOUS LYOPHILIZATES



Figure 5.4: Sucrose (1, 2) - and trehalose (3, 4)-based collapsed (1 and 3) and non-collapsed (2 and 4) lyophilizates.

Figure 5.4 depicts purely amorphous disaccharide-based lyophilizates that were produced by applying a conventional and an aggressive freeze-drying protocol resulting in non-collapsed and collapsed cakes, respectively. Completely collapsed lyophilizates were analyzed in order to provide experimental data on the maximum extent of collapse and in order to evaluate whether this worst case is analytically measurable.

They were classified into non-collapsed and completely collapsed systems by their macroscopic appearance.

3 SPECIFIC SURFACE AREA (SSA) DETERMINATION

The specific surface area (SSA) was analyzed using BET gas adsorption. Since specific surface areas of lyophilizates are small, krypton was used as the adsorbate gas.

3.1 PARTIALLY CRYSTALLINE LYOPHILIZATES

Figure 5.5 displays the specific surface areas of lyophilizates consisting of different ratios of mannitol to sucrose as determined by gas adsorption (black bars). As discussed above, stepwise reduction of the amount of mannitol resulted in different extents of macroscopic collapse. The degree of collapse as determined by visual inspection is included in the graph as well and is represented by open diamonds.

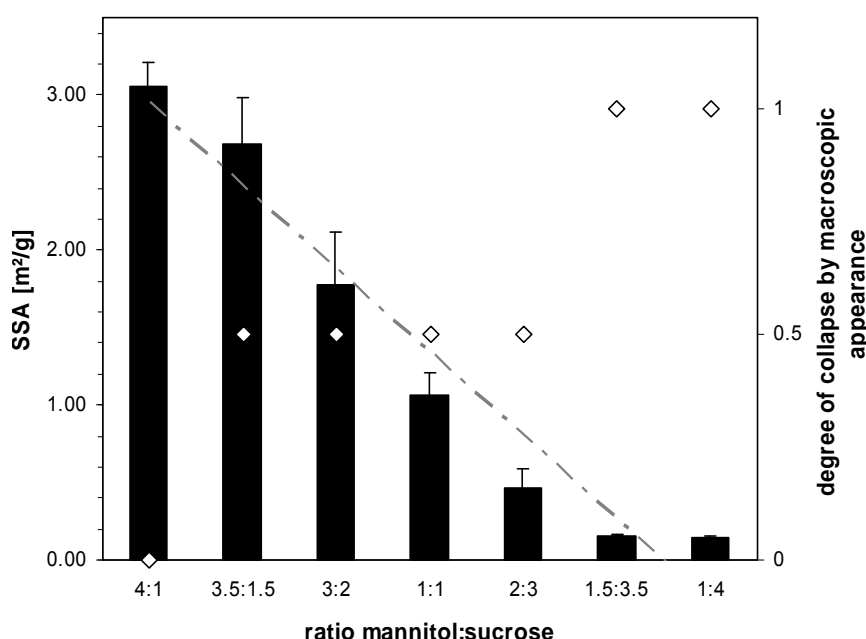


Figure 5.5: Specific surface area of lyophilizates consisting of various ratios of mannitol to sucrose as determined by BET krypton gas adsorption (black bars) compared to the degree of collapse determined by visual inspection of the cake appearance (open diamonds).

SSA-values are average values of three independent measurements of two different lyophilized batches. The grey dashed line is a linear fit of the decrease of SSA resulting in a correlation coefficient of $r^2 = 0.9455$; omitting the lowest SSA (M:S 1:4) that is obviously below the level of quantification leads to $r^2 = 0.9817$.

Most noticeably, a stepwise decrease of specific surface area with decreasing amount of mannitol is observed. Using the specific surface area as analytic measure, partially collapsed cakes can be classified in more detail than by visual inspection of the cake appearance as described in the previous section (only three classes, i.e. non-collapsed, partially collapsed and completely collapsed).

Interestingly, there is a linear relationship between the specific surface area and the amount of mannitol that can be related to the degree of collapse. Experimental data is in good agreement with literature²¹⁻²³. A specific surface area of $3.6 \text{ m}^2/\text{g}$ was reported for freeze-dried Met-hGH-trehalose samples²² and values ranging from $2.0 \text{ m}^2/\text{g}$ to $2.9 \text{ m}^2/\text{g}$ for freeze-dried sucrose-HES systems²³. The specific surface area of foam-dried materials that

macroscopically resemble collapse-dried lyophilizates, were reported to be between $0.04 \text{ m}^2/\text{g}$ and $0.17 \text{ m}^2/\text{g}$ ²¹. Thus there is a good consistence with experimental data as well. Apparently, the further differentiation between the two completely collapsed systems (formulated at a mannitol to sucrose ratio of 1.5: 3.5 and 1: 4) was below the resolution of the method. This was most probably due to limitations regarding the minimum surface area. However, from a practical point of view this discrimination is not important, since both systems are completely collapsed based on visual evaluation. In contrast, the thorough assessment of the mean specific surface area of a given formulation and the clear definition of a maximum allowable decrease in specific surface area is of high importance and could render the approval of lyophilizates more fact-based.

3.2 AMORPHOUS LYOPHILIZATES

The specific surface areas of purely amorphous sucrose- and trehalose-based lyophilizates that were either non-collapsed or completely collapsed were analyzed as well. Table 5.2 lists the experimental data. Specific surface areas are in good agreement with literature reports ($0.62 \pm 0.03 \text{ m}^2/\text{g}$ ²⁴ and $1.21 \pm 0.02 \text{ m}^2/\text{g}$ ²¹ for freeze-dried sucrose cakes, and $1.7 \text{ m}^2/\text{g}$ for freeze-dried trehalose cakes²²). The specific surface areas of the completely collapsed cakes were not relevantly different from the ones determined above that additionally contained a small amount of mannitol and they are as well in good agreement with literature reports on foam-dried materials²¹.

Table 5.2: SSA of trehalose- and sucrose-based lyophilizates both immediately after freeze-drying and after 2 weeks of storage at 50 °C.

excipient	appearance	SSA [m^2/g] immediately after FD	SSA [m^2/g] after 2 weeks at 50°C
sucrose	initially non-collapsed	0.82 ± 0.01	0.31 ± 0.01
	initially collapsed	0.14 ± 0.00	0.19 ± 0.01
trehalose	initially non-collapsed	1.13 ± 0.06	1.05 ± 0.03
	initially collapsed	0.09 ± 0.00	0.09 ± 0.00

BET gas adsorption analysis was performed a second time after two weeks of storage at elevated temperatures that caused the sucrose-based systems to undergo a remarkable degree of shrinkage, referred to as collapse during storage throughout this thesis. The occurrence of collapse was well reflected in an approximately 2.6 fold decreased specific surface area and could be accurately quantified, pointing towards the potential of the method to reliably quantify shrinkage and collapse both during lyophilization and during subsequent storage.

Trehalose-based lyophilizates that did not macroscopically collapse during storage did not show any alteration in specific surface area after two weeks. The SSA of initially collapsed lyophilizates remained unchanged during storage as well.

4 MERCURY POROSIMETRY

4.1 PARTIALLY CRYSTALLINE LYOPHILIZATES

According to the collapse-model stated by Pikal et al., collapse is caused by viscous flow of the glassy matrix over the distance of a pore-radius, leading to closure of pores². Hence, a collapsed material is less porous than a non-collapsed lyophilizate.

The decrease in porosity with the onset of collapse has been thoroughly described in literature^{25,26} and has been applied to the quantification of the extent of collapse¹⁶. A common method to assess the pore size distribution of porous materials is mercury intrusion porosimetry, where the extent of mercury intrusion into a porous matrix is monitored as a function of applied pressure. The pore radius can then be calculated using the Washburn equation²⁷. Rambhatla and co-workers characterized the shrinkage of sucrose-cakes during freeze-drying and observed a simultaneous decrease in pore volume with increasing degree of shrinkage and decreasing specific surface area⁷, but they did not apply the method to quantify the degree of shrinkage.

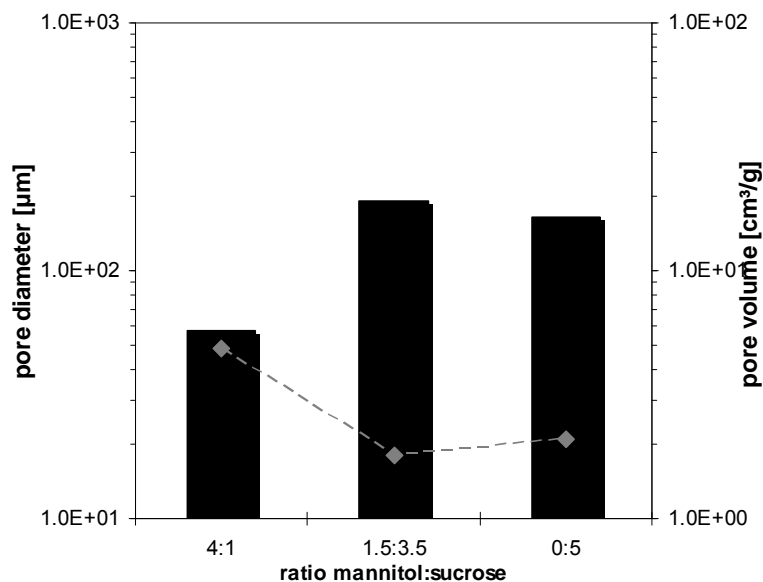


Figure 5.6: Mean pore diameter (bars) and mean pore volume (diamonds) as determined by Hg-porosimetry measurements.

Figure 5.6 depicts the mean pore diameter and the mean pore volume of representative mannitol-sucrose (M:S) formulations that are non-collapsed (M:S 4:1), partially collapsed (M:S 1.5:3.5) or completely collapsed (M:S 0:5), respectively. Distinctly, an increase in the mean pore diameter and hence also a decrease in the absolute mean pore volume can be perceived with the onset of collapse. This is in good agreement with Rambhatla⁷, who

described collapse as viscous flow over a finite distance in a certain time. Thus smaller pores are more prone to collapse in a defined period of time than larger pores and collapse first. Interestingly, the difference in pore characteristics between partially collapsed and completely collapsed cakes is not very distinct, although the lyophilizates are macroscopically greatly different. This might be related to the fact that collapsed lyophilizates lack a noteworthy cake structure. This probably causes a deviation of the prevalent pore shape from the cylindrical pore model that is assumed for the calculation of the pore geometrics from mercury intrusion data. In addition, pore collapse during the intrusion measurement or a change of the contact angle of mercury to the collapsed sugar matrix might affect the analysis²⁸. However, as completely collapsed cakes can be unambiguously identified by macroscopic appearance, the exact characterization of partially collapsed cakes is of much more importance.

In summary, a correlation between the extent of macroscopic partial collapse and the decrease of pore volume as well as pore diameter could be shown, similar to the correlation of specific surface area and collapse. However, comparing the change of analytic measure with the degree of collapse, the specific surface area decreased more than 15-fold, whereas the pore volume is reduced just 2.3-fold. Hence, the specific surface area provides a more sensitive analytic measure in order to accurately quantify slight forms of collapse.

5 HELIUM PYCNOMETRY

With the onset of collapse, the glassy system undergoes viscous flow that decreases its specific volume and increases its density. Thus the powder density and the porosity, i.e. the ratio of pore-volume to total volume, can be applied to characterize collapsed systems and to evaluate the extent of collapse.

A decrease in porosity and an increase in bulk density was described by Krokida et al. for dried plant materials with increasing drying temperatures¹⁶. An effect of drying method on the true density was described for disaccharide-based formulations^{21,29}. For freeze-dried products that are lyophilized in vials, both the apparent (bulk) density taking the dimensions of the cake into consideration, as well as the true density as determined by helium pycnometry, that is related to the internal degrees of freedom and that thus reflects the molecular mobility within the glassy solid, are of importance.

In the present study, the effect of cake collapse on both the volume and the density of the intact cake and the lyophilized powder were investigated.

5.1 EFFECT OF COLLAPSE ON THE INTACT CAKE: PARTIALLY CRYSTALLINE LYOPHILIZATES

5.1.1 POROSITY

In an attempt to quantify the degree of cake shrinkage, the complete lyophilizate was transferred into the pycnometer chamber and the cake volume was determined. In order to evaluate whether there is a continuous decrease of specific volume with increasing degree of macroscopic collapse, samples consisting of various ratios of mannitol to sucrose (Figure 5.1) were analyzed. Figure 5.7 depicts a completely collapsed cake (1) and a non-collapsed cake (2) as an example. Clearly, the greatly altered structure of the collapsed lyophilizate can be recognized.

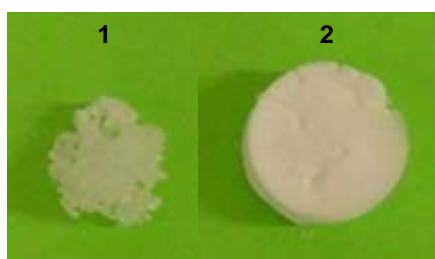


Figure 5.7: A completely collapsed lyophilizate formulated at a mannitol to sucrose ratio of 1:4 (1) and a non-collapsed cake formulated at a mannitol to sucrose ratio of 4:1 (2).

A steady decrease in specific volume was observed with increasing degree of collapse (data not shown).

As a further measure for the degree of collapse the parameter ε is introduced in equation (5.1). It resembles the calculation of the porosity; however, since the geometric volume of each collapsed cake, which is usually assessed by measuring the cake with a caliper gauge, would be hard to measure, a fixed volume V_t (the geometric volume of the non-collapsed cake) was always taken as a reference. For this reason, the calculated value ε is called apparent porosity rather than porosity. The total volume V_t was determined by measuring the geometric dimensions of a non-collapsed cake (height and diameter) with a caliper gauge.

The true volume V_c of cakes collapsed to different degrees was determined by helium pycnometry. The apparent porosity ε then refers to the fraction of pore volume in the complete cake as compared to a non-collapsed cake. In addition, the decrease in specific volume is also considered in equation (5.1).

$$\varepsilon = 1 - \frac{V_c}{V_t} \quad (5.1)$$

Figure 5.8 A depicts the apparent porosities of differently collapsed cakes. An almost linear decrease in apparent product porosity is observed with increasing degree of collapse, i.e. from mannitol to sucrose ratios from 4:1 (designated 4 in Figure 5.8 A) to 1:4 (designated 0.25 in Figure 5.8 A). However, the lyophilizate containing the lowest amount of mannitol,

thus the highest degree of collapse showed a deviating apparent porosity. This was most probably for two reasons: The occurrence of foaming in the maximally collapsed system might cause an increase in volume and the re-opening of formerly closed pores opposing the effect of collapse. In addition, results were distorted by the fact that foamed samples could not be completely removed from the vial, resulting in decreased absolute samples masses.

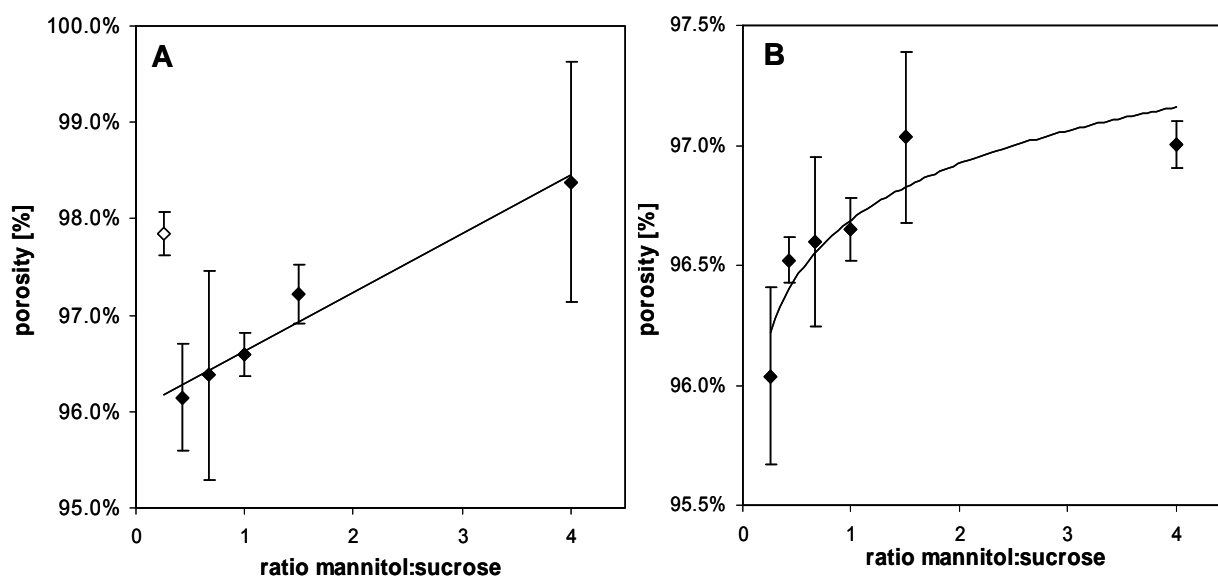


Figure 5.8: Porosity of mannitol-sucrose-based lyophilizates calculated using the true and the geometrical volume (A) and the true and apparent density (B); $n = 3$.

The geometric volume was determined from a non-collapsed cake.

open diamond: completely collapsed formulation, porosity increased because of the onset of foaming.

In order to correct for the variable samples masses of completely collapsed cakes, the true density and the apparent density rather than the volumes were applied to calculate ε according to equation (5.2).

$$\varepsilon = 1 - \frac{\rho_{bs}}{\rho_{ps}} \quad (5.2)$$

Where ρ_{bs} is the bulk or apparent density calculated from the geometric dimensions of the cake and its weight and ρ_{ps} is the true density of the solid determined by helium pycnometry. Figure 5.8 B displays the density-based apparent porosities versus the mannitol-sucrose-ratio, showing a continuous decrease of apparent porosity with decreasing mannitol-amount and thus increasing degree of collapse.

Thus pycnometry measurements further confirmed mercury porosimetry measurements and the hypothesis that collapse leads to closure of pores and thus a decreased porosity, providing a further method applicable to the quantification of collapse. However, as already observed during mercury porosimetry measurements, the change in porosity, observed upon the onset of collapse is less pronounced than the variation in the specific surface area, rendering the method less sensitive. There are no porosity values of disaccharide based lyophilizates available in literature, but Krokida et al. reported a decrease in porosity ranging

between 70 % and 95 % upon drying at various temperatures both below and above the collapse temperature¹⁶.

5.1.2 DENSITY

Regarding the true densities of complete cakes as determined by helium pycnometry, interestingly, densities decreased with increasing degree of collapse, in contrast to the widespread opinion that collapse leads to an increase in bulk density¹⁶. Table 5.3 lists the helium densities for different mannitol-sucrose ratios.

Table 5.3: Specific surface area (SSA), density and porosity of lyophilizates comprising of different ratios mannitol to sucrose (average +/- SD, n = 3 (BET measurements)/ n = 2 (density measurements)).

ratio mannitol:sucrose	SSA \pm SD [cm ² /g] ^{a)}	density \pm SD [g/cm ³] ^{b)}
4	3.06 \pm 0.16	1.880 \pm 0.062
2.33	2.68 \pm 0.30	1.772 \pm 0.052
1.5	1.78 \pm 0.34	1.683 \pm
1	1.07 \pm 0.14	1.683 \pm 0.066
0.67	0.47 \pm 0.12	1.668 \pm 0.172
0.43	0.16 \pm 0.01	1.620 \pm 0.045
0.25	0.15 \pm 0.01	1.430 \pm 0.136

a) determined by BET krypton gas adsorption

b) determined by helium pycnometry analyzing the intact, not-ground cake

As it is discussed in detail in the following section, true powder density, analyzing ground powder rather than the intact cake, indeed was increased in collapsed cakes.

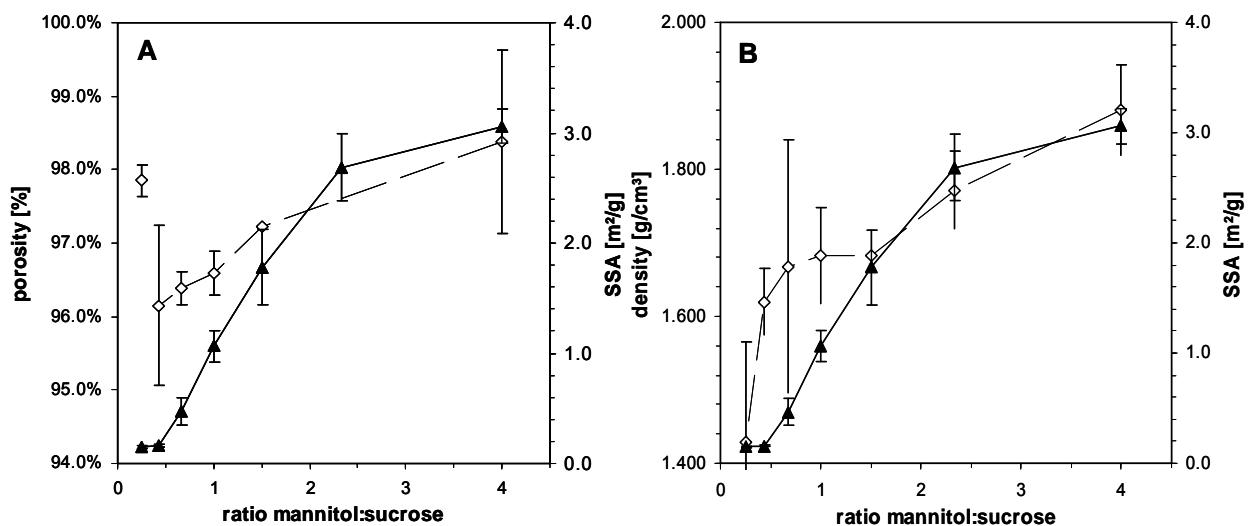


Figure 5.9: correlation of SSA (triangles) as determined by Krypton gas adsorption with porosity (diamonds) (A) and true helium-density (diamonds) (B) as determined by Helium-pycnometry for lyophilizates composed of different ratios of mannitol to sucrose.

Thus the apparent decrease in density observed during analysis of intact cakes was caused by the collapse of surface pores resulting in the formation of air-filled cavities simulating a

decrease in density. A similar observation was reported by Rahman et al. regarding the drying of apples³⁰.

Interestingly, both material properties, i.e. the decrease in porosity and density correlated qualitatively well with the degree of collapse as measured by the specific surface area, as depicted in Figure 5.9 A and B. As the change in density is more pronounced than the change in porosity, the density seemed to be a more sensitive analytic measure, but still, the specific surface area remained the most sensitive material property for the quantification of cake collapse.

5.2 EFFECT OF COLLAPSE ON THE PARTICLE DENSITY: AMORPHOUS LYOPHILIZATES

The effect of collapse on the true density of the glassy solid was investigated analyzing the ground lyophilizate rather than the intact cake, in order to avoid biasing the results by the non-detection of enclosed cavities. The lyophilizates were ground in an agate mortar in a dry environment in order to avoid the disturbance by residual water that is extensively reported in literature to adversely affect pycnometric measurements³¹.

As the density is inversely related to the free volume of the system, the free volume can be estimated from density data. According to the free volume model, material transport in amorphous solids occurs by movement of a molecule from one void to another, thus the free volume is directly related to the probability of transport and thus the molecular mobility³².

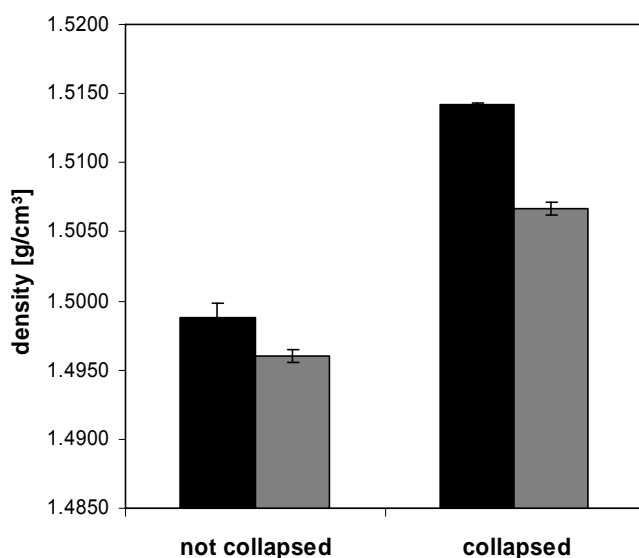


Figure 5.10: helium-densities of non-collapsed and collapsed sucrose (black bars) and trehalose (grey bars) lyophilizates; n = 3, each samples was measured 20 times.

Therefore assessing the density information regarding the free volume and the molecular mobility that is closely related to protein stability can be assessed as well. While this is beyond the scope of this chapter, the glassy dynamics of collapsed and non-collapsed protein lyophilizates will be discussed in Chapter 9 of this thesis.

Figure 5.10 depicts the densities of collapsed and non-collapsed sucrose- and trehalose-based lyophilizates that were ground prior to analysis. Most noticeably, a sharp increase in density with the onset of collapse is observed. Measured densities are in good agreement with literature reports on densities for freeze-dried sucrose-protein systems^{21,33}. It is frequently described in literature, the onset of collapse strongly increases the density of the dried material^{16,25,34}.

6 SUMMARY AND CONCLUSION

In order to establish an analytical method describing the degree of collapse that allows to put the decision whether a material has collapsed or not and if so to what extent in a more scientific way, different techniques were evaluated that analytically assess material properties that are known to change with the onset of collapse. The specific surface area, the pore diameter and volume, the specific volume, the density and the apparent porosity all show some degree of correlation to the macroscopically determined degree of collapse and thus they provide the possibility to evaluate and to quantify the degree of collapse. However, given to the fact that the specific surface area experiences the most pronounced change upon collapse, BET krypton gas adsorption has turned out to be the most sensitive analytical method for the quantification of collapse.

7 REFERENCES

1. Tsourouflis, S., Flink, J.M., and Karel, M. Loss of structure in freeze-dried carbohydrates solutions: effect of temperature, moisture content and composition. *Journal of the Science of Food and Agriculture*, **27** (6): 509-519 (1976)
2. Pikal, M.J. and Shah, S. The collapse temperature in freeze drying: dependence on measurement methodology and rate of water removal from the glassy phase. *International Journal of Pharmaceutics*, **62** (2-3): 165-186 (1990)
3. Lueckel, B., Helk, B., Bodmer, D., and Leuenberger, H. Effects of formulation and process variables on the aggregation of freeze-dried interleukin-6 (IL-6) after lyophilization and on storage. *Pharmaceutical Development and Technology*, **3** (3): 337-346 (1998)
4. MacKenzie, A.P. The physico-chemical basis for the freeze-drying process. *Developments in Biological Standardization*, **36** (Int. Symp. Freeze-Drying Biol. Prod.): 51-67 (1977)
5. Passot, S., Fonseca, F., Barbouche, N., Marin, M., arcon-Lorca, M., Rolland, D., and Rapaud, M. Effect of Product Temperature During Primary Drying on the Long-Term Stability of Lyophilized Proteins. *Pharmaceutical Development and Technology*, **12** (6): 543-553 (2007)
6. To, E.C. and Flink, J.M. 'Collapse', a structural transition in freeze dried carbohydrates. I. Evaluation of analytical methods. *Journal of Food Technology*, **13** (6): 551-565 (1978)
7. Rambhatla, S., Obert, J.P., Luthra, S., Bhugra, C., and Pikal, M.J. Cake shrinkage during freeze drying: a combined experimental and theoretical study. *Pharmaceutical Development and Technology*, **10** (1): 33-40 (2005)
8. Overcashier, D.E., Patapoff, T.W., and Hsu, C.C. Lyophilization of Protein Formulations in Vials: Investigation of the Relationship between Resistance to Vapor Flow during Primary Drying and Small-Scale Product Collapse. *Journal of Pharmaceutical Sciences*, **88** (7): 688-695 (1999)
9. Burin, L., Jouppila, K., Roos, Y.H., Kansikas, J., and Buera, M.P. Retention of beta -galactosidase activity as related to Maillard reaction, lactose crystallization, collapse and glass transition in low moisture whey systems. *International Dairy Journal*, **14** (6): 517-525 (2004)
10. Prado, S.M., Buera, M.P., and Elizalde, B.E. Structural collapse prevents beta-carotene loss in a supercooled polymeric matrix. *J Agric Food Chem*, **54** (1): 79-85 (2006)
11. Buera, M.P. and Karel, M. Effect of physical changes on the rates of nonenzymic browning and related reactions. *Food Chem.*, **52** (2): 167-173 (1994)
12. Katekawa, M.E. and Silva, M.A. Drying rates in shrinking medium: Case study of banana. *Braz.J.Chem.Eng.*, **24** (4): 561-569 (2007)
13. Hwang, M.P. and Hayakawa, K.I. Bulk densities of cookies undergoing commercial baking process. *J.Food.Sci.*, **45** 1400-1402,1407 (1980)
14. Aguilera, J.M., Levi, G., and Karel, M. Effect of water content on the glass transition and caking of fish protein hydrolyzates. *Biotechnology Progress*, **9** (6): 651-654 (1993)
15. Levi, G. and Karel, M. Volumetric shrinkage (collapse) in freeze-dried carbohydrates above their glass transition temperature. *Food Research International*, **28** (2): 145-151 (1995)
16. Krokida, M.K., Karathanos, V.D., and Maroulis, Z.B. Effect of freeze-drying conditions on shrinkage and porosity of dehydrated agricultural products. *Journal of Food Engineering*, **35** 369-380 Elsevier Science Limited (1998)
17. MacKenzie, A.P. Collapse during freeze drying - qualitative and quantitative aspects. *Freeze Drying Adv.Food Technol., [Int.Course]*, 277-307 (1975)
18. Rassis, D., Nussinovitch, A., and Saguy, I.S. Oxidation of Encapsulated Oil in Tailor-Made Cellular Solid. *Journal of Agricultural and Food Chemistry*, **48** (5): 1843-1849 (2000)

19. Chatterjee, K., Shalae, E.Y., and Suryanarayanan, R. Partially crystalline systems in lyophilization: II. Withstanding collapse at high primary drying temperatures and impact on protein activity recovery. *Journal of Pharmaceutical Sciences*, **94** (4): 809-820 (2005)
20. Johnson, R.E., Kirchoff, C.F., and Gaud, H.T. Mannitol-sucrose mixtures-versatile formulations for protein lyophilization. *Journal of Pharmaceutical Sciences*, **91** (4): 914-922 (2002)
21. Abdul-Fattah, A.M., Truong-Le, V., Yee, L., Nguyen, L., Kalonia, D.S., Cicerone, M.T., and Pikal, M.J. Drying-induced variations in physico-chemical properties of amorphous pharmaceuticals and their impact on stability (I): stability of a monoclonal antibody. *Journal of Pharmaceutical Sciences*, **96** (8): 1983-2008 (2007)
22. Abdul-Fattah, A.M., Lechuga-Ballesteros, D., Kalonia, D.S., and Pikal, M.J. The impact of drying method and formulation on the physical properties and stability of methionyl human growth hormone in the amorphous solid state. *Journal of Pharmaceutical Sciences*, **97** (1): 163-184 (2008)
23. Webb, S.D., Cleland, J.L., Carpenter, J.F., and Randolph, T.W. Effects of annealing lyophilized and spray-lyophilized formulations of recombinant human interferon-gamma. *Journal of Pharmaceutical Sciences*, **92** (4): 715-729 (2003)
24. Bhatnagar, B.S., Pikal, M.J., and Bogner, R.H. Study of the individual contributions of ice formation and freeze-concentration on isothermal stability of lactate dehydrogenase during freezing. *Journal of Pharmaceutical Sciences*, **97** (2): 787-803 (2008)
25. Anglea, S.A., Karathanos, V., and Karel, M. Low-temperature transitions in fresh and osmotically dehydrated plant materials. *Biotechnol.Prog.*, **9** (2): 204-209 (1993)
26. Bellows, R.J. and King, D.J. Product collapse during freeze drying of liquid foods. *AIChE Symposium Series*, **69** (132): 33-41 (1973)
27. Washburn, E.W. Note on a Method of Determining the Distribution of Pore Sizes in a Porous Material. *Proceedings National Academy of Sciences USA*, **7** (4): 115-116 (1921)
28. Lawrence, G.P. Measurement of pore sizes in fine-textured soils: a review of existing techniques. *Journal of Soil Science*, **28** (4): 527-540 (1977)
29. Bhugra, C., Rambhatla, S., Bakri, A., Duddu, S.P., Miller, D.P., Pikal, M.J., and Lechuga-Ballesteros, D. Prediction of the onset of crystallization of amorphous sucrose below the calorimetric glass transition temperature from correlations with mobility. *Journal of Pharmaceutical Sciences*, **96** (5): 1258-1269 (2007)
30. Rahman, M.S., Al-Zakwani, I., and Guizani, N. Pore formation in apple during air-drying as a function of temperature: Porosity and pore-size distribution. *Journal of the Science of Food and Agriculture*, **85** (6): 979-989 (2005)
31. Sun, C. A novel method for deriving true density of pharmaceutical solids including hydrates and water-containing powders. *Journal of Pharmaceutical Sciences*, **93** (3): 646-653 (2004)
32. Turnbull, D. and Cohen, M.H. Free-volume model of the amorphous:glass transition. *Journal of Chemical Physics*, **34** 120-125 (1961)
33. Wang, B., Tchessalov, S., Warne, N.W., Cicerone, M.T., and Pikal, M.J. Impact of Sucrose level on Storage Stability of Proteins in Freeze-dried Solids: II. Correlation of Aggregation Rate with protein Structure and Molecular Mobility. *Journal of Pharmaceutical Sciences*, **9999 published online** (9999): n/a-n/a (2008)
34. Krokida, M.K. and Maroulis, Z.B. Structural properties of dehydrated products during rehydration. *International Journal of Food Science and Technology*, **36** (5): 529-538 (2001)

CHAPTER 6

EFFECT OF RESIDUAL MOISTURE ON IGG₀₁-STABILITY IN THE LYOPHILIZED STATE

1 INTRODUCTION

The effect of residual water on the stability of dried protein pharmaceuticals is extensively described in literature¹⁻⁸. Water acts as a plasticizer of the amorphous state, decreasing T_g and thereby increasing molecular mobility at a given storage temperature. Furthermore, water can participate directly in degradation reactions either as a reactant (i.e. hydrolysis) or as a catalyst. Moreover, water can serve as a solvent or reaction medium⁹. On the other hand, there are reports describing decreased protein stabilities at low residual moisture levels as well. This phenomenon is referred to as over-drying^{1,4,7}.

While investigating the effect of lyophilizate collapse on protein stability it is important to closely monitor the residual moisture, in order to avoid mixing up two different phenomena – the effect of residual moisture and the possible effect of collapse. Due to the different freeze drying protocols used to prepare collapsed and non-collapsed lyophilizates, exactly equal setting of residual moisture levels in both cakes might not always be perfectly feasible. In order to be able to estimate the potential impact of differing residual moisture levels on IgG₁-stability, a comprehensive investigation was performed. For this purpose, (non-collapsed) lyophilizates with a range of different residual moisture levels from 0.7 % to 6.3 % were produced by performing freeze-drying at different primary and secondary drying shelf temperatures. All samples were produced in one freeze-drying run in order to eliminate the risk of batch to batch heterogeneities affecting the investigation. With the intention to closely mimic the existence of inherently different residual moisture levels, residual moistures were set to different values by freeze-drying at different shelf temperatures rather than by incubating lyophilized samples in defined humidity atmospheres over saturated salt solutions. Residual moisture levels were determined using the Karl Fischer direct extraction-set-up. In addition, moisture values were assessed using Near Infrared (NIR) spectroscopy, to allow for a direct correlation of residual moisture and protein-stability by first non-destructively analyzing the moisture followed by the analysis of a stability indicating parameter, such as protein aggregation by HP-SEC and secondary structure by FTIR spectroscopy.

2 PHYSICOCHEMICAL MATERIAL-PROPERTIES

The IgG₁ was formulated at 4 mg/mL in 50 mg/mL trehalose and 0.04 % polysorbate 20 in a 10 mM sodium succinate buffer at a pH of 5.5. Samples were stored at 40 °C and 50 °C for up to six months and samples were analyzed every month. Reference samples were stored at 2-8 °C in the refrigerator.

Table 6. 1: Lyophilizate formulations investigated at different residual moisture contents.

excipient	concentration
IgG01	4.0 mg/mL
trehalose	50.0 mg/mL
polysorbate 20	0.4 mg/mL
sodium succinate, pH 5.5	2.7 mg/mL

2.1 CAKE APPEARANCE

After freeze-drying, all lyophilizates were white and no shiny patches or collapse was observed, regardless of the residual moisture level (Figure 6.1 A). After storage at 40 °C and 50 °C, in the highest moisture class (6.3 %) collapse occurred to different extents, ranging from slight shrinkage to melt-back (Figure 6.1 B vials 1-4). Lyophilizates with lower residual moisture contents did not show any change in macroscopic appearance upon storage.



Figure 6.1: IgG01 lyophilizates immediately after freeze-drying with average residual moisture contents of 6.3 % (1), 3.3 % (2), 1.8 % (3) and 0.7 % (4) (A) and after 6 months of storage at 50°C (B) with average residual moisture contents of 6.3 % (1-4), 3.3 % (5), 1.8 % (6) and 0.7 % (7).

All lyophilizates remained white and no browning indicating the occurrence of glycation, was observed in any of the lyophilizates.

2.2 RESIDUAL MOISTURE

Figure 6.2 shows the residual moisture contents of the four moisture classes referred to as RM 1 to RM 4 as determined by Karl Fischer direct methanol extraction (A) and by NIR spectroscopy (B).

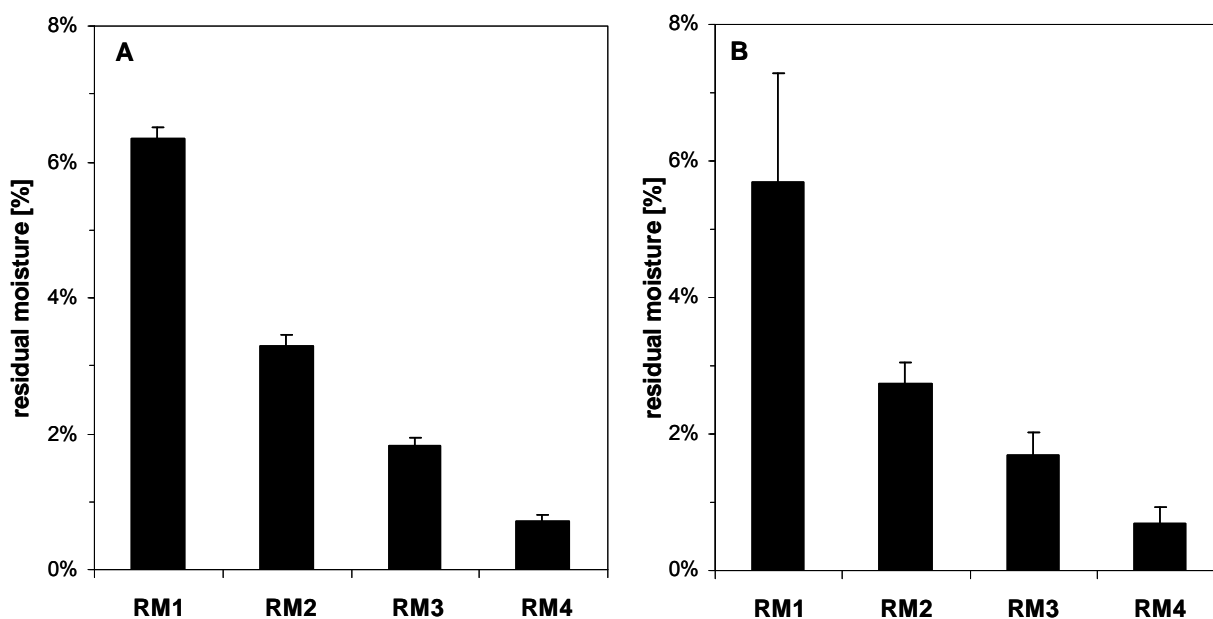


Figure 6.2: Residual moisture levels of the four residual moisture classes after freeze-drying as determined by Karl Fischer direct methanol extraction (A) and NIR spectroscopy (B).

Bars represent the calculated average of six vials \pm SD (Karl Fischer direct methanol extraction) and 50 vials (NIR spectroscopy), respectively.

The four moisture classes were distinctly different, i.e. error bars were not overlapping, and an overall good consistency was observed between the two analytical techniques. In the two upper moisture classes RM 1 and RM 2, NIR spectroscopy resulted in slightly lower average residual moisture values and larger standard deviations than Karl Fischer (5.7 % versus 6.3 % and 2.7 % versus 3.3 % for RM1 and RM2, respectively). This most probably reflected the size of the sample set (6 vials in Karl Fischer analysis versus 50 vials in NIR analysis) and the slightly increased inhomogeneity in sublimation and desorption during freeze-drying due to the larger impact of edge effects and radiation during lyophilization at lower temperatures used for the preparation of higher residual moisture levels.

However, both techniques confirmed the preparation of four sample sets with significantly different residual moisture levels.

Figure 6.3 depicts the development of residual moisture contents during storage at 50 °C. Interestingly, the highest residual moisture class showed a pronounced decrease in average residual moisture content within one month of storage. This was most probably caused by water vapor permeability of the rubber stopper or by transfer of residual water from the lyophilizate to the dried stopper. In contrast, the lyophilizates with the lowest residual moisture content (RM 4) showed a steady increase of residual moisture content during storage. This phenomenon is commonly observed during storage of freeze-dried products at elevated temperatures and is most likely also caused by water vapor permeability of the stopper and by transfer of moisture from the stopper to the dried cake^{6,10,11}.

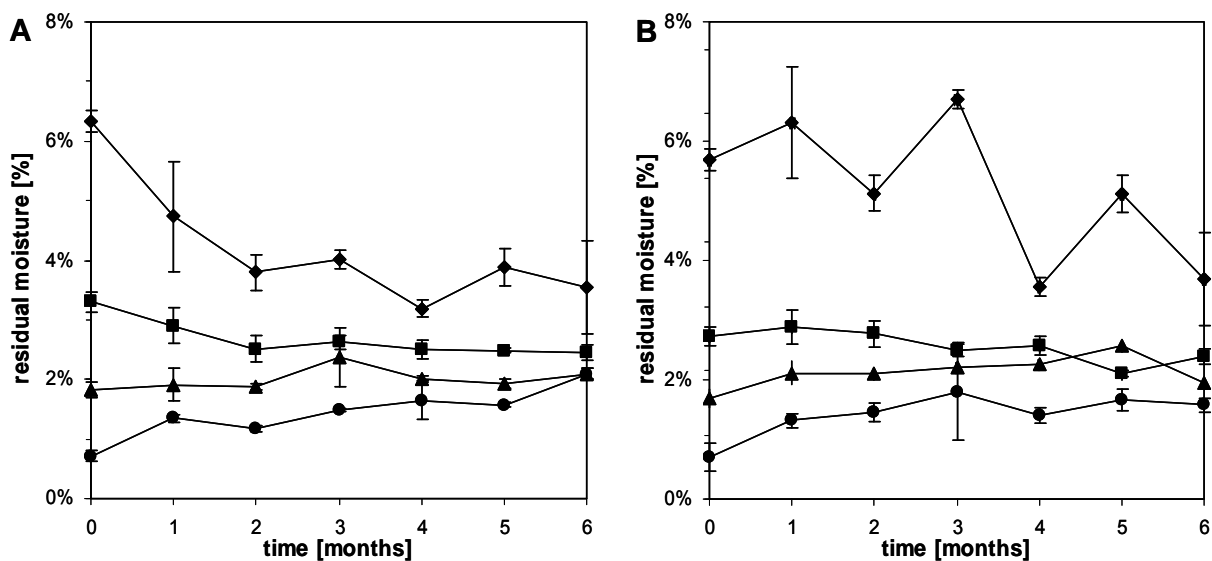


Figure 6.3: Residual moisture contents during storage at 50 °C as determined by Karl Fischer direct extraction (A) and NIR spectroscopy (B) for lyophilizates at different residual moisture levels.

RM1 (diamonds), RM2 (squares), RM3 (triangles) and RM4 (circles).

Depicted values are calculated average values of three (Karl Fischer) and 15 (NIR) independent measurements, respectively.

NIR spectroscopy showed a similar trend to Karl Fischer moisture analysis (Figure 6.3 B), although the observed decrease in residual moisture contents in the highest moisture class (RM1) was less pronounced. This again reflects the slightly increased inhomogeneity at high residual moisture contents.

Residual moisture contents also changed during storage at 40 °C and during storage at 2 - 8 °C, but the alteration was less pronounced (representative data of the highest and the lowest residual moisture class summarized in Table 6. 2).

The bottom line of the observed course of residual moisture contents is a convergence of the four initially significantly different classes. However, the four classes remain relevantly different throughout the investigated storage period.

Table 6. 2: Variation of residual moisture contents during storage: residual moisture levels of the highest (RM1) and the lowest (RM4) moisture class prior to storage and after 6 months of storage at the different storage temperatures.

storage time	storage temperature	residual moisture [%] by Karl Fischer		by NIR spectroscopy	
		RM1	RM4	RM1	RM4
0 month	n.a.	6.33 ± 0.17%	0.71 ± 0.10%	5.69 ± 1.59%	0.70 ± 0.24%
6 months	2-8°C	5.19 ± 1.08%	0.86 ± 0.06%	5.08 ± 1.07%	0.78 ± 0.12%
	40°C	4.36 ± 0.74%	1.56 ± 0.10%	4.93 ± 1.92%	1.59 ± 0.14%
	50°C	3.54 ± 0.79%	1.66 ± 0.04%	3.69 ± 1.81%	1.57 ± 0.12%

The consistency between average residual moisture contents determined by NIR and Karl Fischer, respectively, is summarized in Figure 6.4. Figure 6.4 shows representative residual

moisture values of the RM 1 and RM 4 samples determined by either Karl Fischer (solid bars) or NIR (striped bars) during storage at 2-8 °C and 50 °C

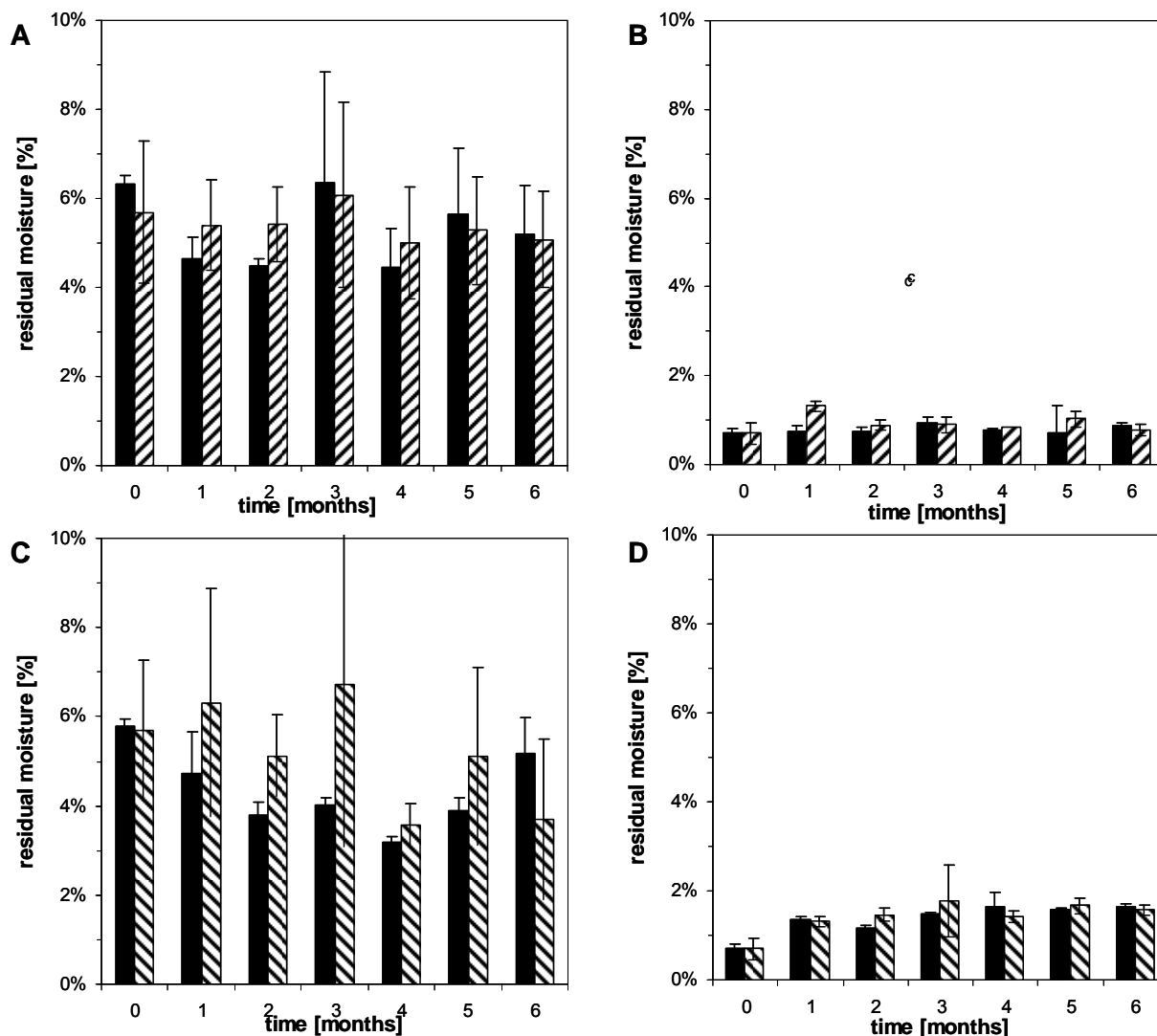


Figure 6.4: Comparison of residual moisture contents determined by Karl Fischer direct extraction (solid bars) with residual moisture contents determined by NIR spectroscopy (striped bars) in high RM-samples (RM1) stored at 2-8 °C (A) and at 50 °C (C) and low RM-samples (RM4) stored at 2-8 °C (B) and 50 °C (D). Karl Fischer n = 3, NIR n = 15.

In addition to the already discussed changes in residual moisture levels during storage, a decreasing agreement between NIR and KF results in high-moisture samples stored at 50 °C (Figure 6.4 C) catches the eye. The decrease of reproducibility and correlation between the two techniques coincides with the onset of collapse in high moisture samples. As NIR spectra are recorded in diffuse reflectance, the technique is sensitive to the matrix of the analyzed sample¹². As calibration was performed with non-collapsed samples, the occurrence of collapse alters the matrix and causes a deterioration of the NIR spectra most probably due to scattering effects.

Figure 6.5 A depicts NIR diffuse reflectance spectra of cakes that show collapse to different extents (as shown in the figure-part B). The increase of noise in the spectral region that was

used to calculate the residual moisture content (marked by a red circle in Figure 6.5 A) is clearly visible. As measurements are performed in the center of the vial bottom and as the measurement probe is small, minor extents of collapse as represented by cake A in Figure 6.5 are well tolerated by the method, as indicated by correlating residual moisture contents (3.8 % by NIR and 3.6 % by KF). With increasing extent of collapse, however, results become more and more different. Thus the onset of complete collapse results in a bias of NIR-based residual moisture results and can be regarded as the limit for the applicability of the method.

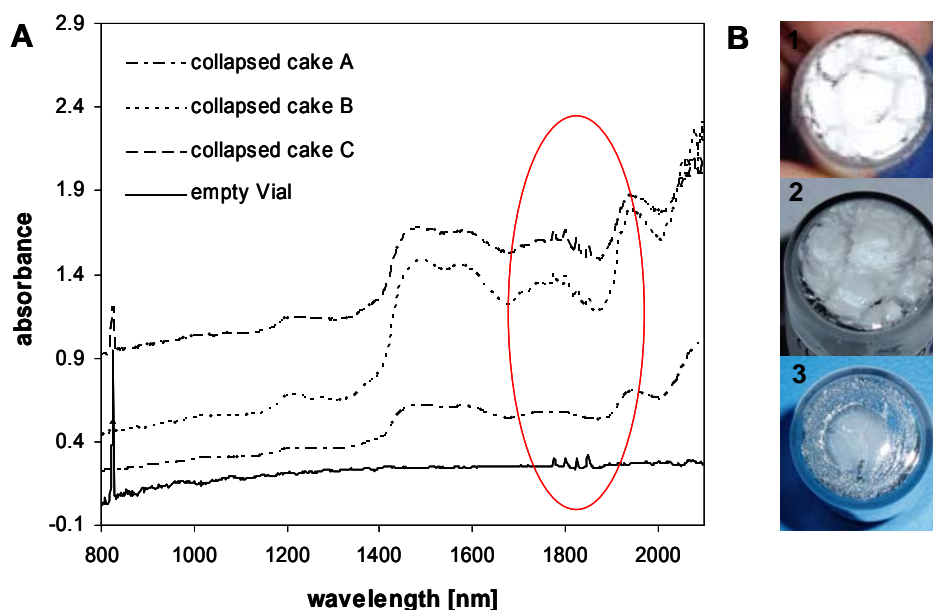


Figure 6.5: NIR spectra of collapsed lyophilizates (A) and macroscopic appearance of the corresponding lyophilizates through the vial-bottom (B).

Cake A: Figure B1 (3.8 % residual moisture determined by NIR versus 3.6 % by KF); cake B: Figure B2 (5.5 % by NIR versus 3.8 % by KF); cake C: Figure B3 (7.4 % by NIR and 4.2 % by KF). Spectral region used for the calculation of residual moisture contents is marked by a red circle.

2.3 GLASS TRANSITION & CRYSTALLIZATION

An important quality parameter of a lyophilized product is its glass transition temperature. It applies to good freeze-drying practice that lyophilizates are kept well below their glass transition during storage¹³. As different solid state degradation kinetics are often observed below and above the glass transition, accelerated stability studies should also be performed in the glassy state¹⁴.

It is well-known that water acts as a plasticizer of the amorphous state, lowering the glass transition temperature by approximately 10 K for each percent of moisture retained^{15,16}. Figure 6.6 A shows DSC thermograms of the lyophilizates comprising different residual moisture contents. Clearly, the decrease of glass transition temperatures with increasing residual moisture levels can be observed. Table 6.3 summarizes the glass transition temperatures ranging from approximately 50 °C to 85 °C. This range is in good agreement

with literature, reporting T_g -values from 40 °C to 100 °C within a moisture range of 0.5 % to 6.5 %¹⁷. The lyophilizates comprising the highest residual moisture content, namely RM 1, show an average T_g of 52.5 °C. Although this value is close to the highest storage temperature of 50 °C, investigations are still performed in the glassy state. However, as these values represent average values, the occurrence of collapse in some vials of the highest residual moisture class RM 1 indicated that these vials were stored above their T_g resulting in the occurrence of shrinkage.

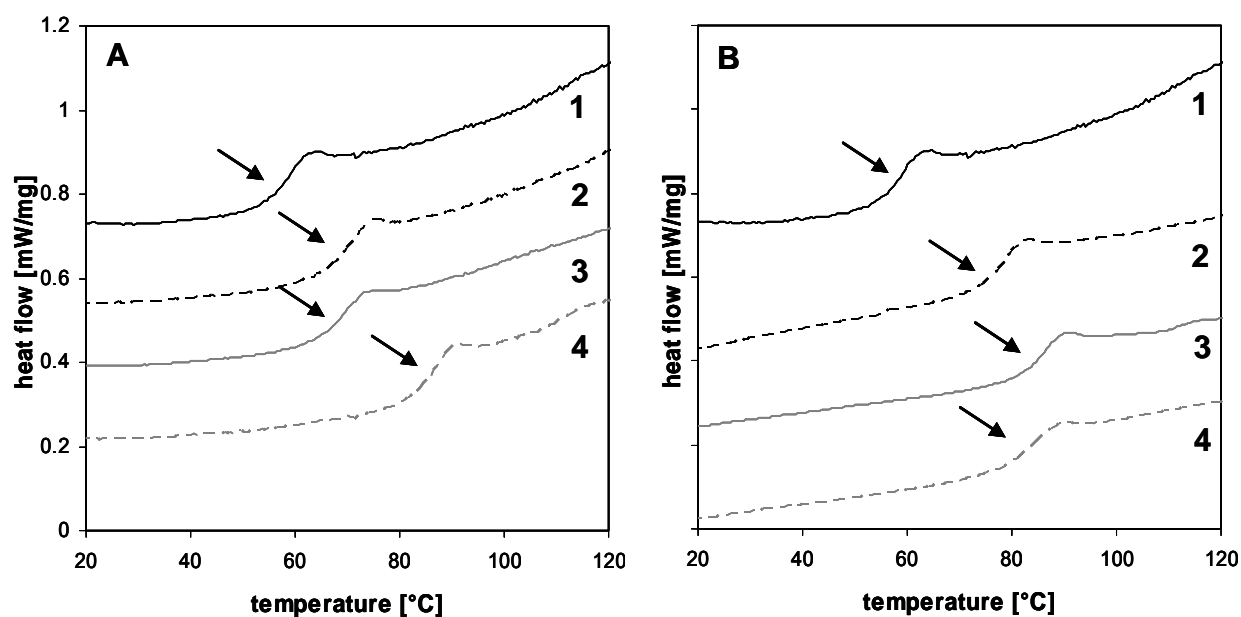


Figure 6.6: DSC thermograms of trehalose-based IgG₀₁ lyophilizates comprising different residual moisture levels (1: 6.3 % (RM1); 2: 3.3 % (RM2); 3: 1.8 % (RM3); 4: 0.7 % (RM4)) after freeze-drying (A) and after 6 months storage at 50 °C (B).

Glass transitions are marked by arrows.

Figure 6.6 B shows DSC thermograms of samples that were stored for six months at 50 °C. Most obviously, all samples remained amorphous and no crystallization occurred as no melting endotherms could be observed in the thermograms. This finding was further confirmed by XRD analysis, showing no diffractions (spectra not shown) indicating that all the lyophilizates were completely X-ray amorphous despite the onset of collapse in some samples that was reported to be associated with an increased susceptibility towards crystallization^{18,19}.

The decreased residual moisture levels of the RM 1 and RM 2-samples after storage were reflected in increased glass transition temperatures after storage as compared to the glass transition temperatures prior to storage (Table 6.3). Glass transition temperatures of the RM 3 samples (average moisture content 1.8 %) could not be clearly correlated to their residual moisture level. The low T_g observed prior to storage (68.1 °C) might most probably be regarded as outlier. No strong increase of residual moisture content occurred during storage of the RM3-samples and the T_g determined after storage (84.5 °C) is in good agreement with published T_g -values for trehalose at a moisture content of approximately

2 %²⁰. RM 4-Lyophilizates also showed low T_g -values after freeze-drying regarding their residual moisture content. Now clear depression of T_g was observed upon storage despite the considerable increase in residual moisture content. However, the measured T_g after storage corresponds well to published T_g values¹⁶. Thus the slightly low T_g prior to storage might be due to water absorption during sample preparation and might be regarded as outlier as well.

Table 6.3: Glass transition temperatures after freeze-drying and after 6 months of storage at 50 °C as determined by DSC as compared to residual moisture contents as determined by Karl Fischer direct methanol extraction (average \pm SD, n = 2 for DSC and n = 3 for KF experiments).

residual moisture level	$T_g \pm SD$ [°C] after 6 months @		Residual Moisture KF [%] after 6 months @	
	after freeze- drying	50°C	after freeze- drying	50°C
RM1	52.5 \pm 6.9	72.9 \pm 0.5	6.33 \pm 0.17	3.54 \pm 0.79
RM2	70.5 \pm 0.8	79.5 \pm 4.0	3.30 \pm 0.17	2.44 \pm 0.13
RM3	68.1 \pm 0.5	84.5 \pm 0.1	1.82 \pm 0.13	2.10 \pm 0.10
RM4	84.2 \pm 1.0	83.9 \pm 2.7	0.71 \pm 0.10	1.66 \pm 0.04

Summarizing, trehalose remained amorphous throughout the investigated period, allowing for acting as a water substitute according to the water-replacement-theory. Thus possibly observed differences in IgG₁-stability can be assigned to the differences in residual moisture content and are not affected by differences in excipient-stability.

3 PHYSICAL PROTEIN STABILITY OF IGG₀₁ IN RECONSTITUTED LYOPHILIZATES

Physical protein stability was monitored using HP-SEC and asymmetrical flow field flow fractionation (AF4). Figure 6.7 shows the amount of monomer during storage at elevated and reference temperatures as determined by HP-SEC. No loss of monomer occurred during the freeze-drying process (98.8 % \pm 0.1 % prior to lyophilization).

During subsequent storage at 2-8 °C and 40 °C, no relevant decrease in monomer content was observed (Figure 6.7 B). During storage at 50 °C, monomer contents slightly decreased. However, there was no significant difference in the monomer contents between the different residual moisture classes.

Trehalose-lyophilizates with the highest residual moisture content (RM 1) showed faintly more strongly reduced monomer contents, but results were not significantly different to monomer contents of the lowest residual moisture level (p = 0.5 in a two-tailed unpaired t-test).

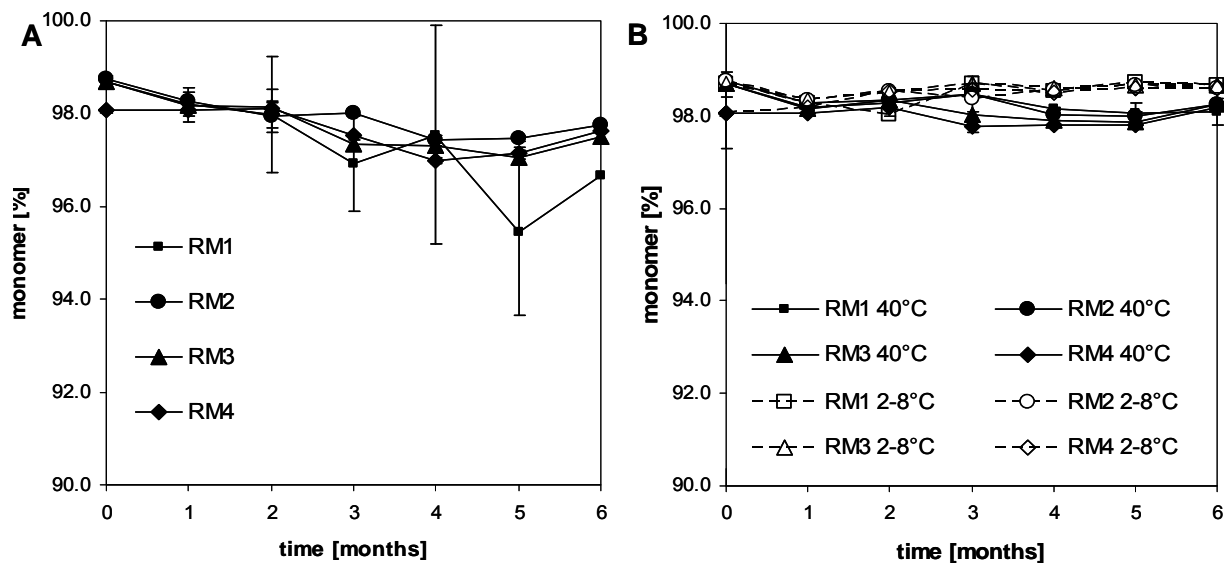


Figure 6.7: IgG₀₁ monomer as determined by HP-SEC during storage at 50 °C (A) and during storage at 40 °C and 2-8 °C (B); average \pm SD, n = 2.

As IgG₀₁ recovery in all HP-SEC experiments was complete, the existence of larger and insoluble aggregates in the investigated samples could be excluded. The absence of larger particles was further confirmed by AF4 experiments that showed comparable results to HP-SEC experiments (data not shown). SDS-PAGE further confirmed that no relevant fractions of aggregates were formed. No additional bands could be observed above the mAb main band as compared to IgG₀₁ bulk that was included in every gel as a standard (SDS-PAGE gels not shown).

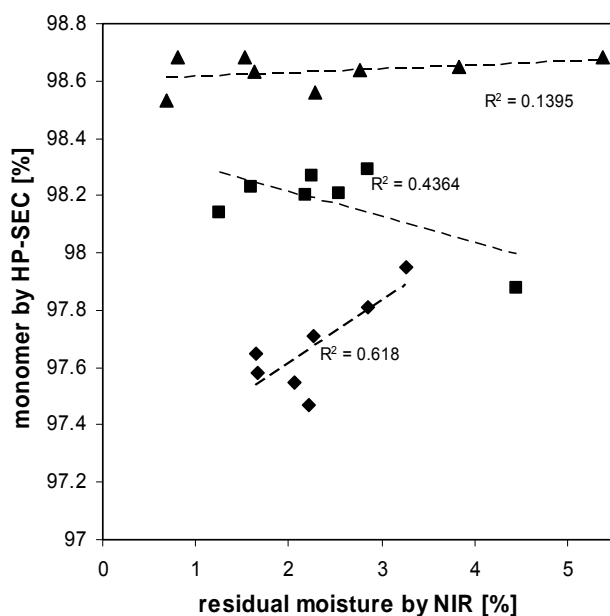


Figure 6.8: Correlation of residual moisture content and physical stability: residual moisture contents as determined by NIR-spectroscopy versus IgG monomer content of the same lyophilizate after 6 months of storage at 50 °C (diamonds), 40 °C (squares) and 2-8 °C (triangles).

NIR spectroscopy as a non-destructive technique for the determination of residual moisture contents, allowed for the direct correlation of the residual moisture content and the

aggregation level. Figure 6.8 displays the mAb-monomer content as determined by HP-SEC versus the residual moisture content of the same lyophilizate, which was previously determined using NIR spectroscopy.

No correlation of residual moisture content and physical IgG stability as determined by HP-SEC could be stated as indicated by the low correlation coefficients displayed in Figure 6.8. The same lack of correlation was observed after 1, 2, 3, 4 and 5 months of storage (data not shown). But it is important to notice that not all samples could be included in the correlation, because lyophilizates comprising the highest levels of residual moisture collapsed during storage at elevated temperatures. As outlined above, the onset of gross collapse affected the accuracy of the NIR signal and thus the determination of water content prior to HP-SEC analysis was not feasible.

However, as the IgG₀₁ did not show relevant aggregation during the period of investigation as depicted in Figure 6.7, even the highest moisture levels did not relevantly affect IgG₀₁ stability, despite the difficulties in correlation.

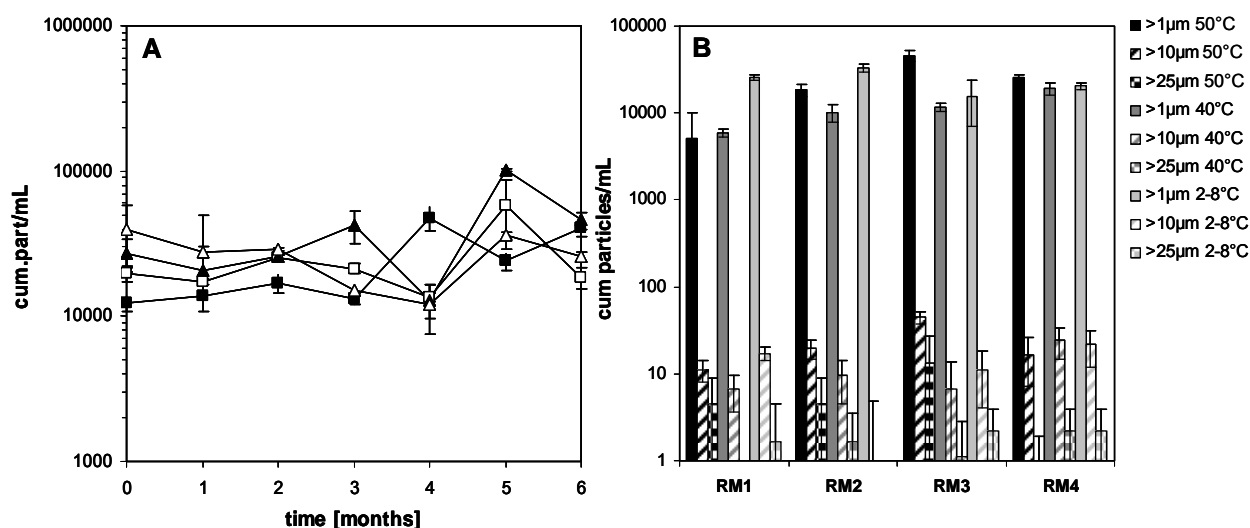


Figure 6.9: Sub-visible particles larger 1 µm as determined by light obscuration during storage at 50 °C (A) (RM1: filled squares, RM2: open squares, RM3: filled triangles, RM4: open triangles); sub-visible particles after 6 months of storage at 50 °C, 40 °C and 2-8 °C (B).

Average \pm SD, n = 2.

The formation of sub-visible and visible particles was monitored using light obscuration analysis. Figure 6.9 A displays the course of particle formation during storage at 50 °C. Particles larger 1 µm are displayed here as they are considered as indicative for protein instability²¹. Figure 6.9 B summarizes the particulate matter after 6 months of storage at different temperatures including the particle classes specified in the pharmacopeias (larger 10 µm and larger 25 µm). Most remarkably, all samples showed particle numbers well below the specifications given in the pharmacopoeias (less than 6000 particles > 10 µm, less than 600 particles > 25 µm)^{22,23} and no distinct increase of particles was observed during storage.

Although slight differences between the different moisture classes were observed, no clear correlation can be inferred between residual moisture content and particle formation.

Because all samples proved to be remarkably stable, dynamic light scattering (DLS), a technique sensitive to trace amounts of aggregates²⁴, was performed in order to further characterize the mAb solutions regarding the formation of small amounts of high molecular weight species.

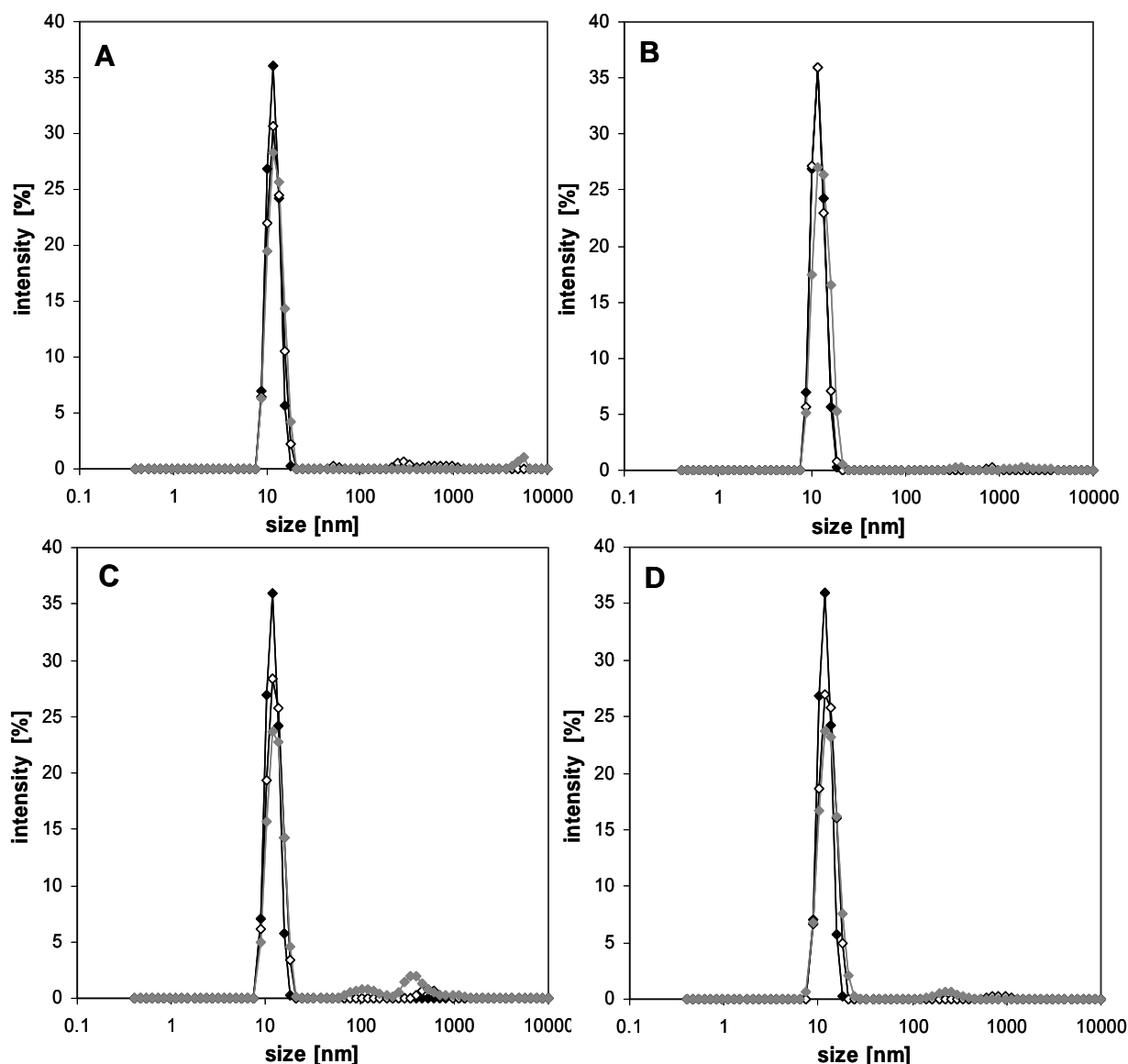


Figure 6.10: Size distribution by intensity of scattered light as determined by DLS of IgG₀₁ stored in lyophilizates with 6.3 % (A), 3.3 % (B), 1.8 % (C) and 0.7 % residual moisture after 3 (open symbols) and 6 months (grey symbols) of storage at 50 °C as compared to the solution prior to lyophilization (black symbols).

Each graph is the calculated average of two independent samples.

Interestingly, IgG₀₁ stored at lower residual moisture contents showed distinct signs of higher molecular weight (hmw) species (100 – 300 nm; Figure 6.10 C and D) after 6 months of storage at 50 °C. In contrast, IgG₀₁ stored at higher moisture contents showed no distinct hmw-fractions. This was further reflected in the mean particle size expressed by the Z-

average: IgG₀₁ reconstituted from lyophilizates with 6.3 % and 3.3 % residual moisture showed Z-average values of 12.6 nm and 13.1 nm, respectively, after 6 months of storage at 50 °C: This indicated no change as compared to the Z-average of 13.2 nm measured prior to freeze-drying and matches the hydrodynamic diameter of a mAb monomer²⁵ In contrast IgG₀₁ stored at 1.8 % and 0.7 % residual moisture exhibited Z-average-values of 19.1 nm and 21.0 nm, respectively, indicating that small amounts of hmw species were present.

However, the observed hmw fractions were small, because no second fraction could be detected in the more relevant size distribution by volume (data not shown). Also, the polydispersity indices (PDI) of the analyzed samples ranging from 0.19 to 0.28 (PDI prior to lyophilization was 0.19) indicated that the hmw-fractions present in the samples were small.

Turbidity of reconstituted lyophilizates was low, ranging from 2.0 to 2.3 FNU (data not shown) for all the samples. This further confirms the absence of insoluble aggregates.

4 CONFORMATIONAL STABILITY OF IGG₀₁ IN RECONSTITUTED LYOPHILIZATES

In addition to physical protein stability, conformational stability was analyzed as well. FTIR spectroscopy was used to assess the secondary structure and intrinsic tryptophan fluorescence spectroscopy was accomplished to get further insight into the tertiary structural changes of the IgG. Figure 6.11 A displays the area-normalized amide I FTIR second derivative transmission spectra of 4 mg/mL IgG₀₁ stored at 50 °C at various residual moisture levels for 6 months as compared to a standard IgG₀₁ solution. The main band at 1639 cm⁻¹ can be assigned to intramolecular β -sheet structures and the bands at 1687 cm⁻¹ and 1612 cm⁻¹ are associated with intermolecular β -sheet structures according to Costantino et al.²⁶. IgGs are mainly composed of β -sheet structures (approximately 70 %) with the remaining part consisting mostly of turn-structures. A detailed description of the assignment of secondary structural elements to the FTIR second derivative spectral bands is given in Chapter 7, section 2.1.4.

Examining Figure 6.11 A, most remarkably, no secondary structural differences between IgG₀₁ stored at different residual moisture contents for 6 months and an IgG₀₁ standard (protein bulk) are observed. Most important, no intensity-increase of the bands at 1612 cm⁻¹ and 1687 cm⁻¹ occurred, indicating that no intermolecular β -sheet structures, a secondary structural element frequently observed in aggregated species^{27,28}, were formed during storage.

Figure 6.11 B depicts intrinsic tryptophan fluorescence spectra of IgG₀₁ reconstituted from lyophilizates comprising different residual moisture levels prior to storage and after 6 months of storage at 50 °C as compared to IgG₀₁ standard (IgG₀₁ bulk) and the IgG₀₁ formulated drug product prior to lyophilization.

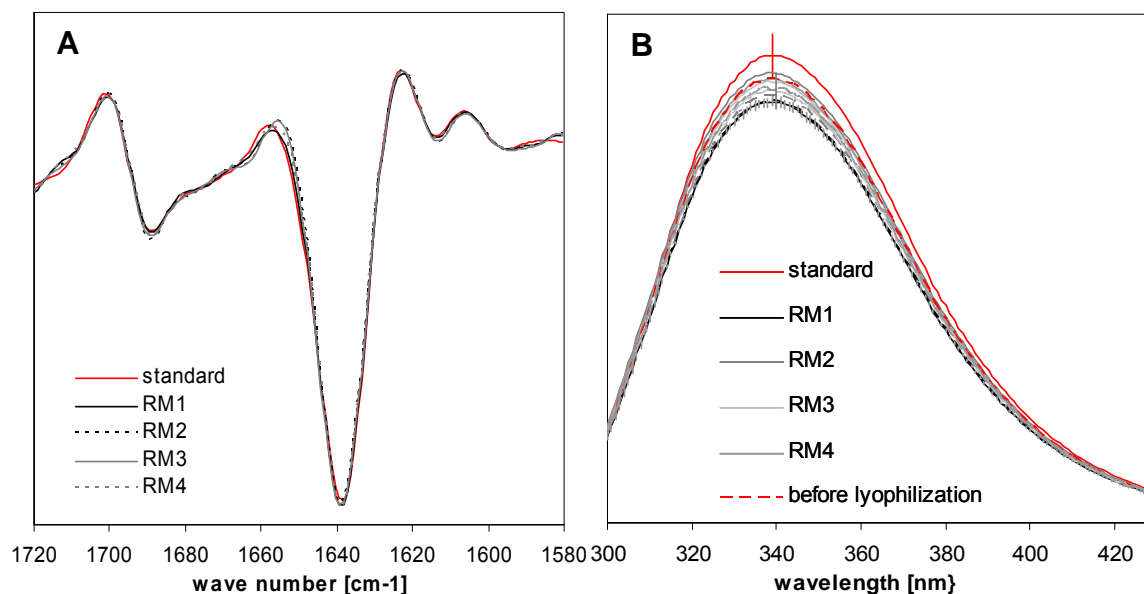


Figure 6.11: Area-normalized second derivative FTIR transmission spectra of 4 mg/mL IgG₀₁ (A) and intrinsic protein fluorescence emission spectra of 0.05 mg/mL IgG₀₁ (B) after storage at 50 °C for 6 months in the solid state and reconstitution.

All spectra are calculated average spectra of two independent measurements.

Figure 6.12 B: solid lines represent samples after 6 months of storage, dashed lines represent samples after freeze-drying, prior to storage; vertical bars represent the standard deviation of selected data points.

All spectra show an emission maximum at 338 nm that corresponds to values reported in literature for IgGs²⁹. A more detailed discussion of the assignment of tertiary structural elements to the IgG₀₁ fluorescence spectra is given in Chapter 7, section 2.1.4. No shift in the emission maximum occurred during storage, indicating that no major changes in the tryptophan-environment and thus the IgG tertiary structure took place. However, slight variations in fluorescence intensity were observed. These fluctuations were not regarded as significant, because they were within the standard deviation of the measurements, as indicated by the error bars depicted for selected data points in Figure 6.11 B.

5 EXCURSUS: DISTRIBUTION OF RESIDUAL MOISTURE IN COLLAPSED AND ELEGANT CAKES

Besides increased residual moisture levels another frequently raised concern regarding collapsed lyophilizates is the risk of inhomogeneous moisture distribution and the formation of high moisture areas^{30,31}. The residual moisture determined by Karl Fischer analysis is an average value of the complete cake. In order to investigate the distribution of moisture within the lyophilized cake and in order to evaluate the impact of collapse on this distribution, lyophilizates that were collapsed to different degrees were produced by the stepwise reduction of the content of the crystalline bulking agent mannitol and by concomitant increase of the amorphous protective agent sucrose. Figure 6.12 displays the investigated samples that are part of the so-called “collapse-series” described in Chapter 5. Formulation 1 resulted in non-collapsed cakes, lyophilizates from formulation 2 were partially collapsed and

lyophilizates from formulation 3, 4 and 5 were completely collapsed. In contrast to the cakes referred to in Chapter 5, these cakes were produced in 10 R vials in order to allow for a division into core and wall fraction or top and bottom fraction of the lyophilized cake, respectively.



Figure 6.12: Lyophilizates consisting of different ratios of mannitol to sucrose having collapsed to different extents.

1 – mannitol (M):sucrose (S) 4:1, 2 – M:S 1:1, 3 – M:S 1.5:3.5, 4 – M:S 1:4, 5 – M:S 0:5; samples were prepared in 10 R vials with a fill volume of 5 mL.

The risk of the existence of high moisture areas is supposed to be especially high at the core and at the bottom of the cake, as drying proceeds from top to bottom and from wall to core³². Thus lyophilizates were divided into a top and bottom region by cutting them in a dry nitrogen atmosphere and then determining the residual moisture content by Karl Fischer direct methanol extraction separately for each part. Also, a core and a wall sample were prepared by punching the cake in the center (again in a dry nitrogen atmosphere) and separately determining the residual moisture contents as well.

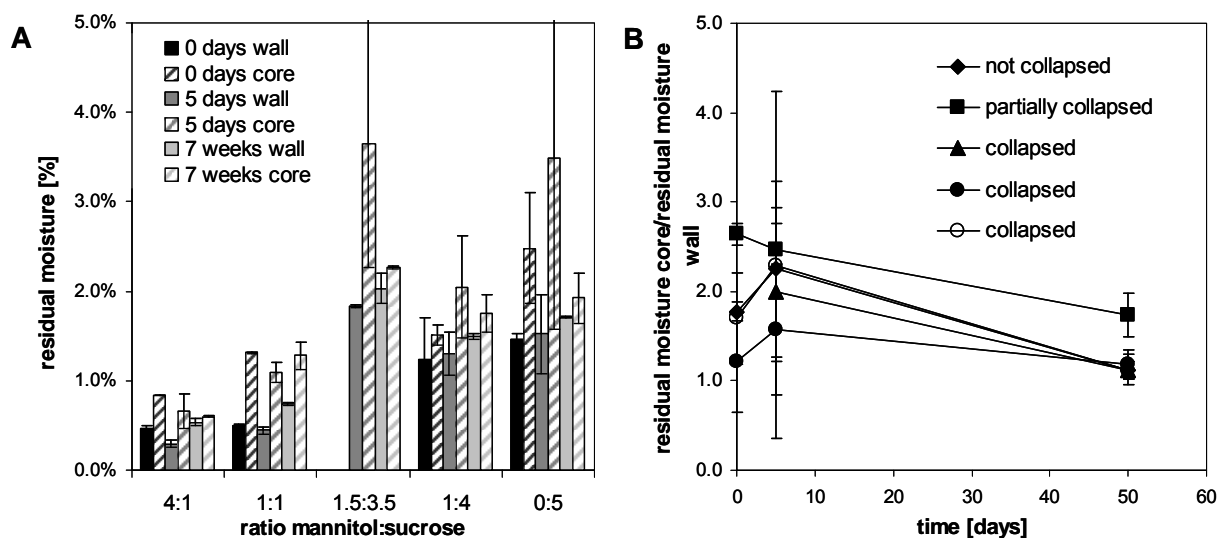


Figure 6.13: Residual moisture contents of the wall and the core section of cakes that collapsed to different extents: absolute residual moistures (A) and the ratio of residual moisture contents from the core and the wall-section (B) immediately after lyophilization and after 5 and 50 days of storage at 2-8 °C. M:S 4:S – not collapsed, M:S 1.1– partially collapsed, M:S 1.5:3.5/ M:S 1:4/ M:S 0:5 – completely collapsed.

There were no relevant differences in residual moisture contents comparing top and bottom of the lyophilizates (data not shown). In contrast, when comparing core and wall section of the lyophilized cakes, distinct differences were observed (Figure 6.13). A similar observation was reported earlier by Pikal et al³². Interestingly, this discrepancy was observed no matter

whether the cakes collapsed or not, although the difference was less pronounced in the non-collapsed cakes. The strongest difference was observed in partially collapsed cakes.

Upon storage this gradient in residual moisture dissipated, but it was still discernible after 5 days of storage at 2-8 °C. However, after 50 days of equilibration time, residual moisture was evenly distributed throughout the cake, except for partially collapsed cakes that still showed some disparity.

Completely collapsed cakes thus did not show a relevantly increased inhomogeneity in residual moisture distribution as compared to non-collapsed cakes.

In addition, even the highest local residual moisture contents did not exceed 6.3 %, a moisture content that has previously been shown not to adversely affect IgG₀₁ stability (see section 2 of this chapter). Thus even if locally increased residual moisture contents could not be detected by Karl Fischer analysis of the complete cake, a local damage of mAb stability due to increased moisture contents is not regarded critical.

6 SUMMARY AND CONCLUSION

While investigating the effect of collapse on protein stability, it is of utmost importance to closely monitor the residual moisture content of the lyophilized cakes in order to avoid mixing up a possible effect of collapse and the effect of moisture on solid state protein stability, the latter being well-described in literature to adversely affect protein stability¹⁻⁸. IgG₀₁ stability in the lyophilized state was studied over a wide range of residual moisture contents (0.7 % to 6.3 %) in order to evaluate the exact effect of moisture on IgG₀₁ stability and in order to assess the impact of subtle differences in moisture contents of collapsed and non-collapsed lyophilizates observed during this thesis.

Trehalose-based non-collapsed IgG₀₁ lyophilizates were stored at 40 °C and 50 °C for up to six months and reference samples were stored at 2-8 °C. By using NIR spectroscopy as a non-destructive tool for 100 % residual moisture analysis, a direct correlation of residual moisture and stability-indicating parameters, such as aggregate level or secondary structure, could be performed.

There was no effect of residual moisture on IgG₀₁ stability observed. All samples showed comparable physical and conformational protein stability over the investigated residual moisture range and no correlation between residual moisture and any stability parameter could be stated. A similar observation was made by Breen et al. who also described no effect of residual moisture on physical mAb-stability¹. However, due to water vapor permeability of the rubber stopper, water contents in high-residual moisture lyophilizates decreased and water contents in low-residual moisture samples increased during storage, thereby narrowing the actually investigated residual moisture range. Nevertheless, the analyzed moisture range still covered all relevant residual moisture levels usually observed during lyophilization and in this thesis.

Summarizing, slight differences in residual moisture levels that were observed between collapsed and non-collapsed lyophilizates in some studies of this thesis, are not regarded as critical, as no relevant effect of residual moisture on IgG₀₁ stability was observed using a wide range of moisture levels. However, in order to keep collapsed and non-collapsed lyophilizates as close as possible, residual moisture contents should be maintained as similar as possible.

7 REFERENCES

1. Breen, E.D., Curley, J.G., Overcashier, D.E., Hsu, C.C., and Shire, S.J. Effect of moisture on the stability of a lyophilized humanized monoclonal antibody formulation. *Pharmaceutical Research*, **18** (9): 1345-1353 (2001)
2. Chang, L., Shepherd, D., Sun, J., Tang, X., and Pikal, M.J. Effect of sorbitol and residual moisture on the stability of lyophilized antibodies: Implications for the mechanism of protein stabilization in the solid state. *Journal of Pharmaceutical Sciences*, **94** (7): 1445-1455 (2005)
3. Earle, J.P., Bennett, P.S., Larson, K.A., and Shaw, R. The effects of stopper drying on moisture levels of Haemophilus influenzae conjugate vaccine. *Developments in Biological Standardization*, **74** (Biol. Prod. Freeze-Drying Formulation): 203-210 (1992)
4. Hsu, C.C., Ward, C.A., Pearlman, R., Nguyen, H.M., Yeung, D.A., and Curley, J.G. Determining the optimum residual moisture in lyophilized protein pharmaceuticals. *Developments in Biological Standardization*, **74** (Biol. Prod. Freeze-Drying Formulation): 255-271 (1992)
5. Jiang, S. and Nail, S.L. Effect of process conditions on recovery of protein activity after freezing and freeze-drying. *European Journal of Pharmaceutics and Biopharmaceutics*, **45** (3): 249-257 (1998)
6. Lueckel, B., Helk, B., Bodmer, D., and Leuenberger, H. Effects of formulation and process variables on the aggregation of freeze-dried interleukin-6 (IL-6) after lyophilization and on storage. *Pharmaceutical Development and Technology*, **3** (3): 337-346 (1998)
7. Pikal, M.J., Dellerman, K., and Roy, M.L. Formulation and stability of freeze-dried proteins: effects of moisture and oxygen on the stability of freeze-dried formulations of human growth hormone. *Developments in Biological Standardization*, **74** (Biol. Prod. Freeze-Drying Formulation): 21-38 (1992)
8. Towns, J.K. Moisture content in proteins: its effects and measurement. *Journal of Chromatography, A*, **705** (1): 115-127 (1995)
9. Lai, M.C. and Topp, E.M. Solid-state chemical stability of proteins and peptides. *Journal of Pharmaceutical Sciences*, **88** (5): 489-500 (1999)
10. House, J.A. and Mariner, J.C. Stabilization of rinderpest vaccine by modification of the lyophilization process. *Developments in Biological Standardization*, **87** 235-244 (1996)
11. Jennings, T.A. Managing the risk of residual moisture on lyophilized products from elastomer closures. *J.Process Anal.Chem.*, **10** (2): 44-49 (2008)
12. Lin, T.P. and Hsu, C.C. Determination of residual moisture in lyophilized protein pharmaceuticals using a rapid and non-invasive method: near infrared spectroscopy. *PDA journal of pharmaceutical science and technology / PDA*, **56** (4): 196-205 (2002)
13. Hancock, B.C., Shamblin, S.L., and Zografi, G. Molecular mobility of amorphous pharmaceutical solids below their glass transition temperatures. *Pharmaceutical Research*, **12** (6): 799-806 (1995)
14. Duddu, S.P. and Dal Monte, P.R. Effect of glass transition temperature on the stability of lyophilized formulations containing a chimeric therapeutic monoclonal antibody. *Pharmaceutical Research*, **14** (5): 591-595 (1997)
15. Angell, C.A. Formation of glasses from liquids and biopolymers. *Science (Washington, D.C.)*, **267** (5206): 1924-1935 (1995)
16. Hatley, R.H.M. Glass fragility and the stability of pharmaceutical preparations-excipient selection. *Pharmaceutical Development and Technology*, **2** (3): 257-264 (1997)
17. Kawai, K. and Suzuki, T. Stabilizing Effect of Four Types of Disaccharide on the Enzymatic Activity of Freeze-dried Lactate Dehydrogenase: Step by Step Evaluation from Freezing to Storage. *Pharmaceutical Research*, **24** (10): 1883-1890 (2007)
18. Burin, L., Jouppila, K., Roos, Y.H., Kansikas, J., and Buera, M.P. Retention of beta -galactosidase activity as related to Maillard reaction, lactose crystallization, collapse and glass transition in low moisture whey systems. *International Dairy Journal*, **14** (6): 517-525 (2004)

19. Te Booy, M.P.W.M., De Ruiter, R.A., and De Meere, A.L.J. Evaluation of the physical stability of freeze-dried sucrose-containing formulations by differential scanning calorimetry. *Pharmaceutical Research*, **9** (1): 109-114 (1992)
20. Adler, M. and Lee, G. Stability and Surface Activity of Lactate Dehydrogenase in Spray-Dried Trehalose. *Journal of Pharmaceutical Sciences*, **88** (2): 199-208 (1999)
21. Carpenter, J.F., Randolph, T.W., Jiskoot, W., Crommelin, D.J.A., Middaugh, C.R., Winter, G., Fan, Y.X., Kirshner, S., Verthelyi, D., Kozlowski, S., Clouse, K.A., Swann, P.G., Rosenberg, A., and Cherney, B. Overlooking subvisible particles in therapeutic protein products: gaps that may compromise product quality. *Journal of Pharmaceutical Sciences*, **98** (4): 1201-1205 (2009)
22. Ph.Eur. 2.9.19. Particulate contamination: Sub-visible particles, 6th edition. *European Directorate for the Quality of Medicine (EDQM)* (2008)
23. USP 2008 USP/NF general chapter <788> particulate matter in injections. *Ed. Rockville, MD: United States Pharmacopoeial Convention* (2008)
24. Demeester, J., De Smedt, S.S., Sanders, N.N., and Haustraete, J. Light scattering. *Biotechnology: Pharmaceutical Aspects*, **3** (Methods for Structural Analysis of Protein Pharmaceuticals): 245-275 (2005)
25. Mahler, H.C., Mueller, R., Friess, W., Delille, A., and Matheus, S. Induction and analysis of aggregates in a liquid IgG1-antibody formulation. *European Journal of Pharmaceutics and Biopharmaceutics*, **59** (3): 407-417 (2005)
26. Costantino, H.R., Andya, J.D., Shire, S.J., and Hsu, C.C. Fourier-transform infrared spectroscopic analysis of the secondary structure of recombinant humanized immunoglobulin G. *Pharmaceutical Sciences*, **3** (3): 121-128 (1997)
27. Costantino, H.R., Schwendeman, S.P., Griebenow, K., Klibanov, A.M., and Langer, R. The Secondary Structure and Aggregation of Lyophilized Tetanus Toxoid. *Journal of Pharmaceutical Sciences*, **85** (12): 1290-1293 (1996)
28. Dong, A., Prestrelski, S.J., Allison, S.D., and Carpenter, J.F. Infrared Spectroscopic Studies of Lyophilization- and Temperature-Induced Protein Aggregation. *Journal of Pharmaceutical Sciences*, **84** (4): 415-424 (1995)
29. Taschner, N., Mueller, S.A., Alumalla, V.R., Goldie, K.N., Drake, A.F., Aebi, U., and Arvinte, T. Modulation of antigenicity related to changes in antibody flexibility upon lyophilization. [Erratum to document cited in CA136:107411]. *Journal of Molecular Biology*, **312** (3): 579(2001)
30. Bellows, R.J. and King, D.J. Product collapse during freeze drying of liquid foods. *AIChE Symposium Series*, **69** (132): 33-41 (1973)
31. MacKenzie, A.P. Collapse during freeze drying - qualitative and quantitative aspects. *Freeze Drying Adv. Food Technol., [Int. Course]*, 277-307 (1975)
32. Pikal, M.J. and Shah, S. Intravial distribution of moisture during the secondary drying stage of freeze drying. *PDA journal of pharmaceutical science and technology / PDA*, **51** (1): 17-24 (1997)

CHAPTER 7

EFFECT OF COLLAPSE ON PROTEIN STABILITY I: STABILITY AFTER FREEZE-DRYING

1 INTRODUCTION

In the production of lyophilized products it is common thinking that the occurrence of collapse has to be avoided by any means. The most severe concern regarding the onset of collapse is its suspected detrimental effect on protein stability. As discussed in detail in the general introduction of this thesis there are only few investigations dealing with the effect of the collapse on protein stability and even fewer pointing out a clear negative effect. What is more, some investigations acted out on this subject suggest that collapse itself does not necessarily result in loss of protein stability¹⁻³.

Because there is no comprehensive study on the effect of collapse on protein stability carried out with a broad range of analytical tools performed so far, it is the objective of this chapter to investigate the impact of the onset of collapse during the freeze-drying run on the stability of protein pharmaceuticals. An ample set of analytical techniques was used to provide profound data to allow a scientific-based evaluation of possible effects of collapse.

While investigating the effects of collapse on protein stability, it is important to closely monitor the residual moisture content of the cakes in order to avoid mixing up two different phenomena – the collapse itself and the storage at high residual moisture contents, which is thoroughly reported in literature to destabilize proteins^{4,5}.

An antibody of the IgG₁-class was used as a model protein because antibodies currently are the largest and most important class of protein pharmaceuticals on the market. L-Lactic Dehydrogenase (LDH) was used as a second model protein because of its well reported sensitivity towards the various stress situations during freeze-drying⁶⁻¹⁰. A third model protein was investigated with PA₀₁, an important protein pharmaceutical which formulation is reported to easily undergo partial collapse and therefore is difficult to freeze-dry.

2 IgG₀₁

A monoclonal antibody of the IgG1-class was used as model protein. Antibodies currently are the largest and most important class of biopharmaceuticals. There are more than 30 approved antibodies on the US market¹¹ and an estimated 200 or more antibody products are in development¹². Despite the homogeneity of large parts of their molecular structure, each antibody requires personalized development strategies. Although antibodies usually are remarkably stable towards various degradation pathways and can often be sufficiently stabilized to be marketed in the liquid state, there are antibody products that have to be lyophilized to ensure satisfactory stability. The importance of the addition of an adequate stabilizing excipient has been reported by several researchers^{4,13,14}, demonstrating the protein's sensitivity towards stress situations arising during freeze-drying. Thus a compromised formulation, as it is worried about with the onset of collapse, would result in detectable changes in physical or chemical protein stability.

2.1 AMORPHOUS SYSTEMS

Freeze-dried formulations usually require an amorphous excipient for the adequate stabilization of the protein active ingredient¹⁵. They serve as a water substitute by hydrogen-bonding to the protein molecule and thereby stabilizing its three-dimensional structure (water replacement hypothesis)¹⁶⁻¹⁸. Furthermore, they serve as a glassy matrix separating protein molecules from each other and reducing the molecular mobility of other reactive species (vitrification hypothesis)¹⁹⁻²¹. Sometimes a crystalline component, such as mannitol or glycine is added to increase the mechanical stability of the cake^{1,22,23}.

Each additional ingredient renders the system more complex. Because the effect of collapse on protein stability is not yet well understood, investigations were first carried out in formulations comprising of just an amorphous excipient. These formulations are both typical examples of freeze-drying formulations and not too complex to allow a sound investigation of just the effect of collapse on protein stability. In a second step, investigations were carried out on partially crystalline formulations as well, because partially crystalline systems are the second important formulation principle of freeze-drying formulations. The results obtained from these investigations shall be discussed in section 2.2.

Amorphous formulations composed of either sucrose or trehalose (serving as both cryo- and lyo-protectants) were investigated, because they are most commonly used for freeze-dried formulations^{24,25}. Two different pH values were investigated: pH 5.5 and pH 3.5. The pH range from 5 – 6.5 has been reported to be the most appropriate for most antibody products and is most commonly used in marketed formulations¹². However, in our studies it was found that the IgG₀₁ exhibits a greater sensitivity towards stress situations during freeze-drying at more acidic conditions (Figure 7.1).

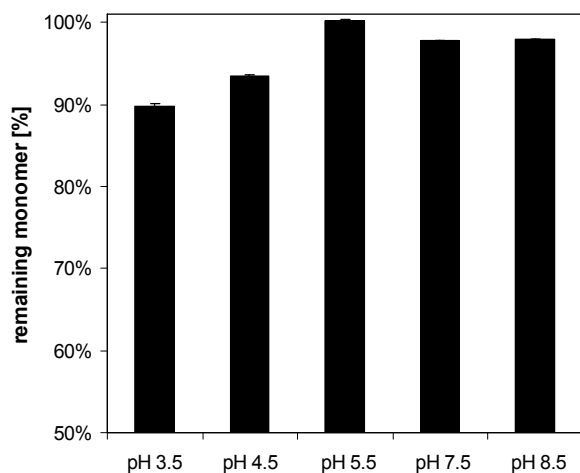


Figure 7.1: Remaining IgG₀₁ monomer after freeze-drying at different pH-values as compared to the monomer content prior to lyophilization as determined by HP-SEC (average \pm SD, n = 2).

IgG₀₁ was formulated at a concentration of 4 mg/mL in 10 mM sodium-succinate buffer at different pH values, as indicated.

Table 7.1 lists the detailed composition of the formulations used for the investigations.

Table 7.1: Amorphous IgG₀₁ formulations analyzed for the investigation of the effect of collapse on IgG₀₁ stability.

ID	cryo-/lyoprotectant	[%]	pH
1	sucrose	5%	5.5
2	sucrose	5%	3.5
3	trehalose	5%	5.5
4	trehalose	5%	3.5

The formulations were freeze-dried to gain collapsed lyophilizates using the aggressive drying cycle developed for the controlled generation of collapsed lyophilizates as described in Chapter 3 and Chapter 4 of this thesis. Pharmaceutically elegant, non-collapsed lyophilizates were produced using more gentle, conventional freeze-drying cycles as described in Chapter 3 (refer to cycles used to freeze-dry sucrose and trehalose based formulations).

2.1.1 PHYSICOCHEMICAL CHARACTERISTICS OF LYOPHILIZATES

Figure 7.2 depicts representative lyophilizates formulated at pH 5.5 obtained after gentle freeze-drying (A) and aggressive freeze-drying (B), respectively.

Lyophilizates formulated at pH 3.5 appeared identical.

While investigating the effect of collapse on protein stability it is most important to compare cakes having comparable residual moisture levels in order to avoid mixing up the effect of residual moisture and the effect of collapse. High residual moisture levels are thoroughly reported to adversely affect protein stability^{5,26,27}.

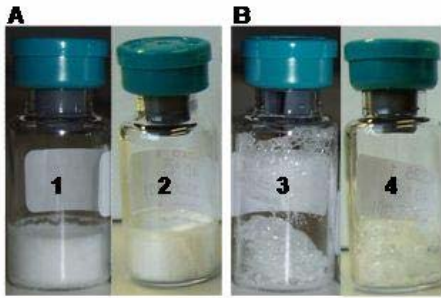


Figure 7.2: Lyophilizates obtained after gentle freeze-drying (A) and aggressive freeze-drying (B), respectively; lyophilizates contained either sucrose (vial 1, 3) or trehalose (vial 2, 4).

Lyophilizates were composed of 4 mg/mL IgG₀₁, 50 mg/mL sucrose or trehalose, 0.04 % Tween 20 in 10 mM sodium succinate buffer pH 5.5.

Lyophilizates formulated at pH 3.5 showed exactly the same appearance and are hence not additionally depicted.

Figure 7.3 depicts the residual moisture levels of the freeze-dried cakes investigated. The residual moisture levels of collapsed and elegant sucrose based cakes were perfectly comparable as can be seen from the overlapping error bars. Concerning the trehalose based lyophilizates there is a more distinct difference in residual moisture levels. As collapsed and non-collapsed lyophilizates were produced with two different drying protocols, the exact adjustment was not perfectly feasible here. However, as discussed in Chapter 6, a detailed investigation on the effect of residual moisture level on the stability of the IgG₀₁ was performed and no strong sensitivity of the IgG₀₁ towards the level of residual moisture between 0.7 and 6.3 % was found. Therefore the residual moisture levels of collapsed (1.6 % and 1.7 % for pH 5.5 and pH 3.5, respectively) and elegant (0.4 %) cakes, presented in Figure 7.3, can be regarded as comparable.

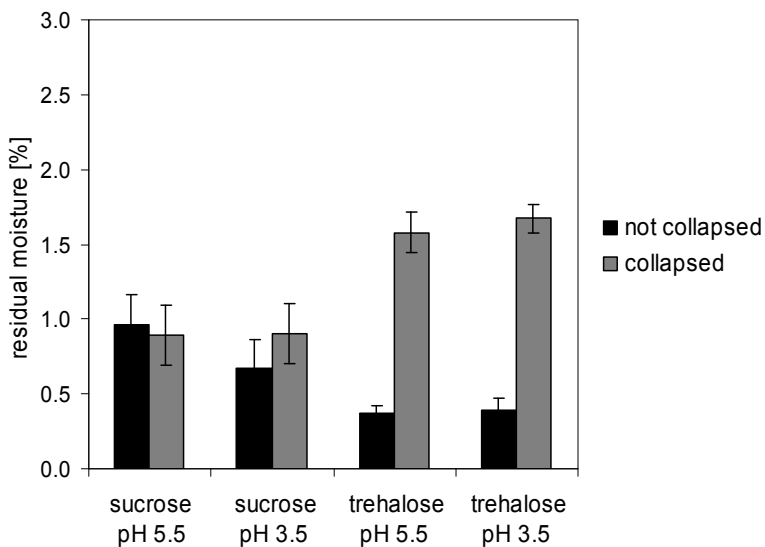


Figure 7.3: Residual moisture contents of collapsed and non-collapsed lyophilizates as determined by coulometric Karl Fischer titration in a headspace set-up (average \pm SD, n = 3).

In addition, collapsed lyophilizates having higher residual moisture contents than non-collapsed cakes constitutes the worst case scenario for collapse, which is commonly associated with resulting in lyophilizates with high residual moisture contents.

The lyophilizates were reconstituted with water and the protein stability was analyzed. A major concern regarding collapsed lyophilizates is the prolonged reconstitution time due to the decreased surface area and the increased density^{28,29}.

Table 7.2: Reconstitution times of collapsed lyophilizates after addition of 1 mL of purified water.

formulation	appearance	reconstitution time [s]
sucrose pH 5.5	not collapsed	20
sucrose pH 5.5	collapsed	9
sucrose pH 3.5	not collapsed	14
sucrose pH 3.5	collapsed	11
trehalose pH 5.5	not collapsed	10
trehalose pH 5.5	collapsed	15
trehalose pH 3.5	not collapsed	8
trehalose pH 3.5	collapsed	15

Table 7.2 shows the reconstitution times of the lyophilizates investigated. All lyophilizates were reconstituted in significantly less than one minute no matter whether the material has collapsed or not. There were no significant differences in the time needed for complete dissolution.

2.1.2 PHYSICAL PROTEIN STABILITY OF IGG₀₁ IN RECONSTITUTED LYOPHILIZATES

An important degradation pathway of lyophilized antibody formulations is aggregation^{4,14,30}. Pathways and induction factors of protein aggregation have been reviewed recently³¹. There are various aggregation pathways which may differ between proteins and may as well be different for the same protein regarding different stress conditions applied³². Protein aggregation most often has been described using the Lumry-Eyring two state model, stating that the protein first undergoes a reversible conformational change increasing its susceptibility to aggregate and then irreversibly aggregates³³⁻³⁵.

Aggregates can be either mediated through physical association of protein molecules without changes in the primary structure (physical, non-covalent aggregation) or by formation of new covalent bonds (chemical covalent aggregation) leading either directly to cross-linked multimers or altering the protein's propensity to form aggregates³⁶. Chemical aggregation is mediated most commonly by the formation of disulfide bonds but cross-linking via other functional groups such as amide groups have been reported as well³⁷. Furthermore, chemical reactions such as oxidation can alter the protein's primary structure and alter its aggregation behavior. Reaction with carbohydrates during the Maillard reaction can result in high molecular weight sugar-protein adducts considered as aggregates as well.

Initial protein aggregates are soluble but become insoluble as they exceed a certain size^{35,38}. The transition usually is smooth and differently made by different detection methods for visible and sub-visible particles or by aggregate size³⁹. Soluble aggregates may be redissolved but insoluble aggregate formation usually irreversible. Mahler et al. recently

proposed the classification into soluble aggregates including tetramers, ≥ 10 mer oligomers, aggregates from approx. 20 nm to 1 μm , insoluble particles from 1 – 25 μm and larger insoluble particles^{31,39-41}.

As the existence of insoluble particles in a parenteral pharmaceutical product causes severe quality and safety concerns, the analysis of particulate matter is of utmost importance^{42,43}. Because particles can be caused by insoluble aggregation, the thorough analysis of the aggregation behavior is crucial during biopharmaceutical dosage form development.

Since the formation of insoluble aggregates often is preceded by the formation of soluble aggregates the detection not only of insoluble but also soluble aggregates is important. A sensitive and reliable tool for the detection and quantification of soluble aggregates is high pressure size exclusion chromatography (HP-SEC)⁴⁴. The protein is injected into a gel with a defined pore size and separated by its size and therefore molecular weight while permeating through the pores.

Figure 7.4 depicts the remaining monomer fraction of IgG₀₁ reconstituted from collapsed and non-collapsed lyophilizates, respectively. The bar chart clearly shows a high monomer recovery for all formulations investigated (> 98 % for all the formulations). There was no significant difference in the monomer fractions of collapsed and non-collapsed lyophilizates and there was no such difference between formulations formulated at pH 3.5 and pH 5.5 either. As the recovery from HP-SEC experiments was complete, the existence of relevant amounts of insoluble aggregates could be excluded.

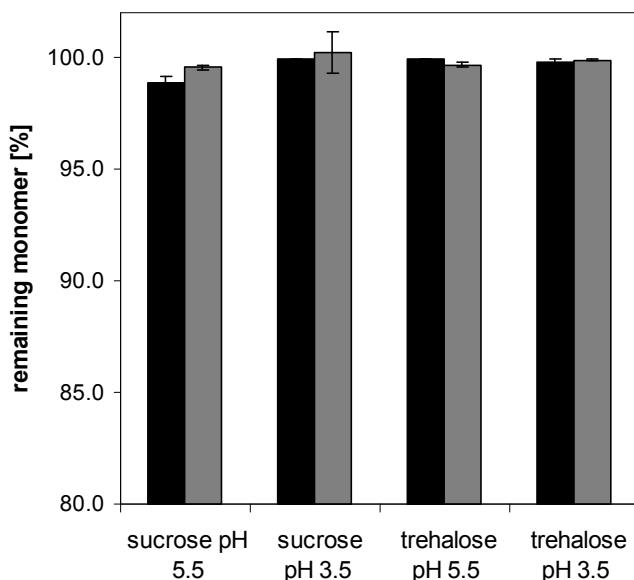


Figure 7.4: Remaining IgG₀₁ monomer after freeze-drying to collapsed (grey bars) and elegant (black bars) lyophilizates, respectively, as compared to the amount of monomer present in the solution prior to freeze-drying as determined by HP-SEC (average \pm SD, n = 2).

Asymmetric flow field flow fractionation (AF4) is another tool to analyze the physical stability of protein pharmaceuticals. As described in detail in Chapter 3, the main advantage of the AF4 technology is the large range of particle sizes that can be analyzed. Therefore sample

filtration or centrifugation prior to analysis (that is obligatory in HP-SEC sample preparation) can be omitted. As a result, soluble as well as insoluble components of a formulation, i.e. soluble and insoluble protein aggregates can be investigated. AF4 was applied as an orthogonal analytical technique for HP-SEC analysis during this thesis.

Figure 7.5 shows the AF4 fractogram of the IgG₀₁-sucrose formulation before freeze-drying and after reconstitution of collapsed and non-collapsed lyophilizates, respectively. AF4 results further confirmed HP-SEC findings: All formulations showed mostly monomer and small fractions of dimer and a fragment eluting before the monomer. There was no significant difference in the amount of monomer detectable between the samples and results were in good agreement with results obtained from HP-SEC measurements. There were no insoluble aggregates present in all the formulations as no high molecular weight fraction could be separated, further confirming HP-SEC results.

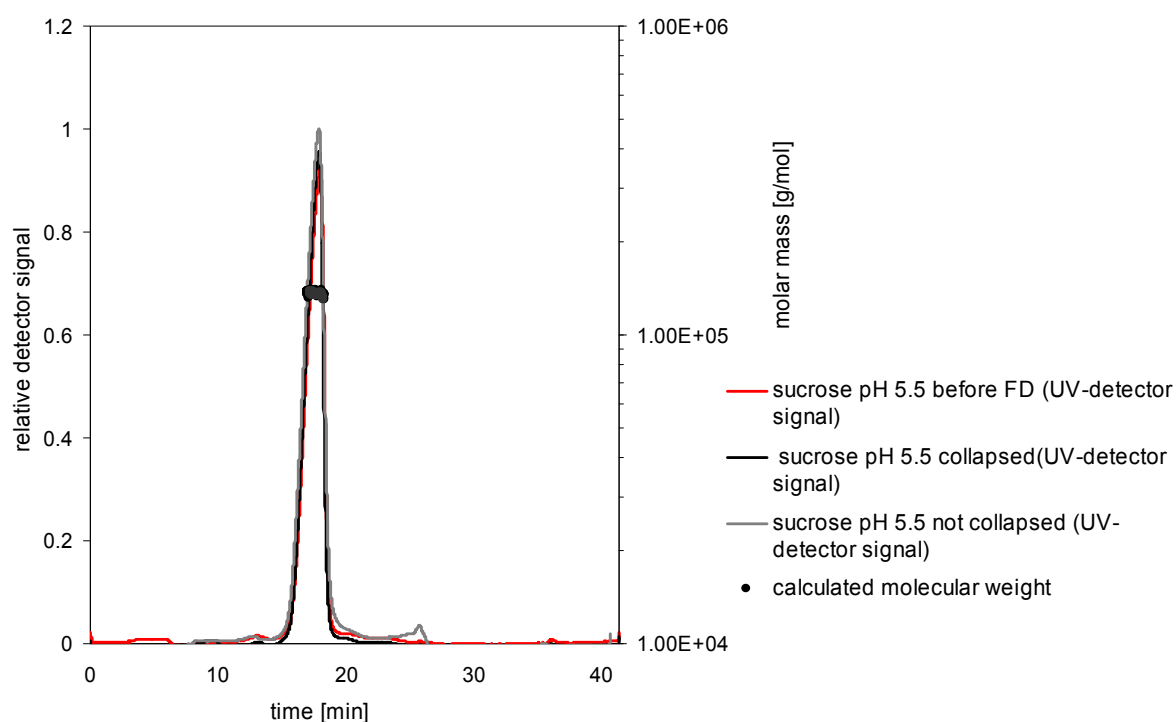


Figure 7.5: Typical AF4 fractogram of 10 µg IgG₀₁ before and after freeze-drying using either a gentle or an aggressive drying cycle.

In order to further characterize the particulate attributes of the reconstituted lyophilizates, turbidity and light obscuration experiments were performed. Table 7.3 lists the turbidity values and the number of characteristic particle classes.

Turbidity measurements present a simple but sensitive tool for the detection of insoluble aggregates in protein solutions⁴⁵. As the measurements were accomplished using a nephelometric set-up, excellent accuracy is achieved even at low absolute turbidity values⁴⁶. All solutions showed turbidity lower or equal to 2 FNU. According to the European Pharmacopoeia solutions that show a degree of opalescence lower than that of reference 1,

i.e. a turbidity of 3.2 FNU are considered as clear^{46,47}. Thus all solutions were clear, indicating that no relevant amounts of particles were present in the investigated solutions.

Light obscuration allows the analyses of sub-visible particles ranging from 1 – 200 μm . Particles are characterized by size and a relative size distribution can be obtained as well. Light obscuration has been used for the characterization of protein aggregation^{39,48}. A limitation of the method is the analysis of stretched particles and fibrils because a globular shape is assumed.

Table 7.3: Turbidity, characteristic particle populations, average particle size and polydispersity index of collapsed and non-collapsed reconstituted lyophilizates.

formulation	appearance	turbidity [FNU] ^{a)}	cumulative particles > 1 μm ^{b)}	cumulative particles > 10 μm ^{b)}	cumulative particles > 25 μm ^{b)}	Z-Average [nm] ^{c)}	PDI ^{c)}
sucrose pH 5.5	not collapsed	1.95 +- 0.17	1620 +- 738	32 +- 11	11 +- 1	12.34	0.189
	collapsed	2.00 +- 0.16	8904 +- 1327	62 +- 11	3 +- 1	16.14	0.202
sucrose pH 3.5	not collapsed	2.01 +- 0.25	1488 +- 973	21 +- 16	6 +- 8	10.94	0.105
	collapsed	1.55 +- 0.30	1544 +- 1021	18 +- 0	5 +- 4	10.78	0.107
trehalose pH 5.5	not collapsed	1.64 +- 0.18	1273 +- 515	7 +- 1	3 +- 1	11.81	0.079
	collapsed	1.61 +- 0.11	1778 +- 719	13 +- 4	1 +- 1	11.81	0.096
trehalose pH 3.5	not collapsed	1.22 +- 0.09	1543 +- 619	38 +- 13	3 +- 3	11.28	0.096
	collapsed	1.33 +- 0.06	1795 +- 547	19 +- 8	9 +- 5	10.95	0.095

a) determined by nephelometric turbidity analysis

b) determined by light obscuration; cumulative particle number per 1 mL

c) determined by dynamic light scattering using cumulants analysis

The European Pharmacopoeia (Ph.Eur.) as well as the United States Pharmacopoeia (USP) lists requirements for particles bigger or equal 10 μm and bigger or equal 25 μm only. For parenteral solutions for injection in containers comprising a volume smaller than 10 mL particle of maximum 6000 and 600, $\geq 10 \mu\text{m}$ and $\geq 25 \mu\text{m}$ respectively are allowed. Table 7.3 lists the cumulative particles $\geq 10 \mu\text{m}$ and $\geq 25 \mu\text{m}$ in 1 milliliter. All the formulations showed particle numbers well below the tolerated limit. There is no clear correlation with the onset of collapse detectable.

Dynamic light scattering (DLS) is another tool to assess the particulate characteristics of protein solutions. Particles in the size range from 1 nm to 1 μm can be analyzed. Thus the IgG₀₁ monomer whose hydrodynamic diameter was determined to be around 10 nm (data not shown) can be directly assessed. Because the scattering intensity increases six-fold with increasing diameter according light scattering offers an extremely sensitive analytical tool for the detection of smallest amounts of aggregates. Aggregate fractions below 0.01 % can be well detected⁴⁹.

Figure 7.6 shows the DLS size distribution by volume of 4 mg/mL mAb-formulations reconstituted after lyophilization to collapsed and non-collapsed lyophilizates. There was no particle fraction detectable in the size range from 100 – 1000 nm (Figure 7.6 B, D) indicating that no aggregated species were present in the formulations. Comparing collapsed and non-collapsed solutions of the same formulation there was no difference detectable. Furthermore

there was no effect of pH detectable. Trehalose-based formulations showed a slightly higher particle size at maximum intensities of 10.1 nm versus 8.7 nm for sucrose-based formulations. This could be assigned to a slightly varied three-dimensional structure of the antibody in the different formulations, as this difference in hydrodynamic radius was already observed in the solution prior to freeze-drying (data not shown). An apparent dependence of the hydrodynamic radius of solution composition and pH has been reported by other researchers⁵⁰.

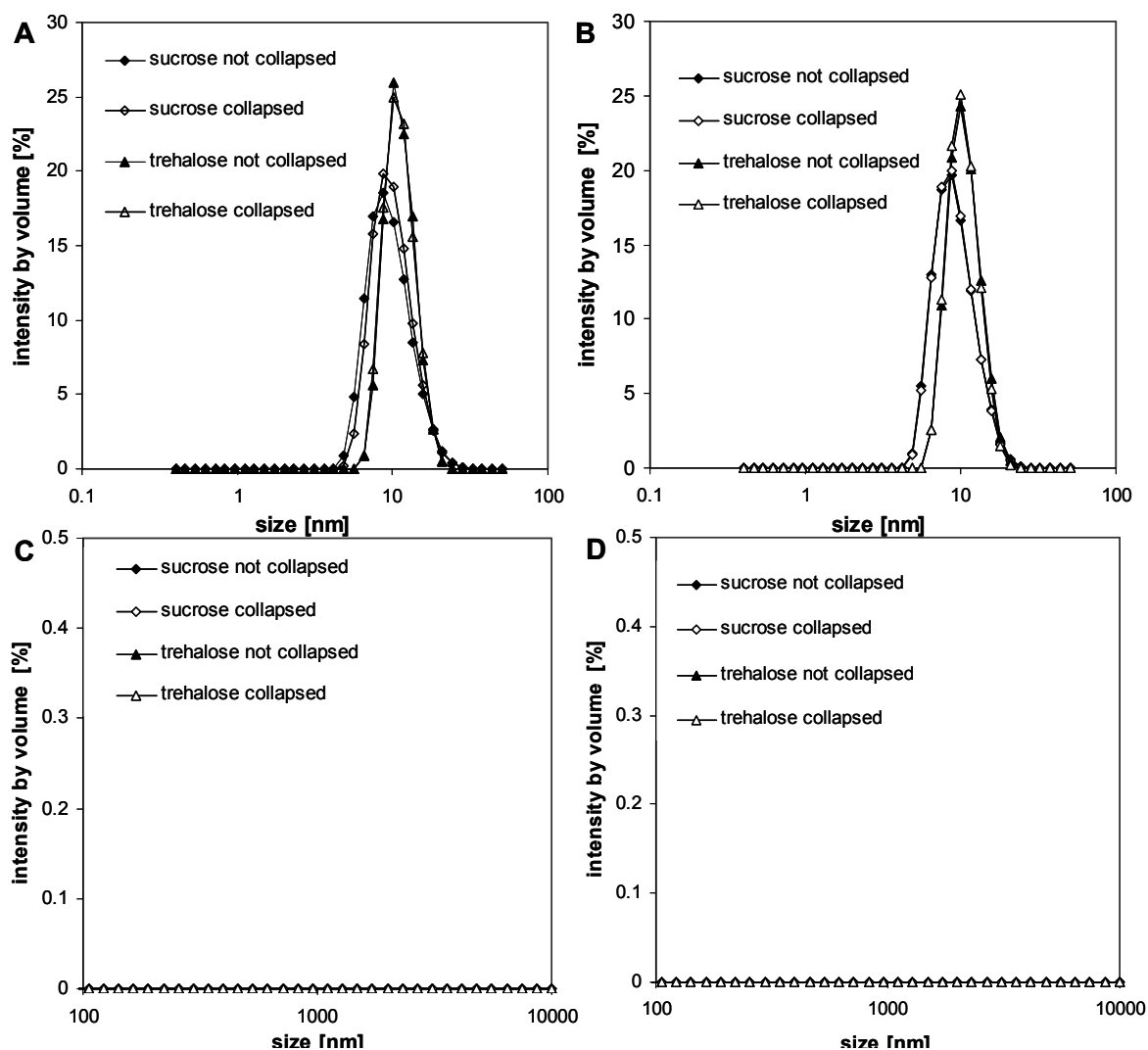


Figure 7.6: DLS size distribution by volume of 4 mg/mL IgG₀₁ formulated with trehalose and sucrose freeze-dried to collapsed and elegant lyophilizates at pH 5.5 (A,C) and pH 3.5 (B,D) (n = 2).

Size distributions from 0.1 – 100 nm are depicted in figures A and B, size distributions from 100 – 10000 nm are depicted in figures C and D.

The size range from 100 to 1000 nm is depicted separately to avoid obscuring the presence of trace amounts of aggregates due to different y-scales.

The size distribution was obtained by fitting a NNLS algorithm to the correlation function.

The size distribution was slightly broader for the sucrose-based formulations, indicating an increased polydispersity, an observation that can be related to the presence of smaller aggregated species that are not resolved from the monomer peak. This is further reflected in the polydispersity index PDI and in the mean particle size (Z-Average) shown in Table 7.3:

The PDI was slightly higher and the Z-Average value was increased as well. The sucrose-formulation at a pH of 5.5 showed a distinct aberration of a polydispersity index of 0.1 which points towards the existence of predominantly monomeric species⁵⁰. But again there was no difference between collapsed and non-collapsed samples. Besides the sucrose pH 5.5 – formulation all other samples were monodisperse, further confirming results obtained from HP-SEC measurements.

The physical stability of collapsed and non-collapsed reconstituted protein lyophilizates was analyzed using a broad set of analytical tools. The existence of soluble and insoluble aggregates was checked with sensitive tools such as turbidity, light obscuration and DLS. Furthermore protein species were characterized concerning their size and molecular weight using HP-SEC and AF4. Additionally, to determine whether aggregation was covalent or non-covalent SDS-PAGE was accomplished (data not shown).

Using these methods no difference in physical stability between collapsed and non-collapsed lyophilizates could be detected.

2.1.3 BINDING ACTIVITY OF IGG₀₁ IN RECONSTITUTED LYOPHILIZATES

Besides the formation of aggregates and particles, the biologic activity is of great interest when dealing with protein pharmaceuticals. The biologic activity of antibodies can reliably be assessed using the surface plasmon resonance (SPR) technology that allows for monitoring the in-vitro binding of the mAb to its specific receptor. Figure 7.7 depicts the binding activities of IgG₀₁ reconstituted from sucrose- and trehalose based collapsed and non-collapsed lyophilizates. All samples showed a binding activity $\geq 91\%$ and no significant differences between collapsed and non-collapsed systems were observed.

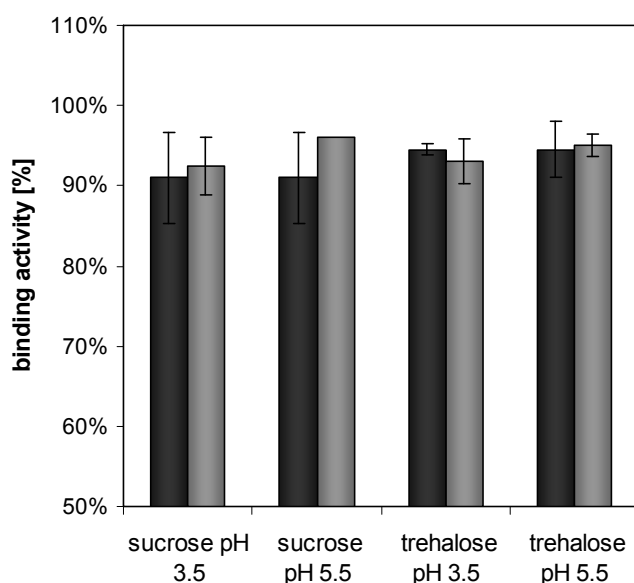


Figure 7.7: Binding activity of IgG₀₁ after reconstitution from collapsed (grey bars) and non-collapsed (black bars) lyophilizates (average \pm SD, n = 2).

Thus binding activity results further confirm findings from physical stability data, pointing towards collapse not having a detrimental effect on IgG₀₁ stability.

2.1.4 CONFORMATIONAL STABILITY OF IGG₀₁ IN RECONSTITUTED LYOPHILIZATES

Besides the physical stability and biologic activity, another important aspect when dealing with protein pharmaceuticals is their conformational stability, i.e. their three-dimensional structure. The biologic function of proteins is inextricably connected to its tertiary and secondary structure. What is more, denaturation as the loss of higher order structure⁵¹ often is a precursor for aggregation or chemical instabilities, as more hydrophobic parts are exposed and a greater flexibility of the whole molecule is experienced in the denatured state. Therefore a careful examination of secondary and tertiary structure elements is crucial during biopharmaceutical drug development.

A well established analytical tool for the investigation of protein secondary structure is Fourier transform infrared (FTIR) spectroscopy. The amide bonds forming the protein's backbone give rise to nine different characteristic bands visible in the mid-infrared region⁵². The most commonly investigated wave number range for the assessment of protein secondary structure is the amide I band from 1600 – 1700 cm^{-152,53}. It is directly related to the backbone conformation and caused by the C=O stretching vibration with minor contributions from the C-N stretching vibration⁵⁴. Depending on the hydrogen bonding pattern of the amide bonds characteristic frequency shifts in the amide I band can be observed. Thus the secondary structure can be deduced.

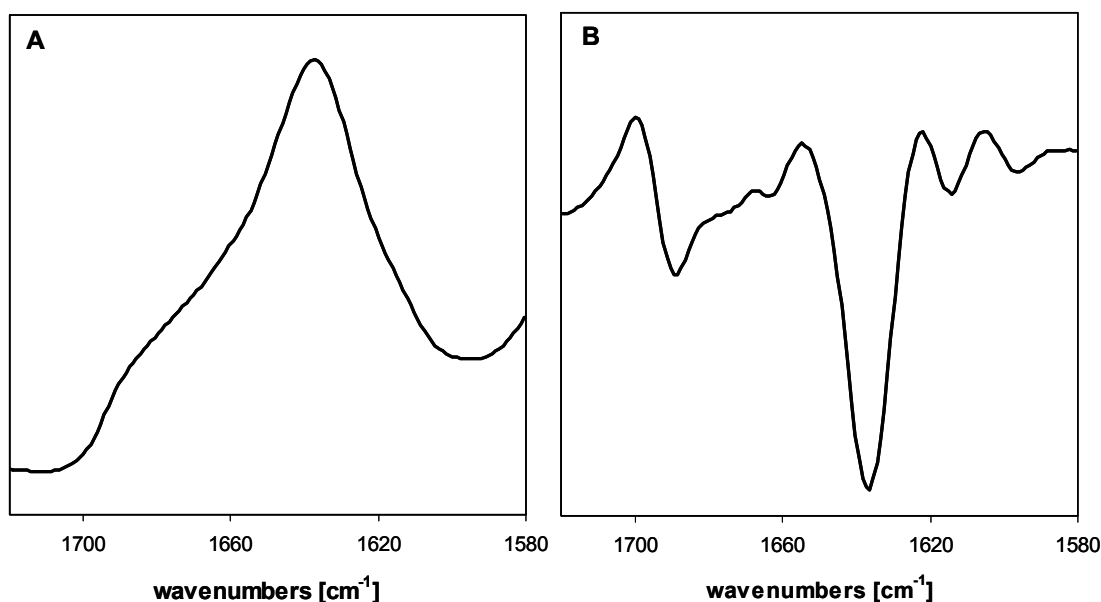


Figure 7.8: FTIR spectra of IgG₀₁ standard solution in 10 mM sodium succinate buffer pH 5.5: Background corrected, area-normalized amide I FTIR-transmission spectrum (A); area-normalized second derivative amide I FTIR transmission spectrum.

Spectra are calculated average spectra of two independent measurements.

As proteins usually are composed of more than one secondary structure type, the amide I band typically is a composite of absorbance arising from the various structural types. Because of this, the amide I band is broad and further mathematical processing has to be applied to gain structural information. The procedure most commonly employed is spectral derivation, based on a method originally described by Savitsky and Golay⁵⁵. Another method commonly applied is Fourier self-deconvolution⁵⁶.

In this work second derivative spectra were used to access structural information. Figure 7.8 shows the original FTIR spectrum of the IgG₀₁ in the amide I band range (A) and the calculated second derivative (B).

Table 7.4: Assignment of FTIR bands in the amide I band to secondary structural elements.

band position [cm-1]	assignment
1697-1686	β -sheet (intermolecular)
1645-37	β -sheet (intramolecular)
1638-1628	β -sheet
1620-1615	β -sheet or side chain (intermolecular)
1680-1676	turns
1667-1660	turns

Table 7.4 presents an assignment of FTIR bands within the amide I band to secondary structural elements as given by Costantino et al^{57,58}. These were in good agreement with previously published data on the general secondary structure of IgGs both from FTIR data⁵⁹⁻⁶¹ and X-ray crystallographic data⁶². The major type of secondary structure is β -sheet and its content is roughly 70 %⁵⁹. The remaining structural elements are unordered structures composed mainly of turn-structures⁵⁷.

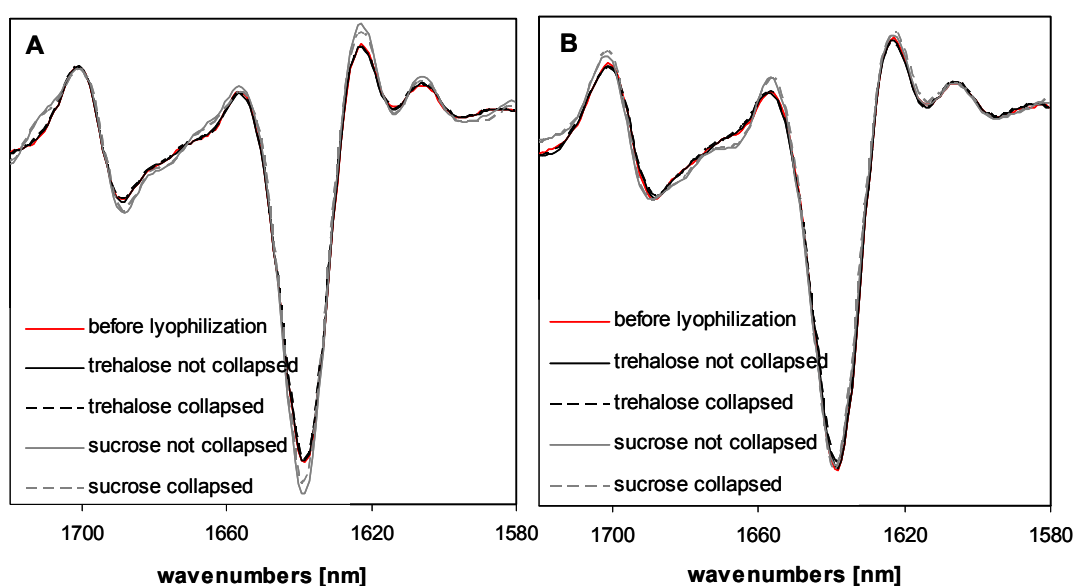


Figure 7.9: Effect of collapse on secondary structure of IgG₀₁: Background-corrected and area-normalized second derivative FTIR transmission spectra of 4 mg/mL IgG₀₁ at a pH of 5.5 (A) and pH of 3.5 (B). Spectra are calculated average spectra of at least two independent measurements.

Figure 7.9 depicts the effect of collapse on the secondary structure of reconstituted solutions of IgG₀₁ at a pH of 5.5 (A) and 3.5 (B), respectively. No clear difference in second derivative spectra was detectable neither between collapsed and non-collapsed formulations nor between the reconstituted lyophilizates and the solution prior to freeze-drying.

As FTIR measurements only assess the secondary structure but a change in tertiary structure may be related to stability as well, intrinsic protein fluorescence experiments were accomplished to further complete the analytical methods set and to check for changes in the tertiary structure of the IgG due to collapse.

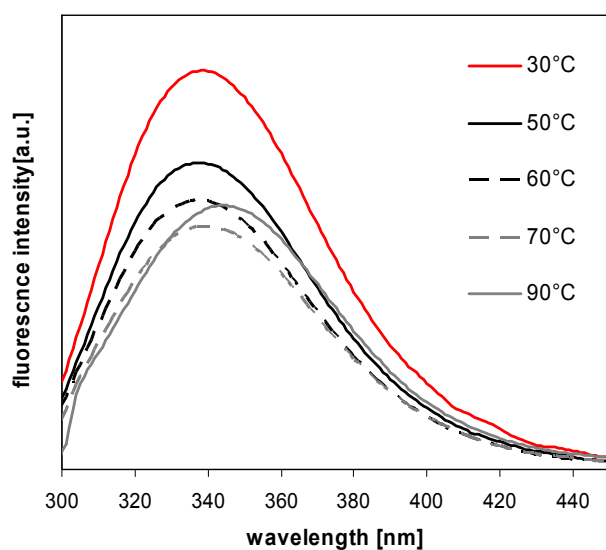


Figure 7.10: Intrinsic protein fluorescence emission spectra of 0.05 mg/mL IgG₀₁ after excitation at 280 nm at increasing temperatures from 30 °C to 90 °C after equilibration at the corresponding temperature.

IgG₀₁ bulk solution was diluted with phosphate buffered saline pH 7.4 to the measurement concentration in order to avoid internal quenching. Spectra were smoothed with a 9 point Savitzky Golay algorithm.

Intrinsic protein fluorescence is caused by the aromatic amino acids of the molecule, i.e. tryptophan, tyrosine and phenylalanine⁶³. The observed fluorescence emission spectrum is composed of the emission spectra of all the amino acids, but tryptophan shows the highest fluorescence intensity and thus the highest contribution to the observed broad band. Tryptophan fluorescence is highly dependent on the local environment with polar surroundings acting as a quencher decreasing the fluorescence intensity⁶³. Thus, intrinsic protein fluorescence can be used to investigate the micro-environment of the protein's aromatic amino acids, i.e. the position of the hydrophobic parts of the protein. Usually these parts are buried deep in the protein molecule but in the denatured state they are exposed to the more hydrophilic surroundings of the aqueous solvents. As a result, the intensity of the intrinsic protein fluorescence is decreased upon denaturation⁶⁴. Because almost all polar protein groups can quench tryptophan fluorescence to some extent⁶⁵, a decrease in fluorescence intensity can already be detected before complete unfolding, when aromatic amino acids are shifted towards the protein exterior and thereby interact with more hydrophilic amino acids. However, this might as well lead to an increase in fluorescence

intensity upon unfolding as the quenching amino acids then will be removed from the tryptophan environment^{66,67}. Thus the reaction upon thermal stress regarding fluorescence quantum yield has to be evaluated for each system separately. A pronounced change in the micro-environment of the aromatic amino acids is reflected in the change of the fluorescence emission spectral maximum. Figure 7.10 shows the fluorescence emission of IgG₀₁ at various temperatures from room temperature up to 90 °C. Most certainly, the IgG₀₁ exhibited a pronounced decrease in quantum yield prior to a shift in emission maximum indicating a gradual unfolding process.

The position of the maximum of the fluorescence spectrum of tryptophan varies from 307 - 353 nm. There are 5 most probable spectral forms of tryptophan residues. In the antibody, as in many proteins, the so-called spectral form II is predominant that exhibits an emission maximum around 340 nm with a band width of ~ 55 nm. The emission maximum is red-shifted as compared to other spectral forms of tryptophan and it is assumed that the fluorophore is at the protein surface and in contact with bound water and other polar groups⁶⁸.

Upon thermal denaturation the maximum of the emission spectrum shifted from 338 nm to 342 nm indicating a more hydrophilic environment of the tryptophan residues. Tryptophan residues in contact with free water molecules as in the completely unfolded state show a $\lambda_{em\ max}$ of 350 nm^{68,69}.

Shifts of the tryptophan emission spectrum are often used to detect structural changes in the protein conformation^{67,70}. Besides the tryptophan emission maximum, the fluorescence intensity and the quantum yield show certain sensitivity towards environmental conditions as well and they are sometimes used as an indicator of structural changes as well^{63,64}.

Table 7.5: $\lambda_{em\ max}$ of IgG₀₁ solutions prior to freeze-drying and after reconstitution of lyophilizates; IgG₀₁ solutions were diluted with formulation buffer to a concentration of 0.05 mg/mL in order to prevent internal quenching; n = 2.

formulation	appearance	$\lambda_{em\ max}$ [nm] before FD	$\lambda_{em\ max}$ [nm] after FD
sucrose pH 5.5	collapsed	337	337
	not collapsed		338
sucrose pH 3.5	collapsed	337	337
	not collapsed		337
trehalose pH 5.5	collapsed	338	338
	not collapsed		338
trehalose pH 3.5	collapsed	337	338
	not collapsed		338

Table 7.5 lists the $\lambda_{em\ max}$ of IgG₀₁ solution both prior to freeze-drying and after reconstitution of collapsed and non-collapsed lyophilizates. No change in $\lambda_{em\ max}$ could be detected indicating that no considerable changes in the protein's conformation took place.

It should be noted that aggregates and denatured protein species may still have a significant amount of secondary structure and therefore will not be distinguishable from native species using FTIR⁷¹. Furthermore, fluorescence parameters are sensitive to local changes of the tryptophan residues' environment only. Thus a change in the environment of other amino acids may be not detectable. Furthermore, as the tryptophan residues are distributed over the whole antibody molecule⁷², fluorescence may fail in detecting a localized change in one tryptophan residue⁶⁷.

To gain further insight into the conformation of the IgG, fluorescence anisotropy experiments were performed for selected formulations. Steady state fluorescence anisotropy gives information about the flexibility of tryptophan residues in the protein molecule and thus information about the protein's hydrodynamic and structural properties. During fluorescence anisotropy experiments the fluorophore is excited with plane polarized light resulting in a selective excitation of fluorophores having an absorption dipole oriented parallel to the electric field vector of the exciting radiation; this process is called photoselection. The fluorescence intensity is detected through a second polarizer oriented either parallel or perpendicular to the first one⁷³. The maximum anisotropy is affected by the probability of a molecule to be excited in a polarized light beam and the angle between absorption and emission dipole. Published values for proteins are around the maximum value of 0.3⁷⁴. The most common reason for a decreased measured anisotropy is rotational diffusion during the time of the excited state. (This is why anisotropy values are affected by the rigidity of the molecule itself and by the fluorescence lifetime. Hence, to gain a real understanding of the protein's dynamics time-resolved measurements are preferable.) This is why small molecular fluorophores in aqueous non-viscous solutions usually exhibit anisotropy values close to zero⁷⁵. Macromolecules show an increased anisotropy because of their increased rotational correlation time caused by their size.

Fluorescence anisotropy measurements are an extremely sensitive tool for the detection of changes in protein structure because the fluorescence lifetimes and the rotational correlation times of most proteins are in the same order of magnitude⁷⁵.

Table 7.6: Fluorescence anisotropy values for 4 mg/mL IgG₀₁ prior to lyophilization and after reconstitution of lyophilizates (average \pm SD, n = 2).

formulation	anisotropy \pm SD	
trehalose pH 5.5	prior to lyophilization	0.050 \pm 0.002
	after lyophilization	0.050 \pm 0.002

Taschner et al. reported an anisotropy value of 0.091 for a monoclonal antibody⁶⁴. They observed a slight decrease of fluorescence anisotropy upon lyophilization to 0.084. Polarization values (that are interrelated to anisotropy) reported by another team are around

0.2 for the native IgG⁶⁷. Upon denaturation with guanidinium hydrochloride a reduction of these polarization values to 0.08 was reported.

Table 7.6 lists the determined anisotropy values for solutions containing the IgG₀₁ in trehalose at a pH of 5.5. No differences in anisotropy values were observed comparing the solutions prior to and after freeze-drying, thus no change in tryptophan flexibility is initiated by freeze-drying. The absolute values are lower than the values reported by Taschner et al⁶⁴, possibly indicating a higher flexibility of tryptophan residues in the investigated antibody.

2.1.5 CONFORMATIONAL STABILITY OF IGG₀₁ IN FREEZE-DRIED CAKES

Besides the investigation of protein structure in the rehydrated lyophilizate, analysis of secondary structure in the dried lyophilizate was accomplished. It is well documented in literature that proteins may readily refold during rehydration yielding native protein spectra despite the partial or complete unfolding in the dried state⁷⁶⁻⁷⁸. Even though native conformation is preserved after immediate reconstitution, the protein may exhibit poor storage stability^{79,80}. It now is common knowledge that preservation of native structure in the dried state is necessary for adequate storage stability of proteins⁸⁰⁻⁸².

Thus investigation of protein secondary structure in the lyophilized state immediately after freeze-drying may be useful in order to predict long-term storage stability. Furthermore, the preservation of native structure in the dried state can be directly correlated with the prevention of aggregation and preservation of activity of labile proteins after rehydration⁷⁶. Comparing protein spectra in the dried state with protein spectra in solution it is important to remember that the absence of water causes spectral changes independent of these associated with conformational changes caused by changes in the vibrational properties of the amide bonds. FTIR spectra of freeze-dried proteins often show band broadening and significant shifts of the band position and intensities of amide I spectral components due to the physical environmental change^{81,83}. However, our analysis was focused on the detection of the formation of new bands around 1620 – 1625 cm⁻¹^{76,81} and around 1680 - 1700 cm⁻¹^{176,83} that can be ascribed to the formation of strong hydrogen-bonded antiparallel intermolecular β -sheet structures that are indicative for protein aggregation.

Figure 7.9 (A) depicts the area-normalized second derivative transmission amide I spectra of various IgG₀₁ formulations in the solid state. Figure 7.9 (B) shows the area-normalized second derivative transmission amide I spectra of both native IgG₀₁ and IgG₀₁ heat denatured as a reference. There were no major changes apparent in the protein secondary structure in the dried and in the solution state, respectively. The bands at 1656 cm⁻¹ and 1623 cm⁻¹ indicating protein aggregation (Figure 7.9 (B)) were not perceptible in the solid state spectra. Only the band at 1675 cm⁻¹ which is assigned to protein aggregation as well and is consistent with published data⁷⁶ was more pronounced in the solid state.

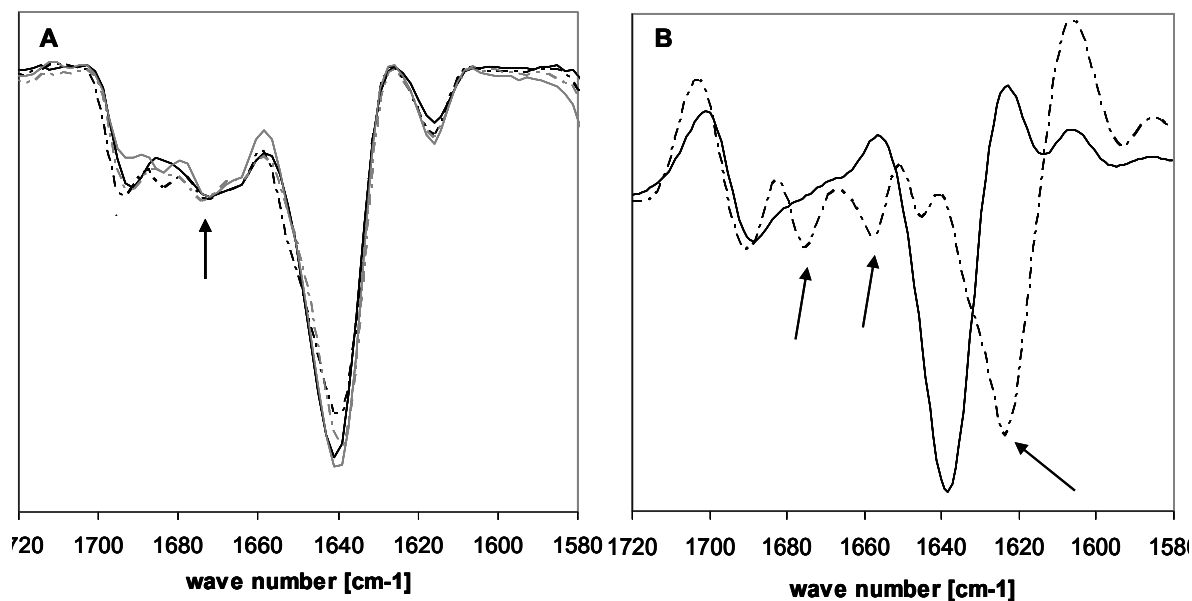


Figure 7.11: Area-normalized second derivative FTIR amide I transmission spectra of IgG₀₁ in the solid state (A) and in aqueous solution (B) (n = 2)

Collapsed (dashed lines) and non-collapsed (solid lines) trehalose- (black lines) and sucrose-based (grey lines) IgG₀₁ (4 mg/mL) formulations at a pH of 5.5(A); IgG₀₁ in sodium-succinate buffer in the native state (solid line) and heat denatured at 80 °C (dashed line) (B).

All formulations exhibited a subtle broadening of bands in the amide I spectral region caused by a broader distribution of conformational states in the dried state.

Comparing collapsed and non-collapsed lyophilizates of the same formulation there were no relevant spectral differences. Collapsed lyophilizates exhibited a very slight shift of the maximum band at 1639 cm⁻¹ towards higher wave numbers at 1640 cm⁻¹. This is assigned to a loss of order in the individual structural elements by some researchers⁸³. In consideration of the fact that the change in band position was small and assigned structural changes were not confirmed by other spectral changes correlated more clearly to secondary structure elements, this was not regarded as significant. Thus the findings from investigations of IgG₀₁ reconstituted solutions were confirmed by analysis of secondary structure in the solid state. No differences between collapsed and non-collapsed lyophilizates could be detected. Regarding the relevance of preservation of native protein structure in the lyophilized state for the long term stability, excellent storage stability is expected for both collapsed and non-collapsed lyophilizates. This assumption will be subject of further investigation in Chapter 8 of this thesis.

2.2 PARTIALLY CRYSTALLINE: FROM ELEGANT TO COMPLETELY COLLAPSED

Besides the application of completely amorphous systems to stabilize proteins in the lyophilized state, partially crystalline systems, comprising of a crystalline bulking agent and a second excipient that remains amorphous and acts as lyo-protectants, are often used⁸⁴⁻⁸⁶. Partially crystalline formulations bear some advantages over completely amorphous systems. The amorphous part of the formulation sufficiently stabilizes the incorporated

protein by water replacement and vitrification. The crystalline part forms a scaffold and allows freeze-drying to be conducted at the eutectic melting temperature of the crystalline component, i.e. temperatures well above the glass transition temperature of the amorphous phase⁸⁵. Thereby a significant reduction of freeze-drying time can be achieved. Thus the use of crystalline bulking agents, such as mannitol or glycine allows the production of mechanical stable and homogeneous cakes with short freeze-drying cycles. It is described in literature that a minimum ratio of crystalline to amorphous component is required in order to prevent collapse at high primary drying temperatures^{1,85}.

In order to extensively investigate the collapse phenomenon and its effect on protein lyophilizates, formulations were investigated comprising of mannitol and sucrose in varying ratios as model system for the important formulation principle of partially crystalline formulations.

Table 7.7 lists the formulations investigated. Formulations were developed according to Johnson et al. describing the collapse behavior of mannitol-sucrose-based formulations⁸⁵. The total solid content was 5 % per weight for all the formulations. The total solid content for freeze-dried formulations usually ranges from 2 – 10 %⁸⁷ by weight, thus 5 % represents an average freeze-dried formulation. Furthermore, isotonic solutions were obtained upon reconstitution.

Solutions contained IgG₀₁ at a concentration of 4 mg/mL as in the amorphous systems described above. The formulation buffer was 10 mM sodium succinate at a pH of 5.5 and 0.4 mg/mL Tween 20 were added. Formulations 1 to 7 were obtained by adding varying amounts of mannitol and sucrose.

The solutions were freeze-dried using either the aggressive drying cycle (protocol 1) or a conventional, gentle drying cycle (protocol 2) as described in the materials and methods section. Table 7.7 also lists the macroscopic cake appearance after freeze-drying that is further graphically summarized in Figure 7.12.

Table 7.7: Composition of partially crystalline formulations and appearance of cakes after freeze-drying with an aggressive or gentle cycle, respectively.

ID	mannitol [%]	sucrose [%]	appearance	
			dried with aggress.protocol	dried with gentle protocol
1	4	1	not collapsed	not collapsed
2	3.5	1.5	partially collapsed	not collapsed
3	3	2	partially collapsed	not collapsed
4	2.5	2.5	partially collapsed	not collapsed
5	2	3	partially collapsed	partially collapsed
6	1.5	3.5	completely collapsed	partially collapsed
7	1	4	completely collapsed	completely collapsed

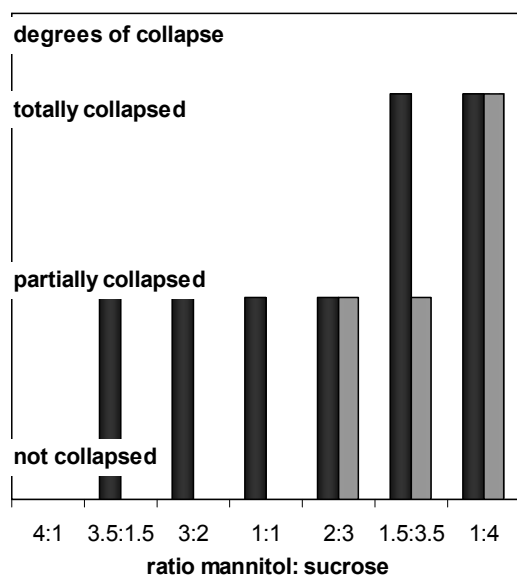


Figure 7.12: Macroscopic appearance of solutions composed of varying ratios of mannitol to sucrose freeze-dried using an aggressive and a gentle protocol, respectively.

Lyophilizates were classified by visual evaluation of the top, wall and bottom section as well as the cross section of the lyophilized cake, as described in detail in Chapter 3.

The depiction of no bar in the figure means that no collapse occurred.

By variation of the ratio of crystalline and amorphous component collapsed, partially collapsed and non-collapsed lyophilizates could be produced using just one drying protocol. Using this set-up the effect of collapse on protein stability could be investigated without the necessity to apply two different drying protocols, a gentle one and an aggressive one. On the other hand, in order to detect a possible effect of drying temperature, two different drying cycles were conducted, a gentle and an aggressive one, both leading to collapsed and non-collapsed lyophilizates. Figure 7.13 shows lyophilizates freeze-dried with the aggressive (A) and the gentle (B) drying-cycle respectively.



Figure 7.13: Lyophilizates comprising various ratios of mannitol to sucrose freeze-dried using an aggressive drying cycle (A) and a gentle freeze-drying cycle (B), respectively.

Freeze-drying cycles as specified in Chapter 3, section 2.1.

Table 7.8 lists the residual moisture levels of the cakes. All cakes showed a homogenous residual moisture distribution as reflected by a small standard deviation. Residual moisture levels of aggressively dried cakes were below 1.5 % no matter whether the cakes were elegant or collapse had occurred. For gently dried cakes partially collapsed cakes showed the highest residual moisture levels and partially and completely collapsed cakes showed an increased standard deviation indicating a less homogeneous drying behavior.

Table 7.8: Residual moisture contents of lyophilizates comprising varying ratios of mannitol to sucrose freeze-dried using an aggressive drying cycle and a gentle freeze-drying cycle, respectively (average \pm SD, n = 2).

ID	gentle drying protocol residual moisture \pm SD [%]	aggressive drying protocol residual moisture \pm SD [%]
1	1.08 \pm 0.02	0.67 \pm 0.00
2	1.25 \pm 0.03	0.69 \pm 0.02
3	1.72 \pm 0.01	0.87 \pm 0.09
4	1.83 \pm 0.08	0.92 \pm -0.01
5	1.75 \pm 0.06	1.11 \pm 0.02
6	2.54 \pm 0.17	1.47 \pm 0.04
7	1.04 \pm 0.29	1.02 \pm 0.02

However, despite observed variations in residual moisture between collapsed and non-collapsed cakes and between cakes produced with the two different protocols, residual moisture levels were regarded as comparable, as no relevant effect of residual moisture content ranging from 0.7 % to 6.3 % on the stability of the IgG₀₁ was observed in a separate investigation (see Chapter 6 for details).

2.2.1 PHYSICO-CHEMICAL CHARACTERISTICS OF LYOPHILIZATES

In the partially crystalline formulations, complete mannitol crystallization on the one hand side and preservation of the amorphous state of sucrose on the other hand side had to be achieved in order to realize optimum stabilization. If mannitol does not crystallize completely during the freeze-drying process uncontrolled crystallization during subsequent storage may take place causing significant stability concerns. Furthermore, since mannitol exists in several polymorphic modifications, metastable polymorphs can be formed that can be transformed into one another during storage. Most critical is the formation of the metastable mannitol hydrate^{88,89} that causes an increase of residual moisture when it is transformed into an anhydrous polymorph. To ensure complete crystallization in a stable modification, annealing steps are frequently employed in lyophilization cycles. But it is crucial to prevent sucrose crystallization because its protein stabilizing abilities are lost upon crystallization. As the aggressive freeze-dry protocol applied here did not include an annealing step, a close check

was important in order to ensure that mannitol completely crystallized in a stable modification to allow for a sound comparison of collapsed and non-collapsed cakes.

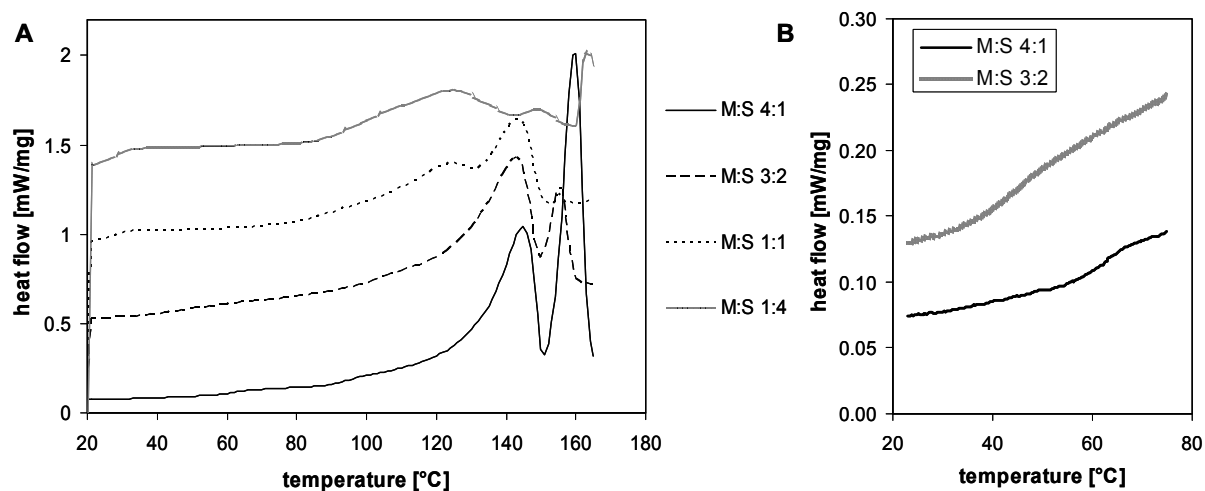


Figure 7.14: DSC heating scans (2nd scan) of lyophilizates with variable ratios of mannitol (M) to sucrose (S) at a total solids content of 5 % freeze-dried with the aggressive protocol, showing melting endotherms of different mannitol polymorphs (A) and magnified to show the glass transition of sucrose (B).

Physicochemical properties of lyophilizates are commonly analyzed using differential scanning calorimetry (DSC) and x-ray powder diffractometry (XRD). With DSC glass transitions and melting events can be characterized. Transformations of polymorphs, crystallization and even dehydration events can be monitored as well^{88,90}. Using XRD polymorphs can be reliably identified. Both techniques can be used to quantify the degree of crystallinity of lyophilizates as well.

Figure 7.14 shows DSC heating scans of lyophilizates containing varying ratios of mannitol to sucrose freeze-dried using the aggressive freeze-drying protocol described in Chapter 3. Crystallization of mannitol was complete for all the formulations because no exothermic event connected to mannitol crystallization (described to be at $\sim 60 - 70$ °C^{91,92}) was observed prior to melting in the first heating scan. Glass transitions of sucrose were sometimes difficult to detect because the higher content of crystalline component. Glass transition temperatures were between 40 and 60 °C for all the formulations depending on the individual residual moisture content, as shown in Figure 7.14 B for representative formulations and listed in Table 7.9. As the samples were stored in the refrigerator at 5 °C, i.e. sufficiently below all glass transition temperatures, the effect of variations in the T_g could be regarded as negligible.

Table 7.9: Glass transition temperatures of mannitol-sucrose-based lyophilizates collapsed to different extents (average \pm SD, n = 2).

ratio mannitol:sucrose	aggressive protocol Tg \pm SD [$^{\circ}$ C]	gentle protocol Tg \pm SD [$^{\circ}$ C]
4:1	61.90 \pm 1.13	41.65 \pm 1.20
3.5:1.5	55.15 \pm 0.35	67.70 \pm 5.66
3:2	45.45 \pm 1.34	60.30 \pm 2.69
1:1	52.05 \pm 9.83	61.60 \pm 2.40
2:3	44.50 \pm 1.56	63.95 \pm 7.14
1.5:3.5	42.05 \pm 0.78	53.35 \pm 5.73
1:4	43.00 \pm 3.39	58.45 \pm 3.61

Mannitol crystallized mainly in the δ -modification with minor contributions from the β -modification as can be seen from the characteristic peak pattern shown in Figure 7.15. With decreasing amount of mannitol the relative amount of β -mannitol increased and the relative amount of δ -mannitol decreased. An overview of characteristic peaks and its assignment to mannitol polymorphs is given and in Table 7.10 as adapted from A. Hawe⁹³.

Table 7.10: Assignment of X-ray diffraction peaks to the different mannitol polymorphs as adapted from A. Hawe.⁹³

mannitol polymorph	main peaks [$^{\circ}2\theta$]	references
α -mannitol	13.6	JCPDS-database
β -mannitol	14.6 16.8 18.8 23.4	JCPDS-database
δ -mannitol	9.7 20.4	JCPDS-database
mannitol hydrate	9.6 17.9	Liao et al. [89]

These findings were further confirmed by the melting endotherms detected by DSC. Pure β -mannitol has a melting point of 165 $^{\circ}$ C and pure δ -mannitol melts at 155 $^{\circ}$ C⁹⁴. Since the investigated lyophilizates not only contain mannitol but different components, the resulting melting points may differ from those reported for pure mannitol (compare⁹⁴). Thus the observed melting points at 145 $^{\circ}$ C and 160 $^{\circ}$ C are in good agreement with literature and represent the melting points of δ - and β -mannitol respectively. It is described in literature that δ -mannitol is transformed into β -mannitol at 130 to 155 $^{\circ}$ C^{95,96}. Accordingly the endothermic event assigned to the melting of δ -mannitol could be described as the melting of δ -mannitol and synchronous transformation into β -mannitol. With decreasing weight fraction of mannitol in the formulation the depression of melting point becomes more pronounced because the relative amount of impurities is increased. This causes a shift of melting point of δ -mannitol to

123 °C as can be seen in the too upper curves in Figure 7.14. With decreasing weight fraction of mannitol the intensity of the melting peak of δ -mannitol decreases.

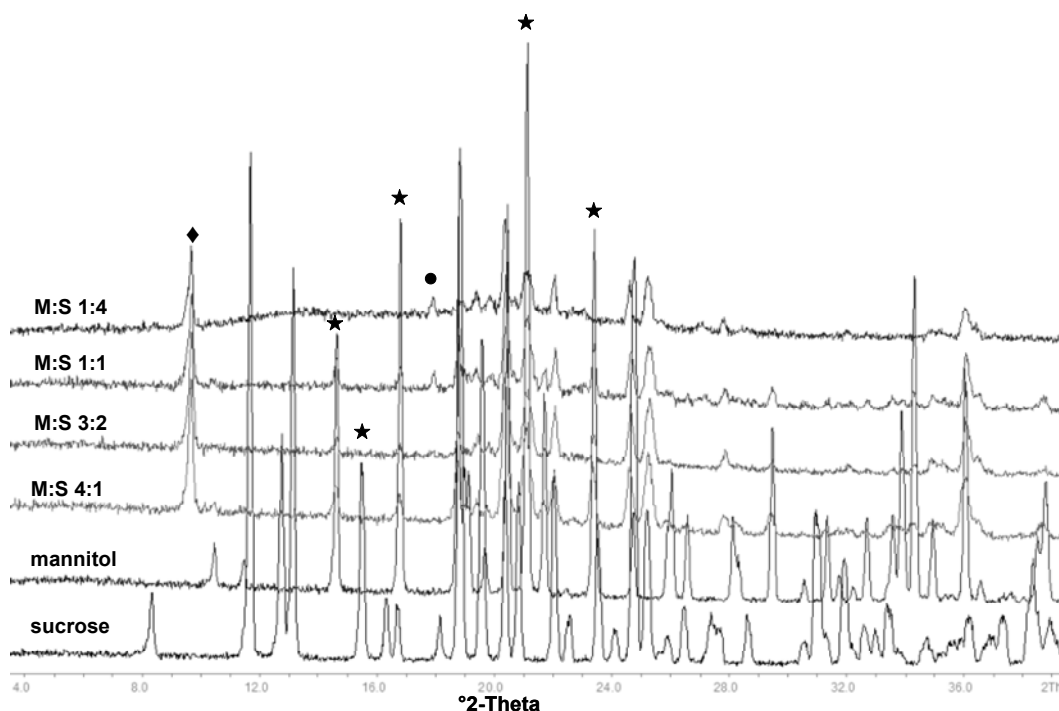


Figure 7.15 : XRD diffraction patterns of lyophilizates with different ratios of mannitol (M) to sucrose (S) at a total solid content of 5 %; characteristic peaks of β - mannitol (★), δ -mannitol (♦) and mannitol hydrate (●) are pointed out.

The broad endothermic event observed in formulations with low mannitol contents that was assigned to the depressed melting point of β -mannitol could be assigned to the dehydration of the mannitol hemihydrate as well. In literature it is described that dehydration takes place at temperatures ~ 80 °C manifested in a very broad peak⁹⁷. This interpretation was further confirmed by the detection of peaks that are characteristic for mannitol hemihydrate in the XRD diffraction patterns at 17.9 2θ ⁹⁷. However, this observation is in disagreement with Johnson et al. who stated that possibly formed mannitol hemihydrate can be eliminated by secondary drying at elevated temperatures, i.e. 40 °C for 13 h at least⁸⁵. According to this report the investigated lyophilizates should not contain any hemihydrate. The authors observed a more distinct endothermic event at 80 °C though. Since the peaks in the diffraction patterns are not very pronounced there may be only a minor amount of mannitol hemihydrate present in the formulations. As the lyophilizates are analyzed immediately after freeze-drying, the potential hazard of transformation of the hydrate during storage is not applicable.

Sucrose was amorphous in all the formulations as deductible from the observed glass transitions and the absence of any characteristic peak in the diffraction patterns.

Lyophilizates freeze-dried with the gentle drying protocol were composed of β - and δ -mannitol fractions as well (data not shown).

2.2.2 PHYSICAL PROTEIN STABILITY OF IGG₀₁ IN RECONSTITUTED LYOPHILIZATES

Physical stability was characterized using HP-SEC. The existence of large amounts of insoluble aggregates could be ruled out because protein recovery was complete. In Table 7.11 the remaining monomer content after freeze-drying and reconstitution of collapsed and non-collapsed lyophilizates of varying composition is shown. Most remarkable, all formulations showed satisfying stability and a remaining monomer fraction of at least 98 % was observed after freeze-drying no matter whether the material has collapsed or not. Thus there is no distinct effect of collapse on soluble aggregate formation of IgG₀₁ observable.

Table 7.11: Remaining monomer as determined by HP-SEC and the extent of collapse as determined by visual evaluation of the macroscopic appearance of collapsed and elegant IgG₀₁ lyophilizates composed of varying ratios of mannitol: sucrose; (average \pm SD, n = 2).

ratio mannitol: sucrose	aggressive protocol		gentle protocol	
	remaining monomer \pm SD [%]	macroscopic appearance	remaining monomer \pm SD [%]	macroscopic appearance
4:1	99.42 \pm 0.20	not collapsed	97.40 \pm 0.02	not collapsed
3.52:5	99.47 \pm 0.09	partially collapsed	99.14 \pm 0.14	not collapsed
3:2	99.41 \pm 0.10	partially collapsed	98.78 \pm 0.06	not collapsed
1:1	99.49 \pm 0.05	partially collapsed	99.18 \pm 0.16	not collapsed
2:3	99.69 \pm 0.12	partially collapsed	99.74 \pm 0.05	partially collapsed
1.5:3.5	99.84 \pm 0.10	completely collapsed	100.66 \pm 0.09	partially collapsed
1:4	99.63 \pm 0.01	completely collapsed	100.37 \pm 0.05	completely collapsed

Comparing lyophilizates freeze-dried using protocol 1 (aggressive) and protocol 2 (gentle), respectively, the effects of formulation and process variables were studied. The cake appearance was unaffected by the applied protocol for the two extreme mannitol-sucrose ratios, i.e. 4:1 and 1:4. At a M:S-ratio of 4:1 the crystalline scaffold formed by the mannitol part of the formulation stabilized the cake to a degree that even drying at extreme high temperatures could not induce collapse. At the opposite M:S-ratio of 1:4 the mannitol fraction was not sufficient to provide a crystalline scaffold and the lyophilizates collapsed even at the low primary drying temperatures applied in the conservative protocol 2. Comparing lyophilizates of the same formulation showing the same degree of collapse, the effect of process variables on protein stability can be studied. As already discussed, no strong effect was observed because overall recovery of monomer was high. The remaining monomer fraction was slightly higher for aggressively dried non-collapsed cakes (M:S ratio 4:1) but slightly lower for aggressively dried total-collapsed cakes (M:S ratio 1:4). Thus no clear effect of process variables could be deduced. Aggressively dried cakes show a slightly increased fraction of remaining monomer as long as cake collapse was not complete. With the onset of complete cake collapse gently dried cakes show a higher monomer fraction.

In order to follow a more scientific based approach to the quantification of collapse and to allow a more detailed evaluation the specific surface area of the cakes was analyzed by BET

Krypton gas adsorption (please see Chapter 5 for details). Figure 7.16 shows the correlation of the remaining monomer fraction of the reconstituted solutions of aggressively freeze-dried IgG₀₁ lyophilizates and the specific surface area of placebo lyophilizates of the same composition determined by BET krypton gas adsorption.

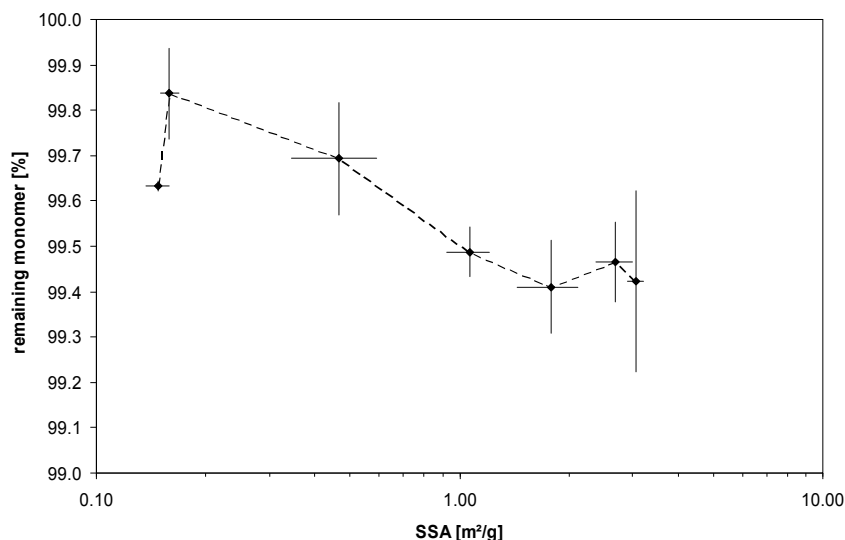


Figure 7.16: Correlation of physical stability with the extent of collapse: Remaining monomer as determined by HP-SEC versus specific surface area as determined by BET krypton gas adsorption of lyophilizates comprising of varying ratios of mannitol (M): sucrose (S) freeze-dried with the aggressive drying protocol.

Remaining monomer: average \pm SD, $n = 2$; specific surface area: average \pm SD, $n = 3$, each measurement was performed pooling 6 vials.

Lyophilizates with small specific surface areas indicating collapse showed a higher proportion of remaining monomer and this value was decreasing with increasing specific surface area. Thus collapsed lyophilizates showed a slightly higher physical stability than elegant lyophilizates. However, differences in remaining monomer were small and all lyophilizates showed good recovery of monomer species after freeze-drying.

To further characterize the physical stability of collapsed and non-collapsed lyophilizates DLS experiments were performed. DLS was chosen as additional analytical tool due to its extreme sensitivity towards smallest amounts of aggregated species⁴⁹. It is important to consider that the size distribution is skewed in favor of larger particles. A drawback of this method is its high sensitivity towards trace amounts of particulate impurities as dust⁴⁹.

Figure 7.17 depicts representative size distributions by intensity of scattered light for IgG₀₁ formulated in four different mannitol to sucrose ratio both prior to freeze-drying (filled symbols) and after lyophilization (open symbols) using protocol 1 (open diamonds) and 2 (open triangles), respectively. The size distribution showed a main particle fraction with a mean particle diameter of 13.5 nm. Hydrodynamic diameters of IgG class antibodies reported in literature are ~ 12 nm^{50,98} thus the main fraction in the described size distributions was composed of IgG monomers. The slightly increased hydrodynamic diameter may be due to the fact that hydrodynamic radii may be overestimated at low ionic strengths⁹⁹.

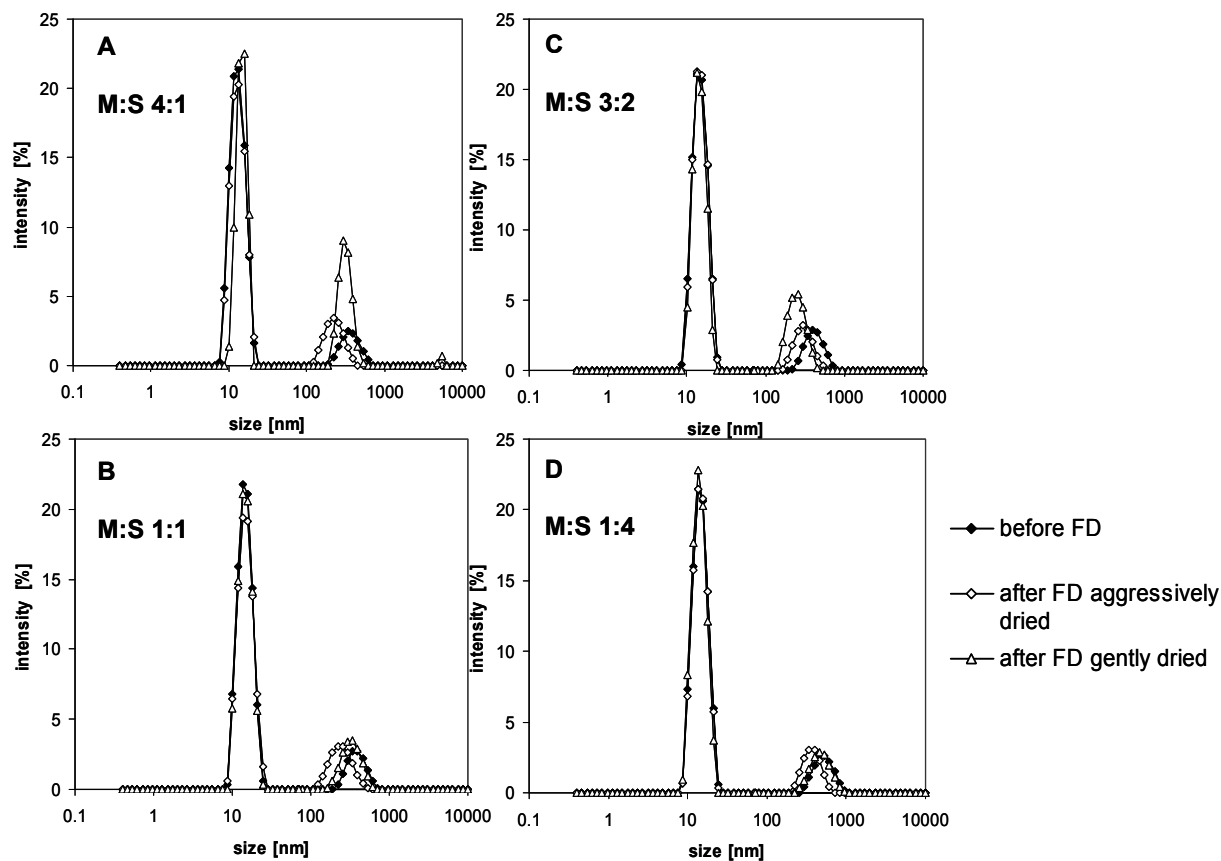


Figure 7.17: DLS size distribution by intensity of scattered light of IgG₀₁ formulations containing various ratios of mannitol (M) to sucrose (S) before lyophilization and after lyophilization and reconstitution using an aggressive or gentle protocol, respectively.

The size distribution was obtained by fitting a NNLS algorithm to the correlation function.

All samples showed a second broader peak between 100 – 1000 nm with a mean particle diameter of 200 – 400 nm, indicating the existence of high-molecular-weight (hmw) species. Due to the relation of particle diameter and scattering intensity this particle fraction appears larger than it actually is. In the more relevant calculated size distribution by volume there was no second particle population detectable (data not shown) and thus the amount of hmw species was not regarded relevant. In addition, as the hmw-species were already observed in the samples prior to freeze-drying, there was no correlation given to the lyophilization process. For the formulations with a mannitol to sucrose ratio of 4:1 and 3:2 the second peak was increased for the gently dried lyophilizates. However, there was no clear correlation neither with the occurrence of collapse nor with the application of a drying protocol.

Table 7.12 summarizes the mean particle size as described by the Z-Average and the polydispersity indices as a measure for the homogeneity of the protein solutions. Most formulations showed a good agreement of the Z-Average and the main particle fraction in the size distribution by intensity as pictured in Figure 7.17. The calculation of the Z-average is based on the linear fit to the autocorrelation function and represents a mean intensity-weighted particle diameter. Calculation of the Z-average is reasonable only when the sample is monomodal and monodisperse. Samples that showed a relevant second peak showed a

deviation between z-average and mean particle size extracted from the size distribution above. The PDIs were between 0.25 and 0.44 for all samples. This indicated that the samples were not monodisperse (as indicated by a PDI higher than 0.1). Samples that showed a second peak of relevant intensity exhibited a higher PDI.

Table 7.12: Mean particle diameter (Z-Average) and polydispersity index (PDI) of IgG₀₁ solutions comprising of variable ratios of mannitol and sucrose after freeze-drying with an aggressive or a gentle drying protocol as determined by DLS.

ratio mannitol:sucrose	freeze-drying protocol	appearance	Z-Average [nm]	PDI
4:1	aggressive	not collapsed	14.86	0.282
	gentle	not collapsed	27.68	0.426
3.5:1.5	aggressive	partially collapsed	13.84	0.246
	gentle	not collapsed	13.75	0.252
3:2	aggressive	partially collapsed	14.85	0.308
	gentle	not collapsed	13.85	0.269
1:1	aggressive	partially collapsed	14.60	0.298
	gentle	not collapsed	14.43	0.300
1.5:3.5	aggressive	partially collapsed	13.95	0.267
	gentle	partially collapsed	16.67	0.435
2:3	aggressive	completely collapsed	13.98	0.289
	gentle	partially collapsed	14.30	0.307
1:4	aggressive	completely collapsed	13.66	0.266
	gentle	completely collapsed	13.39	0.277

Comparing partially crystalline formulations with purely amorphous disaccharide formulations discussed in the previous section, PDI values were significantly higher for the mannitol-sucrose formulations. Amorphous formulations showed PDIs of approximately 0.1 and Z-average values between 11 nm and 12 nm. Only sucrose-based formulations at pH 5.5 showed a slightly increased PDI of 0.2 and Z-average values of 12-16 nm. However, PDI values of the investigated formulations prior to lyophilization already ranged from 0.2 to 0.3 and did not relevantly increase upon freeze-drying.

In summary, there was no significant difference observed between the formulations. Only two gently dried formulations (M:S 4:1 and M:S 1.5:3.5) showed relevantly increased PDI values and mean particle diameters. These findings are in general agreement with the results obtained from size exclusion experiments. Hence, the shorter but more aggressive drying cycle seemed favorable for protein stability, although observed differences were small due to the overall very good stabilization. This is in agreement with authors claiming to minimize freeze-drying time because the process itself might be harmful for the protein¹⁰⁰. Another reason for a decreased stability of formulations freeze-dried with protocol 2 might be the additional annealing step necessary to ensure complete mannitol crystallization. During annealing the sample is held for a certain time above the formulations T_g . The reduced viscosity allows complete crystallization. But the increased mobility may cause adverse reactions as protein aggregation in the freeze-concentrated solute as well. Because an

annealing step is not necessary in the aggressive drying cycle because the high shelf temperatures allow complete crystallization, again this cycle seems superior. A third aspect may be the differences in specific surface area. As discussed in Chapter 5, collapsed lyophilizates showed significantly decreased specific surface areas determined by BET krypton gas adsorption. Surface denaturation is a well known degradation pathway for various proteins^{6,101,102}. The increased stability of an IgG in foam-dried materials with reduced surface area as compared to spray-dried and freeze-dried material has been recently described¹⁰³. Thus the observed differences in stability with the occurrence of collapse might be related to the reduced surface area.

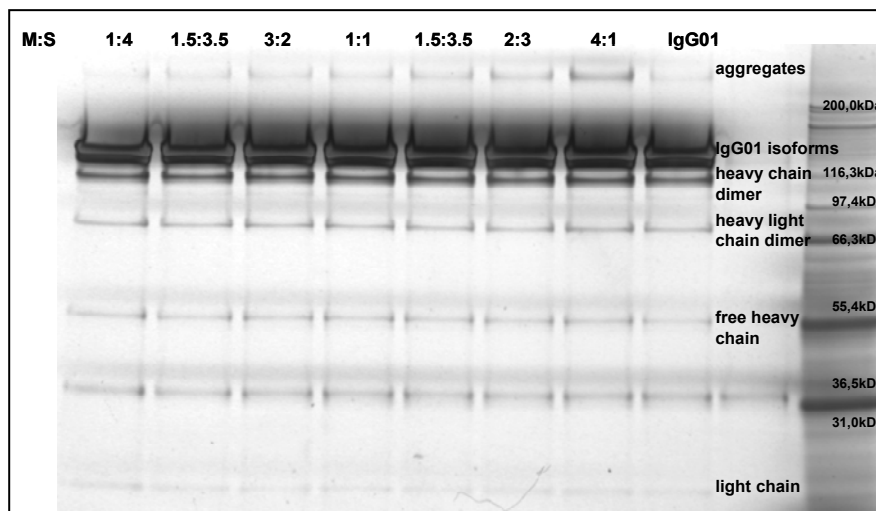


Figure 7.18: Silver-stained SDS-PAGE gel of IgG₀₁ in various formulations containing different ratios of mannitol (M) to sucrose (S) and IgG₀₁ standard (IgG₀₁) after freeze-drying using protocol 1.

In order to further characterize the aggregated species in the IgG₀₁ formulations, SDS-PAGE was performed. Using SDS-PAGE covalent and non-covalent aggregates can be distinguished and sample components are separated by their molecular weight. However, SDS-PAGE analysis of antibodies is complicated by the risk of generating artifacts during sample preparation. Samples are heated to 90 °C in order to facilitate SDS binding to the protein. During heating, disulfide bond cleavage, first between light and heavy chains and later even between the two heavy chains may occur¹⁰⁴.

Figure 7.18 depicts a SDS-PAGE gel of IgG₀₁ aggressively freeze-dried in formulations containing varying amounts of mannitol to sucrose. The most prominent band was the IgG₀₁ monomer, positioned between the marker bands of 116.3 and 200 kDa. The heterogeneity of the band was caused by the different isoforms of the IgG⁸. Besides the monomer band several fragments of the IgG were visible. These might have been formed during sample preparation as discussed above, since HP-SEC experiments detected fragments between 0.7 and 0.9 %. Above the monomer band there was a weak band associated with aggregated species, according to the position relative to the marker presumably dimer. As SDS dissolves non-covalent aggregates, the detected species had to be covalently linked¹⁰⁵.

The varying intensities of the silver stain in the aggregate band may at least partly be due to inhomogeneous staining, because a regular increase in intensity from left to right is observed. This is reflected as well in the dark staining above the monomer band. However, the aggregate band of the formulations with the M:S ratio 4:1 and 2:3 appear to be somewhat more intense indicating an increased amount of aggregates. This is not confirmed by HP-SEC experiments that observe $\sim 0.6\%$ aggregates for all the formulations. This is not confirmed by DLS as well. As silver stained SDS-PAGE gels do not allow quantification due to the non-stoichiometric binding mechanism, no clear trend could be concluded.

All methods used to investigate the physical stability of collapsed, partially collapsed and non-collapsed partially crystalline lyophilizates showed a good stability for all formulations, i.e. high monomer recovery and low amounts of soluble aggregates. The aggregated species were determined to be dimers by SDS-PAGE. Trace amounts of higher molecular weight species that were observed in the DLS size distribution by intensity, were judged as not relevant, because they were not detectable in the volume based size distribution and the intensity based distribution is skewed in favor of large particles. No significant amounts of insoluble aggregates were present in the formulations as further confirmed by complete recovery of IgG₀₁ in HP-SEC experiments.

2.2.3 BINDING ACTIVITY OF IgG₀₁ IN RECONSTITUTED LYOPHILIZATES

Physical protein stability data was further completed by binding activity data determined by surface plasmon resonance spectroscopy, approaching biological activity.

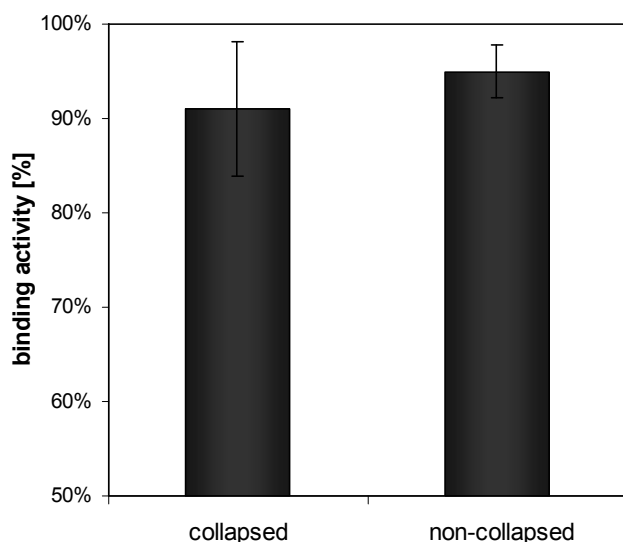


Figure 7.19: Binding activity of IgG₀₁ reconstituted from partially collapsed and non-collapsed mannitol-sucrose-based lyophilizates as determined by surface plasmon resonance spectroscopy (average \pm SD, n = 2).

Partially collapsed lyophilizates were generated by applying the collapse-cycle; non-collapsed lyophilizates were produced with a conventional freeze-drying protocol as described in chapter 3. Lyophilizates were composed of 4 mg/mL IgG₀₁, 35 mg/mL mannitol, 15 mg/mL sucrose, 0.04 % PS20 and 10 mM sodium succinate pH 5.5.

Figure 7.19 shows binding activities of IgG₀₁ reconstituted from partially collapsed and elegant mannitol-sucrose-based lyophilizates.

Although collapsed lyophilizates showed slightly lower binding activities, results were not relevantly different due to the large standard deviation.

2.2.4 CONFORMATIONAL STABILITY OF IGG₀₁ IN RECONSTITUTED LYOPHILIZATES

Conformational stability of the IgG₀₁ was analyzed using FTIR spectroscopy. Figure 7.20 depicts area-normalized second derivative amide I FTIR spectra of selected formulations.

As a reference there are spectra of an IgG₀₁ standard solution and a denatured IgG₀₁ solution (heated to 80 °C) included as well. As can be clearly seen there were no spectral differences between IgG₀₁ prior to freeze-drying and after reconstitution and freeze-drying no matter whether the material has collapsed or not. There was no evidence of the band at 1623 cm⁻¹ indicating intermolecular β -sheet structure and no increase in the bands at 1656 and 1675 cm⁻¹ that are associated with protein aggregation as well.

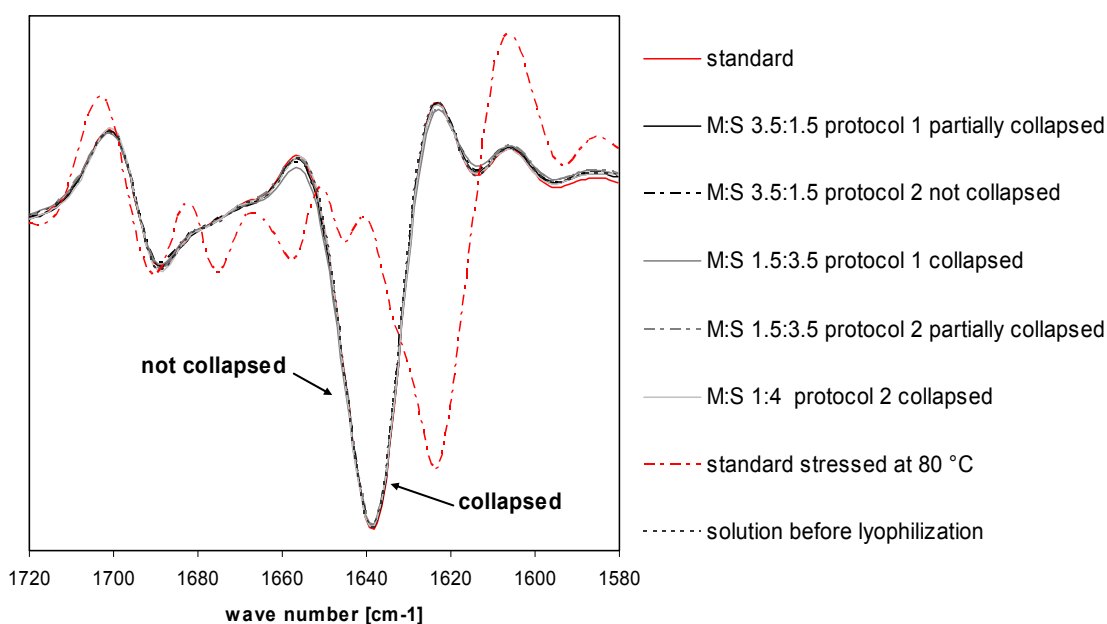


Figure 7.20: Area-normalized second derivative FTIR amide I transmission spectra of 4 mg/mL IgG₀₁ in formulations with variable ratios of mannitol to sucrose at a constant solid concentration of 5 % (n = 2).

However, there are publications indicating that the formation of antibody aggregates cannot be correlated to significant alterations in the secondary structure as assessed by FTIR spectroscopy¹⁰⁶. This might be due to a lack of sensitivity of FTIR spectroscopy (the limit of detection for secondary structural changes is 5 % with the applied method¹⁰⁶) combined with secondary structural changes in only small parts of the protein leading to aggregation. Since spectroscopic techniques only provide general information about the whole sample's secondary structure aggregation might as well be caused by a change in secondary structure of just a small population of molecules that might not be detected.

Another explanation might be the observation of several researchers that antibody aggregation occurs via the molten globule state¹⁰⁷. Thus significant parts of secondary structure will be retained upon aggregation and only changes in tertiary structure might occur. At last it has been reported as well that antibodies aggregate without any detectable change in secondary structure³⁹

However, there also are publications describing significant changes in IgG secondary structure upon drying^{58,83}.

To get a more complete picture of the conformation of the IgG₀₁ after reconstitution from collapsed and non-collapsed lyophilizates, fluorescence spectroscopy studies were performed to assess the antibody's tertiary structure. Figure 7.21 shows the intrinsic protein fluorescence spectra of IgG₀₁ in various formulations comprising of varying ratios of mannitol (M) to sucrose (S) after freeze-drying using the aggressive drying routine. As a reference an IgG₀₁ solution prior to lyophilization is included in the scheme as well.

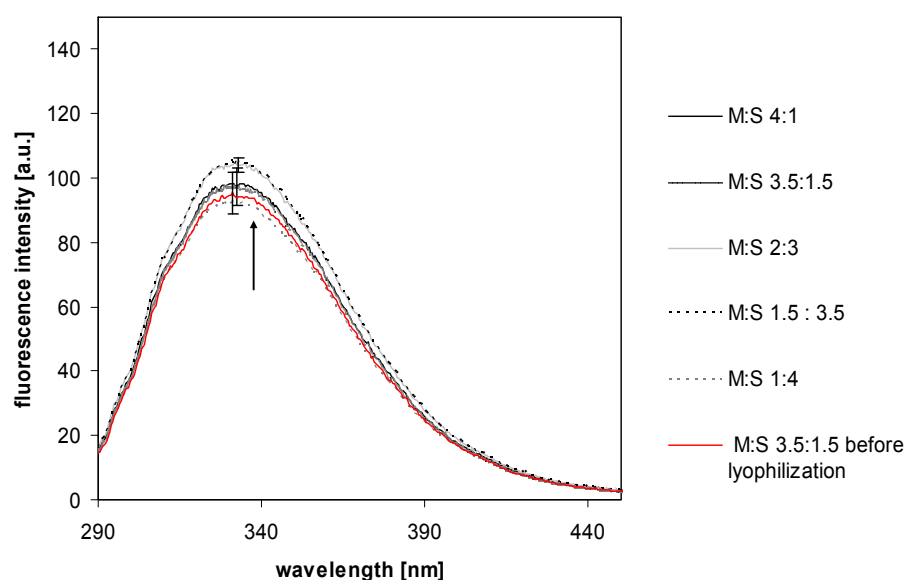


Figure 7.21: Intrinsic protein fluorescence emission spectra of 0.05 mg/mL IgG₀₁ freeze-dried in formulations containing variable ratios of mannitol (M) to sucrose (S) after excitation at 280 nm.

Spectra are calculated average spectra, the standard deviation is depicted for selected data points (black error bars), $n = 3$).

Most evidently all samples showed the same emission maximum at 332 nm. This emission maximum corresponds to the spectral form I of tryptophan as described in literature⁶⁸. It is caused by the indole chromophore of the tryptophan positioned inside the protein globule in a polar but rigid environment. Slight oscillations of the fluorescence intensity are most presumably caused by fluctuations in temperature because temperature was controlled by air-condition rather than a thermostat. The effect of temperature on protein fluorescence is well known (T. Avinte, private communication). Literature describing the use of the fluorescence emission maximum as analytic measure is more numerous and the use of fluorescence intensity as analytic measure is controversial, because fluorescence intensity

can be affected by various factors other than changes in tryptophan microenvironment^{67,70,108}. Error-bars indicating the standard deviation of single spectra around the average spectrum for selected formulations and wavelengths are included in Figure 7.21. The overlapping error-bars indicated that intensities were not significantly different. Thus in summary, the fluctuations in fluorescence intensity were not regarded as relevant.

2.2.5 CONFORMATIONAL STABILITY OF IgG₀₁ IN FREEZE-DRIED CAKES

The conformation of freeze-dried IgG₀₁ was investigated as well. Figure 7.22 depicts the area-normalized second derivative FTIR amide I spectra of IgG₀₁ in the solid state both freeze-dried using a gentle drying protocol and using an aggressive drying protocol. There were no changes in the major band at 1639 cm⁻¹ detectable indicating that the freeze-dried IgG was composed mainly of β -sheet structural elements similar to the IgG in solution. There were no bands at 1623 cm⁻¹ detectable, thus no intermolecular β -sheet structures indicative for aggregation were present. The band at 1675 cm⁻¹ and the band at 1656 cm⁻¹, both associated with aggregation as well, were more pronounced as in the solution state (Figure 7.8 B).

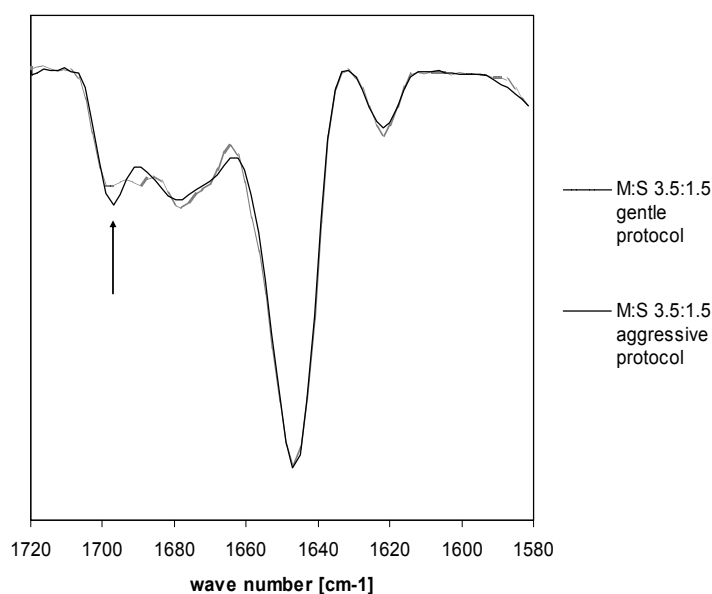


Figure 7.22: Area-normalized 2nd derivative FTIR transmission spectra of the amide I region of 4 mg/mL IgG₀₁ in the solid state (n = 2).

The band at 1675 cm⁻¹ was more pronounced for the aggressively dried IgG₀₁ but the differences were small and most probably were artifacts from spectral processing, as it is well known that derivation disproportional amplifies weak spectral features⁷⁶.

2.2.6 IS THERE A DELAYED EFFECT?

SHORT TERM STRESS STABILITY OF RECONSTITUTED IgG₀₁ LYOPHILIZATES

In order to investigate whether collapse caused subtle changes in protein stability to an extent not detectable with the applied analytical techniques, reconstituted lyophilizates were stored under stress conditions in order to provoke the manifestation of possible stability deficiencies. Samples were stored at 37 °C under permanent agitation at 40 rpm for up to 8 days. Accomplished analytical techniques monitored either physical stability (HP-SEC) or conformational stability (FTIR).

Figure 7.23 displays the IgG₀₁ monomer content in reconstituted lyophilizates during storage. Three representative formulations are depicted as an example (other data not shown). All the formulations showed satisfying stability with high monomer contents after up to 8 days of storage in solution. There were no differences in stability after 8 days. Interestingly, samples reconstituted from collapsed lyophilizates (formulation M:S 1:4) showed higher monomer contents throughout the duration of stress storage. However, this difference was not significant.

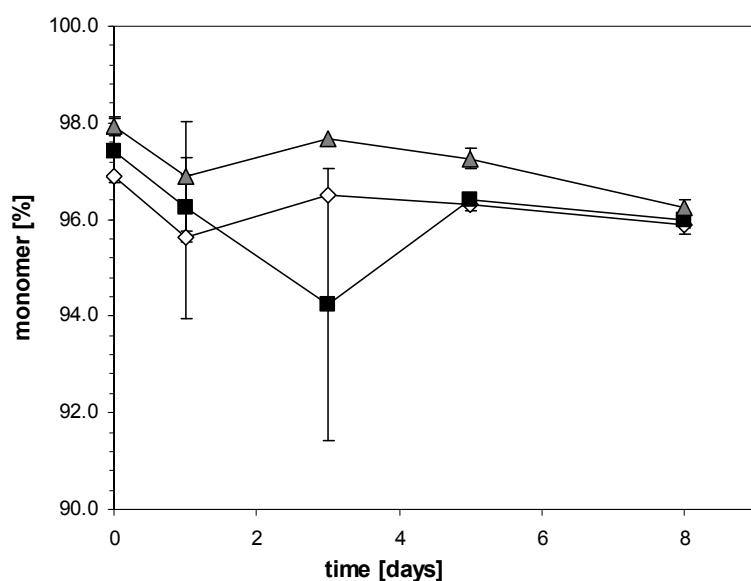


Figure 7.23: IgG₀₁ monomer content as determined by HP-SEC during storage of reconstituted lyophilizates at 37 °C/ 40 rpm for up to 8 days (average \pm SD, n = 2).

Lyophilizates formulated at a mannitol (M): sucrose (S) ratio 3.5:1.5 (diamonds). M:S 1:1 (squares) and M:S 1:4 (triangles).

Figure 7.24 depicts the area-normalized 2nd derivative FTIR transmission spectra. There were no differences detectable between initially collapsed and not-collapsed samples, neither initially nor after stress storage.

Thus the excellent stability observed immediately after freeze-drying both in the solid state and after reconstitution persisted during short time stress storage after reconstitution as well. This further proved the fact that no alterations in either conformation or susceptibility towards

aggregation occurred with the onset of collapse. This hypothesis was further investigated and confirmed in a long term storage stability study discussed in Chapter 8.

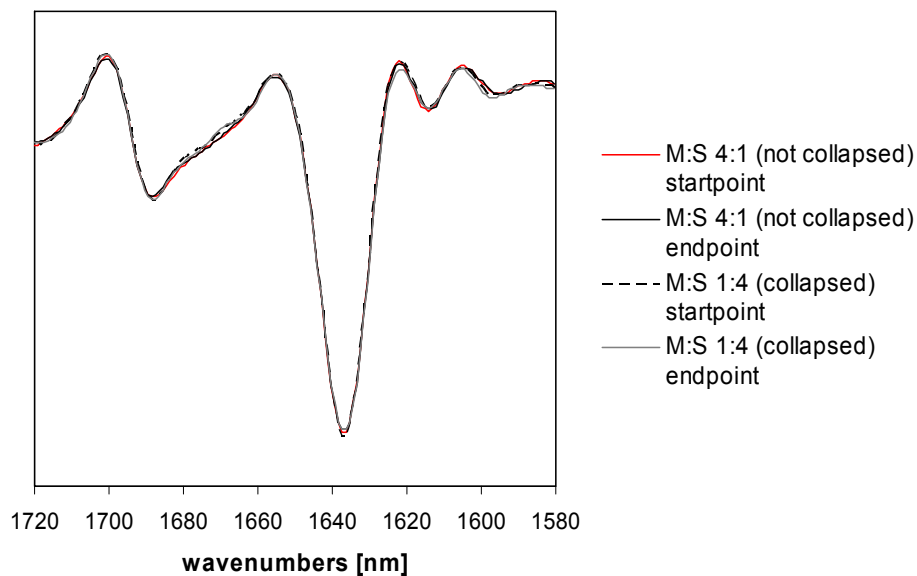


Figure 7.24: Area-normalized 2nd derivative FTIR transmission spectra of the amide I region of 4 mg/mL IgG₀₁ reconstituted from collapsed and non-collapsed lyophilizates after storage at 37 °C/40 rpm for various times.

3 L-LACTIC DEHYDROGENASE (LDH)

In order to further scrutinize the effect of collapse during lyophilization on protein stability L-Lactic-Dehydrogenase (LDH) was investigated as a second model protein. LDH was chosen because of its well described sensitivity towards stress situations arising not only from freeze-drying^{9,109} but also from spray-drying or vacuum-drying^{102,110-112}. It is manifoldly described in literature that drying without a well-stabilizing formulation leads to severe instability reactions². Thus the use of LDH as model system offers the possibility to check the performance of the formulation and the investigated system^{6,113}. Furthermore, with the availability of a photometric activity assay, a key parameter regarding protein stability, the protein's activity, can easily be assessed.

Collapsed and non-collapsed lyophilizates were produced as described in Chapter 3. Collapsed lyophilizates were reproducibly generated using the aggressive collapse-protocol already applied for the production of collapsed IgG₀₁ lyophilizates. Some adaptations in the secondary drying were made to ensure the effective reduction of residual moisture. To enhance drying performance, a stream of dry nitrogen was directed through the drying chamber as described in Chapter 4.

Amorphous as well as partially crystalline formulations were investigated to obtain a representative spectrum of typical freeze-dried formulations¹⁵. Because there are several publications pointing out the importance of poly ethylene glycol (PEG) for the adequate stabilization of LDH^{6,9}, partially crystalline formulations comprising PEG 3350 were investigated. Results of an in-detail investigation on the effect of PEG molecular weight are discussed in section 3.6 of this chapter. This investigation was conducted because some authors described that a minimum molecular weight was required for satisfying LDH stabilization⁸.

To adequately represent amorphous lyophilizates, a formulation containing trehalose, as one of the most often applied disaccharides in lyophilized protein products, was included into the investigation as well²⁴. Because trehalose shows a high glass transition temperature, collapse during storage, as observed during storage of sucrose based lyophilizates (see Chapter 8), had not to be expected. In section 3.5 of this chapter, the results from a study investigating the effect of type of disaccharide (sucrose/ trehalose) on the stabilization of LDH, are discussed.

3.1 PHYSICOCHEMICAL PROPERTIES OF COLLAPSED AND NON-COLLAPSED LYOPHILIZATES

Freeze-dried lyophilizates were either collapsed or elegant, depending on the applied drying protocol. Figure 7.25 A shows a picture of the investigated lyophilizates and Figure 7.25 B lists the corresponding formulations. During conventional freeze-drying lyophilizates

containing sucrose and PEG 3350 (formulation 3) partially collapsed. This allowed the additional comparative investigation of partially collapsed versus completely collapsed lyophilizates.

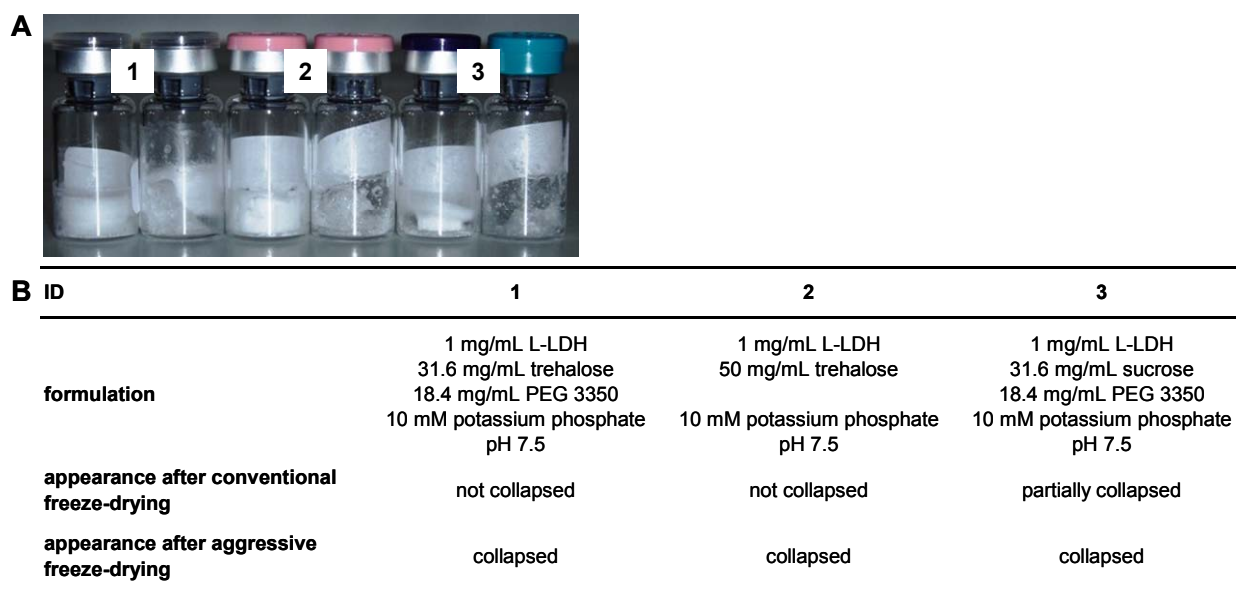


Figure 7.25: Appearance of investigated lyophilizates after aggressive and conventional freeze-drying, respectively (A) and summary of the corresponding formulations and the cake-appearance after freeze-drying (B).

Conventionally freeze-dried lyophilizates: left vial; aggressively freeze-dried lyophilizates right vial (A).

As already discussed in detail above, the prerequisite of a sound comparison of different lyophilized protein products is a comparable residual moisture content, because the adverse effect of moisture on protein stability is well documented in literature^{114,115}. Table 7.13 summarizes the residual moisture levels of the analyzed formulations.

Table 7.13: Physical properties of investigated lyophilizates.

formulation	appearance	residual moisture		$T_g \pm SD [^{\circ}C]^{b)}$	
		$\pm SD [\%]^{a)}$			
trehalose + PEG 3350	not collapsed	0.18% \pm 0.10%	105.45 \pm	2.19	
	collapsed	0.34% \pm 0.05%	109.15 \pm	0.07	
trehalose	not collapsed	0.43% \pm 0.08%	101.1 \pm	0.57	
	collapsed	0.72% \pm 0.09%	90.15 \pm	2.19	
sucrose + PEG 3350	not collapsed	0.82% \pm 0.48%	* \pm	-	*
	collapsed	0.32% \pm 0.14%	72.85 \pm	1.20	

* Determination of glass transition temperatures was not possible due to overlap of the glass transition region and the melting endotherms of PEG modifications.

a) determined by coulometric Karl Fischer titration, $n = 6$

b) determined by differential scanning calorimetry at a scan rate of 10 K/min, $n = 2$

Generally, collapsed cakes showed a higher residual moisture content than the corresponding elegant cakes. However, deviations remained in a range that was previously defined as comparable ($\pm 0.5 \%$). Partially collapsed cakes showed increased water contents

as well. Furthermore, partially collapsed cakes did not dry as homogeneously as elegant or completely collapsed cakes, as could be deduced from increased standard deviations. Partially crystalline cakes showed lower residual moisture levels than amorphous cakes, regardless of the appearance of the lyophilizates. This is probably due to the increased surface area and the less dense structure of crystalline cakes compared to amorphous cakes as already observed by Mattern et al. during vacuum drying of partially crystalline formulations⁷. This behavior is discussed in detail in Chapter 4.

Table 7.13 also lists the glass transition temperatures T_g of the samples. T_g s are determined by the amorphous disaccharides, thus formulation 1 and 2 exhibited higher glass transition temperatures around 100 °C than formulation 3. This is in good agreement with the T_g of trehalose reported in literature (101 °C for freeze-dried trehalose with a residual moisture content of 0.8 %)¹¹⁶. The slightly increased water content of formulation 2 caused the observed decrease in T_g ¹¹⁷. The T_g of formulation 3 could only be analyzed in collapsed cakes, because the glass transition was obscured by the melting endotherm of PEG 3350 at 63 °C^{6,118}. Due to the lower residual moisture in collapsed cakes, the T_g was shifted to higher temperatures. Experimental data is in good agreement with literature values for sucrose (64 °C for freeze-dried sucrose with a residual moisture content of 0.7 %)¹¹⁶.

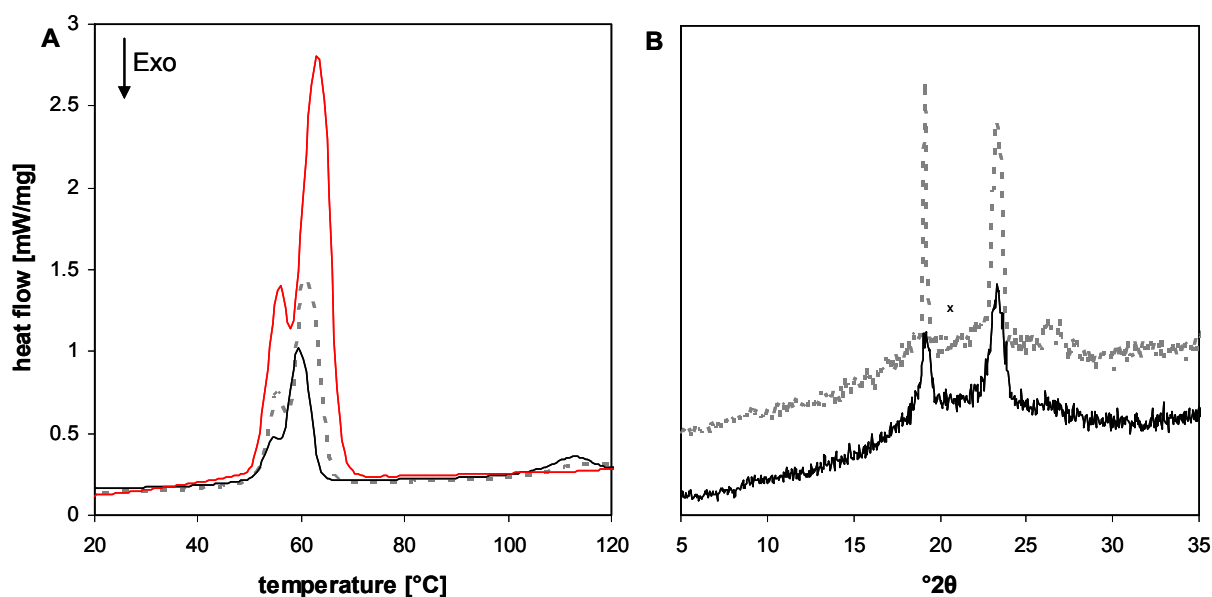


Figure 7.26: Physicochemical characteristics of collapsed (grey-dotted line) and non-collapsed (black solid line) lyophilizates composed of trehalose and PEG 3350: DSC thermograms (A) and X-ray diffractograms (B) ($n = 2$).

The thermogram depicted by a red line in Figure 7.26 A represents PEG 3350 crystalline material.

DSC data showed that disaccharides were amorphous in all the formulations. This was further confirmed by the absence of characteristic signals in the X-ray diffractograms (data not shown). In contrast PEG 3350 crystallized, as indicated by the presence of characteristic melting endotherms in the thermograms^{6,118} (Figure 7.26 A) and by the observation of

characteristic peaks in the X-ray diffractograms (Figure 7.26 B) at 19 and 23 °2θ, respectively¹¹⁸.

In collapsed lyophilizates PEG 3350 seemingly crystallized to a higher extent, as indicated by the higher intensity of both, the melting endotherm and the X-ray diffractions. The crystallinity of PEG was calculated from the melting endotherm according to Izutsu et al.¹¹⁸:

$$\text{crystallinity}[\%] = \frac{\text{heat absorption}_{\text{meltingpeak}} [\text{J}]}{m_{\text{PEG}} [\text{g}] * \text{heat}_{\text{fusion}} [\text{J} / \text{g}]} * 100 \quad (7.1)$$

The heat of fusion was obtained from measurement of pure crystalline PEG and was determined to be 138.4 J/g. This is in satisfying agreement with values reported in literature who reported a heat of fusion of 190.6 J/g for melt quenched PEG 3350¹¹⁹.

Calculated average crystallinities of PEG 3350 were in the order of 100 % for all the formulations except for the non-collapsed trehalose-PEG lyophilizates that are depicted in Figure 7.26. This formulation showed crystallinities around only 60 %. It is well known that crystallization is indicative for phase separation of the phase that crystallized from the remaining matrix. It is furthermore reported in literature that trehalose is more susceptible to phase separation than sucrose²⁴. Thus the observed increased crystallinity can be attributed to phase separation occurring in trehalose-based lyophilizates. This phase separation is apparently more pronounced in collapse-dried cakes. The investigation of the existence and extent of phase separation in the collapsed trehalose PEG lyophilizates was beyond the scope of this study.

However, as no exotherm indicating additional crystallization could be observed in the DSC thermograms, it was concluded that the system was stable and that no uncontrolled crystallization after processing would occur. After thorough assessment the residual moisture and the state of excipients of collapsed and elegant LDH lyophilizates can be regarded as comparable, allowing the further comparative investigation regarding the effect of collapse on protein stability.

3.2 ENZYME ACTIVITY OF LDH IN RECONSTITUTED LYOPHILIZATES

The most important function of enzymes is their catalytic activity. Thus a key analytical tool evaluating protein stability is the recovery of enzymatic activity. LDH catalyzes the reduction of pyruvate to lactate while oxidizing the reduced form of β-nicotinamide adenine dinucleotide (β-NADH) to its oxidized counterpart β-NAD. LDH is an oxidoreductase omnipresent in the cytoplasm of both animals and plants. It allows the regeneration of NAD as vital substance for the glycolysis in the absence of oxygen.

LDH is a tetrameric protein composed of four subunits existing in 2 different types, the M and the H subunit. Thus five isozymes are existent. They differ in their catalytic, physical and immunological properties. Due to the organ-specific distribution of the isozymes, LDH is an

important diagnostic marker. The serum level of a certain subtype of LDH allows drawing conclusions about pathological conditions in certain tissues, e.g. myocardial infarctions and hepatitis.

Because β -NADH measurably absorbs at 340 nm, the consumption of β -NADH and thus the catalytic reaction can be monitored by measuring the decrease of absorption at this wavelength. The catalytic activity of LDH is indispensably connected to the molecules integrity^{120,121}. Thus from activity data conclusions regarding the protein's integrity can be drawn as well.

Figure 7.27 depicts the recovery of enzyme activity in the reconstituted solution after freeze-drying to collapsed (grey bars) and elegant (black bars) lyophilizates.

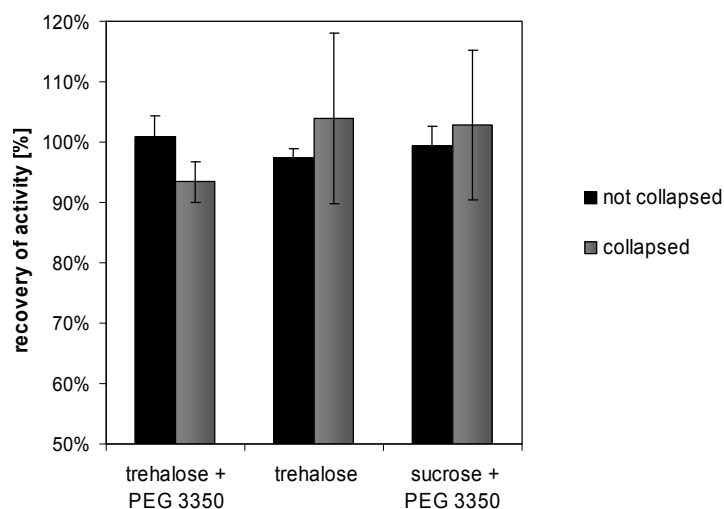


Figure 7.27: Recovery of enzyme activity in the reconstituted solution after freeze-drying to collapsed (grey bars) and non-collapsed (black bars) lyophilizates.

Activities are calculated average values of at least two independent measurements compared to the average activity prior to freeze-drying.

Most obviously LDH stability was well preserved in all the systems, as activities were not strongly decreased as compared to the activities prior to freeze-drying (set to 100 %). Because it is well known from literature, that freeze-drying LDH without a proper formulation results in a severe loss of protein activity, it can be concluded that all the formulations were able to stabilize LDH during freeze-drying and that this ability was not lost with the onset of collapse. The preservation of bioactivity with the onset of collapse has been recently observed by Luthra et al. as well¹²². Interestingly, activities were higher in collapsed lyophilizates than in elegant ones for two of the three investigated formulations (trehalose and sucrose & PEG 3350). These formulations even showed a recovery of enzyme activity larger than 100 %. An increased activity after freeze-drying has also been described by Anchordoquy et al.¹²³. The authors related this phenomenon to changes in the protein's secondary structure upon freeze-drying.

However, regarding the relatively large standard deviations there were no significant differences between the collapsed and non-collapsed cakes.

3.3 PHYSICAL PROTEIN STABILITY OF LDH IN RECONSTITUTED LYOPHILIZATES

To further analyze possible effects caused by the occurrence of collapse in varying formulations of LDH lyophilizates, physical stability of the protein, i.e. the formation of soluble and insoluble aggregates, was assessed. Besides the protein activity the formation of aggregates is a key parameter in protein formulation. Aggregated protein fractions may reduce the product's safety and efficacy⁴². Since aggregates can cause immunogenic responses leading to a loss of activity or – in the worst case – to serious immune reactions¹²⁴, the aggregation status has to be closely monitored and formation of aggregates should be prevented.

Figure 7.28 plots the relative amount of monomer in the soluble fraction of collapsed (grey bars) and non-collapsed (black bars) reconstituted samples. Monomer contents above 90 % were detected. Because activity is inextricably linked to the monomeric protein, a higher monomer content would have been expected from activity data⁹. The higher activity compared to the determined amount of monomer, can be explained with the dissociation of aggregates under the highly diluted conditions (2000 fold) of the activity assay. Once more, collapsed lyophilizates performed slightly better than elegant ones. But again, these differences were not significant.

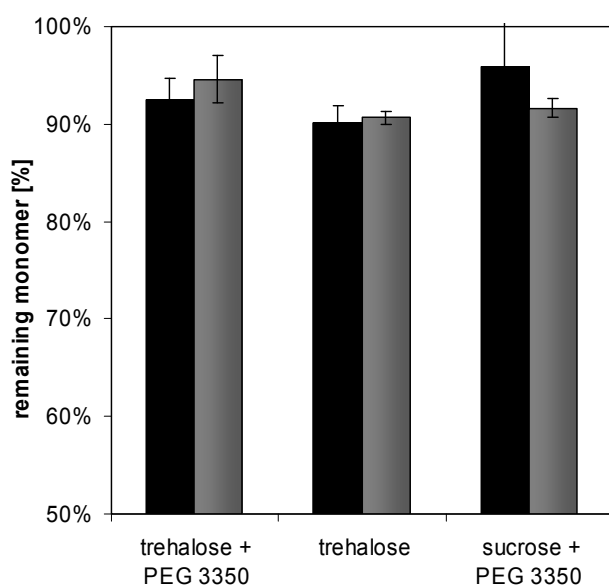
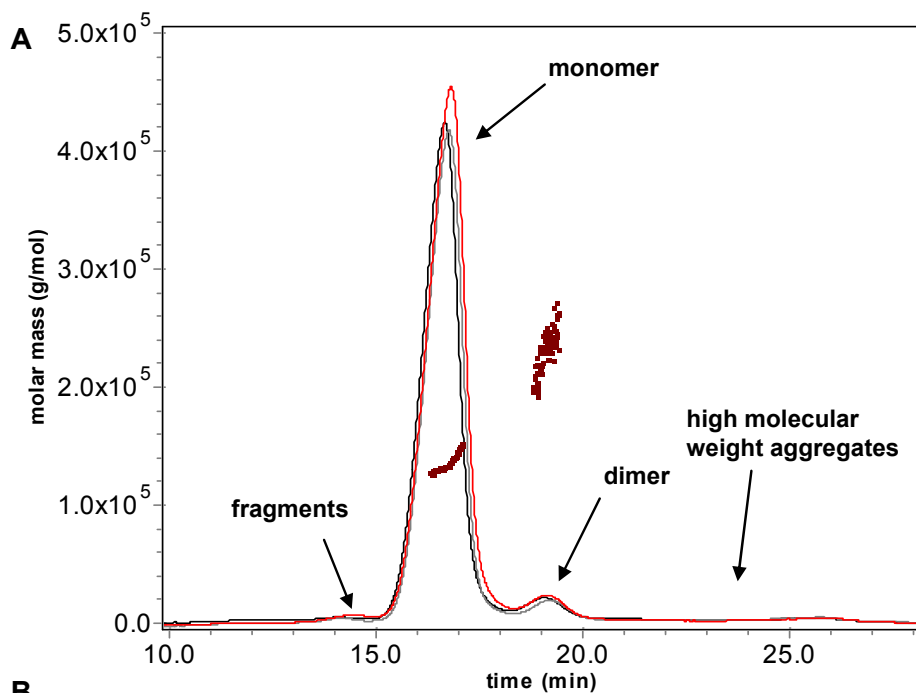


Figure 7.28: Remaining monomer of LDH from collapsed (grey bars) and non-collapsed (black bars) reconstituted lyophilizates, respectively, determined by HP-SEC (average \pm SD, n = 2).

Upon freeze-drying, insoluble aggregates were formed. This was indicated by a decrease in recovery of HP-SEC experiments (data not shown). To further characterize this insoluble aggregate fraction, light obscuration analysis, turbidity measurements and asymmetrical flow field flow fractionation (AF4) experiments were performed.

Figure 7.29 A depicts a representative AF4 fractogram of LDH from collapsed and non-collapsed reconstituted lyophilizates as compared to a freshly dialyzed LDH standard (red

curve). Clearly, well separated monomer and dimer fractions are distinguishable. A small fragmented fraction can be recognized eluting right before the monomer fraction. However, high molecular weight aggregates, as the fraction is small, were not manifested as a peak, but as a broad rise of the baseline after the dimer peak. The molecular weights of the monomer and dimer fraction were determined by multiangle light scattering taking into consideration the concentration from the UV-signal.



formulation	appearance	monomer ± SD [%]	dimer ± SD [%]	hmw aggregates ± SD [%] *
trehalose + PEG 3350	not collapsed	87.06 ± 1.03	5.35 ± 0.33	3.64 ± 1.45
	collapsed	90.26 ± 0.43	5.00 ± 0.04	3.58 ± 0.09
trehalose	not collapsed	88.57 ± 1.50	5.37 ± 0.34	4.77 ± 0.83
	collapsed	88.83 ± -	4.91 ± -	4.75 ± -
sucrose + PEG 3350	not collapsed	88.84 ± 0.67	5.26 ± 0.03	4.30 ± 0.39
	collapsed	88.60 ± 0.67	5.13 ± 0.09	4.84 ± 0.47
LDH standard		89.24 ± 0.65	4.44 ± 1.44	3.57 ± 0.70

* high molecular weight aggregates

Figure 7.29: AF4 fractograms of collapsed (black line) and non-collapsed (grey line) reconstituted lyophilizates formulated with trehalose and PEG 3350 as compared to freshly dialyzed LDH (red line) (A); solid lines represent the UV-signal and dots represent the MALS signal indicating the molecular weight; summary of monomer and aggregated fractions as determined by AF4 (B).

Reported values are average values calculated from 2 independent measurements. Recoveries were approximately 100 % for all the experiments.

The experimental data are well consistent with literature, specifying an average molecular weight of approximately 145 kDa for the monomer fraction and approximately 290 kDa for the dimer fraction. The amount of high molecular weight aggregates and fragments was too

low to allow a reliable determination of the molecular weight. Figure 7.29 B gives a summary of the composition of the investigated reconstituted lyophilizates as determined by AF4.

Results were in good agreement with results obtained from HP-SEC regarding monomer fractions. Dimer fractions were determined slightly higher as compared to HP-SEC experiments. This is consistent with the observation of Gabrielson et al. who observed detectable amounts of monomer upon injection of purified dimer onto an HP-SEC column; Gabrielson et al. explained the partial dissociation of dimers due to shear forces experienced on the column¹²⁵. Higher molecular weight aggregates that were removed from HP-SEC samples during sample preparation that caused the decrease in recovery in HP-SEC experiments could be detected as a broad baseline elevation and eluted upon reduction of the cross-flow starting after 23 minutes runtime (hmw-aggregates in Figure 7.29 B). Comparing collapsed and non-collapsed samples, there was no difference detectable in aggregation behavior. All the samples were composed of mostly monomer, with approximately 5 % dimer and 2 – 3 % higher molecular weight aggregates. There were no aggregates detectable that eluted in the so-called steric-hyperlayer mode indicating very high molecular weights¹²⁶.

Table 7.14 summarizes data regarding the formation of particles in collapsed and non-collapsed LDH lyophilizates. Light obscuration analysis was performed to assess the formation of sub-visible particles¹²⁷. Particle numbers determined in reconstituted lyophilizates were much lower than the limits specified in the pharmacopoeias, but they were markedly higher than particle numbers observed in IgG01 lyophilizates, further highlighting the stronger sensitivity of LDH. Comparing particles $\geq 10 \mu\text{m}$ and $\geq 25 \mu\text{m}$, which are indicated in the pharmacopoeia methods, no relevant differences between collapsed and non-collapsed lyophilizates was observed. However, comparing particles $\geq 1 \mu\text{m}$, which were recently described to be more relevant for protein formulations, differences are observed. PEG-containing formulations showed distinctly increased particle numbers in collapsed lyophilizates. This was further confirmed by increased turbidity values. In contrast, purely amorphous trehalose lyophilizates showed decreased particle numbers in collapsed cakes. Again, this was also reflected in turbidities. Thus no clear trend regarding the effect of collapse on the formation of sub-visible particles could be concluded. However, particle numbers were distinctly lower than in a LDH lyophilizate that was freeze-dried in an inappropriate formulation added as a bench-mark in Table 7.14, except for the purely trehalose-based non-collapsed formulation. Both purely sugar-based cakes (collapsed as well as non-collapsed) showed higher particle numbers for particles $\geq 1 \mu\text{m}$ and $\geq 10 \mu\text{m}$ as compared to the partially crystalline formulations. They exhibited increased turbidity values as well. As this increased level of sub-visible particles was not confirmed by other analytical techniques, this phenomenon possibly was caused by the presence of small air bubbles in

freshly reconstituted lyophilizates, that has been reported elsewhere³¹. The presence of a higher number of air bubbles in freshly reconstituted elegant trehalose-based lyophilizates was shown using micro flow imaging (data not shown).

Table 7.14: Particulate matter in reconstituted collapsed and non-collapsed LDH lyophilizates.

formulation	appearance	particles > 1 $\mu\text{m/ml}$ \pm SD [%] ^{a)}	particles > 10 $\mu\text{m/ml}$ \pm SD [%] ^{a)}	particles > 25 $\mu\text{m/ml}$ \pm SD [%] ^{a)}	turbidity \pm SD [FNU] ^{b)}
trehalose + PEG 3350	prior to FD	63885 \pm 337	3718 \pm 145	583 \pm 61	n.a.
	not collapsed	25282 \pm 683	249 \pm 44	13 \pm 5	6.12 \pm 1.45
	collapsed	33947 \pm 2948	220 \pm 15	12 \pm 7	8.98 \pm 0.11
trehalose	prior to FD	37339 \pm 713	2990 \pm 176	511 \pm 78	n.a.
	not collapsed	150039 \pm 16023	439 \pm 54	24 \pm 11	9.64 \pm 1.07
	collapsed	61951 \pm 354	273 \pm 24	19 \pm 10	8.03 \pm 0.07
sucrose + PEG 3350	prior to FD	47794 \pm 1649	3044 \pm 79	553 \pm 46	n.a.
	not collapsed	23393 \pm 464	256 \pm 76	23 \pm 7	6.87 \pm 2.01
	collapsed	40609 \pm 1132	272 \pm 28	23 \pm 9	10.19 \pm 0.01
LDH freeze-dried in inappropriate formulation		78698 \pm 5386	295 \pm 92	43 \pm 19	n.a.

a) determined by light obscuration, values are calculated average values from 2 measurements

b) determined by nephelometric turbidity measurements, values are calculated average values from 2 measurements

n.a.: not accomplished

A different reconstitution behavior of collapsed and non-collapsed lyophilizates might also affect the observed differences in particle numbers $\geq 1 \mu\text{m}$, as the observed differences were not reflected in neither one of the orthogonal techniques nor in particle size numbers of larger particles.

In summary, no relevant differences in the characteristic properties indicating protein physical stability could be detected, thus the occurrence of collapse during freeze-drying seemingly did not have a negative effect on the physical stability, i.e. the soluble and insoluble aggregation, of LDH. Intriguingly, collapsed lyophilizates exhibited slightly better stability in key analytical parameters, such as activity and amount of remaining monomer. However, as the differences were small, these finding would have to be further confirmed by conformational data (section 3.4) and storage stability data (Chapter 8) to allow for a sound judgment.

3.4 CONFORMATIONAL STABILITY OF LDH IN RECONSTITUTED LYOPHILIZATES

As there is a strong correlation between retention of secondary structure and activity of LDH reported in literature (a linear relationship between the spectral correlation coefficient and the recovery of activity with a correlation of 0.97 was described by Prestrelski et al.⁷⁷), the FTIR analysis is of special interest⁷⁸.

LDH is composed of 36.8 % helical structures, 11.3 % β -sheet structures and 14.3 % turn structures as determined from X-ray diffraction¹²⁸. Figure 7.30 depicts second derivatives of area-normalized FTIR transmission spectra of reconstituted LDH lyophilizates. Figure 7.30

part A compares the three formulations prior to freeze-drying with a LDH standard (LDH type II from rabbit muscle ammonium sulphate suspension, freshly dialyzed over night against 10 mM potassium phosphate buffer pH 7.5). Each Figure B, C, D represents one formulation 1 - 3. The dotted curve in each diagram is a spectrum recorded from a heat denatured LDH standard, whereas the red curves are recorded from the corresponding formulation 1 – 3 prior to freeze-drying.

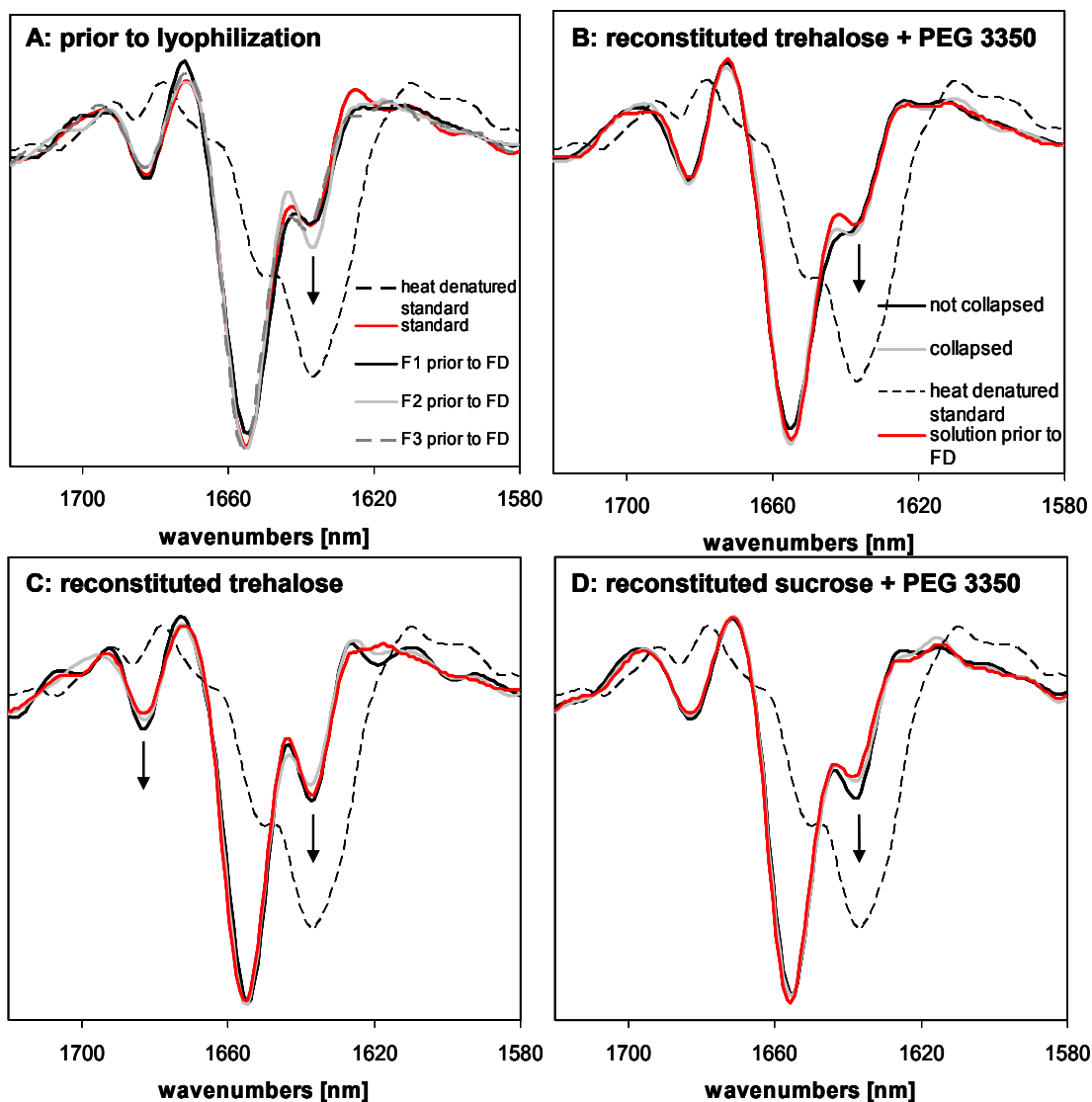


Figure 7.30: 2nd derivative area-normalized FTIR transmission spectra of solutions prior to freeze-drying as compared to standard and heat denatured standard (A) and of reconstituted lyophilizates after freeze-drying to collapsed and non-collapsed lyophilizates (B-D) as compared to the solutions prior to freeze-drying (red line) and to heat denatured LDH standard (dotted line); trehalose & PEG 3350 based lyophilizates (B), trehalose based lyophilizates (C) and sucrose & PEG 3350 based lyophilizates (D). Spectra are calculated average spectra of two independent measurements.

The main band at 1656 cm^{-1} is associated with α -helical structures and the band at 1636 cm^{-1} with β -sheets^{9,113,129}. The origin of bands at higher wavenumbers however, is controversially discussed in literature. Mi et al. ascribe them to either turn structure or β -sheet in accordance with Susi et al.^{9,129}, whereas Prestrelski et al. related a band at 1698 cm^{-1} most probably to

aggregation¹¹³. It is well-described in literature for various proteins, that a band around 1682 cm⁻¹ is associated with intermolecular β -sheet structures that indicate protein aggregation⁷⁶. Thus it was concluded that this might be valid for LDH as well and the band observed at 1683 cm⁻¹ was regarded as indicative for aggregation.

Examining Figure 7.30 B to D, most obviously, all spectra show a high degree of similarity, thus secondary structure was well preserved upon freeze-drying. Furthermore, as there were no drastic differences in the spectra of collapsed and non-collapsed lyophilizates, the onset of collapse did not have a detrimental effect on the protein's conformational stability. There were only small differences in the spectra of reconstituted lyophilizates as compared to the solutions prior to freeze-drying, most pronounced in the band at 1636 cm⁻¹. This increase in β -sheet structure upon drying is a behavior that was observed for various proteins^{76,77} and was explained by the lower degree of hydration required for β -sheet as compared to α -helical structures¹³⁰.

However, more pronounced differences were observed comparing the intensity of that band at 1636 cm⁻¹ in the three different formulations prior to freeze-drying. Formulation 2, i.e. the formulation lacking the addition of PEG 3350, shows the most pronounced band at that wavenumber. This is well consistent with the higher degree of conformational stability of LDH in the presence of PEG observed by Mi et al.⁹. From the comparison of native LDH spectra with heat denatured spectra, a strong increase in the intensity of that band upon thermal unfolding was concluded. Thus the gain in intensity in that band might be indicative for a beginning of unfolding.

Nonetheless, as there were no differences observed in the intensities of the band at 1683 cm⁻¹, no differences regarding the physical stability and soluble aggregation were indicated. This is in agreement with HP-SEC results that did not show a difference in the initial level of aggregation (data not shown).

Table 7.15: Ratios of the intensities of characteristic FTIR 2nd derivative transmission spectral bands.

formulation	β -sheet ratio 1			β -sheet ratio 2		
	intensity at 1683cm-1 /intensity at 1656cm-1			intensity at 1638cm-1 /intensity at 1656cm-1		
	1	2	3	1	2	3
prior to FD	0.05	0.01	0.01	0.23	0.28	0.23
non-collapsed	0.06	0.06	0.02	0.26	0.32	0.32
collapsed	0.07	0.03	0.02	0.26	0.26	0.25
heat denatured standard *			1.12			4.49

* LDH standard heated tot 56 °C for 10 minutes.

In an attempt to more reliably assess the observed slight spectral differences, the ratio between the intensities of the main band at 1656 cm⁻¹ and either the band associated with intermolecular β -sheet at 1683 cm⁻¹ or with the band associated with intramolecular β -sheet

at 1636 cm^{-1} , respectively were calculated according to the calculation of the β -sheet ratio described for an IgG by Abdul-Fattah et al.¹⁰³. Results are listed in Table 7.15. Serving as a benchmark, ratios for heat denatured enzyme were calculated as well.

Calculated ratios were high for the heat-denatured sample but they were small for all the investigated lyophilizates and no relevant difference was observed between the solutions prior to freeze-drying and after reconstitution from either collapsed or non-collapsed lyophilizates. Slightly lower β -sheet ratio 2 values were observed in collapsed lyophilizates for the formulations 2 and 3. A similar tendency could be seen in the β -sheet ratio 1 for formulation 2. However, no differences were observed for the other formulations and as the overall differences were small, no clear trend could be concluded

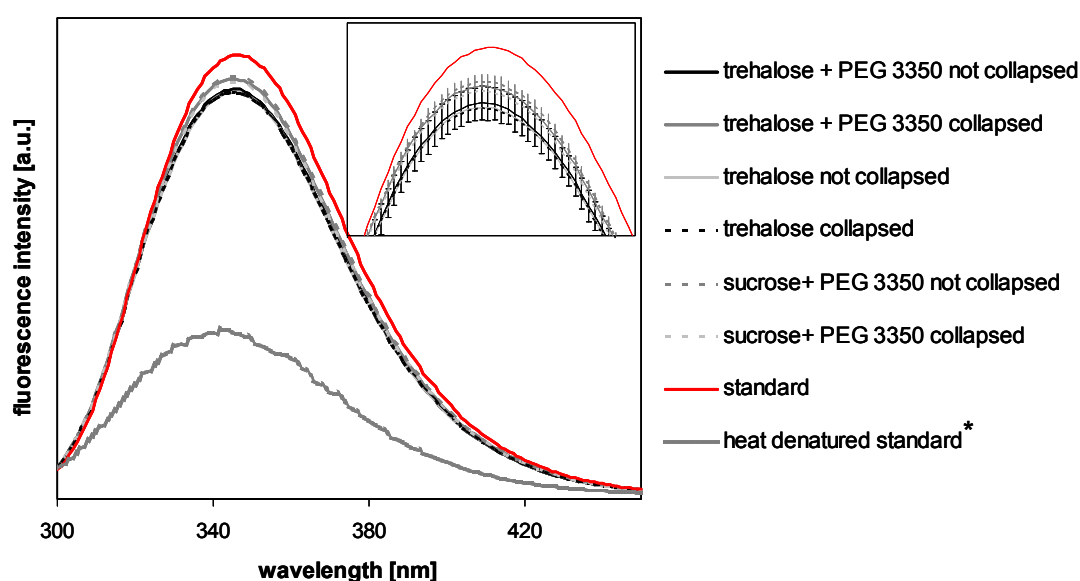


Figure 7.31: Intrinsic protein fluorescence emission spectra after excitation at 280 nm at 20 °C of 0.05 mg/mL LDH after reconstitution from collapsed and non-collapsed lyophilizates.

Reconstituted lyophilizates were diluted with potassium phosphate pH 7.5 to the measurement concentration in order to avoid internal quenching. Spectra are calculated average spectra of 2 independent measurements. The insert shows a magnification of the spectral maxima region including error bars indicating the standard deviation for selected data points.

* Standard was heated to 60 °C during a temperature ramp and intrinsic protein fluorescence was recorded.

To further investigate the effect of collapse on the conformational stability of LDH, tertiary structure was assessed using intrinsic protein fluorescence. Figure 7.31 shows fluorescence emission spectra after excitation at 280 nm of reconstituted collapsed and elegant LDH lyophilizates as compared to standard (red curve) and heat denatured standard (black hatched line).

All samples showed slightly decreased fluorescence intensity after lyophilization as compared to the standard. However, the observed decrease was by far not as pronounced as that observed upon heat denaturation at 60 °C (grey-shaded line in Figure 7.31). No shift in emission maximum was observed upon denaturation. This was reported earlier by Göller et al.¹³¹. The measured emission maximum at 344 nm is in agreement with their data as well.

The insert into Figure 7.31 displays a magnification of the spectral region around the emission maximum at 344 nm, in order to allow for a clearer presentation of the slight differences in fluorescence intensity. Error bars describing the standard deviation of single data points are included for selected formulations. From the overlapping error bars it was concluded that the observed small fluctuations in emission intensity were not significant. To further illustrate this fact Table 7.16 lists the absolute intensities and their standard deviations as well as the intensities normalized for the intensity of a heat-denatured standard, according to a procedure described by Göller et al.¹³¹. Conclusions from the evaluation of the spectra were confirmed in that no significant difference could be observed.

These findings are especially important, because a direct correlation of changes in the fluorescence emission spectra with changes in enzyme activity was reported¹³¹.

Table 7.16: Intrinsic protein fluorescence intensities at the emission maximum at 344 nm, either absolute or normalized to the intensity of a standard solution heat-stressed at 60 °C.

ID	appearance	fluo.int. _{344nm} [a.u.] ± SD	fluo.int. _{344nm sample} / fluo.int. _{344nm denatured} ± SD
1	non-collapsed	187.00 ± 4.60	2.46 ± 0.06
	collapsed	191.99 ± 4.77	2.53 ± 0.06
2	non-collapsed	185.81 ± 2.01	2.45 ± 0.03
	collapsed	195.69 ± 0.85	2.44 ± 0.01
3	non-collapsed	193.15 ± 2.01	2.54 ± 0.03
	collapsed	190.55 ± 4.52	2.51 ± 0.06
standard		185.79 ± 1.71	2.45 ± 0.02

3.5 EXCURSUS I: COMPARISON OF DIFFERENT DISACCHARIDES

Because of the well-described efficacy of trehalose to stabilize proteins in the dried state, a sucrose-based formulation, representing a slightly less effective protective agent, was investigated, in order to ensure, that a possible effect of collapse was not masked by the high efficiency of trehalose.

In literature, trehalose is commonly regarded as the better stabilizer due to several advantages over sucrose. Trehalose glasses exhibit higher glass transition temperatures, thus both freeze-drying and storage can be carried out at higher temperatures¹³². Furthermore, trehalose is less hygroscopic and a reduced increase of residual moisture during storage due to formation of a dihydrate rather than plasticizing of the amorphous phase was reported^{133,134}. Trehalose has a very low chemical reactivity. For example, the hydrolysis rate at 60 °C at low pH was reported to be 1/17000th of the rate for sucrose¹³⁵. The susceptibility to crystallize is strongly reduced as well¹¹⁶. Finally, the absence of internal hydrogen bonds renders the disaccharide more flexible and allows more effective hydrogen bonding than with sucrose¹³⁶. The use of trehalose was first inspired by the observation of

the so-called anhydrobiosis, i.e. the viability of certain organisms after complete dehydration¹³⁷. Since then various investigations pointed out the superior properties of trehalose in the dried-state stabilization of biomaterials as compared to various other excipients including sucrose^{136,138-141}.

Thus it was intended to investigate whether sucrose equally preserves LDH with the onset of collapse. In order to create conditions that allow clear distinction between the disaccharides, the absolute stabilizer content was decreased from 5 % to 1.7 %, because Iwai et al. found, that LDH reacted more sensitive to freeze-drying stresses at lower disaccharide concentrations¹⁴². Anchordoquy et al. found that 0.025 M sucrose led to 60.4 % recovery of activity after freeze-drying, whereas 0.1 M sucrose achieved 87.1 % recovery of activity. Similar results were found for trehalose¹²³. Thus the reduction of sugar concentration from 5 %, i.e. 0.15 M to 1.7 %, i.e. 0.05 M should markedly increase the system's susceptibility towards freeze-drying stresses.

As for all other studies in this thesis, a comparable residual moisture level had to be achieved as prerequisite for the comparative investigation. Table 7.17 lists the residual moisture levels after freeze-drying to collapsed and non-collapsed lyophilizates. Moisture levels were comparably high for all freeze-dried solids.

Table 7.17: Residual moisture levels, sub-visible and visible particles of collapsed and non-collapsed LDH lyophilizates.

excipient	appearance	residual moisture ± SD [%] ^{a)}	cumulative particles > 1 µm / mL ± SD ^{b)}	cumulative particles > 10 µm / mL ± SD ^{b)}	turbidity [FNU] ± SD ^{c)}
sucrose	not collapsed	2.40 ± 0.12	70557 ± 844	178 ± 16	6.23 ± 0.37
	collapsed	2.06 ± 0.40	50022 ± 775	308 ± 31	7.12 ± 0.28
trehalose	not collapsed	2.60 ± 0.05	86617 ± 490	100 ± 9	6.31 ± 0.11
	collapsed	2.81 ± 0.27	60567 ± 453	373 ± 0	6.19 ± 0.06

a) determined by coulometric Karl Fischer titration, n = 2

b) determined by light obscuration analysis, n = 2

c) determined by nephelometric turbidity measurements, n = 2

Table 7.17 also summarizes the results obtained from the analysis of sub-visible particles. Non-collapsed systems showed distinctly lower particle numbers than collapsed lyophilizates regarding particles ≥ 10 µm. In contrast, in the class of particles ≥ 1 µm (that are not specified in the pharmacopoeias but nevertheless are important in the detection of protein aggregates³¹) collapsed systems showed decreased particle numbers. Thus, a trend regarding the preferred formation of small particles at the expense of large particles in collapsed lyophilizates can be concluded. However, as turbidity values were observed to be low, the increased particle numbers might also have been caused by the erroneous detection of air bubbles in the laser beam³¹.

Figure 7.32 displays the activities of reconstituted collapsed and non-collapsed lyophilizates as compared to the activity prior to freeze-drying. Most strikingly, collapsed lyophilizates showed distinctly higher recoveries of activity than non-collapsed systems further confirming

results obtained so far. Moreover, activity of reconstituted collapsed lyophilizates depended on the formulated disaccharide. Interestingly, sucrose based formulations showed a higher activity, in contrast to the often described superior efficacy of trehalose. This was also observed by Anchordoquy et al.¹²³. There was no dependence on formulations observable for non-collapsed systems.

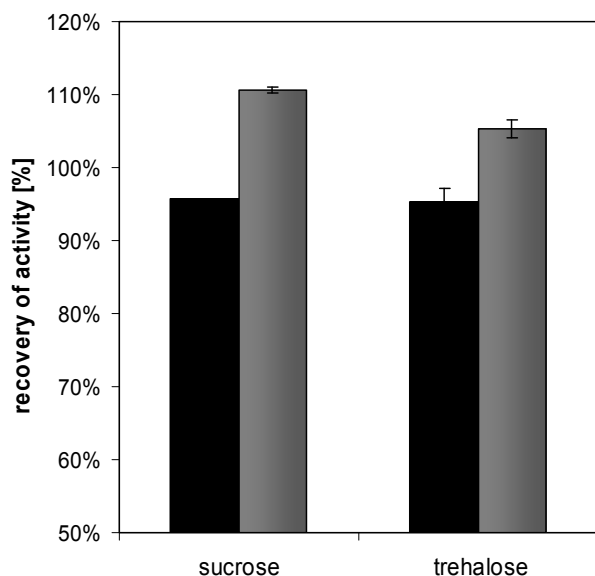


Figure 7.32: Recovery of catalytic activity of LDH after reconstitution from collapsed (grey bars) and non-collapsed (black bars) lyophilizates immediately after freeze-drying (average \pm SD, n = 2).

Figure 7.33 depicts the 2nd derivative FTIR transmission spectra of collapsed and non-collapsed sucrose - (Figure 7.33 A) or trehalose - (Figure 7.33 B) based LDH lyophilizates. Secondary structure was generally well preserved for all the investigated systems, deducible from the overall high degree of spectral similarity. The formation of a new band around 1706 cm^{-1} upon freeze-drying in the presence of sucrose stands out. This band might be of similar origin as the band observed by Prestrelski et al. at 1698 cm^{-1} . The authors stated that this band was most probably related to an aggregated form of LDH¹¹³. As this band was observed to a smaller extent in trehalose based formulations, secondary structure preservation was superior to sucrose-based formulations.

The better preservation of secondary structure in trehalose-based cakes is further manifested in the band at 1638 cm^{-1} , that is associated with intramolecular β -sheet structures. All formulations showed an increase in that band upon freeze-drying, but it was more pronounced for sucrose-based formulations. This is a behavior reported for several proteins^{143,144} and was explained with the lower degree of solvation required for β -sheets¹³⁰. Thus the increased amount of β -sheet structures in sucrose based formulations could be explained with the less effective hydrogen-bonding of sucrose described by Crowe et al.¹⁴⁵. However, there were no structural differences observed between collapsed and non-collapsed lyophilizates in neither of the formulations.

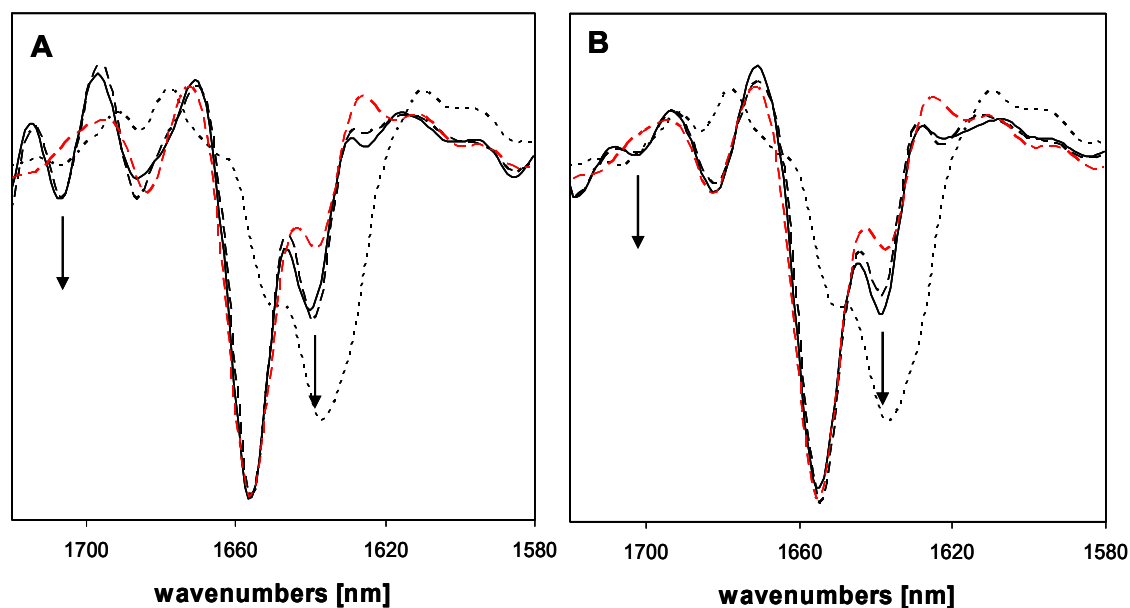


Figure 7.33: Area-normalized 2nd derivative FTIR transmission spectra of collapsed (black dashed) and non-collapsed (black solid) sucrose (A) and trehalose (B) based lyophilizates compared to standard (red) and heat-denatured standard (black dotted).

Bands at 1706 cm^{-1} and 1638 cm^{-1} , indicating changes in LDH secondary structure upon freeze-drying are designated with an arrow.

Spectra are calculated average spectra of two independent measurements. LDH concentration was 1 mg/mL.

In summary, the intention of increasing the formulations' susceptibility towards freeze-drying and collapse-associated stresses in order to get further insight into the possible effect of cake collapse on protein stability was at least partially achieved. Regarding the retention of secondary structure after freeze-drying, sucrose-based formulations showed distinctly less preservation, but no difference between collapsed and non-collapsed lyophilizates was observed in either sucrose- or trehalose-based cakes. Evaluating activity data, collapsed lyophilizates performed markedly better than elegant ones and sucrose based formulations performed better than trehalose based ones

In conclusion there was no clear effect of disaccharide type neither on the preservation of LDH stability during freeze-drying nor on the possible effect of collapse. However, findings from former experiments were further confirmed in that no detrimental effect of collapse on LDH stability was detectable. Moreover, collapsed lyophilizates showed increased recovery of activity, that is an enzyme's key stability-indicating parameter.

3.6 EXCURSUS II: IS THERE A MINIMUM MOLECULAR WEIGHT REQUIRED? EFFECT OF MOLECULAR WEIGHT OF PEG ON THE PRESERVATION OF LDH STABILITY IN COLLAPSED AND NON-COLLAPSED LYOPHILIZATES

There are several publications pointing out the importance of polyethylene glycol for the adequate stabilization of LDH^{6,8-10,113,123,146,147}. PEG acts as a cryo-protectant, preventing dissociation of the native tetramer during freezing^{123,146}. Thus, for optimum stabilization, the combination of PEG with a lyo-protectant, such as sucrose or trehalose, is required^{9,113}. Mi et

al. described increasing protection with increasing molecular weight of PEGs with a minimum molecular weight of PEG required for effective stabilization. PEGs with a molecular weight higher than 8000 Da were shown to fully protect LDH during freezing at concentration lower than 0.01 % whereas lower molecular weight PEGs had to be applied in higher concentrations¹⁰. Izutsu et al. even described a destabilization of LDH by lower molecular weight PEGs (PEG 400) upon freeze-drying despite equal protection during freeze-thawing¹⁴⁷. This behavior was explained by a minimum size required to adequately interact with the protein in a chaperon-like mechanism, stabilizing refolding intermediates and therefore slowing down aggregation¹⁴⁸.

While Anquordoquy et al. described preferential exclusion as the main mechanism of stabilization, Mi et al. identified non-specific, concentration-dependent interactions between PEG and LDH as responsible for the stabilization^{8,123}.

In order to investigate formulations with different capabilities to stabilize LDH, different molecular weight PEGs as excipients were investigated. Additionally to the PEG 3350 formulations shown above, PEG 1500 - and PEG 8000 - based formulations were investigated and compared in regard to their ability to stabilize LDH with and without the occurrence of collapse. All formulations comprised of either sucrose or trehalose as additional lyo-protectant to stabilize LDH in the dried state. Formulations were compared to purely sugar based formulations as a reference.

To maintain collapsibility, PEG was added in a low relative mass ratio of 1.7: 1 sugar to PEG. This ratio was sufficiently low, that no crystalline scaffold could be formed preventing the macroscopic collapse.

3.6.1 RESIDUAL MOISTURE

As already described above, the addition of a crystalline component to an amorphous cake drastically improved the drying performance.

Table 7.18: Residual moistures of collapsed and non-collapsed lyophilizates formulated with PEG of varying molecular weights as determined by coulometric Karl Fischer titration (average \pm SD; n = 2).

excipients	mean M_r of PEG [mol/g]	appearance	residual moisture \pm SD [%]
sucrose + PEG	1500	non-collapsed	0.70 \pm 0.01
		collapsed	0.75 \pm 0.02
	8000	non-collapsed	0.83 \pm 0.05
		collapsed	0.80 \pm 0.05
trehalose + PEG	1500	non-collapsed	0.83 \pm 0.06
		collapsed	1.07 \pm 0.11
	8000	non-collapsed	1.10 \pm 0.12
		collapsed	1.04 \pm 0.04

This was observed by Mattern et al. and was ascribed to the increased surface area and less dense structure of the solid to be dried⁷ (residual moisture levels of purely amorphous cakes are listed in Table 7.17, residual moisture levels of partially crystalline cakes are listed in Table 7.18.). In order to avoid mixing up effects from residual moisture and effects from molecular weight of PEG or collapse, comparable residual moisture levels in the freeze-dried cakes had to be ensured as a prerequisite (Table 7.18).

3.6.2 PHYSICAL PROTEIN STABILITY

Table 7.19 summarizes data concerning the particulate matter of reconstituted collapsed and non-collapsed LDH lyophilizates. Clearly, collapsed lyophilizates showed increased particle numbers upon rehydration. No clear effect of PEG molecular weight could be observed. Turbidity values did not show as clear a trend as the light obscuration data, no effect of either collapse or PEG molecular weight could be detected by turbidity.

Table 7.19: Sub-visible and visible particles of collapsed and non-collapsed lyophilizates formulated with PEG of varying molecular weights (average \pm SD, n = 2).

excipient	mean M _r PEG [g/mol]	appearance	cumulative particles > 1 μ m / mL \pm SD ^{a)}	cumulative particles > 10 μ m / mL \pm SD ^{a)}	turbidity [FNU] \pm SD ^{b)}
sucrose + PEG	1500	not collapsed	43236 \pm 1051	118 \pm 26	6.12 \pm 0.03
		collapsed	46550 \pm 410	143 \pm 14	4.97 \pm 0.04
	8000	not collapsed	14881 \pm 844	50 \pm 5	5.03 \pm 0.21
		collapsed	42711 \pm 285	150 \pm 24	6.22 \pm 0.12
trehalose + PEG	1500	not collapsed	17185 \pm 780	75 \pm 7	6.38 \pm 0.17
		collapsed	47438 \pm 219	243 \pm 19	6.05 \pm 0.21
	8000	not collapsed	21830 \pm 929	52 \pm 2	7.48 \pm 0.11
		collapsed	68266 \pm 127	137 \pm 0	6.4 \pm 0.23

a) determined by light obscuration, n = 2

b) determined by nephelometric turbidity measurements, n = 2

To further assess LDH integrity, SDS-PAGE was performed. Figure 7.34 depicts the effect of PEG molecular weight on the mobility of reconstituted collapse-dried LDH in various formulations. Most strikingly, LDH formulated with PEG 8000 showed faster migrations than LDH in other formulations. This behavior was also observed by Mi et al.. The authors explained the altered electrophoretic mobility with a direct interaction of PEG and LDH, resulting in the coating of the protein with sort of a PEG-shell similar to the enclosing of a glycoprotein. This might lead to a changed molecular weight or SDS-binding behavior causing the altered running pattern¹⁰. This behavior was only reported for PEG 8000 and for PEG 4000 at higher concentrations. Thus the unchanged bands of LDH formulated with PEG 1500 are consistent with Mi's observations.

There was no difference observed between collapsed and non-collapsed samples (data not shown). All samples showed slight aggregation as apparent from the light band above the main band, but there was no relevant difference in the intensities of the band in reconstituted lyophilizates as compared to the standard (lane 3 and lane 8).

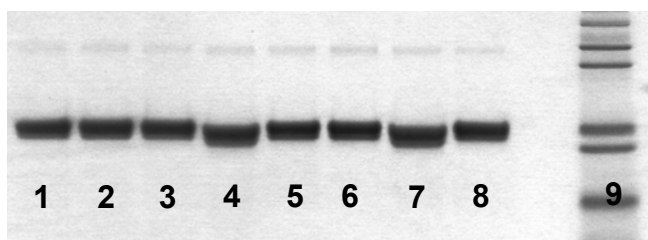


Figure 7.34: SDS-PAGE of LDH after reconstitution from collapsed lyophilizates containing PEG with different molecular weights.

lane 1: trehalose + PEG 1500, lane 2: trehalose, lane 3: LDH standard, lane 4: trehalose + PEG 8000, lane 5: sucrose + PEG 1500, lane 6: sucrose, lane 7: sucrose + PEG 8000, lane 8: LDH standard, lane 9: molecular weight marker.

3.6.3 CONFORMATIONAL STABILITY

Secondary structure was analyzed using FTIR spectroscopy. Figure 7.35 depicts area normalized 2nd derivative transmission spectra of sucrose based (A) and trehalose based (B) formulations. First of all, the presence of the band around 1706 cm⁻¹, that was regarded as related to aggregation¹¹³ in all the spectra stands out. As already observed for the pure sugar formulations, sucrose based systems showed a more pronounced band at 1706 cm⁻¹ (A) than the trehalose based ones (B). Again as observed before, the sucrose-based systems exhibited a higher fraction of β -sheet structures as well, as eminent from the band at 1638 cm⁻¹. Collapsed cakes (represented by solid lines in Figure 7.35) performed slightly worse than elegant cakes for sucrose based formulations, corresponding to the particulate matter data. However, there was no such difference observed for trehalose based systems.

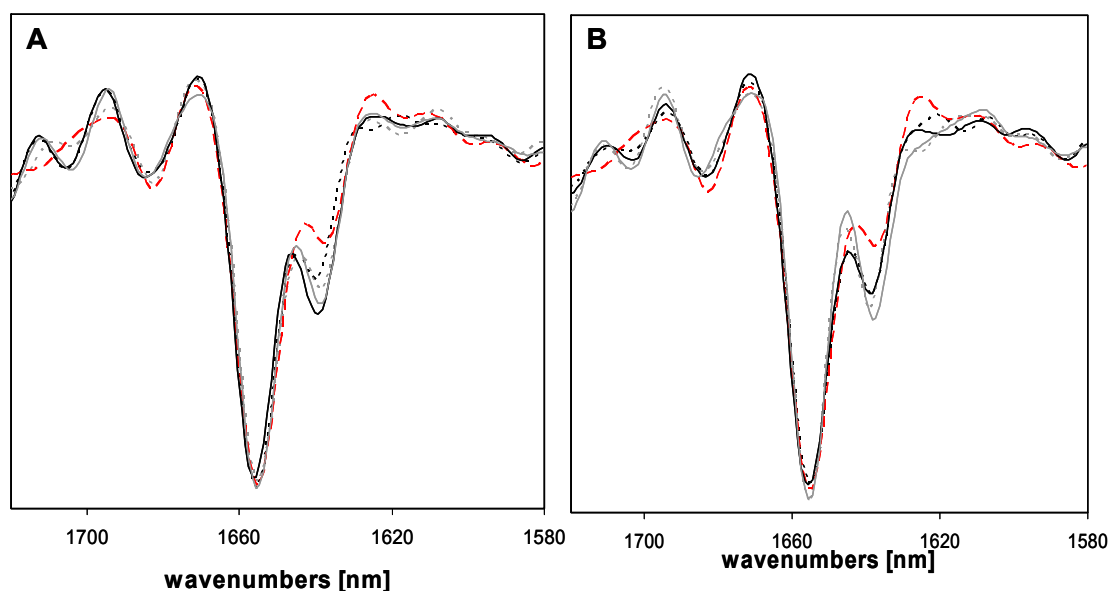


Figure 7.35: Effect of the addition of PEG on sucrose (A) and trehalose (B) based lyophilizates.

Dotted lines represent non-collapsed and solid lines represent collapsed cakes; grey: PEG 1500, black: PEG 8000, red dashed line: standard; (spectra are calculated average spectra, n = 2).

No effect of PEG molecular weight on secondary structure preservation was observed, despite the somewhat reduced band at 1638 cm⁻¹ for LDH formulated with trehalose and PEG 8000 (Figure 7.35 B). The good stability of LDH in presence of low molecular weight

PEGs might be due to the comparably high applied concentrations of PEG. Mi et al. detected a direct interaction of PEG and LDH at concentrations as low as 0.1 % for PEG 4000 or 8000¹⁰. Carpenter et al. and Mi et al. reported 1% PEG 8000 (with the addition of disaccharides) to be sufficient to adequately stabilize LDH during freeze-drying. In another study, Mi et al. found that although 1 % PEG 400 is required for effective cryo-protection, only 0.1 % PEG 3350 and 0.01 % PEG 8000 are sufficiently effective⁸. Thus 1 % PEG, as applied in this investigation, already sufficiently stabilized LDH even at low PEG molecular weight.

3.6.4 ENZYME ACTIVITY

Figure 7.36 shows the effect of different molecular weights of PEG on the recovery of catalytic activity as compared to the activity of the pure saccharide based formulations. Collapsed and non-collapsed samples were compared. Clearly, all formulations yielded high recoveries of activity. Most intriguingly, regardless of the formulation, collapsed lyophilizates always showed a higher relative activity. Some samples even showed higher activities after lyophilization than before. The activation of porcine heart LDH upon lyophilization in the presence of polymers was also observed by Anchordoquy et al. and it was attributed to slight conformational alterations¹²³. However, further investigation of this phenomenon was beyond the scope of the present investigation.

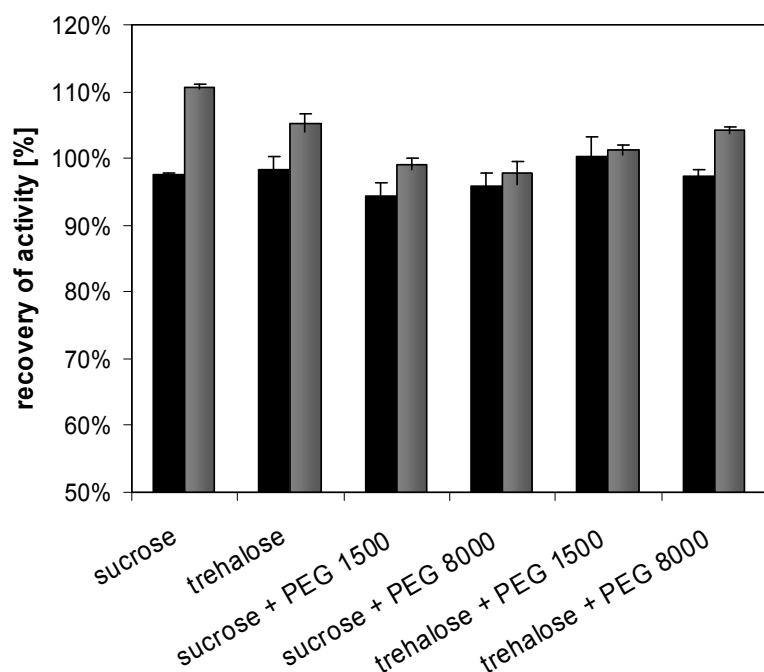


Figure 7.36: Recovery of enzyme activity after freeze-drying various formulations to collapsed (grey bars) and non-collapsed (black bars) lyophilizates (average \pm SD, n=2).

Collapsed lyophilizates showed decreased relative activities in formulations containing PEG, regardless of the molecular weight as compared to formulations without PEG. Non-collapsed freeze-dried systems showed no relevant effect of addition of PEG.

Summarizing, there was no additional stabilizing effect detectable on LDH with the addition of PEG and the requirement for a minimum molecular weight of the added PEG, as described elsewhere, was not confirmed as long as the concentration was maintained higher than 1 %. However, the addition of PEG as a partially crystalline excipient, greatly enhanced drying performance of collapsed cakes, as already described by Mattern et al. for vacuum dried glasses upon the addition of crystalline amino acids⁷. LDH was well stabilized in all the formulations investigated, no matter whether PEG was added or pure disaccharide formulations were used. The onset of collapse did not exert a destabilizing effect on LDH stability; in contrast, relative catalytic activities were increased in cakes that underwent collapse during lyophilization.

3.7 SUMMARY AND CONCLUSION

The good preservation of LDH activity and integrity is in good agreement with other researchers, who did not observe a destabilizing effect of collapse on LDH stability. Luthra et al. reported that structural collapse during primary drying had no effect on LDH recovery¹²², Chatterjee et al. reported no effect of conducting primary drying at temperatures above T_g' as long as a critical weight fraction of crystalline glycine prevents the system from collapsing¹. Jiang et al. investigated the effect of collapse on LDH without the addition of any protective agents and found no sharp decrease of enzyme activity with the onset of collapse, but they observed a gradual decrease in LDH activity with progressing drying because they performed freeze-drying in an incomplete formulation².

The results of the present study allowed the profound evaluation of the effect of collapse on LDH in realistic formulations with the actual observation of structural collapse in contrast to drying above T_g' but without structural collapse. A broad set of analytical tools was applied and various stability indicating parameters were investigated. The generation of a comprehensive set of data could be accomplished and a detailed judgment of the effect of collapse on LDH stability was rendered possible.

Most intriguingly, was the finding, that collapsed lyophilizates not even performed equally well regarding various protein-stability indicating parameters, but they even performed better than non-collapsed lyophilizates concerning several key analytical parameters, such as the activity or monomer recovery. However, particles and turbidity values were found to be slightly increased in collapsed lyophilizates, although the observed trend was not clear. To further confirm these findings storage stability studies were conducted which will be discussed in Chapter 8.

4 TISSUE-TYPE PLASMINOGEN ACTIVATOR (PA₀₁)

The effect of collapse on protein stability was further investigated with a third model protein formulation that is known to be susceptible to partial collapse upon lyophilization. For this purpose recombinant tissue-type Plasminogen-activator (t-PA) was analyzed as a model protein. t-PA is a protein used in an approved biopharmaceutical drug administered to treat blood clots in the management of acute myocardial infarctions, ischemic strokes or pulmonary embolisms¹⁴⁹⁻¹⁵¹. Being an endogenous protein, t-PA is usually secreted by the endothelial cells of blood vessels. The serine protease cleaves plasminogen to plasmin in the presence of fibrin and plasmin then degrades fibrin resulting in the lysis of the fibrin-clots^{152,153}. However, in the incidence of an acute embolism the amount of endogenous t-PA might not be enough to dissolve the thrombus and exogenous t-PA has to be administered.

As t-PA is poorly water-soluble, arginine has to be included in the formulation as a solubility enhancer. The comparably high concentration of arginine creates a dense cake with small pores that is difficult to dry. Furthermore, the addition of a certain amount of sodium chloride is necessary to adequately stabilize the protein. Sodium chloride in turn is well known to decrease a formulations T_g' , increasing its susceptibility to collapse. Taking into account these requirements a formulation that is not easy to freeze-dry results, rendering the thorough investigation of the effect of collapse an interesting subject.

Collapsed and non-collapsed, elegant lyophilizates of identical formulation were produced as usual applying two different protocols, an aggressive collapse cycle and a conventional freeze-drying cycle.

4.1 PHYSICO-CHEMICAL PROPERTIES OF COLLAPSED AND NON-COLLAPSED LYOPHILIZATES

As discussed in detail above, the comparable residual moisture level is a prerequisite for the meaningful investigation of dried protein solids in order to clearly separate effects of moisture and the effects under investigation. Figure 7.37 A lists the residual moisture levels of the investigated cakes. Residual moisture levels were kept higher as usual in freeze-dried formulations. This was done for two reasons. First, Hsu et al. described that t-PA is sensitive to over-drying¹⁵⁴. Second, as it is well known that water adversely affects protein stability, increased water contents were thought to create slightly unfavorable conditions for PA₀₁-stability which possibly would allow a clearer discrimination between collapsed and non-collapsed formulations in terms of aggregation and conformational stability.

The residual moisture contents were almost identical in the collapsed and non-collapsed formulations, allowing a proper comparison regarding the effect of collapse.

Figure 7.37 B shows the visual appearance of the freeze-dried cakes. Interestingly, collapsed PA₀₁ cakes looked different from collapsed IgG₀₁ and LDH cakes. This might be attributable

to the higher glass transition temperature of the maximally freeze-concentrated solution T_g' , that was determined to be -25.4 ± 0.0 °C (data not shown). Another reason might be the denser cake structure with a total solid concentration of approximately 12 % versus 5 – 6 % in the IgG0 and LDH formulations. This led to a less pronounced decrease in viscosity preventing the formation of a foam and just caused a shrinkage as observed for minor degrees of collapse.

The observed glass transition temperature is significantly higher than that reported in literature for arginine solutions (e.g. -41.4 °C for 500 mM L-arginine¹⁵⁵). Although proteins are known to increase a solution's T_g' , a shift of that magnitude is most likely not only caused by the relatively small amount of the protein. Experimental data is in good agreement with literature describing the effect of H_3PO_4 on L-arginine in frozen solutions. A significant shift towards higher temperatures is described upon the addition of H_3PO_4 ¹⁵⁵. As the formulation's pH was adjusted by the addition of H_3PO_4 the observed T_g' is caused by the same phenomenon.

A

appearance	residual moisture		
	[%] \pm SD ^{a)}	T_g [°C] \pm SD ^{b)}	Δc_p [J/(g*K)] ^{b)}
not collapsed	3.70 ± 0.12	84.00 ± 1.56	0.63 ± 0.03
collapsed	3.91 ± 0.25	82.80 ± 0.42	0.65 ± 0.04

a) determined by coulometric Karl Fischer titration, $n = 3$

b) determined by differential scanning calorimetry at a heating rate of 10 K/min, $n = 2$

B

Figure 7.37: Residual moistures and glass transition parameters of collapsed and non-collapsed PA₀₁ lyophilizates (A), appearance of PA₀₁ cakes after gentle (left vial) and aggressive (right vial) freeze-drying, respectively (B).

Glass transition temperatures showed the same effect of H_3PO_4 and were in good agreement with literature^{111,155}. They were furthermore in a comparable range as expected from the similar residual moisture levels.

4.2 CATALYTIC ACTIVITY OF PA₀₁ IN RECONSTITUTED LYOPHILIZATES

Catalytic activity of the reconstituted enzyme solutions was assessed using the Clot lysis assay described by Carlson et al.¹⁵⁶. Fibrinogen, plasminogen, thrombin and t-PA were mixed in a micro-centrifuge in-situ generating a fibrin clot and activating plasminogen by t-PA at the same time. The lysis of the clot was monitored photometrically measuring the optical density at 340 nm. The precision of the assay was described to be 5 %.

Figure 7.38 displays the clot-lytic activities of PA₀₁ after reconstitution from collapsed and non-collapsed lyophilizates, respectively. Freeze-drying somewhat affected the enzyme stability, as the activity after freeze-drying was reduced by approximately 3 and 5 % for non-collapsed and collapsed cakes, respectively. Collapse-drying thus seems to exhibit a more

pronounced adverse effect on protein stability; however, as the observed differences are below the precision initially described for the method¹⁵⁶, the samples are not regarded as significantly different. In consequence it can be concluded that collapse exerts no detrimental effect on PA₀₁ activity.

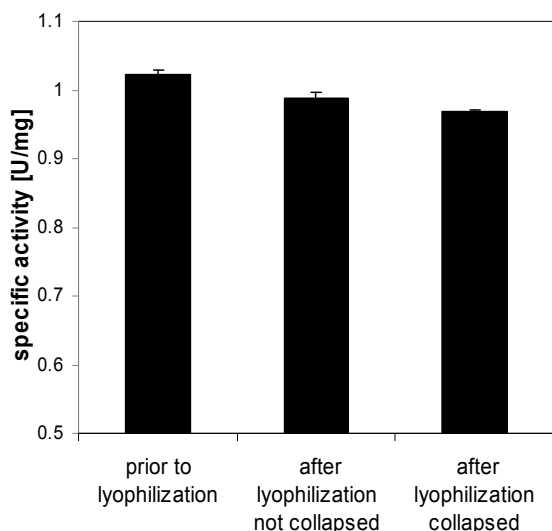


Figure 7.38: Activity of PA₀₁ after reconstitution from collapsed and non-collapsed lyophilizates as compared to the enzyme activity prior to freeze-drying as determined by the clot lysis assay (average \pm SD, n = 2).

4.3 PHYSICAL STABILITY OF PA₀₁ IN RECONSTITUTED LYOPHILIZATES

Physical stability was assessed by HP-SEC. Because t-PA non-specifically binds to the HPLC-column via a hydrophobic interaction, HP-SEC could only be conducted in the presence of SDS. As non-covalent aggregates might be dissolved in SDS-containing media, aggregates determined by this method mostly represent covalent aggregates and consequently the actual total amount of soluble aggregates might be higher¹⁵⁷.

Figure 7.39 depicts the amount of remaining monomer as compared to the amount of monomer prior to lyophilization (99.70 % PA₀₁-monomer prior to freeze-drying) after gentle and aggressive freeze-drying, respectively (left y-axis). Remaining monomer fractions were high, indicating excellent stability for both systems. Interestingly, recovery of monomer is even higher for collapsed samples. However, as the absolute difference is small (2%) and the relative sample composition is identical (98.6 % monomer for both systems, data not shown), results are not regarded as relevantly different.

Findings were further confirmed by the amount of 1-chain material. PA₀₁ is present in either a one chain or a two chain form that results from proteolytic cleavage of the molecule between Arg 275 and Ile 276 by plasmin¹⁵⁸. The protein is initially produced as one continuous chain in the endothelium. During fibrinolysis, the protein is cleaved by plasmin, creating a heavy (A) chain and a light (B) chain. While the heavy chain carries out the fibrin-binding and thus

ensures the clot-specific activation of plasminogen, the light chain implements the serine protease activity activating plasminogen¹⁵⁹.

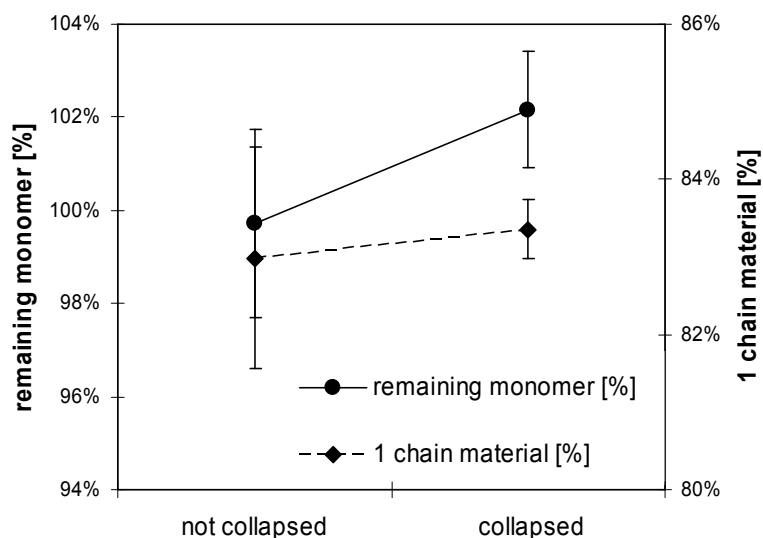


Figure 7.39: Remaining monomer and integrity as indicated by the fraction of 1 chain material of reconstituted collapsed and non-collapsed PA₀₁ lyophilizates (average \pm SD, n = 2).

MacDonald et al. found that the isolated light chain exhibits full t-PA activity but lacks the stimulation of activity in the presence of fibrin¹⁶⁰. Thus the two chain material lacks the clot-specificity of plasminogen-activation. The amount of 1-chain material was high in both systems and did not relevantly differ from the composition prior to freeze-drying (79.98 ± 1.22 %).

To further assess aggregation and fragmentation, SDS PAGE was performed using both non-reducing and DL-dithiothreitol (DTT)-reducing conditions. Figure 7.40 depicts a non-reduced gel comparing reconstituted lyophilizates to standard PA₀₁ (lane 6).

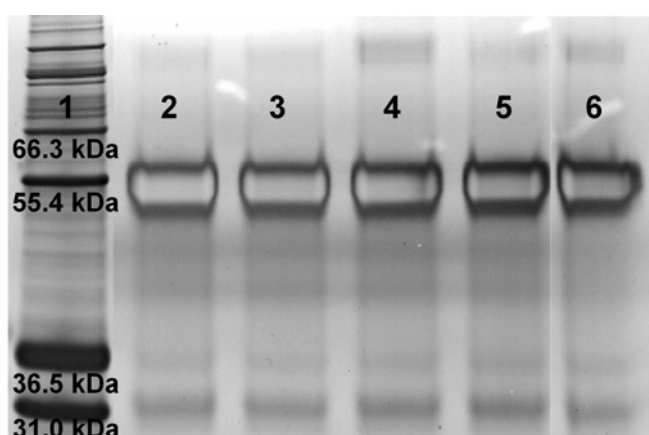


Figure 7.40: Silver-stained SDS-PAGE of 0.5 μ g PA₀₁ after reconstitution from collapsed and non-collapsed lyophilizates, respectively.

Lane 1: molecular weight marker, lane 2 & 3: PA₀₁ from non-collapsed cake, lane 4 & 5: PA₀₁ from collapsed cake, lane 6: PA₀₁ standard.

The observed electrophoretic pattern is in good agreement with literature, describing a band at approximately 60 kDa representing the monomer one-chain material and two lighter bands at around 30 kDa representing the monomer two-chain material.

The observed heterogeneity of the monomer band might be due to the fact that t-PA is a glycoprotein. The molecule contains three glycosylation sites¹⁶¹ and two variants exist, one with three and one with just two sites glycosylated. This fact in addition to the variation in carbohydrate structures and variations in the sialic acids content of certain carbohydrates leads to a variety of glycoforms¹⁶². As it is well known from antibodies, this causes small deviations in the electrophoretic behavior leading to the observed heterogeneity in the main band⁸. A pale band at approximately 140 kDa indicated a small fraction of aggregates.

The existence of predominantly one chain material is regarded as stability-indicating. As shown in Figure 7.39 (right y-axis), the amount of one chain material was high, further corroborating good preservation of protein integrity. Again, there was no relevant difference between collapsed and non-collapsed material.

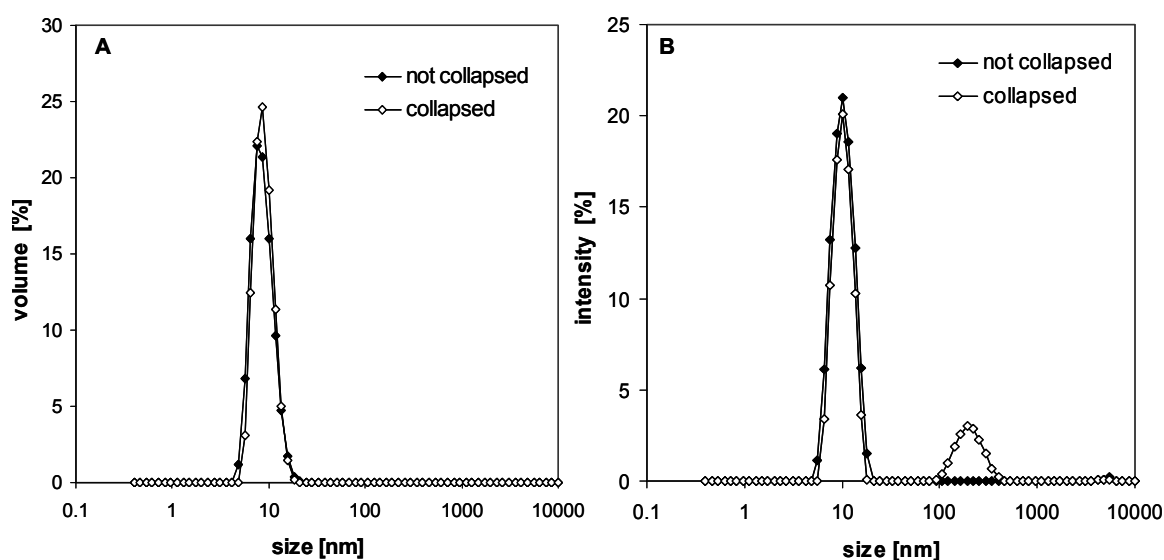


Figure 7.41: Physical stability of reconstituted PA₀₁ lyophilizates as determined by dynamic light scattering; size distribution by volume (A) and by intensity of scattered light (B), respectively (n = 2).

The size distribution was obtained by fitting a NNLS algorithm to the correlation function.

To analyze the presence of any insoluble aggregates, dynamic light scattering experiments were performed. Figure 7.41 illustrates the size distribution by volume (Figure 7.41 A) and by intensity (Figure 7.41 B), respectively. As discussed in detail above, the intensity distribution presents a much more sensitive tool to detect trace amounts of high molecular weight species, as the intensity of scattered light increases six-fold with the object's diameter. Size distributions by volume were identical for both systems, collapsed and non-collapsed, respectively. However, the size distribution by intensity indicated the presence of small amounts of a high molecular weight species with a diameter between 100 and 600 nm in collapsed samples. This was reflected in an increased PDI (0.275 for non-collapsed versus 0.347 for collapsed lyophilizates). However, as these findings were not reflected by either a

decreased recovery in HP-SEC experiments or by the volume size distribution, the mass fraction has to be small.

To further investigate particulate matter, light obscuration and turbidity measurements were performed. Table 7.20 lists the results. All the samples showed very low particle numbers well below the limits required by the pharmacopoeias. Turbidities were very low as well. There were no differences between collapsed and non-collapsed lyophilizates. Furthermore the solutions were all colorless upon reconstitution.

Table 7.20: Sub-visible particles and turbidities of PA₀₁ solutions reconstituted from collapsed and non-collapsed lyophilizates.

appearance	color ^{a)}	cumulative particles > 1 $\mu\text{m/ml} \pm \text{SD}$ ^{b)}	cumulative particles > 10 $\mu\text{m/ml} \pm \text{SD}$ ^{b)}	cumulative particles > 25 $\mu\text{m/ml} \pm \text{SD}$ ^{b)}	turbidity [FNU] $\pm \text{SD}$ ^{c)}
non-collapsed	colourless	3022 \pm 82	20 \pm 5	0 \pm 0	0.55 \pm 0.03
collapsed	colourless	2379 \pm 217	21 \pm 17	0 \pm 0	0.56 \pm 0.08

a) determined comparing reconstituted solution to standard solutions of defined color, $n = 2$

b) determined by light obscuration, $n = 2$

c) determined by nephelometric turbidimetry, $n = 2$

4.4 CONFORMATIONAL STABILITY OF PA₀₁ IN RECONSTITUTED LYOPHILIZATES

The structure of t-PA is closely linked to its biologic activity. The glycoprotein is composed of two kringle-domains. The kringle-2 domain contains a lysine binding site that is supposed to control the interaction between t-PA and fibrin¹⁶³.

Because PA₀₁ is formulated with arginine, FTIR spectroscopy could not be employed to study the protein's secondary structure as the PA₀₁ signal is obscured by the signal from the amino acid arginine¹⁵⁷. In order to assess the conformational stability of PA₀₁, the protein's tertiary structure was monitored using UV 2nd derivative absorption spectroscopy. As absorption in the near UV-region between 250 and 320 nm is predominantly governed by the absorption of the aromatic amino acid side-chains, there is no interference of arginine. Although the zero order spectra of proteins are usually broad, they are in fact composed of multiple overlapping spectra arising primarily from the absorbance of phenylalanine (245-270 nm), tyrosine (265-285 nm) and tryptophan (265-295 nm)¹⁶⁴. Using resolution-enhancement techniques, such as 2nd derivative analysis, single peaks can be determined. The position of these peaks is sensitive to the polarity of the microenvironment of the aromatic amino acids. Therefore 2nd derivative UV absorption spectroscopy can be used to assess the tertiary structure of proteins¹⁶⁵. Shifts to shorter wavelengths usually indicate an increased environmental polarity¹⁶⁵. However, the intensity of the peaks can give useful structural information as well. Usually the so-called a/b ratio is used to assess the exposure of tyrosine to bulk solvent¹⁶⁶. The ratio r of the distance between the minimum at 283 nm and the maximum at 287 nm (a) and the distance between the minimum and maximum at 290 and 295 nm (b) is calculated.

However, the ratios obtained for native proteins are reported to vary widely from protein to protein and the extent of change in r-value upon denaturation can not be generalized either¹⁶⁷.

Figure 7.42 displays second derivative UV-spectra of PA₀₁ both prior to lyophilization (A) and after freeze-drying and subsequent reconstitution (B).

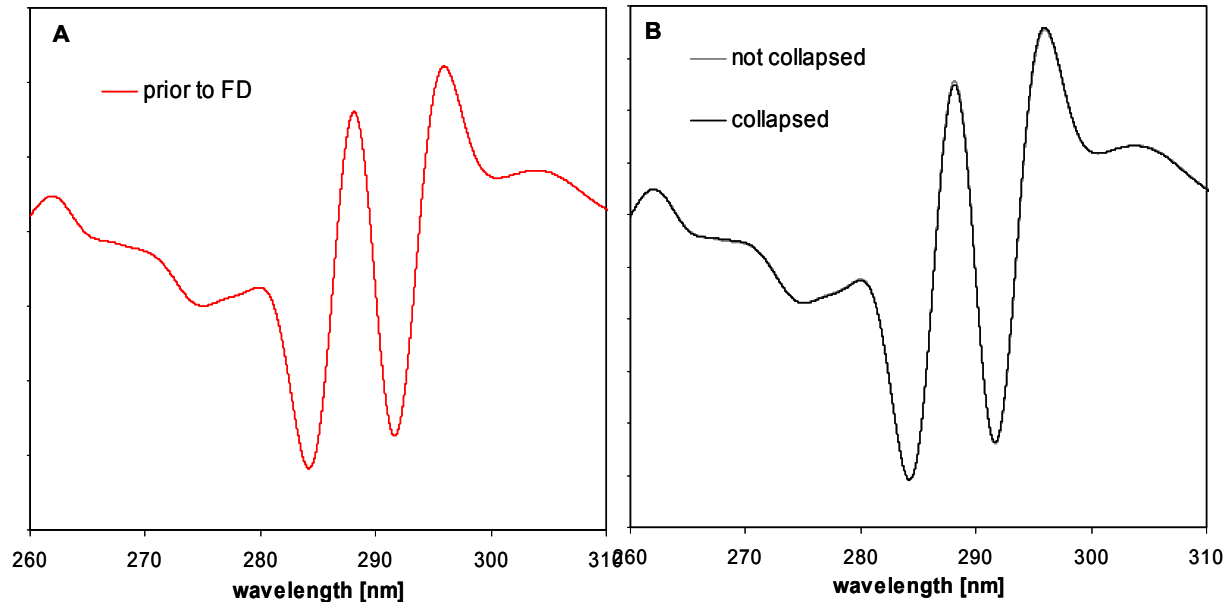


Figure 7.42: UV 2nd derivative spectra of PA₀₁ samples prior to lyophilization (0.25 mg/mL) (A) and after freeze-drying to collapsed and non-collapsed lyophilizates (0.1 mg/mL), respectively (B) (n = 2).

Two major valleys were manifest in the derivative spectra, one at 284.5 nm arising from both tryptophan and tyrosine absorbance and one at 292 m arising from tryptophan absorbance^{164,168}

Comparing PA₀₁ reconstituted from collapsed and non-collapsed cakes, the curves were congruent. There was no difference detectable neither in the single peak position nor in the intensities or the a/b ratio.

Thus freeze-drying has no impact on PA₀₁ tertiary structure, no matter whether the material collapses or not.

Summarizing the effect of collapse on PA₀₁ stability, cakes of similar residual moistures resulted, proving once more the possibility to obtain sufficiently dry material despite the onset of collapse. Collapse had no measurable relevant effect on clot lysis activity. Protein integrity was not compromised by the occurrence of collapse either and soluble and insoluble aggregation was absolutely comparable. The tertiary structure of PA₀₁, as assessed by UV 2nd derivative absorption spectroscopy, was determined to be identical to the structure prior to lyophilization, no matter whether the material collapsed or not. Thus the fact that lyophilizate collapse during freeze-drying has no detrimental effect on protein stability that had already been shown for an IgG and a sensitive model protein, LDH, was shown for a third protein, the pharmaceutically relevant tissue plasminogen activator PA₀₁.

5 FINAL SUMMARY AND CONCLUSION

The objective of the present study was to investigate the effect of collapse during freeze-drying on protein lyophilizates. For this purpose, three structurally different model proteins were analyzed: An antibody of the IgG₁-class, representing the currently largest and most important group of biopharmaceuticals. A protein that is a marketed biopharmaceutical product, referred to as PA₀₁, which is formulated in a dense lyophilized cake that is known to be difficult to freeze-dry. L-Lactic Dehydrogenase, because of its well-documented sensitivity towards the various stress situations arising during freeze-drying.

Investigations were performed using different formulations including both purely amorphous disaccharide- or amino acid-based formulations and partially crystalline mannitol- or PEG-based formulations, representing the most commonly used freeze-drying formulations. Collapsed lyophilizates were intentionally generated in a reproducible manner by application of an aggressive freeze-drying protocol, referred to as collapse-drying, and were compared to non-collapsed lyophilizates of identical formulation.

In order to clearly distinguish between the effect of collapse and the effect of residual moisture, collapsed and non-collapsed formulations of comparable residual moisture levels were produced. It was found that reconstitution times of collapsed lyophilizates were not significantly prolonged.

In addition to the investigation of completely collapsed and non-collapsed lyophilizates, various intermediate collapse states were analyzed as well. This was achieved by stepwise variation of the ratio of mannitol to sucrose, resulting in lyophilizates with increasing degree of collapse upon decreasing amount of mannitol.

The formulations were analyzed regarding both, the physicochemical properties of the excipients, such as the glass transition and the crystallinity, and the protein stability, including the formation of aggregates, the secondary and tertiary structure and the biological activity. Excipients were found to be insensitive towards the onset of collapse: amorphous excipients remained amorphous and crystalline excipients remained crystalline with the onset of collapse.

The first model protein, an IgG₁, was stabilized in both purely amorphous sucrose- and trehalose-based formulations as well as in partially crystalline mannitol-sucrose-based formulations. The amount of soluble remaining monomer was above 97 %, regardless of collapse. These findings were confirmed by various analytical techniques concerning the formation of soluble and insoluble aggregates. The conformational stability of the IgG, i.e. the secondary and tertiary structure was unaffected by the onset of collapse as well.

To verify the observed trend that collapse had no effect on IgG₀₁ stability, lyophilizates formulated at a decreased pH of 3.5 where the IgG₀₁ was found to be more sensitive towards

freeze-drying stresses (compared to pH 5.5 in the original formulation) were also analyzed, and the absence of a strong negative effect of collapse was further confirmed.

Studies on L-LDH further confirmed the observed trend. Sucrose- and trehalose-based formulations with and without the addition of different molecular weight PEGs were investigated. Recoveries of activity were complete regardless of collapse, and there were no relevant differences observed in remaining monomer contents (all > 90 %) or secondary and tertiary structural stability. Collapsed PEG-disaccharide-based LDH lyophilizates showed slightly increased sub-visible particle numbers, but collapsed purely trehalose-based lyophilizates showed decreased sub-visible particle numbers as compared to non-collapsed cakes, thus no clear trend could be concluded. Trehalose was slightly more effective in preserving LDH secondary structure. An effect of PEG molecular weight on the enzyme's stability could not be confirmed.

The occurrence of partial collapse in sucrose-PEG 3350-based lyophilizates also had no negative effect on LDH stability.

Experiments on the third model protein, PA₀₁, led to a similar conclusion. An arginine-based formulation was investigated that was prepared at rather high, but comparable residual moisture levels, in order to create slightly unfavourable conditions that should allow clear discrimination between collapsed and non-collapsed lyophilizates regarding aggregation and conformational stability of PA₀₁. No difference was observed concerning aggregation of PA₀₁. Remaining monomer contents were above 98 % regardless of collapse. This was supported by techniques such as light obscuration and dynamic light scattering, all indicating the absence of relevant amounts of insoluble aggregates. No difference in tertiary structure upon collapse was detected. In addition, the clot-lytic activity of the protein was not significantly different after reconstitution from collapsed and non-collapsed cakes.

Summarizing, no clear detrimental effect of collapse on protein stability could be detected using a comprehensive experimental approach. Most intriguingly, in some cases, proteins from reconstituted collapsed cakes performed even slightly better in key stability-indicating parameters, such as the level of remaining monomer and the recovery of catalytic activity. The observed trend is further evaluated investigating the effect of collapse on long-term storage stability that is discussed in chapter 8 of this thesis.

6 REFERENCES

1. Chatterjee, K., Shalae, E.Y., and Suryanarayanan, R. Partially crystalline systems in lyophilization: II. Withstanding collapse at high primary drying temperatures and impact on protein activity recovery. *Journal of Pharmaceutical Sciences*, **94** (4): 809-820 (2005)
2. Jiang, S. and Nail, S.L. Effect of process conditions on recovery of protein activity after freezing and freeze-drying. *European Journal of Pharmaceutics and Biopharmaceutics*, **45** (3): 249-257 (1998)
3. Wang, D.Q., Hey, J.M., and Nail, S.L. Effect of collapse on the stability of freeze-dried recombinant factor VIII and α -amylase. *Journal of Pharmaceutical Sciences*, **93** (5): 1253-1263 (2004)
4. Roy, M.L., Pikal, M.J., Rickard, E.C., and Maloney, A.M. The effects of formulation and moisture on the stability of a freeze-dried monoclonal antibody-vinca conjugate: a test of the WLF glass transition theory. *Developments in Biological Standardization*, **74** (Biol. Prod. Freeze-Drying Formulation): 323-340 (1992)
5. Towns, J.K. Moisture content in proteins: its effects and measurement. *Journal of Chromatography, A*, **705** (1): 115-127 (1995)
6. Carpenter, J.F., Prestrelski, S.J., and Arakawa, T. Separation of freezing- and drying-induced denaturation of lyophilized proteins using stress-specific stabilization. I. Enzyme activity and calorimetric studies. *Archives of Biochemistry and Biophysics*, **303** (2): 456-464 (1993)
7. Mattern, M., Winter, G., Rudolph, R., and Lee, G. Formulation of proteins in vacuum-dried glasses. Part 1. Improved vacuum-drying of sugars using crystallizing amino acids. *European Journal of Pharmaceutics and Biopharmaceutics*, **44** (2): 177-185 (1997)
8. Mi, Y., Wood, G., Thoma, L., and Rashed, S. Effects of polyethylene glycol molecular weight and concentration on lactate dehydrogenase activity in solution and after freeze-thawing. *PDA journal of pharmaceutical science and technology / PDA*, **56** (3): 115-123 (2002)
9. Mi, Y. and Wood, G. The application and mechanisms of polyethylene glycol 8000 on stabilizing lactate dehydrogenase during lyophilization. *PDA journal of pharmaceutical science and technology / PDA*, **58** (4): 192-202 (2004)
10. Mi, Y., Wood, G., and Thoma, L. Cryoprotection mechanisms of polyethylene glycols on lactate dehydrogenase during freeze-thawing. *AAPS Journal*, **6** (3): e22(2004)
11. Piggee, C. Therapeutic antibodies coming through the pipeline. *Analytical Chemistry*, **80** (7): 2305-2310 (2008)
12. Wang, W., Singh, S., Zeng, D.L., King, K., and Nema, S. Antibody structure, instability, and formulation. *Journal of Pharmaceutical Sciences*, **96** (1): 1-26 (2007)
13. Cleland, J.L., Lam, X., Kendrick, B., Yang, J., Yang, T.H., Overcashier, D., Brooks, D., Hsu, C., and Carpenter, J.F. A specific molar ratio of stabilizer to protein is required for storage stability of a lyophilized monoclonal antibody. *Journal of Pharmaceutical Sciences*, **90** (3): 310-321 (2001)
14. Andya, J.D., Hsu, C.C., and Shire, S.J. Mechanisms of aggregate formation and carbohydrate excipient stabilization of lyophilized humanized monoclonal antibody formulations. *Pharmaceutical Sciences*, **5** (2): No(2003)
15. Schwegman, J.J., Hardwick, L.M., and Akers, M.J. Practical formulation and process development of freeze-dried products. *Pharmaceutical Development and Technology*, **10** (2): 151-173 (2005)
16. Carpenter, J.F. and Crowe, J.H. An infrared spectroscopic study of the interactions of carbohydrates with dried proteins. *Biochemistry*, **28** (9): 3916-3922 (1989)
17. Carpenter, J.F., Crowe, J.H., and Arakawa, T. Comparison of solute-induced protein stabilization in aqueous solution and in the frozen and dried states. *Journal of Dairy Science*, **73** (12): 3627-3636 (1990)
18. Liao, Y.H., Brown, M.B., Quader, A., and Martin, G.P. Protective Mechanism of Stabilizing Excipients Against Dehydration in the Freeze-Drying of Proteins. *Pharmaceutical Research*, **19** (12): 1854-1861 (2002)

19. Chang, L., Shepherd, D., Sun, J., Tang, X., and Pikal, M.J. Effect of sorbitol and residual moisture on the stability of lyophilized antibodies: Implications for the mechanism of protein stabilization in the solid state. *Journal of Pharmaceutical Sciences*, **94** (7): 1445-1455 (2005)
20. Chang, L., Shepherd, D., Sun, J., Ouellette, D., Grant, K.L., Tang, X., and Pikal, M.J. Mechanism of protein stabilization by sugars during freeze-drying and storage: Native structure preservation, specific interaction, and/or immobilization in a glassy matrix? *Journal of Pharmaceutical Sciences*, **94** (7): 1427-1444 (2005)
21. Slade, L. and Levine, H. Beyond water activity: recent advances based on an alternative approach to the assessment of food quality and safety. *Critical Reviews in Food Science and Nutrition*, **30** (2-3): 115-360 (1991)
22. Chatterjee, K., Shalaev, E.Y., and Suryanarayanan, R. Partially crystalline systems in lyophilization: I. Use of ternary state diagrams to determine extent of crystallization of bulking agent. *Journal of Pharmaceutical Sciences*, **94** (4): 798-808 (2005)
23. Shalaev, E.Y. and Franks, F. Changes in the physical state of model mixtures during freezing and drying: impact on product quality. *Cryobiology*, **33** (1): 14-26 (1996)
24. Carpenter, J.F., Pikal, M.J., Chang, B.S., and Randolph, T.W. Rational design of stable lyophilized protein formulations: some practical advice. *Pharmaceutical Research*, **14** (8): 969-975 (1997)
25. Pikal, M.J. Freeze-drying of proteins: process, formulation, and stability. *ACS Symposium Series*, **567** 120-133 *ACS Symposium Series* (1994)
26. Breen, E.D., Curley, J.G., Overcashier, D.E., Hsu, C.C., and Shire, S.J. Effect of moisture on the stability of a lyophilized humanized monoclonal antibody formulation. *Pharmaceutical Research*, **18** (9): 1345-1353 (2001)
27. Duddu, S.P. and Dal Monte, P.R. Effect of glass transition temperature on the stability of lyophilized formulations containing a chimeric therapeutic monoclonal antibody. *Pharmaceutical Research*, **14** (5): 591-595 (1997)
28. Bellows, R.J. and King, C.J. Freeze-drying of aqueous solutions: Maximum allowable operating temperature. *Cryobiology*, **9** (6): 559-561 (1972)
29. Tsourouflis, S., Flink, J.M., and Karel, M. Loss of structure in freeze-dried carbohydrates solutions: effect of temperature, moisture content and composition. *Journal of the Science of Food and Agriculture*, **27** (6): 509-519 (1976)
30. Ressing, M.E., Jiskoot, W., Talsma, H., van Ingen, C.W., Beuvery, E.C., and Crommelin, D.J. The influence of sucrose, dextran, and hydroxypropyl-beta-cyclodextrin as lyoprotectants for a freeze-dried mouse IgG2a monoclonal antibody (MN12). *Pharmaceutical Research*, **9** (2): 266-270 (1992)
31. Mahler, H.C., Friess, W., Grauschopf, U., and Kiese, S. Protein Aggregation: Pathways, Induction Factors and Analysis. *Journal of Pharmaceutical Sciences*, (2008)
32. Roberts, C.J. Non-native protein aggregation kinetics. *Biotechnology and Bioengineering*, **98** (5): 927-938 (2007)
33. Andrews, J.M. and Roberts, C.J. A Lumry-Eyring Nucleated Polymerization Model of Protein Aggregation Kinetics: 1. Aggregation with Pre-Equilibrated Unfolding. *Journal of Physical Chemistry B*, **111** (27): 7897-7913 (2007)
34. Fields, G.B., Alonso, D.O.V., Stigter, D., and Dill, K.A. Theory for the aggregation of proteins and copolymers. *Journal of Physical Chemistry*, **96** (10): 3974-3981 (1992)
35. Fink, A.L. Protein aggregation: folding aggregates, inclusion bodies and amyloid. *Folding Des.*, **3** (1): R9-R23 (1998)
36. Finke, J.M., Roy, M., Zimm, B.H., and Jennings, P.A. Aggregation events occur prior to stable intermediate formation during refolding of interleukin 1beta. *Biochemistry*, **39** (3): 575-583 (2000)

37. Strickley, R.G. and Anderson, B.D. Solid-state stability of human insulin. II. Effect of water on reactive intermediate partitioning in lyophiles from pH 2-5 solutions: stabilization against covalent dimer formation. *Journal of Pharmaceutical Sciences*, **86** (6): 645-653 (1997)
38. Uversky, V.N., Karnoup, A.S., Khurana, R., Segel, D.J., Doniach, S., and Fink, A.L. Association of partially-folded intermediates of staphylococcal nuclease induces structure and stability. *Protein Science*, **8** (1): 161-173 (1999)
39. Mahler, H.C., Mueller, R., Friess, W., Delille, A., and Matheus, S. Induction and analysis of aggregates in a liquid IgG1-antibody formulation. *European Journal of Pharmaceutics and Biopharmaceutics*, **59** (3): 407-417 (2005)
40. Carpenter, J.F., Kendrick, B.S., Chang, B.S., Manning, M.C., and Randolph, T.W. Inhibition of stress-induced aggregation of protein therapeutics. *Methods in Enzymology*, **309** (Amyloid, Prions, and Other Protein Aggregates): 236-255 (1999)
41. Philo, J.S. Is any measurement method optimal for all aggregate sizes and types? *AAPS Journal*, **8** (3): E564-E571 (2006)
42. Schellekens, H. Immunogenicity of therapeutic proteins: clinical implications and future prospects. *Clinical Therapeutics*, **24** (11): 1720-1740 (2002)
43. Schellekens, H. Factors influencing the immunogenicity of therapeutic proteins. *Nephrol., Dial., Transplant.*, **20** (Suppl. 6): vi3-vi9 (2005)
44. Wang, W. Protein aggregation and its inhibition in biopharmaceutics. *International Journal of Pharmaceutics*, **289** (1-2): 1-30 (2005)
45. Wang, Y.J., Shahrokh, Z., Vemuri, S., Eberlein, G., Beylin, I., and Busch, M. Characterization, stability, and formulations of basic fibroblast growth factor. *Pharmaceutical Biotechnology*, **9** (Formulation, Characterization, and Stability of Protein Drugs): 141-180 (1996)
46. Ph.Eur. 2.2.1 Clarity and degree of opalescence of liquids, 6th edition. *European Directorate for the Quality of Medicine (EDQM)*, (2008)
47. Hawe, A. and Friess, W. Stabilization of a hydrophobic recombinant cytokine by human serum albumin. *Journal of Pharmaceutical Sciences*, **96** (11): 2987-2999 (2007)
48. Kerwin, B.A., Akers, M.J., Apostol, I., Moore-Einsel, C., Etter, J.E., Hess, E., Lippincott, J., Levine, J., Mathews, A.J., Revilla-Sharp, P., Schubert, R., and Looker, D.L. Acute and Long-Term Stability Studies of Deoxy Hemoglobin and Characterization of Ascorbate-Induced Modifications. *Journal of Pharmaceutical Sciences*, **88** (1): 79-88 (1999)
49. Demeester, J., De Smedt, S.S., Sanders, N.N., and Hastraete, J. Light scattering. *Biotechnology: Pharmaceutical Aspects*, **3** (Methods for Structural Analysis of Protein Pharmaceuticals): 245-275 (2005)
50. Saluja, A., Badkar, A.V., Zeng, D.L., Nema, S., and Kalonia, D.S. Ultrasonic storage modulus as a novel parameter for analyzing protein-protein interactions in high protein concentration solutions: correlation with static and dynamic light scattering measurements. *Biophysical Journal*, **92** (1): 234-244 (2007)
51. Manning, M.C., Patel, K., and Borchardt, R.T. Stability of protein pharmaceuticals. *Pharmaceutical Research*, **6** (11): 903-918 (1989)
52. Bandekar, J. Amide modes and protein conformation. *Biochimica et Biophysica Acta, Protein Structure and Molecular Enzymology*, **1120** (2): 123-143 (1992)
53. Cooper, E.A. and Knutson, K. Fourier transform infrared spectroscopy investigations of protein structure. *Pharmaceutical Biotechnology*, **7** (Physical Methods to Characterize Pharmaceutical Proteins): 101-143 (1995)
54. Van De Weert, M., Hering, J.A., and Haris, P.I. Fourier transform infrared spectroscopy. *Biotechnology: Pharmaceutical Aspects*, **3** (Methods for Structural Analysis of Protein Pharmaceuticals): 131-166 (2005)
55. Savitzky, A. and Golay, M.J.E. Smoothing and differentiation of data by simplified least squares procedures. *Analytical Chemistry*, **36** (8): 1627-1639 (1964)

56. Kauppinen, J.K., Moffatt, D.J., Mantsch, H.H., and Cameron, D.G. Fourier self-deconvolution: a method for resolving intrinsically overlapped bands. *Applied Spectroscopy*, **35** (3): 271-276 (1981)
57. Costantino, H.R., Andya, J.D., Shire, S.J., and Hsu, C.C. Fourier-transform infrared spectroscopic analysis of the secondary structure of recombinant humanized immunoglobulin G. *Pharmaceutical Sciences*, **3** (3): 121-128 (1997)
58. Maury, M., Murphy, K., Kumar, S., Mauerer, A., and Lee, G. Spray-drying of proteins: effects of sorbitol and trehalose on aggregation and FT-IR amide I spectrum of an immunoglobulin G. *European Journal of Pharmaceutics and Biopharmaceutics*, **59** (2): 251-261 (2005)
59. Chen, B., Bautista, R., Yu, K., Zapata, G.A., Mulkerrin, M.G., and Chamow, S.M. Influence of Histidine on the Stability and Physical Properties of a Fully Human Antibody in Aqueous and Solid Forms. *Pharmaceutical Research*, **20** (12): 1952-1960 (2003)
60. Byler, D.M. and Susi, H. Examination of the secondary structure of proteins by deconvolved FTIR spectra. *Biopolymers*, **25** (3): 469-487 (1986)
61. Fu, F.N., DeOliveira, D.B., Trumble, W.R., Sarkar, H.K., and Singh, B.R. Secondary structure estimation of proteins using the amide III region of Fourier transform infrared spectroscopy: application to analyze calcium-binding-induced structural changes in calsequestrin. *Applied Spectroscopy*, **48** (11): 1432-1441 (1994)
62. Levitt, M. and Greer, J. Automatic identification of secondary structure in globular proteins. *Journal of Molecular Biology*, **114** (2): 181-239 (1977)
63. Jiskoot, W., Visser, A.J.W.G., Herron, J.N., and Sutter, M. Fluorescence spectroscopy. *Biotechnology: Pharmaceutical Aspects*, **3** (Methods for Structural Analysis of Protein Pharmaceuticals): 27-82 (2005)
64. Taschner, N., Mueller, S.A., Alumalla, V.R., Goldie, K.N., Drake, A.F., Aebi, U., and Arvinte, T. Modulation of antigenicity related to changes in antibody flexibility upon lyophilization. [Erratum to document cited in CA136:107411]. *Journal of Molecular Biology*, **312** (3): 579(2001)
65. Chen, Y. and Barkley, M.D. Toward understanding tryptophan fluorescence in proteins. *Biochemistry*, **37** (28): 9976-9982 (1998)
66. Hawe, A., Friess, W., Sutter, M., and Jiskoot, W. Online fluorescent dye detection method for the characterization of immunoglobulin G aggregation by size exclusion chromatography and asymmetrical flow field flow fractionation. *Analytical Biochemistry*, **378** (2): 115-122 (2008)
67. Jiskoot, W., Bloemendal, M., Van Haeringen, B., Van Grondelle, R., Beuvery, E.C., Herron, J.N., and Crommelin, D.J.A. Non-random conformation of a mouse IgG2a monoclonal antibody at low pH. *European Journal of Biochemistry*, **201** (1): 223-232 (1991)
68. Ladokhin, A.S. Fluorescence Spectroscopy in Peptide and Protein Analysis. *Encyclopedia of Analytical Chemistry* (2000)
69. Welfle, K., Misselwitz, R., Hausdorf, G., Hohne, W., and Welfle, H. Conformation, pH-induced conformational changes, and thermal unfolding of anti-p24 (HIV-1) monoclonal antibody CB4-1 and its Fab and Fc fragments. *Biochimica et Biophysica Acta, Protein Structure and Molecular Enzymology*, **1431** (1): 120-131 (1999)
70. Tanaka, N., Nishizawa, H., and Kunugi, S. Structure of pressure-induced denatured state of human serum albumin: a comparison with the intermediate in urea-induced denaturation. *Biochimica et Biophysica Acta, Protein Structure and Molecular Enzymology*, **1338** (1): 13-20 (1997)
71. Sharma, V.K. and Kalonia, D.S. Temperature- and pH-Induced Multiple Partially Unfolded States of Recombinant Human Interferon-alpha 2a: Possible Implications in Protein Stability. *Pharmaceutical Research*, **20** (11): 1721-1729 (2003)
72. Schreiber, A.B., Strosberg, A.D., and Pecht, I. Fluorescence of tryptophan residues in homogenous rabbit antibodies. Variability in quantum yields and degree of exposure to solvent. *Immunochemistry*, **15** (4): 207-212 (1978)

73. Jiskoot, W., Hlady, V., Naleway, J.J., and Herron, J.N. Application of fluorescence spectroscopy for determining the structure and function of proteins. *Pharmaceutical Biotechnology*, **7** (Physical Methods to Characterize Pharmaceutical Proteins): 1-63 (1995)
74. Cantor, C.R. and Schimmel, P.R. *Biophysical Chemistry of Macromolecules, Pt. 3: The Behavior of Biological Macromolecules*. 624 *W H Freeman & Co* (1980)
75. Lakowicz, J.R. *Principles of Fluorescence Spectroscopy*. 496 *Springer, Berlin* (1983)
76. Dong, A., Prestrelski, S.J., Allison, S.D., and Carpenter, J.F. Infrared Spectroscopic Studies of Lyophilization- and Temperature-Induced Protein Aggregation. *Journal of Pharmaceutical Sciences*, **84** (4): 415-424 (1995)
77. Prestrelski, S., Tedeschi, N., Arakawa, T., and Carpenter, J.F. Dehydration-induced conformational transitions in proteins and their inhibition by stabilizers. *Biophysical Journal*, **65** (2): 661-671 (1993)
78. Prestrelski, S.J., Arakawa, T., and Carpenter, J.F. Structure of proteins in lyophilized formulations using Fourier transform infrared spectroscopy. *ACS Symposium Series*, **567** (Formulation and Delivery of Proteins and Peptides): 148-169 (1994)
79. Chang, B.S., Beauvais, R.M., Dong, A., and Carpenter, J.F. Physical factors affecting the storage stability of freeze-dried interleukin-1 receptor antagonist: glass transition and protein conformation. *Archives of Biochemistry and Biophysics*, **331** (2): 249-258 (1996)
80. Prestrelski, S.J., Pikal, K.A., and Arakawa, T. Optimization of lyophilization conditions for recombinant human interleukin-2 by dried-state conformational analysis using Fourier-transform infrared spectroscopy. *Pharmaceutical Research*, **12** (9): 1250-1259 (1995)
81. Carpenter, J.F., Prestrelski, S.J., and Dong, A. Application of infrared spectroscopy to development of stable lyophilized protein formulations. *European Journal of Pharmaceutics and Biopharmaceutics*, **45** (3): 231-238 (1998)
82. Izutsu, K., Yoshioka, S., and Takeda, Y. The effects of additives on the stability of freeze-dried b-galactosidase stored at elevated temperature. *International Journal of Pharmaceutics*, **71** (1-2): 137-146 (1991)
83. Tian, F., Middaugh, C.R., Offerdahl, T., Munson, E., Sane, S., and Rytting, J.H. Spectroscopic evaluation of the stabilization of humanized monoclonal antibodies in amino acid formulations. *International Journal of Pharmaceutics*, **335** (1-2): 20-31 (2007)
84. Izutsu, K. and Kojima, S. Excipient crystallinity and its protein-structure-stabilizing effect during freeze-drying. *Journal of pharmacy and pharmacology*, **54** (8): 1033-1039 (2002)
85. Johnson, R.E., Kirchhoff, C.F., and Gaud, H.T. Mannitol-sucrose mixtures-versatile formulations for protein lyophilization. *Journal of Pharmaceutical Sciences*, **91** (4): 914-922 (2002)
86. Pikal, M.J., Dellerman, K.M., Roy, M.I., and Riggin, R.M. The effects of formulation variables on the stability of freeze-dried human growth hormone. *Pharmaceutical Research*, **8** (4): 427-436 (1991)
87. Franks, F. Freeze-drying of bioproducts: putting principles into practice. *European Journal of Pharmaceutics and Biopharmaceutics*, **45** (3): 221-229 (1998)
88. Yu, L., Milton, N., Groleau, E.G., Mishra, D.S., and Vansickle, R.E. Existence of a Mannitol Hydrate during Freeze-Drying and Practical Implications. *Journal of Pharmaceutical Sciences*, **88** (2): 196-198 (1999)
89. Cavatur, R.K. and Suryanarayanan, R. Characterization of phase transitions during freeze-drying by in situ X-ray powder diffractometry. *Pharmaceutical Development and Technology*, **3** (4): 579-586 (1998)
90. Te Booy, M.P.W.M., De Ruiter, R.A., and De Meere, A.L.J. Evaluation of the physical stability of freeze-dried sucrose-containing formulations by differential scanning calorimetry. *Pharmaceutical Research*, **9** (1): 109-114 (1992)
91. Gombas, A., Szabo-Revesz, P., Regdon, G., Jr., and Eroes, I. Study of thermal behaviour of sugar alcohols. *Journal of Thermal Analysis and Calorimetry*, **73** (2): 615-621 (2003)

92. Hawe, A. and Friess, W. Physico-chemical lyophilization behavior of mannitol, human serum albumin formulations. *European Journal of Pharmaceutical Sciences*, **28** (3): 224-232 (2006)
93. Hawe, A. Studies on Stable Formulations for a Hydrophobic Cytokine. *Dissertation Ludwig-Maximilians-Universität München* (2006)
94. Telang, C., Suryanarayanan, R., and Yu, L. Crystallization of D-mannitol in binary mixtures with NaCl: phase diagram and polymorphism. *Pharmaceutical Research*, **20** (12): 1939-1945 (2003)
95. Burger, A., Henck, J.O., Hetz, S., Rollinger, J.M., Weissnicht, A.A., and Stottner, H. Energy/temperature diagram and compression behavior of the polymorphs of D-mannitol. *Journal of Pharmaceutical Sciences*, **89** (4): 457-468 (2000)
96. Yoshinari, T., Forbes, R.T., York, P., and Kawashima, Y. Moisture induced polymorphic transition of mannitol and its morphological transformation. *International Journal of Pharmaceutics*, **247** (1-2): 69-77 (2002)
97. Liao, X., Krishnamurthy, R., and Suryanarayanan, R. Influence of Processing Conditions on the Physical State of Mannitol-Implications in Freeze-Drying. *Pharmaceutical Research*, **24** (2): 370-376 (2007)
98. Ahrer, K., Buchacher, A., Iberer, G., and Jungbauer, A. Thermodynamic stability and formation of aggregates of human immunoglobulin G characterized by differential scanning calorimetry and dynamic light scattering. *Journal of Biochemical and Biophysical Methods*, **66** (1-3): 73-86 (2006)
99. Hernandez-Contreras, M., arcon-Waess, O., and Medina-Noyola, M. Rotational-translational electrolyte friction on nonspherical particles. *Journal of Chemical Physics*, **106** (6): 2492-2501 (1997)
100. Tang, X. and Pikal, M.J. Design of Freeze-Drying Processes for Pharmaceuticals: Practical Advice. *Pharmaceutical Research*, **21** (2): 191-200 (2004)
101. Hsu, C.C., Nguyen, H.M., Yeung, D.A., Brooks, D.A., Koe, G.S., Bewley, T.A., and Pearlman, R. Surface denaturation at solid-void interface-a possible pathway by which opalescent particulates form during the storage of lyophilized tissue-type plasminogen activator at high temperatures. *Pharmaceutical Research*, **12** (1): 69-77 (1995)
102. Adler, M. and Lee, G. Stability and Surface Activity of Lactate Dehydrogenase in Spray-Dried Trehalose. *Journal of Pharmaceutical Sciences*, **88** (2): 199-208 (1999)
103. Abdul-Fattah, A.M., Truong-Le, V., Yee, L., Nguyen, L., Kalonia, D.S., Cicerone, M.T., and Pikal, M.J. Drying-induced variations in physico-chemical properties of amorphous pharmaceuticals and their impact on stability (I): stability of a monoclonal antibody. *Journal of Pharmaceutical Sciences*, **96** (8): 1983-2008 (2007)
104. Hunt, G. and Nashabeh, W. Capillary electrophoresis sodium dodecyl sulfate nongel sieving analysis of a therapeutic recombinant monoclonal antibody: A biotechnology perspective. *Analytical Chemistry*, **71** (13): 2390-2397 (1999)
105. Shire, S.J., Shahrokh, Z., and Liu, J. Challenges in the development of high protein concentration formulations. *Journal of Pharmaceutical Sciences*, **93** (6): 1390-1402 (2004)
106. Schuele, S., Friess, W., Bechtold-Peters, K., and Garidel, P. Conformational analysis of protein secondary structure during spray-drying of antibody/mannitol formulations. *European Journal of Pharmaceutics and Biopharmaceutics*, **65** (1): 1-9 (2007)
107. Van De Weert, M., Haris, P.I., Hennink, W.E., and Crommelin, D.J.A. Fourier transform infrared spectrometric analysis of protein conformation: Effect of sampling method and stress factors. *Analytical Biochemistry*, **297** (2): 160-169 (2001)
108. Sharma, V.K. and Kalonia, D.S. Steady-state tryptophan fluorescence spectroscopy study to probe tertiary structure of proteins in solid powders. *Journal of Pharmaceutical Sciences*, **92** (4): 890-899 (2003)
109. Izutsu, K., Yoshioka, S., and Terao, T. Effect of mannitol crystallinity on the stabilization of enzymes during freeze-drying. *Chemical & Pharmaceutical Bulletin*, **42** (1): 5-8 (1994)

110. Franks, F., Hatley, R.H.M., and Mathias, S.F. Materials science and the production of shelf-stable biologicals. *BioPharm (Eugene, Oreg.)*, **4** (9): 38, 40-2, 55 (1991)
111. Mattern, M., Winter, G., Kohnert, U., and Lee, G. Formulation of proteins in vacuum-dried glasses. II. Process and storage stability in sugar-free amino acid systems. *Pharmaceutical Development and Technology*, **4** (2): 199-208 (1999)
112. Miller, D.P., Anderson, R.E., and De Pablo, J.J. Stabilization of lactate dehydrogenase following freeze-thawing and vacuum-drying in the presence of trehalose and borate. *Pharmaceutical Research*, **15** (8): 1215-1221 (1998)
113. Prestrelski, S.J., Arakawa, T., and Carpenter, J.F. Separation of freezing- and drying-induced denaturation of lyophilized proteins using stress-specific stabilization. II. Structural studies using infrared spectroscopy. *Archives of Biochemistry and Biophysics*, **303** (2): 465-473 (1993)
114. Liu, W.R., Langer, R., and Klivanov, A.M. Moisture-induced aggregation of lyophilized proteins in the solid state. *Biotechnology and Bioengineering*, **37** (2): 177-184 (1991)
115. Roos, Y. and Karel, M. Plasticizing effect of water on thermal behavior and crystallization of amorphous food models. *Journal of Food Science*, **56** (1): 38-43 (1991)
116. Hatley, R.H.M. Glass fragility and the stability of pharmaceutical preparations-excipient selection. *Pharmaceutical Development and Technology*, **2** (3): 257-264 (1997)
117. Angell, C.A. Formation of glasses from liquids and biopolymers. *Science (Washington, D.C.)*, **267** (5206): 1924-1935 (1995)
118. Izutsu, K.i., Yoshioka, S., and Kojima, S. Increased stabilizing effects of amphiphilic excipients on freeze-drying of lactate dehydrogenase (LDH) by dispersion into sugar matrixes. *Pharmaceutical Research*, **12** (6): 838-843 (1995)
119. Morris, K.R., Knipp, G.T., and Serajuddin, A.T.M. Structural properties of polyethylene glycol-polysorbate 80 mixture, a solid dispersion vehicle. *Journal of Pharmaceutical Sciences*, **81** (12): 1185-1188 (1992)
120. Bartholmes, P., Durchschlag, H., and Jaenicke, R. Molecular properties of lactic dehydrogenase under the conditions of the enzymic test. Sedimentation analysis and gel filtration in the microgram and nanogram range. *European Journal of Biochemistry*, **39** (1): 101-108 (1973)
121. Zettlmeissl, G., Rudolph, R., and Jaenicke, R. Rate-determining folding and association reactions on the reconstitution pathway of porcine skeletal muscle lactic dehydrogenase after denaturation by guanidine hydrochloride. *Biochemistry*, **21** (17): 3946-3950 (1982)
122. Luthra, S., Obert, J.P., Kalonia, D.S., and Pikal, M.J. Investigation of drying stresses on proteins during lyophilization: differentiation between primary and secondary-drying stresses on lactate dehydrogenase using a humidity controlled mini freeze-dryer. *Journal of Pharmaceutical Sciences*, **96** (1): 61-70 (2006)
123. Anchordoquy, T.J., Izutsu, K.i., Randolph, T.W., and Carpenter, J.F. Maintenance of Quaternary Structure in the Frozen State Stabilizes Lactate Dehydrogenase during Freeze-Drying. *Archives of Biochemistry and Biophysics*, **390** (1): 35-41 (2001)
124. Rosenberg, A.S. Effects of protein aggregates: an immunologic perspective. *AAPS Journal*, **8** (3): E501-E507 (2006)
125. Gabrielson, J.P., Brader, M.L., Pekar, A.H., Mathis, K.B., Winter, G., Carpenter, J.F., and Randolph, T.W. Quantitation of aggregate levels in a recombinant humanized monoclonal antibody formulation by size-exclusion chromatography, asymmetrical flow field flow fractionation, and sedimentation velocity. *Journal of Pharmaceutical Sciences*, **96** (2): 268-279 (2006)
126. Litzen, A., Walter, J.K., Krischollek, H., and Wahlund, K.G. Separation and quantitation of monoclonal antibody aggregates by asymmetrical flow field-flow fractionation and comparison to gel permeation chromatography. *Analytical Biochemistry*, **212** (2): 469-480 (1993)
127. Pavanetto, F., Genta, I., Conti, B., Modena, T., and Montanari, L. Aluminum, cadmium and lead in large volume parenterals: contamination levels and sources. *International Journal of Pharmaceutics*, **54** (2): 143-148 (1989)

128. Baumruk, V., Pancoska, P., and Keiderling, T.A. Predictions of secondary structure using statistical analyses of electronic and vibrational circular dichroism and Fourier transform infrared spectra of proteins in H₂O. *Journal of Molecular Biology*, **259** (4): 774-791 (1996)
129. Susi, H. and Byler, D.M. Resolution-enhanced Fourier transform infrared spectroscopy of enzymes. *Methods in Enzymology*, **130** (Enzyme Struct., Pt. K): 290-311 (1986)
130. Costantino, H.R., Schwendeman, S.P., Griebenow, K., Klibanov, A.M., and Langer, R. The Secondary Structure and Aggregation of Lyophilized Tetanus Toxoid. *Journal of Pharmaceutical Sciences*, **85** (12): 1290-1293 (1996)
131. Goller, K. and Galinski, E.A. Protection of a model enzyme (lactate dehydrogenase) against heat, urea and freeze-thaw treatment by compatible solute additives. *Journal of Molecular Catalysis B: Enzymatic*, **7** (1-4): 37-45 (1999)
132. Green, J.L. and Angell, C.A. Phase relations and vitrification in saccharide-water solutions and the trehalose anomaly. *Journal of Physical Chemistry*, **93** (8): 2880-2882 (1989)
133. Aldous, B.J., Auffret, A.D., and Franks, F. The crystallization of hydrates from amorphous carbohydrates. *Cryo-Letters*, **16** (3): 181-186 (1995)
134. Crowe, L.M., Reid, D.S., and Crowe, J.H. Is trehalose special for preserving dry biomaterials? *Biophysical Journal*, **71** (4): 2087-2093 (1996)
135. Moelwyn-Hughes, E.A. Kinetics of the hydrolysis of certain glucosides (salicin, arbutin and phlorhizin). *Transactions of the Faraday Society*, (advance proof): (1928)
136. Roser, B. Trehalose drying: a novel replacement for freeze-drying. *BioPharm (Eugene, Oreg.)*, **4** (8): 47-53 (1991)
137. Crowe, J.H., Clegg, J.S., and Editors. *Biological Systems*.357(1978)
138. Crowe, J.H., Crowe, L.M., Carpenter, J.F., and urell Wistrom, C. Stabilization of dry phospholipid bilayers and proteins by sugars. *Biochemical Journal*, **242** (1): 1-10 (1987)
139. Leslie, S.B., Israeli, E., Lighthart, B., Crowe, J.H., and Crowe, L.M. Trehalose and sucrose protect both membranes and proteins in intact bacteria during drying. *Applied and Environmental Microbiology*, **61** (10): 3592-3597 (1995)
140. Uritani, M., Takai, M., and Yoshinaga, K. Protective effect of disaccharides on restriction endonucleases during drying under vacuum. *Journal of Biochemistry (Tokyo)*, **117** (4): 774-779 (1995)
141. Miller, D.P., De Pablo, J.J., and Corti, H. Thermophysical properties of trehalose and its concentrated aqueous solutions. *Pharmaceutical Research*, **14** (5): 578-590 (1997)
142. Iwai, J., Ogawa, N., Nagase, H., Endo, T., Loftsson, T., and Ueda, H. Effects of various cyclodextrins on the stability of freeze-dried lactate dehydrogenase. *Journal of Pharmaceutical Sciences*, **96** (11): 3140-3143 (2007)
143. Costantino, H.R., Griebenow, K., Mishra, P., Langer, R., and Klibanov, A.M. Fourier-transform infrared spectroscopic investigation of protein stability in the lyophilized form. *Biochimica et Biophysica Acta, Protein Structure and Molecular Enzymology*, **1253** (1): 69-74 (1995)
144. Griebenow, K. and Klibanov, A.M. Lyophilization-induced reversible changes in the secondary structure of proteins. *Proceedings of the National Academy of Sciences of the United States of America*, **92** (24): 10969-10976 (1995)
145. Crowe, J.H., Crowe, L.M., and Jackson, S.A. Preservation of structural and functional activity in lyophilized sarcoplasmic reticulum. *Archives of Biochemistry and Biophysics*, **220** (2): 477-484 (1983)
146. Anchordoquy, T.J. and Carpenter, J.F. Polymers protect lactate dehydrogenase during freeze-drying by inhibiting dissociation in the frozen state. *Archives of Biochemistry and Biophysics*, **332** (2): 231-238 (1996)

147. Izutsu, K.i., Yoshioka, S., and Terao, T. Stabilizing effect of amphiphilic excipients on the freeze-thawing and freeze-drying of lactate dehydrogenase. *Biotechnology and Bioengineering*, **43** (11): 1102-1107 (1994)
148. Cleland, J.L., Hedgepeth, C., and Wang, D.I.C. Polyethylene glycol enhanced refolding of bovine carbonic anhydrase B. Reaction stoichiometry and refolding model. *Journal of Biological Chemistry*, **267** (19): 13327-13334 (1992)
149. Semba, C.P., Weck, S., Razavi, M.K., Tuomi, L., and Patapoff, T. Tenecteplase: stability and bioactivity of thawed or diluted solutions used in peripheral thrombolysis. *Journal of Vascular and Interventional Radiology*, **14** (4): 475-479 (2003)
150. Albers, G.W., Bates, V.E., Clark, W.M., Bell, R., Verro, P., and Hamilton, S.A. Intravenous tissue-type plasminogen activator for treatment of acute stroke: the standard treatment with alteplase to reverse stroke (stars) study. *JAMA, J.Am.Med.Assoc.*, **283** (9): 1145-1150 (2000)
151. Katzan, I.L., Furlan, A.J., Lloyd, L.E., Frank, J.I., Harper, D.L., Hinchey, J.A., Hammel, J.P., Qu, A., and Sila, C.A. Use of tissue-type plasminogen activator for acute ischemic stroke: the Cleveland area experience. *JAMA, J.Am.Med.Assoc.*, **283** (9): 1151-1158 (2000)
152. Pennica, D., Holmes, W.E., Kohr, W.J., Harkins, R.N., Vehar, G.A., Ward, C.A., Bennett, W.F., Yelverton, E., and Seeburg, P.H. Cloning and expression of human tissue-type plasminogen activator cDNA in *E. coli*. *Nature (London)*, **301** (5897): 214-221 (1983)
153. Collen, D. On the regulation and control of fibrinolysis. Edward Kowalski Memorial Lecture. *Thrombosis and Haemostasis*, **43** (2): 77-89 (1980)
154. Hsu, C.C., Ward, C.A., Pearlman, R., Nguyen, H.M., Yeung, D.A., and Curley, J.G. Determining the optimum residual moisture in lyophilized protein pharmaceuticals. *Developments in Biological Standardization*, **74** (Biol. Prod. Freeze-Drying Formulation): 255-271 (1992)
155. Izutsu, K., Fujimaki, Y., Kuwabara, A., and Aoyagi, N. Effect of counterions on the physical properties of l-arginine in frozen solutions and freeze-dried solids. *International Journal of Pharmaceutics*, **301** (1-2): 161-169 (2005)
156. Carlson, R.H., Garnick, R.L., Jones, A.J.S., and Meunier, A.M. The determination of recombinant human tissue-type plasminogen activator activity by turbidimetry using a microcentrifugal analyzer. *Analytical Biochemistry*, **168** (2): 428-435 (1988)
157. Mumenthaler, M., Hsu, C.C., and Pearlman, R. Feasibility study on spray-drying protein pharmaceuticals: recombinant human growth hormone and tissue-type plasminogen activator. *Pharmaceutical Research*, **11** (1): 12-20 (1994)
158. Verstraete, M. and Collen, D. Thrombolytic therapy in the eighties. *Blood*, **67** (6): 1529-1541 (1986)
159. Modi, N.B. Recombinant thrombolytic agents. *Pharm.Biotechnol.(2nd Ed.)*, 327-338 (2002)
160. MacDonald, M.E., Van Zonneveld, A.J., and Pannekoek, H. Functional analysis of the human tissue-type plasminogen activator protein: the light chain. *Gene*, **42** (1): 59-67 (1986)
161. Spellman, M.W., Basa, L.J., Leonard, C.K., Chakel, J.A., O'Connor, J.V., Wilson, S., and Van Halbeek, H. Carbohydrate structures of human tissue plasminogen activator expressed in Chinese hamster ovary cells. *Journal of Biological Chemistry*, **264** (24): 14100-14111 (1989)
162. Thorne, J.M., Goetzinger, K., Chen, A.B., Moorhouse, K.G., and Karger, B.L. Examination of capillary zone electrophoresis, capillary isoelectric focusing and sodium dodecyl sulfate capillary electrophoresis for the analysis of recombinant tissue plasminogen activator. *Journal of Chromatography A*, **744** (1+2): 155-165 (1996)
163. Cleary, S., Mulkerrin, M.G., and Kelley, R.F. Purification and characterization of tissue plasminogen activator kringle-2 domain expressed in *Escherichia coli*. *Biochemistry*, **28** (4): 1884-1891 (1989)
164. Kueltzo, L.A., Ersoy, B., Ralston, J.P., and Middaugh, C.R. Derivative absorbance spectroscopy and protein phase diagrams as tools for comprehensive protein characterization: A bGCSF case study. *Journal of Pharmaceutical Sciences*, **92** (9): 1805-1820 (2003)

165. Mach, H. and Middaugh, C.R. Simultaneous monitoring of the environment of tryptophan, tyrosine, and phenylalanine residues in proteins by near-ultraviolet second-derivative spectroscopy. *Analytical Biochemistry*, **222** (2): 323-331 (1994)
166. Ragone, R., Colonna, G., Balestrieri, C., Servillo, L., and Irace, G. Determination of tyrosine exposure in proteins by second-derivative spectroscopy. *Biochemistry*, **23** (8): 1871-1875 (1984)
167. Kuiltzo, L.A. and Middaugh, C.R. Ultraviolet absorption spectroscopy. *Biotechnology: Pharmaceutical Aspects*, **3** (Methods for Structural Analysis of Protein Pharmaceuticals): 1-25 (2005)
168. Kuiltzo, L.A., Wang, W., Randolph, T.W., and Carpenter, J.F. Effects of solution conditions, processing parameters, and container materials on aggregation of a monoclonal antibody during freeze-thawing. *Journal of Pharmaceutical Sciences*, **97** (5): 1801-1812 (2008)

CHAPTER 8

EFFECT OF COLLAPSE ON PROTEIN STABILITY II: STABILITY OF LYOPHILIZATES DURING STORAGE AT ELEVATED TEMPERATURES

1 INTRODUCTION

In the production of protein pharmaceuticals, freeze-drying is frequently applied to stabilize active ingredients that otherwise could not be stabilized. It is well understood that drying alone does not ensure adequate protein stability during processing and subsequent storage and thus various investigations on the effect of formulation parameters have been conducted¹⁻³. However, besides the important effect of formulation the drying process itself can have a tremendous impact as well. No matter whether the process parameters during an established drying protocol are changed or a different drying method is applied, the common result is a change in the product's thermal history, whose effect is well recognized in the polymer and food sciences^{4,5}, but has only recently gained attention in the pharmaceutical industry^{6,7}.

One of the most common process aberrations changing the product's thermal history encountered in freeze-drying is the collapse-phenomenon. The onset of collapse usually is correlated with the loss of pharmaceutical quality⁸⁻¹⁰ and collapsed lyophilizates are regarded as products that lost their ability to be properly dried¹⁰ and that are poorly reconstitutable¹¹. The most severe quality concern is the presumption that protein stability is greatly compromised in collapsed systems¹²⁻¹⁴.

While it was shown in Chapter seven, that collapse has no negative effect on the reconstitution behavior and the protein stability immediately after freeze-drying, results from the investigation of protein-long-term stability in collapsed lyophilizates is presented in the following chapter. Producing lyophilized protein pharmaceuticals, the adequate stabilization of the protein during freeze-drying is of utmost importance. However, the continuation of this stabilization throughout long-term storage is equally important.

While there was no effect of collapse itself on protein storage stability detectable, collapsed lyophilizates have been reported to be more prone to crystallization than non-collapsed cakes^{15,16}. Other researchers describe compromised storage stability due to increased residual moisture levels in collapsed cakes¹³, but as the collapse-dried lyophilizates investigated in this thesis do not show increased residual moistures, this factor can be excluded for the investigated lyophilizates. In contrast, Wang and co-workers found that lyophilizates that collapsed during freeze-drying did not show reduced storage stability and

some collapsed formulations performed even better than non-collapsed ones in terms of biological activity of rFVIII¹⁷. A similar observation was made by Chatterjee et al. who did not see a compromised biological activity of LDH no matter whether freeze-drying was performed above or below T_g' ¹⁸.

Interestingly, a clearly impaired long-term storage stability was observed by Passot et al. for lyophilizates that were freeze-dried above the T_g' although no effect on protein stability could be detected immediately after freeze-drying, pointing out the importance of long-term storage stability studies. However, this compromised stability was not clearly correlated to the collapse phenomenon, because systems that did not collapse because of the use of crystalline bulking agents showed a decreased stability as well¹⁹.

Another aspect possibly affecting protein stability might be the specific surface area (SSA). As was discussed in Chapter 5, the specific surface area is greatly reduced with the onset of collapse and so is the system's porosity. There are several reports dealing with the effect of SSA on protein stability, pointing out an increased stability in less porous matrices^{20,21}.

Finally, the effect of collapse on the system's thermal history that is discussed in detail in Chapter 9 of this thesis might have a tremendous effect on the long-term stability as well. As it was found that collapse-dried cakes exhibit greatly increased structural relaxation times, degradation reactions that are coupled to viscosity might be greatly retarded in these systems, actually increasing stability in collapsed cakes in analogy to foam-dried systems as compared to conventionally freeze-dried systems²⁰.

Although protein pharmaceuticals are usually stored refrigeratedly, elevated temperatures may be encountered accidentally during shipping, storage and prior to application. The robustness of the system towards variations in temperature and its tolerance against high temperatures may be increased in collapsed systems; obviously, they are not sensitive to collapse during storage above their glass transition temperature, as they are already collapsed. In addition, they may have an increased fragility as a result of the altered thermal history, rendering them less sensitive towards crystallization during temporary storage at elevated temperatures^{22,23}.

Given the contrary reports on the effect of collapse and collapse-associated material properties, a comprehensive study concerning the effect of cake collapse during lyophilization on the long-term storage stability of proteins was conducted including IgG₀₁, LDH and PA₀₁ as model proteins with quite different properties in terms of thermal stability and sensitivity towards freeze-drying stresses.

2 IgG₀₁

IgG₀₁ was analyzed as a model protein representing the currently most important class of biopharmaceuticals. Amorphous and partially crystalline formulations were stored at 40 °C and 50 °C for up to 15 weeks, respectively. In order to increase the antibody's sensitivity towards freeze-drying stresses, a formulation at a decreased pH of 3.5 was also included into the investigation.

2.1 AMORPHOUS SYSTEMS I - TREHALOSE-BASED LYOPHILIZATES: THE EFFECT OF COLLAPSE DURING LYOPHILIZATION

Trehalose-based IgG₀₁ lyophilizates were investigated at two different pH values as explained above (Chapter 7). Because trehalose has a strongly reduced susceptibility towards acid catalyzed hydrolysis, called inversion, compared to sucrose²⁴, the degradation of excipients due to the low pH value is most unlikely to occur, allowing the unbiased assessment of IgG₀₁ stability at low pH. Table 8.1 lists the investigated trehalose-based formulations.

Table 8.1: Investigated IgG₀₁ formulations.

ID	excipient	concentration
1	IgG01	4.0 mg/mL
	trehalose	50.0 mg/mL
	polysorbate 20	0.4 mg/mL
	sodium succinate, pH 5.5	2.7 mg/mL
2	IgG01	4.0 mg/mL
	trehalose	50.0 mg/mL
	polysorbate 20	0.4 mg/mL
	sodium succinate, pH 3.5	2.7 mg/mL

Collapsed lyophilizates were produced using the collapse-cycle described in Chapter 3. Non-collapsed lyophilizates were freeze-dried using a conventional lyophilization protocol that is also described in Chapter 3.

2.1.1 PHYSICOCHEMICAL CHARACTERISTICS OF LYOPHILIZATES

The macroscopic appearance of the freeze-dried cakes was not significantly altered during storage at elevated temperatures. Figure 8.1 exemplarily shows non-collapsed (A) and collapsed (B) trehalose lyophilizates formulated at pH 5.5 after storage at elevated temperatures for 15 weeks. No shrinkage or discoloration can be observed. Lyophilizates formulated at pH 3.5 looked identically (data not shown).

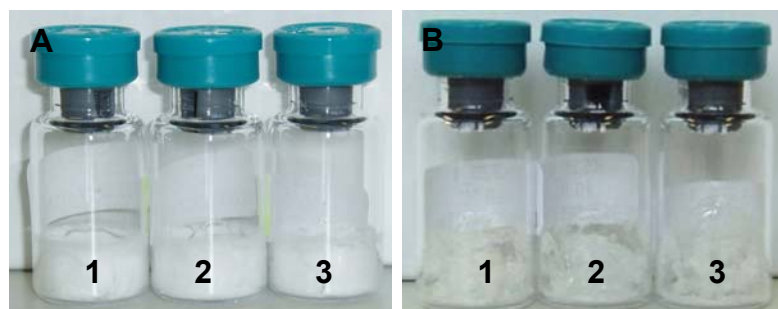


Figure 8.1: Non-collapsed (A) and collapsed (B) trehalose-based lyophilizates containing 4 mg/mL IgG₀₁ after 15 weeks of storage at 2-8 °C (1), 40 °C (2) and 50 °C (3), respectively.

Table 8.2 summarizes the physicochemical properties of the investigated lyophilizates after 15 weeks of storage at various temperatures. Slight increases in residual moisture levels were observed for the samples stored at 40 °C and 50 °C. The increase in residual moisture upon storage at elevated temperatures is commonly reported in literature²⁵.

Table 8.2: Physicochemical properties of trehalose lyophilizates after 15 weeks of storage.

pH	appearance	storage temperature [°C]	residual moisture [%] ^{a)}	Tg [°C] ^{b)}	Δc_p [J/gK] ^{b)}	characteristic XRD peaks ^{c)}
5.5	non-collapsed	2-8°C	0.61 ± 0.06	77.1 ± 14.1	0.458 ± 0.214	no peaks
		40°C	0.97 ± 0.01	100.0 ± 27.6	0.412 ± 0.240	no peaks
		50°C	1.03 ± 0.03	88.0 ± 1.6	0.464 ± 0.088	no peaks
	collapsed	2-8°C	1.55 ± 0.03	85.8 ± 0.9	0.551 ± 0.031	no peaks
		40°C	1.84 ± 0.08	82.6 ± 1.1	0.729 ± 0.034	no peaks
		50°C	1.81 ± 0.14	82.5 ± 1.1	0.528 ± 0.045	no peaks
3.5	non-collapsed	2-8°C	0.57 ± 0.09	66.8 ± 39.5	0.682 ± 0.341	no peaks
		40°C	1.03 ± 0.06	85.3 ± 29.3	0.537 ± 0.139	no peaks
		50°C	1.06 ± 0.06	80.2 ± 3.2	0.516 ± 0.004	no peaks
	collapsed	2-8°C	1.74 ± 0.04	77.2 ± 1.6	0.606 ± 0.100	no peaks
		40°C	1.88 ± 0.04	76.1 ± 1.8	0.601 ± 0.028	no peaks
		50°C	1.82 ± 0.14	77.1 ± 0.4	0.475 ± 0.013	no peaks

a) determined by Karl Fischer direct methanol extraction set-up'

b) determined by differential scanning calorimetry

c) determined by powder x-ray diffraction

However, the uptake of water did not cause the residual moisture levels within one formulation to differ beyond the range of ± 0.5 % that was previously defined as acceptable. But comparing collapsed and not collapsed lyophilizates, differences larger than the specified range are observed. The effect of residual moisture, which is commonly reported to adversely affect protein stability, on freeze-dried IgG₀₁ was thoroughly investigated in the range of 0.7 % to 6.3 % residual moisture in a separate study. The results of this study are discussed in Chapter 6 of this thesis. No effect of residual moisture within this range could be

detected on the physical and conformational stability of the IgG₀₁. According to these findings, the slighter differences in residual moisture observed in this sample set can be regarded as negligible.

Glass transition temperatures were between 70.7 °C and 77.2 °C at the beginning of long-term storage (see Chapter 7 for details) and they did not relevantly change during storage either and they were in good agreement with literature reports for freeze-dried trehalose (90 ± 7.0 °C at a residual moisture content of 2.0 ± 1.4 %²⁶). Most importantly glass transition temperatures of all samples were well above the highest storage temperature at 50 °C, indicating that all samples remained in the glassy state during storage.

Neither DSC results nor X-ray powder diffractograms showed any signs of trehalose crystallization upon storage. Interestingly, ΔC_p -values were identical no matter whether the material collapsed or not. As the extent of change in heat capacity at the glass transition is an indication of the system's fragility, this points towards collapse having no effect on this system's fragility. This observation is discussed in detail in the following Chapter 9.

In summary, all investigated lyophilized systems remained physico-chemically stable during storage. No crystallization or excessive uptake of water occurred and all samples stayed in the glassy state during the whole period of storage allowing the accurate comparison of collapsed and non-collapsed lyophilizates.

2.1.2 PHYSICAL PROTEIN STABILITY OF IGG₀₁ IN RECONSTITUTED LYOPHILIZATES

Physical protein stability, i.e. the formation of soluble and insoluble aggregates was assessed with a variety of analytical techniques. Table 8.3 summarizes results obtained from light obscuration, dynamic light scattering and turbidity measurements after 15 weeks of storage at 50 °C.

Table 8.3: Particulate matter of reconstituted trehalose based IgG₀₁ lyophilizates stored at 50 °C for 15 weeks.

pH appearance	5.5		3.5	
	not collapsed	collapsed	not collapsed	collapsed
particles > 1 µm/mL ^{a)}	3421 ± 445	2098 ± 243	18586 ± 340	9956 ± 189
particles > 10 µm/mL ^{a)}	7 ± 8	23 ± 14	23 ± 3	22 ± 6
particles > 25 µm/mL ^{a)}	0 ± 0	4 ± 4	2 ± 1	0 ± 0
turbidity [FNU] ^{b)}	1.73 ± 0.27	1.45 ± 0.04	1.51 ± 0.28	1.31 ± 0.08
Z average [nm] ^{c)}	12.45 ± 0.07	11.85 ± 0.07	11.20 ± 0.00	11.40 ± 0.00
PDI ^{c)}	0.126 ± 0.005	0.090 ± 0.001	0.121 ± 0.004	0.145 ± 0.004

a) determined by light obscuration

b) determined by nephelometric turbidity measurements

c) determined by dynamic light scattering using cumulants analysis

Regarding the light obscuration data, particles larger 10 µm and larger 25 µm that are specified in the pharmacopoeias are listed besides particles larger 1 µm that are better suited to give insight into particles caused by protein aggregation²⁷. Immediately after freeze-drying,

collapsed samples showed comparable particle numbers (1273 ± 515 and 1543 ± 619 particles larger $1 \mu\text{m}$ in collapsed pH 5.5 and pH 3.5 samples, respectively as compared to 1778 ± 719 and 1795 ± 547 particles larger $1 \mu\text{m}$ in non-collapsed pH 5.5 and pH 3.5 samples, respectively). Most notably, all formulations remained remarkably stable upon storage. No relevant amounts of particles larger than $25 \mu\text{m}$ could be detected and only low numbers of particles larger $10 \mu\text{m}$. Concerning particles larger $1 \mu\text{m}$, samples reconstituted from non-collapsed lyophilizates exhibited larger particle numbers than samples reconstituted from collapsed cakes, indicating a higher stability of collapsed cakes. Samples formulated at a pH of 3.5 most certainly showed higher particle numbers than samples formulated at pH 5.5, because it was shown beforehand, that the IgG₀₁ is less stable at acidic pH.

However, the observed trend was not confirmed by turbidity measurements or DLS results. All samples were clear and monodisperse, as indicated by a low turbidity and a Z-average-value at the size of an IgG monomer around 10 nm. Polydispersity indices of around 0.1 indicated the monodispersity of the samples.

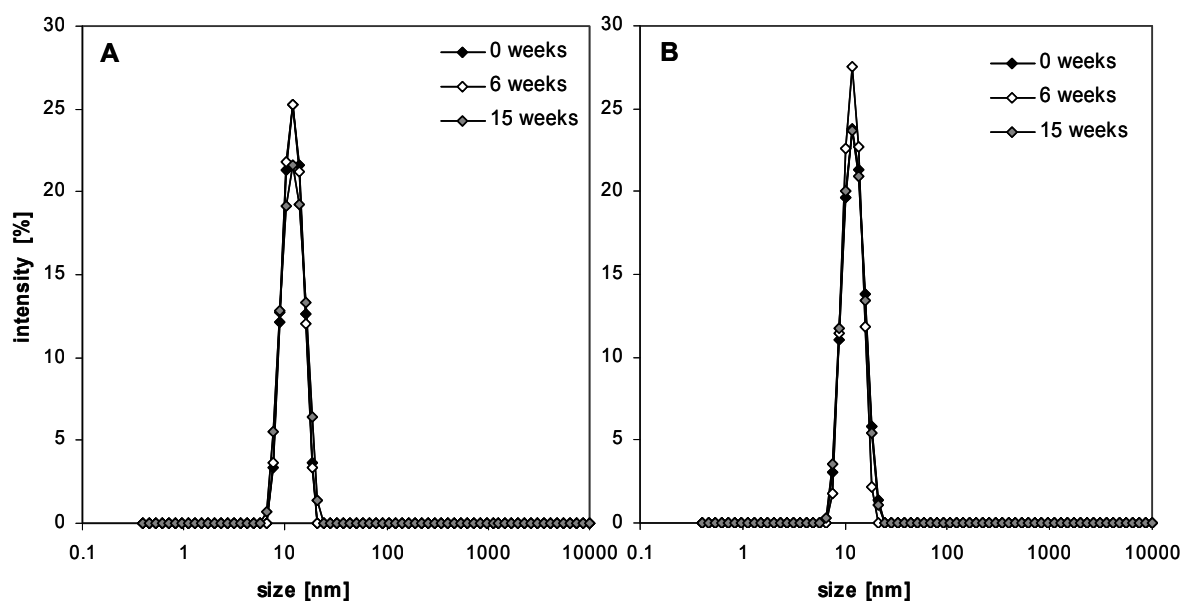


Figure 8.2: Size distribution by intensity of scattered light determined by DLS after 0, 6, and 15 weeks of storage at $50 \text{ }^\circ\text{C}$ in collapsed (A) and non-collapsed (B) trehalose-based lyophilizates formulated at pH 3.5; $n = 2$.

The size distribution was obtained by fitting a NNLS algorithm to the correlation function.

To further demonstrate the excellent stability of both collapsed and not collapsed lyophilizates, Figure 8.2 depicts the size distributions by intensity as determined by dynamic light scattering after 0, 6 and 15 weeks of storage at $50 \text{ }^\circ\text{C}$ in collapsed (Figure 8.2 A) and non-collapsed (Figure 8.2 B) lyophilizates. Because the intensity of scattered light strongly increases with particle size, DLS is an extremely sensitive tool to monitor the formation of smallest amounts of aggregated species²⁸. Figure 8.2 clearly shows only one peak around

10 nm that can be assigned to the hydrodynamic diameter of the IgG monomer. No signals are observed in the higher size range, further confirming the absence of aggregated species. Similar observations were made for systems stored at 40 °C and 2-8 °C and for all analyzed time points in between, i.e. after 2, 4, 6, 9, 12 and 15 weeks of storage.

Table 8.4: Aggregation of IgG₀₁ after storage at 50 °C for 15 weeks.

pH	appearance	remaining monomer [%] ± SD ^{a)}	soluble aggregates [%] ± SD ^{a)}	monomer AF4 [%] ± SD ^{b)}	hmw aggregates [%] ± SD ^{b)}
5.5	not collapsed	94.63 ± 1.44	1.23 ± 0.03	96.37 ± 0.35	1.09 ± 0.29
	collapsed	98.31 ± 3.12	0.96 ± 0.08	98.56 ± 0.53	0.90 ± 1.12
3.5	not collapsed	96.51 ± 0.33	2.28 ± 0.02	93.75 ± 0.75	2.61 ± 0.30
	collapsed	96.30 ± 1.10	1.71 ± 0.01	94.08 ± 0.52	2.09 ± 1.05

a) determined by HP-SEC

b) determined by AF4

Excellent stability is pointed out by HP-SEC results as well. Remaining monomer contents were above 94 % for all the formulations as listed in Table 8.4. Monomer contents determined by AF4 measurements were very similar to the ones determined by HP-SEC, further confirming that HP-SEC-results were not skewed by the dissociation of soluble aggregates during HP-SEC analysis due to high shear forces during column passage – a problem that has been reported elsewhere^{29,30}. The complete recovery in HP-SEC experiments further confirmed the absence of relevant amounts of insoluble aggregates that would have been removed during sample-preparation and would have caused a decrease in recovery.

IgG₀₁ formulated at pH 3.5 showed slightly decreased monomer contents in the AF4 results. A compromised stability at pH 3.5 was expected, because a decreased melting point T_m was measured prior to this study (data not shown) and reports from literature point out a decreased stability of IgG antibodies at decreased pH values^{31,32}. Furthermore, soluble as well as insoluble high molecular weight aggregates were increased in IgG₀₁ formulations at lower pH.

Interestingly, collapsed lyophilizates showed lower amounts of soluble as well as insoluble aggregates, indicating a higher degree of stabilization in collapsed lyophilizates as compared to non-collapsed cakes.

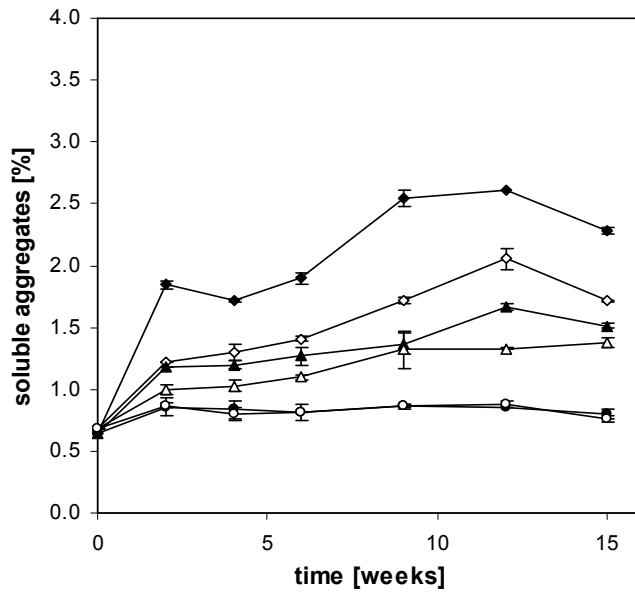


Figure 8.3: Soluble aggregates as determined by HP-SEC during storage at 50 °C (diamonds), 40 °C (triangles) and 2-8 °C (circles) in collapsed (open symbols) and non-collapsed (closed symbols) trehalose-based lyophilizates, respectively (average +/- SD, n = 2).

Figure 8.3 exemplarily shows the amount of soluble aggregates in trehalose-based lyophilizates formulated at pH 3.5 as determined by HP-SEC during storage at 50, 40 and 2 - 8 °C. Although the absolute amount of aggregates remained low during the whole period of storage, non-collapsed lyophilizates showed significantly higher amounts of aggregated fractions than collapsed lyophilizates during storage at 50 °C and 40 °C. Reference samples stored in the refrigerator did not relevantly aggregate throughout the investigated period of time.

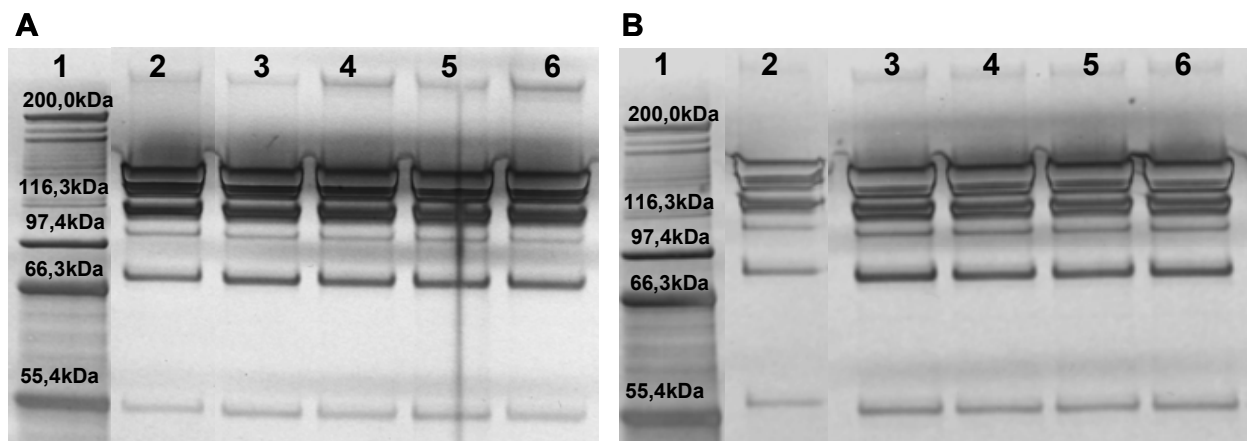


Figure 8.4: SDS-PAGE of IgG₀₁ stored for 15 weeks at 50 °C (A) and 2-8 °C (B).

lane 1: molecular weight standard, lane 2: IgG₀₁ standard, lane 3: pH 5.5 collapsed, lane 4: pH 3.5 collapsed, lane 5: pH 5.5 not collapsed, lane 6: pH 3.5 not collapsed.

Excellent stability was further proven by SDS-PAGE (Figure 8.4): No relevant difference could be detected between the electrophoretic pattern of IgG₀₁ standard (lane 2) and IgG₀₁ reconstituted from collapsed (lane 3 & 4) and non-collapsed (lane 5 & 6) cakes, respectively. As observed before, the slightly more intense band at the very top of the gel, above 200 kDa,

in the lanes of the pH 3.5 samples indicates an increased amount of aggregates present in these formulations. Furthermore, comparing samples formulated at pH 5.5 in lane 3 and lane 5, the aggregate band in lane 5, i.e. the non-collapsed sample, is slightly darker as well.

Significant fragmentation was observed in all the formulations. This is most probably caused by the sample preparation as described by Harris et al.³³ and not due to stability issues, because IgG₀₁ standard also showed this degradation to a similar extent.

Summarizing, despite the overall high stability, a trend pointing out a greater stability of IgG₀₁ in collapsed lyophilizates could be observed. Samples stored at 40 °C and reference samples stored at 2-8 °C exhibited high stability as well and showed a similar trend to the samples stored at 50 °C.

2.1.3 BINDING ACTIVITY OF IgG₀₁ IN RECONSTITUTED LYOPHILIZATES

The biologic activity of reconstituted IgG₀₁ solutions was approached by determining the binding activity of the mAb to a specific receptor using surface plasmon resonance (SPR) spectroscopy. Figure 8.5 displays binding activities of IgG₀₁ reconstituted from collapsed and non-collapsed trehalose-based lyophilizates after freeze-drying and after 15 weeks of storage at 40 °C and 50 °C, respectively.

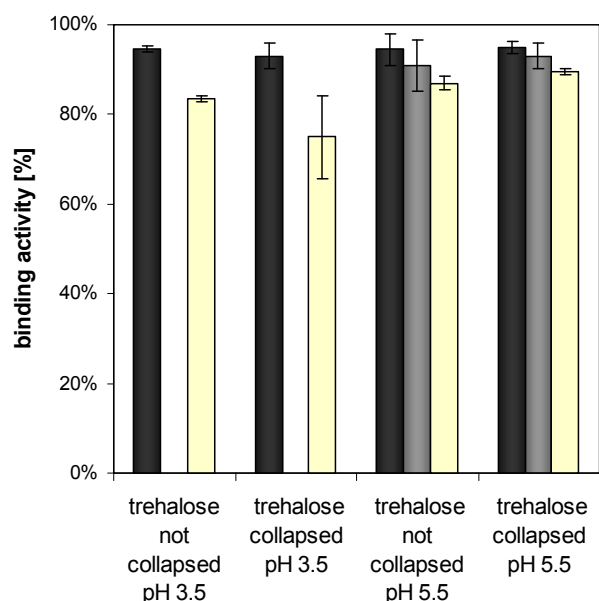


Figure 8.5: Binding activity of IgG₀₁ as determined by surface plasmon resonance spectroscopy (average +/- SD, n = 2).

Binding activity after lyophilization (black bars), after 15 weeks of storage at 40 °C (grey bars) and after 15 weeks of storage at 50 °C (white bars).

After lyophilization, all formulations showed a comparable binding activity of > 93 %. After storage, all formulations showed decreased binding activities, in contrast to the observed very high physical stability. However, binding activities were above 75 % for all the formulations. Lyophilizates formulated at a pH of 5.5 showed no relevant difference between collapsed and non-collapsed cakes. Regarding formulations at pH 3.5 in contrast, a decreased binding activity in collapsed systems was observed. However, there was no

significant difference between collapsed and non-collapsed samples, as standard deviations were high.

Thus binding activity data further confirmed findings from physical protein stability, that there could be no strong negative effect of collapse concluded and collapsed lyophilizates performed equally well as elegant cakes.

2.1.4 CONFORMATIONAL STABILITY OF IgG₀₁ IN RECONSTITUTED LYOPHILIZATES

To complete investigations on the effect of collapse on IgG₀₁ stability during storage at elevated temperature, conformational stability was taken into consideration as well. To assess secondary structure, FTIR transmission spectroscopy was applied and to evaluate the tertiary structure, fluorescence spectroscopy was employed. Figure 8.6 exemplarily depicts typical spectra obtained from the analysis of samples that were stored at 50 °C for 15 weeks. Samples stored at 40 °C and reference samples stored at 2-8 °C showed similar results.

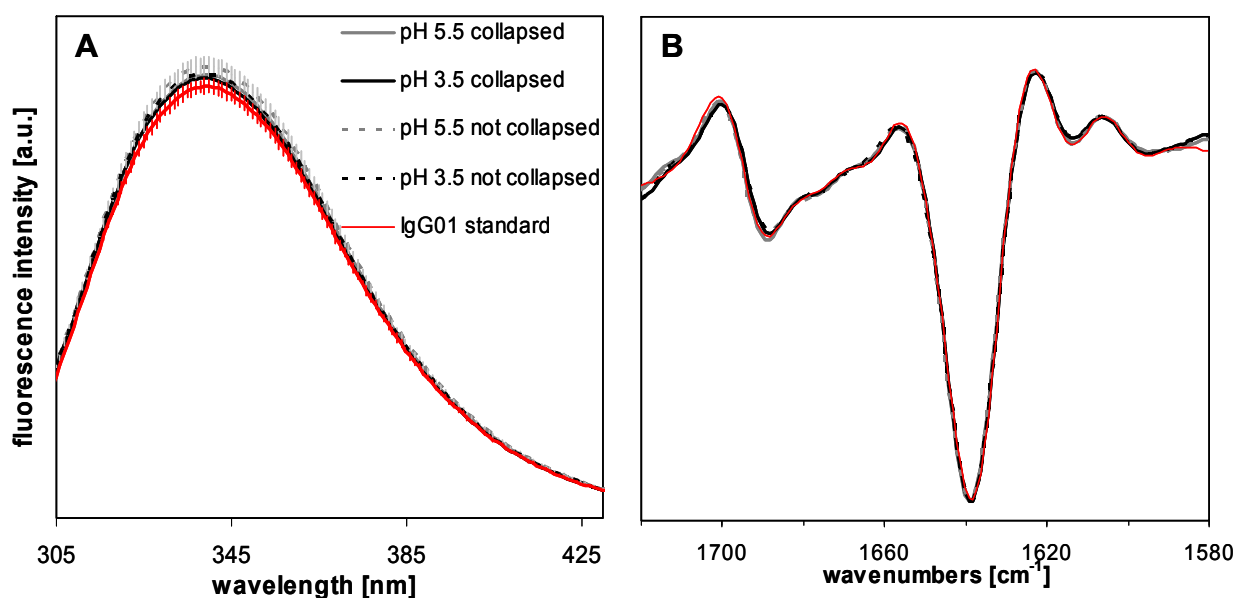


Figure 8.6: Conformational stability after storage at 50 °C for 15 weeks: Intrinsic protein fluorescence spectra of 50 µg/mL IgG₀₁ formulated with trehalose at different pH-values reconstituted from collapsed and non-collapsed lyophilizates, respectively (A); area-normalized 2nd derivative FTIR transmission spectra of 4 mg/mL IgG₀₁; n = 2.

Spectra are calculated average spectra of at least two independent measurements.

IgG₀₁ reconstituted from trehalose-based cakes formulated at a pH of 5.5 that were collapsed (grey solid line) and non-collapsed (grey dotted line) and reconstituted from trehalose-based cakes formulated at a pH of 3.5 that were collapsed (black solid line) and non-collapsed (black dotted line).

Clearly, there are no changes in either the secondary or the tertiary structure of the IgG₀₁ detectable. Figure 8.6 A depicts fluorescence spectra of IgG₀₁ reconstituted from stored trehalose lyophilizates, either collapsed or non-collapsed, after excitation at 280 nm as compared to a standard solution that was not stored. No change in emission maximum is observed, indicating that no major change in the local environment of the tryptophan

molecules occurred. As indicated by the overlapping error bars, slight differences observed in the fluorescence intensities are not significant.

Figure 8.6 B shows the second derivative of FTIR transmission spectra of IgG₀₁ reconstituted from collapsed and non-collapsed trehalose lyophilizates as compared to a standard that was not stored. Undoubtedly, the position of the main band at 1639 cm⁻¹, indicating intramolecular β -sheet structures, was not altered throughout storage in collapsed and non-collapsed systems. Furthermore, there was no change in the intensity of the bands at 1656 cm⁻¹ and at 1675 cm⁻¹, that are associated with the formation of intermolecular β -sheet structures and protein aggregation.

To sum up the findings of the investigation of conformational stability of IgG₀₁ in collapsed and non-collapsed trehalose lyophilizates, complete preservation of both, secondary and tertiary structure was found in all the systems, no matter whether the material collapsed or not.

2.1.5 SUMMARY AND CONCLUSION

Summing up the lessons learned from the investigation of trehalose-based IgG₀₁ lyophilizates at 40 °C and 50 °C for up to 15 weeks, findings from the comparative investigation of collapsed and non-collapsed cakes immediately after freeze-drying were further confirmed. No negative effect of collapse on the IgG₀₁ stability could be detected applying various analytical tools assessing both the physical protein stability in terms of aggregation and the conformational stability. All investigated systems showed a high degree of stability regarding the formation of soluble and insoluble aggregates. Secondary and tertiary structure remained unchanged after storage. Interestingly, collapsed lyophilizates showed a slightly but significantly decreased extent of protein aggregation as compared to non-collapsed systems.

Besides the stability of the antibody, excipient stability was also taken into consideration. Trehalose remained physically stable in the amorphous state and no crystallization or hydrolysis occurred. Furthermore, both systems remained in the glassy state as they were stored well below their glass transition temperatures throughout the period of investigation.

Given the high storage temperatures results obtained during the comparatively short period of storage were granted relevance. Samples stored at 40 °C and 2-8 °C showed similar results further confirming the trend observed in the samples stored at 50 °C.

2.2 AMORPHOUS SYSTEMS II – SUCROSE-BASED LYOPHILIZATES: THE EFFECT OF COLLAPSE DURING STORAGE

To get further insight into the effect of lyophilizate collapse on the stability of protein drugs, another typical protein formulation employed for lyophilization, comprising sucrose as protective agent was investigated. Formulations were identical to the trehalose-based formulations described in the previous section, except for the substitution of trehalose by sucrose. Hence, 4 mg IgG₀₁ were formulated with 50 mg sucrose and 0.04 mg polysorbate 20 in a 10 mM sodium succinate buffer at two different pH values, namely pH 3.5 and pH 5.5. Collapsed and non-collapsed lyophilizates of equal composition were produced using an aggressive and a more gentle freeze-drying protocol, as described in Chapter 3. Samples were stored for 15 weeks at 40 °C and 50 °C and reference samples were stored in the refrigerator at 2-8°C. MAB- as well as excipient-stability was investigated after 0, 2, 4, 6, 9, 12 and 15 weeks of storage with a wide array of analytical methods.

2.2.1 PHYSICOCHEMICAL CHARACTERISTICS OF LYOPHILIZATES

After freeze-drying both non-collapsed and collapsed lyophilizates exhibited comparable residual moisture levels and glass transition temperatures were in good accordance as well (Table 8.5). With residual moisture levels at 1 %, the produced lyophilizates represent a typical freeze-dried product, whose residual moisture levels usually range from below 1 % to 3 %³⁴.

Table 8.5: Calorimetric characteristics and residual moisture levels of sucrose-based lyophilizates after freeze-drying.

appearance	formulation- pH	T _g ± SD[°C]	Δc _p [J/gK]	residual moisture ± SD [%]
non-collapsed	5.5	63.8 ± 2.8	0.1 ± 0.0	1.0 ± 0.2
collapsed		56.7 ± 0.1	0.5 ± 0.1	0.9 ± 0.2
non-collapsed	3.5	67.9 ± 7.1	0.1 ± 0.0	0.7 ± 0.2
collapsed		56.3 ± 8.2	0.6 ± 0.4	0.9 ± 0.2

With glass transition temperatures between 56 °C and 68 °C, storage of all lyophilizates is conducted in the glassy state, although the offset to the highest storage temperature at 50 °C is not very distinct.

Residual moisture levels slightly increased during storage as shown in Figure 8.7. This is a phenomenon frequently observed during storage of freeze-dried solids and it is caused by either moisture transfer from the stoppers or by water vapor permeability of the container closure system^{13,25}. However, moisture contents remained below 1.4 % in all the samples. Thus they were still in a well-acceptable range for lyophilized products^{34,35}.

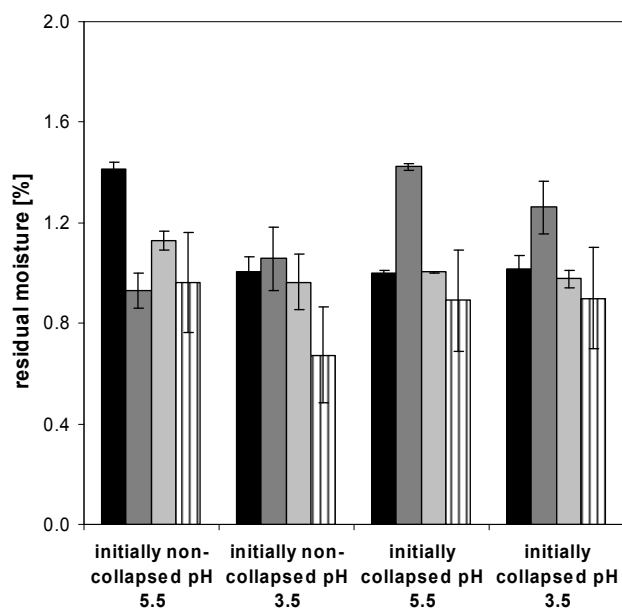


Figure 8.7: Residual moisture levels in lyophilizates stored for 15 weeks at 2-8 °C (black bars), 40 °C (dark grey bars) and 50 °C (light grey bars) as compared to the residual moisture level immediately after freeze-drying (striped bars) (average \pm SD, n = 3).

COLLAPSE DURING STORAGE

After freeze-drying, aggressively dried lyophilizates were collapsed and conventionally dried lyophilizates appeared as elegant, non-collapsed cakes. However, after two weeks of storage at 40 °C and 50 °C, the initially non-collapsed lyophilizates had collapsed as well. Figure 8.8 shows collapsed and non-collapsed lyophilizates that were stored for 2 weeks. The picture displays initially non-collapsed lyophilizates that were stored at either 2-8 °C (vial 1 and 4) or 50 °C (vial 2 and 5) as well as initially collapsed lyophilizates that were stored at 50 °C (vials 3 and 6). Initially collapsed lyophilizates stored at 2-8 °C are not depicted because no difference in the macroscopic appearance of these lyophilizates stored at 2-8 °C and 50 °C was observed.



Figure 8.8: Macroscopic appearance of collapsed and non-collapsed lyophilizates stored for 2 weeks at 2 - 8 °C (1 and 4) and 50 °C (2, 3, 5 and 6), respectively.

Vials 1-3 (crimped with a turquoise cap) were formulated at pH 5.5, vials 4-6 (crimped with a transparent cap) were formulated at pH 3.5.

Comparing initially non-collapsed lyophilizates stored at 2-8 °C and 50 °C, a marked difference was observed. Samples stored at elevated temperatures showed a dramatic shrinkage, reducing the lyophilizate to a tablet-like structure at the vial center. Lyophilizates

stored at 40 °C showed a similar behavior (data not shown). This shrinkage was described as volume relaxation by Duddu et al.³⁶ and is termed “collapse during storage” throughout this thesis.

In order to assess the change in cake appearance with an analytic parameter, the extent of collapse was characterized by the decrease in specific surface area as determined by BET krypton gas adsorption analysis (for details see Chapter 5). Figure 8.9 displays the specific surface areas (SSA) of initially non-collapsed and initially collapsed sucrose-based lyophilizates. The SSA determined for non-collapsed lyophilizates of 0.82 m²/g is in good agreement with values reported in literature for carbohydrate lyophilizates freeze-dried with a protocol including an annealing step (0.74 m²/g for Met-hGH-trehalose formulations⁷, 0.60 m²/g and 0.81 m²/g for IgG-sucrose formulations with and without surfactant, respectively²⁰).

Specific surface areas of collapsed lyophilizates have not yet been described in literature. However, Abdul-Fattah et al. determined the SSA of foam-dried carbohydrate systems to be between 0.04 m²/g and 0.17 m²/g depending on the mass ratio of protein to stabilizer (either 1:4 or 1:19 respectively)²⁰. These data are in good agreement with SSA determined for collapsed lyophilizates. Because the collapse-drying protocol results in lyophilizates that macroscopically resemble foam-dried materials, this consistence can be regarded as a confirmation.

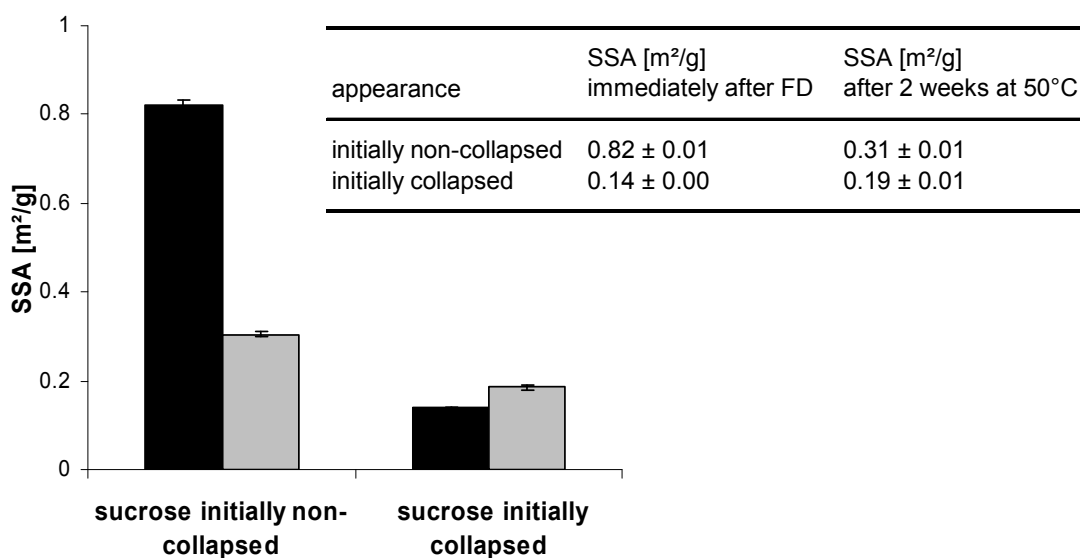


Figure 8.9: Specific surface area (SSA) as determined by BET krypton gas adsorption of initially collapsed and initially non-collapsed sucrose lyophilizates immediately after freeze-drying (black bars) and after two weeks of storage at 50 °C (grey bars), respectively (average +/- SD, n = 2).

Whereas the SSA of initially collapsed lyophilizates remained rather unchanged upon storage at 50 °C, initially non-collapsed lyophilizates exhibited a dramatic decrease in SSA by a factor of approximately 2.6. This decrease in surface area coincides with the onset of

collapse in the initially non-collapsed systems and can be used to quantify the degree of collapse.

However, lyophilizates that collapsed during storage still showed higher SSA than initially collapsed lyophilizates.

Table 8.6: Reconstitution times of initially collapsed and non-collapsed lyophilizates after different times of storage at elevated temperatures.

appearance	pH	reconstitution time after FD [s]	reconstitution time after 2 weeks [s]
storage at 50°C			
initially non-collapsed	5.5	20	164
	3.5	14	1200
initially collapsed	5.5	9	11
	3.5	9	15
storage at 40°C			
initially non-collapsed	5.5		30
	3.5		64
initially collapsed	5.5		7
	3.5		7

The onset of collapse was accompanied by a dramatic change of the physicochemical properties. One major concern regarding the occurrence of collapse is the greatly prolonged reconstitution time^{10,37,38}. This was shown not to be true for intentionally collapsed lyophilizates (see Table 7.2). However, lyophilizates that collapsed during storage exhibited remarkably increased reconstitution times (Table 8.6). Reconstitution times did not drastically change during continuing storage (data not shown).

CRYSTALLIZATION OF SUCROSE

Another tremendous change occurred regarding the physical state of the major stabilizing excipient, sucrose. The generally accepted mechanism of stabilization by disaccharides is the so-called water-replacement³⁹. It is common knowledge, that the disaccharide existing in the amorphous state is a prerequisite for adequate formation of hydrogen-bonds to replace the sublimed water. A widespread analytical technique to study the physical state of materials is X-ray powder diffraction (XRD)^{40,41}. Figure 8.10 and Figure 8.11 display XRD-diffraction patterns of lyophilizates stored for different periods of time. Looking at the bottom diffraction patterns (designated 1 and representing the states of the samples after freeze-drying prior to storage), all lyophilizates are amorphous. During subsequent storage at 50 °C however, crystallization occurred. The diffraction patterns nominated 2 – 4 represent the physical state of samples stored for 2, 9 and 15 weeks at 50 °C, respectively.

Comparing the patterns recorded after 2 weeks of storage, thus after the collapse of initially non-collapsed lyophilizates during storage at elevated temperatures, samples collapsed

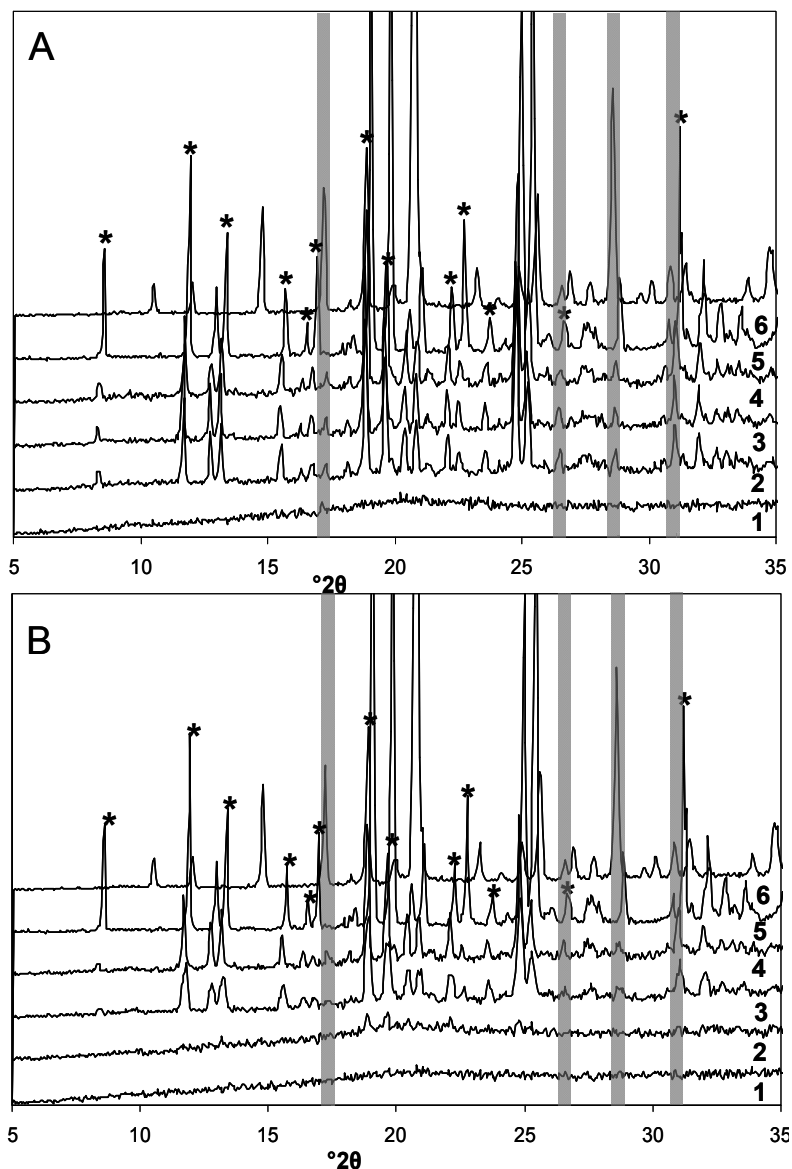


Figure 8.10: X-ray diffraction patterns of initially non-collapsed (A) and initially collapsed (B) sucrose-based lyophilizates formulated at a pH of 3.5 after different periods of storage at 50 °C as compared to crystalline sucrose and glucose.

1: stored for 0 weeks, 2: stored for 2 weeks, 3: stored for 9 weeks, 4: stored for 15 weeks, 5: crystalline sucrose, 6: crystalline glucose; asterisks mark characteristic diffractions of sucrose, characteristic glucose-diffractions are shaded grey.

during storage are crystallized whereas initially-collapsed cakes show only small diffractions indicating that crystallization occurred to a distinctly minor extent.

By comparing the observed diffractions with XRD patterns of purely crystalline sucrose (pattern 5 in Figure 8.10 and Figure 8.11), it was concluded that the initially amorphous disaccharide crystallized within two weeks of storage at 50 °C. Initially non-collapsed samples stored at 40 °C that collapsed likewise, also crystallized, but X-ray diffractions were not as pronounced as in the samples stored at 50 °C (data not shown). Initially collapsed cakes were completely X-ray amorphous after storage at 40 °C for 2 weeks. Thus the occurrence of collapse during storage and crystallization coincided in the investigated samples.

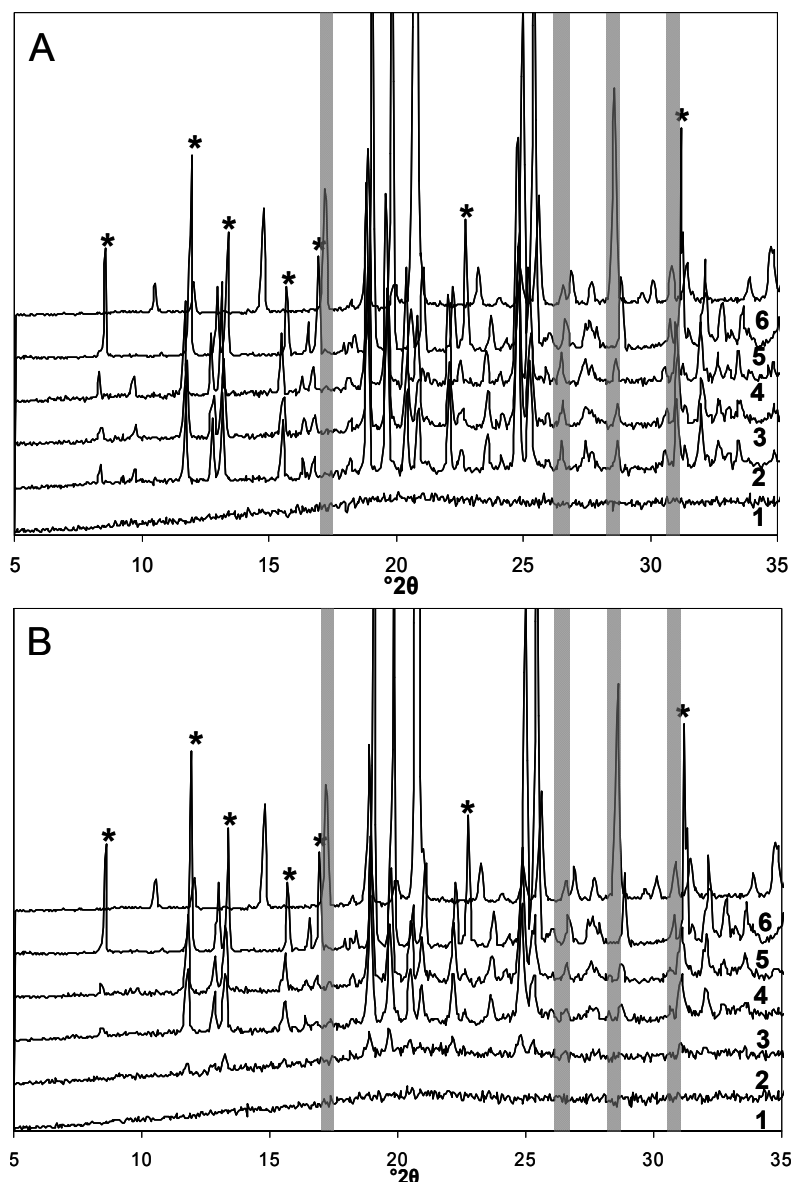


Figure 8.11: X-ray diffraction patterns of initially non-collapsed (A) and initially collapsed (B) sucrose-based lyophilizates formulated at a pH of 5.5 after different periods of storage at 50 °C as compared to crystalline sucrose and glucose

1: stored for 0 weeks, 2: stored for 2 weeks, 3: stored for 9 weeks, 4: stored for 15 weeks, 5: crystalline sucrose, 6: crystalline glucose; asterisks mark characteristic diffractions of sucrose, characteristic glucose-diffractions are shaded grey.

Crystallization is a result of two independent phenomena, i.e. nucleation and crystal growth⁴² of which the nucleation rate is rate-controlling⁴³. The susceptibility towards crystallization is affected by thermodynamic and kinetic factors.

It is well described in literature that sucrose readily crystallizes during storage above its glass transition temperature^{22,43}. Above T_g , molecular mobility is sufficiently increased to allow the rapid formation of nuclei and subsequent crystallization. Sucrose is reported to be especially prone to crystallization²². However, as the investigated samples were stored close to their glass transition temperatures, but not above them, this only partly explains the observed crystallization. More importantly, as collapsed and non-collapsed samples have comparable glass transition temperatures (with collapsed cakes exhibiting slightly lower T_g s, i.e. $56.7 \pm$

0.1 °C and 56.3 ± 8.2 °C for pH 5.5 and pH 3.5, respectively, as compared to 63.8 ± 2.8 °C and 67.9 ± 7.1 °C for pH 5.5 and pH 3.5 in non-collapsed cakes), the experienced difference in the rate of crystallization can not be explained.

Another important factor influencing crystallization is the molecular mobility, i.e. both global α -dynamics and local β -dynamics. A clear coupling between molecular mobility and crystallization kinetics has been described by various researchers⁴⁴⁻⁴⁶. Mobility may affect crystallization by imparting the movement of the whole system towards the more stable crystalline form by nucleation within glassy substates of higher mobility⁴². Thus a decreased molecular mobility stabilizes the system towards crystallization by impeding nucleation. As discussed in detail in Chapter 9, the structural relaxation times of collapsed and non-collapsed sucrose-based lyophilizates were found to be significantly different, with collapsed systems showing tremendously increased structural relaxation times. This was explained by differences in thermal histories and the annealing effect exerted by collapse-drying. In contrast, increased nucleation upon annealing that was observed in trehalose glasses by Surana et al. and was explained with an augmented β -mobility during abidance at elevated temperatures facilitating the formation of nuclei⁴⁷ was not observed in collapsed lyophilizates, because no differences in the β -mobility was observed either.

Sample preparation also affects crystallization. Besides its effect on the glassy dynamics of a material by affecting its thermal history^{6,20,48}, differences in mechanical stress experienced during production and differences in the induction of nuclei influence crystallization⁴². It was reported that low-temperature drying processes, such as freeze-drying, lead to the formation of less stable glasses with more nuclei than e.g. spray-dried glasses. This leads to an accelerated crystallization⁴⁴. Thus the conventional, lower-temperature freeze-drying cycle applied to produce non-collapsed lyophilizates might have resulted in stronger nucleation, further boosting crystallization.

Recently, the importance of surface crystallization has been described. Indomethacin showed a significantly higher extent of crystallization at larger surface areas⁴⁹ and the effect of cracks in melt-quenched material accelerating crystallization has been observed. As shown above, non-collapsed cakes do have strongly increased specific surface areas, thus this might be a third factor amplifying crystallization from non-collapsed cakes.

Summarizing, non-collapsed cakes showed an increased propensity to crystallize during storage close to of their glass transition temperature as compared to collapsed lyophilizates, despite the comparability of residual moisture content and glass transition temperature. This could be correlated to an increased structural relaxation time in collapsed systems. Additionally, the increased induction of nuclei during conventional freeze-drying and the increased surface area of elegant cakes may contribute to the boosted crystallization.

Lyophilizates that collapsed during storage were completely crystalline after 2 weeks of storage at 50 °C, as can be deduced from the absence of a glass transition or a crystallization exotherm in the DSC thermograms depicted in Figure 8.14 A and Figure 8.14 C. In initially collapsed samples crystallinity slowly increased and cakes formulated at a pH of 3.5 were completely crystalline after 15 weeks of storage. Cakes formulated at a pH of 5.5 remained partially amorphous throughout the whole period of storage, as indicated by the appearance of a glass transition and a crystallization exotherm at 100-110 °C⁵⁰ in the first DSC heating scan (data not shown).

Due to this occurrence of devitrification during the DSC experiment exact quantification of sucrose crystallization using the area under the curve of the melting endotherm as analytic measure was not possible.

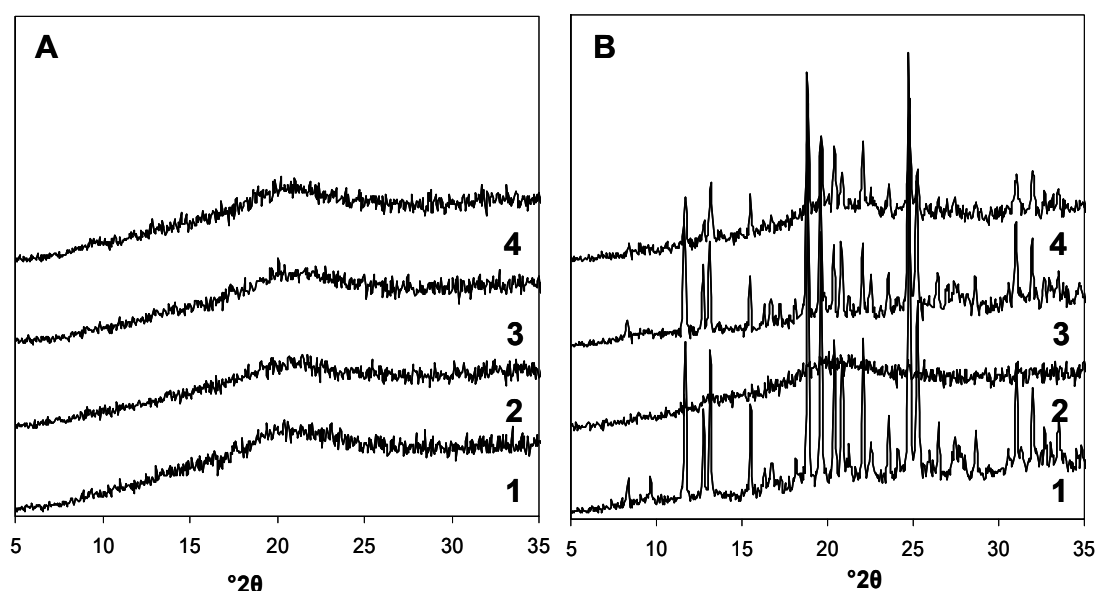


Figure 8.12: X-ray diffraction patterns of samples stored for 15 weeks at 2-8 °C (A) and 40 °C (B).
1: non-collapsed pH 5.5, 2: collapsed pH 5.5, 3: non-collapsed pH 3.5, 4: collapsed pH 3.5.

Samples stored at 40 °C crystallized as well, but the rate of crystallization was slower than at 50 °C. Figure 8.12 B shows the XRD patterns of lyophilizates stored at 40 °C for 15 weeks. Clearly, initially collapsed samples showed less intensive diffractions as samples collapsed during storage. Initially collapsed lyophilizates formulated at pH 5.5 even remained completely X-ray amorphous. Thus samples stored at 40 °C further confirmed the observed trend, namely, that samples formulated at pH 3.5 crystallized faster than samples formulated at pH 5.5 and samples that collapsed during storage crystallized faster than samples that collapsed during freeze-drying. All samples stored at 2-8 °C remained amorphous throughout the period of investigation (Figure 8.12 A).

SUCROSE-HYDROLYSIS

Regarding the XRD patterns in Figure 8.10 and Figure 8.11, another alteration besides the crystallization stands out. Comparing the sample peak patterns with the diffraction pattern of crystalline glucose (trace 6 in all Figures) and fructose (data not shown), the gradual formation of glucose and fructose is noticeable from the appearance of characteristic peaks at 17.2, 26.6, 28.6 and 30.8 °2 θ (grey shaded areas in Figure 8.10 and Figure 8.11).

This observation is further confirmed by the detection of characteristic melting endotherms of glucose and fructose in the DSC thermograms (Figure 8.13 and Figure 8.14). Figure 8.13 shows DSC thermograms of samples stored for 2 weeks at 50 °C, thus after the occurrence of collapse during storage. Clearly, two different melting endotherms can be observed. Samples formulated at pH 5.5 show a melting endotherm at 165 °C that can be attributed to the melting of crystalline sucrose (160 – 186 °C^{51,52}). Samples formulated at pH 3.5 in contrast show a reduced melting endotherm at 153 °C that can be attributed to the melting of glucose (150 °C⁵³). Additionally, they show a second weak melting endotherm at 120 °C that can be attributed to fructose (120 °C⁵⁴). Thus in samples formulated at a more acidic pH, sucrose was hydrolyzed and the corresponding monosaccharides glucose and fructose were formed. From the melting enthalpy of the corresponding peak the amount of monosugar present can be estimated. Melting enthalpies of glucose and fructose are slightly higher in lyophilizates that collapsed during storage, indicating an increased sucrose-inversion. In addition, X-ray diffractions assigned to glucose and fructose were more pronounced in cakes that collapsed during storage (Figure 8.10).

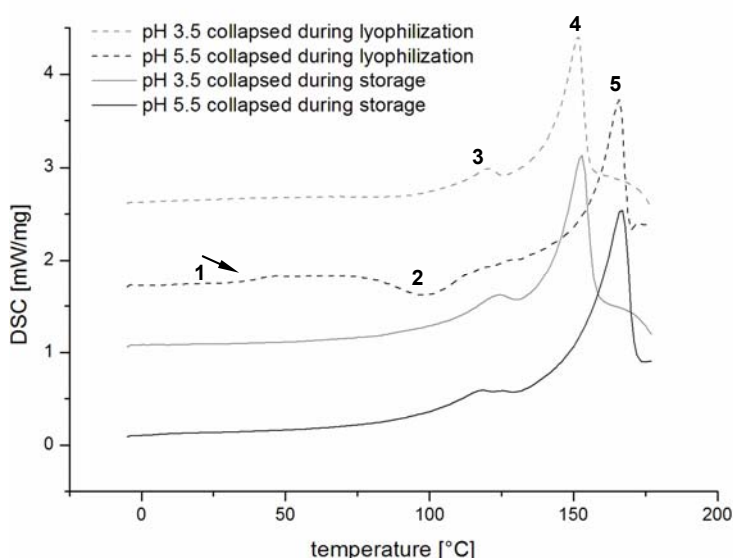


Figure 8.13: DSC thermograms of sucrose-based lyophilizates after 2 weeks of storage at 50°C.

1: sucrose glass transition, 2: sucrose crystallization, 3: fructose melting, 4: glucose melting, 5: sucrose melting

Samples formulated at pH 5.5 eventually hydrolyzed as well, but the extent of inversion was low. Regarding the X-ray diffraction patterns only peaks around 26.6 °2 θ and 28.6 °2 θ were detectable. These peaks however, are difficult to clearly be assigned to glucose in a sucrose-

containing system because they are in close vicinity to sucrose-diffractions. The most detached and thus significant peak at $17.2^\circ 2\theta$ is not observed in any of the samples. In addition no explicit glucose melting endotherm was observed in DSC thermograms (Figure 8.14 A and Figure 8.14 B). However, as the melting endotherms of glucose and sucrose were close to each other, the melting endotherm of small amounts of glucose might be hidden in the larger melting endotherm of sucrose.

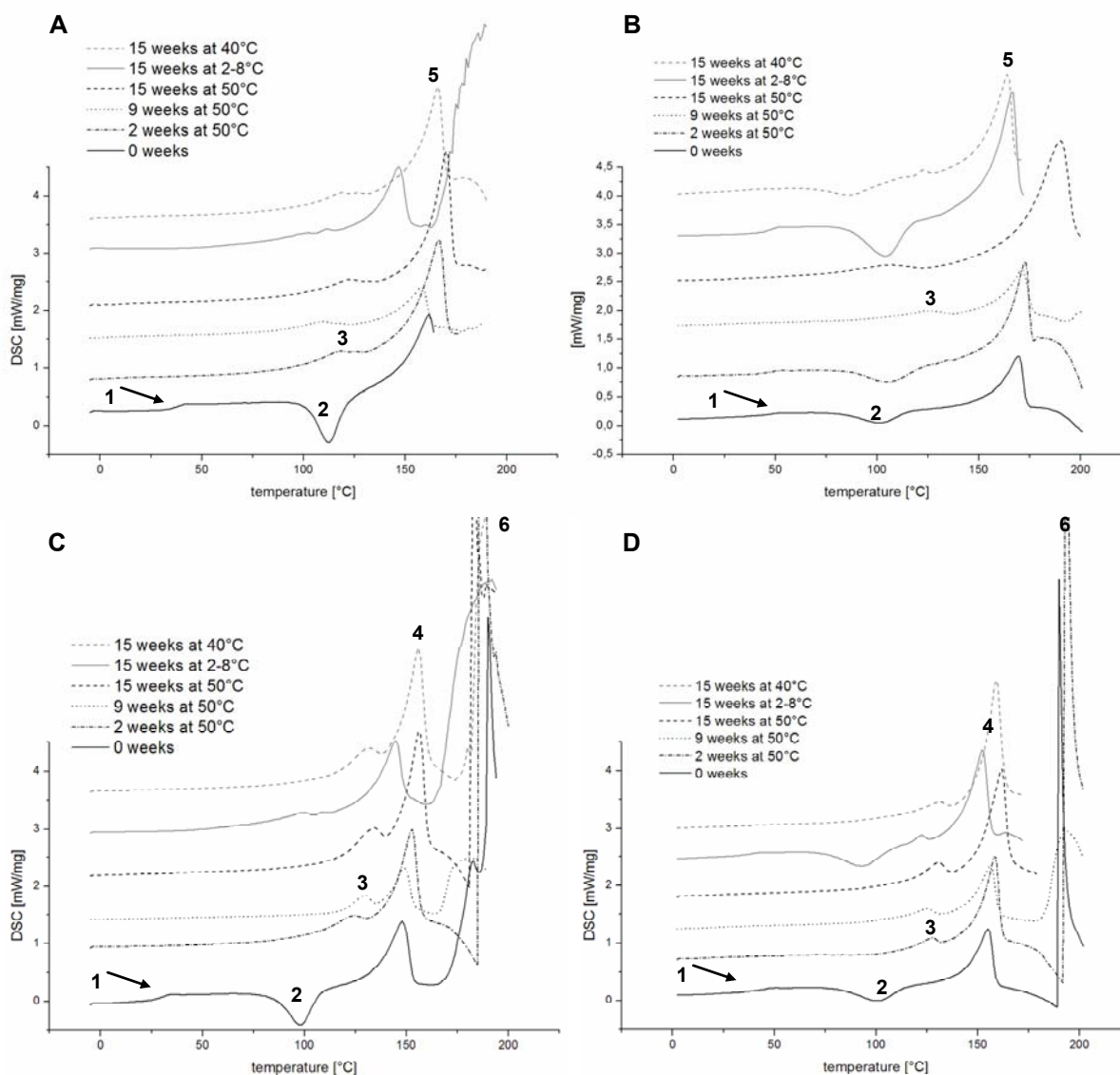


Figure 8.14: DSC thermograms of sucrose-based lyophilizates formulated at pH 5.5 that are initially non-collapsed (A) and initially collapsed (B) and of lyophilizates formulated at pH 3.5 that are initially non-collapsed (C) and initially collapsed (D) after different periods of storage.

1: sucrose glass transition, 2: sucrose crystallization, 3: fructose melting, 4: glucose melting, 5: sucrose melting, 6: thermal decomposition.

The origin of the broad peak around 115°C however is unclear. It may be attributed to the formation of fructose, further confirming the minor hydrolysis in pH 5.5 – samples, but it may as well be caused by water loss or breaking of hydrogen bonds prior to melting as suggested by Reynhardt⁵⁵.

Despite the ambiguousness of hydrolysis at pH 5.5, the trend that cakes that collapsed during storage decomposed earlier, was observed again.

Regarding DSC data, the observed melting endotherms are generally low as compared to reported melting points. Although melting endotherms of disaccharides are melting ranges rather than melting points, the observed temperatures of fusion are located at the lower end of that range (160-192 °C for sucrose, 146-165 °C for glucose, 102-132 °C for fructose⁵¹). As the melting endotherms of sugars are sensitive to water, impurities and crystallinity⁵¹, these rather low temperatures might be due to the fact that the investigated lyophilized systems are mixtures rather than pure saccharides. The fact that crystallization was not complete might contribute to the deviating melting temperatures as well. Decomposition occurring concomitantly with melting was also reported to affect the melting temperature of sugars⁵¹. As thermal decomposition was observed to start at around 180 °C (thermal event 6 in Figure 8.14 C and Figure 8.14 D), this might also affect the melting temperature of sucrose.

Sucrose hydrolysis is an acid-catalyzed cleavage reaction that starts with the protonation of the oxygen forming the disaccharide-bond followed by the cleavage of that bond and the formation of glucose and fructose. Sucrose is especially prone to hydrolysis, because the bond-energy of its disaccharide-bond is comparatively high (> 115 kJ/mol²⁴) as compared to trehalose for example (< 4 kJ/mol²⁴). The generated mono-saccharides glucose and fructose are so-called reducing sugars that can react with amino-groups in proteins in a reaction called Maillard-reaction causing severe instabilities that will be discussed in the following section.

The hydrolysis of sucrose during freezing and freeze-drying and during subsequent storage in the dried state in the presence of acidic compounds has been described by various researchers. Lund et al. observed a constant inversion-rate during freezing due to the concentration of hydrogen ions during freeze-concentration⁵⁶. Degradation of sucrose was also observed during freeze-drying starting at the end of primary drying and the reaction rate was reported to increase with decreasing water content (as the reaction is a condensation with water formed as one of the products) and with decreasing pH (as hydrogen ions catalyze the reaction)⁵⁷. During storage in the lyophilized state, the initial concentration of hydrogen ions, i.e. the initial pH prior to lyophilization was found to be the key factor controlling the sucrose hydrolysis rate⁵⁸⁻⁶⁰. Other authors however pointed out the importance of the solid-state acidity rather than the initial solution pH^{61,62}. The maximum extent of the reaction was argued to be limited by the amount of acid present⁵⁹. Water activity also had an effect on the reaction rate most probably through its effect on pH⁵⁸ and through the stabilization of the protonated monosugars formed during hydrolysis⁵⁹. The glass transition temperature and the term $T-T_g$ in contrast did not significantly affect the rate of reaction^{58,59} nor did the molecular mobility determined by isothermal microcalorimetry⁶².

To sum up findings regarding the hydrolysis of sucrose, inversion was observed in lyophilizates during storage at elevated temperatures. The extent of degradation correlated with the initial pH of the lyophilized solution, i.e. samples formulated at pH 3.5 showed a higher degree of hydrolysis than samples formulated at pH 5.5. Interestingly, samples that collapsed during storage showed accelerated degradation compared to samples that were initially collapsed. It is reported that the inversion of sucrose can be related to collapse phenomena observed during storage at elevated temperatures⁵⁹. Because the first time point in this investigation was after two weeks of storage as commonly performed during storage stability studies of lyophilizates, the onset of collapse during storage and the inversion of sucrose were conjointly detected, thus a clear assignment of cause and effect cannot be exerted at this point. A detailed investigation dealing with that topic will be discussed at the end of this section.

NON-ENZYMATIC BROWNING/ MAILLARD-REACTION

The observed sucrose-hydrolysis is of special relevance because the formed glucose and fructose can react with proteins to form covalent modifications. The formation of adducts of glucose and amino groups in the side chain of proteins via the so-called Maillard reaction, i.e. a condensation of the aldehyde group of the reducing sugar and the primary amino groups of proteins are described both in the liquid state⁶³ and in the lyophilized state^{64,65}. In addition, increased serine cleavage was observed in human relaxin via a cyclic intermediate in the presence of glucose⁶⁴. Glycated proteins have been related to severe diseases such as diabetes or vascular diseases and glycation might have implications on the stability, safety and efficacy of therapeutic proteins as well⁶³.

The Maillard reaction, also termed glycation or nonenzymatic browning is divided into several stages. In the first stage a Schiff's base is formed that then is transformed into a ketoamine termed Amadori compound. The reaction then proceeds via fluorescent intermediate products to eventually form colored melanoidins⁶⁶. The progression of the reaction can be monitored by a variety of analytical techniques, such as mass spectrometry⁶⁷, boronate affinity chromatography⁶³, fluorescence spectroscopy⁶⁸ or spectrophotometrically at 280 nm and 420 nm. But first of all, the detection of gradual browning during storage is a first indication of the occurrence of Maillard reaction.

Because the exact chemical characterization of the glycated protein was out of the scope of the present investigation, the occurrence of browning was regarded as indicative for the formation of Maillard adducts and the extent of discoloration was assessed by visual inspection. Figure 8.15 shows lyophilizates stored for 15 weeks at different temperatures. Distinctly, a brown discoloration is observed in lyophilizates formulated at pH 3.5 (Figure 8.15 C and D). Interestingly, samples that collapsed during storage turned brownish after storage at 40 °C and 50 °C, whereas the same formulation but initially collapsed during

drying showed a discoloration just after storage at 50 °C. This is further reflected in the observed yellowish color of the lyophilizate formulated at pH 5.5 stored at 50 °C that collapsed during storage whereas the corresponding initially collapsed cake remains unchanged.



Figure 8.15: Lyophilizates stored for 15 weeks at elevated temperatures.

sucrose pH 5.5 initially non-collapsed (A) and initially collapsed (B), sucrose pH 3.5 initially non-collapsed (C) and initially collapsed (D) stored at 2-8 °C (leftmost vial in each sub-Figure), 40 °C (middle vial in each sub-Figure) and 50 °C (rightmost vial in every sub-Figure).

Table 8.7 summarizes the first detection of browning in the lyophilizates. Cakes that collapsed during storage clearly showed an earlier incidence of brown discoloration as compared to cakes that collapsed during processing. This is in good agreement with the different extents and rates of sucrose hydrolysis observed earlier by DSC and XRD.

Table 8.7: Occurrence of browning in lyophilizates stored at different temperatures as determined by visual inspection.

appearance	pH	browning	browning	browning
		stored at 2-8°C	stored at 40°C	stored at 50°C
collapsed during storage	3.5 -		after 4 weeks	after 2 weeks
collapsed during lyophilization	-		-	after 6 weeks
collapsed during storage	5.5 -		after 6 weeks	after 6 weeks
collapsed during lyophilization	-		-	-

The observed accelerated browning at 50 °C as compared to 40 °C is in good agreement with the reported temperature dependence following Arrhenius kinetics that can be modeled using the WLF equation⁶⁹. The degradation following WLF kinetics indicates the importance of the glass transition for the Maillard reaction kinetics. Being a diffusion controlled reaction, the decrease in viscosity above the glass transition greatly accelerates the reaction⁷⁰.

Besides this effect, the occurrence of collapse and crystallization⁷¹ frequently encountered above the glass transition greatly accelerates the reaction.

As it was shown that collapse-dried systems exhibit greatly increased structural relaxation times as compared to non-collapsed systems, this might explain the different extents of brown pigment formation in the initially collapsed cakes. However, Hill et al. investigated the effect of different thermal histories on the rate of nonenzymatic browning, but they found, that differences in glassy dynamics rapidly diminished upon storage and reaction rates were not relevant different for most of the products studied⁷². Interestingly though, the rate of glucose consumption was decreased about 20 % in aged samples. The glucose consumption in differently collapsed systems will be discussed at the end of that section.

A decreased porosity was also related to a decreased rate of glucose consumption^{73,74}, offering a further explanation for the better performance of collapse-dried systems as they have been shown to have a greatly decreased porosity (Chapter 5). In contrast, Buera et al. reported an increase in nonenzymatic browning rate due to shrinkage, presumably because of a minimization of diffusion paths of the reactants^{58,75}. Thus most probably, there can be different effects of collapse on the rate of nonenzymatic browning (NEB): slow-down of the reaction due to a decrease in porosity on the one hand and an acceleration of the reaction due to a converging of reacting species on the other hand. This might well explain the different behavior of samples that collapsed during freeze-drying and during storage. Initially collapsed samples show a greatly reduced porosity that significantly slows down the browning rate. Samples collapsed during storage on the other hand have a higher porosity but still the reactive species are kept close together, thus the effects that increase the reaction rate prevail. In addition, the increased degree of crystallinity that is known to accelerate browning rates as well, further boosts the nonenzymatic browning rates in lyophilizates collapsed during storage.

Water content also plays a vital role: There is a residual moisture content at which the reaction rate reaches a maximum. Below this water content, reaction rates increase due to the plasticizing effect of water on the diffusion-controlled reaction. Above a certain water content, the reaction is slowed down, most probably due to the fact, that water is a reaction product of the condensation reaction, thus moving the equilibrium to the educt side^{70,76}. Although the average water contents of initially collapsed and initially non-collapsed samples were not relevantly different, crystallization might have increased the residual moisture of the remaining amorphous phase thus further increasing browning rates.

Summarizing the physicochemical stability of initially collapsed and initially non-collapsed sucrose-based lyophilizates, most importantly, the initially non-collapsed samples collapsed during storage at 40 °C and 50 °C. Thereby the scope of the investigation was shifted from comparing collapsed and non-collapsed lyophilizates to comparing two different appearances

of collapse. Although samples had comparable residual moisture levels and glass transition temperatures, physicochemical properties were quite different. Sucrose crystallized during storage and the rate and the extent of crystallization were greatly increased in systems that collapsed during storage. These samples were completely crystalline after 2 weeks of storage at 50°C whereas samples that initially collapsed during processing remained at least partially amorphous throughout the period of investigation (15 weeks) (pH 5.5) and until the 9th weeks of storage (pH 3.5), respectively.

In addition to the observed physical instability, chemical degradation occurred as well. Sucrose was hydrolyzed and the reducing sugars glucose and fructose were formed. This reaction was more pronounced in the lyophilizates formulated at pH 3.5, because the degradation is acid-catalyzed. Again, also in the samples at pH 3.5, when collapsed during storage they showed an increased instability and inversion rates were greatly augmented.

The formed monosaccharides reacted in the Maillard reaction with the incorporated antibody leading to glycation of the protein (as will be discussed later) and formation of brown pigments that are noticed by the brown discoloration of the lyophilizates. The rate of browning was again greatly increased in lyophilizates collapsed during storage.

Thus systems, that collapsed during storage at elevated temperatures were both physically and chemically less stable than lyophilizates that were intentionally collapsed during freeze-drying. Furthermore the preservation of the incorporated antibody was greatly reduced as well, because the Maillard reaction between the degraded excipient and the active ingredient proceeded more rapid. The effect of the sucrose degradation, namely the protein stability in both collapsed systems during storage will be discussed in detail in the following section.

2.2.2 PHYSICAL PROTEIN STABILITY OF IgG₀₁ IN RECONSTITUTED LYOPHILIZATES

As in the investigation of the effect of collapse immediately after freeze-drying (Chapter 7), the stability of the freeze-dried, reconstituted antibody was analyzed regarding the physical stability, i.e. the formation of soluble and insoluble aggregates and particles.

Figure 8.16 displays the amount of remaining soluble IgG₀₁ monomer during storage at 40 °C and 50 °C, respectively, as determined by HP-SEC. In the Figure, lyophilizates that collapsed during storage are represented by open symbols and cakes that collapsed during drying are represented by closed symbols. Most noticeably, a distinct decrease in monomer content is observed for the two systems that underwent collapse during storage at elevated temperatures. Protein stability in the initially collapsed lyophilizates formulated at pH 3.5 was greatly reduced throughout the storage period as well (Figure 8.16 A).

Monomer contents in the lower pH-samples decreased to almost zero after two weeks and 6 weeks of storage at 50 °C in storage-collapsed and drying-collapsed samples, respectively. This was accompanied by a tremendous decrease of recovery to almost zero as well, indicating the formation of insoluble aggregates. The detection of insoluble aggregates

coincided with the appearance of distinct browning, thus presumably, the occurrence of Maillard reaction strongly affected protein stability resulting in severe aggregation.

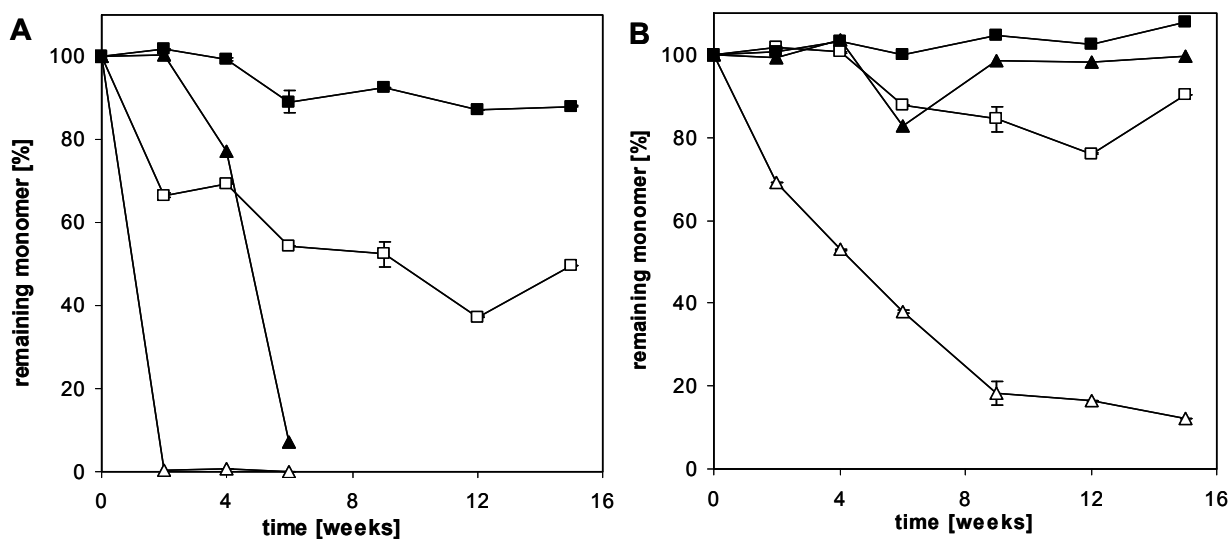


Figure 8.16: Decrease in IgG₀₁ soluble monomer content during storage of lyophilizates at 50 °C (A) and 40 °C (B) for up to 15 weeks determined by HP-SEC of reconstituted lyophilizates as compared to the monomer content immediately after lyophilization (average \pm SD, n = 2).

Initially non-collapsed sucrose-based lyophilizates pH 5.5 (open square) and pH 3.5 (open triangle) and initially collapsed sucrose-based lyophilizates pH 5.5 (closed squares) and pH 3.5 (closed triangles).

Crystallization could be ruled out as responsible factor for the remarkable instability in the pH 3.5 samples, because storage-collapsed lyophilizates formulated at pH 5.5 that showed the same degree of crystallinity (100%) as the cakes formulated at pH 3.5, did not exhibit such a strong decrease in monomer content. However, the gradual decrease of antibody monomer in these samples indicated a nevertheless negative impact of crystallization on physical protein stability that is thoroughly reported in literature⁷⁷⁻⁷⁹. Interestingly there was no sharp decrease in protein recovery with the onset of visual browning after 6 weeks of storage in these samples as observed in the pH 3.5 samples. The lower intensity of the brown color formation indicated that the extent of Maillard reaction was not as pronounced as in pH 3.5 samples (see Table 8.7). The remaining monomer content after 15 weeks of storage at 50 °C was 49.7 ± 0.1 % in pH 5.5 lyophilizates collapsed during storage. In contrast, preservation of antibody monomer was distinctly higher in pH 5.5 cakes that were intentionally collapsed by collapse-drying. Monomer contents after the same period of storage were 87.9 ± 0.2 %. Stability of samples stored at 40 °C further confirmed results gained so far and pointed out the importance of nonenzymatic browning as stability-compromising. Antibody stability was well preserved in lyophilizates that were initially collapsed, regardless of the pH. Lyophilizates that collapsed during subsequent storage showed a gradual decrease of monomer contents during storage that was more pronounced at a lower pH. This is consistent with the observation of discoloration – there was no browning observed in initially collapsed samples whereas samples collapsed during storage turned brown after four and six weeks, respectively.

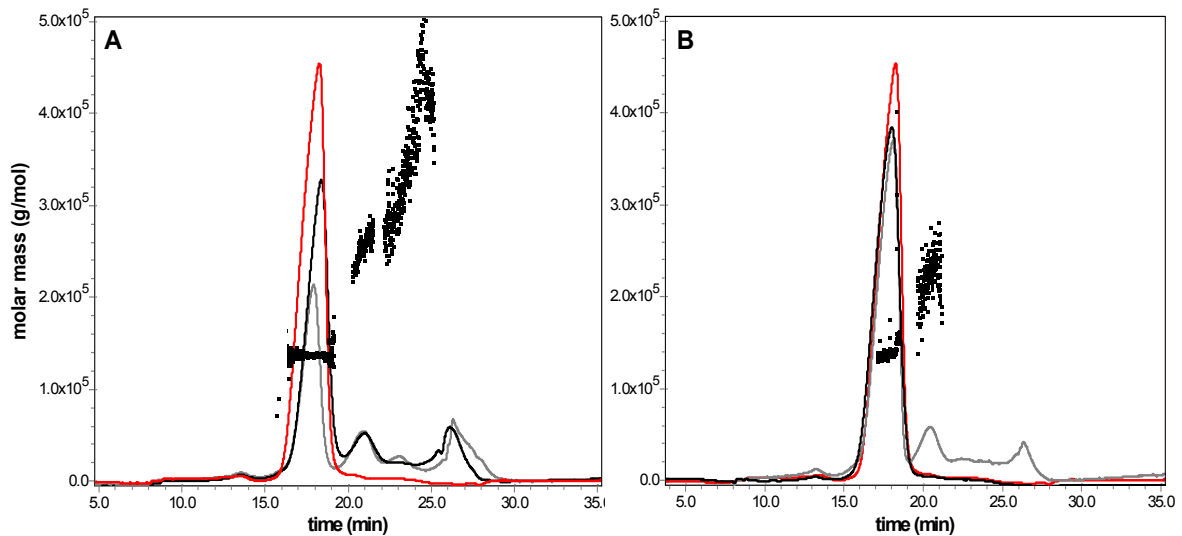


Figure 8.17: AF4 fractograms of 10 µg IgG₀₁ reconstituted from initially non-collapsed (A) and collapsed (B) lyophilizates either immediately after freeze-drying (red curve) or after 2 (black curves) and 15 (grey curves) weeks of storage at 50 °C, respectively.

Initially non-collapsed lyophilizates collapsed during storage at 50 °C.

Molecular weight of IgG₀₁ monomer, dimer and higher molecular weight aggregates as determined by static light scattering are depicted as back dots. Concentration was determined from the UV-absorption depicted as lines.

Samples stored refrigerated at 4 °C remained stable throughout the whole storage period and did not relevantly change. Monomer contents were approximately 100 % for all the formulations and the soluble aggregate content ranged between 0.70 and 0.82 % after 15 weeks of storage.

To further characterize the aggregated species that cannot be assessed by HP-SEC, as indicated by the drop in recovery in HPLC-experiments, analysis by asymmetric flow field flow fractionation (AF4) was carried out in parallel. Figure 8.17 depicts AF4 fractograms of samples formulated at pH 5.5 that collapsed either during storage (A) or during lyophilization (B). Clearly the formation of dimers and higher molecular weight species can be detected, eluting after the IgG monomer peak. Samples that collapsed during storage exhibited significant amounts of aggregated species after two weeks of storage that is also the onset of collapse, whereas samples that were initially collapsed were composed of mostly monomer, further illustrating the different states of degradation in the differently collapsed samples.

Figure 8.18 depicts fractograms of samples formulated at pH 3.5 that collapsed either during freeze-drying or during subsequent storage at 50 °C. Immediately after freeze-drying, the antibody was well stabilized in both systems and only monomeric species were present (red curves in Figure 8.18). However, with the onset of collapse during storage, the amount of monomer was greatly reduced (black curve in Figure 8.18 A), and significant amounts of dimer and higher molecular weight species up to molecular weights of 10⁸ kDa were detected. The tremendous drop in monomer content coincides with the detection of browning. Storage in the collapsed state led to further degradation.

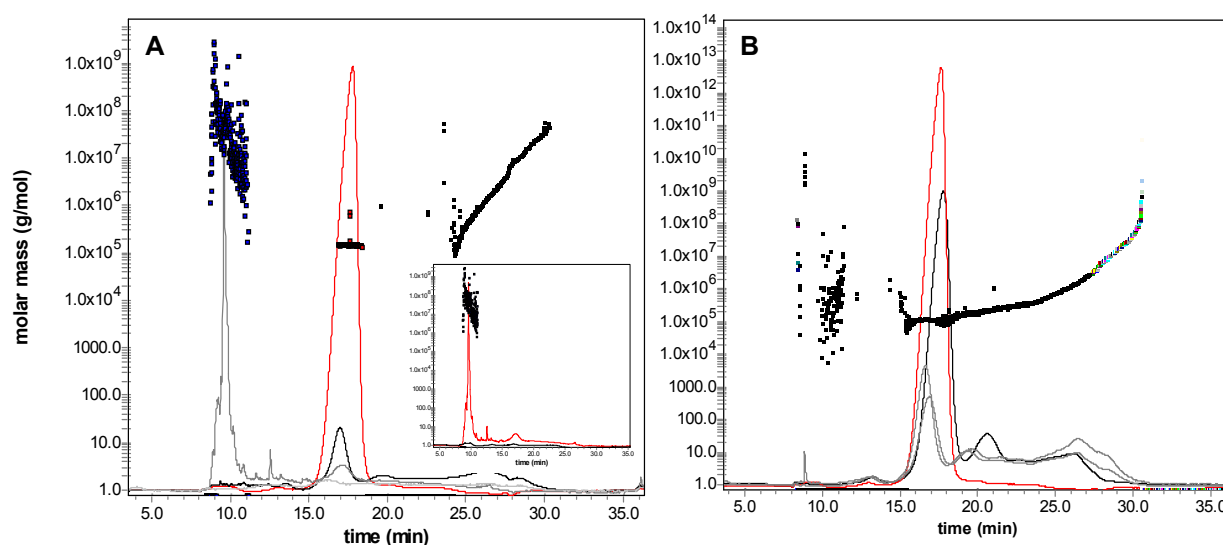


Figure 8.18: AF4 fractograms of 10 μg IgG₀₁ reconstituted from pH 3.5 sucrose-based lyophilizates collapsed during storage after storage for 0 (red line), 2 (black line), 4 (dark grey line) and 15 (light grey line) weeks at 50 °C (A); comparison of filtrated (black line) and not filtrated (red line) sample after 4 weeks of storage at 50 °C to illustrate the presence of insoluble aggregates (insert in Figure part A); AF4 fractograms of 10 μg IgG₀₁ reconstituted from pH 3.5 sucrose-based lyophilizates collapsed during freeze-drying after storage for 0 (red line), 4 (black line), 6 (dark grey line) and 15 (light grey line) weeks at 50 °C (B).

After 4 weeks of storage the major part of the sample is composed of high molecular weight aggregates that are too large to be retarded by the system's cross flow. These aggregates elute in the steric hyperlayer mode in the void peak (dark grey line in Figure 8.18 A). A comparison between an unfiltered sample (red line in insert in Figure 8.18 A) and one that has been filtrated through a 0.2 μm syringe filter (black line insert in Figure 8.18 A) shows that only insoluble aggregates are present in the sample, because after filtration no relevant amounts of protein can be detected. In contrast, systems that collapsed during lyophilization show significant amounts of monomer after 4 weeks of storage at 50 °C (black line Figure 8.18 B), although dimers and hmw aggregates are present as well. The occurrence of browning after 6 weeks of storage is accompanied by a distinct decrease in monomer content (dark grey curve in Figure 8.18 B).

Comparing the sample composition of the two collapsed systems after 15 weeks of storage, there is still a relevant amount of monomer detectable in samples that were intentionally collapsed during freeze-drying whereas there is no more monomer detectable in system's that collapsed during storage.

These findings are further summarized in Figure 8.19 that shows the course of monomer and hmw aggregate species in lyophilizates formulated at pH 3.5 during storage at elevated temperatures. Clearly, the degradation of monomer and the formation of hmw aggregates are more accelerated in systems that collapsed during storage (full circles in Figure 8.19) at elevated temperatures than in systems that were intentionally collapsed during drying (open circles in Figure 8.19). A distinct drop in monomer content was observed to occur

concomitantly with the onset of visual browning after 2 and 6 weeks, respectively in both systems. After 15 weeks of storage the system that collapsed during storage was too degraded to allow for reliable quantification of mAb-monomer and aggregated species, whereas in systems collapsed during drying 29 % mAb-monomer remained in solution.

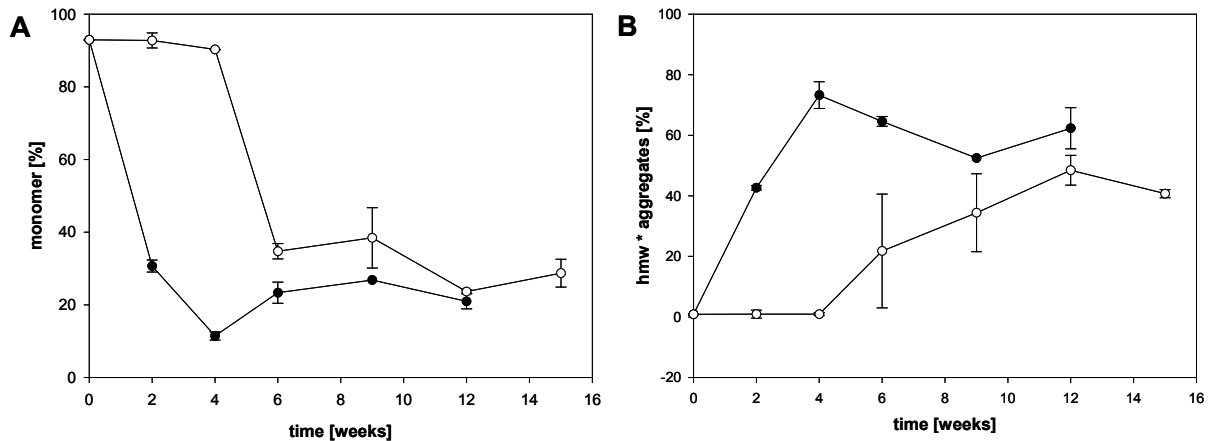


Figure 8.19: Decrease of IgG₀₁ monomer content and increase of high molecular weight aggregates content in initially non-collapsed (full circles) and initially collapsed (open circles) pH 3.5-sucrose-based lyophilizates as determined by AF4 during storage at 50 °C for up to 15 weeks (average \pm SD, n = 2).

* hmw aggregates = high molecular weight aggregates

Physical protein stability, namely the formation of insoluble aggregates and particles was further analyzed using the light obscuration technique that quantifies particles in the size range from 1 μ m to 200 μ m.

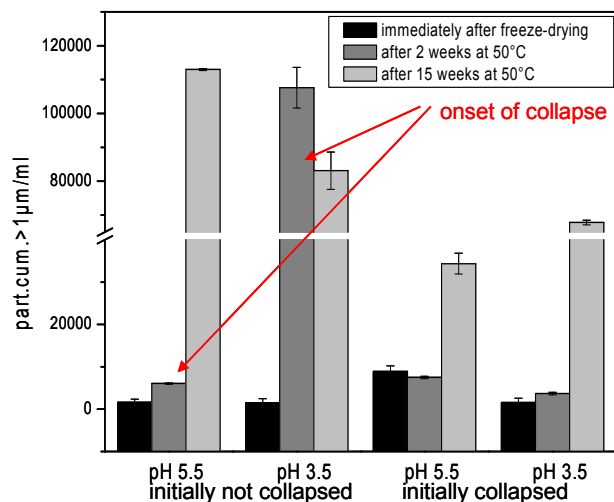


Figure 8.20: Subvisible particles $\geq 1 \mu$ m in IgG₀₁-samples (4 mg/mL) reconstituted from initially non-collapsed and collapsed sucrose-based lyophilizates analyzed either immediately after freeze-drying or after 2 and 15 weeks of storage at 50 °C, respectively (average \pm SD, n = 2).

Samples that were initially non-collapsed collapsed during storage at 50 °C.

Figure 8.20 displays the number of sub-visible particles larger than 1 μ m after freeze-drying and during storage. After freeze-drying particle numbers were low, confirming results obtained from HP-SEC and AF4 that protein stability was maintained during processing. After two weeks of storage, i.e. upon the occurrence of collapse in the initially non-collapsed

samples, particle numbers in pH 3.5 samples were greatly increased, indicating the formation of insoluble aggregates that were also observed in AF4 experiments. In contrast, storage in already collapsed lyophilizates did not have an effect on the particle numbers after the same period of storage.

Interestingly, the onset of collapse in samples formulated at pH 5.5 did not seem to have a severe effect on IgG stability in terms of particle formation; however, after 15 weeks of storage, particle numbers were greatly increased as well. Analyzing dynamic light scattering (DLS) data which can be regarded as a most sensitive tool for the detection of trace amounts of aggregated species, the formation of species besides the antibody monomer becomes noticeable after the occurrence of collapse after two weeks of storage: Figure 8.21 A compares the DLS intensity size distribution of pH 5.5 samples after lyophilization (black symbols) and after the onset of collapse after two weeks of storage at 50 °C (grey symbols). Clearly, a deformation of the monomer peak and the formation of additional larger species can be seen. In contrast there were only minor alterations in the size distributions of collapse-dried samples after two weeks of storage (Figure 8.21 B). Thus DLS results indicate the formation of small amounts of aggregated species with the occurrence of collapse after 2 weeks of storage and can be regarded as predictive for the strong particle formation observed during subsequent storage and for the increased aggregation rate of storage-collapsed lyophilizates as compared to initially collapsed samples.

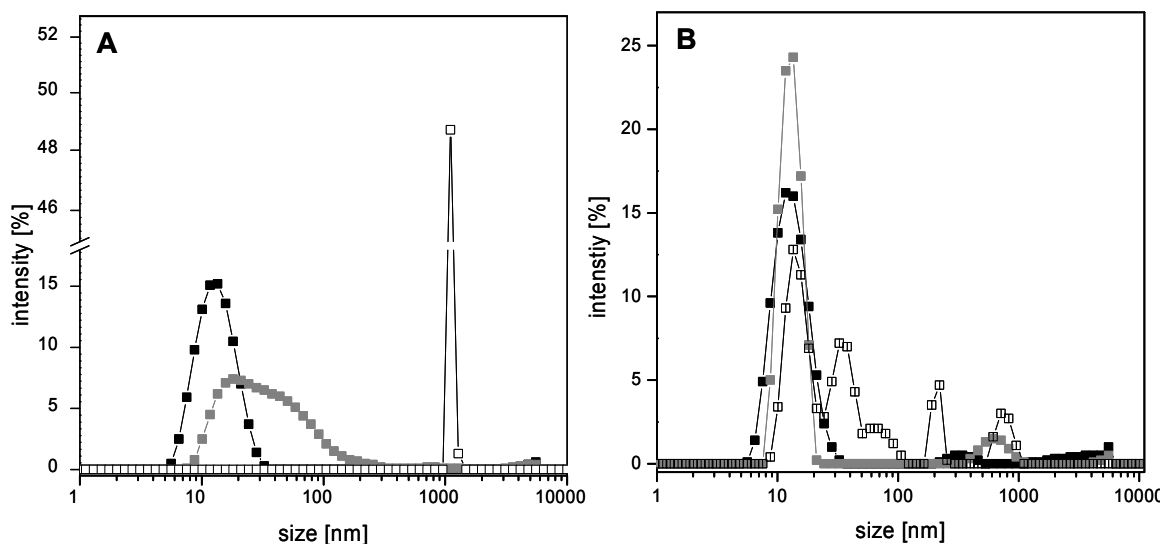


Figure 8.21: DLS size distribution by intensity of 4 mg/mL IgG₀₁ reconstituted from initially non-collapsed (A) and initially collapsed (B) lyophilizates immediately after freeze-drying (black squares) and after 2 (grey squares) and 15 (open squares) weeks of storage at 50 °C, respectively.

Curves are calculated average values from two measurements. The size distribution was obtained by fitting a NNLS algorithm to the correlation function.

Samples are formulated in sucrose at a pH of 5.5.

Collapse in initially non-collapsed lyophilizates occurred after 2 weeks of storage, thus the grey and the open squares in Figure A actually represent IgG₀₁ reconstituted from lyophilizates that underwent collapse during storage.

However, the observed change was not very distinct and it was not observed in the more relevant volume distribution.

Samples that were stored at 40 °C and underwent collapse during 2 weeks of storage as well did not show a dramatic increase in particle numbers immediately with the onset of collapse, i.e. after two weeks. Furthermore, there were no changes detected in the DLS size distributions after 2 weeks, as additionally indicated by the low polydispersity indices (0.18 and 0.16 for initially non-collapsed and collapsed samples formulated at pH 5.5 and 0.15 and 0.18 for samples formulated at pH 3.5, respectively). This might point out, that the mere occurrence of collapse itself was not instantly detrimental for protein stability. Storage conditions at 40 °C were not harsh enough to allow for an immediate discrimination between initially collapsed and non-collapsed lyophilizates. However, particle numbers increased during subsequent storage and storage-collapsed cakes became clearly distinguishable from process-collapsed cakes (Table 8.8).

Interestingly, alterations in the DLS size distribution were detected at the same time, a brown discoloration could be noticed, i.e. after four weeks for the pH 3.5 samples (PDI 0.4) and after 6 weeks for the pH 5.5 samples (PDI 0.2) stored at 40 °C. Thus the occurrence of the Maillard reaction seemed to strongly compromise protein stability. This theory was further confirmed by the first detection of aggregated species in initially collapsed pH 3.5 samples after 6 weeks of storage when stored at 50 °C (PDI 0.46) concomitantly with the detection of browning.

However, samples that showed no discoloration eventually exhibited alterations in the DLS size distribution, indicating that the glycation was not the only degradation pathway during storage.

During continuing storage, particle numbers further increased. Figure 8.20 depicts particle numbers after 15 weeks of storage and Table 8.8 summarizes data concerning particulate matter of samples stored for 15 weeks at various temperatures. Lyophilizates that collapsed during storage at 50 °C showed strongly increased particle numbers as compared to the same formulation that was initially collapsed during processing. This difference was especially pronounced regarding large particles $\geq 10 \mu\text{m}$ and $\geq 25 \mu\text{m}$. This was further illustrated by a dramatic increase of the Z-average and the polydispersity index and the turbidity of the reconstituted solutions. Most obviously, samples formulated at pH 3.5 exhibited higher particle numbers and higher turbidities, being in good agreement with the degree of sucrose inversion and the extent of nonenzymatic browning.

Table 8.8: particulate matter in initially non-collapsed and initially collapsed lyophilizates stored at various temperatures for 15 weeks.

pH	appearance	storage temperature [°C]	particles > 1 µm/mL ^{a)}	particles > 10 µm/mL ^{a)}	particles > 25 µm/mL ^{a)}	turbidity [FNU] ^{b)}	Z average [nm] ^{c)}	PDI ^{c)}
5.5	non-collapsed	2-8	475 ± 81	23 ± 3	2 ± 1	1.4 ± 0.1	11.90	0.11
	collapsed during storage	40	15750 ± 150	15 ± 3	2 ± 1	2.7 ± 0.1	19.15	0.35
	collapsed during storage	50	112974 ± 264	89238 ± 842	45578 ± 2120	1300 ± 00	1.98E+07	0.41
	collapsed	2-8	1004 ± 270	8 ± 3	3 ± 4	2.5 ± 0.1	11.20	0.11
	collapsed	40	1089 ± 36	78 ± 12	30 ± 11	1.5 ± 0.1	11.80	0.12
	collapsed	50	34375 ± 2446	211 ± 19	25 ± 11	6.9 ± 0.7	137.3	0.302
3.5	non-collapsed	2-8	246 ± 5	13 ± 3	8 ± 3	1.4 ± 0.3	11.10	0.12
	collapsed during storage	40	35409 ± 4293	203 ± 27	69 ± 6	39.6 ± 0.7	99.30	0.47
	collapsed during storage	50	83132 ± 5508	5949 ± 661	1240 ± 382	187.8 ± 27.4	1.31E+07	0.82
	collapsed	2-8	9900 ± 801	41 ± 9	13 ± 5	1.6 ± 0.3	12.15	0.13
	collapsed	40	13029 ± 503	78 ± 31	7 ± 3	2.0 ± 0.1	19.15	0.35
	collapsed	50	67828 ± 668	1079 ± 12	156 ± 48	95.5 ± 9.6	159.4	0.562

a) determined by light obscuration

b) determined by nephelometric turbidity measurements

c) determined by dynamic light scattering using cumulants analysis

Lyophilizates stored at 40 °C further confirmed results obtained so far. Again, the lower pH-system was less stable and showed increased particle numbers and turbidities, with the cakes that collapsed during storage showing higher values than cakes that initially collapsed during freeze-drying. Systems formulated at pH 5.5 showed only moderately increased Z-averages, PDIs and particle numbers and turbidities were below 3 FNU. At 40 °C and pH 5.5, differences between those systems that collapsed during storage and those that collapsed during processing were subtle, but measurable. At 2-8 °C, where no collapse during storage occurred, even increased particle numbers were observed in collapsed lyophilizates, but turbidity values and DLS data showed no relevant difference between collapsed and non-collapsed cakes. This further highlights the importance of lyophilizate storage at controlled conditions well below the system's T_g . In contrast, collapse-dried systems are less sensitive towards storage at elevated temperatures.

Figure 8.22 exemplarily shows the course of turbidities during storage at 50 °C (A) and 40 °C (B) to illustrate the progression of particulate matter characteristics during storage at elevated temperatures. The development of experimental data assessed by DLS and light obscuration is well consistent with the turbidity course presented here and it is therefore omitted for the sake of clarity.

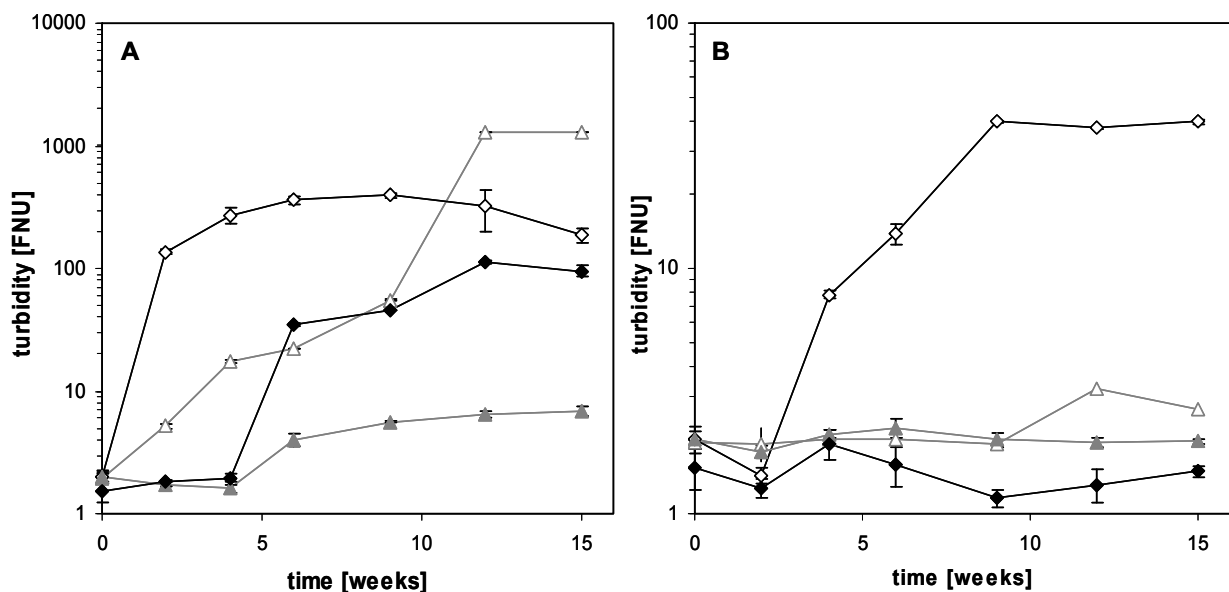


Figure 8.22: Turbidity during storage at 50 °C (A) and 40 °C (B) in samples that collapsed during storage (open symbols) and during freeze-drying (closed symbols) formulated at pH 3.5 (diamonds) and pH 5.5 (triangles); $n = 2$.

Figure 8.22 A clearly shows the rapid turbidity increase in samples that collapsed during storage (open symbols). Systems formulated at pH 3.5 showed higher absolute turbidity values with a more rapid increase than samples formulated at pH 5.5 being in good agreement with light obscuration and DLS data. The decrease in turbidity at the end of the investigated period might be caused by non-linearity of turbidities at very high absolute values as well as by the formation of large particles that were sedimented during analysis.

pH 3.5-samples that collapsed during freeze-drying showed increased turbidity values after 6 weeks of storage, thus again coinciding with the start of browning.

Samples that were stored at 40 °C are displayed in Figure 8.22 B and further confirmed the observed trend that samples formulated at pH 3.5 were less stable than samples formulated at pH 5.5 and that systems that collapsed during storage were less stable than samples that collapsed during lyophilization.

Samples stored at 2 – 8 °C exhibited low turbidities that did not exceed 2 FNU throughout the entire storage period (Table 8.8).

2.2.3 BINDING ACTIVITY OF IgG₀₁ IN RECONSTITUTED LYOPHILIZATES

An important property of protein pharmaceuticals is their biologic activity. The binding activity to a specific receptor of the mAb was assessed using surface plasmon resonance spectroscopy as an analytical technique to approach the biologic activity of protein pharmaceuticals. Figure 8.23 depicts binding activities of IgG₀₁ in reconstituted sucrose-based lyophilizates that are formulated at a pH of 5.5 after freeze-drying and after 15 weeks of storage at 40 °C and 50 °C, respectively.

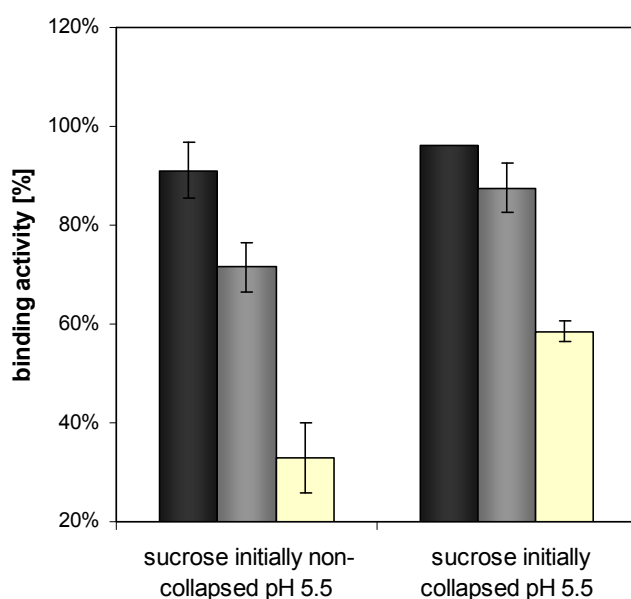


Figure 8.23: Binding activity of IgG₀₁ as determined by surface plasmon resonance spectroscopy (average +/- SD, n = 2).

Binding activity after lyophilization (black bars), after 15 weeks of storage at 40 °C (grey bars) and after 15 weeks of storage at 50 °C (white bars).

Immediately after freeze-drying, the binding activity of IgG₀₁ in collapsed and non-collapsed lyophilizates is not relevantly different. Upon storage at elevated temperatures, a pronounced decrease in binding activity is observed. In contrast to the comparable activity of the un-stored cakes, a significant difference in binding activity is clearly visible. Collapsed lyophilizates showed a better IgG₀₁ preservation at both 40 °C and 50 °C storage temperature. This further confirms findings from physical protein stability data and from excipient stability data as well.

Lyophilizates formulated at a decreased pH of 3.5 were too degraded to be analyzed after 15 weeks of storage and thus are not depicted here.

2.2.4 CONFORMATIONAL STABILITY OF IgG₀₁ IN RECONSTITUTED LYOPHILIZATES

In addition to assessing the physical protein stability of IgG₀₁ with a variety of analytical techniques, the conformational stability was included into the investigation as well using Fourier-Transform infrared transmission spectroscopy.

The prevalent secondary structure element in monoclonal antibodies of the IgG1 class is β -sheet structure^{80,81}. Figure 8.24 A shows second derivative FTIR transmission spectra of reconstituted IgG₀₁ lyophilizates after freeze-drying. The main band at 1639 cm⁻¹ can be assigned to intramolecular β -sheet structures and the band at 1686 cm⁻¹ can be assigned to β -sheet structures as well⁸²⁻⁸⁴. Obviously, the secondary structure is well preserved during both conventional freeze-drying and collapse-drying, as no difference to the IgG₀₁ bulk can be observed (red line).

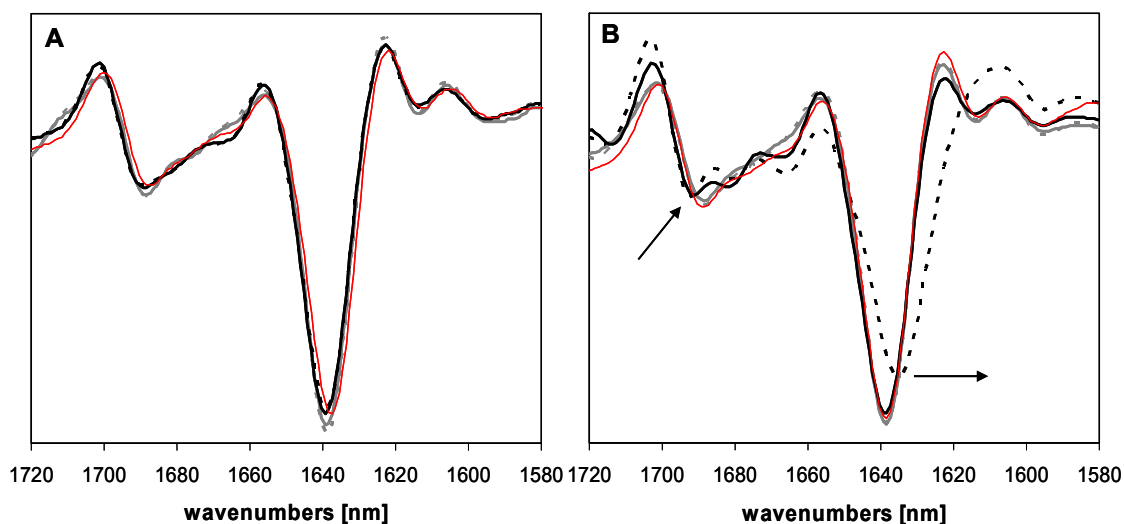


Figure 8.24: Area-normalized 2nd derivative FTIR transmission spectra of 4 mg/mL IgG₀₁ reconstituted from initially collapsed and initially non-collapsed lyophilizates immediately after freeze-drying (A) and after 2 weeks of storage at 50 °C, i.e. after the onset of collapse during storage (B).

IgG₀₁ standard (red line), IgG₀₁ in sucrose pH 5.5 (grey lines) and pH 3.5 (black lines) collapsed during freeze-drying (solid line) and during storage at elevated temperatures (dashed line).

Figure 8.24 B depicts the second derivative FTIR spectra after two weeks of storage at 50 °C, thus after the onset of collapse during storage. With the onset of collapse, distinct alterations in secondary structure can be observed in the pH 3.5-sample. The main band is shifted towards lower wave lengths (1635 cm⁻¹) and additional bands at 1692 cm⁻¹, 1679 cm⁻¹ and 1665 cm⁻¹ are formed. Similar alterations were also observed in heat denatured antibody samples (see Figure 7.10 B) and can be assigned to turn-structures and intermolecular β -sheet structures^{81,85,86}. The formation of β -sheet structures is commonly observed in dried protein products due to the lower degree of hydrogen-bonding as compared to α -helical

structures^{87,88}. In addition, β -sheet structures indicate increased degrees of protein-protein interactions and thus they are frequently encountered in aggregated protein species.

Due to the crystallization of sucrose, the disaccharide's hydrogen-bonding-capacity to the antibody is compromised and the protein's secondary structure is altered due to this lack of interaction with the stabilizer. The impact of saccharide-crystallization on the preservation of the antibody's native conformation is further demonstrated by the coincidence of the first detection of structural deteriorations in pH 3.5 lyophilizates collapsed during freeze-drying after 9 weeks of storage at 50 °C (shift of main band to 1635 cm^{-1} ; data not shown) and the complete crystallinity of sucrose as determined by DSC (as indicated by the absence of a glass transition and a crystallization exotherm) at the same point of time.

In addition, as the observed change in secondary structure concurs with the onset of browning, the observed deteriorations may be related to glycation as well. However, there was no alteration in secondary structure observed for the pH 3.5-formulation that collapsed during freeze-drying until after nine weeks of storage, whereas nonenzymatic browning could already be visually detected after 6 weeks, indicating that crystallization had a greater impact on the conformation and that secondary structure was less sensitive towards protein-glycation than aggregation and particle formation. The fact that aggregated species were not reflected by alterations of secondary structure is consistent with reports referring to the observation that IgG aggregation may proceed without alterations in secondary structure^{82,89}.

Figure 8.24 A depicts second derivative spectra of samples stored for 15 weeks at 50 °C. Lyophilizates that collapsed during storage formulated at pH 3.5 were too degraded to be analyzed, because there was no soluble protein left after the filtration step mandatory in sample-preparation. In contrast, the same formulation that collapsed during lyophilization contained enough residual soluble protein, but secondary structure was greatly altered as well, as indicated by the band-shifts and additional bands discussed above.

Lyophilizates that were formulated at pH 5.5 did not show any alteration of their secondary structure, despite the observation of browning and the formation of significant amounts of aggregates, further pointing towards the formation of native-like aggregates.

Samples that were stored at 40 °C further qualitatively confirmed the trend observed in samples stored at 50 °C. pH 3.5-samples that collapsed during storage showed slight changes in secondary structure that were apparent in the formation of the additional bands at 1692 cm^{-1} , 1679 cm^{-1} and 1665 cm^{-1} after two weeks of storage (data not shown). After six weeks of storage the red shift of the major band became detectable and was well discernable after 12 weeks (data not shown). Figure 8.25 B shows samples after 15 weeks of storage at 40 °C. Samples that collapsed during storage formulated at pH 3.5 showed the described shift of the main band and the additional bands between 1665 and 1692 cm^{-1} associated with aggregation. The same formulations that were intentionally collapsed during

freeze-drying showed only minor spectral alterations missing the red-shift. However the additional aggregation-related bands were detectable as well, indicating that some conformational deterioration occurred.

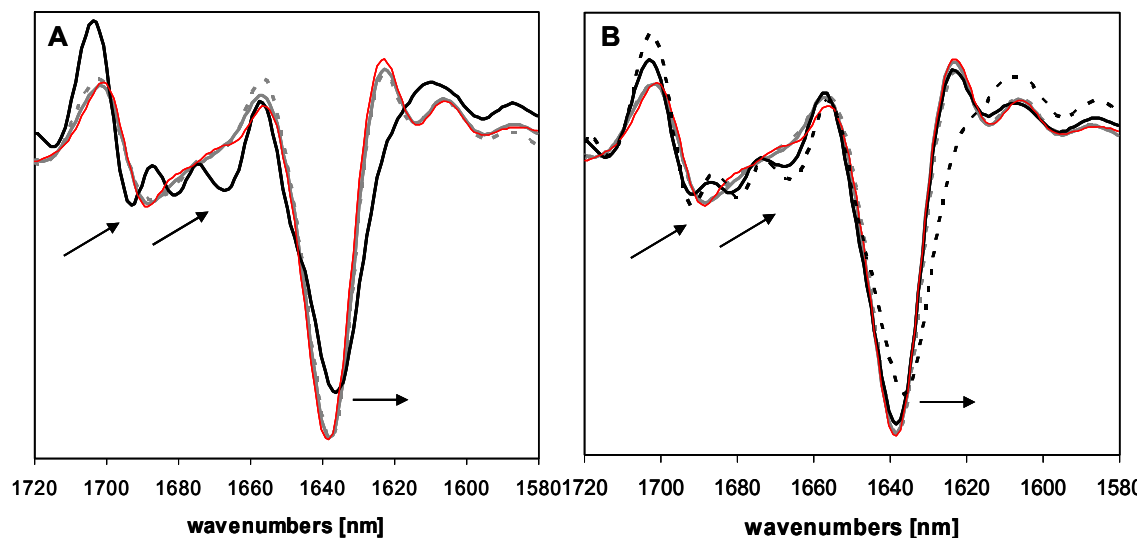


Figure 8.25: Area-normalized 2nd derivative FTIR transmission spectra of reconstituted lyophilizates that collapsed either during lyophilization or during subsequent storage after storage at 50 °C (A) and 40 °C (B) for 15 weeks, respectively.

standard IgG₀₁ (red line), sucrose pH 5.5 collapsed during lyophilization (grey solid line) and during storage (grey dashed line), sucrose pH 3.5 collapsed during lyophilization (black solid line) and during storage (black dashed line).

Samples that were stored at 2-8 °C did not show any deviation from standard spectra.

2.2.5 EXCURSUS: IN-DEPTH INVESTIGATION OF CRYSTALLIZATION AND NON-ENZYMATIC BROWNING IN INITIALLY COLLAPSED AND INITIALLY NON-COLLAPSED SUCROSE-BASED LYOPHILIZATES

In order to get further insight into the differences in the rates and extents of sucrose crystallization and degradation, sucrose-based IgG₀₁ lyophilizates formulated at pH 3.5 were produced a second time and protein and excipient stability was monitored more closely during storage at 50 °C, i.e. samples were analyzed after 3, 7, 10, 14, 21 and 28 days. Initially non-collapsed lyophilizates collapsed during storage at 50 °C within 3 days.

Table 8.9 summarizes the physical properties of the freeze-dried cakes at the beginning and after storage at 50 °C for 28 days. Residual moisture levels were well comparable allowing for a sound comparison of the two differently freeze-dried systems. Residual moisture levels did not relevantly increase during storage at 2-8 °C and 50 °C.

Glass transition temperatures were approximately at the storage temperature, i.e. the samples were actually stored in the rubbery state, allowing for the certain observation of crystallization events at experimental timescales. The slightly lower average glass transition temperature observed in the non-collapsed lyophilizates at the beginning of the storage period was most probably caused by increased residual moisture levels in the samples that were analyzed in DSC experiments as compared to the average residual moisture, as the

residual moisture showed a considerable standard deviation. This was further corroborated by the identical glass transition temperatures observed in samples that were stored at 2-8 °C for 28 days, i.e. in an environment in which no moisture uptake would be expected.

Table 8.9: Residual moisture and glass transition temperatures of the sample set.

appearance	storage temperature [°C]	storage time [days]	Tg ± SD [°C] ^{a)}	residual moisture ± SD [%] ^{b)}
initially non-collapsed	-	0	46.9 ± 1.8	1.3 ± 0.7
	2-8	28	49.8 ± 1.3	- ^{d)}
	50	28	- ^{c)}	1.1 ± 0.3
initially collapsed	-	0	57.8 ± 0.1	1.4 ± 0.1
	2-8	28	49.4 ± 5.2	- ^{d)}
	50	28	50.4 ± 0.1	1.7 ± 0.1

a) determined by DSC

b) determined by coulometric Karl Fischer titration

c) no glass transition was detectable after storage at 50 °C

d) as no significant increase in residual moisture was observed during storage at 50°C, no increase was expected during storage at 2-8 °C and therefore Karl Fischer was not accomplished on these samples.

After 28 days of storage at 50 °C, the initially non-collapsed samples had completely crystallized and no glass transition could be detected. In contrast, initially collapsed samples remained at least partially amorphous.

The extent of crystallization during storage was monitored using differential scanning calorimetry (DSC) as a commonly applied technique for this purpose⁹⁰. The amount of amorphous sucrose still present in the lyophilizates was quantified using the area of the crystallization exotherm observed during DSC heating scans as analytical measure.

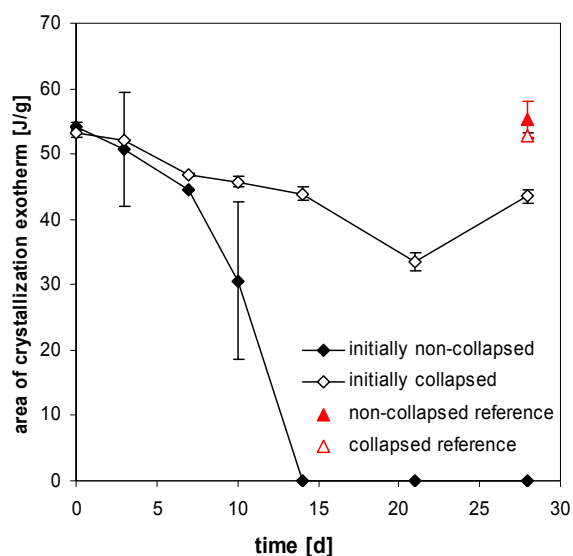


Figure 8.26: Extent of sucrose-crystallization: area of crystallization-exotherm as determined by DSC during storage at 50 °C in initially non-collapsed (closed diamonds) and initially collapsed (open diamonds) lyophilizates.

As a reference, open and closed triangles represent the area of the crystallization exotherm in initially collapsed and non-collapsed lyophilizates, respectively, that were stored for 28 days at 2-8 °C.

Figure 8.26 depicts the course of crystallization during storage of initially collapsed and storage-collapsed lyophilizates. Lyophilizates that collapsed during storage at elevated temperatures were completely crystalline after 14 days of incubation at 50 °C, whereas samples that were initially collapsed during freeze-drying remained amorphous throughout the 28 days under investigation. Reference samples that were stored in the refrigerator remained amorphous as well (red symbols in Figure 8.27). A qualitative correlation between the onset of crystallization and the drying technique applied to produce the amorphous solid sucrose was also observed by Bhugra et al.⁴⁴.

Interestingly, the onset of collapse (no matter when) was not accompanied by complete crystallization, as described by te Booy and coworkers^{43,91} and there was no sharp acceleration of crystallization observed with the onset of collapse.

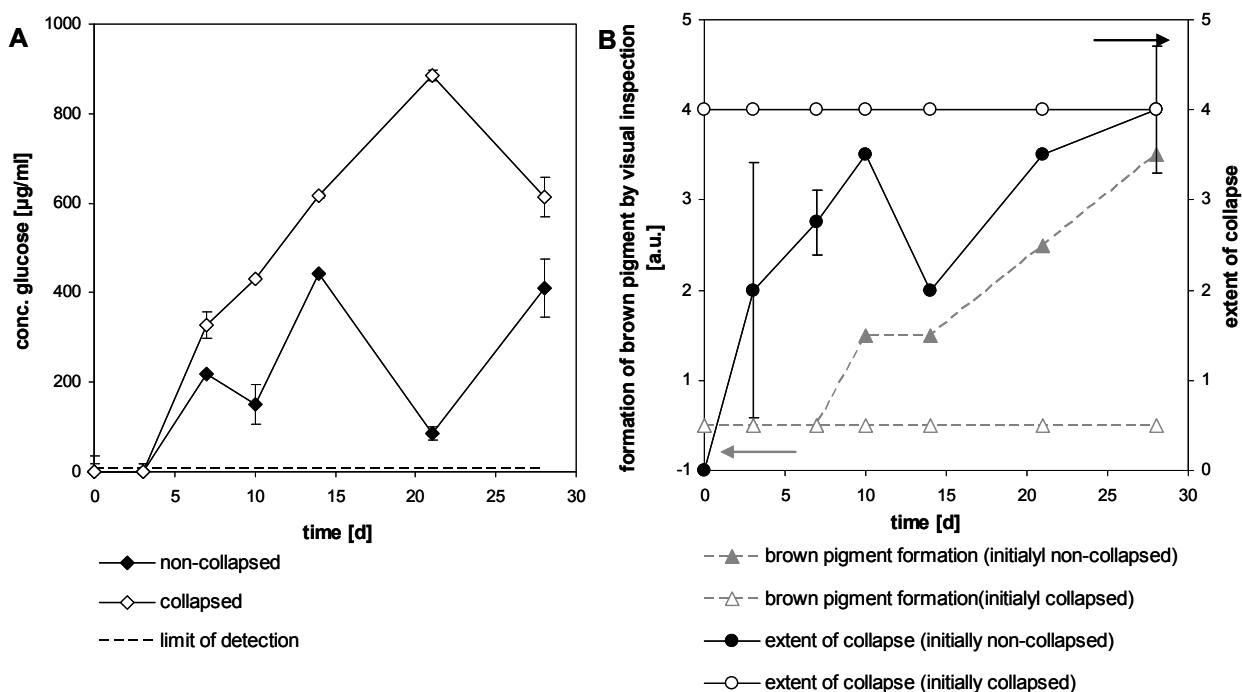


Figure 8.27: Formation of glucose during storage at 50 °C in initially non-collapsed and initially collapsed lyophilizates as determined by the Trinder-assay (A); formation of brown pigment and the extent of collapse of initially non-collapsed and initially collapsed lyophilizates during storage at 50 °C as determined by visual evaluation of cake appearance and color (average +/- SD, n = 2).

Besides the crystallization behavior the chemical degradation of sucrose, i.e. the acid-catalyzed hydrolysis was studied as well. The extent of sucrose-inversion was monitored by detecting the formed glucose using the Trinder-assay⁶¹. The Trinder-assay is enzyme-based and monitors the formation of a pink dye that is formed by oxidation with hydrogen peroxide, in turn generated in a reaction with glucose. Figure 8.27 A shows the amount of glucose that is formed during storage at 50 °C. In contrast to observations of Flink⁵⁷ no sucrose-hydrolysis occurred during the freeze-drying process. Interestingly, no sharp increase in glucose formation with the onset of collapse was observed.

After 7 days of storage, the formation of glucose was detected for the first time in both sample-types. Most noticeable, glucose amounts in initially collapsed cakes were actually higher than in storage-collapsed cakes. This is in strong contrast to the trend observed during the 15 weeks storage stability-study that indicated a more rapid sucrose degradation and nonenzymatic browning in initially non-collapsed cakes. Analyzing the onset and the extent of non-enzymatic browning by visually assessing the color-formation, the rapid discoloration of the storage-collapsed cakes catches the eye. Figure 8.27 B displays the color of the lyophilizates and the extent of collapse both ranked on a scale from zero (colorless, not collapsed) to four (strong brown discoloration, completely collapsed).

Interestingly, the development of browning was in sharp contrast to the determined amount of glucose. Whereas collapse-dried lyophilizates showed higher glucose-concentrations indicating a more pronounced sucrose hydrolysis in these systems, browning was more prominent in storage-collapsed cakes. Indeed, there was no browning at all detectable in collapse-dried cakes after 28 days of storage at 50°C. Figure 8.28 shows lyophilizates that were stored for zero, three or 28 days at 50 °C. Clearly, cakes that collapsed during storage show a yellow discoloration after 28 days of storage, whereas initially collapsed cakes remained white.

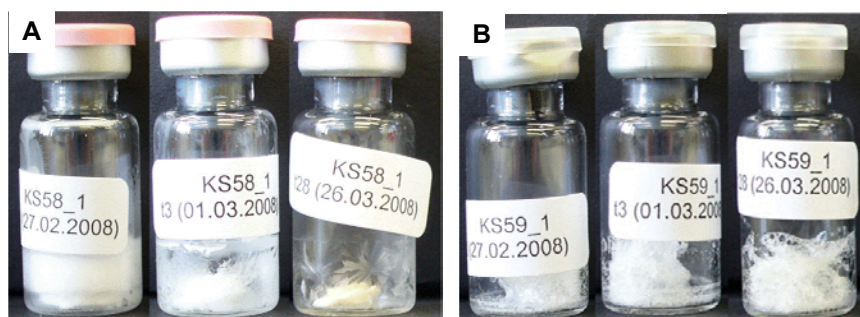


Figure 8.28: Appearance and color of initially non-collapsed (A) and initially collapsed (B) sucrose-based lyophilizates after storage at 50 °C for 0, 3 and 28 days.

Browning in storage-collapsed cakes started after 10 days of storage and steadily increased during subsequent storage (Figure 8.28 B). With intensifying discoloration the amount of remaining soluble monomer as determined by HP-SEC rapidly decreased (Figure 8.29), pointing towards the formation of insoluble glucose-protein adducts in the Maillard reaction. Monomer fractions remained high in initially collapsed samples. Along with the absence of any browning this indirectly indicated that no glycation of the antibody and consecutive reactions leading to insoluble colored products took place.

This is most extraordinary, because hydrolysis of sucrose occurred most probably to a comparable extent as in systems that collapsed during storage, as glucose contents determined using the Trinder kit were high. However, the subsequent reaction of the reducing sugar with the IgG was strongly retarded in collapse-dried cakes. This caused the

absolute amount of glucose to be higher in collapse-dried systems, because glucose-consumption was decreased.

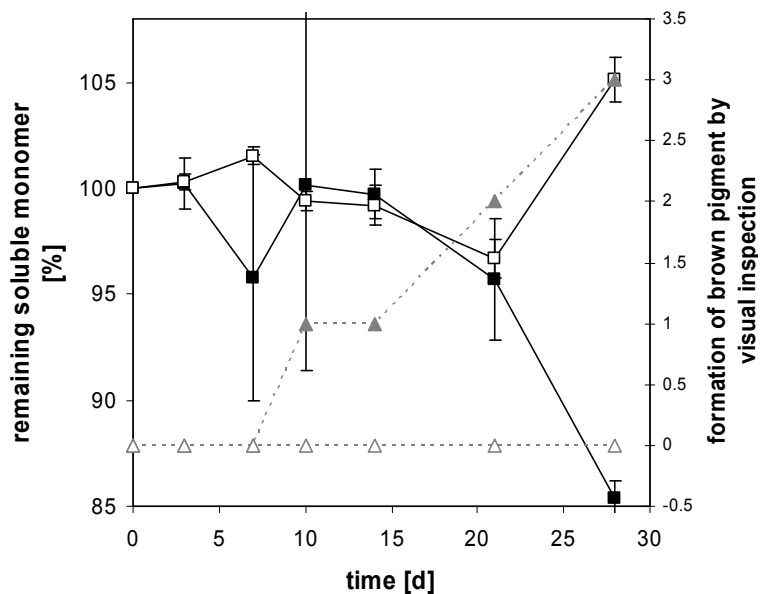


Figure 8.29: Remaining soluble IgG₀₁ monomer as determined by HP-SEC during storage of initially collapsed (open squares) and initially non-collapsed (closed squares) sucrose-based lyophilizates compared to the extent of browning determined by visual inspection of initially collapsed (open triangles) and initially non-collapsed (closed triangles) lyophilizates.

This observation might be explainable by the differences in the glassy dynamics of the two systems that are explicitly discussed in Chapter 9 of this thesis. Collapse-dried systems were found to exhibit tremendously increased structural relaxation times as compared to conventionally dried initially non-collapsed systems. As α -relaxations (frequently referred to as structural relaxation time) are correlated with translational diffusion within a glassy matrix and as they are often described to be coupled to diffusion-controlled reactions, a high degree of coupling to the Maillard reaction can be expected. The reaction depends on the condensation of the aldehyde group of a reducing sugar with the amino-group of a protein. The latter is a large species whose movements are highly coupled to the viscosity of the glassy matrix system^{36,92}. In contrast, the initial step of acid-catalyzed sucrose-hydrolysis that is based on the protonation of the glycosidic bond is not expected to be strongly coupled to α -relaxation dynamics but rather to β -dynamics, because the diffusing species are comparably small⁴⁵. Thus there is no pronounced difference observed in the rate of sucrose hydrolysis but there is a tremendous difference on the rate of Maillard reaction.

Besides the effect of glassy dynamics, the already discussed differences in specific surface area might contribute to the stronger extent of nonenzymatic browning in storage-collapsed systems, because the initial steps of the Maillard reaction were described to occur in pores⁷⁴. In addition the increased crystallinity in these samples might further account for the higher amounts of glycated products, because it was described that crystallization further boosts the course of the Maillard reaction⁹³.

2.2.6 SUMMARY AND CONCLUSION

Initially non-collapsed and initially collapsed sucrose-based lyophilizates showed comparable physical and conformational protein stability as well as residual moisture levels and glass transition temperatures. However, during storage at elevated temperatures in the vicinity of the systems' glass transition, initially non-collapsed lyophilizates tremendously shrunk, i.e. they underwent collapse during storage.

The onset of collapse during storage was accompanied by a vast change in the physicochemical properties of sucrose and the stability of the antibody. Upon collapse, sucrose completely crystallized. In contrast, sucrose in initially collapsed cakes remained at least partly amorphous throughout the whole storage period. In addition to physical instabilities, sucrose was also chemically degraded at high temperatures, i.e. sucrose was hydrolyzed and the reducing sugars glucose and fructose were formed. These monosaccharides then reacted in the so-called Maillard-reaction, probably resulting in a glycation of the antibody. Although the rate and extent of sucrose hydrolysis were probably comparable in storage-collapsed and initially collapsed lyophilizates, the rate and extent of nonenzymatic browning was tremendously different. Lyophilizates that collapsed during storage showed strongly increased amounts of aggregated antibody and a distinct brown discoloration indicating the occurrence of the Maillard reaction, whereas in lyophilizates that were initially collapsed glucose was formed but not consummated in the glycation.

The presumable glycation of IgG₀₁ in turn led to a strongly increased formation of soluble and insoluble aggregates. In addition, glycation caused a dramatic change in secondary structure manifested by an initially increased β -sheet content leading to complete unfolding.

The greatly retarded crystallization of sucrose and the hindered Maillard reaction in collapse-dried cakes could be correlated to the greatly reduced molecular mobility and the increased fragility in these glasses that are discussed in detail in Chapter 9 of this thesis. Because both, crystallization and the Maillard reaction, are at least partly diffusion-controlled and the diffusing species are comparably large in the case of the protein involved, they may be well correlated to α -relaxation dynamics. As the Maillard reaction was described to be initiated in pores, the greatly reduced porosity in collapsed cakes as indicated by the reduced specific surface area (Figure 8.9), may contribute to this retardation as well. Furthermore, as it is known that crystallization greatly accelerates the rate of nonenzymatic browning, the reduced extent of sucrose crystallinity may play a role as well.

In summary, collapsed lyophilizates that were intentionally collapsed during processing showed greatly enhanced stability during storage at elevated temperatures in the vicinity of the glass transition. In contrast, conventionally dried non-collapsed lyophilizates collapsed during storage and showed enormous instabilities during subsequent storage. Thus, initially collapsed lyophilizates are more robust during storage at elevated temperatures and offer

better protein stabilization considering both physical and conformational stability, and presumably also a better chemical stability.

Collapsed and non-collapsed lyophilizates stored at 2-8 °C, where no collapse during storage occurred, remained equally stable during the investigated period of time (15 weeks). This highlights the importance of controlled storage conditions well below the glass transition temperature for conventionally freeze-dried lyophilizates. In contrast, intentionally collapsed lyophilizates that were found to be more robust towards storage at elevated temperatures might offer the possibility to be stored at room temperature.

2.3 PARTIALLY CRYSTALLINE SYSTEMS: THE EFFECT OF PARTIAL COLLAPSE

Besides the investigation of purely amorphous trehalose- and sucrose-based formulations, a partially crystalline formulation was analyzed as well in terms of the effect of partial collapse on long-term protein stability.

The use of crystalline bulking agents such as mannitol or glycine is frequently described in the development of freeze-dried protein formulations. During freezing or annealing those excipients crystallize to form a crystalline matrix that increases the mechanical stability of the freeze-dried cake and even prevents the occurrence of macroscopic collapse. Upon the occurrence of so-called micro-collapse, the crystalline excipient acts as a crystalline scaffold, maintaining the macroscopic cake structure while the amorphous phase collapses^{94,95}. Chatterjee and coworkers investigated the effect of freeze-drying substantially above T_g' in such systems and found that LDH activity was well preserved¹⁸.

They also found that there is a minimum weight ratio of crystalline to amorphous formulation component required for the system to reliably withstand collapse at high drying temperatures¹⁸, thus by reducing this weight ratio, the system's susceptibility towards collapse can be altered. This fact was exploited in the present investigation: By slightly decreasing the weight fraction of the crystalline bulking agent mannitol and concomitantly increasing the weight fraction of the amorphous stabilizer sucrose, partially collapsed lyophilizates could be produced by freeze-drying with the collapse-cycle described in Chapter 3. Table 8.10 summarizes the investigated formulation. The same formulation was also conventionally freeze-dried, resulting in non-collapsed cakes. The samples were stored at 40 °C and 50 °C for 15 weeks and vials were analyzed after 2, 4, 6, 9, 12 and 15 weeks of storage. Reference samples were stored at 2-8 °C.

Table 8.10: Partially crystalline formulation freeze-dried to non-collapsed and partially collapsed cakes to investigate the effect of partial collapse on protein stability.

IgG01	4 mg/mL
mannitol	35 mg/mL
sucrose	15 mg/mL
sodium succinate pH 5.5	2.7 mg/mL

After freeze-drying, non-collapsed lyophilizates appeared as mat-white, stable cakes whose dimensions correspond exactly to the inner dimensions of the vial. Partially collapsed cakes were slightly shrunken and in the cross section, cavities were observed.



Figure 8.30: Appearance of non-collapsed (A) and partially collapsed (B) mannitol-sucrose-based lyophilizates after storage at various temperatures for 15 weeks.

Lyophilizates stored at 2-8 °C (leftmost vial), 40 °C (middle vial) and 50 °C (rightmost vial).

Appearance did not change during storage (Figure 8.30) and no collapse during storage occurred.

2.3.1 PHYSICOCHEMICAL CHARACTERISTICS OF LYOPHILIZATES

Table 8.11 lists the physicochemical properties of mannitol-sucrose-based lyophilizates. After freeze-drying, residual moisture levels were low (0.9 ± 0.1 % for non-collapsed and 0.1 ± 0.0 % for partially collapsed cakes, respectively). The distinctly decreased amount of residual water in partially collapsed cakes is expectable, considering the high drying temperatures applied in the collapse-cycle. It is well known, that the addition of crystalline excipients greatly enhances drying efficiency due to an increased porosity^{18,96}. Furthermore, the decrease in specific surface area (SSA), that renders the drying less effective, is less pronounced in the case of partially collapsed systems (2.68 ± 0.30 m²/g for partially collapsed cakes versus 3.06 ± 0.16 m²/g for non-collapsed cakes composed of mannitol and sucrose in a ration of 4:1; see Chapter 5). However, it must be recognized that there will be an uneven moisture distribution with much higher water contents in the amorphous phase¹⁸. Residual moisture contents did not relevantly increase during storage in the non-collapsed samples. However, they more strongly increased in the partially collapsed samples, most probably due to the lower initial water content and thus the higher concentration gradient between the stoppers and the surroundings and the cake. Residual moisture levels increased more strongly during storage at elevated temperatures and were most likely caused by moisture transfer from stoppers and water vapor permeability of the closure system, as frequently observed during storage of freeze-dried solids²⁵. Residual moisture levels increased during the first two weeks of storage (0.43 ± 0.01 % and 0.35 ± 0.15 % in partially collapsed lyophilizates stored at 40 °C and 50 °C, respectively), resulting in comparable moisture levels between partially collapsed and non-collapsed lyophilizates during the remaining stability study, therefore antibody stability results were not distorted by a difference in residual moisture contents.

Table 8.11: Physicochemical properties of mannitol-sucrose lyophilizates after storage for 15 weeks at various temperatures.

appearance	storage temperature [°C]	residual moisture [%] ± SD ^{a)}	Tg [°C] ^{b)}	characteristic melting endotherms [°C] ^{c)}	characteristic XRD peaks [°2θ] ^{c)}
non-collapsed	2-8	1.16 ± 0.02	37.1	134.7; 150.8	9.7; 20.4
	40	1.17 ± 0.01	34.3	138.6; 151.9	9.7; 20.4
	50	0.98 ± 0.01	40.3	138.8; 152.1	9.7; 20.4
partially collapsed	2-8	0.27 ± 0.01	55.3	137.6; 153.7	9.7; 20.4
	40	0.64 ± 0.01	46.7	137.8; 154	9.7; 20.4
	50	0.51 ± 0.17	42.3	138.4; 152.6	9.7; 20.4

a) determined by coulometric Karl Fischer titration

b) determined by differential scanning calorimetry

c) determined by X-ray powder diffraction

Glass transition temperatures of the amorphous sucrose phase were 53.6 °C and 66.0°C in elegant and partially collapsed cakes, respectively, immediately after lyophilization. The higher glass transition temperatures in collapsed cakes correspond to the lower residual moisture. The slightly reduced experimental glass transition values as compared to literature values for freeze-dried sucrose with a comparable residual moisture level (63 ± 1 °C⁹¹) might indicate the announced uneven moisture distribution with higher moisture levels in the amorphous sucrose part of the lyophilizate and lower moisture levels in the crystalline mannitol part.

Glass transition values decreased during storage due to the increase in residual moisture. Eventually, storage at elevated temperatures was carried out no longer in the glassy state but at the transition to the rubbery state. However, no macroscopic collapse appeared as can be seen from Figure 8.30.

Mannitol crystallized during freeze-drying and both drying protocols resulted in the formation of the δ -mannitol modification as determined by X-ray powder diffraction (XRD). No reflections of either α - or β -mannitol could be detected (data not shown). In the DSC thermograms, δ -mannitol was first transformed to β -mannitol at 130-140 °C and the in-situ formed β -mannitol then melts at 150-158 °C. The melting points are lowered as compared to those of pure mannitol due to the presence of sucrose and buffer salts, but they are in good agreement with melting temperatures observed by Hawe et al.⁹⁷. The mannitol polymorphs remained stable during storage in contrast to the observations of Yu et al who observed a transformation to α - and β -mannitol⁹⁸, but again in agreement with Hawe et al.⁹⁷.

2.3.2 PHYSICAL PROTEIN STABILITY OF IGG₀₁ IN RECONSTITUTED LYOPHILIZATES

Protein stability was monitored using HP-SEC to detect the formation of soluble aggregates and indirectly (using the recovery data) the formation of insoluble aggregates. Figure 8.31

displays the decrease of remaining soluble monomer and the increase in soluble aggregates during storage at 40 °C and 50 °C.

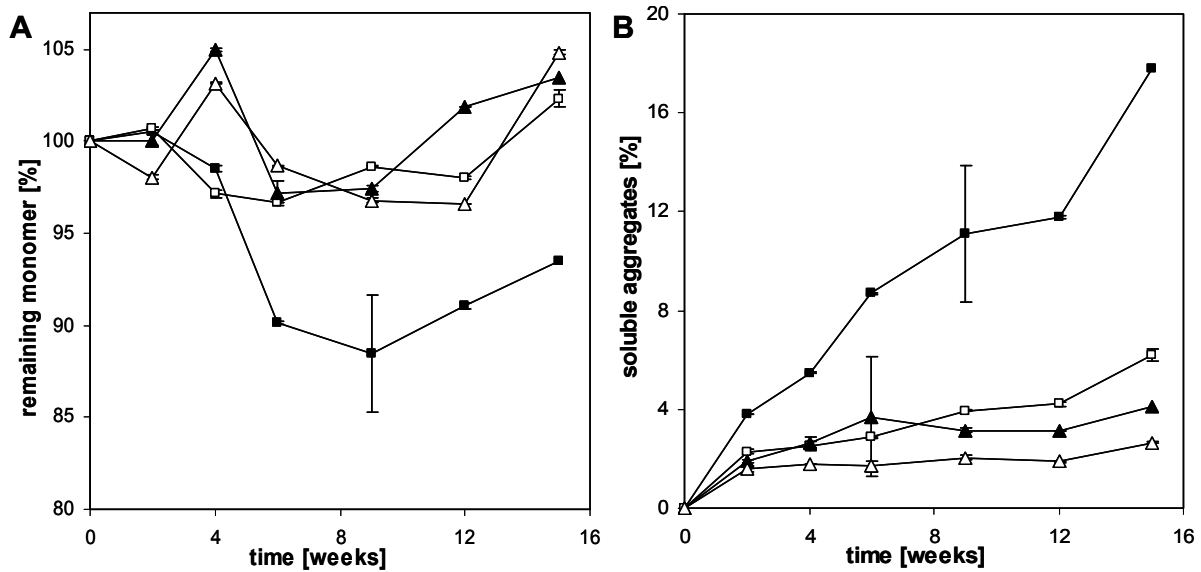


Figure 8.31: Remaining monomer (A) and soluble aggregates (B) of IgG₀₁ (4 mg/mL) reconstituted from non-collapsed (full symbols) and partially collapsed (open symbols) mannitol-sucrose lyophilizates during storage at 40 °C (triangles) and 50 °C (squares).

Non-collapsed and partially collapsed samples that were stored at 40 °C showed a similar behavior. Remaining monomer contents were high allowing for no significant discrimination. Regarding the amount of soluble aggregates that is formed during storage, partially collapsed lyophilizates exhibit slightly lower amounts of aggregated species. This trend is more pronounced in samples stored at 50 °C. Non-collapsed cakes clearly show reduced amounts of remaining monomer and distinctly increased quantities of aggregated species. These findings were further confirmed by AF4-analysis as an orthogonal technique to investigate the formation of soluble and insoluble aggregates in IgG lyophilizates (data not shown).

Table 8.12: Particulate matter of mannitol-sucrose lyophilizates after storage at 50 °C for 15 weeks.

appearance	particles > 1 µm/mL ^{a)}	particles > 10 µm/mL ^{a)}	particles > 25 µm/mL ^{a)}	turbidity [FNU] ^{b)}	Z average [nm] ^{c)}	PDI ^{c)}
non-collapsed	1970 ± 79	68 ± 5	28 ± 3	3.1 ± 0.2	21.30	0.37
partially collapsed	1584 ± 86	27 ± 12	3 ± 3	2.0 ± 0.3	15.60	0.23

a) determined by light obscuration

b) determined by nephelometric turbidity measurements

c) determined by dynamic light scattering

To further assess the physical stability, i.e. the formation of insoluble aggregates and particles, light obscuration, dynamic light scattering and turbidity measurements were accomplished. Table 8.12 summarizes results from these techniques after 15 weeks of storage at 50 °C. Noticeably, particle numbers were slightly increased in lyophilizates that

were conventionally freeze-dried. This was further reflected by increased turbidity values and increased Z-Averages and polydispersity indices. This trend was observed throughout the whole period of investigation, but for the sake of clarity, only the endpoint is depicted here.

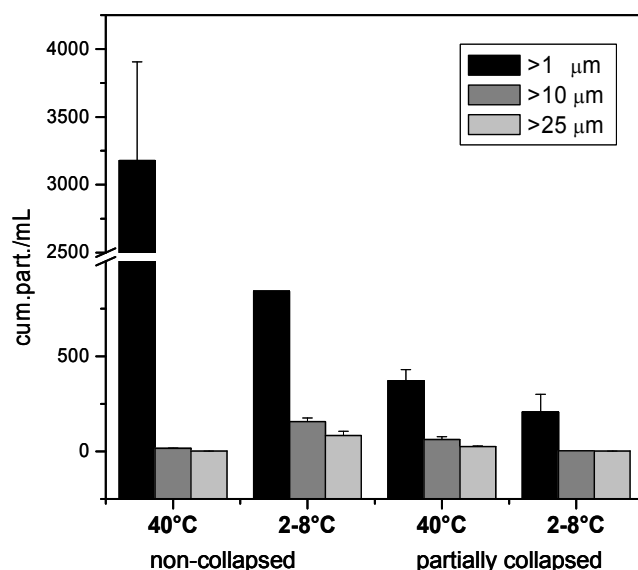


Figure 8.32: Particle size distribution of non-collapsed and partially collapsed mannitol-sucrose lyophilizates stored for 15 weeks at 40 °C and 2-8 °C, respectively.

cum. part./mL: cumulative particles per milliliter

In order to check whether the observed differences are related to the slightly higher glass transition temperatures of partially collapsed cakes, data for samples stored at 40 °C and at 2-8 °C, that were certainly stored below the glass transition temperature are displayed in Figure 8.32. The trend observed at 50 °C can also be noticed here – non-collapsed lyophilizates showed higher particle numbers than partially collapsed lyophilizates.

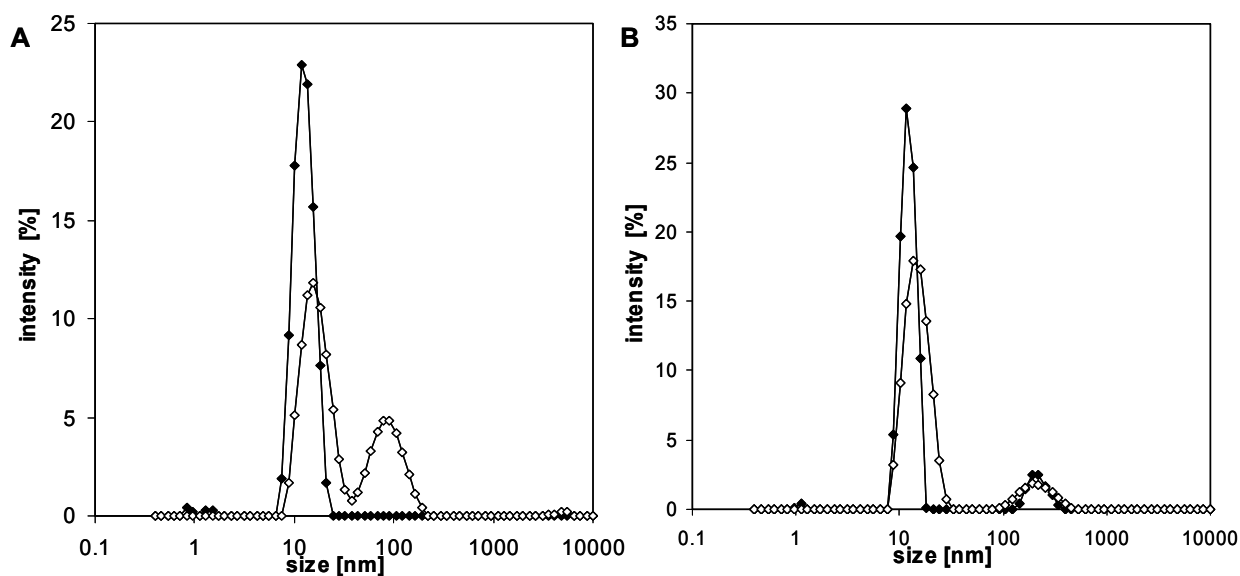


Figure 8.33: DLS size distribution by intensity of IgG₀₁ reconstituted from non-collapsed (A) and partially collapsed (B) lyophilizates after freeze-drying (closed symbols) and after 15 weeks of storage at 50 °C (open symbols).

The size distribution was obtained by fitting a NNLS algorithm to the correlation function.

In DLS, IgG₀₁ in partially collapsed cakes appeared to be slightly less stable than non-collapsed cakes immediately after freeze-drying. This was indicated by the detection of a second peak in the DLS size distribution by intensity between 100 nm and 500 nm (Figure 8.33 B), that was absent in the non-collapsed samples (Figure 8.33 A). However, during subsequent storage at elevated temperatures, IgG stability was better preserved in partially collapsed cakes, as indicated by the unaltered peak assigned to large, high molecular weight species.

In contrast, a prominent peak between 30 nm and 300 nm was formed in the non-collapsed sample. However, the observed differences were only marginal. Comparing the more relevant size distributions by volume no differences could be observed (Figure 8.34)

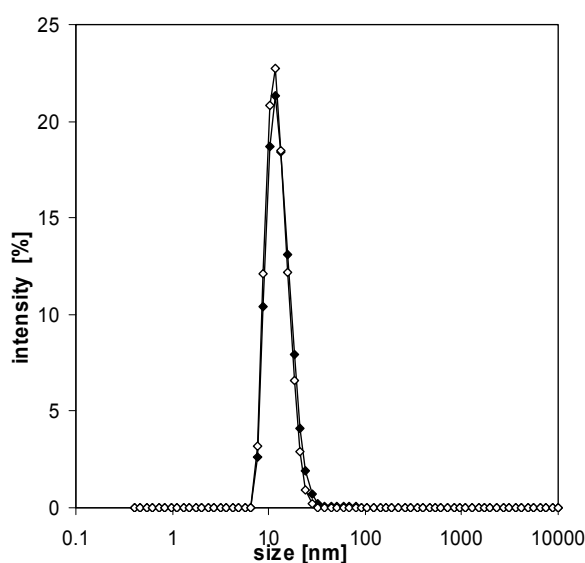


Figure 8.34: DLS size distribution by volume of IgG₀₁ reconstituted from non-collapsed (closed symbols) and partially collapsed (open symbols) lyophilizates after 15 weeks of storage at 50 °C.

The size distribution was obtained by fitting a NNLS algorithm to the correlation function.

The observed trend was further confirmed by increased turbidity of partially collapsed lyophilizates at the beginning of storage as compared to non-collapsed cakes (2.60 ± 0.4 versus 1.3 ± 0.1) that did not relevantly change during storage whereas turbidity in the non-collapsed system increased (Table 8.12).

To sum up the findings regarding the physical stability of IgG₀₁ stored in non-collapsed and partially collapsed mannitol-sucrose-based lyophilizates, the formation of soluble and insoluble aggregates during stress storage was slightly enhanced in non-collapsed systems as compared to partially collapsed ones, although immediately after freeze-drying, the formation of sub-visible and visible particles was increased in partially collapsed cakes.

2.3.3 BINDING ACTIVITY OF IgG₀₁ IN RECONSTITUTED LYOPHILIZATES

The preservation of biologic activities after freeze-drying to partially collapsed and elegant lyophilizates was addressed by determining the binding activity to a specific receptor of IgG₀₁ using surface plasmon resonance spectroscopy. Figure 8.35 displays binding activities

immediately after lyophilization as compared to the activity after 15 weeks of storage at 50 °C.

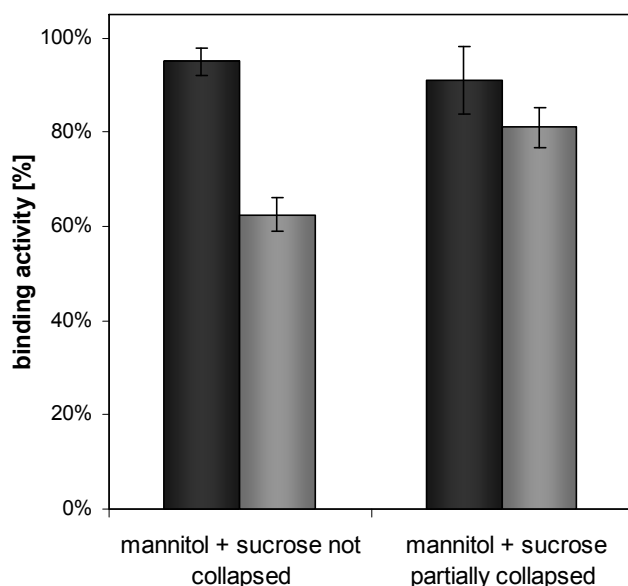


Figure 8.35: Binding activity of IgG₀₁ as determined by surface plasmon resonance spectroscopy (average +/- SD, n = 2).

Binding activity after lyophilization (black bars) and after 15 weeks of storage at 50 °C (grey bars).

Although binding activities in collapsed cakes appear to be slightly lower than in elegant ones immediately after freeze-drying, being in good agreement with physical protein stability data, results cannot be regarded as significantly different due to overlapping error bars. Evidently, binding activities decreased during storage at 50 °C. Interestingly, partially collapsed lyophilizates exerted a higher degree of IgG₀₁ stabilization as indicated by the higher significantly higher binding activities. This is again in good agreement with findings from physical stability data.

2.3.4 CONFORMATIONAL STABILITY OF IGG₀₁ IN RECONSTITUTED LYOPHILIZATES

In addition to physical stability considerations, conformational stability, i.e. the preservation of the native state was analyzed. Secondary structure was investigated using FTIR spectroscopy. Figure 8.36 displays second derivative FTIR transmission spectra of IgG₀₁ reconstituted from non-collapsed (A) and partially collapsed (B) lyophilizates after different times of storage. There were no differences between the spectra detectable, indicating that no alterations of the secondary structure occurred. This is consistent with the observed low levels of aggregated species and the overall good stability. However, slight differences in the formation of soluble and insoluble aggregates were not reflected in the secondary structure, pointing out the decreased sensitivity of FTIR to detect subtle changes in antibody formulations that has been described elsewhere^{82,99}.

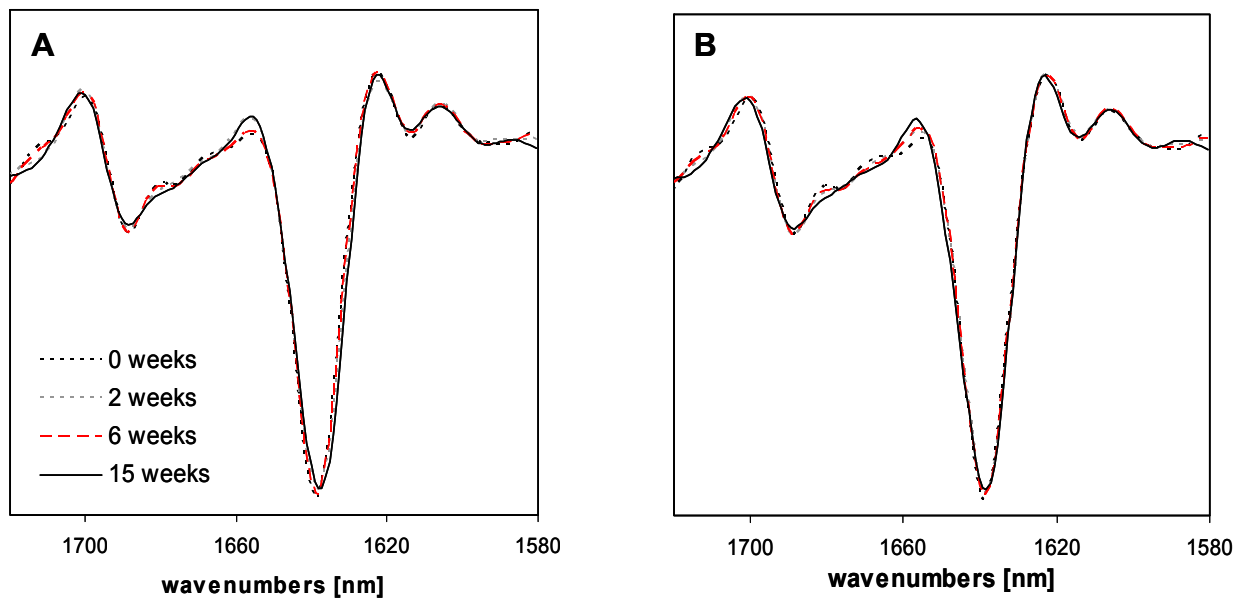


Figure 8.36: Area-normalized FTIR second derivative transmission spectra of 4 mg/mL IgG₀₁ reconstituted from non-collapsed (A) and partially collapsed (B) mannitol-sucrose lyophilizates after different periods of storage at 50 °C.

Spectra are calculated average spectra of two independent measurements.

In contrast, intrinsic tryptophan fluorescence spectroscopy showed clear differences between partially and non-collapsed mannitol-sucrose-systems. Figure 8.37 shows the fluorescence emission spectra immediately after freeze-drying (solid lines) and after 15 weeks of storage at 50 °C (dashed lines) as compared to IgG₀₁ standard (red line).

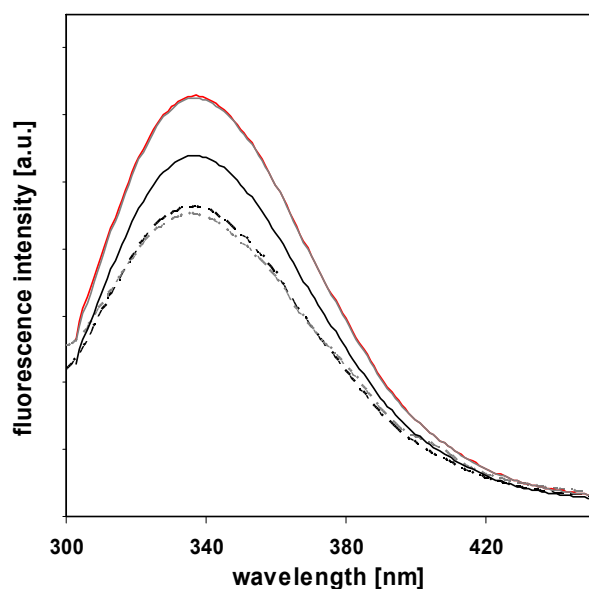


Figure 8.37: Intrinsic tryptophan fluorescence of 50 µg/mL IgG₀₁ after reconstitution from non-collapsed (black curves) and partially collapsed (grey curves) mannitol-sucrose-based lyophilizates immediately after lyophilization (solid lines) and after 15 weeks of storage at 50 °C (dashed lines).

There was no shift in emission maximum detectable, indicating that no major changes in tertiary structure occurred. However, there is a decrease in fluorescence intensity observed. Most noticeably, partially collapsed cakes showed complete preservation of tertiary structure

after freeze-drying whereas non-collapsed cakes showed slight perturbations as indicated by a slightly decreased fluorescence quantum yield.

During storage, fluorescence intensities further decreased and initially observed differences between the two systems assimilated, indicating a comparable degree of tertiary structure deterioration after 15 weeks of storage (dashed lines in Figure 8.37).

2.3.5 SUMMARY AND CONCLUSION

Summarizing the findings from the comparative investigation of non-collapsed and partially collapsed lyophilizates that were partially crystalline, results gained from the comparison of differently collapsed partially collapsed cakes immediately after lyophilization, that were discussed in Chapter 7 of this thesis, could be confirmed. The long-term storage stability of IgG₀₁ in partially collapsed cakes was not compromised by partial collapse.

Interestingly, partially collapsed lyophilizates provide slightly better stabilization, as indicated by increased remaining soluble monomer contents. This further confirms the observed trend investigating trehalose- and sucrose-based lyophilizates.

Thus the intentional evocation of collapse during freeze-drying applying a collapse-drying cycle leads to lyophilizates that are more robust towards storage at elevated temperatures, namely that cannot experience collapse during storage as they are already collapsed. More important, by applying collapse-drying, more stable lyophilizates can be produced that show both an increased physicochemical excipient-stability, namely retarded crystallization and retarded nonenzymatic browning, as well as increased protein stability, namely better preservation of physical and conformational antibody integrity.

3 L-LACTIC DEHYDROGENASE (LDH)

To further confirm the findings regarding the effect of collapse on protein stability gained during the IgG₀₁ studies and to test the universality of these findings, L-lactic Dehydrogenase (LDH) was investigated as a second, sensitive model protein. LDH was chosen because of its well-documented sensitivity to the stress situations during freezing^{100,101} and drying^{102,103}, as well as during storage under unfavorable conditions^{18,78}. Additionally, various publications using LDH as a model protein allow for a sound classification and evaluation of the effect of collapse on LDH's biological, physical and conformational stability properties.

Table 8.13 lists the investigated LDH formulations. Two partially crystalline and one purely amorphous formulation were chosen, reflecting the most commonly used freeze-drying formulations. The two most frequently used disaccharides trehalose and sucrose were applied as lyo-protectants. Polyethylene glycol (PEG) 3350 was used as cryo-protectant, because there are several publications pointing out the importance of PEGs for the stabilization of LDH^{102,104,105}. The total amount of solid was maintained constant for all the formulations (5.2 %) and was approximately the same as in the IgG₀₁ formulations (5.7 %).

Table 8.13: Investigated freeze-dried LDH formulations.

ID	excipient	concentration
1	LDH	1.00 mg/mL
	PEG 3350	18.44 mg/mL
	trehalose	31.56 mg/mL
	10 mM sodium phosphate buffer, pH 7.5	
2	LDH	1.00 mg/mL
	trehalose	50.00 mg/mL
	10 mM sodium phosphate buffer, pH 7.5	
3	LDH	1.00 mg/mL
	PEG 3350	18.44 mg/mL
	sucrose	31.56 mg/mL
	10 mM sodium phosphate buffer, pH 7.5	

LDH was purchased as ammonium sulphate suspension and dialyzed over night against 10 mM sodium phosphate buffer. Formulations were prepared immediately before freeze-drying to prevent LDH degradation. Solutions were filled into sterilized 2R vials and freeze-dried using either a conservative or an aggressive freeze-drying protocol as described in Chapter 3. This procedure allowed the production of non-collapsed and collapsed lyophilizates of exactly the same composition.

Samples were stored at 25 °C and 40 °C for up to 26 weeks and reference samples were stored in the refrigerator at 2 °C to 8 °C for the same period of time. Samples were analyzed immediately after freeze-drying and after 2, 4, 6, 9, 15 and 26 weeks of storage.

3.1 PHYSICOCHEMICAL PROPERTIES OF COLLAPSED AND NON-COLLAPSED LYOPHILIZATES

Figure 8.38 A depicts the different freeze-dried formulations (1 – 3, see Table 8.13) after lyophilization with the conservative, gentle drying protocol (left vial of each formulation) and the aggressive, collapse-drying protocol (right vial). Formulations 1 and 2 resulted in non-collapsed and collapsed lyophilizates. However, gently freeze-dried cakes of formulation 3 (sucrose and PEG 3350) partially collapsed during the process as visible from the shrunken cake dimensions.



Figure 8.38: Macroscopic appearance of LDH-lyophilizates of varying composition after freeze-drying with a conservative drying protocol (left vial of each formulation) and an aggressive drying-protocol (right vial of each formulation) immediately after freeze-drying (A) and after 26 weeks of storage at 40 °C (B).

1: PEG 3350 + trehalose, 2: trehalose, 3: PEG 3350 + sucrose.

Given the low shelf temperatures and chamber pressures this partial collapse was unexpected and most probably happened during ramping up the shelf temperature from the primary drying temperature at – 20 °C to the secondary drying temperature at 10 °C. Due to inhomogeneous drying, cakes in the center of the shelf remained slightly moister and their decreased T_g was then exceeded causing the partial collapse.

However, although this was initially not planned, it allows widening the scope of the investigation to the effect of partial collapse on LDH stability.

Figure 8.38 B shows the lyophilizates after 26 weeks of storage at 40 °C. No change in macroscopic appearance can be observed.

Figure 8.39 depicts the residual moisture levels of lyophilizates stored for 26 weeks at the various storage temperatures and compares them to the residual moisture immediately after production.

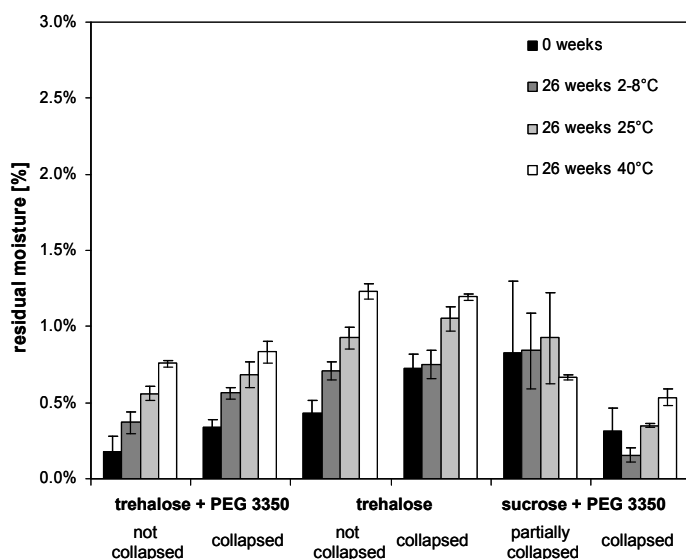


Figure 8.39: Residual moisture levels of lyophilizates immediately after freeze-drying and after 26 weeks of storage at 2-8 °C, 25 °C and 40 °C as determined by coulometric Karl Fischer titration; average \pm SD, $n = 3$.

Initial residual moisture levels were in the range of 0.2 % to 0.8 % and non-collapsed and collapsed lyophilizates of the same formulation showed deviations in their residual moistures between 0.1 % and 0.5 %. Thus they comply with the tolerated fluctuation of 0.5 % specified prior to storage as described in the materials and methods section. Standard deviations were low except for the partially collapsed lyophilizates. The observed inhomogeneity of drying corresponds to the often expressed concern that collapse leads to irregular residual moisture distributions¹⁰. However, completely collapsed lyophilizates showed narrow distributions of residual moisture levels, suggesting that complete collapse intentionally provoked by collapse-drying might be superior to partial collapse regarding the homogeneity of drying. Most obviously, residual moisture levels increased during storage and the water uptake was more pronounced at higher storage temperatures. This is a phenomenon regularly observed during storage of freeze-dried samples¹⁰⁶ and it is often caused by either water transfer from the stoppers into the lyophilizate or by water vapor permeability of the stoppers²⁵. However, residual moisture levels never exceeded 1.2 %, thus remaining in a range widely acknowledged as acceptable for freeze-dried solids (below 1 % to usually 3 % residual moisture)³⁴. There was no relevant difference in the water uptake of collapsed and non-collapsed lyophilizates.

Table 8.14 summarizes the calorimetric properties of lyophilizates stored at 2-8 °C and at 40 °C for 26 weeks as determined by DSC. Most importantly, the uptake of water did not lead to a decrease of the glass transition temperature below the storage temperature, thus all

systems remained in the glassy state. However, the increased residual moisture level indeed led to a decrease in glass transition temperatures by about 10 °C for all the samples. The glass transition temperature could not be determined in sucrose-PEG-based lyophilizates because the glass transition was obscured by the melting endotherm of PEG at 55 – 60 °C¹⁰⁷.

Table 8.14: Differential scanning calorimetric properties of LDH lyophilizates after 26 weeks of storage at 2-8 °C and 40 °C, respectively.

formulation	appearance	storage temperature [°C]	T _g prior to storage [°C] ± SD	T _g [°C] ± SD	T _m PEG [°C] ± SD	Δc _p [J/gK] ± SD
trehalose + PEG 3350	non-collapsed	2-8	105.5 ± 2.2	91.0 ± 0.0	57.8 ± 0.2	0.179 ± 0.101
	collapsed		109.2 ± 0.1	107.3 ± 1.0	61.9 ± 0.4	0.312 ± 0.008
trehalose	non-collapsed		101.1 ± 0.6	100.6 ± -	-	0.478 ± -
	collapsed		90.2 ± 2.2	91.7 ± 1.8	-	0.409 ± 0.134
sucrose + PEG 3350	non-collapsed		- *	- *	55.7 ± 4.8	- *
	collapsed		72.9 ± 1.2	75 ± 0.1	55.1 ± 0.4	0.171 ± 0.132
trehalose + PEG 3350	non-collapsed	40		96.5 ± 0.7	56.9 ± 0.2	0.567 ± 0.045
	collapsed			96.8 ± 1.4	61.0 ± 0.1	0.316 ± 0.042
trehalose	non-collapsed			91.3 ± 4.2	-	0.719 ± 0.320
	collapsed			87.1 ± 0.0	-	1.112 ± 0.601
sucrose + PEG 3350	non-collapsed			- *	56.5 ± 2.8	- *
	collapsed			- *	60.9 ± 1.4	- *

* Glass transition temperatures could not be determined due to the overlap of the glass transition event and the PEG melting endotherm.

The melting endotherm of PEG remained unchanged over the whole period of storage and ranged between 55 °C and 60 °C. Calculated PEG crystallinities using the formula described by Izutsu et al.¹⁰⁸ were in the range of 100 % for all the samples (data not shown) using the enthalpy of melting of completely crystalline PEG 3350 bulk material as a reference.

Figure 8.40 A shows the DSC thermograms of collapsed (grey lines) and non-collapsed (black lines) trehalose-PEG-based lyophilizates prior to storage and after 26 weeks of storage at 40 °C. No change in the position and intensity of the PEG melting endotherm can be observed. In the right part of the graph, between approximately 90 °C and 110 °C, the baseline shift indicating the trehalose glass transition can be recognized. The crystallinity of PEG is further confirmed by XRD measurements as depicted in Figure 8.40 C: Two prominent peaks are observed at 19 °2θ and 23 °2θ that are assigned to crystalline PEG¹⁰⁸. The small peaks at 26.2 °2θ and 27.1 °2θ that are present in most of the samples can be related to the crystallization of the buffer salt potassium phosphate (reference: JCPDS-database). Peaks remained unchanged during the period of investigation.

Figure 8.40 B shows the DSC thermograms of collapsed (grey lines) and non-collapsed (black lines) trehalose-based lyophilizates both prior to storage and after 26 weeks of storage. Again, the decrease in glass transition temperature due to the increase in residual moisture can be observed. Interestingly, the extent of thermal overshoot, indicating the

degree of enthalpy relaxation, remained roughly unchanged in non-collapsed samples (0.7 ± 0.1 after drying versus 0.8 ± 0.03 after storage) whereas it increased in collapsed samples (0.5 ± 0.1 versus 1.6 ± 0.8). The thermal overshoot was determined by the extrapolation of the baseline after the glass transition.

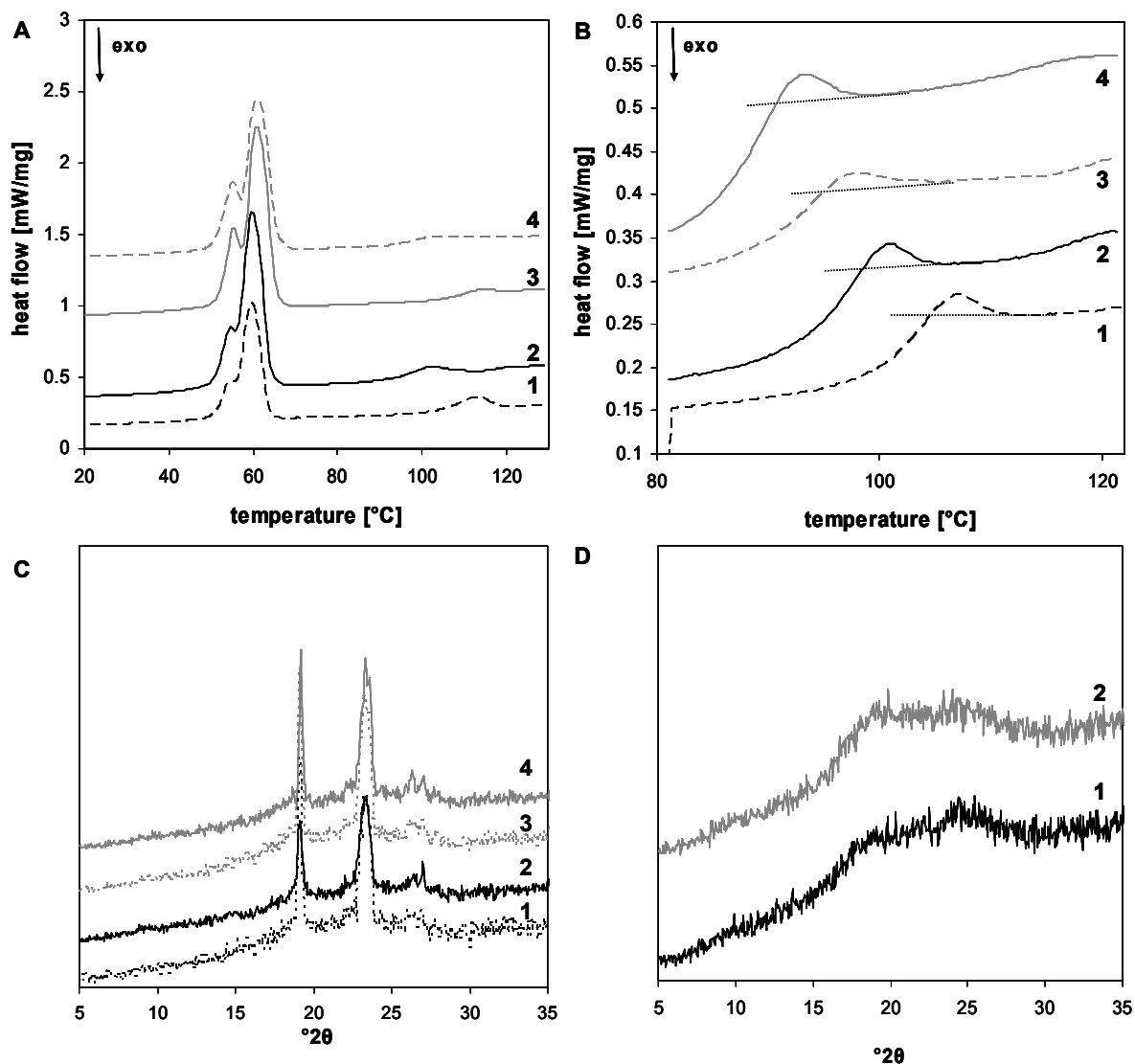


Figure 8.40: DSC thermograms of trehalose-PEG-based lyophilizates (A) and trehalose-based lyophilizates (B); X-ray diffractograms of trehalose-PEG-based lyophilizates (C) and trehalose-based lyophilizates (D).

1: non-collapsed not stored, 2: non-collapsed stored for 26 weeks at 40 °C, 3: collapsed not stored, 4: collapsed stored for 26 weeks at 40 °C; Figure D: 1: non-collapsed stored for 26 weeks at 40 °C, 2: collapsed stored for 26 weeks at 40 °C; all graphs are calculated average values of two independent measurements.

No melting endotherms of trehalose were observed indicating that trehalose remained amorphous throughout the whole period of storage. This was further confirmed by the absence of any characteristic diffraction in the X-ray diffractograms (Figure 8.40 D). To sum up the physicochemical properties of trehalose-PEG-based and purely trehalose-based lyophilizates, all samples remained stable throughout the whole period of storage, i.e., no crystallization occurred and all systems were stored in the glassy state well below the glass transition temperature. Findings presented above for samples stored at 40 °C were confirmed

by samples stored at 25 °C and 2-8 °C and samples analyzed after 2, 4, 6, 9 and 15 weeks all showed the same results as the samples analyzed after 26 weeks as presented here.

Figure 8.41 A shows the X-ray diffractograms of completely collapsed (grey line) and partially collapsed (black line) sucrose-PEG-based lyophilizates stored for 26 weeks at 40 °C and completely collapsed and partially collapsed samples prior to storage (dotted grey and black lines, respectively).

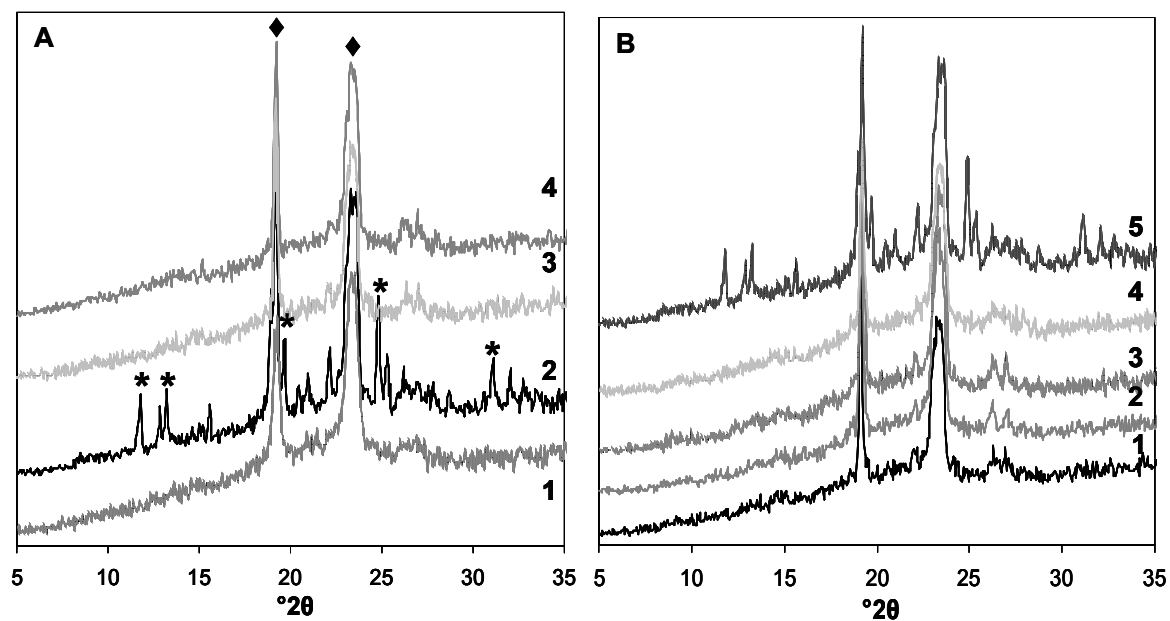


Figure 8.41: X-ray diffractograms of sucrose-PEG-based lyophilizates partially collapsed not stored (1) and stored for 26 weeks at 40 °C (2) as well as completely collapsed not stored (3) and stored for 26 weeks/40 °C (4) (A); X-ray diffractograms of partially collapsed sucrose-PEG-based lyophilizates stored at 40 °C for 0 (1), 4 (2), 9 (3), 15 (4) and 26 (5) weeks (B).

asterisks (*) mark characteristic X-ray diffraction peaks of sucrose; rhombs (♦) mark characteristic X-ray diffraction peaks of PEG; all graphs are calculated average values of two independent measurements.

Evidently, there are additional X-ray diffractions in the partially collapsed samples stored for 26 weeks at 40 °C besides the peaks at 19 °2θ and 23 °2θ assigned to crystalline PEG. In contrast, no such changes are detectable in the completely collapsed sample. The observed peaks at 11.8 °2θ, 12.8 °2θ, 19.7 °2θ, 24.8 °2θ, 25.2 °2θ and 31.2 °2θ are caused by sucrose that crystallized during storage according to Reynhardt and Chinachoti^{55,109}.

To investigate the onset of crystallization of sucrose in more detail, Figure 8.41 B shows the X-ray diffractograms of partially collapsed sucrose-PEG samples after 0, 4, 9, 15 and 26 weeks of storage at 40 °C. No crystallization was observed at storage periods shorter than 26 weeks. Additionally samples stored at 2-8 °C and 25 °C for various periods of time were analyzed and no crystallization was detected in any of these samples either (data not shown).

Crystallization of sucrose was further confirmed by the presence of a characteristic melting endotherm in the DSC thermograms at 176.8 ± 2.0 °C (data not shown) that can be assigned to the melting of crystalline sucrose (freeze-dried samples melt at 175-185 °C⁹¹; crystalline sucrose melts at 188 °C⁹¹ or at 191.5 ± 0.1 °C⁵¹). However, crystallization was not complete,

because an exothermic event assigned to sucrose crystallization was observed as well. This crystallization exotherm was present in all samples, i.e. in partially and completely collapsed cakes, but it was larger in completely collapsed cakes (17.0 J/g in partially collapsed cakes versus 23.6 J/g in completely collapsed cakes), indicating that initial crystallization (during storage, prior to DSC analysis) was less pronounced in these samples (data not shown). Crystallization occurred at lower temperatures in the partially collapsed cakes (87.6 ± 6.1 °C) than in completely collapsed cakes (117.0 ± 0.3 °C) (data not shown). This is in good agreement with literature describing a correlation between the residual moisture content and the crystallization temperature with increasing residual moistures decreasing the T_{cr} ⁹¹.

PEG crystallinity remained unchanged during storage and crystallinities were approximately 100 % in all samples (data not shown).

Summarizing, sucrose-PEG-based lyophilizates, unlike the two trehalose-based formulations, did not remain completely stable during the whole period of storage. Partially collapsed samples stored at 40 °C showed signs of sucrose crystallization after 26 weeks of storage. In contrast, completely collapsed cakes did not crystallize after the same period of storage, indicating a decreased tendency towards crystallization. This might be related to the different residual moisture contents and thus the different crystallization temperatures. Taking the different production methods into account, differences in the molecular mobility might affect the different crystallization behaviors as well, as it is described by Bhugra et al.⁴⁴.

Nevertheless, most samples (except for partially collapsed sucrose-PEG-based lyophilizates) remained in the glassy state during storage and excipients remained sufficiently stable throughout the time frame of the investigation to allow for a sound comparative investigation regarding the effect of partial and complete collapse on LDH-stability. As crystallization in sucrose-PEG-based cakes was not complete, amorphous sucrose that was sufficient to adequately stabilize the protein may be still present in the system and the effect on protein stability may be negligible.

3.2 ENZYME ACTIVITY OF LDH IN RECONSTITUTED LYOPHILIZATES

3.2.1 COLLAPSED VERSUS NON-COLLAPSED LYOPHILIZATES

An important key parameter describing a protein's stability is its biological activity. LDH is an oxidoreductase that catalyzes the oxidation of β -NADH to NAD^+ while reducing pyruvate to (S)-lactate. Because β -NADH and NAD^+ strongly differ in their absorption at 340 nm, the reaction can be monitored spectrophotometrically. As it is well described in literature that LDH activity strongly decreases upon freeze-drying in inappropriate formulations^{77,103,105,110,111}, LDH activity is a sensitive parameter to monitor the robustness of a formulation.

Figure 8.42 A displays the course of LDH catalytic activity during storage at 40 °C for up to 26 weeks as compared to the catalytic activity prior to freeze-drying. Immediately after freeze-drying, LDH activity was well preserved in all the formulations with a minimum recovery of activity of 93 %.

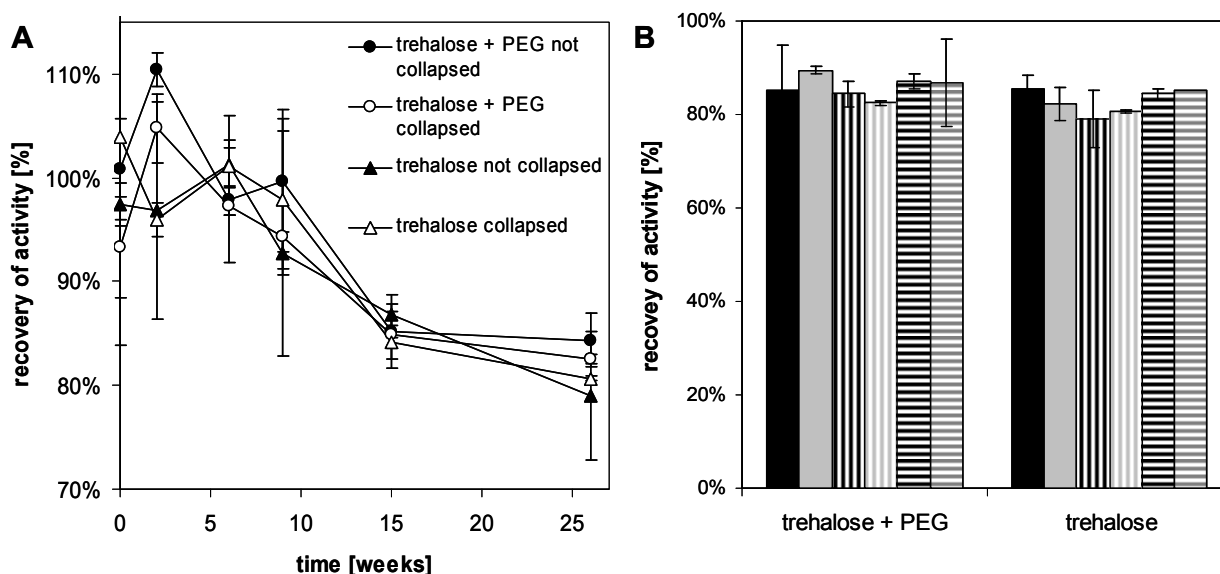


Figure 8.42: Recovery of LDH activity as compared to the activity prior to freeze-drying during storage at 40 °C (A) and after 6 months of storage at 2-8 °C, 25 °C and 40 °C, respectively (B).

Black bar: non-collapsed, stored at 25 °C, grey bar: collapsed stored at 25 °C, black-white striped bar: non-collapsed stored at 40 °C, grey-white striped bar: collapsed stored at 40 °C; black-white horizontally striped: not collapsed stored at 2-8 °C, grey-white horizontally striped: collapsed stored at 2-8 °C; n = 2.

Evidently, activities decreased during storage at 40 °C (Figure 8.42 A). Decreasing activities upon storage were also observed during storage at 25 °C and 2-8 °C. Figure 8.42 B depicts the activity after 26 weeks of storage at 2-8 °C, 25 °C and 40 °C of collapsed and non-collapsed samples, respectively. Recoveries of activity were above 78 % for all formulations and for collapsed and non-collapsed samples alike. There were no significant differences observed between collapsed and non-collapsed samples regarding the biological activity.

3.2.2 COLLAPSED VERSUS PARTIALLY COLLAPSED LYOPHILIZATES

Regarding the preservation of activity in partially collapsed cakes as compared to completely collapsed cakes, Figure 8.43 illustrates the decrease of enzyme activity in sucrose-PEG-based lyophilizates during storage at 40 °C. Recovery of activity after freeze-drying was excellent for both drying procedures. During storage activities decreased more rapidly as in trehalose-based formulations. After 26 weeks of storage, completely collapsed cakes showed a recovery of activity of 78.6 ± 0.3 % whereas partially collapsed cakes showed a lower activity of 72.7 ± 9.1 %. Although these values are not significantly different due to the large standard deviations, higher activities for completely collapsed cakes are observed throughout the whole storage period (Figure 8.43). The observed slower degradation points towards an enhanced stabilization of LDH in completely collapsed cakes as compared to

partially collapsed lyophilizates. However, this trend was not observed during storage at 25 °C.

Regarding the effect of crystallization on LDH activity, there was no sharp decrease in enzyme activity observed with the onset of crystallization in partially collapsed cakes after 26 weeks of storage. Thus an amount of amorphous sucrose sufficient to stabilize LDH remained in the amorphous state.

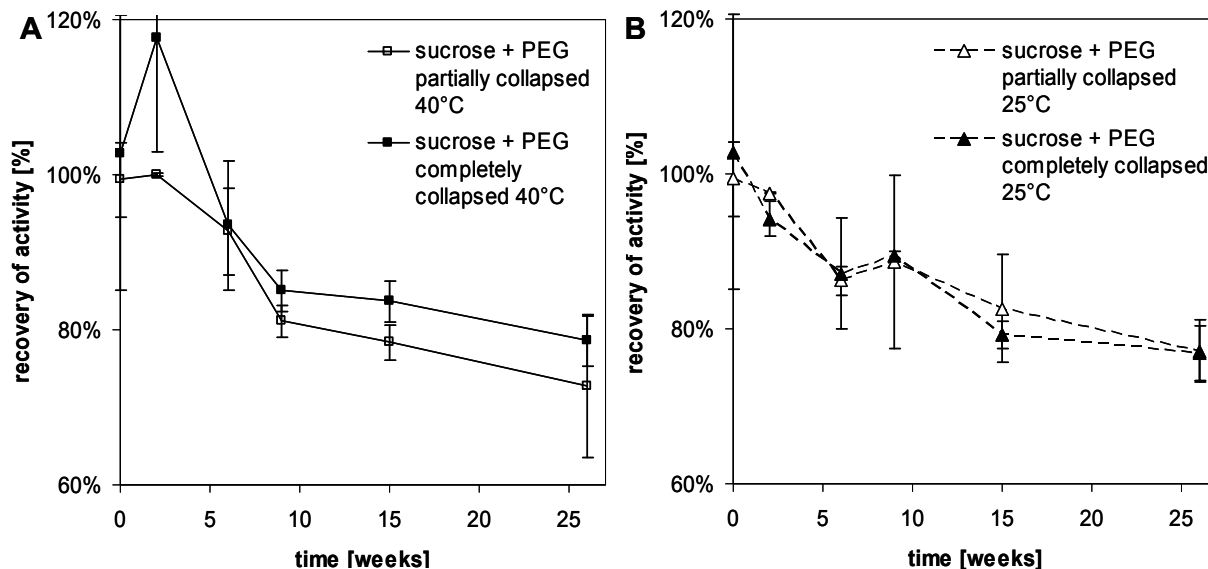


Figure 8.43: Recovery of LDH activity as compared to the activity prior to freeze-drying during storage in partially and completely collapsed sucrose-PEG-based lyophilizates at 40 °C (A) and at 25 °C (B); n = 2.

Trehalose-based formulations showed slightly increased recoveries of activities as compared to sucrose-based formulations, confirming publications describing superior solid-state-stabilizing properties of trehalose as compared to sucrose¹¹². Comparing trehalose-PEG-based lyophilizates and purely trehalose-based lyophilizates, PEG-containing samples showed slightly increased activities as well (84.3 ± 2.6 % versus 79.0 ± 6.2 % for non-collapsed cakes and 82.5 ± 0.5 % versus 80.7 ± 0.2 % for collapsed cakes). This is in agreement with Mi et al., describing the importance of PEG for the adequate preservation of LDH¹⁰². However, the observed effect was small and not consistent throughout the whole period of storage (Figure 8.42).

3.3 PHYSICAL PROTEIN STABILITY OF LDH IN RECONSTITUTED LYOPHILIZATES

LDH stability in collapsed and non-collapsed lyophilizates was further assessed by analyzing the physical stability, i.e. the formation of soluble and insoluble aggregates as well as fragments.

3.3.1 COLLAPSED VERSUS NON-COLLAPSED LYOPHILIZATES: TREHALOSE-BASED FORMULATIONS

Figure 8.44 A shows the remaining soluble LDH monomer during storage at 40 °C as compared to the monomer content prior to freeze-drying determined by HP-SEC. Purely trehalose based lyophilizates are depicted as circles and trehalose-PEG-based cakes are represented by squares, where full symbols represent non-collapsed cakes and open symbols represent collapsed plugs.

LDH physical stability was well preserved during the drying process, as indicated by high remaining monomer contents of higher than 95 % for all the formulations. Obviously, monomer contents decreased during storage. After 4 weeks of storage strongly decreased remaining monomer contents were observed in all the samples that were not confirmed after 6 weeks of storage. As all samples showed the same behavior, most probably an issue in either sample preparation or analysis caused this phenomenon.

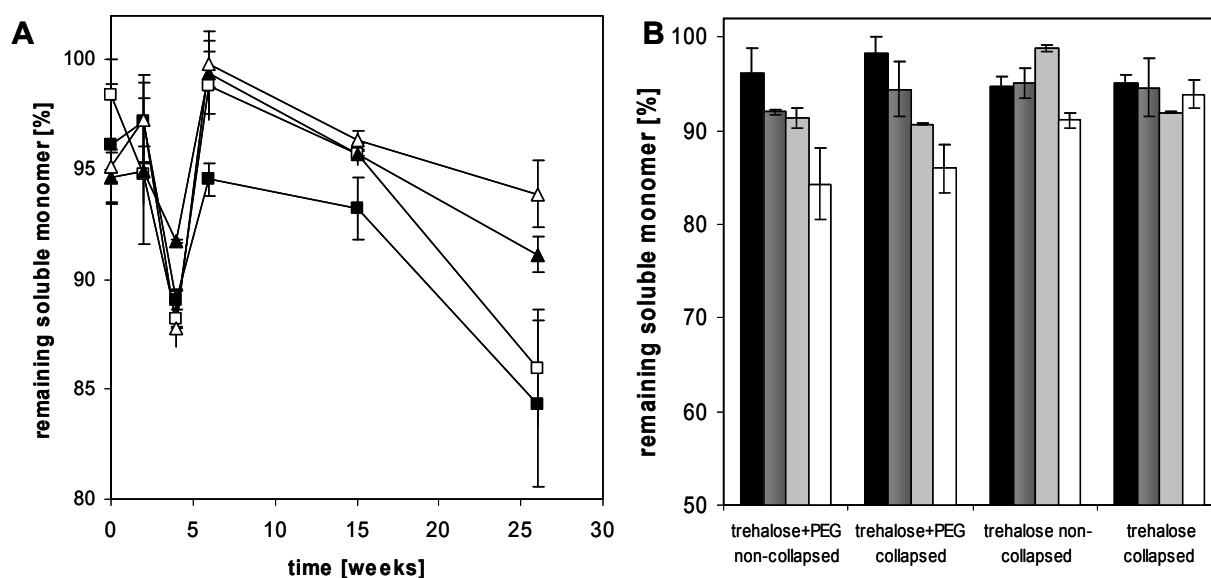


Figure 8.44: LDH remaining soluble monomer during storage at 40 °C as determined by HP-SEC (A) and LDH remaining soluble monomer immediately after freeze-drying and after 6 months of storage at various temperatures as determined by HP-SEC (B).

collapsed (open squares) and non-collapsed (full squares) trehalose-PEG-based lyophilizates and collapsed (open triangles) and non-collapsed (closed triangles) trehalose-based lyophilizates (A); samples after freeze-drying (black bars) and after 6 months of storage at 2-8 °C (dark grey bars), 25 °C (light grey bars) and 40 °C (white bars) (B); average \pm SD, n = 2.

Decreasing monomer contents were also observed in samples stored at 25 °C and 2-8 °C, but to a lesser extent. Figure 8.44 B shows monomer contents of samples stored for 26 weeks at the various temperatures investigated. Interestingly, collapsed lyophilizates showed higher remaining monomer contents as non-collapsed cakes of identical composition, as can be seen from Figure 8.44 A. Although results are not significantly different after 26 weeks of storage, a retarded degradation is observed throughout storage and monomer contents are preserved at significantly higher levels. Regarding samples stored at 25 °C and 2-8 °C, this

observation was not fully confirmed, because results cannot be regarded as significant ($p < 0.05$) (Figure 8.44 B).

In contrast to collapsed versus non-collapsed lyophilizates that showed no relevant differences, formulation apparently did have an impact on LDH physical stability. Trehalose-PEG-based lyophilizates showed clearly decreased remaining monomer contents in comparison to purely trehalose-based lyophilizates, a fact that was not observed in catalytic activity results. PEG-containing systems showed increased levels of fragments, but there was no difference detectable between collapsed and non-collapsed cakes (8.1 ± 1.3 % in non-collapsed and 8.0 ± 0.5 % in collapsed systems). As it is described in literature that LDH is susceptible to subunit dissociation upon exposure to the ice-water interface¹¹³, observed fragmentation might be related to a phase separation phenomenon due to PEG crystallization.

In addition to HP-SEC analysis, aggregation of LDH was investigated using asymmetrical flow field flow fractionation (AF4). Figure 8.45 A shows LDH dimers during storage at 40 °C of collapsed and non-collapsed samples as determined by AF4. In Figure 8.45 B also the amount of high-molecular weight aggregates is depicted. AF4 results further confirmed HP-SEC results and showed an inferior physical stability of PEG-containing formulations as compared to the purely disaccharide-based formulations, as indicated by higher dimer and higher high-molecular-weight aggregate levels (Figure 8.45 A & B: closed symbols refer to non-collapsed lyophilizates and open symbols refer to collapsed lyophilizates).

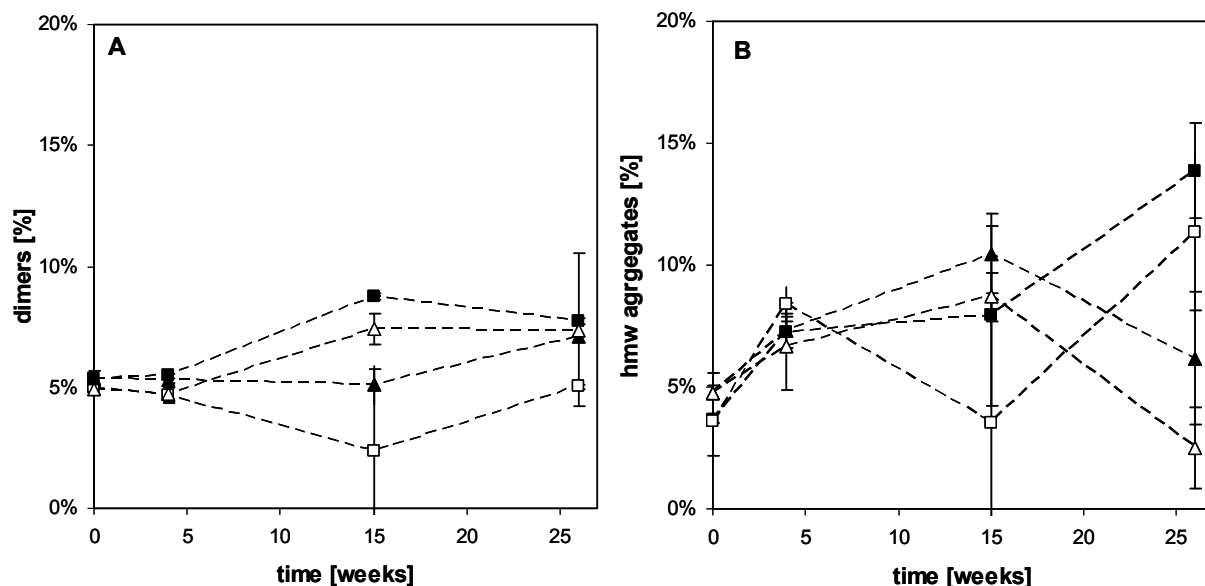


Figure 8.45: LDH aggregation during storage at 40 °C: LDH dimers as assessed by AF4 (black symbols) (A); high molecular weight (hmw) aggregates as assessed by AF4 (B).

non-collapsed (closed symbols) and collapsed (open symbols) trehalose-PG-based (squares) and trehalose-based (triangles) lyophilizates; average \pm SD, $n = 2$.

Interestingly, collapsed lyophilizates show slightly lower aggregate levels than non-collapsed lyophilizates, which was especially pronounced in hmw aggregates (Figure 8.45 B). This may

indicate a superior stabilization of LDH in collapse-dried systems. Regarding the amount of soluble aggregates as determined by HP-SEC, the opposite holds true; collapsed lyophilizates show higher aggregate levels (data not shown). To sum up the aggregation status, collapsed systems seemed to preferentially form soluble aggregates whereas non-collapsed systems show an increased formation of higher molecular weight, probably insoluble, aggregates. Bearing in mind that insoluble aggregates are associated with increased immunogenicity¹¹⁴, collapsed cakes may be regarded as the superior systems.

The insoluble aggregation of LDH was further analyzed by light obscuration. Besides the particle classes $\geq 10 \mu\text{m}$ and $\geq 25 \mu\text{m}$ that are specified in the pharmacopoeias, particles $\geq 1 \mu\text{m}$ were evaluated as well, because it is reported in literature, that the major part of sub-visible particles caused by protein aggregates is often found in the size range below $10 \mu\text{m}$ ^{114,115}. The analysis of small particles became especially important, because the dynamic light scattering analysis was unfeasible due to the interference of PEG, which has a similar hydrodynamic diameter to LDH. Figure 8.46 shows the number of particles $\geq 1 \mu\text{m}$ and $\geq 10 \mu\text{m}$ during storage at 40°C . Figure 8.46 A depicts the turbidity of the reconstituted solutions during storage at 40°C as well.

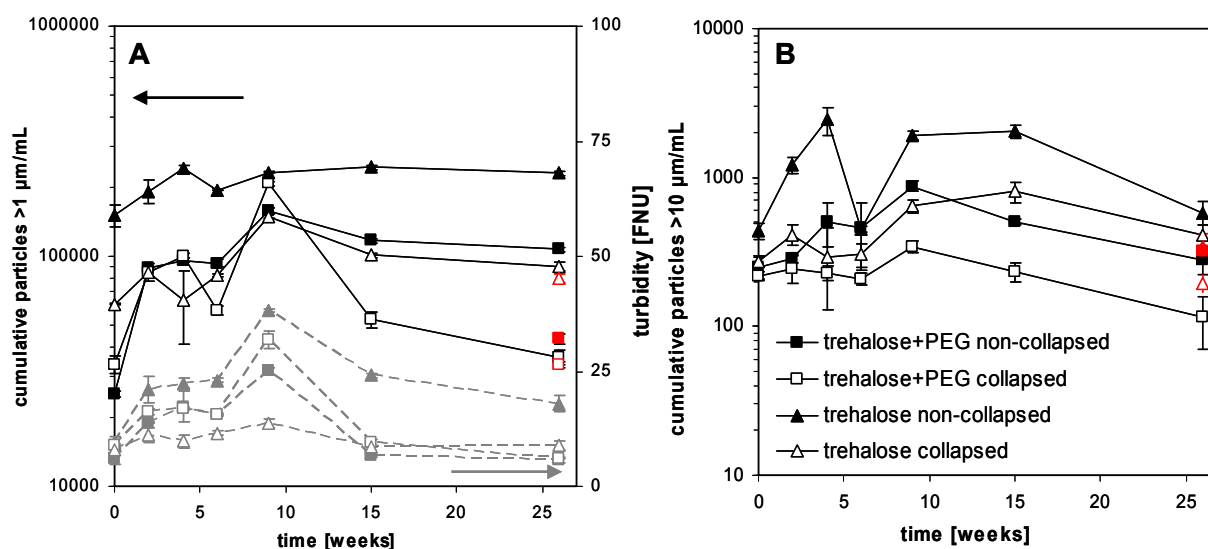


Figure 8.46: Cumulative particle numbers $\geq 1 \mu\text{m}$ as determined by light obscuration and turbidity values as determined by nephelometric turbidity measurements (A) and cumulative particle numbers $\geq 10 \mu\text{m}$ (B) during storage at 40°C .

Black symbols refer to light obscuration data and grey symbols refer to turbidity data; open symbols refer to collapsed samples and closed symbols refer to non-collapsed samples; squares refer to trehalose-PEG-based formulations, triangles refer to trehalose-based formulations, red symbols have the same meaning as black symbols and represent the cumulative particle numbers of reference samples stored at $2\text{--}8^\circ\text{C}$ for 26 weeks; average \pm SD, $n = 2$

Particle numbers did not increase significantly during freeze-drying for trehalose-PEG-based lyophilizates, but it did so in purely trehalose-based cakes ($37\,340 \pm 620$ particles larger $1 \mu\text{m}$ prior to lyophilization versus $150\,039 \pm 16\,023$ particles after conventional freeze-drying and $61\,951 \pm 354$ particles after collapse-drying). During storage particle numbers further increased but this increase was not as pronounced as the rise during freeze-drying. Particle

numbers crossed a maximum after 9 weeks of storage and after that particle numbers slightly decreased. Trends observed for particles $\geq 1 \mu\text{m}$ were also reflected in the particle numbers $\geq 10 \mu\text{m}$ (Figure 8.46 B) and in particle numbers $\geq 25 \mu\text{m}$ (data not shown).

Interestingly, purely trehalose-based formulations showed distinctly higher particle numbers than PEG-trehalose-formulations. Thus PEG, which was observed to have increased aggregate levels in SEC- and AF4-experiments, inhibited the formation of sub-visible particles, whereas purely trehalose-based formulations showed lower soluble aggregate levels, but increased particle levels.

More intriguingly, collapsed lyophilizates showed clearly lower particle numbers than non-collapsed lyophilizates of the same formulation, a trend that was also observed in AF4 results.

Findings from light obscuration analysis were further confirmed by turbidity measurements, although differences were not as distinctive.

3.3.2 COLLAPSED VERSUS PARTIALLY COLLAPSED LYOPHILIZATES: SUCROSE-BASED FORMULATIONS

Figure 8.47 A shows the course of remaining soluble monomer of LDH reconstituted from partially and completely collapsed sucrose lyophilizates during storage at 40 °C. The remaining soluble monomer after production as assessed by HP-SEC was above 95 % for both formulations. Completely collapsed cakes, dried with an aggressive drying-cycle, show a slightly decreased monomer content ($96.2 \pm 1.25 \%$ versus $100.6 \pm 5.7 \%$) but the difference was not significant due to overlapping error bars.

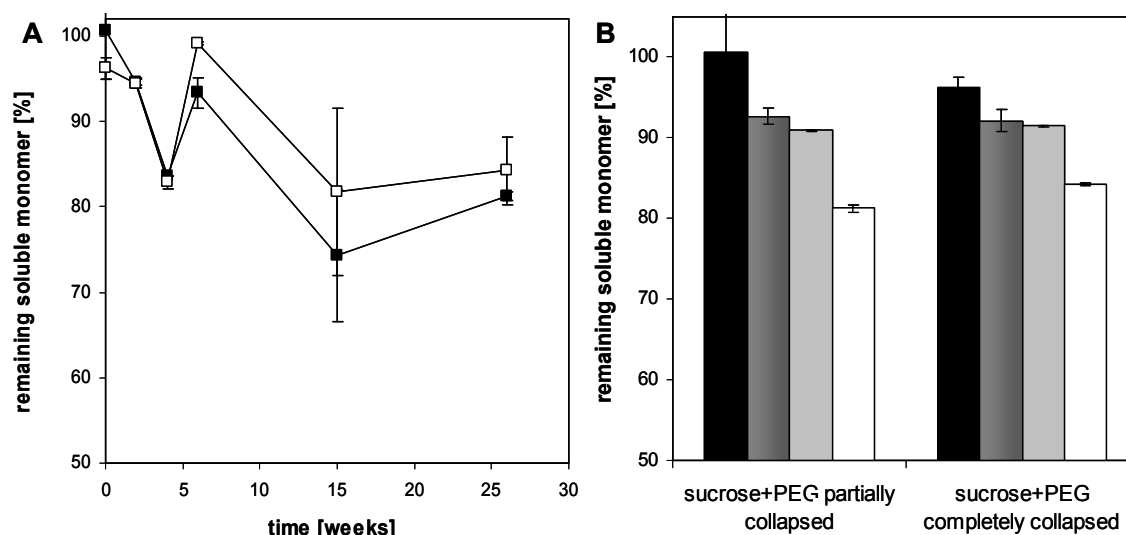


Figure 8.47: LDH remaining soluble monomer during storage at 40 °C as compared to the monomer content prior to freeze-drying as determined by HP-SEC (A) and LDH remaining soluble monomer immediately after freeze-drying and after 6 months storage at various temperatures as determined by HP-SEC (B).

collapsed (open squares) and partially-collapsed (full squares) sucrose-PEG-based lyophilizates (A); samples after freeze-drying (black bars) and after 6 months of storage at 2-8 °C (dark grey bars), 25 °C (light grey bars) and 40 °C (white bars) (B); n = 2.

Remaining monomer contents are identical during subsequent storage, but at six weeks of storage, partially collapsed cakes show significantly lower remaining monomer contents indicating a superior stabilization in collapsed lyophilizates. Although differences during subsequent storage are not significant, a trend can be concluded. This observed course corresponds well to the observed development of catalytic activities.

Figure 8.47 B shows the remaining soluble LDH monomer content after 26 weeks of storage at various temperatures. In comparison to the trehalose-based formulations, the decrease in monomer content during storage time was more pronounced. Samples stored at 25 °C and 2-8 °C showed no relevant difference between completely collapsed and partially collapsed lyophilizates.

Figure 8.48 shows the different aggregated fractions of sucrose-PEG-based LDH lyophilizates during storage at 40 °C as assessed by AF4. Partially collapsed cakes (closed symbols) showed higher amounts of lower molecular weight aggregated species as compared to completely collapsed cakes. Regarding higher molecular weight (hmw) aggregates in contrast, the trend was less clear. Partially collapsed cakes showed lower amounts of aggregates at the end of the investigated period, but during the course of the storage stability study, partially collapsed cakes frequently showed increased hmw aggregate levels.

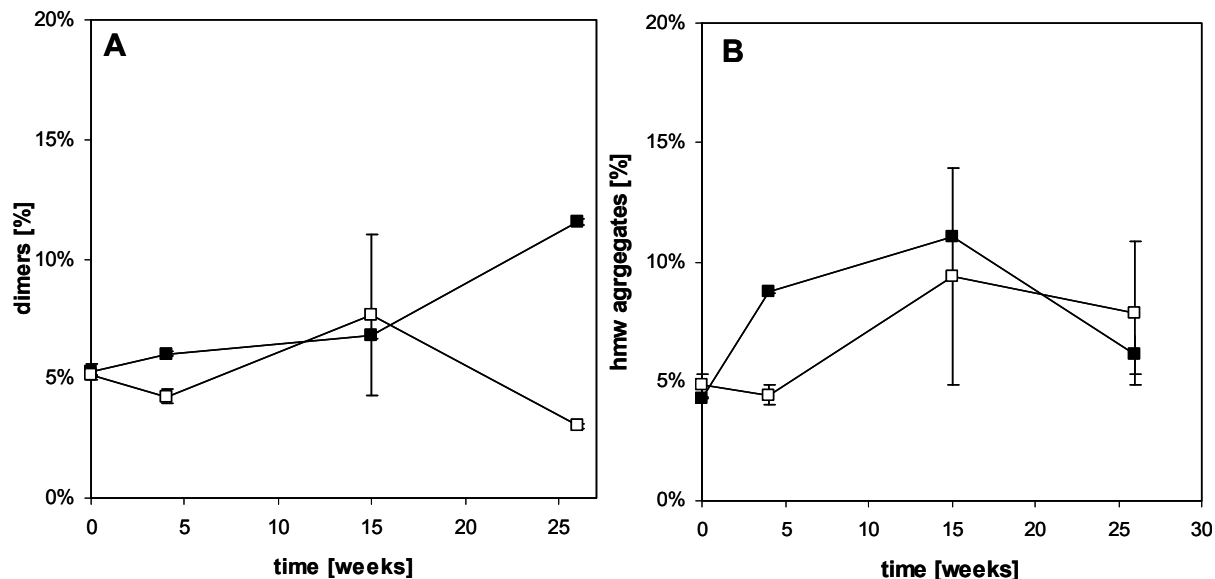


Figure 8.48: LDH aggregation during storage at 40 °C – LDH dimers as assessed by AF4 (black symbols) and soluble aggregates as assessed by HP-SEC (grey symbols) (A); high molecular weight (hmw) aggregates as assessed by AF4 (B).

partially-collapsed (closed squares) and completely-collapsed (open squares) sucrose-PEG-based lyophilizates; n = 2.

Figure 8.49 displays the course of particle numbers and turbidities of sucrose-PEG-based lyophilizates during storage at 40 °C. The table included in Figure 8.49 lists the state of particulate matter after 26 weeks of storage at 2-8 °C and 40 °C. Compared to the initial level of particles $\geq 1 \mu\text{m}$ immediately after lyophilization ($23,393 \pm 464$) (for details see Chapter 7)

partially collapsed lyophilizates showed a distinct increase during storage at 40 °C and this was also observed for particles $\geq 10 \mu\text{m}$ (256 ± 76 after lyophilization). In contrast, completely collapsed samples, that initially exhibited higher particle numbers ($40,609 + 1132$ particles $\geq 1 \mu\text{m}$; 272 ± 28 particles $\geq 10 \mu\text{m}$), did not show distinctly increased particle numbers at the end of the storage period.

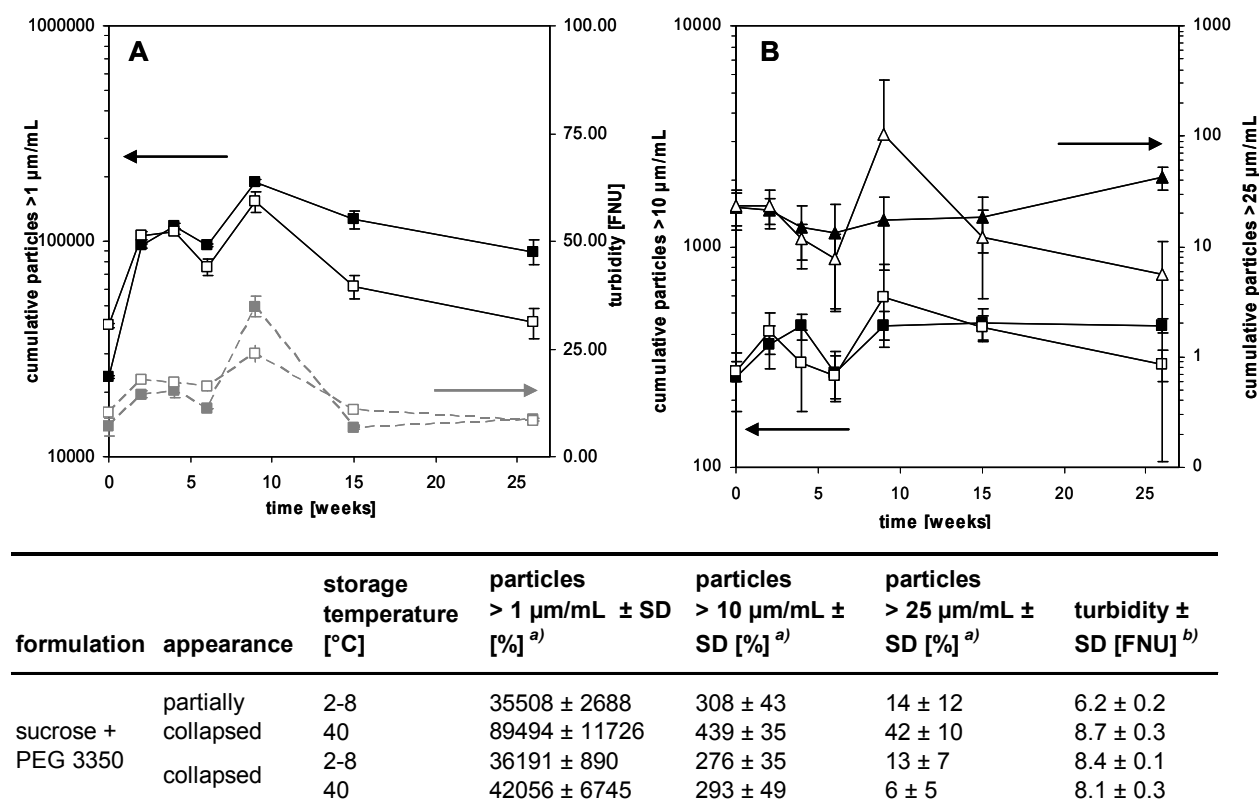


Figure 8.49: Cumulative particle numbers $\geq 1 \mu\text{m}$ as determined with light obscuration and turbidity values as determined with nephelometric turbidity measurements (A) and cumulative particle numbers $\geq 10 \mu\text{m}$ (squares) and $\geq 25 \mu\text{m}$ (triangles) (B) during storage at 40 °C.

Black symbols refer to light obscuration data and grey symbols refer to turbidity data; open symbols refer to collapsed samples and closed symbols refer to partially collapsed samples; $n = 2$.

Samples stored at 25 °C (data not shown) and 2-8 °C (table in Figure 8.49) did not allow for a discrimination of partially and completely collapsed lyophilizates.

To sum up the findings from LDH physical stability, completely collapsed systems clearly showed higher remaining monomer contents and lower levels of aggregated species fractions (dimers and high molecular weight aggregates as determined by AF4) during storage at 40 °C. Regarding the formation of sub-visible particles, collapsed systems also showed distinctly decreased particle numbers. Turbidity values further confirmed the findings, but they were not as explicit.

Lyophilizates stored at 25 °C and 2-8 °C did not allow for a clear discrimination between collapsed and non-collapsed cakes. However, this further highlights that collapsed cakes do not perform worse than non-collapsed cakes at relevant storage conditions.

Comparing the different cryo- and lyo-protectants, namely sucrose and trehalose with and without the addition of PEG 3350, the formation of soluble aggregates was strongly reduced in the purely disaccharide-based formulation, but the formation of sub-visible particles was more effectively suppressed in PEG-containing formulations. The increased particle formation in PEG-free systems could be related to the cryoprotective mechanism exerted by PEG, preventing LDH denaturation at ice-interfaces^{105,116}. Sucrose was a less effective protective agent than trehalose.

In conclusion, collapsed systems offered a slightly higher potential of LDH stabilization during storage at elevated temperatures. Partially collapsed systems however, had a clearly reduced stabilizing ability and performed worse than non-collapsed systems. Thus by the intentional introduction of collapse, the accidental occurrence of partial collapse during a conservative freeze-drying run can be reliably avoided and consequently also the risk of a compromised storage stability.

3.4 CONFORMATIONAL STABILITY OF LDH IN RECONSTITUTED LYOPHILIZATES

In order to complement investigations on LDH physical stability, the protein's conformational stability was analyzed as well. It is well described in literature, that LDH secondary structure and its catalytic activity are closely coupled¹¹⁷ and that the preservation of the native conformation during drying is mandatory for adequate stabilization

3.4.1 COLLAPSED VERSUS NON-COLLAPSED LYOPHILIZATES: TREHALOSE-BASED LYOPHILIZATES

Figure 8.50 shows the FTIR second derivative spectra of reconstituted LDH in the amide I region.

The secondary structural alterations of LDH during the freeze-drying run were negligible. All formulations showed a slight increase in β -sheet structure, that is commonly reported for freeze-dried formulations due to the lower degree of hydrogen-bonding to water as compared to α -helical structures⁸⁷. They are discussed in detail in Chapter 7 of this thesis. Figure 8.50 describes the change in secondary structure during lyophilizate storage at 40 °C. Samples stored at 2-8 °C and 25 °C behaved similarly (data not shown).

The main bands at 1656 cm^{-1} and 1638 cm^{-1} arise from α -helical and β -sheet structures, respectively⁸⁰. Figure 8.50 A and Figure 8.50 B show LDH reconstituted from non-collapsed and collapsed trehalose-PEG-based lyophilizates, respectively, Figure 8.50 C and Figure 8.50 D display LDH from non-collapsed and collapsed purely trehalose-based lyophilizates, respectively. Considering the spectra recorded immediately after lyophilization (red spectra in Figure 8.50), PEG-containing systems generally showed lower degrees of β -sheet structures immediately after freeze-drying, as indicated by the lower intensity of the

band around 1638 cm^{-1} . This was also described by Prestrelski et al, who observed full structural preservation only in systems containing PEG¹¹⁸.

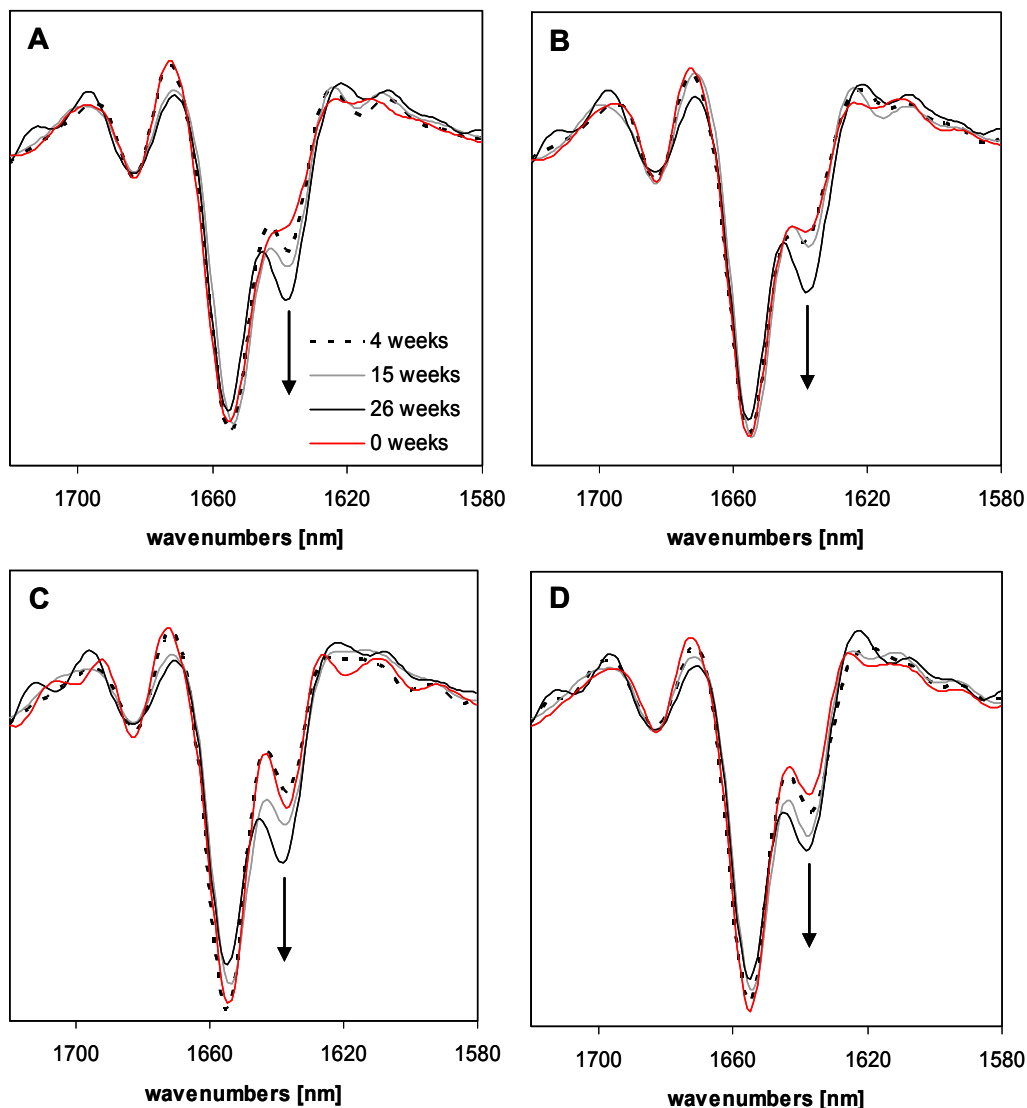


Figure 8.50: Preservation of LDH secondary structure: Area-normalized second derivative FTIR transmission spectra of non-collapsed (A, C) and collapsed (B, D) trehalose-PEG- (A, B) and purely trehalose- (C, D) based lyophilizates after 0, 4, 15 and 26 weeks of storage at $40\text{ }^{\circ}\text{C}$; Spectra are calculated average spectra of two independent measurements ($n = 2$).

All systems showed increasing β -sheet contents during storage at $40\text{ }^{\circ}\text{C}$ as indicated by increasing intensities of the band at 1638 cm^{-1} . Comparing LDH secondary structure to a heat denatured sample (see Figure 7.29), a strong augmentation of that band upon thermal denaturation can be observed. Thus one may consider an intensity-increase as predictive for a beginning of unfolding.

To further point out the spectral changes upon storage, Figure 8.51 A displays the ratios of the main band at 1656 cm^{-1} to the band at 1638 cm^{-1} as adapted from Abdul-Fattah et al.²⁰ and Figure 8.51 B presents the ratio of the main band at each time point as compared to the intensity of that band prior to lyophilization as described by Wang et al.¹¹⁹.

Most obviously, the ratio $1656/1638\text{ cm}^{-1}$ increased during storage. Purely trehalose-based systems (triangles) showed higher ratios as PEG-trehalose-based systems in non-collapsed systems, confirming conclusions from the visual inspection of the spectra. However, collapsed systems did not show a significantly different ratio between systems with or without the addition of PEG. Interestingly, collapsed systems generally showed a decreased ratio, indicating a decreased extent of β -sheet formation after 26 weeks of storage. The findings were further confirmed by comparing the intensity of the main band at various time points to the main band prior to lyophilization (Figure 8.51 B). PEG-containing systems resulted in ratios close to 1, indicating almost complete preservation of native conformation, whereas ratios for purely trehalose-based formulations were slightly decreased. All collapsed systems showed better structural conservation than non-collapsed systems of the same composition.

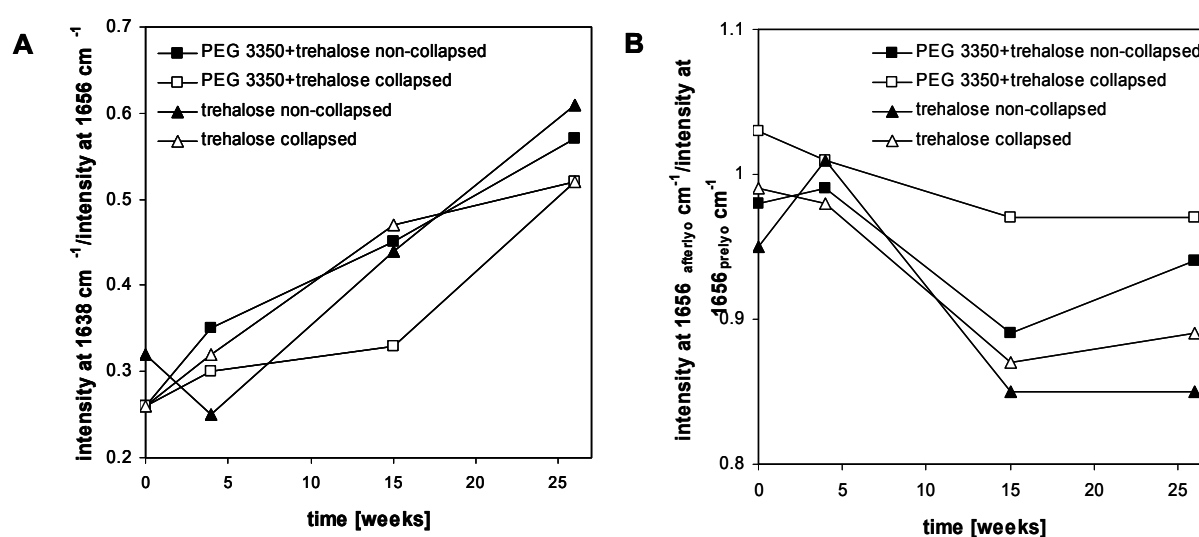


Figure 8.51: Preservation of LDH secondary structure during storage at 40 °C: ratio of the intensity of the main band at 1656 cm^{-1} to the intensity of the band at 1638 cm^{-1} (A); ratio of the intensity of the main band at 1656 cm^{-1} after defined periods of storage in the solid state as compared to the intensity of the main band prior to lyophilization (B).

Figure 8.52 displays intrinsic tryptophan fluorescence spectra of collapsed and non-collapsed LDH lyophilizates after varying periods of storage. During lyophilization, tertiary structure was completely preserved and no deviation from the LDH standard could be observed. The emission maximum at 344 nm is in agreement with literature¹²⁰ and classifies LDH tryptophan residues as appertained to the spectral form II in which the indole chromophore is located at the protein surface which is commonly observed in many proteins¹²¹. During storage, fluorescence intensity decreases, but no shift in the emission maximum is observed, indicating that no major tertiary structural changes occurred. However, it is described in literature that LDH denaturation is not associated with a shift of the emission maximum¹²⁰. Comparing the decrease in intensity to that observed in a heat denatured LDH standard (see Figure 7.30), the detected decrease during storage was by far not that pronounced, further confirming, that no major tertiary structural changes occurred.

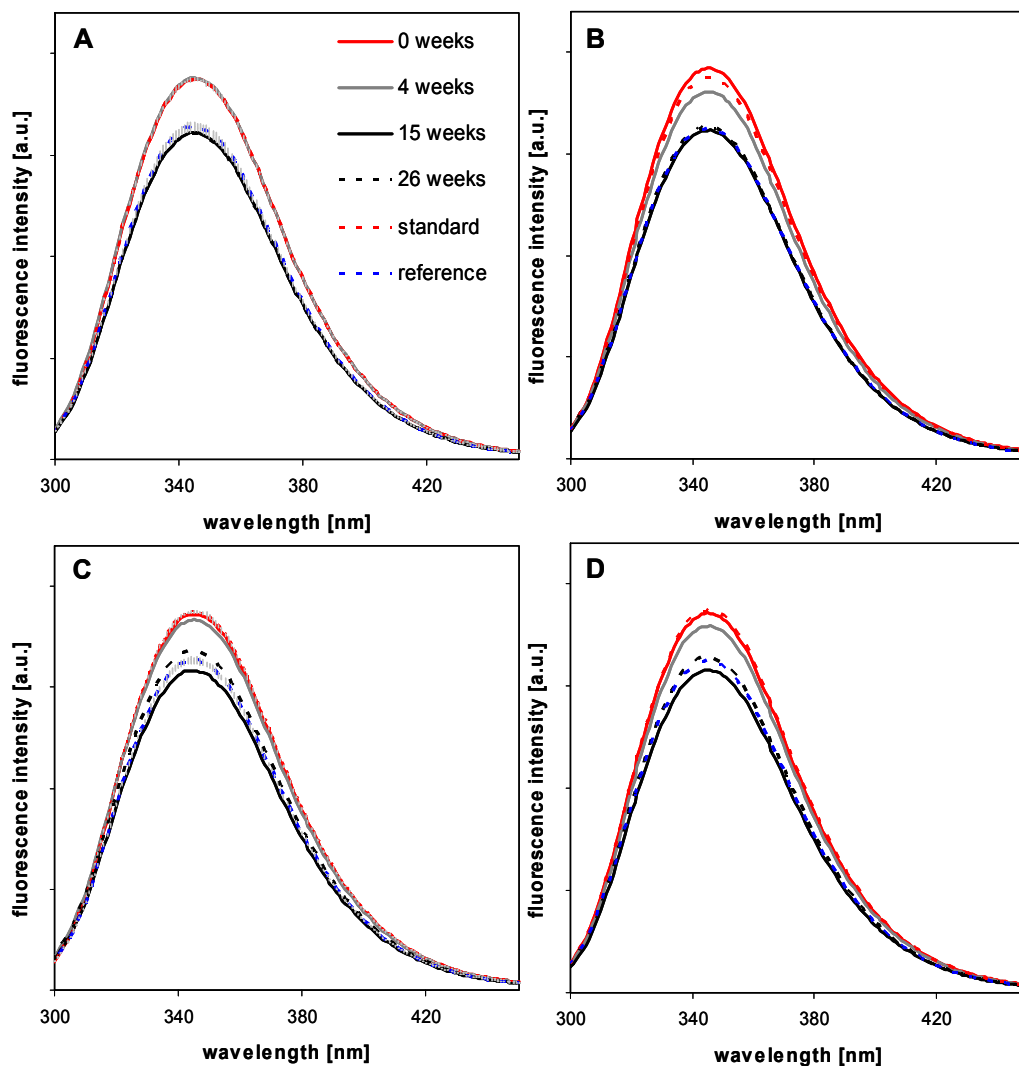


Figure 8.52: Intrinsic protein fluorescence emission spectra of LDH stored for different periods of time in trehalose + PEG-based non-collapsed (A), collapsed (B), purely trehalose-based non-collapsed (C) and collapsed (D) lyophilizates, respectively.

Excitation wavelength was 280 nm, measurements were performed at a constant temperature of 20 °C; spectra are calculated average spectra of two independent measurements ($n = 2$).

Comparing collapsed and non-collapsed lyophilizates of the same formulation (A versus B/trehalose-PEG and C versus D/trehalose), collapsed systems already showed a pronounced decrease in fluorescence intensity after 4 weeks, whereas the intensity of the non-collapsed systems remained similar to the LDH standard. However, after 6 weeks of storage at 40 °C, intensities of non-collapsed systems went down as well (Figure 8.53) and remained similar to that of the collapsed systems throughout the remaining storage period. Spectra collected after 2, 6 and 9 weeks of storage, as well as samples stored at 25 °C and 2-8 °C are not included in Figure 8.52 for the sake of clarity of the diagram, but they showed similar results and further confirmed the depicted trends.

Reference samples stored at 2-8 °C for 26 weeks showed fluorescence intensities comparable to the fluorescence intensities of samples stored at elevated temperatures,

indicating that slight perturbations of tertiary structure were not related to elevated temperature stress.

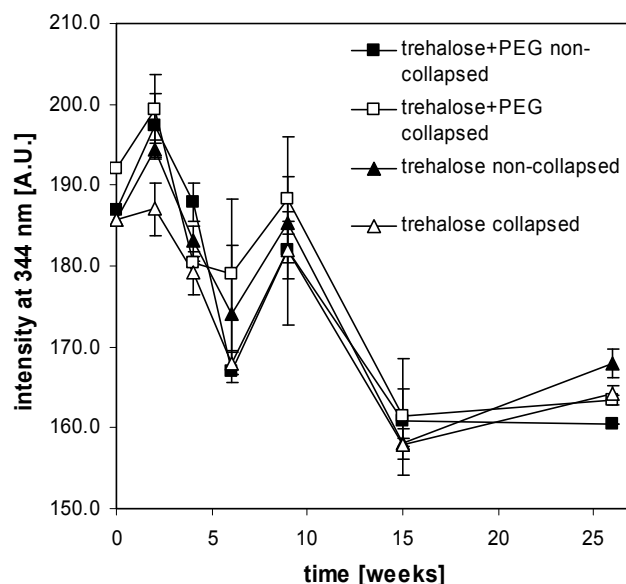


Figure 8.53: Intrinsic tryptophan fluorescence intensity at the emission maximum at 344 nm after excitation at 280 nm during storage at 40 °C; n = 2.

3.4.2 COLLAPSED VERSUS PARTIALLY COLLAPSED LYOPHILIZATES: SUCROSE-BASED LYOPHILIZATES

Figure 8.54 depicts second derivative FTIR transmission spectra of LDH reconstituted from partially collapsed (A) and completely collapsed (A) sucrose-PEG-based lyophilizates. As observed for the trehalose-based lyophilizates, the intensity of the band at 1638 cm^{-1} increased during storage.

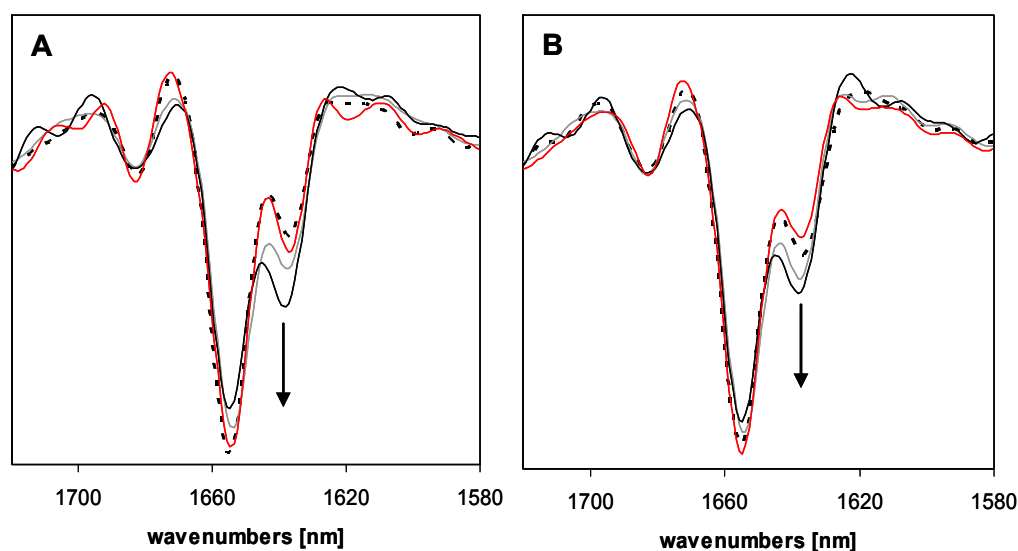


Figure 8.54: Preservation of LDH secondary structure: Area-normalized second derivative FTIR transmission spectra of partially collapsed (A) and completely collapsed (B) sucrose-PEG-based lyophilizates after 0, 4, 15 and 26 weeks of storage at 40 °C.

0 weeks (red curve), 4 weeks (black dotted curve), 15 weeks (grey curve), 26 weeks (black curve) of storage at 40 °C; spectra are calculated average spectra of two independent measurements (n = 2).

Figure 8.55 depicts the ratios calculated as described above. In contrast to findings from physical stability data, completely collapsed cakes exhibit slightly less preserved native conformation as indicated by higher intensities of the band at 1638 cm^{-1} and decreased intensities of the band at 1656 cm^{-1} . However, overall structural alterations were small, as indicated by a high normalized peak height ratio.

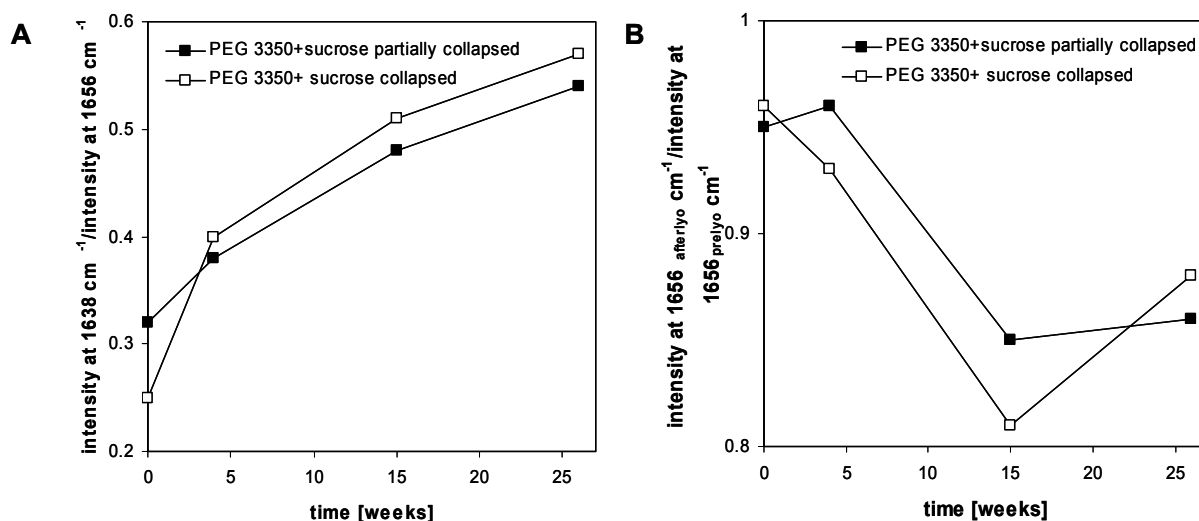


Figure 8.55: Preservation of LDH secondary structure during storage at $40\text{ }^{\circ}\text{C}$: ratio of the intensity of the main band at 1656 cm^{-1} and the intensity of the band at 1638 cm^{-1} , for LDH reconstituted from two different formulations (A); ratio of the intensity of the main band at 1656 cm^{-1} after defined periods of storage in the solid state as compared to the intensity of the main band prior to lyophilization (B).

Fluorescence spectroscopic data pointed into a similar direction. As found for the trehalose-based systems, there was no alteration in fluorescence emission observed immediately after lyophilization.

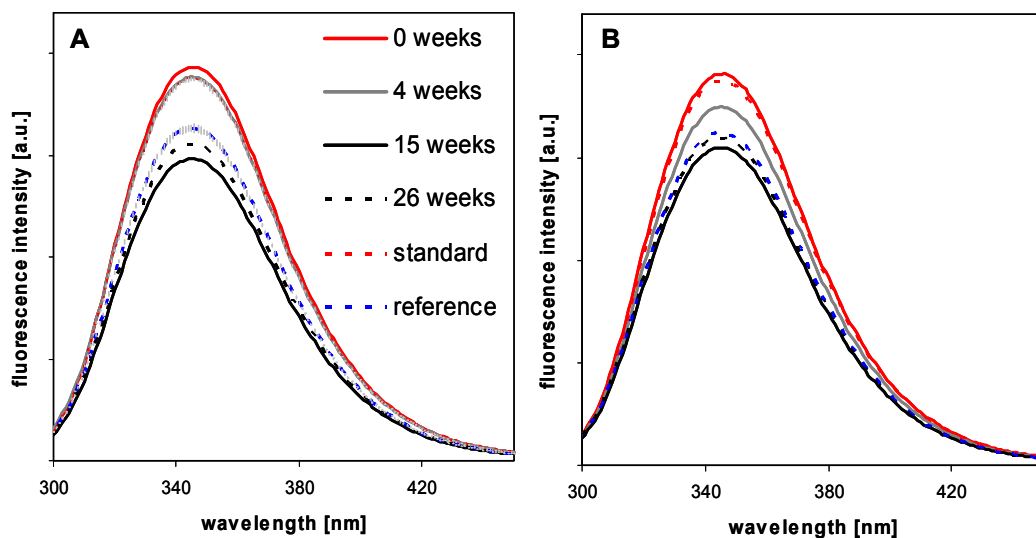


Figure 8.56: Intrinsic protein fluorescence emission spectra of reconstituted LDH stored for different periods of time at $40\text{ }^{\circ}\text{C}$ in sucrose-PEG-based partially collapsed (A) and completely collapsed (B) lyophilizates; $n = 2$.

During storage however, fluorescence intensity decreased, but, as for the trehalose cakes, no shift in emission maximum was observed. This decrease in fluorescence intensity was developed more pronounced in completely collapsed cakes after 4 weeks of storage at 40 °C (Figure 8.56 A).

However, considering the decrease of fluorescence intensity throughout the complete storage time at 40 °C, as depicted in Figure 8.57, a large standard deviation at the 4 weeks time point is observed. Considering the further development of fluorescence intensities, partially collapsed systems showed fluorescence intensities comparable to collapsed cakes after 6 weeks of storage and they remained comparable throughout the remaining storage time. Partially collapsed cakes even exhibited slightly decreased quantum yields (Figure 8.57), but intensities were not relevantly different.

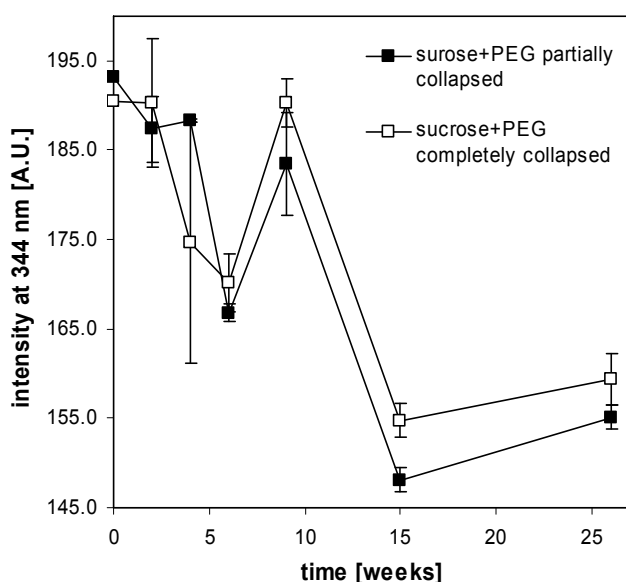


Figure 8.57: Intrinsic tryptophan fluorescence intensity at the emission maximum at 344 nm after excitation at 280 nm during storage at 40 °C; n = 2.

Comparing sucrose- and trehalose based systems, findings from physical stability data were further confirmed, indicating a decreased stabilizing potential of sucrose.

To sum up the findings from the conformational stability assessment, the preservation of native conformation, regarding both secondary and tertiary structure, was high for all the formulations, no matter whether the material had collapsed or not.

Regarding secondary structure, all formulations experienced an increase in the band at 1638 cm^{-1} in the second derivative FTIR-transmission spectra, that is associated with β -sheet structures and can be regarded as a precursor for denaturation, as it is the major band in the thermally denaturated state. Trehalose-based formulations showed better native-state preservation in collapsed systems, whereas sucrose-based formulations indicated a slightly inferior performance of completely collapsed systems as compared to partially collapsed systems.

Tertiary structure as assessed by intrinsic tryptophan fluorescence did not show as explicit results as secondary structure. All formulations showed a decrease in fluorescence intensity upon storage, but there were no significant differences between collapsed and non-collapsed systems.

3.5 SUMMARY AND CONCLUSION

The effect of lyophilizate collapse on protein stability was investigated using LDH as a second, sensitive model protein. Completely collapsed as well as partially collapsed cakes were included in this examination and samples were stored for up to 6 months (26 weeks) at elevated temperatures, i.e. at 25 °C and 40 °C. Reference samples were stored at 2-8 °C. Protein stability was assessed analyzing biological activity, the formation of soluble and insoluble aggregates as well as conformational stability as sensitive stability parameters. To further complete the investigation, excipient stability was examined as well.

Excipients remained stable and analysis was carried out in the glassy state, as indicated by a glass transition temperature well above the highest storage temperature, allowing for a sound evaluation of the effect of collapse on LDH stability. Partially collapsed, sucrose-containing lyophilizates however, had crystallized to some extent after 26 weeks of storage at 40 °C, but there was sufficient amorphous sucrose left to adequately stabilize LDH, as no sharp drop in LDH activity was observed.

LDH catalytic activity was minimum 70 % for all the formulations after 26 weeks of storage at 40 °C, thus given the extreme sensitivity of LDH as a model protein, enzyme stabilization was satisfying throughout the period of storage. There was no significant difference between collapsed and non-collapsed systems.

Regarding LDH physical stability, remaining monomer contents were greater than 80 % for all the formulations after 26 weeks of storage at 40 °C. Collapsed systems showed distinctly higher monomer contents and lower amounts of higher molecular weight aggregates than non-collapsed systems of identical formulation. Soluble aggregates as determined by HP-SEC were slightly increased in collapsed cakes, pointing towards the preferred formation of soluble aggregates at the expense of insoluble aggregates. This was further confirmed by strongly reduced numbers of sub-visible particles in collapsed systems as compared to non-collapsed systems.

Comparing the different formulations, PEG-containing lyophilizates showed a distinctly reduced formation of sub-visible particles as determined by light obscuration, but they also showed an increased formation of soluble aggregates, as indicated by decreased remaining monomer contents and increased fractions of dimers and hmw aggregates. The opposite held true for purely trehalose-based formulations. Given the potential risk of severe immunogenicity reactions due to insoluble aggregates, PEG-containing formulations have to

be regarded as superior, further confirming publications by Mi et al. and Prestrelski et al. who described the importance of PEG for adequate LDH stabilization^{102,118}.

Conformational LDH stability was assessed by FTIR- and intrinsic tryptophan fluorescence-spectroscopy. Generally, overall native conformation preservation was good. All samples showed an increase in β -sheet structure and a decrease in tryptophan fluorescence intensity, which indicates a higher polarity in the tryptophan environment that is possibly associated with a positioning closer to the molecules surface, but alterations were small. Regarding the trehalose-based formulations, collapsed systems clearly showed a better preservation of secondary structure, but there were no significant differences in tertiary structural preservation. Sucrose-based systems showed no relevant difference in the structural stability of partially collapsed and completely collapsed cakes.

To sum up findings from the LDH storage stability study, there was no negative effect of collapse on LDH stability observed. Collapsed systems not even performed equally well during storage at elevated temperatures, but performed better concerning several key stability indicating parameters, such as the formation of soluble and insoluble aggregates. Regarding other important parameters, e.g. the native state preservation and the enzymatic activity, collapsed cakes preserved LDH as well as non-collapsed cakes.

Thus findings gained from the investigation of the effect of collapse on IgG₀₁ storage stability could be confirmed using LDH as a more sensitive model protein that did show clear degradation throughout the storage period and that therefore allowed for a clear discrimination of the different levels of stability if there would have been any.

4 TISSUE-TYPE PLASMINOGEN ACTIVATOR (PA₀₁)

In order to complement the investigations on the effect of lyophilizate collapse on the long term stability of a monoclonal antibody and L-Lactic Dehydrogenase, tissue-type plasminogen-activator (PA₀₁) was evaluated as a third model protein. PA₀₁ is marketed in an approved pharmaceutical drug, thus findings are of remarkable interest for the practical application.

Because PA₀₁ is poorly water soluble, L-arginine is an important formulation component to enhance the molecule's solubility. The addition of comparably high amounts of L-arginine creates a relatively high concentrated freeze-dry solution (approximately 9 %) that is difficult to dry and prone to partial collapse. Furthermore, the addition of L-arginine changes the collapse-behavior of the system, because no foam is formed upon collapse-drying but a sponge-like structure (see Figure 7.36 B). Thus investigating PA₀₁ should enlarge our knowledge about a collapsed system with a different macroscopic and microscopic texture.

In Chapter 7, the effect of cake-collapse on PA₀₁ integrity immediately after lyophilization was discussed. Comparable stability was observed for elegant and collapsed cakes. In the following section, results regarding the PA₀₁ stability during storage at elevated temperatures are discussed. Collapsed and non-collapsed, elegant lyophilizates of identical composition were produced by freeze-drying PA₀₁ bulk solution either with a collapse-protocol or with a conventional freeze-drying protocol, as described in Chapter 3. Samples were stored for 15 weeks at 50 °C and reference samples were stored at 2-8 °C. After 0, 4, 9 and 15 weeks the stability of the protein as well as that of the excipients were analyzed using a broad set of analytical tools, taking into account biological, physical and conformational stability.

4.1 PHYSICO-CHEMICAL PROPERTIES OF COLLAPSED AND NON-COLLAPSED LYOPHILIZATES

Figure 8.58 depicts PA₀₁ cakes after storage at 50 °C for 15 weeks. Cake appearance remained unchanged during storage at 50 °C and no collapse of the elegant cakes occurred during storage.



Figure 8.58: Macroscopic appearance of collapsed and non-collapsed PA₀₁ lyophilizates after storage. Non-collapsed (left) and collapsed (right) lyophilizates after storage at 50 °C for 15 weeks.

Reconstitution times were not relevantly different for collapsed and non-collapsed cakes (< one minute) and they did not change during storage either.

Glass transition temperatures of collapsed and non-collapsed cakes were well comparable after freeze-drying (T_g was 84.0 ± 1.6 °C in non-collapsed versus 82.8 ± 0.4 °C in collapsed cakes). During storage, glass transition temperatures slightly decreased, as shown in Figure 8.59 A (black lines). This was most probably caused by the small increase in residual moisture (Figure 8.59 A, grey dashed lines), observed during storage at elevated temperatures. This is a phenomenon frequently observed during storage of freeze-dried solids^{25,122}. Because the vials were sealed in aluminum bags to prevent moisture uptake from the surroundings due to water vapor permeability of the stoppers, the increase in residual moisture was most likely caused by the transfer of water from the stoppers into the lyophilizate. However, the observed increase in residual moisture was small (3.7 ± 0.1 % and 3.91 ± 0.3 % at the beginning of the storage period in non-collapsed and collapsed cakes, respectively; 4.5 ± 0.1 % and 4.3 ± 0.1 % in non-collapsed and collapsed cakes, respectively after 15 weeks of storage at 50 °C). Importantly, collapsed and non-collapsed lyophilizates showed comparable residual moisture level that did not differ more than the previously specified deviation of 0.5 %.

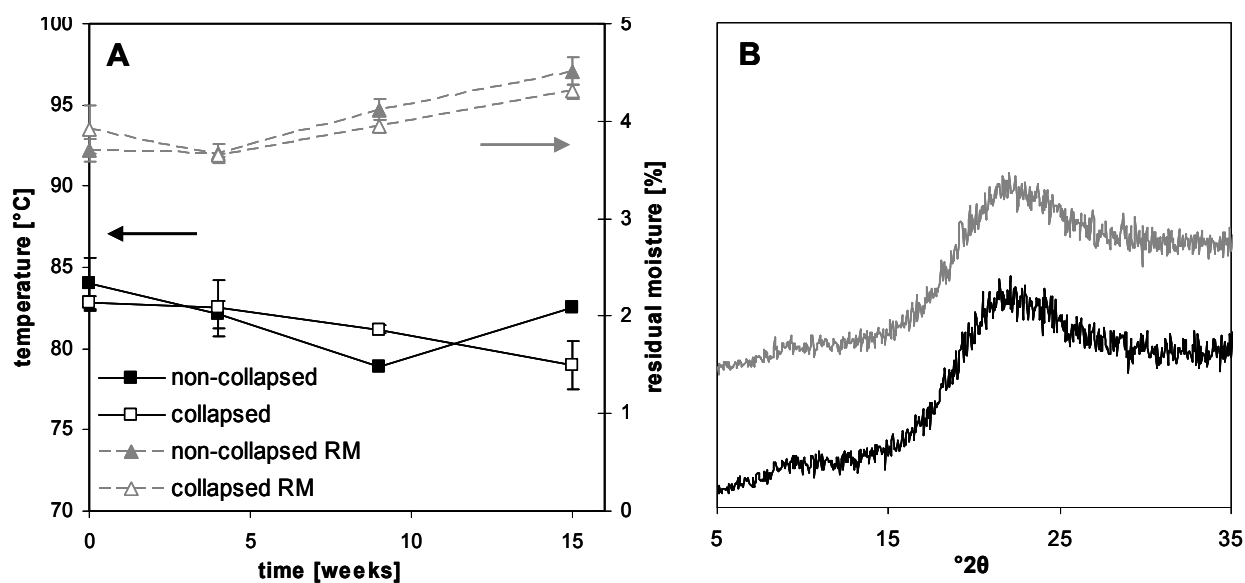


Figure 8.59: Residual moisture levels and glass transition temperatures of collapsed and non-collapsed PA₀₁ lyophilizates during storage at 50 °C (A) and X-ray diffraction pattern after 15 weeks of storage at 50 °C (B); n = 2.

Samples stored at 2-8 °C behaved similarly, since the residual moisture increase was not as pronounced (4.0 ± 0.1 % and 4.0 ± 0.0 % after 15 weeks of storage in non-collapsed and collapsed cakes, respectively) as after storage at 50 °C. Consistently, the glass transition temperatures decreased as well. However, irrespective of the observed decrease, all formulations had glass transition temperatures well above the storage temperature of 50 °C.

Thus all systems remained in the glassy state throughout the storage period, allowing for a sound investigation that is not affected by the transition from the glassy to the rubbery state. Excipients remained amorphous, as indicated by the absence of any diffraction in the X-ray analysis (Figure 8.59 B) and by the absence of characteristic melting endotherms in the DSC thermograms (data not shown).

To sum up the physicochemical properties of collapsed and non-collapsed lyophilizates during storage at 2-8 °C and 50 °C, all components remained stable throughout the investigation period, i.e. they remained amorphous and well in the glassy state, thus allowing a sound investigation of the effect of collapse on PA₀₁ long-term stability.

4.2 CATALYTIC ACTIVITY OF PA₀₁ IN RECONSTITUTED LYOPHILIZATES

The most critical quality-indicating parameter of a biotechnological drug is its biological activity. Physiologically, PA₀₁ activates plasminogen in the presence of fibrin and the formed plasmin then leads to clot lysis. Clinically, PA₀₁ is used as an emergency drug in the management of acute myocardial infarctions, acute massive pulmonary embolisms and acute ischemic strokes¹²³.

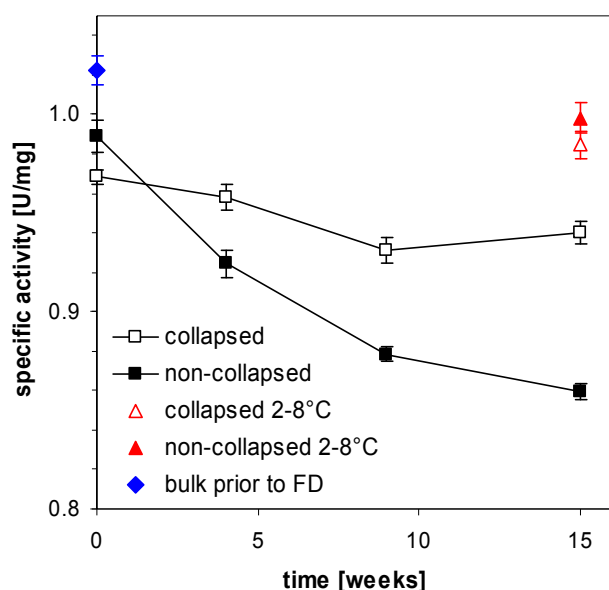


Figure 8.60: Activity of PA₀₁ after reconstitution from collapsed and non-collapsed lyophilizates during storage at 50 °C as compared to the enzyme activity prior to freeze-drying and to the activity of samples stored at 2-8 °C as determined by the clot lysis assay.

The assay was performed using reconstituted solutions from two different vials for each formulation.

The *in vitro* catalytic activity was determined according to the assay described by Carlson et al¹²⁴, by mixing PA₀₁, fibrinogen, plasminogen and thrombin and monitoring the optical density at 340 nm indicating the presence of insoluble material. Figure 8.60 displays the catalytic activity of PA₀₁ reconstituted from collapsed and non-collapsed lyophilizates after defined periods of storage at 50 °C.

Freeze-drying caused a decrease in catalytic activity as compared to the activity prior to lyophilization (blue diamond). PA₀₁ reconstituted from collapsed lyophilizates immediately after freeze-drying showed lower catalytic activity than PA₀₁ reconstituted from elegant cakes, but the difference was below the described assay-accuracy of 5 %¹²⁴. However, during storage at 50 °C, clot-lytic activity decreased more rapidly in non-collapsed systems. After 15 weeks of storage collapsed cakes showed an activity of 0.94 ± 0.01 U/mg whereas the activity in non-collapsed cakes had decreased to 0.86 ± 0.00 U/mg. Activity in samples stored at 2-8 °C did not relevantly change and there was no significant difference between collapsed and elegant cakes (0.99 ± 0.01 U/mg and 1.00 ± 0.01 mg in collapsed and non-collapsed cakes, respectively). Interestingly, the initially observed slight difference between collapsed and elegant cakes was not confirmed upon storage, but in contrast, collapsed cakes showed a better stabilization of PA₀₁ during storage at elevated temperatures.

4.3 PHYSICAL PROTEIN STABILITY OF PA₀₁ IN RECONSTITUTED LYOPHILIZATES

PA₀₁ stability in collapsed and non-collapsed lyophilizates was assessed by monitoring physical protein stability, i.e. the formation of soluble and insoluble aggregates. Figure 8.61 shows the decrease of the remaining soluble monomer (Figure 8.61 A) and the concurrent increase of dimers and higher molecular weight (hwm) aggregates (Figure 8.61 B) during storage in collapsed (open symbols) and elegant (closed symbols) lyophilizates.

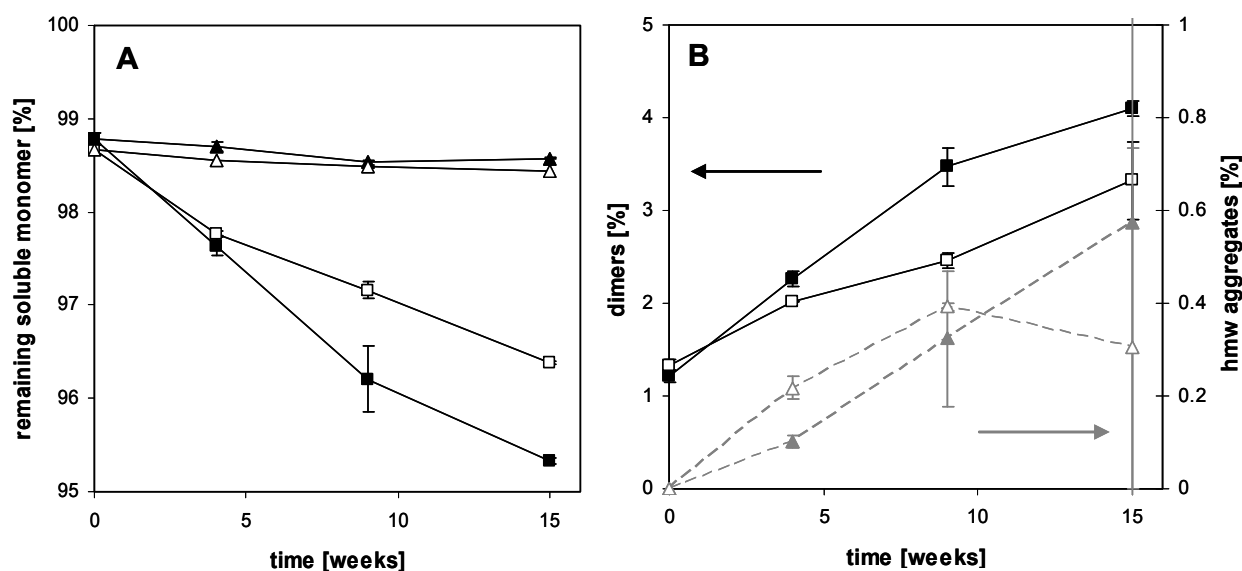


Figure 8.61: Remaining PA₀₁ soluble monomer reconstituted from collapsed (open symbols) and non-collapsed (full symbols) lyophilizates stored at 2-8 °C (triangles) and 50 °C (squares) for up to 15 weeks as determined by HP-SEC (A); PA₀₁ dimers (black symbols) and higher molecular weight aggregates (grey symbols) reconstituted from collapsed (open symbols) and non-collapsed (full symbols) cakes during storage at 50 °C as determined by HP-SEC (B); (average ± SD, n = 2).

After either collapse-drying or conventional freeze-drying, PA₀₁ stability was well preserved and monomer contents were high (98.9 ± 0.1 % and 98.7 ± 0.1 % in non-collapsed and collapsed lyophilizates, respectively).

During storage at 2-8 °C (triangles), all samples remained stable and no aggregated species were formed during the period of investigation ($98.6 \pm 0.0\%$ and $98.5 \pm 0.0\%$ remaining monomer in non-collapsed and collapsed systems, respectively). In contrast, samples stored at 50 °C showed a distinct monomer-decrease (squares). Collapsed cakes showed higher monomer contents than non-collapsed cakes after the same storage time ($95.3 \pm 0.0\%$ and $96.4 \pm 0.0\%$ remaining monomer in non-collapsed and collapsed cakes, respectively, after 15 weeks of storage). This was further reflected in higher amounts of dimers observed in elegant cakes. However, the formation of hmw aggregated species was slightly more pronounced in collapsed cakes (grey open triangles in Figure 8.61 B). However, the amount of formed hmw aggregates was small ($< 0.6\%$) and differences between the samples were not significant due to large standard deviations indicated by overlapping error bars.

Besides the formation of aggregated species, the creation of so-called two-chain material is an important quality parameter of PA₀₁ as well. Physiologically, PA₀₁ initially is produced as one continuous chain that is cleaved by plasmin to form a heavy chain that includes the fibrin-binding site and a light chain that performs the plasminogen-activation. The two formed chains are connected by disulphide bonds. As a drug product, amide bond-cleavage and formation of the two chains has been observed during storage¹²⁵. The two-chain material exerts full plasminogen activation activity but lacks the clot-specificity of the reaction. Thus an increasing amount of two-chain material is regarded as quality-compromising.

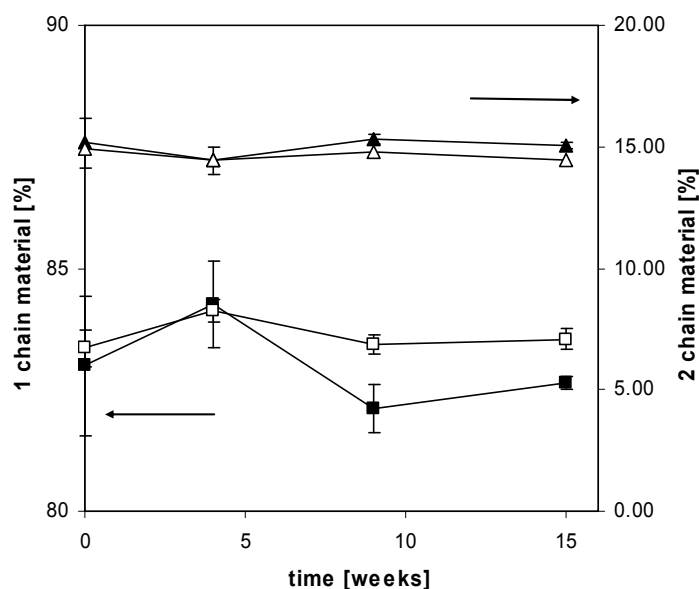


Figure 8.62: Integrity of PA₀₁ as indicated by the fraction of one-chain and two-chain material of PA₀₁ reconstituted from collapsed (open symbols) and non-collapsed (closed symbols) cakes during storage at 50 °C as determined by HP-SEC after DTT incubation; n = 2.

Figure 8.62 depicts the relative amount of one-chain and two-chain material during storage at 50 °C in both collapsed and non-collapsed cakes as determined by size exclusion chromatography after reductive cleavage of the disulphide bond connecting the heavy and the light chain. Besides the formation of one- and two-chain material, small amounts of

further-degraded products, eluting after the two-chain material was also observed but is not considered in the Figure. Collapse-drying results in comparable levels of one-chain material as conservative freeze-drying ($83.3 \pm 0.4\%$ and $83.0 \pm 1.4\%$ in collapsed and non-collapsed cakes, respectively). During storage, the amount of two-chain PA_{01} slightly increases, but all samples show high amounts of intact PA_{01} at the end of the investigated period of storage, i.e. $82.6 \pm 0.4\%$ in elegant plugs and $83.6 \pm 0.2\%$ in collapsed ones. As already observed for the formation of aggregated species, collapsed systems performed slightly better and showed significantly higher amounts of intact PA_{01} during storage at elevated temperatures. Figure 8.63 displays the course of specific activity in comparison to the amount of remaining soluble PA_{01} monomer (A) and the amount of one-chain material (B). There is a good correlation between the three stability parameters, all pointing towards a slightly superior stability of collapsed cakes as compared to non-collapsed conventionally freeze-dried cakes.

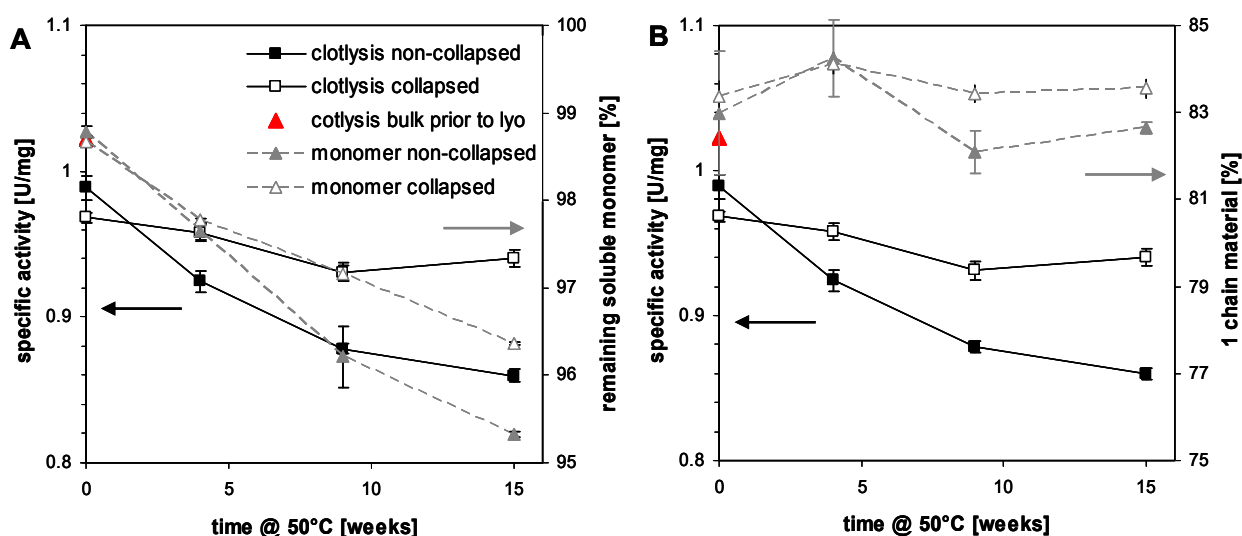


Figure 8.63: Comparison of the course of specific activity to the amount of remaining monomer content as determined by HP-SEC (A) and to the amount of one-chain material determined by HP-SEC after reductive cleavage of disulphide bonds with DTT (B) during storage at 50 °C.

Specific activity as determined by the clot lysis assay is represented by black symbols and monomer and one-chain material content as determined by HP-SEC is represented by grey symbols; collapsed cakes are represented by open symbols and non-collapsed cakes are represented by closed symbols.

PA_{01} integrity and aggregation was also assessed using SDS-PAGE both under non-reducing and dithiothreitol (DTT)-reducing conditions. Figure 8.64 depicts SDS-PAGE patterns of PA_{01} samples in both non-reduced and reduced form after different periods of storage at 50 °C.

The main band in both gels can be assigned to PA_{01} monomer with a molecular weight of 64 kDa. The two bands at approximately 38-35 kDa represent the PA_{01} two-chain material. Because the two chains are usually linked via a disulphide bond that is cleaved by DTT, the two bands representing the heavy and the light PA_{01} chain fragments are more intense in the DTT-reduced gel. However, probably due to disulphide bond cleavage by SDS, similar to the formation of fragments observed in mAb-SDS-PAGE³³, two-chain material is noticeable in the

non-reduced gels as well. There is no change observed in the intensity of the two-chain material bands during storage and also there is no difference observed between collapsed and non-collapsed cakes. These findings point out that differences observed during HP-SEC analysis were small and collapsed and non-collapsed lyophilizates adequately preserved PA₀₁ integrity.

Comparing the intensity of the bands representing aggregated species at the top of the gels, a strengthening is observed with increasing storage time, but there is no clear difference observed between collapsed and non-collapsed material. Because non-reduced and DTT-reduced gels show comparable band-coloration one can conclude that aggregates are not dissolved upon reduction, thus non-reducible, covalently linked aggregates are present in the lyophilizates.

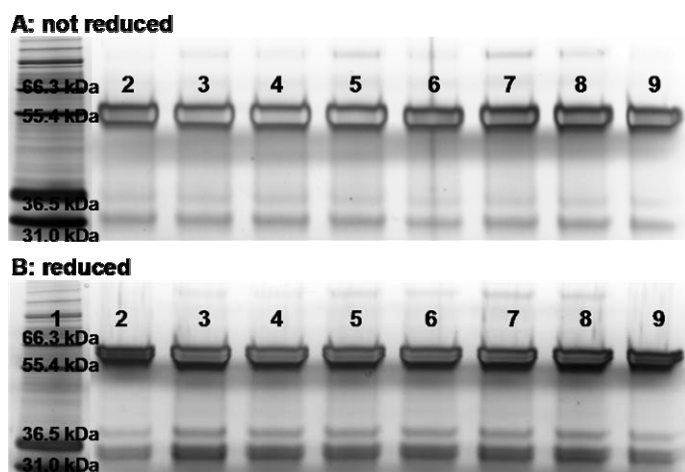


Figure 8.64: Silver-stained SDS-PAGE patterns of PA₀₁ stored for different periods of time at 50 °C under non-reducing (A) and DTT-reducing (B) conditions.

lane 1: marker, lane 2: standard, lane 3: non-collapsed after 4 weeks at 50 °C, lane 4: collapsed after 4 weeks at 50 °C, lane 5: non-collapsed after 9 weeks at 50 °C, lane 6: collapsed after 9 weeks at 50 °C, lane 7: non-collapsed after 15 weeks at 50 °C, lane 8: collapsed after 15 weeks at 50 °C, lane 9: standard.

Besides the formation of soluble aggregated species, that can be detected and classified using gel permeation chromatography, the formation of insoluble aggregates and the formation of visible and sub-visible particles are of utmost importance. Dynamic light scattering (DLS) and light obscuration were used to detect the formation of such particles and to further characterize these particles.

Figure 8.65 depicts size distributions of PA₀₁ samples stored for different periods of time at 50 °C that are determined by DLS using either the intensity of scattered light directly or the intensity corrected for the size of the scattering particles, called volume distribution.

The size distributions in Figure 8.65 all show a main peak at approximately 10 nm that represents the PA₀₁ monomer. Additional peaks between approximately 50 nm and 1000 nm that are assigned to aggregated species are observed in varying intensities as well. Comparing the intensity size distributions of non-collapsed and collapsed lyophilizates (Figure 8.65 A and Figure 8.65 C), distinct aggregate peaks (ranging from 100 nm to

1000 nm) are noticeable in collapsed cakes after lyophilization whereas they are not discernable in non-collapsed cakes until after 15 weeks of storage. The higher polydispersity of the collapsed samples was reflected in the slightly increased PDI values (0.366 and 0.429 in elegant and collapsed systems, respectively) as well as the Z-Averages (11.47 nm and 12.31 nm for elegant and collapsed cakes, respectively). However, the amount of these aggregated species is small and they are not detectable in the more relevant volume distribution (Figure 8.65 B and Figure 8.65 D).

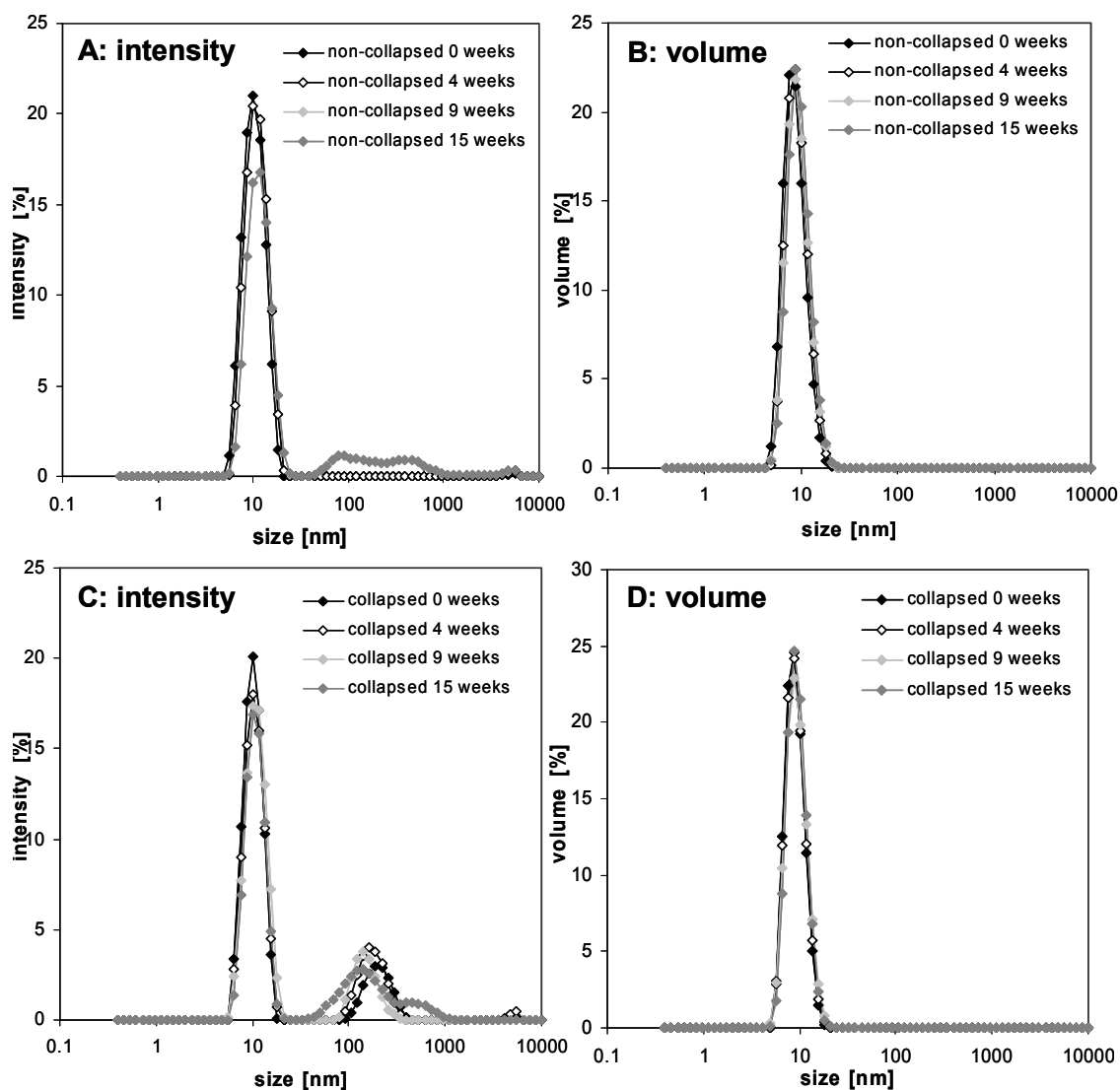


Figure 8.65: Physical protein stability of reconstituted PA₀₁ lyophilizates as determined by dynamic light scattering; size distribution by intensity of scattered light (A, C) and by volume (B, D) of non-collapsed (A, B) and collapsed (C, D) lyophilizates, respectively after different times of storage at 50 °C; n = 2.

The size distribution was obtained by fitting a NNLS algorithm to the correlation function.

Samples stored at 2-8 °C further confirmed observations made in samples stored at elevated temperatures and trace amount of aggregates were detected earlier during storage in collapsed cakes than in non-collapsed cakes.

The formation of insoluble aggregates and sub-visible particles was further analyzed using the light obscuration technique that detects particles in the range of 1 μm to 200 μm.

Figure 8.66 shows the numbers of particles $\geq 1 \mu\text{m}$ and $\geq 10 \mu\text{m}$ during storage at 50°C . Particles $\geq 25 \mu\text{m}$ were not present in all the samples and for all time points and storage temperatures. In contrast to DLS data, collapsed cakes showed slightly lower particle numbers than elegant cakes at the beginning of the storage period (3022 ± 82 and 2379 ± 218 particles larger $1 \mu\text{m}$ in non-collapsed and collapsed cakes, respectively). Most strikingly, particles did not relevantly increase during storage in both formulations (3256 ± 82 and 2065 ± 462 particles $\geq 1 \mu\text{m}$ in elegant and collapsed cakes, respectively after 15 weeks at 50°C). Again, collapsed cakes showed lower particle numbers than elegant lyophilizates. However, during the course of the stability study elegant cakes showed distinctly decreased particle numbers, rendering the definite evaluation, whether collapsed or non-collapsed lyophilizates are more stable in terms of particle formation, difficult.

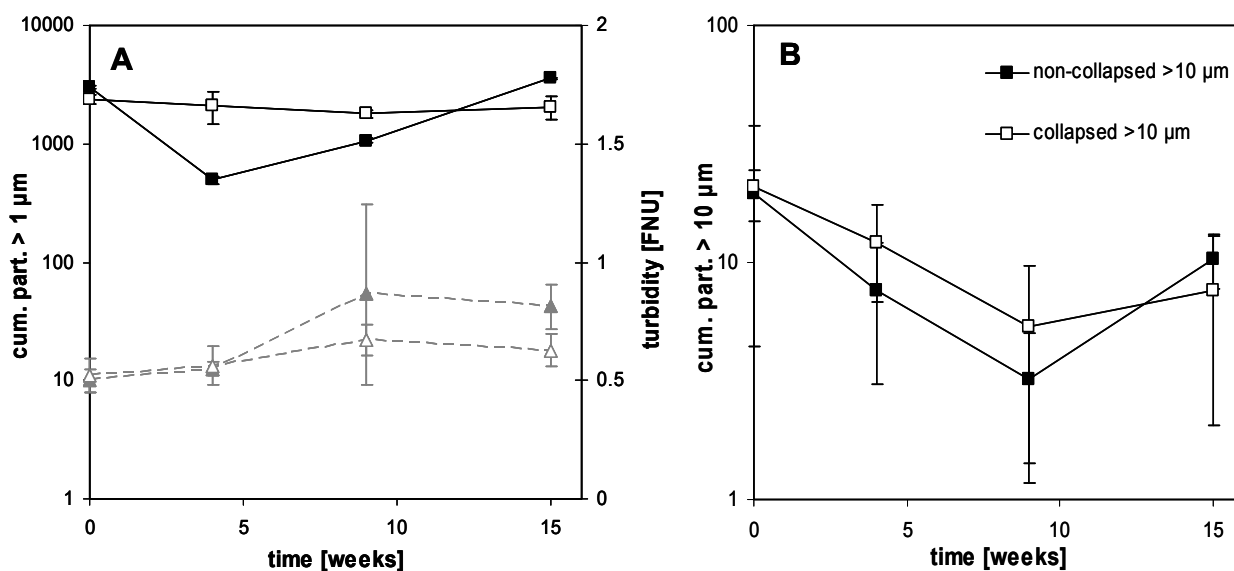


Figure 8.66: Subvisible particles larger $1 \mu\text{m}$ and turbidities (A) and particles larger $10 \mu\text{m}$ (B) of PA_{01} solutions reconstituted from collapsed and not collapsed lyophilizates after different periods of storage at 50°C .

Particle numbers $\geq 1 \mu\text{m}$ (A) and $\geq 10 \mu\text{m}$ (B) are represented by black symbols and turbidity values are represented by grey symbols; collapsed cakes are represented by open symbols and non-collapsed cakes are represented by closed symbols; average \pm SD, $n = 2$.

Turbidity values were below one FNU for all samples (grey triangles in Figure 8.66) further reflecting the low particle numbers. Non-collapsed cakes showed slightly increased turbidities, but given the overlapping error bars, results were not relevantly different. As t-PA was reported to be sensitive towards denaturation at solid-void interfaces by Hsu et al.²¹, the slightly decreased turbidities could be related to the lower surface area of collapsed cakes that was described in detail in Chapter 5 of this thesis.

To sum up the findings from the analysis of particulate matter of PA_{01} stored in collapsed and non-collapsed lyophilizates, acquired data was ambiguous. Whereas DLS pointed towards slightly increased levels of aggregated species between 30nm and 1000 nm in collapsed cakes, light obscuration analysis showed slightly decreased particle numbers of particles

$\geq 1 \mu\text{m}$ in collapsed cakes. However, light obscuration data was not consistent throughout the period of investigation and non-collapsed systems showed decreased particle numbers after 4 and 9 weeks of storage as compared to collapsed cakes. When DLS data was evaluated using the more relevant volume size distribution no difference between collapsed and non-collapsed cakes was observed. Turbidity data as well showed no relevant differences. Considering the entire data-set, there is no clear difference between collapsed and non-collapsed systems regarding particle formation. Thus no negative effect of collapse was observed.

In a further attempt to comprehensively distinguish PA_{01} stability in collapsed and non-collapsed lyophilizates, the color of the reconstituted solution was analyzed. This assay investigates the extent of yellow discoloration by comparison with yellow standard solutions and it is reported to be sensitive towards PA_{01} instability reactions (private communication). Figure 8.67 shows the color of PA_{01} solutions after different periods of storage at 50°C . Non-collapsed cakes distinctly show a discoloration after 9 weeks of storage whereas collapsed cakes remain colorless until 15 weeks of storage.

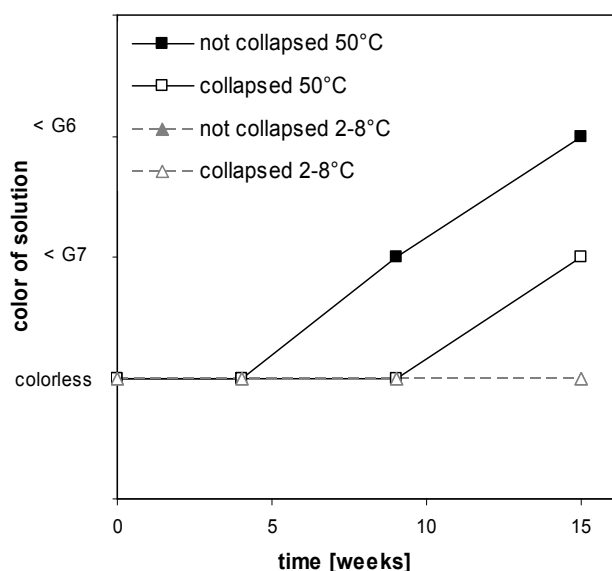


Figure 8.67: Color of PA_{01} solution after reconstitution from collapsed and non-collapsed lyophilizates after various periods of storage at 50°C and $2-8^\circ\text{C}$, respectively; $n = 2$.

4.4 CONFORMATIONAL STABILITY OF PA_{01} IN RECONSTITUTED LYOPHILIZATES

To complete the analysis of the effect of cake-collapse on PA_{01} stability, the tertiary structure was investigated by analyzing shifts in the peak positions of tryptophan and tyrosine in the second derivative of UV-absorption spectra, as described by Kuelzto et al.^{126,127}.

Figure 8.68 shows second derivative UV-absorption spectra of PA_{01} reconstituted from non-collapsed (A) and collapsed (B) lyophilizates after different periods of storage. Derivative spectra of non-collapsed systems remained unchanged during storage.

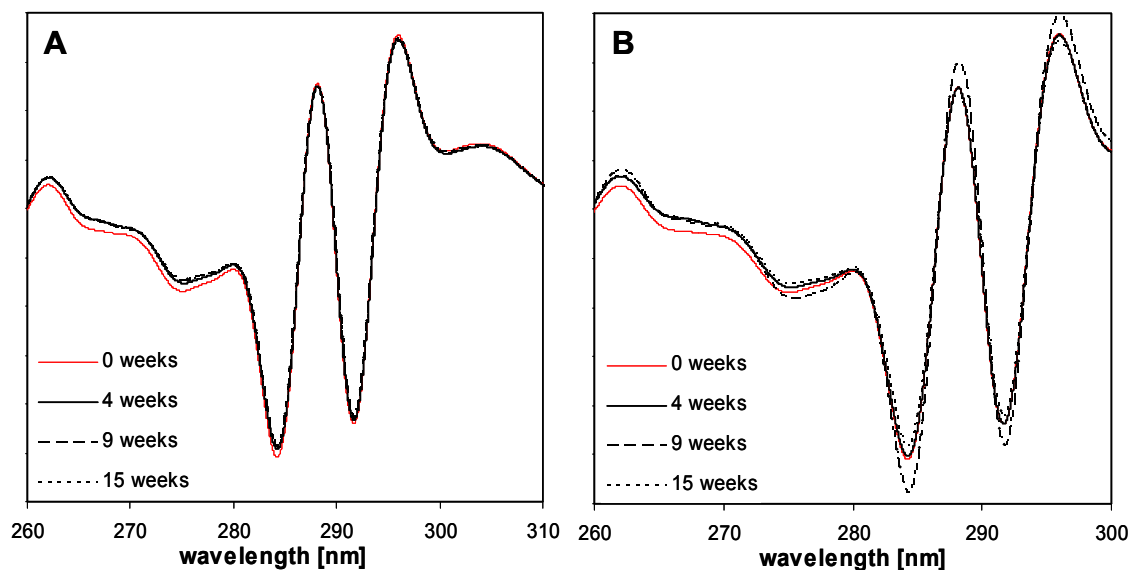


Figure 8.68: UV 2nd derivative absorption spectra of PA₀₁ reconstituted from non-collapsed (A) and collapsed (B) lyophilizates stored for different periods of time at 50 °C.

All spectra are calculated average spectra of two independent measurements ($n = 2$).

The slight offsets observed between the spectra recorded immediately after freeze-drying (0 weeks) and the spectra recorded during subsequent storage were most probably caused by a variation of equipment parameters, as it was also observed in comparison to non-stored standards recorded at the various time points of analysis after storage.

Table 8.15: Characteristic peak positions in UV 2nd derivative absorption spectra of PA₀₁ stored for different periods of time in collapsed and non-collapsed lyophilizates.

ID	storage temperature [°C]	storage time [weeks]	Tyr/Trp-peak position [nm]	Trp-peak position [nm]
non-collapsed	2-8	0	284.24 ± 0.01	291.66 ± 0.00
		4	284.23 ± 0.00	291.69 ± 0.00
		9	284.24 ± 0.01	291.69 ± 0.01
		15	284.24 ± 0.01	291.68 ± 0.01
collapsed		0	284.23 ± 0.01	291.65 ± 0.01
		4	284.24 ± 0.01	291.68 ± 0.00
		9	284.24 ± 0.00	291.66 ± 0.00
		15	284.24 ± 0.00	291.67 ± 0.00
non-collapsed	50	0	284.24 ± 0.01	291.66 ± 0.00
		4	284.24 ± 0.01	291.68 ± 0.00
		9	284.24 ± 0.00	291.68 ± 0.00
		15	284.25 ± 0.01	291.69 ± 0.01
collapsed		0	284.23 ± 0.01	291.65 ± 0.01
		4	284.24 ± 0.00	291.67 ± 0.00
		9	284.31 ± 0.09	291.74 ± 0.10
		15	284.25 ± 0.00	291.69 ± 0.01
PA01 standard	-	-	284.23 ± 0.00	291.69 ± 0.00

This becomes further plausible comparing the positions of the two major peaks in the second derivatives that are correlated to the microenvironment of tryptophan and tyrosine¹²⁸ as listed

in Table 8.15. No shifts were discernible comparing lyophilizates immediately after freeze-drying and after the different periods of storage at 50 °C indicating that PA₀₁ tertiary structure was not altered during storage.

Regarding the second derivative spectra of collapsed lyophilizates, the baseline shift between the spectra after production and after storage was observed as well. Additionally, slight fluctuations in the peak-intensity were observed. But as there was no shift in the peak positions observed, these were most likely caused by slight differences in the protein concentration. What is more, as the intensities equally changed in both peaks, the a/b ratio describing the degree of tyrosine solvent-exposure¹²⁹ remained unaffected.

Thus in summary, tertiary structure was well preserved in both, non-collapsed, elegant and collapsed lyophilizates.

4.5 SUMMARY AND CONCLUSION

PA₀₁, serving as a third, pharmaceutically relevant model protein, was freeze-dried to elegant and collapsed lyophilizates and stored for up to 15 weeks at 50 °C to evaluate the effect of lyophilizate collapse on various stability-indicating parameters, i.e. the biologic activity, physical and conformational integrity and the formation of soluble and insoluble aggregates. Interestingly, the arginine-containing cakes showed a different collapse behavior than the disaccharide-based cakes investigated previously, allowing for the analysis of a different form of collapse.

The investigated lyophilizates were dried to residual moisture contents of approximately 4 %, because PA₀₁ was argued to be sensitive to over-drying¹²². Glass transition temperatures were above 80 °C and physicochemical characteristics remained constant throughout the storage period, thus samples remained in the amorphous state throughout the investigation. Most importantly, collapsed and non-collapsed samples were well comparable in their physicochemical qualities.

Clotlytic activity was slightly reduced upon freeze-drying and it further decreased during storage. However, collapsed cakes, that initially showed a somewhat reduced catalytic activity, preserved PA₀₁-activity significantly better and showed an 8.6 % higher activity after 15 weeks of storage at 50 °C compared to elegant cakes.

Physical protein stability of collapsed and non-collapsed cakes was well comparable after freeze-drying, but collapsed systems showed 1 % higher remaining monomer levels after 15 weeks of storage at 50 °C. This trend was further reflected by a decreased formation of dimers. However, the formation of sub-visible particles did not show a clear trend. DLS analysis revealed the existence of trace amounts of aggregated species in collapsed samples throughout the storage period, whereas high molecular weight species in non-collapsed cakes were not detectable until after 15 weeks of storage. Light obscuration measurements in contrast showed a slightly decreased amount of particles in collapsed

cakes stored at 50 °C, while the overall formation of particles was low. PA₀₁ integrity, i.e. the formation of two-chain material by bond-cleavage was not relevantly altered during storage.

The stability of PA₀₁ was further monitored by assessing the color of the reconstituted solution and a more rapid discoloration was observed in non-collapsed lyophilizates.

Tertiary structure that was analyzed by second derivative UV-absorption spectroscopy was not altered within the investigated period of time and there was no difference in the microenvironment of tryptophan and tyrosine detected; neither in collapsed nor in non-collapsed cakes.

To sum up findings from the investigation of PA₀₁-stability over 15 weeks of storage at 50 °C regarding the effect of collapse during freeze-drying, there was no negative effect of collapse observed. Collapsed PA₀₁-lyophilizates performed equally well as non-collapsed lyophilizates. In key stability-indicating parameters, such as catalytic activity and the preservation of monomeric PA₀₁, collapsed cakes performed even slightly better than non-collapsed cakes.

5 FINAL SUMMARY AND CONCLUSION

The long-term storage stability of collapsed and non-collapsed protein lyophilizates was investigated using three different model proteins. An IgG₁ monoclonal antibody was included into the investigation to represent the most widely used class of protein pharmaceuticals at the moment. Furthermore, L-Lactic Dehydrogenase (LDH) was analyzed, because of its well-known sensitivity towards the various stress situations arising during freeze-drying and subsequent storage. PA₀₁ was included as a third model protein and also as a marketed protein pharmaceutical that is known to be difficult to freeze-dry and to be prone to partial collapse.

The proteins were formulated in different formulations intended to represent the most frequently used and most important stabilizers for lyophilization. Completely amorphous formulations, comprising the lyo-protectants sucrose and trehalose as well as the amino-acid arginine were investigated along with partially crystalline formulations that additionally contained mannitol or polyethylene glycol. Collapsed and non-collapsed lyophilizates of identical composition were produced using an aggressive drying protocol, termed collapse-drying and a conventional, gentle freeze-drying protocol. All lyophilizates were produced in a way that yielded comparable residual moisture levels to allow for the clear discrimination of effects of residual moisture, which is thoroughly documented to adversely affect protein stability, and effects of collapse. Samples were then stored at elevated temperatures (25 °C, 40 °C, 50 °C) for up to 6 months and protein as well as excipient stability was assessed at regular intervals (after 2, 4, 6, 9, 12, 15 and 26 weeks) using a broad set of analytical tools.

Briefly summarized, results gained from the investigation of protein stability immediately after lyophilization (discussed in Chapter 7) could be further confirmed: no negative effect of collapse on protein stability was detected. Even more, collapse-dried cakes exhibited increased protein stability.

Of the investigated IgG₀₁ lyophilizates, trehalose-based formulations at pH 5.5 and pH 3.5 well preserved IgG₀₁ stability, indicated for example by monomer contents above 94 % after 15 weeks of storage at 50 °C and no detectable alterations in secondary or tertiary structure. But despite this overall good stability, collapsed lyophilizates slightly better preserved the antibody, as indicated by slightly decreased soluble aggregate fractions and lower levels of sub-visible particles.

Similar results were obtained for partially crystalline mannitol-sucrose-based lyophilizates that were partially and non-collapsed, respectively. IgG₀₁ stability was slightly better preserved in collapse-dried, partially collapsed cakes, as indicated for example by decreased sub-visible particle numbers and higher fluorescence intensities indicating better preservation of tertiary structure.

The most remarkable demonstration of a tremendously enhanced stability of collapse-dried lyophilizates was observed during storage of collapsed and non-collapsed sucrose-based lyophilizates in the vicinity of their glass transition temperature. Initially non-collapsed lyophilizates collapsed during storage at elevated temperatures and this onset of collapse during storage was accompanied by a clear change in physicochemical stability of both the excipient sucrose and the antibody. Upon the onset of collapse during storage sucrose completely crystallized, whereas initially collapsed lyophilizates remained at least partially amorphous throughout the period of investigation, in sharp contrast to the widespread concern that collapsed cakes are more prone to crystallize during storage^{15,91,93}. Besides this physical instability, sucrose was also chemically degraded, i.e. inversion and the formation of the reducing sugars glucose and fructose occurred. The monosaccharides then reacted with the antibody in the so-called Maillard-reaction presumably resulting in the formation of glycated antibody-species that in turn were greatly prone to aggregation and lead to the formation of high levels of soluble and insoluble aggregates. While the rate of hydrolysis of sucrose was comparable in initially collapsed and storage-collapsed cakes, there was a distinct difference in the rate and the extent of nonenzymatic browning with initially collapsed cakes showing a clearly retarded reaction rate. This difference in the reaction rate most probably related to the strongly decreased molecular mobility in collapsed cakes as indicated by greatly increased structural relaxation times that are discussed in detail in Chapter 9 of this thesis. Because the Maillard reaction is a partially diffusion-controlled reaction, the rate of reaction may be well correlated to the system's global glassy dynamics and may therefore be slowed down in collapsed cakes. Since on the other hand the hydrogen-ions participating in the hydrolysis of sucrose are relatively small, this reaction is likely not coupled to global dynamics but rather to local dynamics, which were found not to be relevantly different in collapsed and non-collapsed cakes. Furthermore, as the Maillard-reaction is known to be initiated in pores⁷⁴, the decreased specific surface area of collapsed cakes might contribute to the retardation as well, along with the reduced degree of crystallinity in collapsed cakes that is also so known to accelerate the rate of glycation¹³⁰. The decreased crystallization rate may also be related to the reduced global mobility as observed by Bhugra et al⁴⁴.

Thus it was shown, that there is no detrimental effect of collapse on long-term IgG stability. Moreover, intentionally collapsed lyophilizates using collapse-drying are more robust towards storage at elevated temperatures and show a greatly enhanced stability.

LDH stability was assessed in both partially-crystalline and purely amorphous collapsed and non-collapsed lyophilizates with respect to enzymatic activity, physical and conformational stability. Furthermore, partially collapsed sucrose-PEG lyophilizates were compared to completely collapsed lyophilizates. Collapsed lyophilizates appeared to better preserve LDH physical protein stability and native conformation and there was no relevant difference in the

preservation of the catalytic activity. Partially collapsed cakes showed the least degree of stabilization. In addition sucrose-crystallization occurred in the partially collapsed cakes. This further demonstrates the benefit of the concerted production of collapsed lyophilizates in order to prevent the onset of accidental collapse – either during storage at elevated temperatures or during the secondary stage of the freeze-drying run.

Thus results from the IgG experiments were further confirmed – the onset of collapse during lyophilization did not compromise the long-term storage stability of LDH.

PA₀₁ as the third model protein also confirmed the results obtained from the investigations of long-term storage stability of IgG₀₁ and LDH. Arginine-based collapsed and non-collapsed cakes were produced and analyzed with respect to PA₀₁ biologic activity, as well as to PA₀₁ physical and conformational stability. Clot lytic activity was significantly higher in collapsed cakes after 15 weeks of storage at 50 °C and the formation of soluble aggregates was decreased. There was no change observed in the tertiary structure as assessed by UV second derivative spectroscopy.

In summary, the comparable degree of stabilization of IgG₀₁, LDH and PA₀₁ in collapsed and non-collapsed lyophilizates immediately after freeze-drying was further confirmed by investigating the long-term storage stability. It turned out that in some cases, stabilization was found to be even more than comparable, i.e. stability in collapsed cakes was superior to stability in non-collapsed cakes. Thus collapse-drying can provide a mean to produce lyophilizates that are more robust towards storage at elevated temperatures. This higher stability is due to the fact that collapse-dried lyophilizates cannot further collapse during storage at high temperatures and that they offer a higher degree of stabilization during storage at high temperatures. Finally, concerns usually related to collapsed products, such as prolonged reconstitution times, high residual moisture contents and the susceptibility towards crystallization were shown not to apply to collapse-dried lyophilizates.

6 REFERENCES

1. Carpenter, J.F. and Izutsu, K. Freezing- and Drying- induced Perturbations of Protein Structure and Mechanisms of Protein Protection by Stabilizing Additives. 146-186 *Freeze-Drying/ Lyophilization of Pharmaceutical and Biological Products (Drugs and the Pharmaceutical Sciences Volume 137)* (2004)
2. Cleland, J.L., Lam, X., Kendrick, B., Yang, J., Yang, T.H., Overcashier, D., Brooks, D., Hsu, C., and Carpenter, J.F. A specific molar ratio of stabilizer to protein is required for storage stability of a lyophilized monoclonal antibody. *Journal of Pharmaceutical Sciences*, **90** (3): 310-321 (2001)
3. Costantino, H.R., Pikal, M.J., and Editors. *Lyophilization of Biopharmaceuticals (Biotechnology: Pharmaceutical Aspects)*. Springer, Berlin (2004)
4. Monsoor, M.A. Effect of drying methods on the functional properties of soy hull pectin. *Carbohydr.Polym.*, **61** (3): 362-367 (2005)
5. az-Maroto, M.C., Perez-Coello, M.S., and Cabezudo, M.D. Effect of different drying methods on the volatile components of parsley (*Petroselinum crispum* L.). *Eur.Food Res.Technol.*, **215** (3): 227-230 (2002)
6. Abdul-Fattah, A.M., Kalonia, D.S., and Pikal, M.J. The challenge of drying method selection for protein pharmaceuticals: product quality implications. *Journal of Pharmaceutical Sciences*, **96** (8): 1886-1916 (2007)
7. Abdul-Fattah, A.M., Lechuga-Ballesteros, D., Kalonia, D.S., and Pikal, M.J. The impact of drying method and formulation on the physical properties and stability of methionyl human growth hormone in the amorphous solid state. *Journal of Pharmaceutical Sciences*, **97** (1): 163-184 (2008)
8. Franks, F. Freeze-drying of bioproducts: putting principles into practice. *European Journal of Pharmaceutics and Biopharmaceutics*, **45** (3): 221-229 (1998)
9. Jennings, T.A. *Lyophilization: Introduction and Basic Principles*. Informa Healthcare (1999)
10. MacKenzie, A.P. Collapse during freeze drying - qualitative and quantitative aspects. *Freeze Drying Adv.Food Technol., [Int.Course]*, 277-307 (1975)
11. Bellows, R.J. and King, D.J. Product collapse during freeze drying of liquid foods. *AIChE Symposium Series*, **69** (132): 33-41 (1973)
12. Fonseca, F., Passot, S., Cunin, O., and Marin, M. Collapse Temperature of Freeze-Dried *Lactobacillus bulgaricus* Suspensions and Protective Media. *Biotechnology Progress*, **20** (1): 229-238 (2004)
13. Lueckel, B., Helk, B., Bodmer, D., and Leuenberger, H. Effects of formulation and process variables on the aggregation of freeze-dried interleukin-6 (IL-6) after lyophilization and on storage. *Pharmaceutical Development and Technology*, **3** (3): 337-346 (1998)
14. Passot, S., Fonseca, F., arcon-Lorca, M., Rolland, D., and Marin, M. Physical characterisation of formulations for the development of two stable freeze-dried proteins during both dried and liquid storage. *European Journal of Pharmaceutics and Biopharmaceutics*, **60** (3): 335-348 (2005)
15. Darcy, P. and Buckton, G. The influence of heating/drying on the crystallization of amorphous lactose after structural collapse. *International Journal of Pharmaceutics*, **158** (2): 157-164 (1997)
16. Izutsu, K., Yoshioka, S., and Kojima, S. Physical stability and protein stability of freeze-dried cakes during storage at elevated temperatures. *Pharmaceutical Research*, **11** (7): 995-999 (1994)
17. Wang, D.Q., Hey, J.M., and Nail, S.L. Effect of collapse on the stability of freeze-dried recombinant factor VIII and α -amylase. *Journal of Pharmaceutical Sciences*, **93** (5): 1253-1263 (2004)
18. Chatterjee, K., Shalaev, E.Y., and Suryanarayanan, R. Partially crystalline systems in lyophilization: II. Withstanding collapse at high primary drying temperatures and impact on protein activity recovery. *Journal of Pharmaceutical Sciences*, **94** (4): 809-820 (2005)

19. Passot, S., Fonseca, F., Barbouche, N., Marin, M., arcon-Lorca, M., Rolland, D., and Rapaud, M. Effect of Product Temperature During Primary Drying on the Long-Term Stability of Lyophilized Proteins. *Pharmaceutical Development and Technology*, **12** (6): 543-553 (2007)
20. Abdul-Fattah, A.M., Truong-Le, V., Yee, L., Nguyen, L., Kalonia, D.S., Cicerone, M.T., and Pikal, M.J. Drying-induced variations in physico-chemical properties of amorphous pharmaceuticals and their impact on stability (I): stability of a monoclonal antibody. *Journal of Pharmaceutical Sciences*, **96** (8): 1983-2008 (2007)
21. Hsu, C.C., Nguyen, H.M., Yeung, D.A., Brooks, D.A., Koe, G.S., Bewley, T.A., and Pearlman, R. Surface denaturation at solid-void interface-a possible pathway by which opalescent particulates form during the storage of lyophilized tissue-type plasminogen activator at high temperatures. *Pharmaceutical Research*, **12** (1): 69-77 (1995)
22. Hatley, R.H.M. Glass fragility and the stability of pharmaceutical preparations- excipient selection. *Pharmaceutical Development and Technology*, **2** (3): 257-264 (1997)
23. Surana, R., Pyne, A., and Suryanarayanan, R. Effect of Preparation Method on Physical Properties of Amorphous Trehalose. *Pharmaceutical Research*, **21** (7): 1167-1176 (2004)
24. Schebor, C., Burin, L., Del Pilar Buera, M., and Chirife, J. Stability to hydrolysis and browning of trehalose, sucrose and raffinose in low-moisture systems in relation to their use as protectants of dry biomaterials. *Lebensm.-Wiss. Technol.*, **32** (8): 481-485 (1999)
25. House, J.A. and Mariner, J.C. Stabilization of rinderpest vaccine by modification of the lyophilization process. *Developments in Biological Standardization*, **87** 235-244 (1996)
26. McGarvey, O.S., Kett, V.L., and Craig, D.Q.M. An Investigation into the Crystallization of α,α -Trehalose from the Amorphous State. *Journal of Physical Chemistry B*, **107** (27): 6614-6620 (2003)
27. Mahler, H.C., Friess, W., Grauschopf, U., and Kiese, S. Protein Aggregation: Pathways, Induction Factors and Analysis. *Journal of Pharmaceutical Sciences*, (2008)
28. Demeester, J., De Smedt, S.S., Sanders, N.N., and Hastraete, J. Light scattering. *Biotechnology: Pharmaceutical Aspects*, **3** (Methods for Structural Analysis of Protein Pharmaceuticals): 245-275 (2005)
29. Gabrielson, J.P., Brader, M.L., Pekar, A.H., Mathis, K.B., Winter, G., Carpenter, J.F., and Randolph, T.W. Quantitation of aggregate levels in a recombinant humanized monoclonal antibody formulation by size-exclusion chromatography, asymmetrical flow field flow fractionation, and sedimentation velocity. *Journal of Pharmaceutical Sciences*, **96** (2): 268-279 (2006)
30. Hawe, A., Friess, W., Sutter, M., and Jiskoot, W. Online fluorescent dye detection method for the characterization of immunoglobulin G aggregation by size exclusion chromatography and asymmetrical flow field flow fractionation. *Analytical Biochemistry*, **378** (2): 115-122 (2008)
31. Welfle, K., Misselwitz, R., Hausdorf, G., Hohne, W., and Welfle, H. Conformation, pH-induced conformational changes, and thermal unfolding of anti-p24 (HIV-1) monoclonal antibody CB4-1 and its Fab and Fc fragments. *Biochimica et Biophysica Acta, Protein Structure and Molecular Enzymology*, **1431** (1): 120-131 (1999)
32. Hatta, H., Tsuda, K., Akachi, S., Kim, M., and Yamamoto, T. Productivity and some properties of egg yolk antibody (IgY) against human rotavirus compared with rabbit IgG. *Bioscience, Biotechnology, and Biochemistry*, **57** (3): 450-454 (1993)
33. Harris, R.J., Shire, S.J., and Winter, C. Commercial manufacturing scale formulation and analytical characterization of therapeutic recombinant antibodies. *Drug Development Research*, **61** (3): 137-154 (2004)
34. Guideline for the Determination of Residual Moisture in Dried Biological Products. *Center for Biologics Evaluation and Research (CBER), Food and Drug Administration* (1990)
35. Towns, J.K. Moisture content in proteins: its effects and measurement. *Journal of Chromatography, A*, **705** (1): 115-127 (1995)

36. Duddu, S.P., Zhang, G., and Dal Monte, P.R. The relationship between protein aggregation and molecular mobility below the glass transition temperature of lyophilized formulations containing a monoclonal antibody. *Pharmaceutical Research*, **14** (5): 596-600 (1997)
37. Bellows, R.J. and King, C.J. Freeze-drying of aqueous solutions: Maximum allowable operating temperature. *Cryobiology*, **9** (6): 559-561 (1972)
38. Tsourouflis, S., Flink, J.M., and Karel, M. Loss of structure in freeze-dried carbohydrates solutions: effect of temperature, moisture content and composition. *Journal of the Science of Food and Agriculture*, **27** (6): 509-519 (1976)
39. Carpenter, J.F., Crowe, J.H., and Arakawa, T. Comparison of solute-induced protein stabilization in aqueous solution and in the frozen and dried states. *Journal of Dairy Science*, **73** (12): 3627-3636 (1990)
40. Saleki-Gerhardt, A., Ahlneck, C., and Zografi, G. Assessment of disorder in crystalline solids. *International Journal of Pharmaceutics*, **101** (3): 237-247 (1994)
41. Shah, B., Kakumanu, V.K., and Bansal, A.K. Analytical techniques for quantification of amorphous/crystalline phases in pharmaceutical solids. *Journal of Pharmaceutical Sciences*, **95** (8): 1641-1665 (2006)
42. Bhugra, C. and Pikal, M.J. Role of thermodynamic, molecular, and kinetic factors in crystallization from the amorphous state. *Journal of Pharmaceutical Sciences*, **97** (4): 1329-1349 (2008)
43. Saleki-Gerhardt, A. and Zografi, G. Non-isothermal and isothermal crystallization of sucrose from the amorphous state. *Pharmaceutical Research*, **11** (8): 1166-1173 (1994)
44. Bhugra, C., Rambhatla, S., Bakri, A., Duddu, S.P., Miller, D.P., Pikal, M.J., and Lechuga-Ballesteros, D. Prediction of the onset of crystallization of amorphous sucrose below the calorimetric glass transition temperature from correlations with mobility. *Journal of Pharmaceutical Sciences*, **96** (5): 1258-1269 (2007)
45. Pikal, M.J. Mechanisms of Protein Stabilization during Freeze-Drying and Storage: The Relative Importance of Thermodynamic Stabilization and Glassy State Relaxation Dynamics.(3): 63-108 *Freeze-Drying/ Lyophilization of Pharmaceutical and Biological Products (Drugs and the Pharmaceutical Sciences Volume 137)* (2004)
46. Shamblin, S.L., Hancock, B.C., and Pikal, M.J. Coupling Between Chemical Reactivity and Structural Relaxation in Pharmaceutical Glasses. *Pharmaceutical Research*, **23** (10): 2254-2268 (2006)
47. Surana, R., Pyne, A., and Suryanarayanan, R. Effect of Aging on the Physical Properties of Amorphous Trehalose. *Pharmaceutical Research*, **21** (5): 867-874 (2004)
48. Shamblin, S.L., Tang, X., Chang, L., Hancock, B.C., and Pikal, M.J. Characterization of the Time Scales of Molecular Motion in Pharmaceutically Important Glasses. *Journal of Physical Chemistry B*, **103** (20): 4113-4121 (1999)
49. Wu, T. and Yu, L. Surface Crystallization of Indomethacin Below Glass Transition Temperature. *Pharmaceutical Research*, **23** (10): 2350-2355 (2006)
50. Beckett, S.T., Grazia Francesconi, M., Geary, P.M., MacKenzie, G., and Maulny, A.P.E. DSC study of sucrose melting. *Carbohydrate Research*, **341** (15): 2591-2599 (2006)
51. Hurtta, M., Pitkaenen, I., and Knutinen, J. Melting behaviour of D-sucrose, D-glucose and D-fructose. *Carbohydrate Research*, **339** (13): 2267-2273 (2004)
52. Shallenberger, R.S. and Birch, G.G. Sugar Chemistry.218 AVI. Westport Conn (1975)
53. Raemy, A. and Schweizer, T.F. Thermal behavior of carbohydrates studied by heat flow calorimetry. *Journal of Thermal Analysis*, **28** (1): 95-108 (1983)
54. Orsi, F. Kinetic studies on the thermal decomposition of glucose and fructose. *Journal of Thermal Analysis*, **5** (2): 329-335 (1973)

55. Reynhardt, E.C. An NMR, DSC, and x-ray investigation of the disaccharides sucrose, maltose, and lactose. *Molecular Physics*, **69** (6): 1083-1097 (1990)
56. Lund, D.B., Fennema, O.R., and Powrie, W.D. Enzymic and acid hydrolysis of sucrose as influenced by freezing. *Journal of Food Science*, **34** (4): 378-382 (1969)
57. Flink, J.M. Nonenzymatic browning of freeze-dried sucrose. *Journal of Food Science*, **48** 539-542 (1983)
58. Buera, M.d.P., Chirife, J., and Karel, M. A study of acid-catalyzed sucrose hydrolysis in an amorphous polymeric matrix at reduced moisture contents. *Food Research International*, **28** (4): 359-365 (1995)
59. Shalaev, E.Y., Lu, Q., Shalaeva, M., and Zografis, G. Acid-catalyzed inversion of sucrose in the amorphous state at very low levels of residual water. *Pharmaceutical Research*, **17** (3): 366-370 (2000)
60. Karel, M. and Labuza, T.P. Nonenzymic browning in model systems containing sucrose. *Journal of Agricultural and Food Chemistry*, **16** (5): 717-719 (1968)
61. Alkhamis, K.A. Influence of solid-state acidity on the decomposition of sucrose in amorphous systems. *International Journal of Pharmaceutics*, **362** (1-2): 74-80 (2008)
62. Chatterjee, K., Shalaev, E.Y., Suryanarayanan, R., and Govindarajan, R. Correlation between chemical reactivity and the Hammett acidity function in amorphous solids using inversion of sucrose as a model reaction. *Journal of Pharmaceutical Sciences*, **97** (1): 274-286 (2008)
63. Fischer, S., Hoernschemeyer, J., and Mahler, H.C. Glycation during storage and administration of monoclonal antibody formulations. *European Journal of Pharmaceutics and Biopharmaceutics*, **70** (1): 42-50 (2008)
64. Li, S., Patapoff, T.W., Overcashier, D., Hsu, C., Nguyen, T.H., and Borchardt, R.T. Effects of reducing sugars on the chemical stability of human relaxin in the lyophilized state. *Journal of Pharmaceutical Sciences*, **85** (8): 873-877 (1996)
65. Tarelli, E., Corran, P.H., Bingham, B.R., Mollison, H., and Wait, R. Lysine vasopressin undergoes rapid glycation in the presence of reducing sugars. *Journal of Pharmaceutical and Biomedical Analysis*, **12** (11): 1355-1361 (1994)
66. Silvan, J.M., van de Lagemaat, J., Olano, A., and del Castillo, M.D. Analysis and biological properties of amino acid derivatives formed by Maillard reaction in foods. *Journal of Pharmaceutical and Biomedical Analysis*, **41** (5): 1543-1551 (2006)
67. Fay, L.B. and Brevard, H. Contribution of mass spectrometry to the study of the maillard reaction in food. *Mass Spectrometry Reviews*, **24** (4): 487-507 (2005)
68. Delgado-Andrade, C., Rufian-Henares, J.A., and Morales, F.J. Study on fluorescence of Maillard reaction compounds in breakfast cereals. *Mol.Nutr.Food Res.*, **50** (9): 799-804 (2006)
69. Lievonen, S.M., Laaksonen, T.J., and Roos, Y.H. Nonenzymatic Browning in Food Models in the Vicinity of the Glass Transition: Effects of Fructose, Glucose, and Xylose as Reducing Sugar. *Journal of Agricultural and Food Chemistry*, **50** (24): 7034-7041 (2002)
70. Bell, L.N. Kinetics of non-enzymic browning in amorphous solid systems: distinguishing the effects of water activity and the glass transition. *Food Research International*, **28** (6): 591-597 (1995)
71. Miao, S. and Roos, Y.H. Nonenzymatic browning kinetics in low-moisture food systems as affected by matrix composition and crystallization. *Journal of Food Science*, **70** (2): E69-E77 (2005)
72. Hill, S.A., MacNaughtan, W., Farhat, I.A., Noel, T.R., Parker, R., Ring, S.G., and Whitcombe, M.J. The effect of thermal history on the Maillard reaction in a glassy matrix. *Journal of Agricultural and Food Chemistry*, **53** (26): 10213-10218 (2005)
73. Bell, L.N., Touma, D.E., White, K.L., and Chen, Y.H. Glycine loss and Maillard browning as related to the glass transition in a model food system. *Journal of Food Science*, **63** (4): 625-628 (1998)
74. White, K.L. and Bell, L.N. Glucose loss and Maillard browning in solids as affected by porosity and collapse. *Journal of Food Science*, **64** (6): 1010-1014 (1999)

75. Buera, M.P. and Karel, M. Effect of physical changes on the rates of nonenzymic browning and related reactions. *Food Chem.*, **52** (2): 167-173 (1994)
76. Acevedo, N., Schebor, C., and Buera, M.P. Water-solids interactions, matrix structural properties and the rate of non-enzymatic browning. *Journal of Food Engineering*, **77** (4): 1108-1115 (2006)
77. Chatterjee, K., Shalaev, E.Y., and Suryanarayanan, R. Raffinose Crystallization During Freeze-Drying and Its Impact on Recovery of Protein Activity. *Pharmaceutical Research*, **22** (2): 303-309 (2005)
78. Pyne, A., Chatterjee, K., and Suryanarayanan, R. Solute crystallization in mannitol-glycine systems-implications on protein stabilization in freeze-dried formulations. *Journal of Pharmaceutical Sciences*, **92** (11): 2272-2283 (2003)
79. Sun, W.Q. and Davidson, P. Protein inactivation in amorphous sucrose and trehalose matrixes: effects of phase separation and crystallization. *Biochimica et Biophysica Acta, General Subjects*, **1425** (1): 235-244 (1998)
80. Byler, D.M. and Susi, H. Examination of the secondary structure of proteins by deconvolved FTIR spectra. *Biopolymers*, **25** (3): 469-487 (1986)
81. Costantino, H.R., Andya, J.D., Shire, S.J., and Hsu, C.C. Fourier-transform infrared spectroscopic analysis of the secondary structure of recombinant humanized immunoglobulin G. *Pharmaceutical Sciences*, **3** (3): 121-128 (1997)
82. Maury, M., Murphy, K., Kumar, S., Mauerer, A., and Lee, G. Spray-drying of proteins: effects of sorbitol and trehalose on aggregation and FT-IR amide I spectrum of an immunoglobulin G. *European Journal of Pharmaceutics and Biopharmaceutics*, **59** (2): 251-261 (2005)
83. Susi, H. and Byler, D.M. Resolution-enhanced Fourier transform infrared spectroscopy of enzymes. *Methods in Enzymology*, **130** (Enzyme Struct., Pt. K): 290-311 (1986)
84. Tian, F., Middaugh, C.R., Offerdahl, T., Munson, E., Sane, S., and Rytting, J.H. Spectroscopic evaluation of the stabilization of humanized monoclonal antibodies in amino acid formulations. *International Journal of Pharmaceutics*, **335** (1-2): 20-31 (2007)
85. Dong, A., Prestrelski, S.J., Allison, S.D., and Carpenter, J.F. Infrared Spectroscopic Studies of Lyophilization- and Temperature-Induced Protein Aggregation. *Journal of Pharmaceutical Sciences*, **84** (4): 415-424 (1995)
86. Garidel, P. and Schott, H. Fourier-transform midinfrared spectroscopy for analysis and screening of liquid protein formulations. Part 2: detailed analysis and applications. *Bioprocess International*, **4** (6): 48-50, 52, 54 (2006)
87. Costantino, H.R., Schwendeman, S.P., Griebenow, K., Klibanov, A.M., and Langer, R. The Secondary Structure and Aggregation of Lyophilized Tetanus Toxoid. *Journal of Pharmaceutical Sciences*, **85** (12): 1290-1293 (1996)
88. Griebenow, K. and Klibanov, A.M. Lyophilization-induced reversible changes in the secondary structure of proteins. *Proceedings of the National Academy of Sciences of the United States of America*, **92** (24): 10969-10976 (1995)
89. Schuele, S., Friess, W., Bechtold-Peters, K., and Garidel, P. Conformational analysis of protein secondary structure during spray-drying of antibody/mannitol formulations. *European Journal of Pharmaceutics and Biopharmaceutics*, **65** (1): 1-9 (2007)
90. Saunders, M., Podluis, K., Shergill, S., Buckton, G., and Royall, P. The potential of high speed DSC (Hyper-DSC) for the detection and quantification of small amounts of amorphous content in predominantly crystalline samples. *International Journal of Pharmaceutics*, **274** (1-2): 35-40 (2004)
91. Te Booy, M.P.W.M., De Ruiter, R.A., and De Meere, A.L.J. Evaluation of the physical stability of freeze-dried sucrose-containing formulations by differential scanning calorimetry. *Pharmaceutical Research*, **9** (1): 109-114 (1992)
92. Yoshioka, S., Aso, Y., and Kojima, S. Determination of molecular mobility of lyophilized bovine serum albumin and g-globulin by solid-state ¹H NMR and relation to aggregation-susceptibility. *Pharmaceutical Research*, **13** (6): 926-930 (1996)

93. Burin, L., Jouppila, K., Roos, Y.H., Kansikas, J., and Buera, M.P. Retention of beta -galactosidase activity as related to Maillard reaction, lactose crystallization, collapse and glass transition in low moisture whey systems. *International Dairy Journal*, **14** (6): 517-525 (2004)
94. Chatterjee, K., Shalaev, E.Y., and Suryanarayanan, R. Partially crystalline systems in lyophilization: I. Use of ternary state diagrams to determine extent of crystallization of bulking agent. *Journal of Pharmaceutical Sciences*, **94** (4): 798-808 (2005)
95. Overcashier, D.E., Patapoff, T.W., and Hsu, C.C. Lyophilization of Protein Formulations in Vials: Investigation of the Relationship between Resistance to Vapor Flow during Primary Drying and Small-Scale Product Collapse. *Journal of Pharmaceutical Sciences*, **88** (7): 688-695 (1999)
96. Mattern, M., Winter, G., Rudolph, R., and Lee, G. Formulation of proteins in vacuum-dried glasses. Part 1. Improved vacuum-drying of sugars using crystallizing amino acids. *European Journal of Pharmaceutics and Biopharmaceutics*, **44** (2): 177-185 (1997)
97. Hawe, A. and Friess, W. Physico-chemical lyophilization behavior of mannitol, human serum albumin formulations. *European Journal of Pharmaceutical Sciences*, **28** (3): 224-232 (2006)
98. Yu, L. Nucleation of One Polymorph by Another. *J.Am.Chem.Soc.*, **125** (21): 6380-6381 (2003)
99. Schuele, S., Schulz-Fademrecht, T., Garidel, P., Bechtold-Peters, K., and Friess, W. Stabilization of IgG1 in spray-dried powders for inhalation. *European Journal of Pharmaceutics and Biopharmaceutics*, **69** (3): 793-807 (2008)
100. Nema, S. and Avis, K.E. Freeze-thaw studies of a model protein, lactate dehydrogenase, in the presence of cryoprotectants. *J.Parenter.Sci.Technol.*, **47** (2): 76-83 (1993)
101. Izutsu, K.i., Yoshioka, S., and Terao, T. Stabilizing effect of amphiphilic excipients on the freeze-thawing and freeze-drying of lactate dehydrogenase. *Biotechnology and Bioengineering*, **43** (11): 1102-1107 (1994)
102. Mi, Y. and Wood, G. The application and mechanisms of polyethylene glycol 8000 on stabilizing lactate dehydrogenase during lyophilization. *PDA journal of pharmaceutical science and technology / PDA*, **58** (4): 192-202 (2004)
103. Iwai, J., Ogawa, N., Nagase, H., Endo, T., Loftsson, T., and Ueda, H. Effects of various cyclodextrins on the stability of freeze-dried lactate dehydrogenase. *Journal of Pharmaceutical Sciences*, **96** (11): 3140-3143 (2007)
104. Mi, Y., Wood, G., and Thoma, L. Cryoprotection mechanisms of polyethylene glycols on lactate dehydrogenase during freeze-thawing. *AAPS Journal*, **6** (3): e22(2004)
105. Anchordoquy, T.J., Izutsu, K.i., Randolph, T.W., and Carpenter, J.F. Maintenance of Quaternary Structure in the Frozen State Stabilizes Lactate Dehydrogenase during Freeze-Drying. *Archives of Biochemistry and Biophysics*, **390** (1): 35-41 (2001)
106. Earle, J.P., Bennett, P.S., Larson, K.A., and Shaw, R. The effects of stopper drying on moisture levels of Haemophilus influenzae conjugate vaccine. *Developments in Biological Standardization*, **74** (Biol. Prod. Freeze-Drying Formulation): 203-210 (1992)
107. Carpenter, J.F., Prestrelski, S.J., and Arakawa, T. Separation of freezing- and drying-induced denaturation of lyophilized proteins using stress-specific stabilization. I. Enzyme activity and calorimetric studies. *Archives of Biochemistry and Biophysics*, **303** (2): 456-464 (1993)
108. Izutsu, K.i., Yoshioka, S., and Kojima, S. Increased stabilizing effects of amphiphilic excipients on freeze-drying of lactate dehydrogenase (LDH) by dispersion into sugar matrixes. *Pharmaceutical Research*, **12** (6): 838-843 (1995)
109. Chinachoti, P. and Steinberg, M.P. Crystallinity of sucrose by x-ray diffraction as influenced by absorption versus desorption, waxy maize starch content, and water activity. *Journal of Food Science*, **51** (2): 456-9, 463 (1986)
110. Izutsu, K., Yoshioka, S., and Terao, T. Effect of mannitol crystallinity on the stabilization of enzymes during freeze-drying. *Chemical & Pharmaceutical Bulletin*, **42** (1): 5-8 (1994)

111. Kawai, K. and Suzuki, T. Stabilizing Effect of Four Types of Disaccharide on the Enzymatic Activity of Freeze-dried Lactate Dehydrogenase: Step by Step Evaluation from Freezing to Storage. *Pharmaceutical Research*, **24** (10): 1883-1890 (2007)
112. Crowe, L.M., Reid, D.S., and Crowe, J.H. Is trehalose special for preserving dry biomaterials? *Biophysical Journal*, **71** (4): 2087-2093 (1996)
113. Bhatnagar, B.S., Pikal, M.J., and Bogner, R.H. Study of the individual contributions of ice formation and freeze-concentration on isothermal stability of lactate dehydrogenase during freezing. *Journal of Pharmaceutical Sciences*, **97** (2): 787-803 (2008)
114. Carpenter, J.F., Randolph, T.W., Jiskoot, W., Crommelin, D.J.A., Middaugh, C.R., Winter, G., Fan, Y.X., Kirshner, S., Verthelyi, D., Kozlowski, S., Clouse, K.A., Swann, P.G., Rosenberg, A., and Cherney, B. Overlooking subvisible particles in therapeutic protein products: gaps that may compromise product quality. *Journal of Pharmaceutical Sciences*, **98** (4): 1201-1205 (2009)
115. Hawe, A. and Friess, W. Stabilization of a hydrophobic recombinant cytokine by human serum albumin. *Journal of Pharmaceutical Sciences*, **96** (11): 2987-2999 (2007)
116. Anchordoquy, T.J. and Carpenter, J.F. Polymers protect lactate dehydrogenase during freeze-drying by inhibiting dissociation in the frozen state. *Archives of Biochemistry and Biophysics*, **332** (2): 231-238 (1996)
117. Elkordy, A.A., Forbes, R.T., and Barry, B.W. Study of protein conformational stability and integrity using calorimetry and FT-Raman spectroscopy correlated with enzymatic activity. *European Journal of Pharmaceutical Sciences*, **33** (2): 177-190 (2008)
118. Prestrelski, S.J., Arakawa, T., and Carpenter, J.F. Separation of freezing- and drying-induced denaturation of lyophilized proteins using stress-specific stabilization. II. Structural studies using infrared spectroscopy. *Archives of Biochemistry and Biophysics*, **303** (2): 465-473 (1993)
119. Wang, B., Tchessalov, S., Warne, N.W., and Pikal, M.J. Impact of Sucrose level on Storage Stability of Proteins in Freeze-dried Solids: I. Correlation of Protein-Sugar Interaction With Native Structure Preservation. *Journal of Pharmaceutical Sciences*, **9999 published online** (9999): n/a-n/a (2008)
120. Goller, K. and Galinski, E.A. Protection of a model enzyme (lactate dehydrogenase) against heat, urea and freeze-thaw treatment by compatible solute additives. *Journal of Molecular Catalysis B: Enzymatic*, **7** (1-4): 37-45 (1999)
121. Ladokhin, A.S. Fluorescence Spectroscopy in Peptide and Protein Analysis. *Encyclopedia of Analytical Chemistry* (2000)
122. Hsu, C.C., Ward, C.A., Pearlman, R., Nguyen, H.M., Yeung, D.A., and Curley, J.G. Determining the optimum residual moisture in lyophilized protein pharmaceuticals. *Developments in Biological Standardization*, **74** (Biol. Prod. Freeze-Drying Formulation): 255-271 (1992)
123. Modi, N.B. Recombinant thrombolytic agents. *Pharm. Biotechnol. (2nd Ed.)*, 327-338 (2002)
124. Carlson, R.H., Garnick, R.L., Jones, A.J.S., and Meunier, A.M. The determination of recombinant human tissue-type plasminogen activator activity by turbidimetry using a microcentrifugal analyzer. *Analytical Biochemistry*, **168** (2): 428-435 (1988)
125. Mumenthaler, M., Hsu, C.C., and Pearlman, R. Feasibility study on spray-drying protein pharmaceuticals: recombinant human growth hormone and tissue-type plasminogen activator. *Pharmaceutical Research*, **11** (1): 12-20 (1994)
126. Kueltzo, L.A. and Middaugh, C.R. Structural characterization of bovine granulocyte colony stimulating factor: Effect of temperature and pH. *Journal of Pharmaceutical Sciences*, **92** (9): 1793-1804 (2003)
127. Kueltzo, L.A., Ersoy, B., Ralston, J.P., and Middaugh, C.R. Derivative absorbance spectroscopy and protein phase diagrams as tools for comprehensive protein characterization: A bGCSF case study. *Journal of Pharmaceutical Sciences*, **92** (9): 1805-1820 (2003)
128. Mach, H. and Middaugh, C.R. Simultaneous monitoring of the environment of tryptophan, tyrosine, and phenylalanine residues in proteins by near-ultraviolet second-derivative spectroscopy. *Analytical Biochemistry*, **222** (2): 323-331 (1994)

129. Ragone, R., Colonna, G., Balestrieri, C., Servillo, L., and Irace, G. Determination of tyrosine exposure in proteins by second-derivative spectroscopy. *Biochemistry*, **23** (8): 1871-1875 (1984)
130. Burin, L., Jouppila, K., Roos, Y., Kansikas, J., and Buera, M.P. Color formation in dehydrated modified whey powder systems as affected by compression and T(g). *J Agric Food Chem*, **48** (11): 5263-5268 (2000)

CHAPTER 9

GLASSY DYNAMICS OF COLLAPSED AND NON-COLLAPSED LYOPHILIZATES

1 INTRODUCTION

Freeze-dried protein formulations are usually composed of the protein and one or more amorphous stabilizers. The addition of a crystalline bulking agent merely has cosmetic reasons, just marginally affecting protein stability, e.g. in their effect on the drying behavior and thus the residual moisture level of the freeze-dried cake. Thus freeze-dried formulations are at least partially amorphous and they are physically considered as glasses.

There are two major hypotheses explaining protein stability in the solid state. One is the “water replacement hypothesis”, stating that native structure is preserved upon drying by direct interaction between stabilizer and protein via hydrogen bonds replacing the hydrogen bonds to water molecules that are removed upon drying. By preventing unfolding the protein is thermodynamically stabilized.

There are further stabilization concepts related to native structure preservation during drying and in the solid state. During freezing the protein may be stabilized by preferential exclusion. Upon storage in the solid state the preservation of native conformation can be achieved by simple immobilization in the rigid matrix, similar to the concept of the vitrification hypothesis as described in detail in the general introduction of this thesis.

Preservation of native protein conformation both in the solid state and after reconstitution is regarded as a prerequisite for satisfying protein stabilization.

The second main concept of protein stability in the solid state is the “vitrification hypothesis”, otherwise referred to as “glassy-dynamics-hypothesis”. According to this theory stabilization is governed by kinetic rather than by thermodynamic aspects. The protein, as it is molecularly dispersed in the glassy matrix, is immobilized in a rigid glassy state. Dilution in the glassy matrix separates protein molecules from each other and the strongly reduced molecular mobility inhibits the diffusion of reactive species as well. Thus chemical and physical degradation reactions are strongly slowed down.

In the foregoing chapters it was shown that proteins were well stabilized in collapsed lyophilizates. No change in protein conformation or in the susceptibility towards aggregation could be detected in collapsed lyophilizates as compared to non-collapsed lyophilizates. Thus thermodynamic stabilization concepts presumably remained unaffected by collapse.

To complete the investigation of the effect of collapse on protein-containing lyophilizates, the effect of collapse on kinetic stabilization concepts, i.e. the effect of collapse on the glassy dynamics of amorphous protein lyophilizates, was investigated as well.

Because glasses are not formed by a first order transition but by a mobility transition that has the DSC signature of a second order transition the characteristic properties of the glass are strongly affected by the way it is formed. For example there is a strong effect of the rate of cooling through the glass transition temperature with fast cooling resulting in high enthalpy and thus less stable glasses. There is evidence in literature that the drying method applied to produce amorphous solids affects the solid state properties of glassy systems as well¹⁻³. The effect of drying method is at least partially attributable to the so-called annealing effect:

A system in the glassy state is not in thermodynamic equilibrium. A schematic overview of the glass formation process is given in Figures 1.7 (page 27) and 1.10 (page 32) in the general introduction of this thesis. During glass formation the system is “frozen in”, thereby causing a significant amount of disorder increasing the system’s enthalpy level. During storage the system asymptotically approaches the “equilibrium glassy state” that is the theoretical extension of the super-cooled liquid enthalpy temperature course increasing the system’s degree of order. This process is called relaxation. Changes due to relaxation occur more readily in glasses with higher enthalpy levels.

During annealing, that is controlled storage at an elevated temperature below T_g , molecular mobility is increased to a degree allowing for molecular rearrangement motions causing the system to relax to a certain degree. During subsequent storage the glass will exhibit decreased molecular mobility as compared to non-annealed samples.

Drying at high temperatures, such as spray drying or vacuum drying, was recently reported to exert a similar effect to the described annealing effect⁴. It also leads to more aged glasses produced by these techniques. In contrast, freeze-drying, that is accomplished at low temperatures, has a low annealing affect, leading to less aged glasses showing an increased molecular mobility³⁻⁶.

The occurrence of collapse during a freeze-drying run is usually provoked by a rise in product temperature above the collapse temperature T_c . Thus a collapsed product has been exposed to elevated temperatures during production as compared to non-collapsed samples, causing a change in the system’s thermal history and possibly exerting an effect similar to the described annealing effect. What is more, within this project, collapsed lyophilizates were reproducibly produced by a collapse cycle. To reliably exceed the collapse temperature T_c , high primary and secondary drying temperatures were applied. The non-collapsed lyophilizates were produced by a conventional freeze-drying cycle. Despite the constant cooling rate (0.78 K/min) to ensure comparable glass formation, the two drying procedures

used different drying temperatures that might exert different “annealing effects”, leading to amorphous systems with different properties in term of the glassy dynamics.

Molecular mobility in the glassy state is imparted by several modes. They are most broadly classified into global and local motions. Global motions, otherwise known as structural relaxation or α -relaxations involve larger-scale motions of the magnitude of entire molecules. They are coupled to viscosity and they are associated with the glass transition phenomenon^{7,8}.

Local motions, also known as fast dynamics or secondary relaxations, involve more localized motions of smaller parts of molecules, such as pending functional groups that occur over a broad frequency range anywhere between vibrational and rotational^{9,10}. They can be further classified into β - and γ -relaxations according to their point of emergence in the glassy state. γ -relaxations show lower apparent activation energies and they exist at lower temperatures than β -relaxations. In contrast to α -relaxations β - and γ -relaxations are relevantly observed in the glassy state and impart the mobility well below the glass transition temperature. A special case of β -relaxation is the Johari-Goldstein- β -relaxation that is intermolecular rather than intramolecular¹¹. Regarding disaccharides, it is most probably caused by twisting of mono-sugars around the glycosidic bond¹².

As every (degradation) reaction requires at least some degree of molecular mobility, molecular mobility and reactivity in the glassy solid state are at least partially coupled⁸.

As global dynamics are coupled to viscosity one would expect a relationship between degradation reactions that require the diffusion of larger reactive species through the glass, such as aggregation or non-enzymatic browning, to be coupled to global dynamics¹³⁻¹⁷. Reactions that only require small molecular motions of parts of macromolecules, such as deamidation, or that involve reactive species that are small as compared to the protein and can easily diffuse through the sugar-matrix, such as hydrogen ions or oxygen, are supposed to show a coupling to local dynamics^{9,18-20}.

In order to investigate the effect of collapse on the glassy dynamics of collapsed and non-collapsed lyophilizates and in order to correlate possible differences to observed differences in stability both of excipients and the incorporated protein, global and local dynamics of collapsed and non-collapsed model cakes were analyzed. Two disaccharide formulations, sucrose and trehalose based systems, were tested representing the most relevant amorphous excipients. A monoclonal antibody IgG₀₁ was incorporated as model protein representing the most relevant protein pharmaceutical at the moment.

2 SPECIAL MATERIALS AND METHODS

2.1 FREEZE-DRYING

2.1.1 SOLUTIONS FOR FREEZE-DRYING

Table 9.1 lists the composition of the solutions for freeze-drying. Solutions were prepared as described in detail in chapter 3 section 2.1.2.

Table 9.1: Composition of solutions for freeze-drying.

ID	excipient	concentration
1	IgG ₀₁	4.0 mg/mL
	sucrose	50.0 mg/mL
	polysorbate 20	0.4 mg/mL
	sodium succinate, pH 5.5	2.7 mg/mL
2	IgG01	4.0 mg/mL
	trehalose	50.0 mg/mL
	polysorbate 20	0.4 mg/mL
	sodium succinate, pH 5.5	2.7 mg/mL

2.1.2 COLLAPSED LYOPHILIZATES

Freeze-drying was performed according to the protocol described in chapter 3 section 2.1.3. Additionally, freeze-drying was performed as summarized in Table 9.2 using a FTS Systems Durastop freeze-dryer (Stone Ridge, NY, USA). Solutions were lyophilized in 3 mL serum vials (West Pharmaceutical Services, Lionville, PA, USA) with a fill volume of 1 mL according to the protocol specified in Table 9.2. Product temperatures ranged from -18 °C to -10 °C during the primary drying ramp that provoked lyophilizate collapse, thus well above the collapse temperature at approximately -36 °C. After freeze-drying the chamber was vented with dry nitrogen to a pressure of approximately 600 mbar and the vials were closed with pre-dried (60 °C over night) B2-44 lyophilization stoppers (West, Eschweiler, Germany).

Table 9.2: Parameters of the freeze-drying cycle applied to produce collapsed lyophilizates.

step	ramp [°C/min]	temperature [°C]	pressure [mbar]	hold time [min]
freezing	0.8	-40	-	210
primary/ secondary drying	0.0	-40	2	20
	0.7	45	2	1440
	0.0	45	0.03	1200
	0.2	20	0.03	-

2.1.3 NON-COLLAPSED LYOPHILIZATES

Non-collapsed lyophilizates were produced using the freeze-drying protocol specified in Chapter 3 section 2.1.4 (gentle freeze-drying of sucrose-based IgG₀₁ lyophilizates). In addition to this protocol, lyophilizates were produced with a further protocol comprising an

additional, higher temperature secondary drying step. Table 9.1 summarizes the characteristic parameters.

Table 9.1: Parameters of the freeze-drying cycle applied to produce non-collapsed lyophilizates.

step	ramp [°C/min]	temperature [°C]	pressure [mbar]	hold time [min]
freezing	0.8	-40	-	210
primary/ secondary drying	0.0	-40	0.07	1800
	0.1	-20	0.07	600
	0.5	20	0.07	600
	0.2	35	0.07	600

Solutions were lyophilized in 3 mL serum vials as described above.

2.2 ANNEALING AFTER FREEZE-DRYING

In order to investigate the effect of annealing exerted by freeze-drying at high temperatures during the drying cycle, selected sucrose-based non-collapsed lyophilizates were subjected to a post-drying thermal treatment mimicking the collapse drying-protocol. Vials were placed in a Delta 9023 oven (Delta Design, temperature control ± 0.2 °C) and kept for 24 hours at 45 °C, i.e. the same period of time, the collapsed cakes were dried during primary and secondary drying of the collapse cycle. A beaker with silica gel was put into the oven to reduce the relative humidity. Annealing was performed below the glass transition of the lyophilizates that was determined to be at 61 °C and no collapse occurred during annealing.

2.3 ISOTHERMAL MICROCALORIMETRY (THERMAL ACTIVITY MONITOR (TAM))

A Thermal Activity Monitor (TAM 2277, Thermometric, Jarfalla, Sweden) was used to determine the relaxation time constants below the glass transition temperature. Isothermal microcalorimetry monitors the energy dissipation with time and thus provides a direct measure of the rate of structural relaxation during annealing time.

Samples were prepared in a glove-bag purged with dry nitrogen to minimize moisture uptake during sample handling. Approximately 250 – 350 mg of homogenized lyophilizate was loaded into stainless steel ampoules and sealed in the glove bag. Ampoules containing roughly the same mass of a thermally inert material (crystalline glycine) were used as reference ampoules in order to minimize noise. TAM experiments were carried out at 40°C for at least 70 h. The ampoules were loaded into the equilibration position of the calorimeter and allowed to thermally equilibrate with the instrument for 30 minutes. Then the ampoules were slowly lowered into the measurement position of the calorimeter and release of energy was recorded as a function of time. Due to distortion of the power-signal caused by friction produced during sample loading, data recorded during the first hour of the experiment was not included in the fitting procedure as described elsewhere²¹.

The recorded power-time curve was evaluated by fitting the experimental data to the derivative form of the modified stretched exponential (MSE) equation (9.1). This was accomplished by nonlinear curve fitting (Origin 7.0) and the parameters τ_0 , τ_1 , β were obtained.

$$P = 277.8 \frac{\Delta H_r(\infty)}{\tau_0} \left(1 + \frac{\beta\tau}{\tau_1}\right) \left(1 + \frac{\tau}{\tau_1}\right)^{\beta-2} \times \exp\left[-\left(\frac{t}{\tau_0}\right) \left(1 + \frac{t}{\tau_1}\right)^{\beta-1}\right] \quad (9.1)$$

In the above equation P is the power (in $\mu\text{W/g}$), $\Delta H_r(\infty)$ is the enthalpy relaxation at infinite time calculated according to equation (9.2), 277.8 is a numerical factor due to unit conversion, τ_0 is the relaxation time constant, τ_1 is the relaxation time constant at the “short time limit”, t is the measurement time in hours, β is the Kohlrausch-William-Watts nonexponential constant as described below.

$$\Delta H_r(\infty, T) = \Delta C_p (T_g - T) \quad (9.2)$$

Upon storage at a temperature below T_g a glassy material will undergo relaxation and thereby experience losses in enthalpy (ΔH) and volume (ΔV) as it approaches its equilibrium glassy state. When the aged material is heated through its glass transition the dissipated enthalpy will be fully recovered. This is called enthalpy recovery ΔH_i . $\Delta H_r(\infty)$ describes the maximum enthalpy recovery at a given temperature. It can be determined using DSC. In equation (9.2) T_g is the glass transition temperature, T is the temperature (in the case of TAM it is the experimental storage temperature), ΔC_p is the change in heat capacity at the glass transition temperature.

Structural relaxation is a multi-exponential decay from the glassy state towards the equilibrium state. It is well described by the empirical stretched exponential Kohlrausch-William-Watts equation (9.3)²²:

$$\phi(t) = \exp\left[-\left(\frac{t}{\tau}\right)^\beta\right] \quad (9.3)$$

Where $\Phi(t)$ is the relaxation at the time t, τ is the relaxation time constant and represents the most probable relaxation time and β is the so-called stretch parameter describing the distribution of independently relaxing substates, with β close to zero for a wide distribution of relaxing substates and for β equals one for a uniform relaxation.

For short experimental times with t approaching zero, the time derivative of Φ , the power P, approaches infinity. This discrepancy to the physically reasonable situation could cause inaccuracies in the evaluation of $\Phi(t)$ at short experimental times or in the analysis of slow relaxations²³. With the MSE formalism data obtained from short experimental times can be well described. At long experimental times the MSE equation is reduced to the KWW

equation. Moreover, the MSE equation bears further numerical advantages over the KWW expression and gives more self-consistent τ and β values²³.

The relaxation time τ_D that is equivalent to τ in the KWW equation was calculated from the parameters evaluated from the curve fitting according to equation (9.4).

$$\tau_D = (\tau_D)^{\frac{1}{\beta}} (\tau_1)^{\frac{(\beta-1)}{\beta}} \quad (9.4)$$

It was found by Kawakami et al. that τ and β values obtained from the fitting procedure were too large and too small, respectively but the expression τ^β remained reliable²⁴. Thus this term rather than just τ is used to describe the molecular mobility throughout this work.

Figure 9.1 exemplarily shows the power time data for non-collapsed freeze-dried sucrose obtained at 40 °C and the corresponding MSE fitting line.

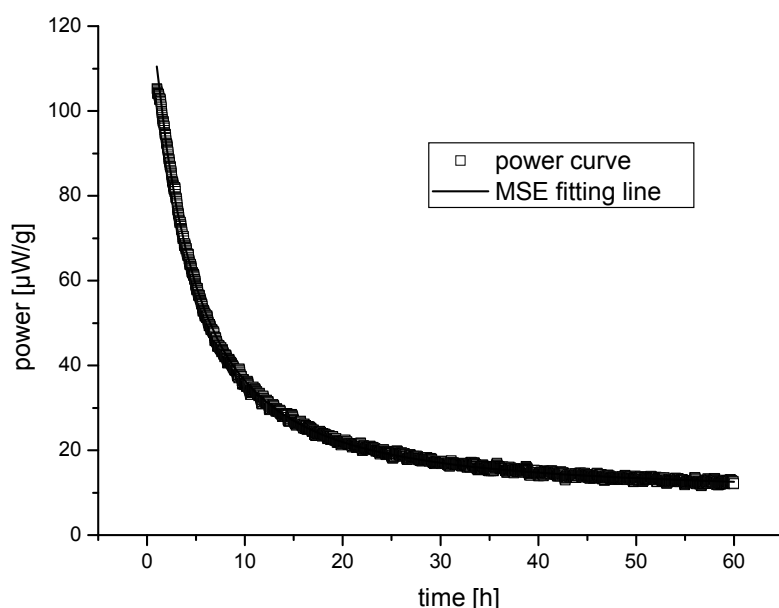


Figure 9.1: Power versus time data from an isothermal microcalorimetry experiment on non-collapsed freeze-dried sucrose lyophilizates at $T_g - 30$ K.

The curve was obtained by fitting the derivative form of the MSE equation to the TAM data ($\chi^2 = 0.32$, $\tau_0 = 35.43 \pm 0.07$ h, $\tau_1 = 7.82 \pm 0.06$ h, $\beta = 0.11 \pm 4.57E-03$, $\Delta H_r = 16.35$ J/g).

2.4 DIELECTRIC RELAXATION SPECTROSCOPY (DRS)

Dielectric relaxation spectroscopy was used to probe global and local dynamics in freeze-dried collapsed and non-collapsed cakes. DRS is particularly useful to analyse different modes of relaxation because of its ability to cover a wide frequency range ($\mu\text{Hz} - \text{GHz}$)^{25,26}.

Sample analysis was performed using a time domain spectrometer (TDS, IMASS, MA, USA)²⁷ that measures the response of a material to an externally applied field, i.e. a step voltage (100 V), as a function of time and subsequently transforms the measured signal into the frequency domain using Laplace transformation. Thus the material's dielectric response is analyzed as a function of frequency ($10^4 - 10^{-4}$ Hz). An equal and opposite voltage was applied to a reference capacitor and the transient difference in the capacitance of sample and reference was analyzed by a charge amplifier.

The applied electrode assembly was developed by the staff of the Institute of Materials Science (Machine Shop IMS, University of Connecticut) as described previously²¹. The established setup was varied slightly in order to adapt for the special requirements of the analysis of hygroscopic sucrose powders. For this purpose the lower electrode was replaced by a mount with a circular recess on the top that held the powder. Thus the thickness of the sample is predefined by the dimensions of the recess (0.0245 cm) and sample handling with the possible risk of moisture uptake could be minimized rendering additional thickness determination with a caliper gauge unnecessary. All sample handling was performed in a glove bag in a dry nitrogen atmosphere.

Between the sample surface and the upper electrode a Teflon sheet (0.14 mm thickness) was inserted to avoid dc-conductivity effects. The upper electrode was tightened with a screw on the top of the electrode assembly in order to ensure good thermal contact between the sample and the electrode and in order to avoid air gaps. The upper electrode was guarded by a built-in Teflon ring to prevent the effects of stray capacitance, edge effects and conductance due to moisture adsorption. Figure 9.2 depicts a schematic drawing of the electrode assembly.

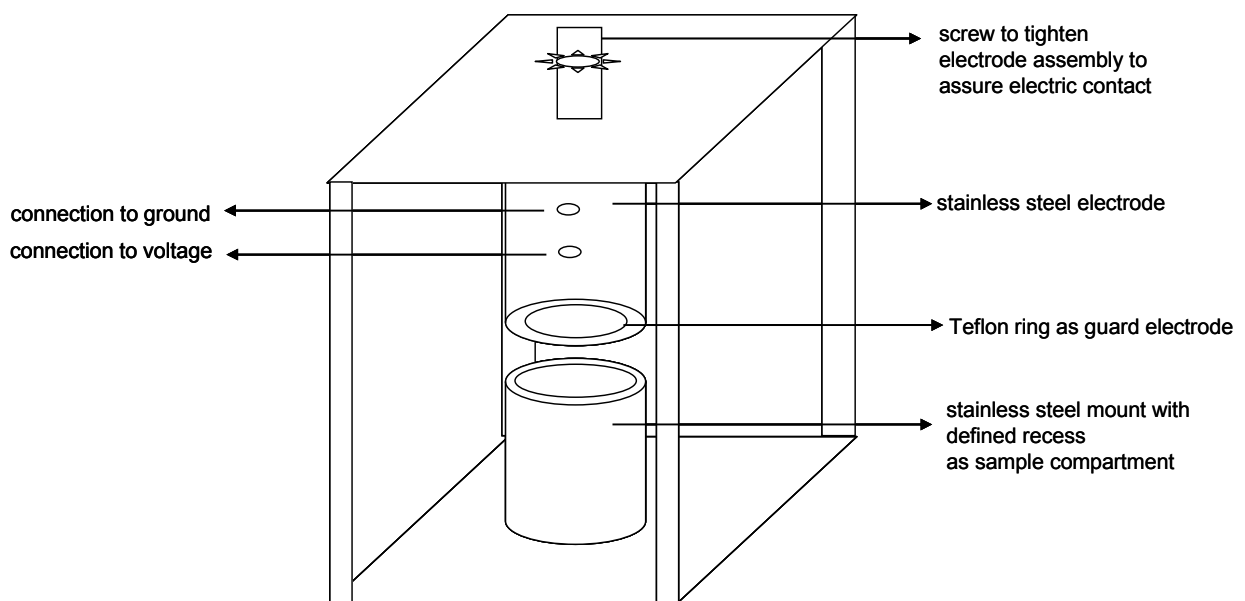


Figure 9.2: Electrode assembly used for dielectric measurements according to²¹ adapted for the analysis of hygroscopic sucrose powders.

The capacitance C was monitored as the overall response was monitored. The capacitance is determined by the sample's permittivity ϵ and the sample geometry, that is the area of the electrode A (1 cm diameter) and the sample thickness d (given by the recess dimension, i.e. 0.0245 cm). Equation (9.5) describes that relationship:

$$C = \frac{A\varepsilon}{d} \quad (9.5)$$

The electrode assembly was placed in an external temperature control device (Delta Design 9023, range -150 – 250 °C, temperature control ± 0.2 °C). To keep humidity low, a beaker with P₂O₅ was introduced into the oven chamber. Experiments were performed beginning at room temperature (= 25 °C) to 85 °C in steps of 5 °C; the sample equilibrated for 5 minutes prior to the measurement. Before each measurement a baseline was collected (before application of voltage) and the baseline was subtracted from the final response.

The charge transient was measured and the resulting capacitance C was calculated according to (9.6)²⁷:

$$C = \frac{Q(t)}{V} \quad (9.6)$$

Q is the charge that flows through the sample, t is time, V is the applied step voltage.

Using equation (9.5) from the capacitance C the sample's permittivity ε or rather the complex permittivity ε^* , as the sample is analyzed with changing frequency, can be calculated. The complex permittivity ε^* is composed of the real part of the permittivity ε' and the imaginary part of the permittivity ε'' as follows:

$$\varepsilon^*(\omega) = \varepsilon'(\omega) + i\varepsilon''(\omega) \quad (9.7)$$

The real part of the complex permittivity ε' corresponds to the dielectric constant of the material and thus describes the ability of the material to store the energy of an applied electric field by polarization of dipoles. The imaginary part of the complex permittivity ε'' describes the ability of the material to dissipate energy of the applied electric field by dielectric loss or through dc-conduction²⁵. Dielectric loss is an alternating current (ac) phenomenon and is caused by the fact that thermally damped dipoles do not respond immediately to an external field but with a characteristic lag time, the relaxation time. If the frequency of the external field is the same as the relaxation time, most energy is dissipated by oscillation of dipoles causing a maximum in the dielectric loss. Thus relaxation times can be determined by accurately identifying the maximum of the imaginary permittivity curve.

In 1929 Debye first described the relaxation behaviour of dielectrics with changing frequency with equation (9.8)²⁸.

$$\varepsilon^* = \varepsilon_\infty + \frac{\Delta\varepsilon}{1 + i\omega\tau_m} \quad (9.8)$$

In this equation ε^* is the complex permittivity, ε_∞ is the real permittivity at the high frequency limit representing instantaneous relaxation behaviour, $\Delta\varepsilon$ is the dielectric increment, i is $\sqrt{-1}$, ω is the angular frequency ($2\pi f$) of the applied field and τ_m is the relaxation time

This empirical model was further developed and adapted to observed differing relaxation behaviours by Cole-Cole²⁹, Cole-Davidson^{30,31} and Havriliak-Negami³². The Havriliak-Negami (HN) equation is the most general equation describing the relaxation behaviour.

$$\varepsilon^*(\omega) = \frac{\Delta\varepsilon}{[1 + (i\omega\tau)^{1-\alpha}]^\beta} + \varepsilon_\infty \quad (9.9)$$

In the HN-equation all the variables and parameters have their usual meaning. α and β are parameters introduced to account for the asymmetry and the broadness of the function, respectively. Special forms of the HN equation are the Cole-Cole equation ($\beta=1$) and the Cole-Davidson equation ($\alpha=0$). The HN equation equals to the Debye equation for $\alpha=0$ and $\beta=1$.

Cole-Cole also showed that for a material exhibiting Debye relaxation the so-called Cole-plot, i.e. a plot of real part of permittivity versus imaginary part of permittivity, results in a semi-circle. Figure 9.3 exemplarily shows a Cole-Cole plot for a not collapsed sucrose lyophilizate. Figure 9.3 A shows the sample at 75 °C exhibiting a semi-circle indicating Debye-type relaxation behaviour. However, the broadness of the observed semi-circle indicates relaxation behaviour characterized by a distribution of relaxation times that is thus best described by the Cole-Cole equation. At lower temperatures (Figure 9.3 B), the Cole-Cole plot shows a slightly asymmetric semi-circle indicating relaxation behaviour that was first described by Cole and Davidson for glycerol^{30,31}.

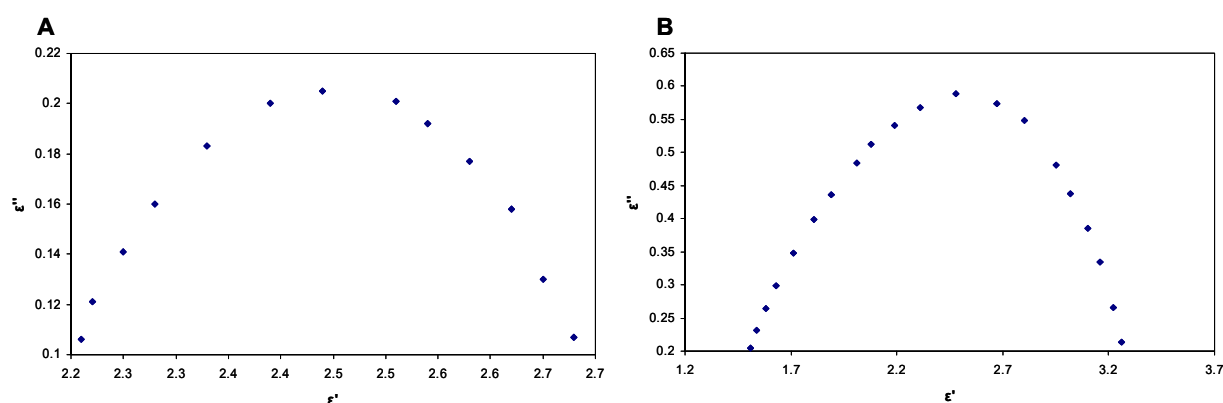


Figure 9.3: Cole-Cole plot for non-collapsed freeze-dried sucrose at 75 °C (A) and at 35 °C (B).

The Cole-Cole equation was used to obtain the relaxation parameters because the observed asymmetry was not very pronounced and only present in samples analyzed at temperatures close to room temperature. However, to make sure that the fitting procedure is correct, the quality of the fits was closely monitored using the χ^2 value.

The relaxation parameter was obtained from simultaneous fitting of the real and the imaginary part of the Cole-Cole equation to the data using nonlinear curve fitting (Origin 7.0). For this purpose the Cole-Cole equation was rewritten to give a term for the real and imaginary component of the permittivity (given in equations (9.10) und (9.11)).

$$\varepsilon' = (\varepsilon_0 - \varepsilon_\infty) \frac{[1 + ((\omega\tau)^\alpha) \cos(0.5\pi\alpha)]}{\left[\left(1 + (\omega\tau)^\alpha * \cos(0.5\pi\alpha)\right)^2 + \left((\omega\tau)^\alpha * \sin(0.5\pi\alpha)\right)^2 \right]} + \varepsilon_\infty \quad (9.10)$$

$$\varepsilon'' = (\varepsilon_0 - \varepsilon_\infty) \frac{[(\omega\tau)^\alpha * \sin(0.5\pi\alpha)]}{\left[\left(1 + (\omega\tau)^\alpha * \cos(0.5\pi\alpha)\right)^2 + \left((\omega\tau)^\alpha * \sin(0.5\pi\alpha)\right)^2 + \left(\frac{\sigma_{dc}}{\omega\varepsilon_0}\right) \right]} \quad (9.11)$$

In the above equations all the parameters have their usual meaning as described earlier. ε_0 is the real permittivity at the lower frequency limit and σ_{dc} is the contribution of dc-conductivity to the permittivity.

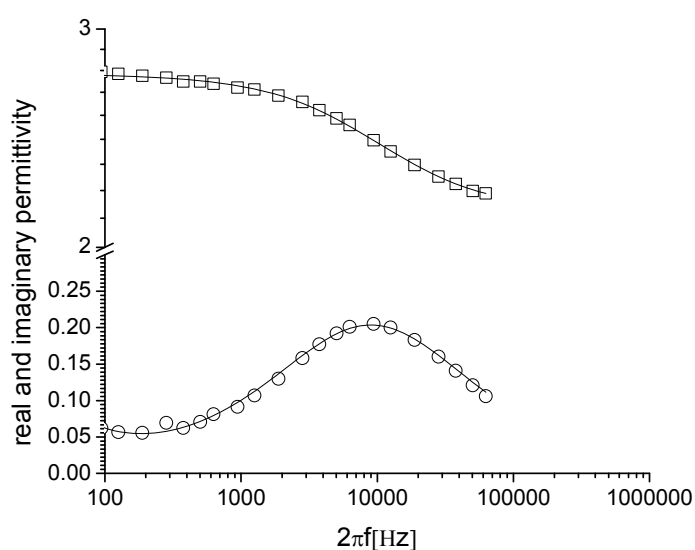


Figure 9.4: Simultaneous fitting of the real and the imaginary components of the Cole-Cole model to the real (open squares) and imaginary (open circles) permittivity of non-collapsed freeze-dried sucrose at 75°C.

$\chi^2 = 3E-05$, $\varepsilon_0 = 2.76229 \pm 0.00294$, $\varepsilon_\infty = 2.12914 \pm 0.00615$, $\square = 0.00011 \pm 2.5205E-6$, $\alpha = 0.72647 \pm 0.00943$, $\sigma_{dc} = 11.3296 \pm 1.15455$.

Figure 9.4 shows an example of for the simultaneous fitting of the data to the Cole-Cole model. The symbols (open squares and circles) represent the data, the solid lines the fit to the model.

2.5 DIFFERENTIAL SCANNING CALORIMETRY (DSC)

Differential Scanning Calorimetry was performed to determine the glass transition temperature T_g and to assess the systems' fragility.

A Q-1000 Differential Scanning Calorimeter equipped with a DSC refrigerated cooling system from TA Instruments Inc. (Newcastle, DE, USA) was used for all the measurements.

2.5.1 DETERMINATION OF T_g AND $\Delta C_p(T_g)$

For T_g -analysis the system was employed in modulated mode. All sample preparation was performed in a dry nitrogen atmosphere with relative humidity controlled to be below 2%. Approximately 5-15 mg powdered lyophilizate were filled into aluminium DSC pans,

compressed into a disc and hermetically sealed. Samples were heated at 2 °C/min to 150 °C with a modulation period and amplitude of 100 s and ± 1 °C, respectively. The glass transition was determined as the midpoint of the step change in reversing heat capacity at T_g . Δc_p was assessed by the offset between the reversing heat capacities of the glass and the supercooled liquid, extrapolated to T_g . Data analysis was done using Universal Analysis Version 4.3A, TA Instruments.

2.5.2 DETERMINATION OF FRAGILITY

For fragility-assessment, DSC scans were performed in standard mode. Samples were prepared as described above and heated from 0 °C to 120 °C applying different heating rates, i.e. 2 K/min, 5 K/min and 10 K/min. The onset and the midpoint of the glass transition as well as the heat capacity change at the glass transition Δc_p were determined from the heat capacity signal as described above.

Experimental data was then plotted according to an Arrhenius type relationship, i.e. log scan rate versus reciprocal glass transition temperature. From the best linear fit the activation energy (ΔH^{DSC}) is calculated. Fragility is determined from equation (9.12), where m is the fragility, ΔH^{DSC} is the activation energy for molecular motions at T_g and R is the gas constant.

$$m = \frac{\Delta H^{DSC}}{(2.303 * R * T_g)} \quad (9.12)$$

2.6 POWDER DENSITY MEASUREMENTS

Density of collapsed and non-collapsed lyophilizates was determined with helium pycnometry using an Accupyc 1330 Gas Pycnometer (Micromeritics, Norcross, GA, USA). Sample preparation and sample handling was performed in a dry nitrogen atmosphere, with the humidity controlled at below 2 %. Lyophilizates were homogenized with a spatula, ground in an agate mortar and transferred into a 1 cm³ aluminium sample cell, the surface was flattened and the sample was slightly compressed with a steel stab and the mass was determined. Then the cell was mounted into the analysis chamber. The sample was first purged with helium for about 30 minutes with the purge fill pressure adjusted to 134 kPa (19.5 psig). Then the sample was analyzed 20 times with the helium equilibration rate set to 34 Pa/min (0.005 psig/min). The pycnometer was tested for accuracy and precision using crystalline sucrose.

2.7 KARL FISCHER RESIDUAL MOISTURE DETERMINATION

Residual moistures were determined using coulometric Karl Fischer titration as described previously (Chapter 3, section 2.4.4) but with an instrument from Denver Instrument Company (Denver, CO, USA).

2.8 SOLID STATE FOURIER TRANSFORM INFRARED (SS-FTIR) SPECTROSCOPY

FTIR spectroscopy studies were performed using a Nicolet Magna IR 760 Spectrometer (Thermo-Nicolet, Madison, WI, USA). Spectra were collected in the solid state from 4000 to 400 cm^{-1} with a total of 120 scans and a resolution of 2 cm^{-1} . Spectra were corrected for contributions of water vapour and carbon dioxide by the subtraction of a background spectrum. Samples were prepared by pressing a ground homogeneous mixture of potassium bromide (approx. 500 mg) and lyophilizate (approx. 10 mg) into a disk. All sample handling, i.e. grinding and filling into the die, was performed in a glove bag in a dry nitrogen atmosphere. A disc was formed by compressing the powder in a Carver press using a pressure of 10000 psi for 2 minutes. During this time vacuum was applied to avoid the sample to get into contact with air and relative humidity. Before spectra collection each specimen was equilibrated for at least 4 minutes to reduce the noise signal of water vapour in the sample compartment.

Spectra were further processed using Omnic software (Nicolet, Madison, WI, USA). Second derivatives of the spectra were calculated using the Savitzky-Golay algorithm (7 points, 3rd polynomial order) and the spectra were 7 point-smoothed. Then the amide I-region of the spectra, ranging from 1600 to 1700 cm^{-1} , was baseline corrected and area-normalized. Spectra were visually compared to each other to check for differences in the secondary structure.

2.9 SPECIFIC SURFACE AREA (SSA) MEASUREMENT

The BET (Brunauer-Emmett-Teller) specific surface area (SSA) was analyzed using a Flowsorb II 2300 BET surface area analyzer (Micromeritics, Norcross, GA, USA) using krypton gas. All sample handling was performed in a dry nitrogen atmosphere. Lyophilizates were homogenized with a spatula and at least 100 mg sample were filled into the sample holder and all samples were degassed for 1 h at 35 °C during krypton purge. Prior to the measurement the equipment was calibrated by a 1-point calibration with 0.1 mol krypton gas.

2.10 HIGH PRESSURE SIZE-EXCLUSION CHROMATOGRAPHY (HP-SEC)

Aggregation of IgG₀₁ was analyzed using HP-SEC. The chromatography system consisted of an HP1100 HPLC pump equipped with a UV multiple wavelength detector, an automatic sampling system and an in-line degasser. Analysis was accomplished using a TSK Gel 3000SWXL column (Tosoh Biosep, Stuttgart, Germany). Assays were performed as described previously (Chapter 3, section 2.3.1).

2.11 POLARIZED LIGHT MICROSCOPY

Samples were routinely checked for the onset of crystallization after completion of TAM-experiments and after storage at elevated temperatures. Samples were immersed in silicone oil and checked for the presence of birefringence using polarized light microscopy.

3 GLOBAL DYNAMICS OF COLLAPSED AND NOT COLLAPSED LYOPHILIZATES

Relaxation from the amorphous solid state towards the lower enthalpy equilibrium glass is mediated by several relaxation modes that can be classified into global and local dynamics. Global dynamics, otherwise known as α -relaxations, involve highly cooperative motions over length scales such as the diameter of a whole molecule. Thus they are coupled to viscosity. α -relaxations are associated with the dynamic glass transition phenomenon and the glass transition is defined as the temperature where global dynamics appear at the timescale of 100 s^{33} . Below the glass transition temperature, α -relaxations occur at much longer timescales eventually exceeding experimental time scales, but there is a significant molecular mobility existent even well below the glass transition.

As all degradation reactions require at least some degree of mobility, a correlation between stability and molecular mobility may well be relevant. The effect of different drying methods on the global dynamics of amorphous solids was recently observed^{1,3}. Collapse, also indicating a change in the sample's thermal history, might have an effect on α -relaxations as well. In order to compare the structural relaxation times of collapsed and non-collapsed lyophilizates different techniques were employed

3.1 GLOBAL DYNAMICS FROM CALORIMETRIC DATA

3.1.1 SUCROSE-BASED FREEZE-DRIED SYSTEMS

The rate of relaxation to the equilibrium state at a certain temperature below the glass transition is affected by the molecular mobility (expressed as relaxation time constant τ , being inversely proportional to the molecular mobility) and the distribution of individually relaxing substates (expressed as the stretch parameter β) as described by the Kohlrausch-William-Watts equation.

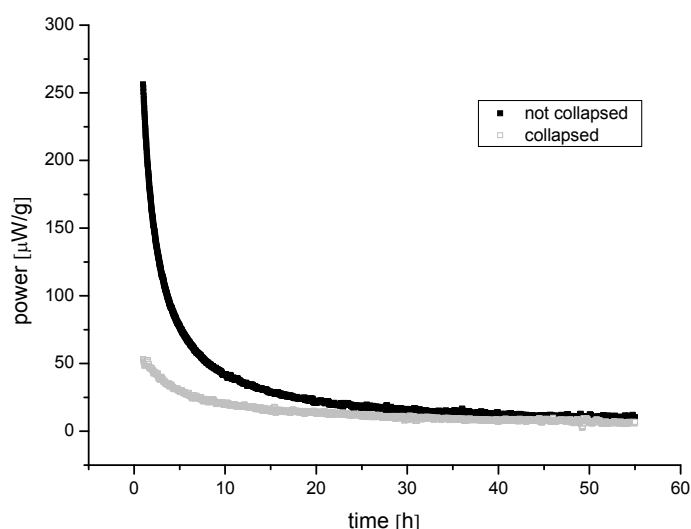


Figure 9.5: Power versus time curves obtained from an isothermal microcalorimetry experiment on collapsed (gray squares) and non-collapsed (black squares) freeze-dried sucrose cakes. Experimental temperature was $40 \text{ }^\circ\text{C}$; power is normalized for sample mass.

Relaxation can be monitored calorimetrically by measuring the rate of energy dissipation with time. Figure 9.5 shows such a power versus time curve (normalized for the sample mass) as determined with isothermal microcalorimetry during incubation at 40 °C for 60 hours. By fitting this curve to the MSE equation as described in detail in the materials and methods section of this chapter, the relaxation time constants were obtained.

Figure 9.6 shows the calculated τ^β values. $\tau^\beta \pm \text{SD}$ rather than just τ was used to compare the relaxation time constants because this measure was found to be more robust²⁴.

Most obviously collapsed lyophilizates show a strongly increased structural relaxation time constant, thus a strongly reduced global molecular mobility. This difference in molecular mobility can be attributed to the differences in the drying temperatures applied in the two freeze-drying cycles. The protocol used to produce collapsed lyophilizates applied higher temperatures in order to exceed the collapse temperature. Once the ice is sublimed and secondary drying has started, this drying at high temperatures may act similar to annealing. The molecular mobility is temporarily increased, allowing controlled relaxation and eventually leading to already aged glasses with improved stability.

This is further confirmed by the pronounced offset in the power dissipation at the beginning of the experiment as can be observed in Figure 9.5: whereas non-collapsed lyophilizates emit power around 250 $\mu\text{W/g}$ at the beginning of the isothermal microcalorimetry experiment, collapsed lyophilizates start at power levels around 50 $\mu\text{W/g}$, indicating a much less energetic and more stable glass.

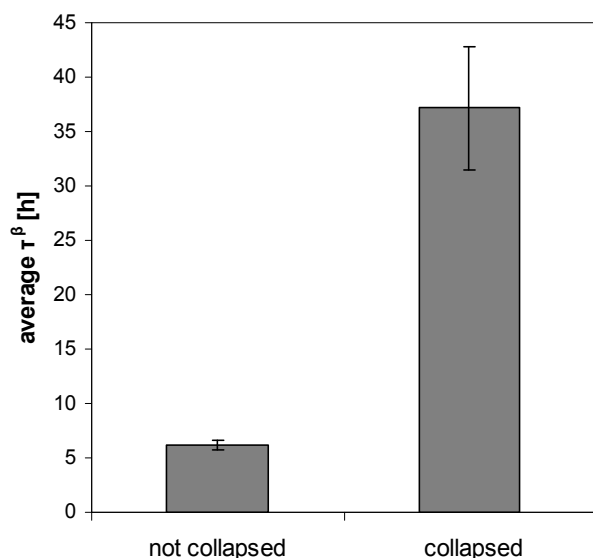


Figure 9.6: Calorimetric structural relaxation times - τ^β for collapsed and non-collapsed sucrose lyophilizates.

$n = 3$ and 5 for non-collapsed and collapsed cakes, respectively.

Table 9.2 lists the average β -values for collapsed and not collapsed lyophilizates as determined by TAM at 40 °C. Collapsed systems showed higher β -values indicating a more homogeneous glass composed of a smaller number of independently relaxing substates²⁴. This is in good agreement with Abdul-Fattah et al., who observed β -values between 0.7 – 0.9

for foam-dried IgG formulations (a drying technique similar to the collapse-cycle applied in this investigation), whereas freeze-dried solids exhibited β -values between 0.2 and 0.3⁵. However, as β -values determined from calorimetric measurements can be subject to experimental error, this data has to be regarded with some caution.

Table 9.2: Calorimetric relaxation times: τ^β and β -values for two batches of collapsed and non-collapsed sucrose-based lyophilizates as determined by TAM-measurements at 40 °C.

collapse status	secondary drying time [h] & temperature [°C]	residual moisture [%] \pm SD	Tg [°C] \pm SD	Tg-T*	$\tau^\beta \pm$ SD	$\beta \pm$ SD
collapsed	24/45	1.8 \pm 0.0	60.79 \pm 0.98	20.8	37.15 \pm 5.65	0.63 \pm 0.16
	44/45	1.1 \pm 0.1	65.02 \pm 0.95	25.0	65.72 \pm 0.51	0.76 \pm 0.10
not collapsed	10/20	1.3 \pm 0.1	60.77 \pm 2.85	20.8	6.23 \pm 0.42	0.32 \pm 0.02
	10/20 + 10/35	0.4 \pm 0.0	70.56 \pm 0.88	30.6	13.93 \pm 2.08	0.47 \pm 0.00

* T is the temperature at which TAM experiments were performed (i.e. 40 °C)

In order to check the general validity of the observed differences in relaxation times between collapsed and not collapsed systems, another batch of sucrose based IgG₀₁ lyophilizates was investigated. The samples were of identical composition but freeze-dried with slight variations in order to investigate the effect of drying temperature.

Collapsed lyophilizates were freeze-dried at 45 °C for 44 hours rather than 24 hours (this was the duration of secondary drying of the first sucrose lyophilizates). Elegant, not collapsed cakes were freeze-dried at 35 °C for 10 hours in addition to the secondary drying step at 20 °C.

Most obviously the prolonged drying times led to reduced residual moistures and increased glass transition temperatures. Table 9.2 summarizes the resulting residual moistures with the first/third line representing the residual moistures and glass transition temperatures of the shorter dried cakes and the second/fourth line representing the residual moistures and glass transition temperatures of the longer dried cakes, respectively. The results are in good agreement with literature stating an increase in glass transition temperature by 10 K for every 1 % residual moisture reductions³⁴.

Table 9.2 also shows the resulting structural relaxation times as determined by isothermal microcalorimetry. It is important to bear in mind the different glass transition temperatures and thus the different values of T_g-T (where T is the temperature the TAM experiment were conducted at), when evaluating the results. Because the second batch of freeze-dried cakes showed higher glass transition temperatures, the value of T_g-T was higher and also the absolute relaxation times are almost twice as long for the second batch. However, comparing collapsed and non-collapsed lyophilizates, the pronounced difference between collapsed and elegant cakes, with the collapsed cakes showing much higher relaxation times, was confirmed for the second batch. β -values in contrast showed only slight effects of longer

drying times. A small increase in β -values indicated more uniformly relaxing glasses for longer dried cakes. Again, the trend observed for the first sample set was confirmed, collapsed cakes showed higher β -values than elegant cakes, suggesting more stable amorphous systems.

3.1.2 TREHALOSE BASED FREEZE-DRIED SYSTEMS

To further investigate the effect of collapse on structural relaxation time, trehalose-based lyophilizates representing another important standard lyo-protectant system were investigated.

Table 9.3: Calorimetric relaxation times - τ^β and β -values for two batches of collapsed and non-collapsed sucrose-based lyophilizates as determined by TAM-measurements at 40 °C.

formulation	collapse status	Tg [K]	$\tau^\beta \pm \text{SD}$ [h]	$\beta \pm \text{SD}$
trehalose	collapsed	72.1	107.8 \pm 34.4	0.67 \pm 0.20
	not collapsed	60.1	45.41 \pm 3.31	0.77 \pm 0.08

Figure 9.7 depicts the average relaxation times for collapsed and non-collapsed lyophilizates, respectively. The results further corroborate the results obtained for sucrose based lyophilizates: collapsed cakes show strongly increased structural relaxation times. Compared to the sucrose based systems, the absolute relaxation time values are higher, because of the much higher glass transition temperatures of trehalose as compared to sucrose³⁵. Table 9.3 lists the relaxation times and β -values. Trehalose glasses show high β -values no matter whether the material has collapsed or not indicating a homogeneous glassy state for both materials.

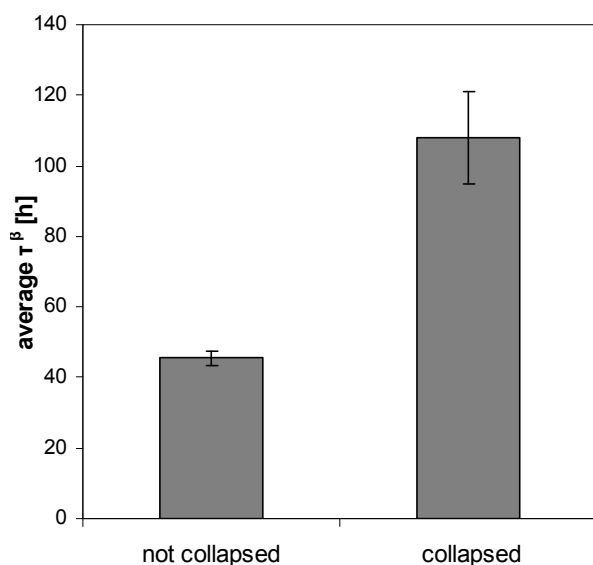


Figure 9.7: Calorimetric structural relaxation times - τ^β for collapsed and non-collapsed trehalose lyophilizates. (n = 4 and 7 for non-collapsed and collapsed cakes, respectively.)

This observation is further confirmed by the power versus time curves shown in Figure 9.8. Both systems exhibit a less pronounced decay of the power versus time curve as compared

to the sucrose based systems. However, the starting power level of the collapsed lyophilizates is again much lower than for the non-collapsed cakes, indicating an even more stable glassy system.

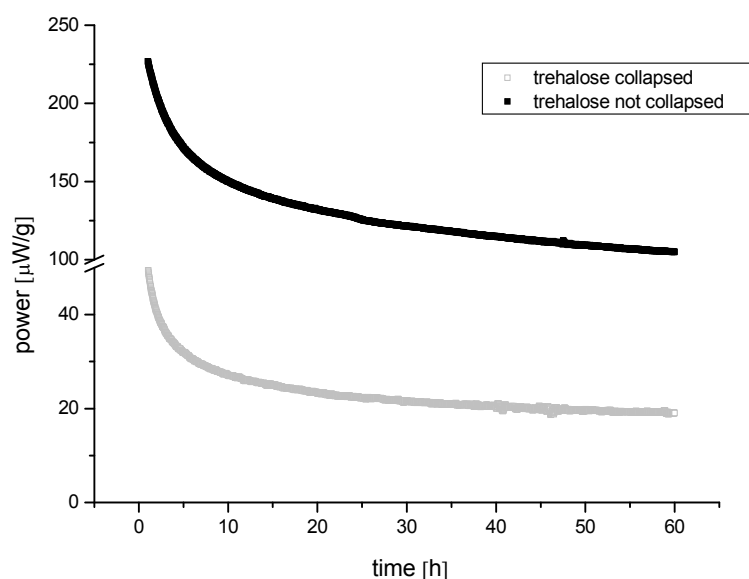


Figure 9.8: Power versus time curves obtained from an isothermal microcalorimetry experiment on collapsed (gray squares) and non-collapsed (black squares) freeze-dried trehalose cakes.

Experimental temperature was 40 °C; power is normalized for sample mass.

These findings coincide with observations made during stability studies comparing collapsed and non-collapsed trehalose lyophilizates described in Chapter 8. A detailed discussion of the possible correlation of molecular mobility analyzed in the systems described in this chapter and stability data observed in foregoing studies for comparable studies will be given in section 6.2 of this chapter.

3.2 GLOBAL DYNAMICS FROM SPECTROSCOPIC DATA

In order to further confirm data obtained from calorimetric measurements, global dynamics were additionally assessed using a spectroscopic technique, i.e. dielectric relaxation spectroscopy (DRS). Because energy dissipation accompanying structural relaxation is small and because it can only be detected using hyper-sensitive instruments that in turn also are hyper-sensitive to disturbances and because these experiments are time-consuming, dielectric relaxation spectroscopy offers some experimental advantages³⁶. Furthermore, DRS more conveniently allow the determination of relaxation times as a function of temperature. This can give further insight into the temperature dependence of global mobility, i.e. the fragility of the glassy system under investigation. As the fragility itself is an important characteristic property of glassy systems it will be discussed in section 5 of this chapter.

3.2.1 EXPERIMENTAL SET-UP: BENEFIT OF THE INSERTION OF A TEFLON-SHEET

In order to suppress polarization and conductivity effects the use of so-called remote electrode systems³⁷ was reported in literature. The insertion of thin sheets of Teflon^{38,39} or

polyethylene³⁷ between the sample and either just the upper electrode or both electrodes was described. The insertion of a poorly conductive material suppressed the so-called quasi dc (direct current) polarization that otherwise obscured the occurring relaxation processes^{38,39}. Quasi dc polarization is a low frequency dispersion (LFD) that is characterized by a high rise and a parallelism of the real and imaginary part of the permittivity at low frequencies⁴⁰. A further characteristic is the satisfaction of the “universal” fractional power law dependency on frequency³⁷. Quasi dc polarization is exhibited by most hydrated powders and commonly observed in sugars and polyalcohols. It is most likely caused by hopping of protons between ionizable groups (such as carboxylic groups) or between hydration water clusters^{12,39}. Yoshioka et al. termed the quasi dc polarization observed in freeze-dried glucose and dextran systems more correctly a “proton-hopping-like process” as there are no carboxylic groups present to allow a real proton-hopping but proton-hopping is thought to occur between hydroxyl groups³⁸. With the use of blocking layers⁴¹ the trespassing of charge from the electrodes into the sample is impeded and the dc conductivity is damped. Furthermore uncontrolled electrode polarization through multiple space charge effects is averted and instead a controlled electrode polarization, called a Maxwell-Wagner process, is induced. Thus the use of inert blocking layers allows the observation of otherwise obscured relaxation processes.

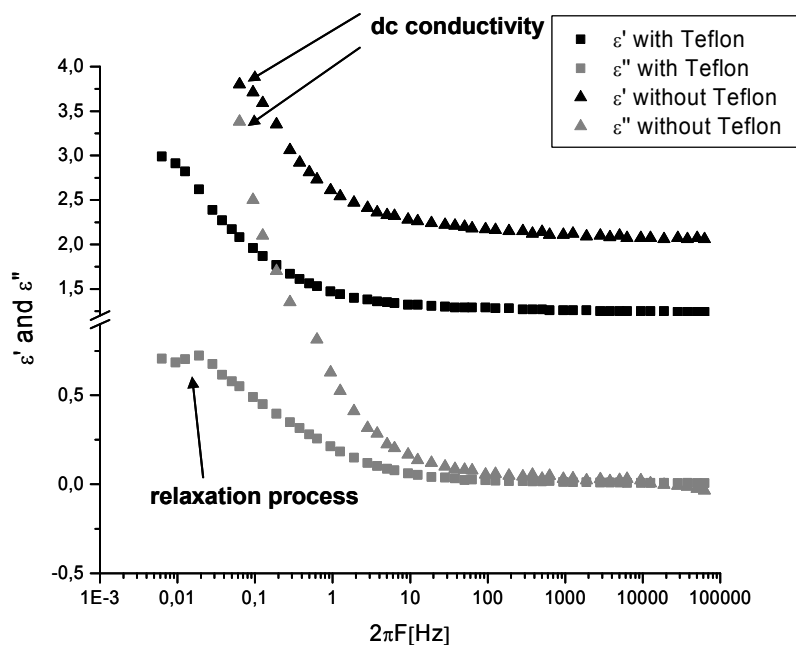


Figure 9.9: Real and imaginary permittivities of freeze-dried sucrose with changing frequencies in the absence and the presence of a Teflon sheet (0.14 mm thick); temperature was 25 °C.

A Maxwell-Wagner process can be described as a capacitor containing two dielectric materials, one with a finite conductivity (e.g. the sample) and one with a low conductivity (e.g. the Teflon). The dielectric response can be fitted to a model accounting for the response of a sample and a term accounting for the response of the Teflon spacers in series. However,

each of the observed relaxation processes can as well be independently fitted to a Cole-Davidson model. Suherman et al. showed that the relaxation time constants calculated with both models are equivalent³⁷. According to that observation, relaxation times in this study were calculated by independently fitting each of the observed processes to a Cole-Cole model.

Figure 9.9 shows the effect of the insertion of a Teflon sheet. Without the Teflon sheet quasi dc polarization, indicated as dc conductivity in the figure, was observed at low frequencies as indicated by the parallel high signal in both real and imaginary permittivities. With the insertion of the Teflon sheet, a peak in the imaginary part of the permittivity ϵ'' can be resolved, indicating a relaxation process.

Suherman et al. investigated the effect of the insertion of PE films between the sample and the electrodes on the determined relaxation times and found a good correlation for relaxation times determined with and without the films³⁷. According to their findings, it was concluded that the insertion of Teflon films did not relevantly alter the determined relaxation times.

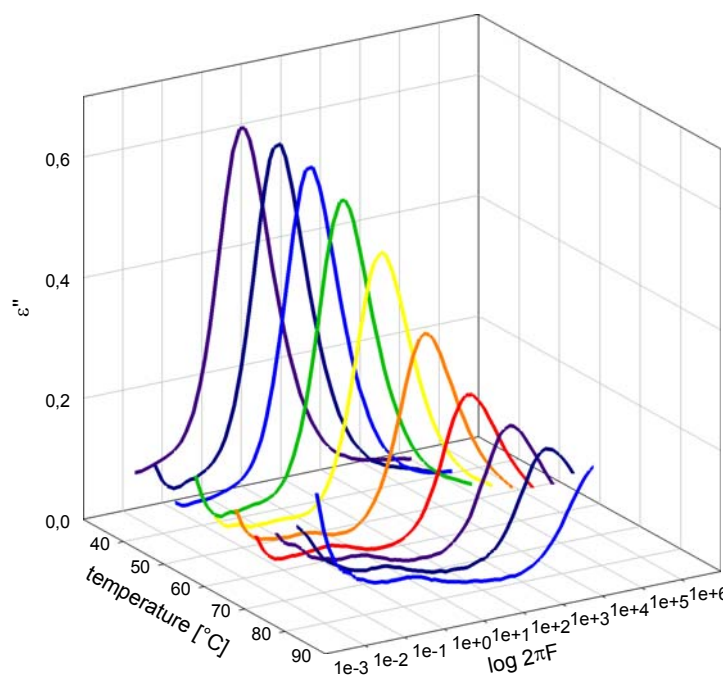


Figure 9.10: Imaginary permittivities of freeze-dried collapsed sucrose with increasing temperature and varying frequencies.

Figure 9.10 exemplarily shows the dielectric loss spectra of collapsed freeze-dried sucrose at varying frequencies and with increasing temperature. Clearly, two peaks can be observed, indicating that two relaxation processes are taking place. The first one is already well developed at room temperature, whereas the second peak first emerges at temperatures close to the glass transition temperature. From temperature dependencies and apparent activation energies, which are discussed in detail later, it is concluded that the first peak can be assigned to β -relaxations whereas the second peak can be assigned to α -relaxations.

These findings will be discussed in the following section (section 4) of this chapter including a detailed examination of the assignment of the observed relaxation processes.

Because this sections deals with the investigation of global dynamics of freeze-dried cakes, observations related to the second peak, which was related to global relaxation processes, will be discussed in this section. Observations concerning the first peak, which was related to local relaxation processes, will be the subject of discussion in the next section, dealing with the local dynamics of lyophilized cakes.

3.2.2 THE α -RELAXATION PROCESS

α -RELAXATION TIMES OF COLLAPSED AND NON-COLLAPSED LYOPHIIZATES

Figure 9.11 shows dielectric loss curves of collapsed and not collapsed sucrose cakes at various temperatures that are normalized for the glass transition temperatures of the respective system in order to account for the slight differences in residual moisture of the investigated systems as described previously^{3,38}. The spectra are truncated to show only the α -relaxation process.

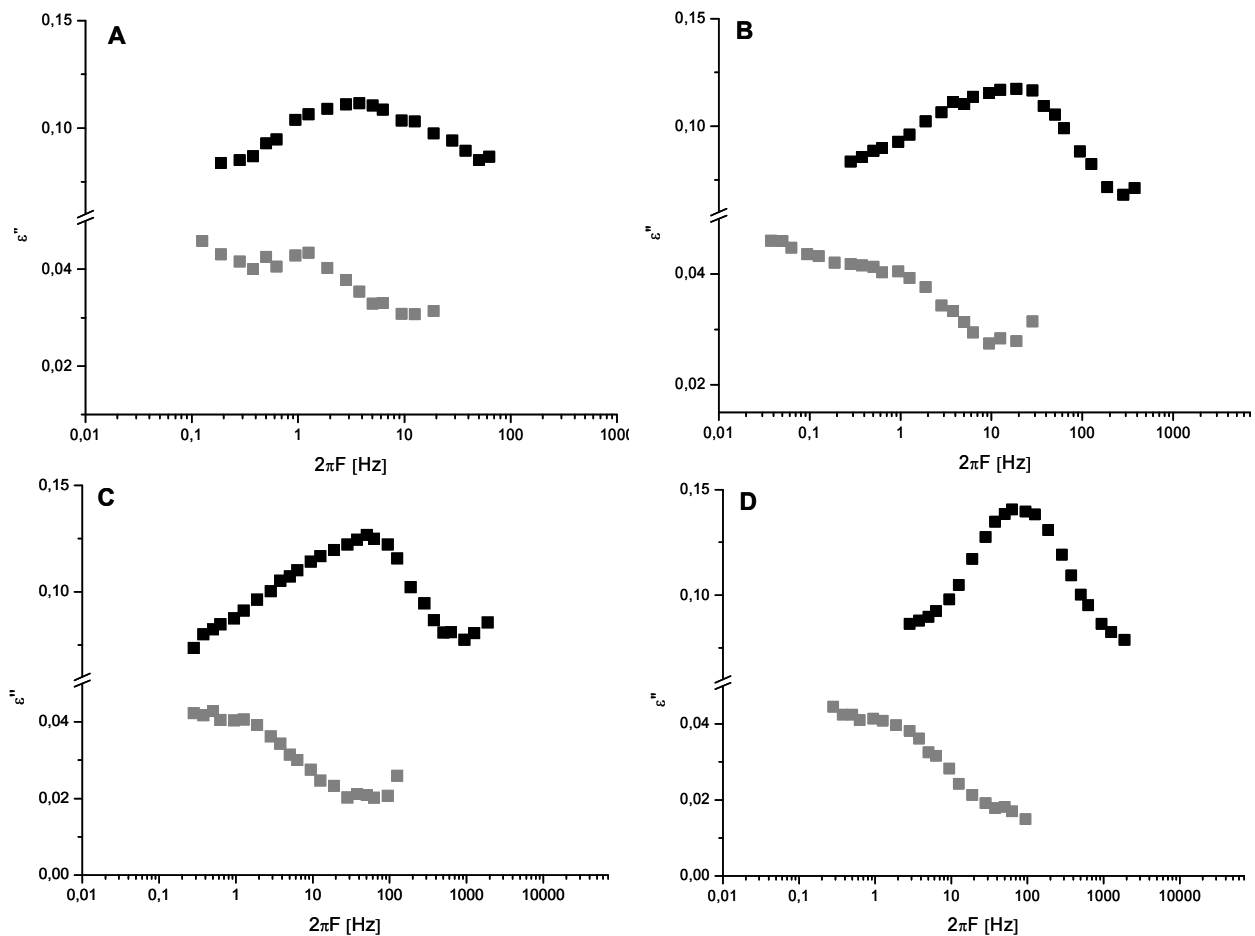


Figure 9.11: Dielectric loss spectra of collapsed (gray squares) and non-collapsed (black squares) freeze-dried sucrose cakes at various temperatures normalized for their distance to T_g ; $T_g/T = 1.09$ (non-collapsed) and 1.08 (collapsed) (A); $T_g/T = 1.00$ (B); $T_g/T = 0.94$ (non-collapsed) and 0.93 (collapsed) (C); $T_g/T = 0.88$ (non-collapsed) and 0.81 (collapsed) (D).

Spectra are calculated mean values of three (not collapsed) and 2 (collapsed) measurements, respectively.

Most notably, dielectric loss curves of non-collapsed cakes show maxima shifted towards higher frequencies as compared to the loss curves determined for collapsed cakes. As the frequency at which the dielectric loss is maximal corresponds to the system's mean relaxation time, this indicates a higher mobility in the non-collapsed lyophilizates. Table 9.4 lists the relaxation times determined from fitting the dielectric loss spectra to the Cole-Cole equation as described above. The relaxation times of the non-collapsed cakes are significantly lower than the relaxation times of the collapsed systems. These findings further confirm the relaxation times determined calorimetrically. However, as α -relaxations first appeared in the dielectric relaxation spectra approximately 5 °C below the system's glass transition, but TAM experiments were performed at least 25 °C below the glass transition temperature, a direct comparison cannot be performed. The differences in calculated relaxation times between collapsed and elegant systems are several orders of magnitude, thus the observed trend, i.e. the collapsed cakes showing a greatly reduced molecular mobility, can be regarded as qualitatively significant, despite the observed inhomogeneities of relaxation behavior in collapsed lyophilizates indicated by a large standard deviation.

Table 9.4: Dielectric relaxation times for collapsed and not collapsed freeze-dried sucrose at various temperatures normalized for the system's T_g s.

T_g/T	τ [s] not collapsed \pm SE	τ [s] collapsed \pm SE
1.02	0.40 \pm 0.23	-
1.00	0.18 \pm 0.12	55.9 \pm 42.9
0.99	0.08 \pm 0.05	1.66 \pm 1.05
0.97	0.02 \pm 0.01	1.61 \pm 1.07
0.96	0.01 \pm -	1.55 \pm 1.02

Regarding the absolute relaxation time constants at the glass transition, it was conspicuous that they were not in the order of 100 s as it is frequently described in the literature³³. This phenomenon was described as well by Bhugra et al.³ and Moynihan et al.⁴².

DIELECTRIC STRENGTH OF COLLAPSED AND NON-COLLAPSED LYOPHIIZATES

Another interesting observation was the difference in dielectric strengths, i.e. the amplitude of the relaxation process, with the non-collapsed system showing a much higher dielectric strength (Figure 9.11). The dielectric strength is a measure of the change in dipole moment upon dielectric polarization. Thus the lower amplitude of the relaxation in the collapsed systems indicated a less pronounced change in dipole moment. This can be explained by a somewhat more restricted mobility in the collapsed state leading to motions occurring on a smaller scale than in the non-collapsed system. A similar explanation was given by Kaminski et al. comparing the β -relaxations of different disaccharides, where restricted mobility due to stronger hydrogen bonds led to restricted rotational mobility around the glycosidic bond¹².

The dielectric strength of the α -relaxation in the non-collapsed sucrose lyophilizates further increased with increasing temperature as indicated by the increasing amplitude of the relaxation peak in Figure 9.11. This behavior is frequently observed and a tentative explanation was given by Ermolina et al.⁴³: At lower temperatures the dipoles preferentially orientate in an antiparallel order to minimize the resulting dipole moment. This orientation is less effective at higher temperatures due to the more randomized motions leading to an increased resulting dipole moment.

However, the amplitude of the relaxation process in the collapsed sucrose system did not remarkably change with increasing temperature. This less pronounced effect of temperature on the reorientational mobility might be related to the system's fragility and will be discussed in the section dealing with the comparison of the fragility of the different systems (section 5.2).

PROOF OF CONCEPT: IDENTIFICATION OF α -RELAXATIONS BY VTF-TEMPERATURE-DEPENDENCE

In order to verify the classification of the observed relaxation process as α -relaxation, the change of relaxation times with varying temperature was analyzed. α -relaxations typically show a temperature dependence well described by the Vogel-Tamman-Fulcher (VTF) equation (equation 1.10) above T_g ⁴⁴. At temperatures significantly below T_g , the modified VTF equation, additionally taking into account the fictive temperature T_f , better describes the temperature-dependence of τ ⁴⁵. Figure 9.12 shows Arrhenius-type plots of the relaxation times estimated for the α -relaxation processes in collapsed and non-collapsed sucrose-based systems. Again, the shorter structural relaxation times in non-collapsed systems can be identified by the curve's offset to lower $\log(\tau)$ values.

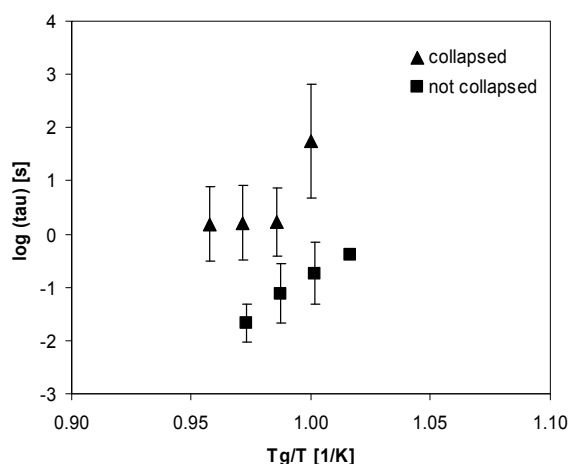


Figure 9.12: Arrhenius-type plot of the relaxation times estimated for α -relaxations in collapsed and non-collapsed sucrose-systems.

$n = 2$ for collapsed cakes; $n = 3$ for non-collapsed cakes; the x-axis displays the inverse temperature that was normalized for T_g rather than the absolute inverse temperature in order to correct for slight differences in T_g between the two systems.

Regarding the non-collapsed lyophilizates (squares in Figure 9.12), the plot of $\log(\tau)$ versus the inverse of temperature that was normalized for T_g (i.e. T_g/T) formed a straight line that

can be described by the VTF equation. A fit of the VTF equation to the experimental data is depicted in Figure 9.14 A. Table 9.5 further lists the fitting parameters for the equation. The limited validity of the VTF-equation at temperatures below T_g has to be taken into account while evaluating these parameters, but as experimental temperatures were not significantly below T_g , qualitative conclusions can be drawn.

In contrast to the non-collapsed lyophilizates, the temperature dependence of structural relaxation times in collapsed systems did not exhibit a linear increase with temperature in the Arrhenius-type plot (Figure 9.12). To further elucidate this observation and to prevent erroneous overall data due to outliers, Figure 9.13 depicts the calculated relaxation times for the respective two analyzed samples instead of the calculated average values that are depicted in Figure 9.12. Figure 9.13 once again emphasizes the heterogeneous relaxation behavior of collapsed samples resulting in a poor reproducibility and large standard deviations. However, both analyzed collapsed samples exhibit a steep decrease of relaxation times upon passing the glass transition temperature, further confirming the observed curve progression in Figure 9.12.

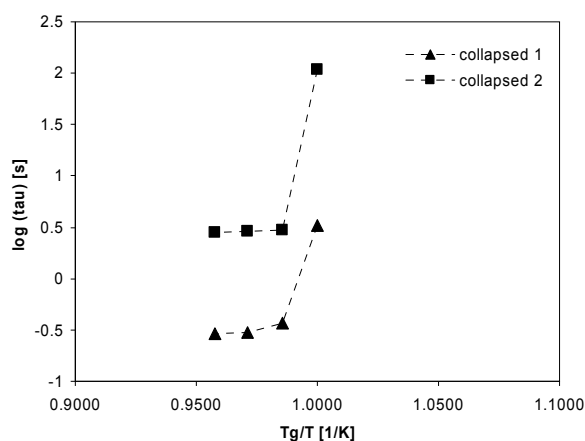


Figure 9.13: Reproducibility of relaxation times estimated for α -relaxations in collapsed systems.

Separate depiction of the α -relaxation times estimated for the two analyzed collapsed samples without calculating the average.

A steep change of relaxation times while traversing the glass transition is typically observed in fragile systems as will be discussed in the section 5 dealing with fragility.

The temperature dependence of α -relaxations in collapsed systems observed in close proximity and above the glass transition can also be described by the VTF equation, as depicted in Figure 9.14 B. The fitting parameters for the VTF equation describing the collapsed system are also given in Table 9.5. Again, the limited validity of the VTF equation below T_g has to be considered.

The parameters given in the VTF-equation are T_0 , often referred to as the zero mobility temperature at which all mobility ceases, and D , a constant directly related to the system's fragility.

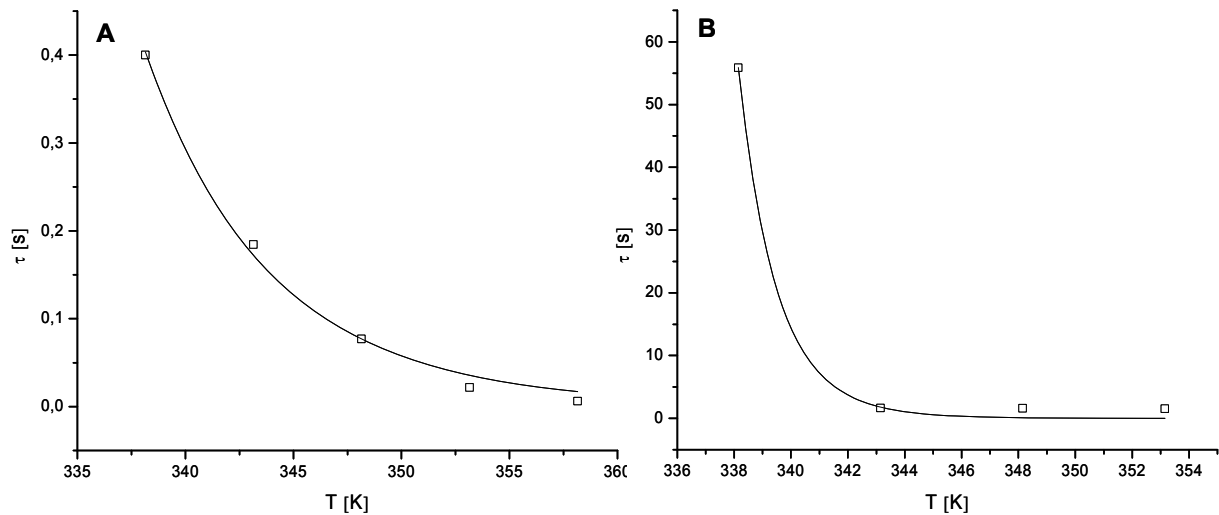


Figure 9.14: α -relaxation times (open symbols) and VTF fits to the experimental data (lines) of non-collapsed (A) and collapsed (B) sucrose-based lyophilizates.

$\chi^2 = 0.00024$ and $r^2 = 0.99544$ for VTF fit of non-collapsed systems; $\chi^2 = 4.6379$ und $r^2 = 0.9979$ for collapsed systems.

The calculated fitting parameters are in good agreement with values observed by other researchers. Shamblin et al. reported a D-value of 7.3 and a T_0 -value of 290 K for sucrose⁴⁵. The importance of the way of preparation on the glassy dynamics is well reflected in the divergent values reported by Kaminski et al.: They also fitted the α -relaxation process of a sucrose-system with the VTF equation resulting in a D-value of 3.2 (calculated from the listed D_T -value by $D = D_T/T_0$) and a T_0 -value of 308 K¹². They prepared amorphous sucrose by quench-melting whereas Shamblin et al. prepared their samples by lyophilization.

The validity of the calculated fitting parameters is further corroborated by the obtained τ_∞ -values. τ_∞ describes the relaxation behavior of the unrestricted material and is most commonly reported to be around $1E-14$ s⁴⁵, which is in good agreement with the calculated results (Table 9.5).

Table 9.5: Fitting parameters for the VTF equations.

appearance	τ_∞ [s]	D [K]	T_0 [K]
non-collapsed	3.76E-15	39	153
collapsed	4.91E-15	6	289

SUMMARY

Global glassy dynamics of collapsed and non-collapsed amorphous lyophilizates were investigated using two different analytical approaches, i.e. calorimetric and spectroscopic techniques. TAM experiments allowed for the determination of the overall structural relaxation time, using DRS local and global dynamics could be analyzed. The later emerging relaxation process in the DRS spectra, discussed in this section, was identified as α -relaxation by the proximity of its manifestation to the glass transition temperature and by its characteristic temperature dependence that is best described by the VTF equation.

Collapsed lyophilizates showed significantly increased structural relaxation times as compared to non-collapsed lyophilizates. Additionally, an altered temperature dependency was detected. This behavior will be the subject of discussion in section 5 of this chapter dealing with the system's fragility.

4 LOCAL DYNAMICS OF COLLAPSED AND NOT COLLAPSED LYOPHILIZATES

In order to get further insight into the glassy dynamics of collapsed and not collapsed lyophilizates, further analysis was performed at temperatures well below the glass transition temperature. At these temperatures the dynamics are mostly governed by the so-called local dynamics of β -relaxations. Whereas the primary or structural α -relaxation involves motions of entire molecules and translational movement of sizeable length, β - or secondary relaxations are more local and most often caused by rotational or vibrational motions of molecular subgroups. As storage of protein lyophilizates is usually performed at temperatures well below the glass transition temperature, β -relaxation processes might determine the dynamics during storage and thus they might be of similar or even greater importance for predicting protein stability than α -relaxations.

Local dynamics can be further classified into β -, γ - and δ -relaxations according to their apparent activation energies and to their characteristic relaxation times, with the δ - and γ -relaxations having lower apparent activation energies and occurring at lower frequencies. γ - and δ -relaxations are only observable at low temperatures deep in the glassy state. Accordingly, β -relaxations show higher apparent activation energies and occur at higher frequencies.

β -relaxations can be further classified into inter- and intra-molecular relaxation processes. They can be differentiated by their sensitivity towards an increase in pressure (e.g. 1 atm as compared to 1 GPa¹¹): the intermolecular processes exhibit sensitivity towards pressure whereas the intramolecular processes do not. Intermolecular β -relaxations are denoted Johari-Goldstein-relaxations¹¹.

The Johari-Goldstein β -relaxation is regarded as a precursor of the structural α -relaxation by some authors^{46,47}.

Besides the secondary relaxations caused by the glass former itself, secondary relaxations can be originated by hydration water⁴⁸. With the use of dielectric relaxation spectroscopy, not only the amount of residual water can be determined, but different types of water, i.e. surface hydration water or bulk water or tightly bound water can be differentiated^{25,41,49}. Taking advantage of this relation, dielectric relaxation spectroscopy can also be used to determine the endpoint of freeze-drying^{25,37}.

Despite the presumable importance of secondary relaxations, their molecular origin is still uncertain. Investigations performed on disaccharides revealed the existence of two secondary relaxations in addition to the primary α -relaxation^{50,51}. The faster one, the γ -relaxation, is prevalently observed in all carbohydrates. It is insensitive towards pressure and the thermodynamic history of the measurement¹². Most probably, γ -relaxations are caused by the rotational mobility of the hydroxyl- and/or hydroxymethyl-groups pending from the monosugar-ring-structure^{12,50-52}. However, there are publications contradicting this

explanation based on NMR measurements⁵³. The β -relaxation is most commonly related to orientational motions of the sugar moieties via the glycosidic bond^{51,54}. In contrast, Noel et al. explained β -relaxations with the rotational motion of pendant groups and motions around C-C bonds within the sugar-ring^{50,51,54}.

β -RELAXATION TIMES OF COLLAPSED AND NON-COLLAPSED LYOPHILIZATES

Figure 9.15 depicts dielectric loss spectra of non-collapsed (A) and collapsed (B) sucrose lyophilizates with increasing temperature. The spectra are truncated to show only the loss caused by secondary β - and γ -relaxations. Loss from primary α -relaxations that was discussed in the previous chapter is not shown.

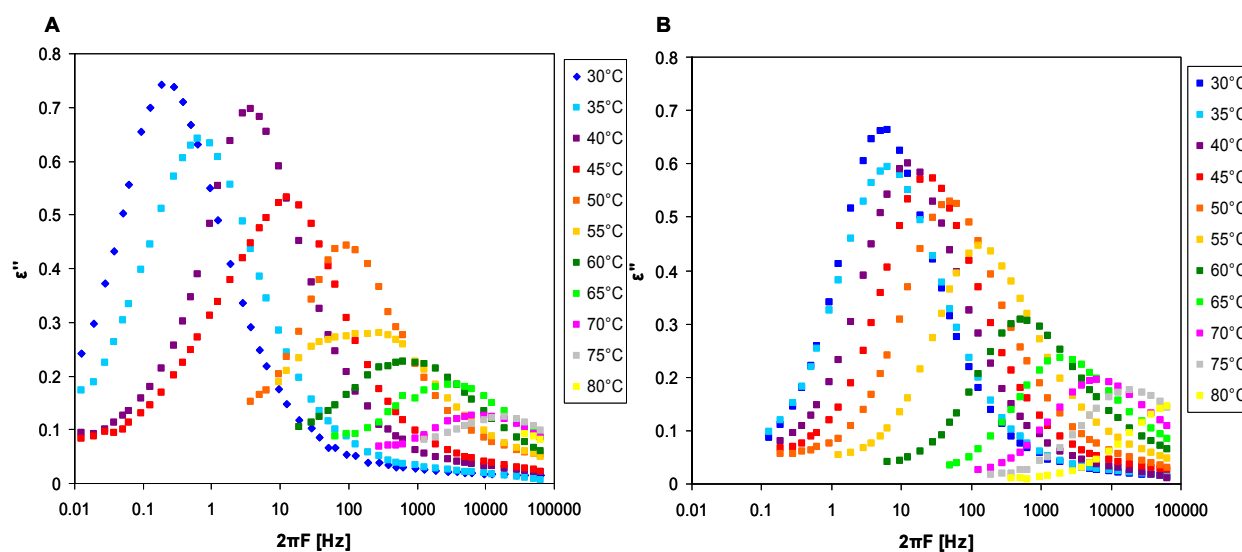


Figure 9.15: Dielectric loss spectra of non-collapsed (A) and collapsed (B) sucrose lyophilizates with increasing temperature.

Spectra are calculated mean spectra of 3 (non-collapsed) and 2 (collapsed) independent measurements, respectively.

Most obviously, only one secondary relaxation is observed for both systems, no matter whether the material was collapsed or not. As measurements were performed starting from room temperature, thus not too deep in the glassy state, and spectra were recorded from 10^{-4} to 10^4 Hz, most probably the detection of the γ -relaxation process was not possible, because it was beyond the analyzed frequency range. This is in good agreement with literature describing the occurrence of γ -relaxations between 10^4 and 10^5 Hz at 263 K¹². Thus the observed relaxation process can be attributed to β -relaxation processes. This assignment can be further confirmed by literature describing β -relaxation processes in sucrose below 10^{-2} Hz at 263 K¹² and around 10^0 Hz and 10^2 Hz between 12 °C and 72 °C⁵¹. A detailed discussion about the identification of the observed relaxation process as β -relaxation is given in the next paragraph.

In order to correctly compare secondary relaxations in collapsed and non-collapsed systems the slightly different glass transition temperatures (70.6 °C and 65.0 °C in non-collapsed and collapsed lyophilizates, respectively) have to be taken into account. Figure 9.16 depicts the

dielectric loss spectra of collapsed (grey symbols) and non-collapsed (black symbols) lyophilizates at different temperatures (A-D) that were normalized to their offset from the glass transition temperature, i.e. the temperature difference to the glass transition is the same.

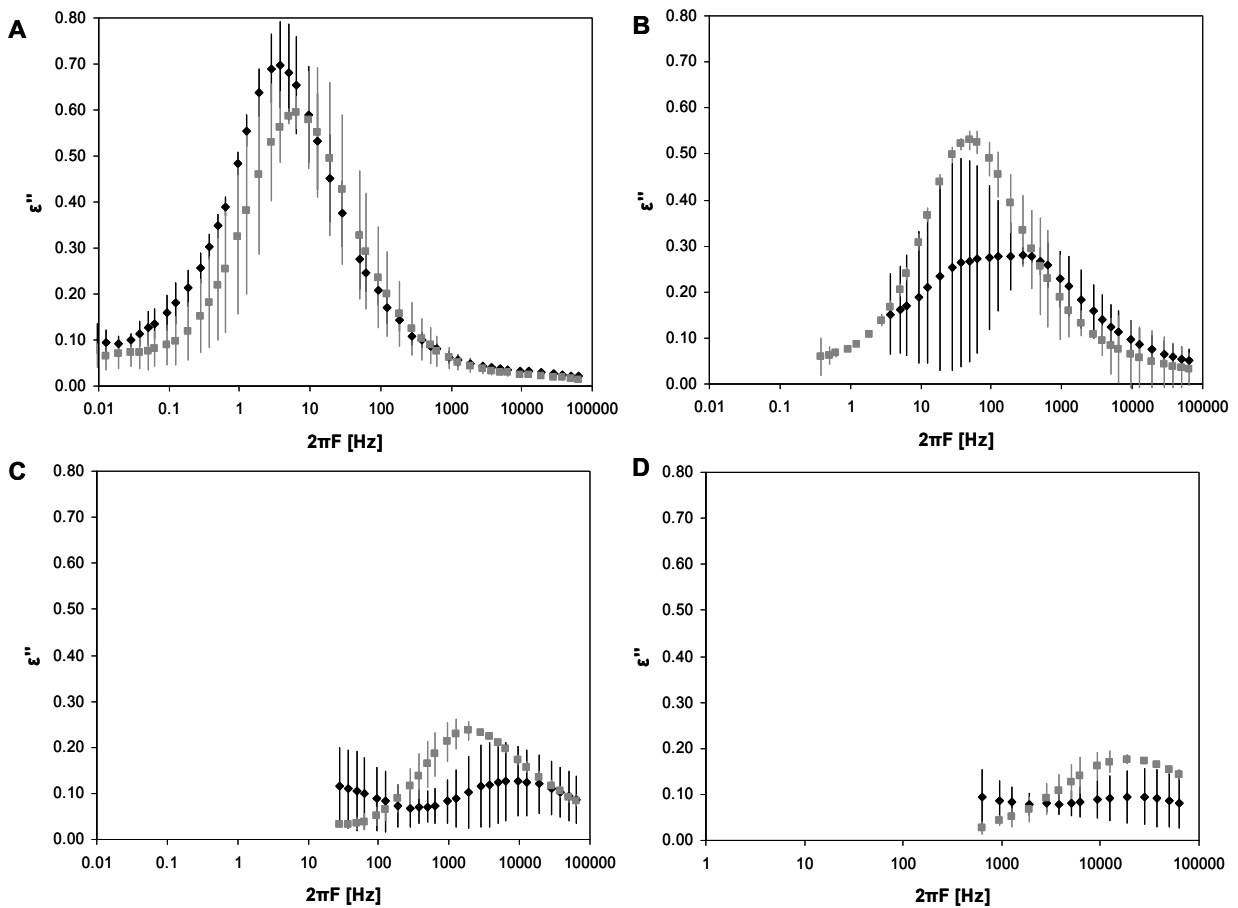


Figure 9.16: DRS spectra T_g -normalized at T_g/T 1.10 (A), 1.05 (B), 1.00 (C), 0.97 (D) for collapsed (grey symbols) and non-collapsed (black symbols) sucrose lyophilizates.

Spectra are average spectra calculate from 2 (collapsed) respectively 3 (non-collapsed) independent measurements. Lines indicate the standard deviation of the individual spectra.

Glass transition temperatures were 65.0 °C for collapsed systems and 70.56 °C for non-collapsed systems.

Initially, non-collapsed cakes show higher dielectric strength and slightly lower relaxation times than collapsed systems. However, with increasing temperature, dielectric strength in non-collapsed cakes rapidly decreases and the loss peak becomes broader. The maximum distinctly shifts towards higher frequencies with increasing temperature. Collapsed lyophilizates also show this observed shift in loss maximum and the decrease in dielectric strength but none of the changes is as pronounced as in the non-collapsed systems. As already observed for global dynamics, collapsed systems showed a heterogeneous relaxation behavior.

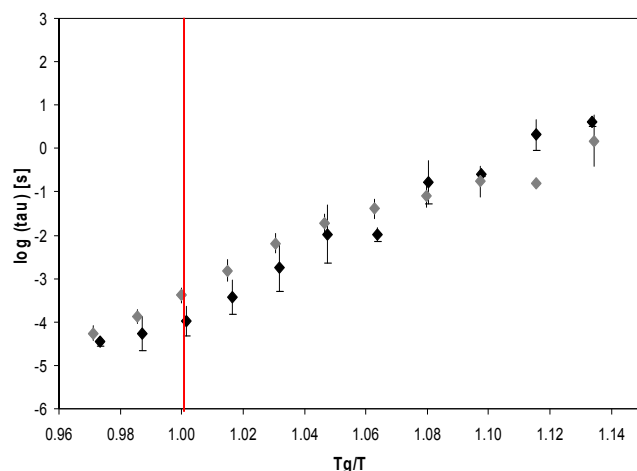


Figure 9.17: Comparison of relaxation times of β -relaxation processes in collapsed (grey symbols) and non-collapsed (black symbols) sucrose lyophilizates versus temperature that has been normalized for T_g . Relaxation times are calculated average values of 3 (non-collapsed) and 2 (collapsed) independent measurements, respectively.

Despite the use of T_g -corrected temperatures, relaxation times at lower temperatures were shorter in collapsed systems as compared to non-collapsed systems. Figure 9.17 displays the logarithm of β -relaxation times versus T_g -corrected temperatures. At temperatures well below the glass transition relaxation time constants are lower for collapsed cakes, but above the glass transition relaxation times are higher for collapsed lyophilizates. However, this difference in relaxation times cannot be regarded as significant, especially given the standard deviations (Table 9.6).

Table 9.6: Calculated β -relaxation times in collapsed and non-collapsed sucrose systems at various temperatures.

T_g/T	τ non-collapsed [s] \pm SD	τ collapsed [s] \pm SD
1.13	4.0107 \pm 0.9629	1.5020 \pm 1.5708
1.12	2.0590 \pm 1.8099	0.1568 \pm -
1.10	0.2522 \pm 0.0217	0.1730 \pm 0.1301
1.08	0.1663 \pm 0.1957	0.0784 \pm 0.0438
1.06	0.0104 \pm 0.0037	0.0403 \pm 0.0198
1.05	0.0105 \pm 0.0144	0.0188 \pm 0.0092
1.03	0.0018 \pm 0.0022	0.0065 \pm 0.0031
1.02	3.63E-04 \pm 3.23E-04	1.53E-03 \pm 8.34E-04
1.00	1.07E-04 \pm 8.96E-05	4.10E-04 \pm 1.56E-04
0.99	5.33E-05 \pm 4.93E-05	1.35E-04 \pm 4.95E-05
0.97	3.50E-05 \pm 7.07E-06	5.50E-05 \pm 2.12E-05

This is in good agreement with literature describing, that the drying method has no effect on β -relaxation behavior of pharmaceutical systems and that α - and β -relaxations are at least partially uncoupled⁵⁵. Further confirmation is given from recent experiments investigating the effect of aging, i.e. annealing on secondary Johari-Goldstein β -relaxations: After aging of various carbohydrate glasses, such as glucose, trehalose and sorbitol, no change in relaxation times was observed^{56,57}.

However, there as well are publications pointing out a distinct effect of thermal history on β -relaxation times similar to the effect on structural α -relaxation times⁵⁸. A pronounced effect was observed for thermal histories resulting in glasses with different densities. Kaminski et al. observed increased β -relaxation times and high activation energies for leucrose glasses prepared by the application of high pressure, resulting in denser materials⁵⁹. A similar observation was made by Sharifi et al. for small organic glass formers⁶⁰. Other relaxation processes that had lower activation volumes and/ or were caused by intramolecular motions, such as γ –relaxations, did not show a pronounced sensitivity towards pressure or density. However, the differing effects of thermal history on β -relaxation processes might be reconciled taking into account the absolute values of change in density in the cited publications. Changes in free volume experienced upon aging most probably are less pronounced than density differences between materials produced at ambient pressures and at 450 MPa. Moreover, investigations performed so far did not analyze freeze-dried systems and did not compare different drying methods. A possible effect of drying method on secondary relaxation times can be deduced from literature comparing reports from Kaminski et al., who observed a β -relaxation at approximately $10^{-1} - 10^0$ Hz at -12 °C for quench-cooled lactose, with Ermolina et al., who reported the observation of β -relaxation in freeze-dried lactose between -50 and 0 °C using the measurement range from 0.1 to 10^6 Hz^{12,61}. This might indicate a more pronounced change in relaxation time for freeze-dried systems as compared to melt-quenched systems. These results could be related to the differences in density between the dried systems, leading to a more variable relaxation span in freeze-dried cakes indicating the increased degrees of freedom. This is in good agreement with the observed larger change in relaxation times in conventionally freeze-dried lyophilizates as compared to collapse-dried lyophilizates.

Table 9.7: Densities of collapsed and non-collapsed sucrose lyophilizates as determined with helium pycnometry; each value is the calculated average of 6 independent measurements, each composed of 20 runs.

appearance	density [g/cm ³] \pm SE
non-collapsed	1.4973 \pm 3.28E-04
collapsed	1.5142 \pm 9.35E-05

The observed relaxation process investigated for the sucrose lyophilizates was classified as Johari-Goldstein-(JG)- β -relaxation, because of the temperature dependence of its relaxation times and its dielectric strength, which will be discussed in detail in the next sections. JG- β -relaxations are relaxations of intermolecular nature whose sensitivity towards pressure indicates a certain activation volume. Hence, an effect of density might well be expected. Table 9.7 shows the densities of collapsed and non-collapsed lyophilizates as determined by helium pycnometry. Collapsed powders show a significantly increased density.

Thus the increased density in collapsed systems might explain the retardation of secondary relaxations observed at higher temperatures, similar to the reports of Ermolina and Kaminski^{59,61}. However, the difference in density between collapsed and non-collapsed systems is not large enough to cause a pronounced deviation in β -relaxation times as observed by Sharifi et al.

DIELECTRIC STRENGTH OF COLLAPSED AND NON-COLLAPSED LYOPHILIZATES

Regarding the dielectric strength, the observed β -relaxation process (Figure 9.16) most notably shows a decreasing dielectric strength with increasing temperature in contrast to structural α -relaxation (Figure 9.11). This is an uncommon behavior for β -relaxations but it was also observed by Kaminski et al^{12,59}. A tentative explanation was given by Ermolina et al., who related the decrease in dielectric strength with a decreased polarizability of the system due to the randomizing effect of temperature combined with the lack of any specific orientation correlation between the two sugar moieties⁶¹.

Dielectric strength initially was higher in non-collapsed cakes, but decreased readily with increasing temperature. Dielectric strength in collapsed cakes, that was initially less pronounced, decreased to a much lesser extent, leading to higher amplitudes at higher temperatures as compared to not collapsed systems.

Diogo and Ramos observed a remarkable decrease in dielectric strength with aging observed for various carbohydrate glasses^{56,57}. Because collapse-drying exerts an annealing- and hence aging-effect, collapsed lyophilizates behaved similar to aged carbohydrate glasses. The authors explained the decrease of dielectric strength with a decreasing number of molecules involved in the secondary relaxation process, caused by the so-called “disappearance of the “islands” of mobility”, i.e. local regions of low density⁶². A second scenario explaining experimental data was that the amplitude of the rotational jumps became smaller with increasing aging time because the material became tighter^{63,64}. This is accompanied by an increase in density and a decrease in free volume during aging. The insensitivity of the relaxation time towards that increase in density despite the comparably large activation volume of Johari-Goldstein- β -relaxations (21.5 ml/mol for leucrose⁵⁹) was explained with the very local nature of that motion, rendering it independent of free volume⁶⁵. Thus the increased density of collapsed lyophilizates (Table 9.7) and the already observed fact that the collapse-drying cycle acted as an annealing step caused a decrease in dielectric strength due to a tighter structure.

PROOF OF CONCEPT: ARRHENIUS-TEMPERATURE-DEPENDENCE OF β -RELAXATIONS

Most clearly, maxima of the dielectric loss spectra are shifted towards higher frequencies with increasing temperature (Figure 9.11). Interestingly, this shift was more pronounced in the non-collapsed systems.

Figure 9.18 displays the temperature dependence of the relaxation processes in a so-called Arrhenius-plot. Obviously, relaxation in both systems could be described by the Arrhenius equation as indicated by the exhibited linear trend. Arrhenius temperature dependence typically is exhibited by β -relaxation processes, although α -relaxations can appear to show an Arrhenius-behavior as well, when studied over a narrow temperature range. But as the analyzed temperature-range is large, the classification of the observed relaxation as β -relaxation is confirmed.

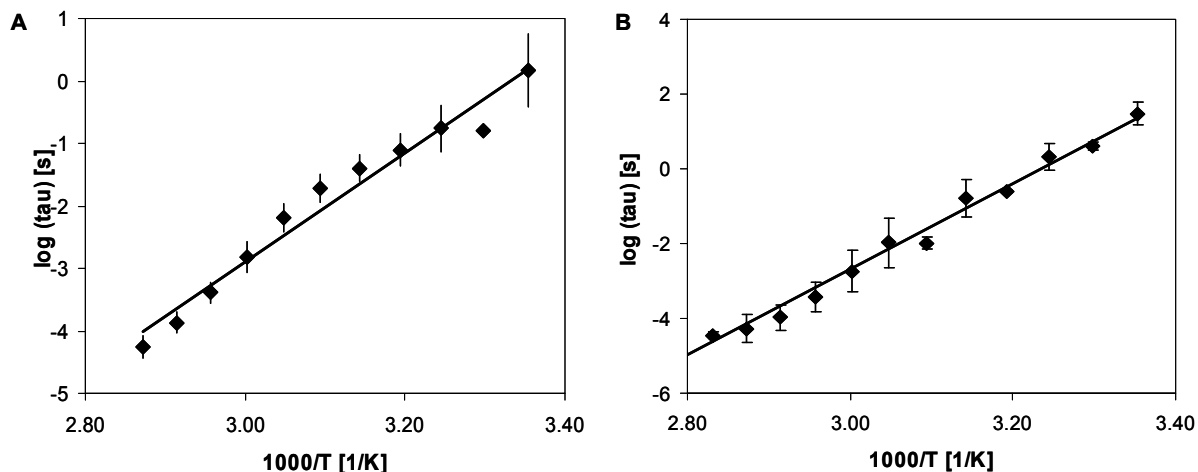


Figure 9.18: Arrhenius-plots of relaxation times of collapsed (A) and non-collapsed (B) sucrose-based systems.

Relaxation times are average values of 2 (collapsed) and 3 (non-collapsed) independent measurements, respectively; r^2 (collapsed) = 0.9665 and r^2 (non-collapsed) = 0.9873.

Table 9.8 lists the apparent activation energies for the β -relaxation calculated from the Arrhenius equation. The determined value for non-collapsed sucrose was in good agreement with β -relaxation activation energies from literature for sucrose^{12,51}, whereas the value determined for collapsed sucrose was slightly lower than literature values. However, as it was significantly higher than activation energies reported for γ -relaxations, the observed relaxation process clearly could be classified as β -relaxation. Also, this value was significantly lower than activation energies reported for α -relaxations (220 kJ/mol)⁶⁶.

Table 9.8: Fitting parameters for the Arrhenius equations describing the temperature dependence of collapsed and non-collapsed sucrose-based freeze-dried systems.

appearance	τ^∞ [s]	E_a [kJ/mol]
non-collapsed	1.03E-37	95.03
collapsed	7.23E-30	72.71

Because the β -relaxation process is most probably generated by a rotational motion of the monosugar-moieties around the glycosidic bond, a higher apparent activation energy of β -relaxations observed for some sugars (e.g. sucrose) was related to a more rigid structure of that bond by Kaminski et al.¹². They observed much higher apparent activation energies for sucrose and trehalose than for other investigated disaccharides. They ascribed that

observation to the existence of one or more hydrogen bonds between the two monosugars, leading to a hindered rotation around the glycosidic linkage. This observation was at least partially confirmed by NMR measurements and theoretical studies. Thus the lower apparent activation energy observed in collapsed sucrose systems might point towards a less rigid structure of the glycosidic bond. However, there is no evidence in literature of the effect of preparation method on β -relaxation activation energies. Activation energies reported for lactose prepared by melt-quenching and freeze-drying, respectively were not significantly different (76 kJ/mol and 72 kJ/mol, respectively)^{12,61}.

PROOF OF CONCEPT II: EFFECT OF RESIDUAL MOISTURE LEVEL ON OBSERVED RELAXATION PROCESSES

In order to verify that the observed relaxation processes were true molecular dipole polarizations within the sucrose glass, additional measurements were performed.

Dealing with lyophilized products a common source of interference is residual moisture. Water can be detected by dielectric relaxation spectroscopy and can even be further differentiated into bound and free (surface) water. In strongly hydrated solids or frozen solutions relaxation processes of water can be directly assessed in the dielectric spectra. Shinyashiki et al. related the β -relaxation observed in fructose-water mixtures to the Johari-Goldstein- β -relaxation of water molecules⁶⁷. The authors described an increasing dielectric strength with increasing temperature and a change in temperature dependence at the glass transition from Arrhenius to a stronger behavior as characteristic properties for this relaxation process. The calculated apparent activation energies for the observed relaxation were approximately the same in all studied excipient-water-systems. That is to say about 50 kJ/mol. The relaxation times of the Johari-Goldstein- β -relaxation of water were reported to be less dependent on the residual water content than the α -relaxation times⁶⁷.

In freeze-dried solids containing only trace amounts of water, quasi dc-polarization as a result of hopping of protons through the hydrogen-bonded network of water molecules can lead to a dielectric response of the material. Usually, this response is quite strong rendering a direct measurement difficult. Thus, the use of the dielectric modulus, i.e. the reciprocal of the complex permittivity, or the use of a remote system with the insertion of Teflon sheets was described^{36,37}.

In order to rule out the possibility of proton-hopping processes as the cause for the observed sub- T_g relaxations, sucrose samples with different residual moisture levels were analyzed. Figure 9.19 depicts the dielectric loss spectra of sucrose-based placebo-lyophilizates with two different residual moisture levels, namely 1.3 and 3.0 % residual moisture, respectively. Two relaxation processes can be observed. The first one is well observable at room temperature and the second one is observable from about 10 °C below the glass transition temperature. Unfortunately, the second relaxation process was masked by dc-conductivity

that was especially pronounced in the high residual moisture sample, so that the effect of residual moisture on α -relaxations can not be investigated. However, it is thoroughly reported in literature, that water acts as a plasticizer of the amorphous structure which enhances structural relaxations⁵⁰. Glass transition temperatures were 60.8 °C and 51.2 °C as determined by DSC for the 1.3 and 3.0 % moisture samples, respectively. This is in good agreement with literature describing the depression of the glass transition temperature by about 10 K for each 1 % increase in moisture³⁵ and a T_g of 63 °C for 1 % residual moisture-freeze-dried sucrose⁶⁸.

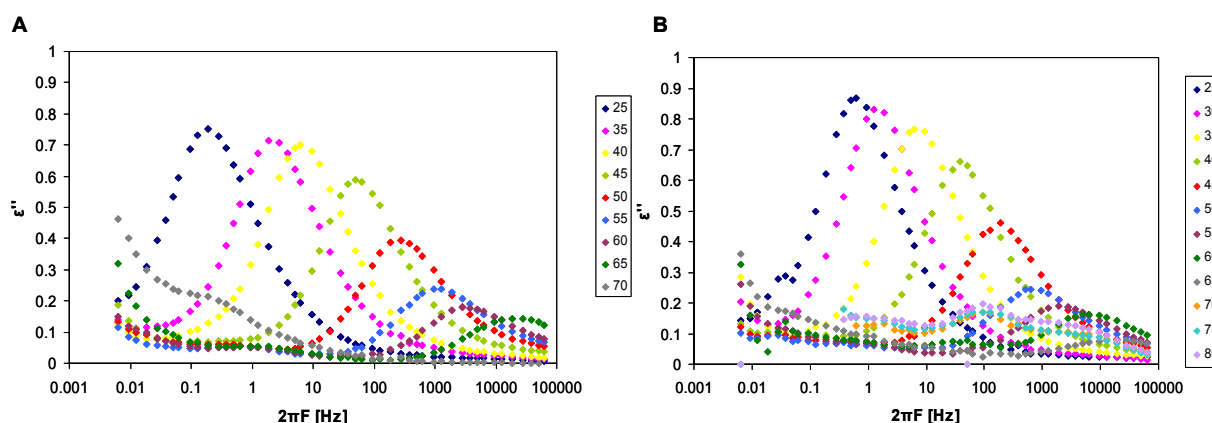


Figure 9.19: Dielectric loss spectra of sucrose-based (placebo) lyophilizates with 1.3 % (A) and 3.0 % (B) residual moisture, respectively.

The dielectric strength of the first relaxation process decreased with increasing temperature whereas that of the second process increased. As discussed in detail above, this leads to the identification of the first process as a β -relaxation and the second as the structural α -relaxation. The β -relaxation was most probably caused by rotational mobility of the mono-sugar-moieties of the sucrose-molecules around the glycosidic bond and it was not caused by proton-hopping or relaxation of water-molecules. This was indicated by the observed decrease in dielectric strength with temperature, where proton-hopping, i.e. a thermally activated process would show an increase⁶⁷.

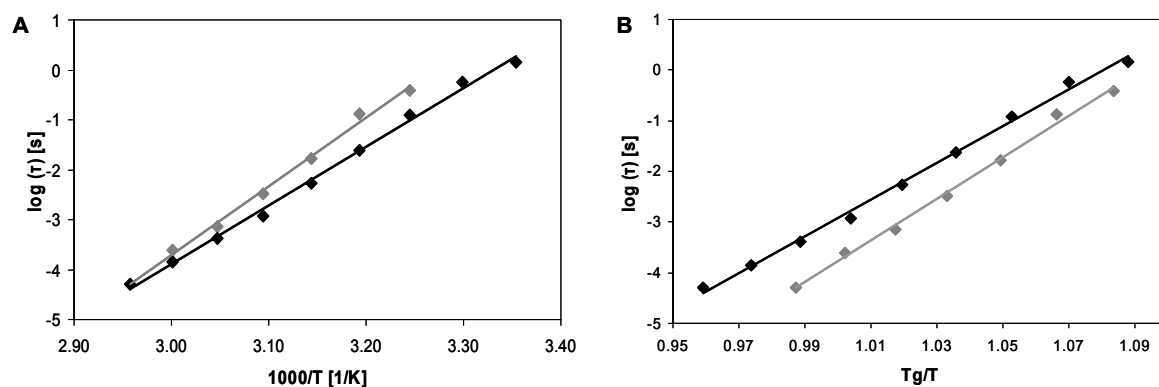


Figure 9.20: Temperature dependence of relaxation times in freeze-dried cakes with 1.3 % (grey symbols) and 3.0 % (black symbols) residual moisture respectively.

Relaxation times are either plotted versus absolute reciprocal temperature (A) or versus reciprocal temperature that was normalized for the offset to T_g (B). r^2 (1.3%) = 0.995; r^2 (3.0 %) = 0.996.

This conclusion was further confirmed by the temperature dependence of the observed secondary relaxation depicted in Figure 9.20. It could be described using the Arrhenius equation with no change in temperature dependence upon passing the T_g as it is described for the β -relaxation of water. However, regarding the proton-hopping process, there are different reports in literature. Yoshioka et al. depict a stronger temperature dependence upon passing the T_g and El Moznine et al. describe a continuous Arrhenius-dependence^{36,38}. Still, the described temperature course of the dielectric strength refuted the likelihood of proton-hopping being the cause for the observed relaxation.

Table 9.9: Relaxation times of the secondary β -relaxation process of sucrose lyophilizates with two different residual moistures.

T_g/T	τ RM 1.3%[s]	τ RM 3.0% [s]
1.07	0.13278	0.57879
1.05	0.01678	0.12268
1.02	0.00073	0.00533
1.00	0.00025	0.00117
0.99	0.00005	0.00041

An intriguing observation was made comparing the absolute secondary relaxation times as listed in Table 9.9. The relaxation times of the sample with the higher residual moisture content were higher than the relaxation times of the dryer sample. This is contrary to what is described in literature concerning the effect of water as a plasticizer of the amorphous phase. However, Cicerone et al. made an observation pointing in a similar direction: They investigated the effect of addition of low- T_g diluents, such as glycerol or sorbitol, to trehalose glasses. The T_g was decreased as expected, but the stability of incorporated horseradish peroxidase and yeast alcohol dehydrogenase was increased. This finding was correlated with the suppression of local dynamics, that was detected by incoherent neutron scattering^{9,19}. An improved stability of a monoclonal antibody upon the addition of low levels of water was also reported by Chang et al⁶⁹.

PROVE OF CONCEPT III: EFFECT OF PROTEIN

After ruling out that residual water caused the observed relaxation processes, the effect of the incorporated protein was investigated as well. To verify that the observed process is caused by the reorientation of sucrose molecules placebo systems lacking the IgG were analyzed. Figure 9.21 depicts dielectric loss spectra of sucrose lyophilizates with (black symbols) and without (grey symbols) IgG₀₁ at two temperatures normalized for their offset to T_g . Both relaxation processes, the α - and the β -relaxation process could be observed in both samples, i.e. with and without protein, although there are slight differences in the position of the maximum losses and the width of the loss peaks. Thus it could be concluded that the observed relaxations were at least mostly caused by sucrose. Because the protein was molecularly dispersed in the sucrose matrix, contributions from the IgG₀₁ to the relaxation

behavior might as well be expected. The observed broadening of the loss peaks in the samples containing protein as compared to the ones lacking protein can be explained by the presence of the IgG: Due to the molecular dispersion of IgG₀₁, the observed relaxation process is in fact a cooperative relaxation of the macromolecule and the carbohydrate system. This results in a broadening of the dielectric loss peak⁷⁰. The slight shift of the maxima of the loss peaks towards lower frequencies observed in the samples without IgG might be correlated to the same phenomenon.

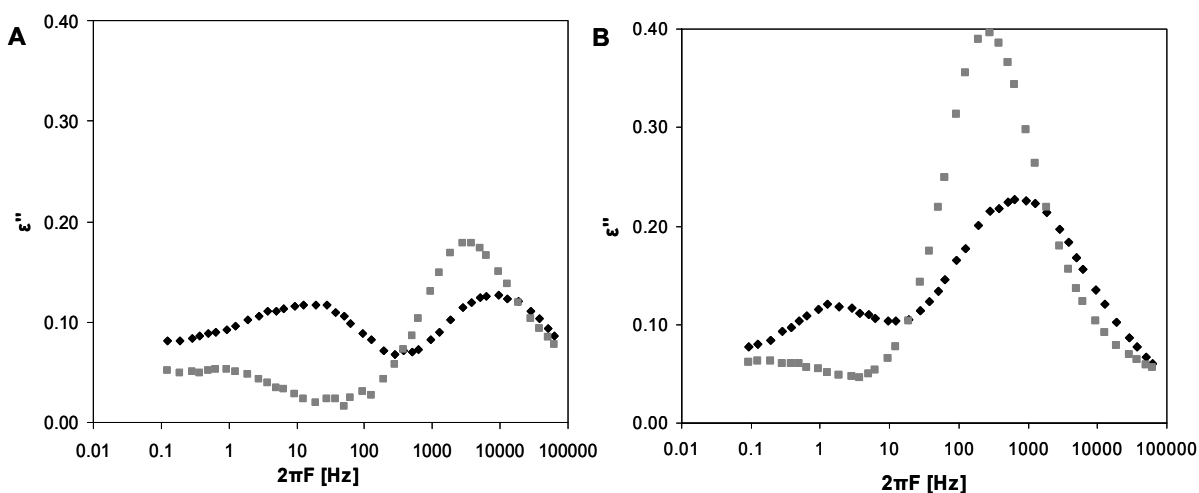


Figure 9.21: Dielectric loss spectra of sucrose lyophilizates with (black symbols) and without (grey symbols) IgG₀₁ at T_g/T 1.00 (A) and 1.03 (B).

PROVE OF CONCEPT IV: EFFECT OF DURATION OF DRYING AT 45 °C

In order to analyze the effect of drying time at 45 °C on the dielectric properties, collapsed sucrose lyophilizates that were freeze-dried for 24 and 44 hours at 45 °C, respectively, were compared. Figure 9.22 shows dielectric loss spectra at 4 different temperatures. Interestingly, samples dried for 44 hours showed slightly decreased β -relaxation times. Unfortunately, α -relaxation times could not be determined for lyophilizates freeze-dried for 24 hours at 45 °C due to dc-conductivity masking the loss peak. Samples dried for a longer time at 45 °C showed slightly decreased dielectric relaxation strength as well.

The observed decrease in dielectric strength could be attributed to the annealing effect that is exerted by drying at 45 °C. However, the slightly decreased β -relaxation times could possibly be related to the lower moisture content in samples dried for a longer time at 45 °C. The water would act as a deplasticizer as described in the previous section. Figure 9.23 shows the temperature dependence of the secondary relaxations, proving the Arrhenius-type character and highlighting the increased relaxation times of samples dried for shorter times. However, the observed differences were small and probably not significant. The absence of a strong effect of the drying time at 45 °C on the observed β -relaxation times further showed that β -relaxation times were not affected by annealing.

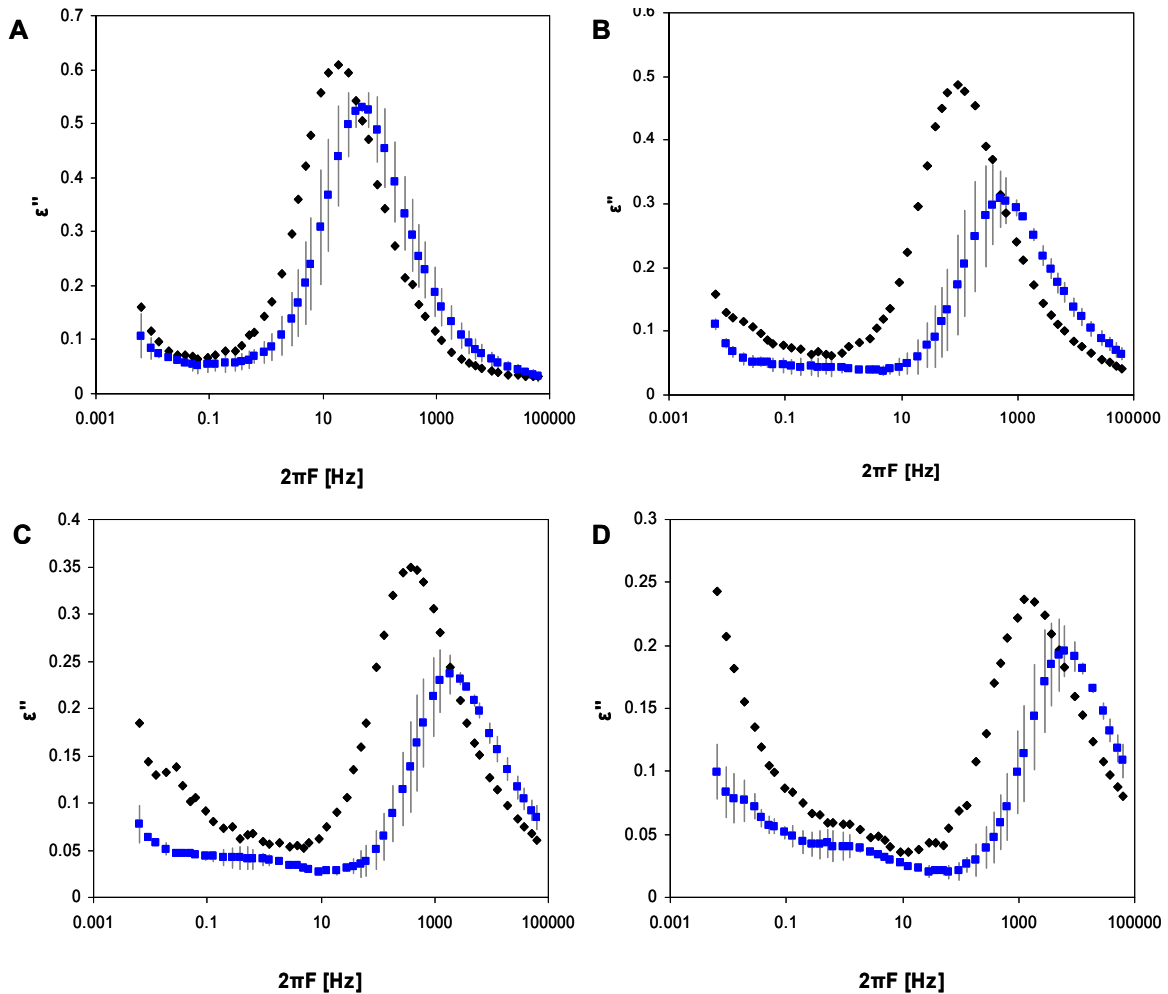


Figure 9.22: Dielectric relaxation spectra of collapsed sucrose lyophilizates that were freeze-dried for 24 (black symbols) and 44 hours (blue symbols), respectively at T_g/T 1.08 (A), 1.02 (B), 1.00 (C) and 0.99 (D).

Spectra of samples dried for 44 hours are calculated average spectra of 2 independent measurements; grey lines indicate the standard deviation.

The larger loss peak at higher frequencies is related to β -relaxations, the smaller loss peak at lower frequencies is related to α -relaxations.

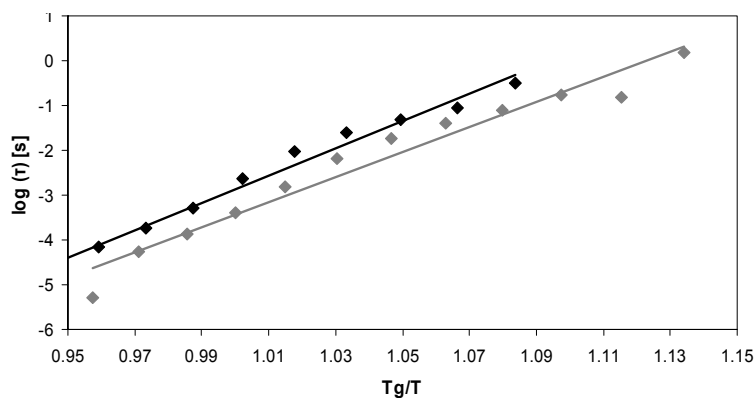


Figure 9.23: Temperature dependence of secondary relaxation of collapsed sucrose dried for 24 h (black symbols) and 44 h (grey symbols) at 45 °C, respectively

5 FRAGILITY OF COLLAPSED AND NOT COLLAPSED LYOPHILIZATES

Besides the structural relaxation time the system's fragility is another important characteristic describing the glass' behaviour during storage. Fragility describes the temperature dependence of molecular motions in glassy systems around their glass transition temperature⁷¹. Thus knowing the fragility of a system gives insight into the change in physical and chemical properties with varying temperature⁷². Especially important is the interrelation of the so-called zero-mobility temperature and the fragility. Whereas there is significant mobility left below the glass transition temperature, the zero-mobility temperature T_0 defines the temperature at which all mobility ceases in an equilibrium glass and below which instability of amorphous systems becomes negligible⁷³. Thus it is argued by some authors that T_0 rather than T_g should be used to predict a system's stability. This is speculated to be especially true for reactions including small molecules³⁵.

According to Angell, glasses can be classified into strong and fragile glasses⁷. Strong glasses show approximately Arrhenius-temperature dependence of molecular motions whereas fragile glasses exhibit a stronger temperature dependence above T_g . Strong and fragile glasses can be visually distinguished in a so-called Kauzmann or fragility plot, in which molecular mobility is plotted versus the inverse of temperature. Strong glass formers would be described by a straight line, whereas fragile glass formers would show a more curved course.

To numerically describe fragility the steepness index m of these fragility plots can be used. The higher the slope, the higher the fragility m . m can as well be calculated from DSC data using equation (9.12) described in the materials and methods part of this chapter. A first approximation of the glass's fragility can be gained from the change in heat capacity at the glass transition Δc_p . Fragile glasses exhibit a large change in heat capacity whereas strong glasses show a smaller Δc_p .

Another analytic measure describing fragility is the so-called Angell's parameter D . It is inversely related to fragility, thus the smaller D the more fragile a material. Of special importance is the linkage of fragility and the zero-mobility temperature (9.13).

$$T_0 = T_g / (1 + (0.0255 * D)) \quad (9.13)$$

According to (9.13) a larger D value leads to a lower T_0 . Because T_0 was defined as the temperature at which all mobility ceases and which is consequently the ultimately safe storage temperature, this would pose the necessity to store at lower temperatures.

Some authors claim that ideal excipients should not only exhibit a high T_g but a high fragility as well.

D can be determined from the Vogel-Tamman-Fulcher (VTF) fit of the structural relaxation time using data above T_g . Because an effect of collapse on the structural relaxation time was observed, an effect of collapse on the system's fragility might as well be expected. To get

further insight into the fragility of collapsed and non-collapsed lyophilizates, experimental data from both, thermal (DSC) and spectroscopic (DRS) analytical methods were used to calculate the fragility.

5.1 FRAGILITY FROM CALORIMETRIC METHODS

A first assumption regarding a material's fragility can be made from the Δc_p at the glass transition. Fragility of glassy materials can then be easily assessed using the heating rate dependency of the glass transition temperature. From the plot in an Arrhenius type diagram of $\log(\text{heating rate})$ versus the reciprocal of the corresponding glass transition temperature, the activation energy for molecular motions at T_g can be calculated. Using equation (9.12), m can be determined. Table 9.10 gives a summary of the calculated variables and lists the fragility indices as calculated from calorimetric data.

Table 9.10: Fragility indices for collapsed and non-collapsed sucrose lyophilizates.

appearance	m
non-collapsed	11
collapsed	125

Clearly, collapsed lyophilizates show increased fragility values as compared to non-collapsed lyophilizates.

5.2 FRAGILITY FROM SPECTROSCOPIC METHODS

To get further insight into the fragility of collapsed and non-collapsed lyophilizates, experimental data from dielectric relaxation spectroscopy was applied to assess fragility using an orthogonal analytical technique. The VTF-fit to describe the temperature dependence of structural relaxation times allows the determination of D , the Angell's parameter. D is directly correlated to the system's fragility with a small D value indicating fragile materials. This approach has seldom been used for pharmaceutically important materials because of experimental difficulties and frequent instabilities of these materials above T_g ⁷¹. Table 9.11 lists the VTF-parameters as determined from the fit of structural relaxation times from DRS data. Non-collapsed lyophilizates showed considerably higher D values as collapsed cakes.

Table 9.11: Parameters from the fit of the VTF equation to the structural relaxation times of sucrose-based collapsed and not collapsed freeze-dried cakes as determined by DRS.

appearance	D	T_0 [K]
non-collapsed	39.0	153.3
collapsed	6.2	289.5

This further confirmed data obtained from calorimetric analysis. As D is inversely related to m , a high D value is correlated to a small m and indicates a strong glass. Thus, elegant

sucrose lyophilizates formed stronger glasses than collapsed systems of the same composition.

The implication of this finding is indicated by the zero-mobility temperature T_0 . As explained in detail above, the existence of significant mobility below the glass transition temperature discredits this temperature as indicative for the estimation of safe storage temperatures. The zero-mobility temperature might be regarded as more indicative to define a storage temperature. A high fragility most familiarly implies a strong decrease in viscosity above the glass transition. At reverse, this means a steeper increase in viscosity below the glass transition as well. Thus, the temperature where all mobility ceases is already reached at higher temperatures.

This is well reflected by Table 9.11, listing the T_0 temperatures from the VTF fit. The T_0 for collapsed lyophilizates was determined at temperatures much higher as for non-collapsed cakes. This gave rise to the assumption that collapsed cakes could be stored at higher temperatures than elegant cakes with regards to preservation of stability of incorporated pharmaceuticals.

6 IS IT JUST ANNEALING OR IS THERE A “COLLAPSE EFFECT”?

6.1 EFFECT OF ANNEALING ON GLASSY DYNAMICS OF NON-COLLAPSED CAKES

The effect of aging or annealing, i.e. exposure to an elevated temperature below T_g for a certain time, on the properties of glassy materials is well known and thoroughly reported in literature. During the time at elevated temperatures, molecular mobility is increased and thus the rate of enthalpy relaxation is increased. After annealing the glass resides at a lower enthalpy level and it is hence more stable than before. As a result, the rate of enthalpy relaxation is decreased during subsequent storage.

The intended use of annealing as a method to increase the storage stability of amorphous pharmaceuticals was reported. Recently, it has been proposed that different drying methods applying various temperature levels during the drying process might affect the glassy dynamics of pharmaceuticals because of differences in the exerted annealing effect⁴. Moreover, it has been described that these differences in glassy dynamics led to differences in storage stability^{1,5,55}.

As described before, the controlled generation of collapsed lyophilizates requires the application of relatively high temperatures for a freeze-drying cycle. But whether collapse was caused intentionally by the application of high drying temperatures or happened accidentally at lower shelf temperatures, e.g. during heating from primary to secondary drying in a conventional freeze-drying cycle, the onset of collapse requires the increase of product temperature above the collapse temperature (although the excess of T_c might be different during collapse-drying and during unintentional occurrence of collapse during a conventional freeze-drying cycle), thus a collapsed lyophilizate most naturally must have been exposed to higher temperatures than a corresponding non-collapsed lyophilizate of identical formulation. Thus collapsed and not collapsed lyophilizates inherently possess different thermal histories.

In order to investigate whether the observed differences in stability (as described in chapter 8) are caused by those different thermal histories and thus by the different degrees of annealing exerted by the different drying protocols or whether there is an additional “collapse-effect”, non-collapsed and collapsed sucrose lyophilizates were compared to non-collapsed lyophilizates that have been annealed, i.e. exposed to elevated temperatures below T_g (approximately 20 K below T_g was reported to be the optimum annealing temperature). By annealing non-collapsed lyophilizates, it was attempted to adjust thermal histories of collapsed and non-collapsed cakes, although it is important to note that annealing of freeze-dried samples at a temperature below their glass transition temperature, as during this experiment, and freeze-drying samples above their collapse temperature, as during collapse-drying, still is a different process. To accomplish this goal, cakes were stored at the same temperature and for the identical period of time (i.e. 24 hours at 45 °C) as the

collapsed cakes were kept during freeze-drying. As the T_g of the non-collapsed lyophilizates was 65 °C, annealing was thus performed 20 K below T_g and optimum annealing conditions were met. Afterwards, glassy dynamics of the three sample systems were compared.

Table 9.12 displays a summary of the characteristic properties regarding the glassy dynamics. Whereas there was a pronounced difference in structural relaxation times of non-collapsed and collapsed sucrose lyophilizates, this offset was significantly reduced after annealing non-collapsed cakes. However, the collapsed lyophilizates still exhibit a higher structural relaxation time, but this difference is not significant anymore, considering the standard deviation.

In contrast to the observed effect of annealing on structural relaxation, there was no effect of annealing on the fragility of the materials. m values calculated from DSC-data gave m -values of 11 and 8 for not collapsed not annealed and annealed samples, respectively, whereas the collapsed lyophilizates showed m values of 23.

Table 9.12: Characteristic properties of collapsed and non-collapsed, annealed and non-annealed sucrose-based lyophilizates.

appearance	annealing	τ^b [h] \pm SD	$\beta \pm$ SD	T_g [°C] \pm SD	m
non-collapsed	-	6.23 \pm 0.68	0.32 \pm 0.02	60.77 \pm 2.85	11
non-collapsed	24 hours/ 45 °C	26.9 \pm 8.0	0.47 \pm 0.24	57.28 \pm 4.49	8
collapsed	24 hours/ 45 °C (during FD)	37.2 \pm 13.8	0.63 \pm 0.16	60.79 \pm 0.98	23

a) determined with isothermal microcalorimetry; temperature of TAM-experiments was 40 °C

b) calculated from the heating rate dependency of the glass transition temperature and using equation (9.12)

Summarizing there is a pronounced effect of annealing on structural relaxation times of not collapsed sucrose lyophilizates. This is in good agreement with observations reported in literature⁷⁴⁻⁷⁶. However, there was no effect of annealing on the fragility observed. Although annealing caused a convergence of relaxation times, annealed non-collapsed systems still exhibited shorter relaxation times than collapsed lyophilizates. Thus the intention to adjust glassy dynamics was only partially achieved.

6.2 CORRELATION OF GLASSY DYNAMICS TO STORAGE STABILITY

To get further insight into the effect of collapse on protein stability in terms of aggregation and to differentiate between contributions from annealing and contributions from a possible “collapse-effect”, a short-term stability was performed. Collapsed and non-collapsed lyophilizates, the latter ones annealed and not annealed, were stored at 40 °C and 50 °C for up to 6 weeks and stability was monitored using HP-SEC and FTIR spectroscopy. These storage conditions were chosen in order to mimic conditions met during the stability study investigating the effect of collapse during storage described in Chapter 8.

Table 9.13 lists the glass transition temperatures and residual moistures of the samples included in the storage stability study. During annealing residual moisture levels slightly

increased and accordingly the glass transition temperatures decreased, but they remained in a comparable range.

Table 9.13: Physical properties of the investigated lyophilizates prior to storage at elevated temperatures.

appearance	annealing	T _g [°C] ± SD	RM [%] ± SD
not collapsed	-	60.77 ± 2.85	1.27 ± 0.06
not collapsed	24h/45°C	57.28 ± 4.49	1.64 ± 0.11
collapsed	24h/45°C (<i>during FD</i>)	60.79 ± 0.98	1.75 ± 0.02

After storage residual moisture levels slightly increased and glass transition temperatures decreased to a comparable degree for all the formulations, as it is frequently reported in literature⁷⁷ (data not shown). Samples remained amorphous upon storage at 40 °C, but upon storage at 50 °C, crystallization occurred, as indicated by the observation of birefringent spots under the polarized light microscope (Figure 9.24 A d-f)). However, all samples remained at least partially amorphous, as a glass transition was observed after storage in all the formulations (data not shown).

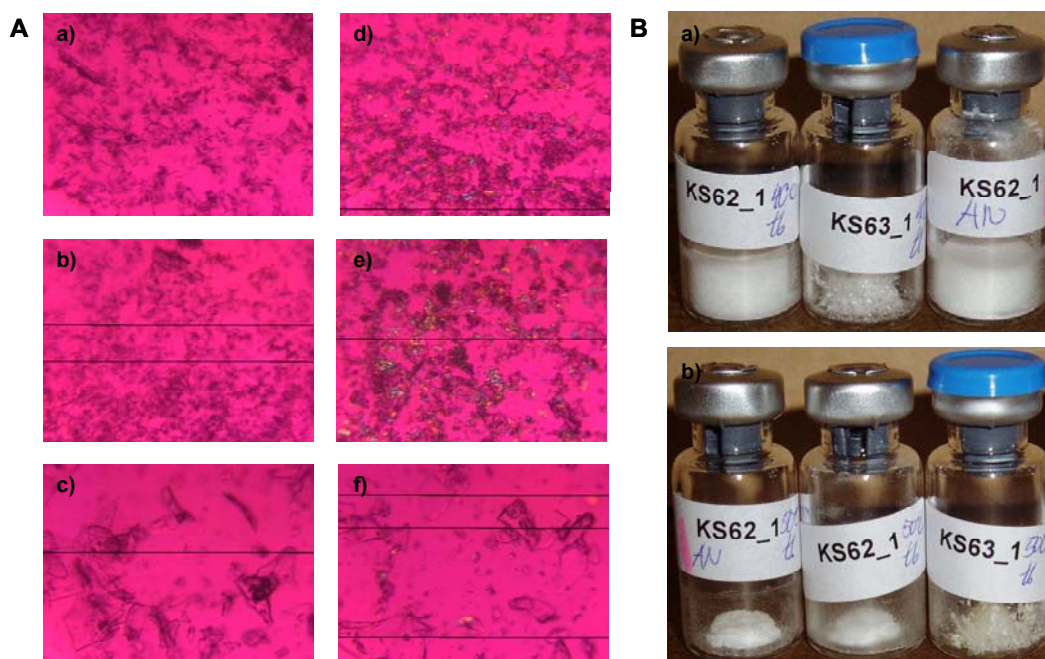


Figure 9.24: A: polarized light microscopic pictures of not collapsed (a, d), not collapsed annealed (b, e) and collapsed (c, f) samples stored for 6 weeks at 40 °C (a-c) and 50 °C (d-f), respectively. B: macroscopic appearance of samples stored for 6 weeks at 40 °C (a) and 50 °C (b), respectively.

Upon storage at 50 °C non-collapsed lyophilizates underwent collapse during storage, no matter whether they had been annealed or not. Collapsed lyophilizates remained macroscopically unchanged. No collapse occurred during storage at 40 °C.

Figure 9.25 depicts the decrease in monomer content during storage at 40 °C and 50 °C, respectively. Most obviously, all samples exhibited little aggregation as indicated by the high

monomer recovery of at least 97.9 %. However, as storage times were short and the IgG₀₁ had been known to be quite stable, this was not surprising.

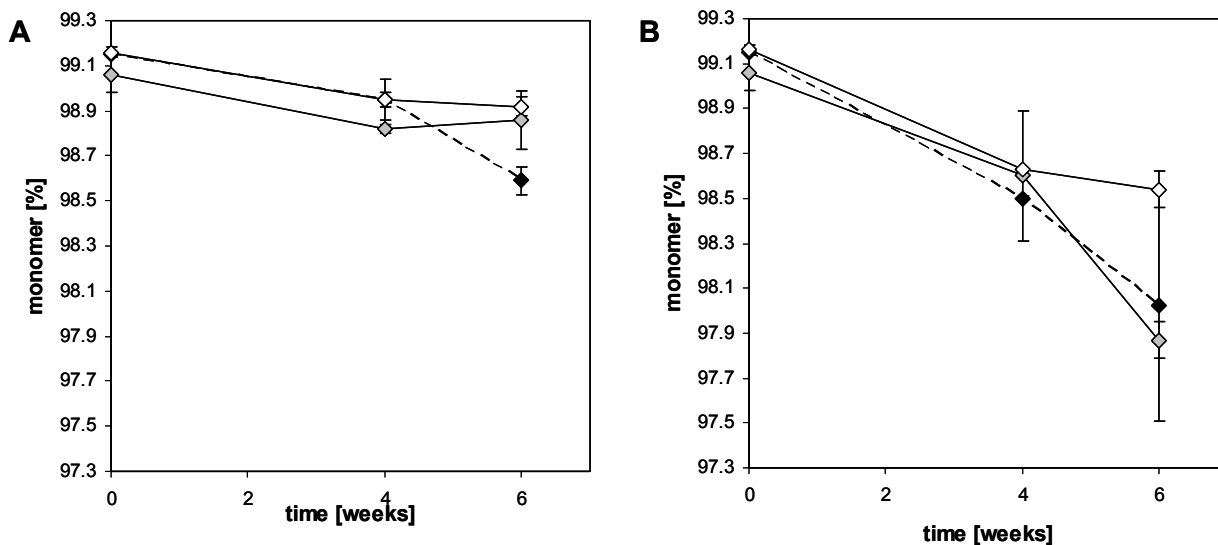


Figure 9.25: IgG₀₁ monomer content during storage at 40 °C (A) and 50 °C (B), respectively, as determined by HP-SEC.

Collapsed (open diamonds), non-collapsed annealed (grey diamonds) and non-collapsed non-annealed (black diamonds) sucrose IgG₀₁ lyophilizates are depicted (average \pm SD, $n = 2$).

Despite the overall little aggregation, differences between the samples could be observed. After storage at 40 °C, collapsed and non-collapsed annealed samples performed slightly better than the non-collapsed non-annealed samples (Figure 9.25 A). In fact the curves describing the decrease of monomer were almost parallel with the non-collapsed annealed sample showing already slightly decreased monomer contents right after processing.

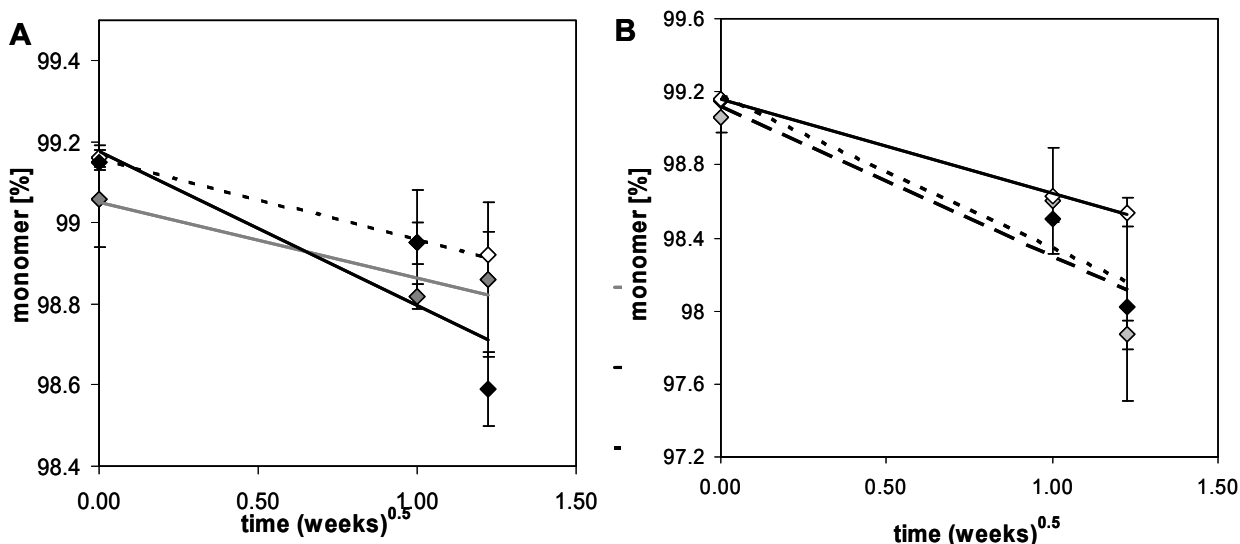


Figure 9.26: Fit of decrease in IgG₀₁ monomer content to stretched exponential kinetics during storage at 40 °C (A) and 50 °C (B) for collapsed (open diamonds), non-collapsed (full diamonds) and non-collapsed annealed (grey full diamonds) lyophilizates. ($n=2$)

40 °C: r^2 (collapsed) = 0.997; r^2 (non-collapsed) = 0.759; r^2 (non-collapsed annealed) = 0.896; 50 °C: r^2 (collapsed) = 0.999; r^2 (non-collapsed) = 0.932; r^2 (non-collapsed annealed) = 0.786

A similar observation was made by Lueckel et al. during annealing during freeze-drying and was related to the increased molecular mobility during annealing that caused an increased level of aggregation⁷⁸. In contrast, during storage at 50 °C (Figure 9.25 B), non-collapsed lyophilizates showed slightly decreased mAb monomer contents as compared to collapsed cakes after six weeks of storage, no matter whether an annealing step was performed or not. However, although results indicated a significant trend, absolute differences in monomer content were small and not relevant.

Aggregation kinetics in amorphous solids often are described by “square root time” or “stretched exponential”⁷⁹ kinetics. Figure 9.26 shows the fits of equation (9.14) to the experimental monomer contents.

$$\%P = P_0 + k\sqrt{t} \quad (9.14)$$

In the above equation P% is the monomer content at a certain point of time, P₀ is the initial level of monomer and k is the apparent rate constant for physical aggregation on the stretched time scale. Table 9.14 summarizes the results of these fits.

Table 9.14: In process degradation of IgG₀₁ and rate constants for aggregation after storage at 40 °C and 50 °C. Initial monomer content of IgG₀₁ before lyophilization was 99.20 ± 0.01 %. n = 2.

appearance	annealing	initial level of monomer (in-process stability) [%]	k at 40°C [%P/(week) ^{0.5}]	k at 50°C [%P/(week) ^{0.5}]
not collapsed	-	99.15 ± 0.01	0.38 ± 0.22	0.84 ± 0.23
not collapsed	24h/45°C	99.06 ± 0.12	0.19 ± 0.06	0.82 ± 0.43
collapsed	24h/45°C (during FD *)	99.16 ± 0.03	0.20 ± 0.01	0.51 ± 0.02

FD: freeze-drying

The rate constants (%/month^{1/2}) were obtained using square root of time kinetics as in Eq. (9.14). The standard error which is the uncertainty in the best fit is also shown.

From Figure 9.26 and Table 9.14 it can be seen that degradation of IgG₀₁ in non-collapsed annealed and collapsed lyophilizates occurred on a similar timescale. In contrast, non-collapsed but non-annealed lyophilizates showed higher degradation rates. Thus it seems that the differences in stability observed between collapsed and non-collapsed lyophilizates observed during former experiments (described in Chapter 8 of this thesis) vanish by annealing non-collapsed lyophilizates and thus adjusting thermal history. However, it has to be noted that overall degradation rates were small and the data set is limited. Also, the relevance during storage at 2-8 °C and 25 °C has to be evaluated in future investigations.

In contrast to observations made during 40 °C-storage, findings from 50 °C-storage drew a different picture. During storage at 50 °C degradation rate constants of non-collapsed cakes were higher than rate constants of collapsed cakes, no matter whether the material had been annealed or not. The increased degradation rate coincides with the onset of collapse during storage. Initially non-collapsed lyophilizates collapsed during storage at 50 °C regardless of initial heat-treatment (Figure 9.24). Thus it seems that the occurrence of collapse during

storage abolished the stabilizing effects of annealing and that there is an additional stabilizing effect of collapse during freeze-drying. This effect might be related to the decreased surface of initially collapsed lyophilizates as compared to both the non-collapsed systems and the systems that collapsed during storage (as described in detail in Chapter 8). Another reason might be an altered total protein surface coverage. A similar effect was described for foam-dried solids that exhibited superior storage stability as compared to freeze- and spray-dried solids. This was explained by decreased local dynamics as well as a decreased protein surface coverage⁵. The remaining differences in global mobility possibly have to be taken into account as well, together with the unchanged fragility of non-collapsed lyophilizates after annealing. Although a high fragility is correlated with a stronger decrease of viscosity above the glass transition temperature, it has been reported that the more fragile trehalose does not crystallize as readily as sucrose upon exceeding T_g ³⁵.

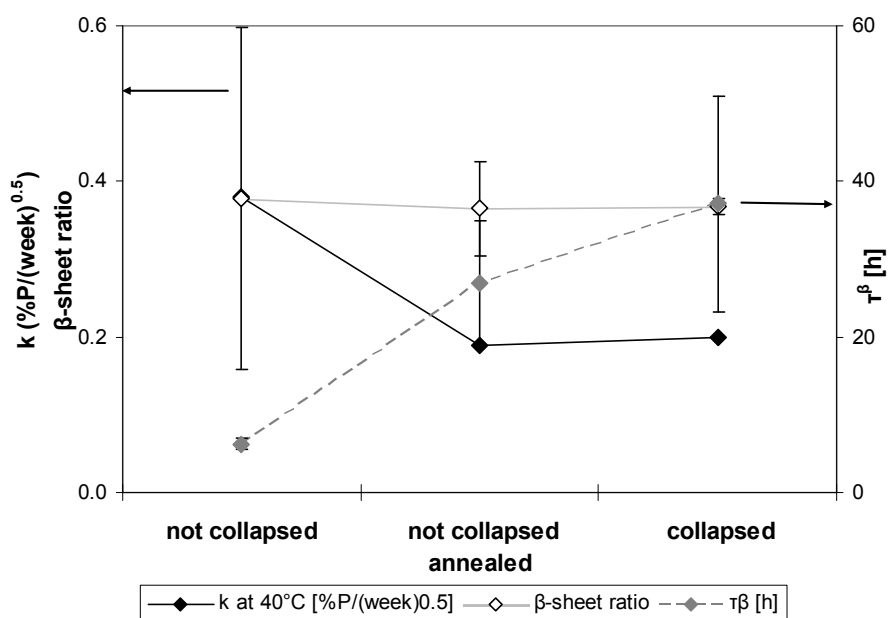


Figure 9.27: Correlation of physical and conformational stability (aggregation rate constants and β -sheet ratio) of collapsed, non-collapsed and non-collapsed annealed lyophilizates at 40 °C to structural relaxation times (τ^β).

Figure 9.27 and Figure 9.28 graphically summarize the discussed findings. At 40 °C there is a qualitative correlation between physical degradation and the structural relaxation time, i.e. the global mobility, whereas at 50 °C this correlation is less clear. The figures also show the β -sheet ratio, to highlight a possible correlation between stability and secondary structure. As described by Abdul-Fattah et al., the ratio of the 2nd derivative FTIR transmission spectra intensities at 1690 cm^{-1} and 1640 cm^{-1} , can be exploited to detect small changes in secondary structure of monoclonal antibodies and proved to be more sensitive than the spectral correlation coefficient^{5,80}. There is no correlation between the secondary structures as reflected in the β -sheet ratios and the degradation kinetics calculated above.

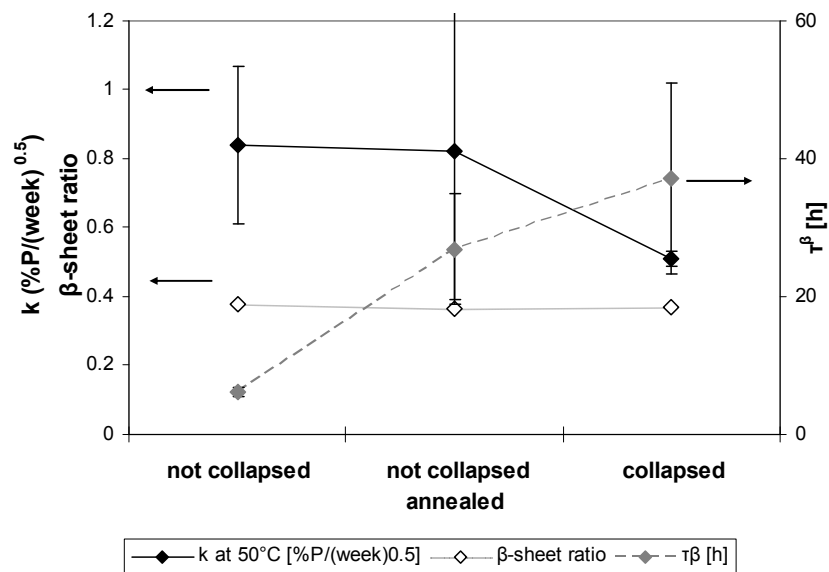


Figure 9.28: Correlation of physical and conformational stability (aggregation rate constants and β -sheet ratio) of collapsed, not collapsed and not collapsed annealed lyophilizates at 50 °C to structural relaxation times (τ^β).

7 SUMMARY

Glassy dynamics of collapsed and non-collapsed sucrose- and trehalose-based lyophilizates containing a mAb of the IgG1-class as a model protein were characterized using both a calorimetric and a spectroscopic analytical technique. Two relaxation processes were detected. The first one, already detectable at room temperature, was identified as a β -relaxation of the Johari-Goldstein-type arising from the rotation of the mono-sugar moieties around the glycosidic bond. This relaxation process proved to be insensitive to the onset of collapse. This finding is consistent with literature describing no effect of drying method on β -relaxations⁴. However, there were differences observed regarding the extent of change in dielectric strength and the degree of frequency shift with varying temperature, with collapsed systems showing a less pronounced dielectric strength and frequency shift. The decreased dielectric strength could be related to the fact that collapsed glasses are more aged than non-collapsed glasses. This was also reflected in the increased powder density of collapsed systems as determined by helium pycnometry.

The second relaxation, emerging at temperatures close to the glass transition temperature, was identified as the structural α -relaxation related to the glass transition phenomenon. A large impact of collapse on structural α -relaxation was found. Collapsed lyophilizates showed strongly increased structural relaxation times. This can be attributed to an annealing effect that was exerted by the drying protocol applied to produce collapsed lyophilizates. A similar effect was observed by Abdul-Fattah et al., who compared foam-dried materials to spray-dried and freeze-dried systems and observed decreased global mobility in materials that were prepared at higher drying temperatures^{1,5,55}.

By the comparative investigation of collapsed, non-collapsed and non-collapsed annealed lyophilizates, it was found that structural relaxation times can be greatly increased by annealing and that differences in structural relaxation times between collapsed and non-collapsed systems vanish by annealing the non-collapsed cakes. Thus the glassy dynamics of non-collapsed glasses can be adapted to that of collapsed glasses by adapting their thermal history. In addition, differences in physical storage stability can be offset as well. However, it was found, that the beneficial effect of annealing is nullified with the occurrence of collapse during storage at elevated temperatures close to T_g . Already initially collapsed lyophilizates are insensitive to storage close to T_g and thus it was concluded that there is another effect additional to the annealing effect that increases stability of collapsed lyophilizates as compared to non-collapsed lyophilizates. An increased stability of protein pharmaceuticals was also reported for foam-dried materials as compared to freeze-dried materials^{1,5,55} and stability was correlated to a reduced protein surface coverage and a reduced specific surface area of the dried material.

Collapsed lyophilizates were also found to be more fragile than non-collapsed lyophilizates. This leads to an increased zero-mobility temperature T_0 that is regarded as more indicative for the choice of a safe storage temperature than T_g by some authors³⁵. Ideal excipients are supposed to have both high T_g s and high fragilities³⁵. Collapsed systems can be regarded as superior to non-collapsed systems with respect to this postulation.

Summarizing, the investigation of global and local glassy dynamics of collapsed and non-collapsed amorphous disaccharide-based lyophilizates allowed for the correlation of differences in the glassy dynamics of collapsed and non-collapsed systems to differences in storage stability regarding the stability of incorporated protein drugs and the stability of excipients that were observed during foregoing storage stability studies. The observation that collapsed lyophilizates show superior stabilizing abilities than non-collapsed systems during storage at elevated temperatures was further confirmed by differences in glassy dynamics that can be correlated to stability.

8 REFERENCES

1. Abdul-Fattah, A.M., Truong-Le, V., Yee, L., Pan, E., Ao, Y., Kalonia, D.S., and Pikal, M.J. Drying-Induced Variations in Physico-Chemical Properties of Amorphous Pharmaceuticals and Their Impact on Stability II: Stability of a Vaccine. *Pharmaceutical Research*, **24** (4): 715-727 (2007)
2. Abdul-Fattah, A.M., Lechuga-Ballesteros, D., Kalonia, D.S., and Pikal, M.J. The impact of drying method and formulation on the physical properties and stability of methionyl human growth hormone in the amorphous solid state. *J.Pharm.Sci.*, **97** (1): 163-184 (2007)
3. Bhugra, C., Rambhatla, S., Bakri, A., Duddu, S.P., Miller, D.P., Pikal, M.J., and Lechuga-Ballesteros, D. Prediction of the onset of crystallization of amorphous sucrose below the calorimetric glass transition temperature from correlations with mobility. *Journal of Pharmaceutical Sciences*, **96** (5): 1258-1269 (2007)
4. Abdul-Fattah, A.M., Kalonia, D.S., and Pikal, M.J. The challenge of drying method selection for protein pharmaceuticals: product quality implications. *Journal of Pharmaceutical Sciences*, **96** (8): 1886-1916 (2007)
5. Abdul-Fattah, A.M., Truong-Le, V., Yee, L., Nguyen, L., Kalonia, D.S., Cicerone, M.T., and Pikal, M.J. Drying-induced variations in physico-chemical properties of amorphous pharmaceuticals and their impact on stability (I): stability of a monoclonal antibody. *Journal of Pharmaceutical Sciences*, **96** (8): 1983-2008 (2007)
6. Mattern, M., Winter, G., Kohnert, U., and Lee, G. Formulation of proteins in vacuum-dried glasses. II. Process and storage stability in sugar-free amino acid systems. *Pharmaceutical Development and Technology*, **4** (2): 199-208 (1999)
7. Angell, C.A. Formation of glasses from liquids and biopolymers. *Science (Washington, D.C.)*, **267** (5206): 1924-1935 (1995)
8. Pikal, M.J. Mechanisms of Protein Satbilization during Freeze-Drying and Storage: The Relative Importance of Thermodynamic Stabilization and Glassy State Relaxation Dynamics.(3): 63-108 (2004)
9. Cicerone, M.T., Tellington, A., Trost, L., and Sokolov, A. Substantially improved stability of biological agents in dried form: the role of glassy dynamics in preservation of biopharmaceuticals. *Bioprocess International*, **1** (1): 36-38, 40, 42, 44, 46 (2003)
10. Cicerone, M.T., Soles, C.L., Chowdhuri, Z., Pikal, M.J., and Chang, L. Fast dynamics as a diagnostic for excipients in preservation of dried proteins. *American Pharmaceutical Reviews*, **8** (6): 22, 24-22, 27 (2005)
11. Ngai, K.L. and Paluch, M. Classification of secondary relaxation in glass-formers based on dynamic properties. *Journal of Chemical Physics*, **120** (2): 857-873 (2004)
12. Kaminski, K., Kaminska, E., Wlodarczyk, P., Pawlus, S., Kimla, D., Kasprzycka, A., Paluch, M., Ziolo, J., Szeja, W., and Ngai, K.L. Dielectric Studies on Mobility of the Glycosidic Linkage in Seven Disaccharides. *Journal of Physical Chemistry B*, **112** (40): 12816-12823 (2008)
13. Duddu, S.P., Zhang, G., and Dal Monte, P.R. The relationship between protein aggregation and molecular mobility below the glass transition temperature of lyophilized formulations containing a monoclonal antibody. *Pharmaceutical Research*, **14** (5): 596-600 (1997)
14. Roy, M.L., Pikal, M.J., Rickard, E.C., and Maloney, A.M. The effects of formulation and moisture on the stability of a freeze-dried monoclonal antibody-vinca conjugate: a test of the WLF glass transition theory. *Developments in Biological Standardization*, **74** (Biol. Prod. Freeze-Drying Formulation): 323-340 (1992)
15. Salnikova, M.S., Middaugh, C.R., and Rytting, J.H. Stability of lyophilized human growth hormone. *International Journal of Pharmaceutics*, **358** (1-2): 108-113 (2008)
16. Yoshioka, S., Tajima, S., Aso, Y., and Kojima, S. Inactivation and Aggregation of beta -Galactosidase in Lyophilized Formulation Described by Kohlrausch-Williams-Watts Stretched Exponential Function. *Pharmaceutical Research*, **20** (10): 1655-1660 (2003)

17. Yoshioka, S., Aso, Y., and Kojima, S. Temperature- and glass transition temperature-dependence of bimolecular reaction rates in lyophilized formulations described by the Adam-Gibbs-Vogel equation. *Journal of Pharmaceutical Sciences*, **93** (4): 1062-1069 (2004)
18. Yoshioka, S., Miyazaki, T., Aso, Y., and Kawanishi, T. Significance of local mobility in aggregation of beta -galactosidase lyophilized with trehalose, sucrose or stachyose. *Pharmaceutical Research*, **24** (9): 1660-1667 (2007)
19. Cicerone, M.T. and Soles, C.L. Fast dynamics and stabilization of proteins: Binary glasses of trehalose and glycerol. *Biophysical Journal*, **86** (6): 3836-3845 (2004)
20. Yoshioka, S., Miyazaki, T., and Aso, Y. beta -Relaxation of Insulin Molecule in Lyophilized Formulations Containing Trehalose or Dextran as a Determinant of Chemical Reactivity. *Pharmaceutical Research*, **23** (5): 961-966 (2006)
21. Bhugra, C., Shmeis, R., Krill, S.L., and Pikal, M.J. Predictions of Onset of Crystallization from Experimental Relaxation Times I-Correlation of Molecular Mobility from Temperatures Above the Glass Transition to Temperatures Below the Glass Transition. *Pharmaceutical Research*, **23** (10): 2277-2290 (2006)
22. Ediger, M.D., Angell, C.A., and Nagel, S.R. Supercooled Liquids and Glasses. *Journal of Physical Chemistry*, **100** (31): 13200-13212 (1996)
23. Liu, J., Rigsbee, D.R., Stotz, C., and Pikal, M.J. Dynamics of pharmaceutical amorphous solids: the study of enthalpy relaxation by isothermal microcalorimetry. *Journal of Pharmaceutical Sciences*, **91** (8): 1853-1862 (2002)
24. Kawakami, K. and Pikal, M.J. Calorimetric investigation of the structural relaxation of amorphous materials: Evaluating validity of the methodologies. *Journal of Pharmaceutical Sciences*, **94** (5): 948-965 (2005)
25. Pearson, D.S. and Smith, G. Dielectric analysis as a tool for investigating the lyophilization of proteins. *Pharmaceutical Science & Technology Today*, **1** (3): 108-117 (1998)
26. Smith, G., Duffy, A.P., Shen, J., and Olliff, C.J. Dielectric Relaxation Spectroscopy and Some Applications in the Pharmaceutical Sciences. *Journal of Pharmaceutical Sciences*, **84** (9): 1029-1044 (1995)
27. Mopsik, F.I. Precision time-domain spectrometer. *Review of Scientific Instruments*, **55** (1): 79-87 (84 A.D.)
28. Debye, P. Polar Molecules. 172(1929)
29. Cole, K.S. and Cole, R.H. Dispersion and absorption in dielectrics. I. Alternating-current characteristics. *Journal of Chemical Physics*, **9** 341-351 (1941)
30. Davidson, D.W. and Cole, R.H. Dielectric relaxation in glycerol. *Journal of Chemical Physics*, **18** 1417(1950)
31. Davidson, D.W. and Cole, R.H. Dielectric relaxation in glycerol, propylene glycol, and n-propanol. *Journal of Chemical Physics*, **19** 1484-1490 (1951)
32. Havriliak, S. and Negami, S. A complex plane representation of dielectric and mechanical relaxation processes in some polymers. *Polymer*, **8** (4): 161-205, appendix (1967)
33. Angell, C.A. Relaxation in liquids, polymers and plastic crystals - strong/fragile patterns and problems. *Journal of Non-Crystalline Solids*, **131-133** (Pt. 1): 13-31 (1991)
34. Hancock, B.C. and Zografi, G. The relationship between the glass transition temperature and the water content of amorphous pharmaceutical solids. *Pharmaceutical Research*, **11** (4): 471-477 (1994)
35. Hatley, R.H.M. Glass fragility and the stability of pharmaceutical preparations-excipient selection. *Pharmaceutical Development and Technology*, **2** (3): 257-264 (1997)

36. El Moznine, R., Smith, G., Polygalov, E., Suherman, P.M., and Broadhead, J. Dielectric properties of residual water in amorphous lyophilized mixtures of sugar and drug. *J.Phys.D: Appl.Phys.*, **36** (4): 330-335 (2003)
37. Suherman, P.M., Taylor, P.M., and Smith, G. Development of a remote electrode system for monitoring the water content of materials inside a glass vial. *Pharmaceutical Research*, **19** (3): 337-344 (2002)
38. Yoshioka, S. and Aso, Y. Glass transition-related changes in molecular mobility below glass transition temperature of freeze-dried formulations, as measured by dielectric spectroscopy and solid state nuclear magnetic resonance. *Journal of Pharmaceutical Sciences*, **94** (2): 275-287 (2005)
39. Sjostrom, J., Swenson, J., Bergman, R., and Kittaka, S. Investigating hydration dependence of dynamics of confined water: Monolayer, hydration water and Maxwell-Wagner processes. *Journal of Chemical Physics*, **128** (15): 154503/1-154503/9 (2008)
40. Jonscher, A.K. Low-frequency dispersion in carrier-dominated dielectrics. *Philos.Mag., [Part] B*, **38** (6): 587-601 (1978)
41. Gross, G.W., Hayslip, I.C., and Hoy, R.N. Dielectric relaxation spectrum of ice measured with linear blocking layers. *Geophysics*, **45** (5): 914-927 (1980)
42. Moynihan, C.T. Structural relaxation and the glass transition. *Rev.Mineral.*, **32** 1-19 (1995)
43. Ermolina, I., Polygalov, E., Bland, C., and Smith, G. Dielectric spectroscopy of low-loss sugar lyophiles: I. A methodical approach to measurement in the frequency domain 10-1-106 Hz. *Journal of Physics D: Applied Physics*, **40** (1): 36-44 (2007)
44. Gangasharan and Murthy, S.S.N. Nature of the Relaxation Processes in the Supercooled Liquid and Glassy States of Some Carbohydrates. *Journal of Physical Chemistry*, **99** (32): 12349-12354 (1995)
45. Shamblin, S.L., Tang, X., Chang, L., Hancock, B.C., and Pikal, M.J. Characterization of the Time Scales of Molecular Motion in Pharmaceutically Important Glasses. *Journal of Physical Chemistry B*, **103** (20): 4113-4121 (1999)
46. Capaccioli, S., Prevosto, D., Kessairi, K., Lucchesi, M., and Rolla, P. Relation between the dispersion of alpha -relaxation and the time scale of beta -relaxation at the glass transition. *Journal of Non-Crystalline Solids*, **353** (41-43): 3984-3988 (2007)
47. Prevosto, D., Capaccioli, S., Sharifi, S., Kessairi, K., Lucchesi, M., and Rolla, P.A. Secondary dynamics in glass formers: Relation with the structural dynamics and the glass transition. *Journal of Non-Crystalline Solids*, **353** (47-51): 4278-4282 (2007)
48. Jansson, H., Bergman, R., and Swenson, J. Dynamics of sugar solutions as studied by dielectric spectroscopy. *Journal of Non-Crystalline Solids*, **351** (33-36): 2858-2863 (2005)
49. Pethig, R. Protein-water interactions determined by dielectric methods. *Annual Review of Physical Chemistry*, **43** 177-205 (1992)
50. Noel, T.R., Parker, R., and Ring, S.G. Effect of molecular structure and water content on the dielectric relaxation behaviour of amorphous low molecular weight carbohydrates above and below their glass transition. *Carbohydrate Research*, **329** (4): 839-845 (2000)
51. Kaminski, K., Kaminska, E., Hensel-Bielowka, S., Chelmecka, E., Paluch, M., Ziolo, J., Wlodarczyk, P., and Ngai, K.L. Identification of the Molecular Motions Responsible for the Slower Secondary (beta) Relaxation in Sucrose. *Journal of Physical Chemistry B*, **112** (25): 7662-7668 (2008)
52. Einfeldt, J., MeiBner, D., and Kwasniewski, A. Molecular interpretation of the main relaxations found in dielectric spectra of cellulose - experimental arguments. *Cellulose (Dordrecht, Neth.)*, **11** (2): 137-150 (2004)
53. Van Dusschoten, D., Tracht, U., Heuer, A., and Spiess, H.W. Site Specific Rotational Mobility of Anhydrous Glucose near the Glass Transition As Studied by 2D Echo Decay 13C NMR. *J.Phys.Chem.A*, **103** (42): 8359-8364 (1999)

54. Einfeldt, J., Meissner, D., and Kwasniewski, A. Comparison of the molecular dynamics of celluloses and related polysaccharides in wet and dried states by means of dielectric spectroscopy. *Macromol.Chem.Phys.*, **201** (15): 1969-1975 (2000)
55. Abdul-Fattah, A.M., Lechuga-Ballesteros, D., Kalonia, D.S., and Pikal, M.J. The impact of drying method and formulation on the physical properties and stability of methionyl human growth hormone in the amorphous solid state. *Journal of Pharmaceutical Sciences*, **97** (1): 163-184 (2008)
56. Diogo, H.P. and Moura Ramos, J.J. Slow molecular mobility in the crystalline and amorphous solid states of glucose as studied by thermally stimulated depolarization currents (TSDC). *Carbohydrate Research*, **343** (16): 2797-2803 (2008)
57. Ramos, J.J.M., Diogo, H.P., and Pinto, S.S. Effect of physical aging on the Johari-Goldstein and alpha relaxations of D-sorbitol: a study by thermally stimulated depolarization currents. *Journal of Chemical Physics*, **126** (14): 144506/1-144506/6 (2007)
58. Ngai, K.L. Do theories of glass transition that address only the alpha -relaxation need a new paradigm? *Journal of Non-Crystalline Solids*, **351** (33-36): 2635-2642 (2005)
59. Kaminski, K., Kaminska, E., Hensel-Bielowka, S., Pawlus, S., Paluch, M., and Ziolo, J. High pressure study on molecular mobility of leucrose. *Journal of Chemical Physics*, **129** (8): 084501/1-084501/5 (2008)
60. Sharifi, S., Prevosto, D., Capaccioli, S., Lucchesi, M., and Paluch, M. Effect of thermodynamic history on secondary relaxation in the glassy state. *Journal of Non-Crystalline Solids*, **353** (47-51): 4313-4317 (2007)
61. Ermolina, I., Polygalov, E., Bland, C., and Smith, G. Dielectric spectroscopy of low-loss sugar lyophiles: II. Relaxation mechanisms in freeze-dried lactose and lactose monohydrate. *Journal of Non-Crystalline Solids*, **353** (47-51): 4485-4491 (2007)
62. Kudlik, A., Benkhof, S., Blochowicz, T., Tschirwitz, C., and Rossler, E. The dielectric response of simple organic glass formers. *Journal of Molecular Structure*, **479** (2-3): 201-218 (1999)
63. Moura Ramos, J.J., Diogo, H.P., and Pinto, S.S. Effect of physical aging on the Johari-Goldstein and alpha relaxations of D-sorbitol: a study by thermally stimulated depolarization currents. *Journal of Chemical Physics*, **126** (14): 144506(2007)
64. Tanaka, H. Origin of the excess wing and slow beta relaxation of glass formers: a unified picture of local orientational fluctuations. *Phys.Rev.E: Stat., Nonlinear, Soft Matter Phys.*, **69** (2-1): 021502/1-021502/10 (2004)
65. Moura Ramos, J.J., Pinto, S.S., and Diogo, H.P. The slow molecular mobility in amorphous trehalose. *Chemphyschem*, **8** (16): 2391-2396 (2007)
66. Dranca, I., Bhattacharya, S., Vyazovkin, S., and Suryanarayanan, R. Implications of Global and Local Mobility in Amorphous Sucrose and Trehalose as Determined by Differential Scanning Calorimetry. *Pharmaceutical Research*, **26** (5): 1064-1072 (2009)
67. Shinyashiki, N., Shinohara, M., Iwata, Y., Goto, T., Oyama, M., Suzuki, S., Yamamoto, W., Yagihara, S., Inoue, T., Oyaizu, S., Yamamoto, S., Ngai, K.L., and Capaccioli, S. The Glass Transition and Dielectric Secondary Relaxation of Fructose-Water Mixtures. *Journal of Physical Chemistry, ACS*(2008)
68. Te Booy, M.P.W.M., De Ruiter, R.A., and De Meere, A.L.J. Evaluation of the physical stability of freeze-dried sucrose-containing formulations by differential scanning calorimetry. *Pharmaceutical Research*, **9** (1): 109-114 (1992)
69. Chang, L., Shepherd, D., Sun, J., Tang, X., and Pikal, M.J. Effect of sorbitol and residual moisture on the stability of lyophilized antibodies: Implications for the mechanism of protein stabilization in the solid state. *Journal of Pharmaceutical Sciences*, **94** (7): 1445-1455 (2005)
70. Pethig, R. Dielectric and Electronic Properties of Biological Materials. *John Wiley & Sons Ltd* (1979)
71. Hancock, B.C., Dalton, C.R., Pikal, M.J., and Shamblin, S.L. A pragmatic test of a simple calorimetric method for determining the fragility of some amorphous pharmaceutical materials. *Pharmaceutical Research*, **15** (5): 762-767 (1998)

72. Hancock, B.C. and Zografi, G. Characteristics and Significance of the Amorphous State in Pharmaceutical Systems. *Journal of Pharmaceutical Sciences*, **86** (1): 1-12 (1997)
73. Hancock, B.C., Shamblin, S.L., and Zografi, G. Molecular mobility of amorphous pharmaceutical solids below their glass transition temperatures. *Pharmaceutical Research*, **12** (6): 799-806 (1995)
74. Abdul-Fattah, A.M., Dellerman, K.M., Bogner, R.H., and Pikal, M.J. The effect of annealing on the stability of amorphous solids: chemical stability of freeze-dried moxalactam. *Journal of Pharmaceutical Sciences*, **96** (5): 1237-1250 (2007)
75. Luthra, S.A., Hodge, I.M., and Pikal, M.J. Investigation of the impact of annealing on global molecular mobility in glasses: optimization for stabilization of amorphous pharmaceuticals. *Journal of Pharmaceutical Sciences*, **97** (9): 3865-3882 (2008)
76. Luthra, S.A., Hodge, I.M., and Pikal, M.J. Effects of annealing on enthalpy relaxation in lyophilized disaccharide formulations: mathematical modeling of DSC curves. *Journal of Pharmaceutical Sciences*, **97** (8): 3084-3099 (2008)
77. Earle, J.P., Bennett, P.S., Larson, K.A., and Shaw, R. The effects of stopper drying on moisture levels of Haemophilus influenzae conjugate vaccine. *Developments in Biological Standardization*, **74** (Biol. Prod. Freeze-Drying Formulation): 203-210 (1992)
78. Lueckel, B., Helk, B., Bodmer, D., and Leuenberger, H. Effects of formulation and process variables on the aggregation of freeze-dried interleukin-6 (IL-6) after lyophilization and on storage. *Pharmaceutical Development and Technology*, **3** (3): 337-346 (1998)
79. Yoshioka, S., Aso, Y., and Kojima, S. Usefulness of the Kohlrausch-Williams-Watts stretched exponential function to describe protein aggregation in lyophilized formulations and the temperature dependence near the glass transition temperature. *Pharmaceutical Research*, **18** (3): 256-260 (2001)
80. Prestrelski, S., Tedeschi, N., Arakawa, T., and Carpenter, J.F. Dehydration-induced conformational transitions in proteins and their inhibition by stabilizers. *Biophysical Journal*, **65** (2): 661-671 (1993)

CHAPTER 10

FINAL SUMMARY AND CONCLUSION

The objective of the present thesis was to investigate the effect of lyophilizate collapse during freeze-drying and after subsequent storage on the stability of incorporated proteins. Interest originated in the fact that collapsed lyophilizates are supposed to have irregularly distributed residual moisture contents, prolonged reconstitution times and inferior protein stability^{1,2}. Thus the release of such product to the market is generally denied. This leads to the common approach during freeze-drying of maintaining the product at low temperatures well below the collapse-temperature, which results in long and therefore expensive production cycles. In contrast, recent publications indicate that the negative effects associated with collapse might in fact be overestimated³⁻⁶. In addition, as deducible from other drying techniques, such as vacuum- or foam-drying, adequate protein stabilization does not necessarily require a porous cake^{7,8}. In the course of our studies, the effect of collapse on protein stability was thus thoroughly investigated by comparing deliberately collapsed with non-collapsed lyophilizates of the same composition.

In **Chapter 1** a general introduction to freeze-drying of biopharmaceuticals is given and special attention is paid to the collapse phenomenon, its mechanism, determinants and the current attitude towards collapse and its effect on proteins. Reviewing literature it becomes apparent that no systematic investigation has been carried out so far with a comprehensive set of analytical tools to determine the effect of collapse on protein stability. Current knowledge is mostly based on observations made in lyophilizates that collapsed accidentally during process- and formulation development.

A second focus is set on solid state stabilization concepts as it was recently described that thermal history has a strong impact on the solid state characteristics and the solid state stability of amorphous dried protein formulations. As in our studies collapsed products underwent higher temperatures than non-collapsed products during processing, a change in thermal history similar to the effect of annealing must be taken into account.

The objectives of this thesis are summarized in **Chapter 2** and the materials and methods used throughout the thesis are specified in **Chapter 3**.

The controlled and reproducible production of collapsed lyophilizates with defined critical material properties, such as the residual moisture content, to be kept comparable to non-collapsed lyophilizates was a categorical prerequisite for the sound comparison of collapsed and non-collapsed lyophilizates. Two approaches to the deliberate production of collapsed lyophilizates can be distinguished: Either a formulation's collapse temperature can be

lowered below the product temperature of an existing freeze-drying protocol, (e.g. by the addition of low molecular weight excipients or by omission of crystalline bulking agents), or the process parameters can be varied in order to exceed the system's collapse temperature. In **Chapter 4** of the thesis, investigations and tentative experiments examining the collapsibility of different excipients commonly applied in freeze-dried formulations were described. To produce collapsed lyophilizates, an aggressive freeze-drying protocol, referred to as the "collapse-cycle", was developed and optimized in order to obtain comparable residual moisture contents in collapsed and non-collapsed cakes. For this purpose, sublimation and desorption behavior of collapsed lyophilizates was extensively characterized using a wide array of process analytical technologies, such as mass spectrometric monitoring of the gas phase composition in the freeze-dryer and sampling throughout the primary drying phase with a sample thief. No strong decrease in sublimation rate was observed with the onset of collapse, but secondary drying was found to be relevantly slowed down. However, using dry nitrogen injections and high secondary drying temperatures, collapsed lyophilizates with residual moisture contents below one percent were produced. Non-collapsed lyophilizates with identical composition and matching residual moisture contents were produced with conventional freeze-drying protocols.

In a second approach, lyophilizates that were collapsed to different extents were produced using the collapse-cycle by stepwise variation of the mass ratio of the crystalline bulking agent mannitol to the amorphous protective agent sucrose. This approach allowed for the comparison of differently collapsed lyophilizates with identical thermal history.

In **Chapter 5** different analytical techniques with the potential to quantify the extent of collapse were evaluated regarding their applicability. The simple classification based upon the evaluation of the macroscopic and microscopic appearance, that has been state of the art so far,⁹ lacked differentiation in terms of partially collapsed cakes and needed improvement. The specific surface area (SSA) as assessed by BET-krypton gas adsorption was found to be the most sensitive method showing a continuous decrease of SSA where visual evaluation could differentiate only into non-collapsed, partially collapsed and completely collapsed cakes. Besides the SSA, density measurements and porosity measurements also proved to be capable of providing an analytical measure for the extent of collapse.

Concerns that collapse leads to high and irregularly distributed residual moisture contents are addressed in **Chapter 6**. Lyophilizates that collapsed to different extents were produced and separated into bottom-, top-, wall- and core-section in a dry nitrogen atmosphere and the moisture content was determined separately for each part. No difference was found between bottom- and top-section, but the core-section was found to have consistently higher moisture

contents. Interestingly higher moisture contents in the core section were found no matter whether the cake had collapsed or not.

Because collapsed and non-collapsed lyophilizates were produced using two different freeze-drying protocols, achieving exactly the same residual moisture content was not always perfectly feasible. In order to estimate to what extent IgG₁-stability could be affected by residual moisture variations, which adversely affect protein stability as reported in literature¹⁰⁻¹³, the effect of moisture on mAb-stability was investigated over a wide range of residual moisture contents (0.7 % to 6.3 %) covering a large span of moisture contents exceeding values observed in collapsed cakes in this thesis. In the entire investigated range, no destabilizing effect of moisture was observed and no correlation between residual moisture content and mAb stability could be concluded. Thus slight differences in residual moisture content that were observed between collapsed and non-collapsed lyophilizates in some studies performed during this thesis, were regarded as not critical in terms of attributing stability differences to collapse.

The effect of collapse on protein stability was extensively investigated by comparing collapsed and non-collapsed lyophilizates of identical composition using a monoclonal antibody of the IgG₁ class representing the currently most important biopharmaceutical product class, L-lactic dehydrogenase (LDH) that is very sensitive towards stress situations arising during freeze-drying and PA₀₁, a commercially available biopharmaceutical product that is known to be challenging in terms of the success of freeze-drying processes, as model proteins. Different formulations representing the most commonly applied freeze-drying excipients, including both purely amorphous disaccharide- and amino acid-based formulations as well as partially crystalline mannitol- or PEG-based formulations were analyzed. Analysis was carried out both immediately after lyophilization (**Chapter 7**) and after up to six months of storage at 2-8 °C, 25 °C, 40 °C or 50 °C (**Chapter 8**). In addition to the investigation of completely collapsed and non-collapsed lyophilizates, IgG₁ in various intermediate collapse states was analyzed as well. By stepwise variation of the ratio of mannitol to sucrose, lyophilizates with increasing degree of collapse were produced.

All formulations were analyzed regarding both, the physicochemical properties of the excipients, such as the glass transition temperature and the crystallinity, and the protein stability, including the formation of soluble and insoluble aggregates, the secondary and tertiary structure and the biologic activity.

After freeze-drying, all proteins were well-stabilized no matter whether the lyophilizates collapsed or not. No detrimental effect of collapse on protein stability was detected. Most intriguingly, in some cases, proteins reconstituted from collapsed cakes performed even better in key stability-indicating parameters, such as the level of remaining monomer or the recovery of catalytic activity.

This trend was further confirmed during storage stability studies. IgG₀₁ was well-stabilized in trehalose-based lyophilizates regardless of whether the cakes were completely collapsed or elegant. In contrast, partially crystalline mannitol-sucrose lyophilizates exhibited a slightly better IgG₀₁ preservation when they were partially collapsed. A remarkable behaviour was observed for sucrose-based IgG₀₁ lyophilizates: Elegant lyophilizates that were stored at 40 °C and 50 °C collapsed during storage and rapidly underwent sucrose crystallization, hydrolysis of sucrose into glucose and fructose and glycation of the IgG₀₁. In contrast, initially, during freeze-drying collapsed sucrose-lyophilizates with identical residual moisture contents and glass transition temperatures showed strongly decreased rates of crystallization and IgG₁-glycation. However, the rate of sucrose hydrolysis was found to be comparable in both systems.

Studies from LDH lyophilizates confirmed the observed trend: Collapsed cakes showed higher degrees of physical protein stability in terms of both soluble and insoluble aggregation and better preservation of both secondary and tertiary structure, but no difference in catalytic activity. Sucrose-PEG-based lyophilizates that partially collapsed during the freeze-drying run showed the least degree of LDH-stabilization, further highlighting the benefit of producing deliberately completely collapsed cakes in order to prevent accidental collapse during the process or subsequent storage.

In PA₀₁ samples, clot lytic activity was significantly increased in collapsed lyophilizates as compared to non-collapsed cakes and the formation of soluble aggregates was decreased. However, stability was well preserved in both systems and differences were subtle, but significant.

Summarizing the main chapters 7 and 8, collapse was shown to not adversely affect protein stability after lyophilization and after long-term storage. Moreover, intentionally collapsed lyophilizates using collapse-drying were found to better preserve protein stability in several key stability-indicating parameters and to be more robust towards storage at elevated temperatures. In addition, concerns usually related to collapsed products, such as prolonged reconstitution times, high residual moisture contents and the susceptibility towards crystallization were shown not to apply to collapse-dried lyophilizates.

The molecular basis for the observed differences in storage stability of collapsed and non-collapsed lyophilizates was elucidated analyzing the glassy dynamics of collapsed and non-collapsed amorphous systems using dielectric relaxation spectroscopy (DRS) and isothermal microcalorimetry as described in **Chapter 9**. Two relaxation processes could be detected. The first one, already detectable at room temperature, was identified as a β -relaxation of the Johari-Goldstein type arising from the rotation of the monosugar moieties around the glycosidic bond. This relaxation was found not to be relevantly different for the two systems, although there were slight dissimilarities referring to the more aged state of the collapsed

sample. The second relaxation, detectable at temperatures close to the glass transition temperature was identified as the structural α -relaxation and it was found to be greatly affected by the onset of collapse. Collapsed lyophilizates showed strongly increased structural relaxation times, which translates into a greatly reduced global mobility. This strongly reduced global mobility can be correlated to the different crystallization and glycation behavior observed during storage of sucrose lyophilizates at elevated temperatures.

As it was recently reported that the drying technology greatly affects a system's thermal history and thereby its molecular mobility, an adjustment of the lyophilizates' thermal histories was realized by annealing the non-collapsed lyophilizates at 45 °C. Annealing indeed resulted in an adaptation of both the structural relaxation time and the physical storage stability of an incorporated IgG (as assessed by HP-SEC). However, the onset of collapse in initially non-collapsed cakes during storage at elevated temperatures close to the T_g nullified the beneficial effect of annealing whereas collapsed lyophilizates were insensitive towards storage close to T_g . Thus there has to be another effect in addition to the annealing effect that increases stability of collapsed lyophilizates as compared to non-collapsed lyophilizates.

It was further found that collapsed systems are more fragile and show higher zero mobility temperatures allowing for storage at higher temperatures.

Summarizing, differences observed in the storage stability of collapsed and non-collapsed lyophilizates could be correlated to a decreased global molecular mobility in collapsed lyophilizates. This was partly attributed to the annealing effect exerted by the collapse-cycle used to produce collapsed cakes. However, as IgG₁ stability could not be completely adapted by annealing non-collapsed cakes an additional stabilizing effect in collapsed cakes is likely.

Taking together conclusions from all the chapters, the effect of collapse on protein stability was extensively investigated using three different model proteins, of whom two were pharmaceutically relevant and one was a sensitive model protein. A representative set of freeze-drying formulations was analyzed. Special attention was paid to keep the residual moisture level of collapsed and non-collapsed cakes comparable and to exclude possible interferences of moisture effects.

The conducted studies provided the basis for a change in paradigm in good freeze-drying practice towards freeze-drying at higher temperatures, thereby shortening drying cycles and greatly enlarging the design space.

In addition, the intentional collapse during collapse-drying might provide a means to avoid accidental collapse either during processing or during subsequent storage. Furthermore, as these cakes appear to be less sensitive towards storage at elevated temperatures they might be stored at room temperature rather than refrigerated, greatly facilitating transportation and

storage. In this context, further studies, especially addressing the advanced characterization of the drying process and the reproducibility and control of the onset of collapse during collapse-drying are of great interest.

REFERENCES

1. Bellows, R.J. and King, C.J. Freeze-drying of aqueous solutions: Maximum allowable operating temperature. *Cryobiology*, **9** (6): 559-561 (1972)
2. MacKenzie, A.P. Collapse during freeze drying - qualitative and quantitative aspects. *Freeze Drying Adv. Food Technol., [Int. Course]*, 277-307 (1975)
3. Chatterjee, K., Shalae, E.Y., and Suryanarayanan, R. Partially crystalline systems in lyophilization: II. Withstanding collapse at high primary drying temperatures and impact on protein activity recovery. *Journal of Pharmaceutical Sciences*, **94** (4): 809-820 (2005)
4. Izutsu, K., Yoshioka, S., and Kojima, S. Physical stability and protein stability of freeze-dried cakes during storage at elevated temperatures. *Pharmaceutical Research*, **11** (7): 995-999 (1994)
5. Jiang, S. and Nail, S.L. Effect of process conditions on recovery of protein activity after freezing and freeze-drying. *European Journal of Pharmaceutics and Biopharmaceutics*, **45** (3): 249-257 (1998)
6. Wang, D.Q., Hey, J.M., and Nail, S.L. Effect of collapse on the stability of freeze-dried recombinant factor VIII and α -amylase. *Journal of Pharmaceutical Sciences*, **93** (5): 1253-1263 (2004)
7. Abdul-Fattah, A.M., Truong-Le, V., Yee, L., Nguyen, L., Kalonia, D.S., Cicerone, M.T., and Pikal, M.J. Drying-induced variations in physico-chemical properties of amorphous pharmaceuticals and their impact on stability (I): stability of a monoclonal antibody. *Journal of Pharmaceutical Sciences*, **96** (8): 1983-2008 (2007)
8. Mattern, M., Winter, G., Kohnert, U., and Lee, G. Formulation of proteins in vacuum-dried glasses. II. Process and storage stability in sugar-free amino acid systems. *Pharmaceutical Development and Technology*, **4** (2): 199-208 (1999)
9. To, E.C. and Flink, J.M. 'Collapse', a structural transition in freeze dried carbohydrates. I. Evaluation of analytical methods. *Journal of Food Technology*, **13** (6): 551-565 (1978)
10. Breen, E.D., Curley, J.G., Overcashier, D.E., Hsu, C.C., and Shire, S.J. Effect of moisture on the stability of a lyophilized humanized monoclonal antibody formulation. *Pharmaceutical Research*, **18** (9): 1345-1353 (2001)
11. Chang, L., Shepherd, D., Sun, J., Tang, X., and Pikal, M.J. Effect of sorbitol and residual moisture on the stability of lyophilized antibodies: Implications for the mechanism of protein stabilization in the solid state. *Journal of Pharmaceutical Sciences*, **94** (7): 1445-1455 (2005)
12. Lueckel, B., Helk, B., Bodmer, D., and Leuenberger, H. Effects of formulation and process variables on the aggregation of freeze-dried interleukin-6 (IL-6) after lyophilization and on storage. *Pharmaceutical Development and Technology*, **3** (3): 337-346 (1998)
13. Towns, J.K. Moisture content in proteins: its effects and measurement. *Journal of Chromatography, A*, **705** (1): 115-127 (1995)

PRESENTATIONS AND PUBLICATIONS ASSOCIATED WITH THIS THESIS

ARTICLES

K. Schersch, O. Betz, P. Garidel, S. Muehlau, S. Bassarab, G. Winter
Systematic investigation of the effect of lyophilizate collapse on pharmaceutically relevant proteins I: Stability after freeze drying
(submitted to *Journal of Pharmaceutical Sciences*, 2009)

POSTER PRESENTATIONS

K. Schersch, O. Betz, P. Garidel, S. Mühlau, S. Bassarab, G. Winter. Effect of cake structure on residual moisture determination of lyophilizates: critical assessment of common methodology. *6th Worldmeeting on Pharmaceutics, Biopharmaceutics and Pharmaceutical Technology*, Barcelona, Spain (2008)

K. Schersch, O. Betz, P. Garidel, S. Mühlau, S. Bassarab, G. Winter. Scrutinizing the effect of collapse during lyophilization: Stability of L-Lactic Dehydrogenase lyophilizates during storage at elevated temperatures. *AAPS Annual Meeting*, San Diego, USA (2007)

K. Schersch, O. Betz, P. Garidel, S. Mühlau, S. Bassarab, G. Winter. New Approaches to quantify the degree of collapse in lyophilizates. *AAPS Annual Meeting*, San Diego, USA (2007)

K. Schersch, O. Betz, P. Garidel, S. Mühlau, S. Bassarab, G. Winter. Stability of Collapsed and Not Collapsed Protein Lyophilizates During Storage at Elevated Temperatures. *Pharmaceutical Sciences World Congress*, Amsterdam, The Netherlands (2007)

K. Schersch, K. Mathis, G. Winter. Ultrasonic Resonator Technology as the New Sensitive Analytical Tool in the Investigation of Collapsed and Not Collapsed Protein Lyophilizates. *Pharmaceutical Sciences World Congress*, Amsterdam, The Netherlands (2007)

K. Schersch, O. Betz, P. Garidel, S. Mühlau, S. Bassarab, G. Winter. Effect of Collapse on Protein-Lyophilizates Using L-Lactic Dehydrogenase as Sensitive Model Protein. *AAPS Annual Meeting*, San Antonio, USA (2006)

K. Schersch, O. Betz, P. Garidel, S. Mühlau, S. Bassarab, G. Winter. Effect of Collapse During Lyophilization and During Storage at Elevated Temperatures on the Stability of Pharmaceutical Protein Lyophilizates. *Freeze Drying of Pharmaceutics and Biologicals*, Garmisch Partenkirchen (2006)

K. Schersch, O. Betz, P. Garidel, S. Mühlau, S. Bassarab, G. Winter. Investigations on the effect of collapse on pharmaceutical protein lyophilizates. *5th World Meeting on Pharmaceutics Biopharmaceutics and Pharmaceutical Technology*, Genf (2006)

CURRICULUM VITAE

KATHRIN BRIGITTE SCHERSCH

PERSONAL DETAILS

Date of birth: 18.12.1979

Place of birth: Kiel

Nationality: German

EDUCATION

since 02/2009	Senior Scientist Novartis Pharma AG, Novartis Biologics, Process Sciences & Production, Pharmaceutical Development/ Basel, Switzerland
03/2005 – 01/2009	Ph.D. Thesis Department of Pharmacy, Pharmaceutical Technology and Biopharmaceutics, Ludwig-Maximilians-University/ Munich, Germany Supervisor: Prof. Dr. Gerhard Winter in cooperation with Boehringer-Ingelheim Pharma GmbH & Co. KG/ Biberach, Germany
05/2008 – 08/2008	Research stay at the University of Connecticut/ CT, USA Department of Pharmaceutical Sciences Supervisor: Prof. Dr. Michael Pikal
03/2005	License to practice as a Pharmacist ("Approbation")
12/2004 – 02/2005	Friesen-Apotheke/ Kiel, Germany
05/2004 – 12/2004	Internship at Bayer HealthCare Company Ltd/ Peking, PR China
11/2003 – 04/2004	Internship in public pharmacy, Enzian-Apotheke/ Munich, Germany
09/1999 – 10/2003	Study of pharmacy Christian-Albrechts-University/ Kiel, Germany Ludwig-Maximilians-University/ Munich, Germany
08/1990 – 06/1999	High School, Gymnasium Elmsenhagen/ Kiel, Germany, Graduation with "Abitur"